

THE MATHS

REVISION



© 2011

© 2011

ACS SYMPOSIUM SERIES **611**

Halon Replacements

Technology and Science

Andrzej W. Miziolek, EDITOR

U.S. Army Research Laboratory

Wing Tsang, EDITOR

National Institute of Standards and Technology

Developed from a symposium sponsored
by the Division of Environmental Chemistry, Inc.
at the 208th National Meeting
of the American Chemical Society,
Washington, DC,
August 21–25, 1994



American Chemical Society, Washington, DC 1995

Halon replacements



Library of Congress Cataloging-in-Publication Data

Halon replacements: technology and science / Andrzej W. Miziolek, editor, Wing Tsang, editor.

p. cm.—(ACS symposium series; 611)

“Developed from a symposium sponsored by the Division of Environmental Chemistry, Inc. at the 208th National Meeting of the American Chemical Society, Washington, D.C., August 21–25, 1994.”

Includes bibliographical references and indexes.

ISBN 0–8412–3327–6

1. Fire extinguishing agents. 2. Halocarbons.

I. Miziolek, Andrzej W., 1950– . II. Tsang, Wing, 1935–
III. American Chemical Society. Meeting (208th: 1994: Washington, D.C.) IV. Series.

TP266.H35 1995
628.9'254—dc20

95–25595
CIP

This book is printed on acid-free, recycled paper.



Copyright © 1995

American Chemical Society

All Rights Reserved. The appearance of the code at the bottom of the first page of each chapter in this volume indicates the copyright owner's consent that reprographic copies of the chapter may be made for personal or internal use or for the personal or internal use of specific clients. This consent is given on the condition, however, that the copier pay the stated per-copy fee through the Copyright Clearance Center, Inc., 222 Rosewood Drive, Danvers, MA 01923, for copying beyond that permitted by Sections 107 or 108 of the U.S. Copyright Law. This consent does not extend to copying or transmission by any means—graphic or electronic—for any other purpose, such as for general distribution, for advertising or promotional purposes, for creating a new collective work, for resale, or for information storage and retrieval systems. The copying fee for each chapter is indicated in the code at the bottom of the first page of the chapter.

The citation of trade names and/or names of manufacturers in this publication is not to be construed as an endorsement or as approval by ACS of the commercial products or services referenced herein; nor should the mere reference herein to any drawing, specification, chemical process, or other data be regarded as a license or as a conveyance of any right or permission to the holder, reader, or any other person or corporation, to manufacture, reproduce, use, or sell any patented invention or copyrighted work that may in any way be related thereto. Registered names, trademarks, etc., used in this publication, even without specific indication thereof, are not to be considered unprotected by law.

PRINTED IN THE UNITED STATES OF AMERICA

American Chemical Society
Library

1155 16th St., N.W.

In Halon Replacements: Miziolek, A., et al.;

ACS Symposium Series, American Chemical Society: Washington, DC, 1997.

1995 Advisory Board

ACS Symposium Series

Robert J. Alaimo
Procter & Gamble Pharmaceuticals

Mark Arnold
University of Iowa

David Baker
University of Tennessee

Arindam Bose
Pfizer Central Research

Robert F. Brady, Jr.
Naval Research Laboratory

Mary E. Castellion
ChemEdit Company

Margaret A. Cavanaugh
National Science Foundation

Arthur B. Ellis
University of Wisconsin at Madison

Gunda I. Georg
University of Kansas

Madeleine M. Joullie
University of Pennsylvania

Lawrence P. Klemann
Nabisco Foods Group

Douglas R. Lloyd
The University of Texas at Austin

Cynthia A. Maryanoff
R. W. Johnson Pharmaceutical
Research Institute

Roger A. Minear
University of Illinois
at Urbana–Champaign

Omkaram Nalamasu
AT&T Bell Laboratories

Vincent Pecoraro
University of Michigan

George W. Roberts
North Carolina State University

John R. Shapley
University of Illinois
at Urbana–Champaign

Douglas A. Smith
Concurrent Technologies Corporation

L. Somasundaram
DuPont

Michael D. Taylor
Parke-Davis Pharmaceutical Research

William C. Walker
DuPont

Peter Willett
University of Sheffield (England)

Foreword

THE ACS SYMPOSIUM SERIES was first published in 1974 to provide a mechanism for publishing symposia quickly in book form. The purpose of this series is to publish comprehensive books developed from symposia, which are usually “snapshots in time” of the current research being done on a topic, plus some review material on the topic. For this reason, it is necessary that the papers be published as quickly as possible.

Before a symposium-based book is put under contract, the proposed table of contents is reviewed for appropriateness to the topic and for comprehensiveness of the collection. Some papers are excluded at this point, and others are added to round out the scope of the volume. In addition, a draft of each paper is peer-reviewed prior to final acceptance or rejection. This anonymous review process is supervised by the organizer(s) of the symposium, who become the editor(s) of the book. The authors then revise their papers according to the recommendations of both the reviewers and the editors, prepare camera-ready copy, and submit the final papers to the editors, who check that all necessary revisions have been made.

As a rule, only original research papers and original review papers are included in the volumes. Verbatim reproductions of previously published papers are not accepted.

Preface

THE DEPLETION OF THE OZONE LAYER is one of the most important environmental challenges facing modern society. Halons, a group of particularly successful and high-performing fire-fighting agents, have been implicated in the ozone catalytic destruction cycles. As a result, U.S. scientists and technologists are working with professionals around the world to identify, develop, test, and evaluate replacement compounds and technologies applicable to a large number of different fire-fighting situations. This problem affects everyone worldwide, and its solution is multidisciplinary involving basic science, applied engineering, and chemistry. Chemistry is central to this overall effort, and therefore a symposium was organized to focus on replacements for ozone-depleting compounds.

Many world experts attended the symposium upon which this book is based and presented their work at the various sessions including Science–Policy Interface, Atmospheric Chemistry of Replacement Compounds, Physical and Chemical Criteria for CFC Replacements, and Halon Replacements: Technology and Science. Coincidentally, this symposium corresponded with the 20th anniversary of the first public presentation (at an ACS meeting) and publication by F. Sherwood Rowland and Mario J. Molina of the theory that links the release of long-lived chlorofluorocarbons with the catalytic destruction of the ozone layer.

After careful consideration of whether to publish a book relating to the symposium, we determined that a book on the Halon replacement problem was particularly relevant and worthwhile and could be organized and presented in a comprehensive single volume. We hope that the readers will agree with us.

The search for acceptable fire-extinguishing Halon replacement compounds and their implementation technologies has proven to be particularly difficult, with no obvious “son of Halon” currently in sight. Both of us are involved in research in this area, and we were struck by the complicated nature of the problem. First, it involves such disparate technical areas including fire science, corrosion science, toxicology, science policy, and atmospheric chemistry. Second, researchers in the field must have command of a wide breadth of technical knowledge. This, however, is the nature of real-world problems.

Viewing the Halon replacement problem as a challenge and opportunity, we have organized the book to incorporate both important technical problems as well as policy issues. As a result, this book will serve as a

reference guide not only for researchers in the field, but also as a useful case study in environmental science and engineering courses. The Halon replacement research and development field is also a good example of how government and industry work together to make policy and reach a common goal.

In some respects this book is a continuation of ACS Symposium Series No. 16, *Halogenated Fire Suppressants*, edited by Richard G. Gann in 1975. An author in our book, Gann continues to play a major role in this field. When Gann's book was published, replacement compounds were clearly not an issue. The question at that time was whether Halon 1301 was the most effective fire suppression compound. Nevertheless, many of the themes presented in that book are discussed in the present volume. Joan Biordi's historical perspective and her perceptive comments are especially noteworthy as they tie in directly to current research. Because of Halon 1301's remarkable properties that allow it to perform its role so well, the need for extensive further research was temporarily put on hold. As a result, little progress has been made over the past 20 years in understanding the properties and actions of Halons.

Because tests on promising near-term substitute compounds have proven them to be inadequate for most applications, the search for Halon replacements has reached a plateau. By reviewing the large number of recent test results, this book presents an opportunity to focus attention on the next generation of replacement compounds and to reformulate our strategy.

Acknowledgments

The military spearheaded the initial effort many years ago of identifying high-performing fire-fighting agents, and this effort produced the Halons. Today, the military continue the search for replacements. It is important to recognize the leadership role of the Department of Defense in the Halon replacement field. Donald M. Dix, Director, Advanced Technology, Office of the Director Defense Research and Engineering (DDR&E) within the Office of the Secretary of Defense, has either funded or helped direct a good portion of the work presented in this book. This same office also directs the other military programs in ozone-depleting compounds (ODC) replacement research.

We are indebted to many people for making this book possible. We thank Karim Ahmed, Mario Molina, and Hillel Magid for helping organize the sessions within the symposium. Ahmed deserves special thanks for organizing a very successful recognition dinner for Rowland and Molina during the symposium. Mary Walker, Program Chair of the Environmental Chemistry Division of the ACS and an enthusiastic supporter, has provided much encouragement. Rose Pesce-Rodriguez and Robert A.

Fifer of the Army Research Laboratory contributed encouragement and management support during the months needed to organize this book. Michael Bennett of the U.S. Air Force Wright Laboratories is recognized for his significant involvement in the aviation agent replacement program. Unfortunately, he was not able to contribute to this book because of his heavy involvement in the Air Force testing program. Naturally, we thank Richard Gann for his encouragement and helpful advice.

We acknowledge the Strategic Environmental Research and Development Program (SERDP) and the U.S. Army's Environmental Quality Basic Research Program for support of Halon replacement projects that have sustained our activities in this area. We thank the staff at ACS books for assisting in the effort. And finally, we thank each author for his or her important technical contributions and timely handling of manuscripts as well as the reviewers for their helpful comments.

ANDRZEJ W. MIZIOLEK
U.S. Army Research Laboratory
AMSRL-WT-PC
Aberdeen Proving Ground, MD 21005-5066

WING TSANG
Chemical Science and Technology Laboratory
Chemical Kinetics and Thermodynamics Division
National Institute of Standards and Technology
Gaithersburg, MD 20899-0001

August 11, 1995

Chapter 1

Halon Replacements: An Overview

Andrzej W. Miziolek¹, Wing Tsang², and John T. Herron²

¹U.S. Army Research Laboratory, AMSRL-WT-PC,
Aberdeen Proving Ground, MD 21005-5066

²Chemical Science and Technology Laboratory, Chemical Kinetics
and Thermodynamics Division, National Institute of Standards
and Technology, Gaithersburg, MD 20899-0001

In 1975 a book was published titled **Halogenated Fire Suppressants** [1] as an ACS Symposium Series monograph. That book was edited by Richard G. Gann, then at the Naval Research Laboratory, and reflected much of the content of a symposium held that year on the same topic in San Antonio, Texas. The monograph contained 15 chapters which were concentrated largely on mechanistic studies of flame inhibition and extinguishment using Halon 1301 (CF₃Br) as well as a few other brominated compounds. The objective of the symposium was to answer the question of whether Halon 1301 was indeed the best compound for fire suppression effectiveness. R.G. Gann started the preface of that book with the quotes: "In many areas of the fire problem, proposed solutions rest on limited experience, shaky assumptions, and guesswork." [2] and "More research is needed on extinguishing agents..., to improve the effectiveness of existing agents and to investigate the chemical and physical mechanisms of new agents." [2] Judging from the content of this, now second book on the subject of fire suppression agents, one can conclude that although much progress has been made in understanding chemical and physical mechanisms of fire extinguishment, we certainly are not there yet.

When the first book was published, the issue of stratospheric ozone depletion had just been raised with the initial emphasis being placed on chlorofluorocarbons (CFCs) as the class of compounds of immediate concern. In due time, it was recognized that the bromine-containing Halons were also destructive to the stratospheric ozone layer, even more so than the CFCs on a molecule-to-molecule comparison basis. Once this connection was made, it was only a matter of time before Halons became a target for regulatory control. In fact, Halons as a class became the first group of compounds

This chapter not subject to U.S. copyright
Published 1995 American Chemical Society

whose production has already been halted (1 January 1994). This accelerated control on an otherwise very successful family of fire extinguishing agents has led to a high degree of urgency in terms of identifying acceptable replacement fire fighting agents. This urgency is being felt most acutely within the military which absolutely needs the high performance fire fighting attributes that the Halons have afforded.

The search for successful replacement compounds, unfortunately, has proven to be most difficult, with no "son of Halon" in sight. The range of requirements that a successful replacement compound(s) has to meet is quite extensive ranging from acceptable environmental properties (Ozone Depletion Potential (ODP), Global Warming Potential (GWP), impact on air quality and environment), to corrosion effects in long term storage, toxicity, proper delivery characteristics, affordability, and, of course, fire extinguishing potential to match the presently used Halons in volume and weight. At this point in time, the research and testing community has evaluated all of the obvious and some of the not so obvious replacement compounds and has found that all of them are lacking for one reason or another, for most applications (particularly the military ones) where high performing agents are required. As mentioned in the preface, we have reached a type of plateau in our search for Halon replacements and thus this is an excellent time to summarize and reflect upon the status of this search.

This book is divided into 5 sections. These are: Environment and Policy; Technology, Testing, and New Approaches; Flame Extinction Phenomenology; Flame Suppression Mechanistic Studies; and Fundamental Supporting Science. The chapters in the first section deal primarily with the basis for the phase-out of the Halon compounds, results of studies on the atmospheric chemistry of potential replacement compounds, and efforts to assess the atmospheric effects of replacement compounds on global ozone levels and climate. The focus of replacement strategies has been to find compounds having very short tropospheric lifetimes with respect to reaction with atmospheric OH radicals or to photolysis. Much effort has gone into determining reaction mechanisms and the subsequent fate of reaction products. The concern here has been that the products of the atmospheric degradation of replacement compounds must themselves not contribute to ozone depletion or climate modification. Homogeneous and heterogeneous processes have therefore been studied in great detail. This kind of research has identified different classes of possible replacement compounds, such as the HFCs or HCFCs, having "satisfactory" regulatory-related properties (at this time) in terms of atmospheric lifetime and the benign nature of the reaction products. However, the search for Halon replacements has not been

restricted to relatively short-lived compounds such as the HFCs or HCFCs, since many fully fluorinated compounds such as the perfluorocarbons (PFCs) have good fire suppressant properties. These compounds have the advantage of not having any effect on the ozone levels. However, they have the disadvantage of possessing extremely long lifetimes, which combined with the fact that they are strong infrared absorbers in the 8-12 micron "window" region, means that they will contribute very significantly to global warming.

Environmental constraints as applied to many of the potential Halon replacements discussed in the chapters mean that other classes of compounds and other "non-chemical" approaches, such as the use of water mists or particulates, are under consideration. The perfluoroalkyl iodides have good properties as fire suppressants, but their atmospheric fate needs considerable further study to establish whether tropospheric degradation leads to harmless by-product formation. The role of iodine in contributing to ozone depletion is now reasonably well-established, and is considered in one of the chapters in this section. Since iodine is more efficient than either bromine or chlorine in ozone depletion, a critical consideration is that the iodine in a fire suppressant not penetrate the stratosphere. There are other classes of compounds which are also potential Halon replacements, such as unsaturated halogen compounds, the halogenated ethers, phosphorus halides, and various metallic compounds. In some cases these compounds or their hydrolysis products are toxic and their atmospheric fates are often not known in detail. Much more laboratory research is therefore required before these can be seriously considered in terms of Halon replacements. It must be recognized that none of the suggested replacement compounds possesses a comparable combination of properties related to fire suppression, minimum-toxicity, and ease of handling than does CF_3Br . Finding a replacement having these properties as well as the property of being atmospherically neutral, presents researchers with an extraordinarily complex and difficult challenge.

Section II addresses a number of the applications, testing, and initial characterization issues of emerging classes of replacement compounds including fluorinated iodines and amines. This section covers the specific Army, Navy, and aircraft requirements as well as the resulting Halon replacement programs being carried out by the military services. However, the military is not the only organization that requires high performance fire extinguishment technology. The Alaskan North Slope gas and oil production facilities have a unique requirement of explosion inertion. This inertion requirement adds yet another challenge for Halon replacement compounds since the chemical and/or physical actions that leads to efficient fire extinguishment

do not necessarily also result in the optimal performance with regard to fire avoidance.

A few of the chapters in Section II address some of the other critical attributes necessary to develop successful Halon replacement compounds, namely toxicology and corrosivity. The toxicology issue pertains to both the effect on humans due to the release of the pure agent, as well as to the possible production of toxic combustion byproducts during use in fire extinguishment. As is pointed out repeatedly throughout the book, present chemically-active candidate replacement agents produce considerably greater quantities of toxic compounds such as HF and CF₂O during use than do the Halons.

Section III contains a number of papers describing laboratory experiments with emphasis on the global behavior of combustion systems in the presence of inhibitors. The results show that the fluorinated compounds which do not contain bromine do not have the fire suppressing capability of Halon 1301. The results also lead to a data base of specific compounds upon which theories can be tested. Particularly noteworthy is the development of a detonation/deflagration tube method for testing the effectiveness of flame fighting agents through the determination of the extent they decelerate the propagating wave and attenuate the hazardous shock that precedes the combustion process. These data represent a new challenge for those who seek to give a physico-chemical explanation of fire suppression. It is very encouraging that the detonation/deflagration tube has been shown to be a good predictor of aircraft dry bay fires. The paper on HF represents a new aspect of the problems arising from the replacement of Halon 1301. The results are a demonstration of the increasing laboratory capability to probe various aspects of the fire situation.

Section IV contains experimental results where chemical species information in appropriate combustion systems (largely premixed laboratory burners) are tested against the results of simulations. The experimental methodology is well established and understood and the results can be considered a crucial test of the validity of the simulations. This is because fits of species information are most sensitive to errors in the hydrocarbon/air/halogen kinetic and thermodynamic data base. Thus, the substantial agreements that have been obtained suggest that the essential features of chemical flame suppression have indeed been captured in the simulation. Therefore, one should have considerable confidence in using the data base as a semi-quantitative predictive tool. For example, one can now successfully differentiate between contributions from dilution, heat capacity, and chemistry in well defined systems. Another use of such data is to test reduced

mechanisms. The task of relating simulations of non-turbulent laboratory flames to actual fires is, perhaps, the most serious challenge.

The last section (V) deals with the fundamental chemistry of fire suppression. Two papers describe the efforts at NIST focussed on the development of a chemical kinetic and thermodynamic information upon which the simulations can be based. These two papers may represent some of the most important contributions in this volume from a general point of view. Certainly, the starting point of all future simulations will be based on the data from these efforts. These papers are notable for their systematic reliance on theory for filling the gaps in the data base. This is due to the increasing reliability of theoretical efforts and the fall-off in experimental efforts in chemical kinetics. Thus, it is significant that in this volume there is only one chapter that contains traditional experimentally-generated chemical kinetic data. This can be contrasted with the situation in the earlier volume edited by Gann [1]. This is unfortunate, since there is a constant need to validate and in many instances calibrate theoretical predictions. This is particularly the case for predictions on the structures and energetics of the transition state. It should be noted that this data base is not restricted to fire suppression. It is indeed applicable to all small organic systems where fluorinated compounds play a role, for example destruction of these fluorinated compounds via incineration. It also forms the fluorinated portion of the data base for systems where fluorine is a component; for example in the incineration of some chemical agents. Furthermore, it can play an important role in predicting the nature of the fluorinated compounds that may be formed during combustion. Finally, because this data base draws on an active research area, its provisional nature must be recognized. One expects that in time accuracy limits will be vastly increased and that predictions will be much more reliable. There is thus a need for a continuing program to upgrade the data base. One notes that the estimated accuracy of the thermodynamics derived from theory is of the order of 8 kJ/mol. For species concentration applications this is equivalent to an error of a factor of 30 at room temperature; 2.5 at 1000 K and 1.6 at 2000 K. Clearly, the simulations should reproduce broad trends under combustion conditions, but cannot be relied on for room temperature applications.

It is quite evident and understandable that the search for Halon replacements has concentrated on chemicals that are near cousins such as the hydrofluorocarbons (HFCs) and perfluorocarbons (PFCs). However, these "chemical-acting" compounds are only one general class of fire extinguishers. The other major class, the "physically-acting" agents/techniques, unfortunately, are not well-represented

in this book. These include particulate or pyrotechnically generated aerosols [3], solid propellant gas generator agents, water and water-based mists, deflagration generated aerosols, and gelled fine particle dry chemicals. The primary reason these are not included in this book is that they are relatively new technologies and techniques and not yet well-studied. Also, in some cases there is the issue of the information being company proprietary [3].

Finally, as a minor point, we would like to address the matter of nomenclature. Over the intervening 20 years since the first book there has been a definite shift from "halon abcde" (see Preface, ref. 1) to "Halon abcde". Perhaps it is due to the developments in the stratospheric ozone depletion field where the compounds have been referred to as "CFCs" not "cfcs". In any event, as the reader will see, we have made no effort to try to impose a standard notation in this book. As far as the editors are concerned, both notations are acceptable, although the argument to keep the notation as originally developed is rather compelling.

References

1. Gann, R.G., Ed., "Halogenated Fire Suppressants", ACS Symposium Series 16, American Chemical Society, Washington, D.C., 1975.
2. "America Burning: The Report of the National Commission on Fire Prevention and Control: U.S. Government Printing Office, Washington, D.C. 20402, 1973.
3. Estee Jacobson, Spectrex Inc., Cedar Grove, NJ, private communication.

RECEIVED August 11, 1995

Chapter 2

The History of the Halon Phaseout and Regulation of Halon Alternatives

Stephen O. Andersen, Karen L. Metchis¹, and Reva Rubenstein

U.S. Environmental Protection Agency, Mail Code 6205J,
401 M Street, S.W., Washington, DC 20460

Halogenated fire agents (Halon 1301, Halon 1211 and Halon 2402) were once thought to be essential for fire safety. However, once their role as potent ozone depleters became scientifically confirmed, fire protection engineers, the military, and regulators rallied world-wide to reevaluate fire protection practices and to develop new chemical and technological solutions. Today, production of halon has ceased in the industrialized world, and less than 20 percent of former uses still require halon. These remaining uses are being served by the existing supplies of halon while research on alternatives continues.

The Montreal Protocol and International Cooperation

The fire protection community has been one of the most important proponents and early implementers of new technology and management to protect the stratospheric ozone layer. This introduction looks back over the last ten years to explain how public, government and industry stakeholders came together on a common and successful global agenda.

Stratospheric ozone is depleted by halons and other ozone-depleting substances. Depletion of ozone allows more harmful ultraviolet radiation to reach the Earth's surface. Increases in UV-B radiation are likely to have substantial adverse effects on human health, including increases in the incidence of, and morbidity from, skin cancer, eye diseases, and infectious diseases (1). Peak global ozone depletion is expected to occur during the next several years, and the stratospheric ozone layer is expected to recover in about 50 years in response to international actions under the Montreal Protocol and its Amendments and Adjustments (2). The early phaseout of halon production produced at least 15 percent of the protection under the Montreal Protocol (3)(4).

¹Corresponding author

This chapter not subject to U.S. copyright
Published 1995 American Chemical Society

The halon production phaseout took effect January 1, 1994 with little disruption because the fire protection community had established global information networks and coordinated halon banks. Halon banks are important because environmentally acceptable alternatives have not been commercialized for some critical fire protection applications representing 15-20% of former uses (5)(6).

In 1985 a small group of countries signed the Vienna Convention of Ozone Layer Protection which is the framework for negotiating the Montreal Protocol. In that document halons are only briefly mentioned in an annex on monitoring of data because earlier analysis had concluded that halon was rarely released and predicted that halon use would decline as computer systems became smaller. In 1986 few substitutes were identified for any of the ozone-depleting substances and it was widely believed that halon uses were all essential. It was hoped that chlorofluorocarbon (CFC) restrictions alone would adequately protect the ozone layer.

By late 1986 the U.S. Environmental Protection Agency (EPA) began to take a new look at halon use. EPA quickly discovered that the National Fire Protection Association (NFPA) planned to mandate full discharge testing of all new Halon 1301 (CF₃Br) systems in order to verify that the controls and hardware properly functioned and that the concentration of halon gas was high enough and contained long enough in the enclosure to extinguish the design fire. The EPA concern was that property owners, insurance companies, and fire authorities might also conclude that older systems should be discharge tested or that all systems should be periodically discharge tested. This action alone would have substantially increased the threat to the ozone layer.

Because halons were not part of any regulatory plan and because fire protection involved human life and property, EPA decided to seek cooperative and collaborative solutions. NFPA managers suggested that EPA contact Gary Taylor, Chair of their Halon 1301 Committee and partner in one of the largest North American fire protection companies. Gary Taylor had worked for DuPont during the early promotion of Halon 1301 and had designed halon systems for some of the most demanding national defense, industrial, and cultural heritage applications. In the late 1970s Mr. Taylor testified before the U.S. Congress that halon use was essential and should not be restricted.

In the first meeting with EPA, Gary Taylor estimated that very little halon was used to actually fight fires but that emissions from testing, training, and accidental discharge were far higher than analysts had calculated. He proposed a plan to investigate halon use, to involve the best global experts in problem solving, and to use market incentives to change the way that engineers and property owners protected against fire risk. He advocated that the full range of stakeholders from chemical manufacturers to building designers and insurance underwriters, fire equipment manufacturers and installers, and military and civilian halon system customers be recruited to participate in developing a solution to the problem. His proposal was that EPA and the fire protection community jointly investigate halon controls with the goal of only acting by broad consensus.

In early 1987 EPA initiated projects with the U.S. Department of Defense and U.S. Air Force. Gary Vest, then the Deputy Assistant Secretary of the Air Force for Environment, Safety and Occupational Health, and then-Captain Edward "Tom" Morehouse of the Air Force Engineering and Services Center, became the first of many military leaders to spearhead halon elimination efforts. By September 1987 the Air Force was confident enough to send Captain Morehouse to Montreal to help make the case that halon should be included in the Protocol. Diplomats reasoned that if the military could reduce their use, so could the civilian sector. Without this endorsement halon production might not have been included in the 1987 Protocol.

Meanwhile, analysis was documenting that less than ten percent of halon emissions were actually for fire fighting (7). EPA, NFPA, and other organizations were now working as a team to educate stakeholders on the importance of eliminating testing, training, and accidental discharges. In Australia the State of Victoria implemented strong controls on halon use and plumbers unions refused to install or service halon systems unless it was deemed essential by a committee of public and private experts. Elsewhere, authorities of jurisdiction were helping eliminate requirements for discharge testing and training with halon.

In 1989 the United Nations Environment Programme (UNEP) organized the first Technology Assessment including the work of the Halon Technical Options Committee, Co-Chaired by Gary Taylor and Tom Morehouse. This Committee of international experts became the catalyst of global efforts.

Slowly even more fundamental change was occurring. Property owners began to use a broader range of strategies to protect property. Computer manufacturers confirmed that, contrary to advertizing claims for halon, most equipment could be protected with water sprinklers. Insurance companies agreed to offer their most favorable rates to ensure property with protection other than halon. Telecommunication companies reduced the need for halon by using cable materials that would not burn. The military began to design weapons systems that did not depend on halon. Broader fire protection engineering considerations and fire prevention began to take precedence over the basic fire extinguishing perspective.

These efforts stimulated other important paradigm shifts. For example, military aircraft designers reevaluated whether space and weight might be better allocated to threat avoidance or weapons rather than fire protection. Commercial aircraft engineers realized that water mist systems might better protect against fires and offer passengers protection from the poisonous gases of combustion.

EPA and the Air Force helped organize the Halon Alternatives Consortium to help identify the most promising research opportunities and worked to prepare markets to accept alternatives and substitutes as they developed. Marine Corps, Navy, and Air Force cooperated to develop the first practical halon recycling equipment and were the first organizations in the world to deploy this equipment. The Navy and Marine Corps teamed up with EPA to teach halon recycling to experts from Argentina, Brazil, Chile, China, Costa Rica, Ecuador, Fiji, Guatemala, India, Malaysia, the Maldives, Mexico, Panama, the Philippines, Thailand, Trinidad and Tobago, Uruguay, and Venezuela.

Halons are still required for 15-20% of the applications they satisfied in 1986. If halons presently contained in existing equipment were never released to the atmosphere, the integrated effective future chlorine loading above the 1980 level is predicted to be 10% less over the next 50 years (8). Thus much work remains to complete the phaseout of halon use. Chemical substitutes to halon for the remaining important uses are an important part of the ultimate solution.

U.S. Regulation of Halons and Halon Substitutes

When the Montreal Protocol was signed in 1987, the Environmental Protection Agency's (EPA) role in stratospheric ozone protection derived from the Clean Air Act of 1977, Part B, section 157(b):

"...the Administrator shall propose regulations for the control of any substance, practice, process or activity (or any combination thereof) which in his judgment may reasonably be anticipated to affect the stratosphere, especially ozone in the stratosphere, if such effect in the stratosphere may reasonably be anticipated to endanger public health or welfare."

This language gave EPA broad latitude but it did not give clear guidance. EPA began developing control strategies based primarily on ozone depletion potential (ODP). A product with an ODP lower than the CFCs was considered to have an advantage over the halons. Thus, FM-100 (HBFC-22B1) with an ODP of 0.74 (9) was investigated as an effective halon substitute. With the enactment of the Clean Air Act Amendments of 1990 (CAAA), Congress provided guidance to EPA by stipulating that any substance with an ODP of 0.2 or greater would be a class I substance and would be subject to the same production phaseout as the CFCs and halons. This effectively eliminated some potential substitutes, such as FM-100, and mixtures using CFCs.

Title VI of the U.S. Clean Air Act of 1990 enacts the U.S. strategy to comply with the Montreal Protocol for protection of the stratospheric ozone layer (10). Title VI is administered by the Stratospheric Protection Division within the Office of Air and Radiation. Section 612 of that Title directs EPA to set up a program, named 'SNAP' or the Significant New Alternatives Policy program, to evaluate any halon substitute or alternative technology to ensure that the substitutes reduce the overall risk to human health and the environment and to promote these substitutes to achieve rapid market acceptance. EPA's goal is to ensure that industry and consumers have ample choices for the diversity of applications in which CFCs and halons are currently used.

EPA adopted a risk balancing approach on health and safety issues by looking at use of the agent in each sector under likely exposure pathways. "The risk to individuals from exposure to halon substitutes is generally from discharges that occur infrequently. Chronic effects are not the usual concern for halon substitutes because when used, these substances are discharged in high concentrations over short periods of time, and thus, are potentially acutely hazardous. Risk from exposure to halon substitutes is accordingly best assessed by analysis of acute toxic effects associated with exposure to these compounds,

such as developmental toxicity and cardiotoxicity. In most instances, cardiotoxicity occurs at lower levels than fetotoxicity, and therefore, unless otherwise warranted by the developmental data, EPA will base the estimates for emergency limits during halon use on the no observable adverse effect level (NOAEL) and lowest observable adverse effect level (LOAEL) reported for epinephrine-sensitized cardiotoxicity in dogs (and in a few instances monkeys). Human heart arrhythmias and sudden death resulting from overexposure to CFCs, halons, other halogenated and nonhalogenated hydrocarbons have been documented in work place settings and in volatile substance abuse (e.g., glue sniffing) (11)."

To assess the safety of an agent for use in a total flooding system, EPA analysts examine the actual design concentration as NFPA defines it (12) (cup burner plus 20%) or in some cases the actual large scale testing design concentration, and compare this value to the cardiotoxic effect levels.

It is a different situation for streaming agents because it is a localized application, and the air exchange further dilutes the concentration of the agent. EPA requires manufacturers to submit data acquired by personal monitoring for the anticipated usage. A device is attached to the breathing zone of a firefighter to collect samples of the actual levels of exposure. The results of these tests show that actual exposure is much lower than what the models predict. Consequently, EPA has listed agents as acceptable, even with LOAEL as low as 1.0 or 2.0 percent (13). In fact, Halon 1211 (CF_2ClBr) has a LOAEL of 1.0 percent which shows that these agents can be used safely by trained firefighters (although there are known incidents of accidental deaths with Halon 1211).

The conditions stipulated under SNAP for use of total flooding agents are patterned after current Occupational Safety and Health Administration (OSHA) requirements for Halon 1301 (CF_3Br) systems. Because OSHA does not currently specify the acceptable exposure levels to the substitute agents, EPA is laying these values out very specifically, and has initiated efforts to work with OSHA as that agency takes steps to amend their regulation of fixed gaseous extinguishing systems (OSHA Regulation 1910.162).

On environmental criteria, EPA first looks at ozone depletion potential. The Clean Air Act specifies that any substance with an ODP of 0.2 or higher must be listed by EPA as a class I substance in the United States and must be phased out of production within seven years of listing.

While the Clean Air Act does not explicitly define a class II substance, by implication it is an agent with an ODP of less than 0.2. The EPA Administrator is to determine if a substance could significantly damage the stratospheric ozone layer. Currently the chemical with the lowest ODP that EPA has listed as a class II substance is HCFC-123 (CF_3CHCl_2) with an ODP of 0.02.

While EPA considers other environmental media besides ozone depletion potential, including aquatic toxicity, air pollution, etc., global warming potential (GWP) and atmospheric lifetime are the key issues in evaluating halon substitutes. Action #40 of President Clinton's Climate Change Action Plan, released November, 1993, directs EPA to minimize unnecessary emissions of greenhouse gases to help meet the national goal of reducing emissions in the year 2000 to 1990 levels. EPA again has adopted a risk balanced approach

between ODP and GWP and the related atmospheric lifetimes of these agents. However, substitute agents with no ODP tend to be moderate to high global warmers, while those with some ODP tend to be low global warmers.

The CAAA directs EPA to "reduce overall risks to human health and the environment (14)." EPA has attempted to characterize emission levels and exposure routes in each use sector in order to minimize environmental impacts. Thus, EPA first looks for the outliers, such as an agent with an extremely long atmospheric lifetime. The perfluorinated carbons (PFCs) are outliers, with atmospheric lifetimes in excess of 3,000 years, and which are virtually indestructible (15). However, because of their extremely favorable toxicity profile, EPA recognizes that they have a role to play in fire protection applications where other agents are not suitable for either technical or safety reasons. Thus, EPA has listed PFCs as acceptable under certain contingent restrictions. Although HFC-23 has a 300 year lifetime (16), EPA recognizes that it is a byproduct of the manufacture of HCFC-22 (CF_2HCl), which will continue to be produced as a feedstock for the manufacture of polymers such as teflon and thus placed no restriction on its use. The acceptance of this agent adds another choice for users in their arsenal of fire protection agents.

In response to environmental and efficacy concerns, fire protection manufacturers are also developing several new alternative technologies, including inert gas systems, water mist systems, and powdered aerosol systems. These nonhalocarbon alternative agents require a different means of determining risk during use. Some of the newer nonhalocarbon alternative agents--the inert gas systems--limit but do not entirely remove the oxygen available to the fire. The most important condition of safe use of such agents is the stipulation that the amount of remaining oxygen in the area is sufficient to maintain Central Nervous System function and that the restriction of oxygen does not impair escape from the area.

Powdered aerosol systems present still other risk assessment issues. The conditions determining the safe use of these agents must account for the potential deposition of very small inhalable particles in the respiratory tract. These powder particles may range from very small and potentially respirable into the alveoli to large particles capable of irritation of the upper nasal passages. The size of the particles may be the most significant factor determining risk. Water mist systems using pure water pose little risk, although additives must be evaluated on a case-by-case basis to determine potential health risks. A concern for both mist and powdered aerosol systems is the visual obscuration which occurs during discharge and which may potentially inhibit the ability to egress the area.

Because the risk analyses of these alternative technologies differs somewhat from the standard EPA risk assessment procedures, EPA has encouraged the formation of ad hoc workshops and medical peer review panels to characterize the risk issues presented by each new technology and to help delineate the appropriate exposure limits for different clinical groups. Workshops and panels have been formed to analyze issues concerning powdered aerosols and water mists. Conditions describing the appropriate use of inert gases with limited oxygen were evaluated by special medical panels. In addition,

EPA solicited guidance from OSHA on these use conditions since OSHA will ultimately determine the proper usage of all fire suppressant systems.

Halon Banking

The EPA's SNAP program has been largely successful in identifying several agents and technologies which can be used in most total flooding and streaming fire protection applications. However, there are still some application areas which pose technical challenges, including aviation, military tanks, some military shipboard uses, and explosion inertion applications. The U.S. military has been a leader in research and development efforts, and has selected HFC-125 (CHF_2CF_3) for the design of systems on new military aircraft. For commercial aircraft, the Federal Aviation Administration (FAA) is spearheading an industry wide R&D effort to identify effective substitutes. However, once an agent is identified for complex systems, much work still remains to design, manufacture and certify not only the fire protection system but the entire redesign of, for example, the aircraft itself.

To serve existing equipment that cannot be cost-effectively retrofitted, EPA encourages halon banking programs. The Department of Defense maintains such a bank for mission critical systems, managed by the Defense Logistics Agency, which also serves as the buffer needed while new agents are identified and systems developed for new platforms. In the commercial sector, users have undertaken similar actions to redeploy and bank halon. Private-sector business have sprung up to work the halon recycling market, and the non-profit Halon Recycling Corporation plays an important role in aiding buyers and sellers of halon both in the U.S. and abroad.

Conclusion

The collaborative efforts of industry, military, end-users, and regulators described in this chapter is a success story. Not only has this community of professionals and citizens contributed significantly to ozone layer protection, but they have gone the extra length to recognize the broader environmental implications of chemical use and fire fighting practices. Environmental protection, in this case, has truly evolved to pollution prevention and stewardship of the earth's ecosystem.

Literature Cited

1. J.D. Longstreth et al., "Effects of Increased Solar Ultraviolet Radiation on Human Health" in *Environmental Effects of Ozone Depletion: 1994 Assessment*, ed. J.C. van der Leun (Nairobi, Kenya: United Nations Environment Programme, Nov. 1994), pp. 23-48.

2. Solomon, S., Wuebbles, D., et al., "Ozone Depletion Potentials, Global Warming Potentials, and Future Chlorine/Bromine Loading" In *Scientific Assessment of Ozone Depletion: 1994*; Coauthors, Albritton, Daniel L., Watson, Robert T., and Aucamp, Piet J.; World Meteorological Organization: Geneva, Switzerland, 1994; pp. 13.9-13.13.
3. U.S. Environmental Protection Agency. *Risk Screen on the use of Substitutes for Class I Ozone Depleting Substances: Fire Suppression and Explosion Protection*. Washington, D.C.: EPA, March 1994. p. 2-2 to 2-4.
4. U.S. Environmental Protection Agency. Global Change Division. "Integrated Assessment Model" and from "Atmospheric and Health Effects Framework" model run for *Regulatory Impact Analysis*. Washington, D.C.: U.S. EPA, 1987; 1992.
5. Taylor, Gary. "Halon Bank Management - A Rationale to Evaluate Future World Supplies." In *Proceedings of the Second International Conference on Halons and the Environment*. Geneva, Switzerland: CFPA Europe/NFPA, Sept. 28, 1990.
6. Environment Canada. *Halon Bank Management - A Rationale for Canada*. March 15, 1990.
7. *Halon Fire Extinguishing Agents Technical Options Report to the United Nations Environment Programme Technology Review Panel*. Gary Taylor and Major E. Thomas Morehouse Jr., Co-Chairmen. Toronto, Canada: June, 1989), p. 9.
8. Solomon S., Wuebbles D., et al.; "Ozone Depletion Potentials, Global Warming Potentials, and Future Chlorine/Bromine Loading" in *Scientific Assessment of Ozone Depletion: 1994*; Coauthors Albritton, Daniel L., Watson, Robert T., and Aucamp, Piet J.; World Meteorological Organization: Geneva, Switzerland, 1994; p. 13.13.
9. Ozone Secretariat. *Handbook for the Montreal Protocol on Substances that Deplete the Ozone Layer*. Nairobi, Kenya: United Nations Environment Programme. Third edition, Aug. 1993. p. 27.
10. *Clean Air Act*. U.S. Code, Title VI, vol. 42, secs. 7450 et seq. (1990).
11. Rubenstein, Reva. "Human health and environmental toxicity issues for evaluation of halon replacements." *Toxicology Letters*. (1993), 68, pp. 21-24.
12. National Fire Protection Association. *NFPA 12A: Halon 1301 Fire Extinguishing Systems*. Quincy, Massachusetts: NFPA, 1992. p. 12A-11.
13. U.S. Environmental Protection Agency. Significant New Alternatives Policy Program, rulemakings and notices. 59 FR 13044 (March 18, 1994); 59 FR 44240 (August 26, 1994); 60 FR 3318 (January 13, 1995).
14. *Clean Air Act*. U.S. Code, vol. 42, secs. 7401 et seq. "Title VI", sec. 612(a), (1990).
15. Ravishankara, A.R. et al. "Atmospheric Lifetimes of Long-Lived Halogenated Species." *Science*. **January 8, 1993**, 259, pp.194-199.
16. Du Pont Fluorochemicals. "EPA SNAP Submission for HFC-23." Jan. 1993.

RECEIVED June 12, 1995

Chapter 3

Atmospheric Chemistry and Environmental Impact of Hydrofluorocarbons and Hydrochlorofluorocarbons

Timothy J. Wallington¹, William F. Schneider¹, Ole J. Nielsen²,
Jens Sehested², Douglas R. Worsnop³, W. J. De Bruyn^{4,5},
and Jeffrey A. Shorter^{4,6}

¹Ford Research Laboratory, Mail Drop SRL-3083, 20000 Rotunda Drive,
Dearborn, MI 48121-2053

²Section for Chemical Reactivity, Environmental Science and Technology
Department, Risø National Laboratory, DK-4000 Roskilde, Denmark

³Center for Chemical and Environmental Physics,

Aerodyne Research, Inc., 45 Manning Road, Billerica, MA 01821-3976

⁴Department of Chemistry, Boston College, Chestnut Hill, MA 02167

We review the available data concerning the atmospheric chemistry and environmental impact of a series of important hydrofluorocarbons (HFCs) and hydrochlorofluorocarbons (HCFCs). HFCs have no impact on stratospheric ozone. HCFCs have ozone depletion potentials which are 10-100 times less than CFCs. The direct global warming potentials of HFCs and HCFCs are approximately an order of magnitude less than those of the CFCs they replace. At the concentrations expected from their atmospheric degradation, none of the oxidation products of HFCs or HCFCs are noxious or toxic (e.g., the concentration of CF_3COOH in rainwater will be 3-4 orders of magnitude lower than that reported to have an impact on plants).

Recognition of the adverse impact of chlorofluorocarbons (CFCs) on stratospheric ozone (1) has prompted an international effort to replace CFCs with environmentally acceptable alternatives (2). Hydrofluorocarbons (HFCs) and hydrochlorofluorocarbons (HCFCs) are two classes of CFC replacements. For example, HFC-134a (CF_3CFH_2) is a replacement for CFC-12 (CF_2Cl_2) in domestic refrigeration and automobile air conditioning units. HCFC-22 (CHF_2Cl) is a replacement for CFC-12 in industrial refrigeration units. HCFC-141b is a replacement for CFC-11 in foam blowing applications. HFCs and HCFCs are volatile and insoluble in water. Following release

⁵Rosenstiel School of Marine and Atmospheric Science, University of Miami, Miami, FL 23149

⁶Mission Research Inc., Nashua, NH 03062

into the environment these compounds will reside in the atmosphere where they will be oxidized into a variety of degradation products.

The choice of HFCs and HCFCs is motivated by a number of factors, not least of which is that in contrast to CFCs, HFCs and HCFCs contain one or more C-H bonds. Hence, HFCs and HCFCs are susceptible to attack by OH radicals in the lower atmosphere (troposphere). HFCs do not contain chlorine and so have no ozone depletion potential associated with the well established chlorine catalytic cycles. While HCFCs contain chlorine, the delivery of this chlorine to the stratosphere is relatively inefficient because of the efficient scavenging of HCFCs by OH radicals in the troposphere. To define the environmental impact of HFCs and HCFCs, their ability to destroy stratospheric ozone, to contribute to potential global warming, and to produce noxious degradation products must be assessed. To address these issues a detailed knowledge of their atmospheric chemistry is required. Atmospheric chemistry includes reactions in gaseous and aqueous phases together with any relevant heterogeneous processes. We present here an overview of the atmospheric chemistry and environmental impact of a series of important HFCs and HCFCs.

Gas Phase Chemistry

The gas phase atmospheric chemistry of HFCs and HCFCs can be divided into two parts: reactions that convert the halogenated compound into halogenated carbonyl species and reactions that remove these carbonyl compounds.

Conversion of Haloalkanes into Halogenated Carbonyl Compounds. Reaction with OH radicals is the dominant loss process for all HFCs and HCFCs, accounting for > 90% of the fate of these compounds. In the stratosphere photolysis and reaction with Cl and O(¹D) atoms make minor contributions to the overall loss. A substantial kinetic database exists concerning the reaction of OH radicals with HFCs and HCFCs (3). From these data atmospheric lifetimes can be calculated. HFC and HCFC lifetimes range from 2 to 411 years and are listed in Table I along with those for CFC-11 and CFC-12 for comparison.

A generic scheme for the atmospheric oxidation of a C₂ haloalkane is given in Figure 1. Values in parentheses are order of magnitude lifetime estimates. Reaction with OH radicals gives a halogenated alkyl radical which reacts with O₂ to give the corresponding peroxy radical (RO₂). Peroxy radicals can react with three important trace species in the atmosphere: NO, NO₂, and HO₂ radicals. The importance of these reactions is dictated by the abundances of NO, NO₂, and HO₂ radicals and by the rates of the reactions of RO₂ radicals with these species. In the troposphere the concentrations of NO, NO₂, and HO₂ are approximately (2.5–10) × 10⁸ cm⁻³ (2).

The peroxy radicals derived from HFCs and HCFCs react rapidly with NO to give NO₂ and an alkoxy radical RO (4,5). The atmospheric lifetime of peroxy radicals with respect to reaction with NO is 3 to 7 minutes (4,5).

Peroxy radicals react rapidly with NO₂ to give alkyl peroxy nitrates (RO₂NO₂). By analogy to the measured rate of reaction of CF₂ClO₂ and CF₃CH₂O₂ radicals with NO₂ (5,6) the lifetime of RO₂ radicals with respect to reaction with NO₂ is approximately 10 minutes. Alkyl peroxy nitrates are thermally unstable and decompose to regenerate RO₂ radicals and NO₂ (7,8). At room temperature in one atmosphere of air the peroxy nitrates derived from HCFC-22 and HFC-134a have lifetimes of 24 seconds (8)

and < 90 seconds (9), respectively. Thermal decomposition dominates the atmospheric chemistry of halogenated alkyl peroxy nitrates.

Peroxy radicals react with HO₂ radicals to give hydroperoxides and in some cases carbonyl products. The relative importance of the hydroperoxide and carbonyl forming channels is uncertain (10). Product data are available for two haloperoxy radicals: CH₂FO₂ and CF₃CFHO₂. Reaction of CH₂FO₂ radicals with HO₂ gives 30% yield of the hydroperoxide, CH₂FOOH, and 70% yield of the carbonyl product, HC(O)F (10). In the reaction of CF₃CFHO₂ with HO₂ radicals less than 5% of the carbon-containing products appear as the carbonyl CF₃C(O)F and, by inference, > 95% of the reaction proceeds to give the hydroperoxide CF₃CFHOOH or the alkoxy radical CF₃CFHO (11). There is considerable uncertainty in the mechanism of reaction of haloperoxy radicals with HO₂ radicals. The observed carbonyl product in the CH₂FO₂ + HO₂ reaction could be a result of the reaction proceeding via a concerted process involving a six-membered ring transition state or via a stepwise process with the formation of an alkoxy radical which subsequently undergoes reaction with O₂. More work is needed in this area.

Table I: Atmospheric Lifetimes, Ozone Depletion Potential, and Halocarbon Global Warming Potentials

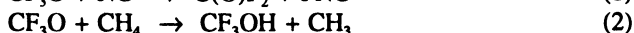
Compound	Lifetime ^a (years)	ODP ^b	HGWP ^c
HFC-23 (CF ₃ H)	411	0	7.7
HFC-32 (CH ₂ F ₂)	6.7	0	0.094 ^d
HFC-125 (CF ₃ CF ₂ H)	26	0	0.58
HFC-134a (CF ₃ CFH ₂)	14	0	0.27
HFC-143a (CF ₃ CH ₃)	40	0	0.74
HCFC-22 (CHF ₂ Cl)	14	0.047	0.36
HCFC-123 (CF ₃ CCl ₂ H)	1.5	0.016	0.019
HCFC-124 (CF ₃ CFClH)	6.0	0.018	0.096
HCFC-141b (CFCl ₂ CH ₃)	7.1	0.085	0.092
HCFC-142b (CF ₂ ClCH ₃)	17.8	0.053	0.36
CFC-11 (CFCl ₃)	60	1.0 ^e	1.0 ^e
CFC-12 (CF ₂ Cl ₂)	105	0.95	3.1
CO ₂			0.00076 ^f

^aAverage of values given by Derwent et al., page 124 (2). ^bAverage of values given in Table 4 of Fisher et al. (71). ^cAverage of values given in Table 5 of Fisher et al. (77). ^dEstimated from lifetime to be midway between HCFCs 124 and 141b. ^eBy definition. ^fSee text.

Reactions of CF_3CFHO_2 and $\text{CF}_2\text{ClCH}_2\text{O}_2$ radicals with HO_2 proceed with rates that are comparable to those of the simplest alkyl peroxy radicals, CH_3O_2 and $\text{C}_2\text{H}_5\text{O}_2$ (11,12). In contrast, $\text{CF}_3\text{CCl}_2\text{O}_2$ radicals react approximately 3 times more slowly (13). It seems reasonable to conclude that the peroxy radicals formed from HFCs and HCFCs react with rates similar to those measured for CF_3CFHO_2 , $\text{CF}_2\text{ClCH}_2\text{O}_2$, and $\text{CF}_3\text{CCl}_2\text{O}_2$ (i.e., in the range $2-7 \times 10^{-12} \text{ cm}^3 \text{ molecule}^{-1} \text{ s}^{-1}$). Using an HO_2 concentration of $10^9 \text{ molecule cm}^{-3}$ then gives a lifetime of 2 to 8 minutes for CX_3CXYO_2 radicals with respect to reaction with HO_2 . As discussed by Atkinson (2), the hydroperoxide CX_3CXyOOH is expected to be returned to the CX_3CXyO_x radical pool via reaction with OH and photolysis (2). The fate of the carbonyl product $\text{CX}_3\text{C(O)X}$ produced in the $\text{CX}_3\text{CXyO}_2 + \text{HO}_2$ reaction is discussed later.

Numerous product studies of halocarbon oxidation have shown that the atmospheric fate of the alkoxy radical, CX_3CXyO , is either decomposition or reaction with O_2 (5,14,15,16,17,18,19,20,21,22,23,24). Decomposition can occur either by C-C bond fission or Cl atom elimination. Reaction with O_2 is only possible when an α -H atom is available (e.g. in CF_3CFHO). In the case of the alkoxy radicals derived from HFC-32, HFC-125, and HCFC-22, only one reaction pathway available. Hence, CHF_2O radicals react with O_2 to give C(O)F_2 (25), $\text{CF}_3\text{CF}_2\text{O}$ radicals decompose to give CF_3 radicals and C(O)F_2 (16,18,19), and CF_2ClO radicals eliminate a Cl atom to give C(O)F_2 (26,27). The alkoxy radicals derived from HFC-143a, HCFC-123, HCFC-124, HCFC-141b and HCFC-142b all have two or more possible fates, but one loss mechanism dominates in the atmosphere. For HCFCs 123 and 124 the dominant process is elimination of a Cl atom to give $\text{CF}_3\text{C(O)Cl}$ (14,18,22) and $\text{CF}_3\text{C(O)F}$ (16,18), respectively. For HFC-143a, HCFC-141b, and HCFC-142b reaction with O_2 dominates, giving CF_3CHO (5), CFCl_2CHO (23,28), and CF_2ClCHO (23,28), respectively. The case of HFC-134a is the most complex. Under atmospheric conditions, the alkoxy radical derived from HFC-134a, CF_3CFHO , decomposes [to give CF_3 radicals and HC(O)F] and reacts with O_2 [to give $\text{CF}_3\text{C(O)F}$ and HO_2 radicals] at comparable rates (15,17,29).

Before moving on to consider the fate of the carbonyl products, it is appropriate to discuss the atmospheric fate of CF_3O radicals. The usual modes of alkoxy radical loss are not possible for CF_3O radical. Reaction with O_2 and decomposition via F atom elimination are both thermodynamically impossible under atmospheric conditions (30). CF_3O radicals react with NO (31,32,33,34), hydrocarbons (35,36,37,38,39,40,41,42) and possibly water vapor (43).



Reaction with NO yields C(O)F_2 . C(O)F_2 does not react with any gas phase trace atmospheric species and its photolysis is slow (44). C(O)F_2 is removed from the atmosphere by incorporation into water droplets and hydrolysis to give CO_2 and HF and by photolysis in the upper stratosphere to give FCO radicals and F atoms. FNO photolyses to give NO and a F atom (45). F atoms reversibly form FO_2 radicals by combining with O_2 , and also react with CH_4 and H_2O to give HF which will be rained out of the atmosphere. Reaction of CF_3O radicals with hydrocarbons such as CH_4 or with gas phase H_2O produces CF_3OH . The $\text{CF}_3\text{O-H}$ bond is unusually strong (120 kcal mole⁻¹) and is not expected to be attacked by any trace atmospheric radical species (43,46) or to be cleaved photolytically (47). CF_3OH undergoes heterogeneous

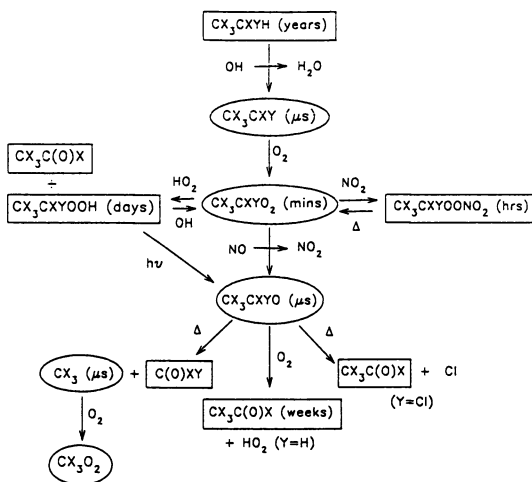


Figure 1:

Generalized scheme for the atmospheric oxidation of a halogenated organic compound, CX_3CXyH ($X, Y = H, Cl, \text{ or } F$). Transient radical intermediates are enclosed in ellipses, and products with less transitory existence are given in the boxes.

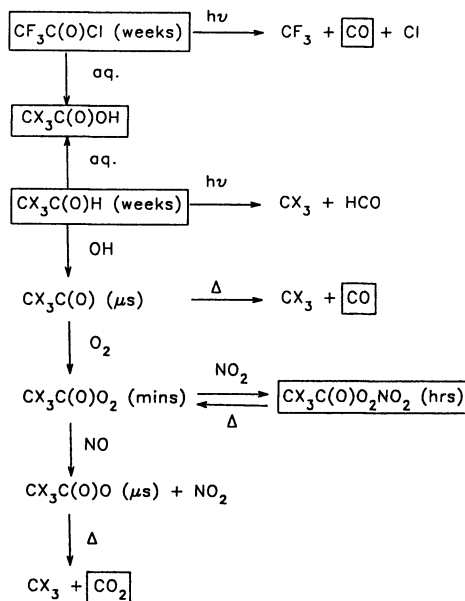


Figure 2:

Generalized scheme for the gas phase atmospheric chemistry of $CX_3C(O)H$ and $CF_3C(O)Cl$.

decomposition to give $C(O)F_2$ and HF and/or is incorporated into atmospheric water droplets (48).

While there has been speculation that CF_3O radicals could participate in catalytic ozone destruction cycles (49), recent studies have shown that the reaction of CF_3O radicals with ozone is too slow to be of significance (34,50,51,52,53,54).

Reactions of Halogenated Carbonyl Intermediates. Thus far the oxidation of the title halocarbons into halogenated carbonyl products has been discussed. While the gas phase oxidation mechanisms are complex, the carbonyl products are well established and are given in Table II.

Table II: Gas-Phase Atmospheric Degradation Products

Compound	Carbon Containing Degradation Products
HFC-23 (CF_3H)	$C(O)F_2$, CF_3OH
HFC-32 (CH_2F_2)	$C(O)F_2$
HFC-125 (CF_3CF_2H)	$C(O)F_2$, CF_3OH
HFC-134a (CF_3CFH_2)	$HC(O)F$, CF_3OH , $C(O)F_2$, $CF_3C(O)F$
HFC-143a (CF_3CH_3)	$CF_3C(O)H$, CF_3OH , $C(O)F_2$, CO_2
HCFC-22 (CHF_2Cl)	$C(O)F_2$
HCFC-123 (CF_3CCl_2H)	$CF_3C(O)Cl$, CF_3OH , $C(O)F_2$, CO
HCFC-124 (CF_3CFClH)	$CF_3C(O)F$
HCFC-141b ($CFCl_2CH_3$)	$CFCl_2CHO$, $C(O)FCl$, CO , CO_2
HCFC-142b (CF_2ClCH_3)	CF_2ClCHO , $C(O)F_2$, CO , CO_2

The carbonyl products represent a convenient break point in our discussion. The sequence of gas phase reactions that follow from the initial attack of OH radicals on the parent halocarbon are sufficiently rapid that heterogeneous and aqueous processes play no role. In contrast, the lifetimes of the carbonyl products [e.g., $HC(O)F$, $C(O)F_2$, $CF_3C(O)F$] are relatively long. As discussed in the following section, incorporation into water droplets followed by hydrolysis plays an important role in the removal of halogenated carbonyl compounds (55). In the case of $HC(O)F$, $C(O)F_2$, $FC(O)Cl$, and $CF_3C(O)F$ reaction with OH radicals (56) and photolysis (44) are too slow to be of any significance. These compounds are removed entirely by incorporation into water droplets.

The gas phase oxidation mechanism for $CX_3C(O)H$ and $CF_3C(O)Cl$ is shown in Figure 2. For $CX_3C(O)H$ species reaction with OH radicals is important (57). The lifetimes of $CF_3C(O)H$, $CF_2ClC(O)H$, and $CFCl_2C(O)H$ with respect to OH attack have been estimated to be 24, 19, and 11 days, respectively (57). As discussed by Scollard et al. (57), photolysis is probably also an important sink for $CF_3C(O)H$, $CF_2ClC(O)H$,

and $\text{CFCl}_2\text{C}(\text{O})\text{H}$. Finally, scavenging by water droplets probably plays a role in the atmospheric fate of these halogenated aldehydes. For $\text{CF}_3\text{C}(\text{O})\text{Cl}$, reaction with OH is not possible. Photolysis of $\text{CF}_3\text{C}(\text{O})\text{Cl}$ is important (24,58) and competes with incorporation of $\text{CF}_3\text{C}(\text{O})\text{Cl}$ into water droplets.

As shown in Figure 2, photolysis of $\text{CF}_3\text{C}(\text{O})\text{Cl}$ yields CF_3 radical, CO, and Cl (24). In addition, trace amounts (< 1% yield) of CF_3Cl were reported (24). CF_3Cl is a long-lived compound that efficiently transports chlorine from the lower atmosphere to the stratosphere. However, the low yield of CF_3Cl from $\text{CF}_3\text{C}(\text{O})\text{Cl}$ photolysis renders this pathway of negligible environmental significance. The photolysis of $\text{CF}_3\text{C}(\text{O})\text{H}$ in air produces a substantial yield of CF_3H [preliminary data suggests a 56% yield (59)]. It seems reasonable to suppose that $\text{CF}_2\text{ClC}(\text{O})\text{H}$ and $\text{CFCl}_2\text{C}(\text{O})\text{H}$ also photolyze to give significant yields of CF_2ClH and CFCl_2H , respectively. CF_2ClH and CFCl_2H both have shorter atmospheric lifetimes than the parent HCFCs (141b and 142b) (2) from which they may be derived. From the viewpoint of assessing the environmental impact of these compounds, the potential formation of CF_2ClH and CFCl_2H is then of little consequence. In contrast, CF_3H is approximately an order of magnitude more persistent than HFC-143a. Hence, the formation of CF_3H via the photolysis of $\text{CF}_3\text{C}(\text{O})\text{H}$ has important ramifications concerning the global warming potential of HFC-143a. Further work is needed in this area.

$\text{CF}_3\text{C}(\text{O})$, $\text{CF}_2\text{ClC}(\text{O})$, and $\text{CFCl}_2\text{C}(\text{O})$ radicals can either react with O_2 or dissociate to give CO and a halogenated methyl radical. The relative importance of dissociation increases with the number of Cl atoms. Reaction with O_2 is essentially the sole atmospheric fate of $\text{CF}_3\text{C}(\text{O})$ radicals (60,61), while decomposition accounts for 21% of the loss of $\text{CF}_2\text{ClC}(\text{O})$ radicals and 61% of the loss of $\text{CFCl}_2\text{C}(\text{O})$ radicals at 298 K in 740 Torr of air (28). The reaction of $\text{CX}_3\text{C}(\text{O})$ radicals with O_2 yields $\text{CX}_3\text{C}(\text{O})\text{O}_2$ radicals, which can react with NO or NO_2 . Reaction with NO_2 gives a halogenated acetyl peroxy radical which undergoes thermal decomposition (60,61) to regenerate $\text{CX}_3\text{C}(\text{O})\text{O}_2$. Reaction with NO gives a $\text{CX}_3\text{C}(\text{O})\text{O}$ radical which rapidly dissociates to give CX_3 radicals and CO_2 (61).

Heterogeneous and Aqueous Phase Chemistry

The final step in removal of any species from the atmosphere involves heterogeneous deposition to the earth's surface. Removal processes include wet deposition via rainout (following uptake into tropospheric clouds) and dry deposition to the earth's surface, principally to the oceans. The rates of these processes are largely determined by the species' chemistries in aqueous solution. For the viability of CFC replacements, the question is whether the rate of removal of any degradation product is slow compared to the OH reaction-limited lifetime of the parent compounds listed in Table I. Heterogeneous lifetimes of the parent compounds themselves are on the order of hundreds of years because of their low aqueous solubility and reactivity.

As discussed in the preceding sections, the species listed in Table III are degradation products of the parent HFC and HCFC compounds that have removal rates in the gas phase (via reaction or photolysis) that are slow enough (days or longer) for heterogeneous processing to be significant. All the halogen containing species are thought to undergo aqueous interactions that are "fast enough" for efficient wet and dry deposition

(62). For example, although the acid halides are relatively insoluble in water, they do hydrolyze to produce the acids HX and $CX_3C(O)OH$ (see Table III). Since the acids are very water soluble, hydrolysis removes the halides from the gas phase irreversibly.

Table III: Aqueous-Phase Atmospheric Degradation Products

Compound	$H^*k_{hyd}^{1/2}$ ($M \text{ atm}^{-1} \text{ s}^{-1/2}$)	Lifetime		Degradation Products
		Clouds (days)	Ocean (years)	
$C(O)F_2$	6 ^a	5-10	0.3-1.5	HF, CO_2
$C(O)ClF$	$\approx 2^b$	5-20	0.5-5.0	HF, HCl, CO_2
$CF_3C(O)F$	4 ^a	5-15	0.3-3.0	$CF_3C(O)OH$, HF
$CF_3C(O)Cl$	1 ^a	5-30	1.0-9.0	$CF_3C(O)OH$, HCl
$HC(O)F$		150-1500 ^c	80 ^c	HF, $HCOOH$

^aValues measured by DeBruyn et al. (64). George et al. (63) have reported higher values; quoted lifetimes should be considered as upper limits. ^bInterpolation of data for $C(O)Cl_2$ and $C(O)F_2$. ^cConservative estimate based on $k_{hyd} = 0.01^{-1}$ (69).

The problem is that it is difficult to measure the relevant aqueous kinetics of such species. Atmospheric removal rates depend on both solubility (expressed in terms of the Henry's law constant, H , $M \text{ atm}^{-1}$) and hydrolysis rate (k_{hyd} , s^{-1}). Because these species do not form stable aqueous solutions, neither parameter is simply measurable in bulk solution. As a result, laboratory determinations involve heterogeneous processes that typically measure combinations of H and k_{hyd} . Estimation of atmospheric lifetimes requires deconvolution of these parameters.

For the halocarbonyls, [$C(O)F_2$, $CF_3C(O)F$, and $CF_3C(O)Cl$, in particular] there has been much effort to measure the relevant aqueous kinetics including techniques utilizing droplets (55,63), bubbles (64), wetted wall reactors (65), and aerosol chambers (65). The results of these experiments are summarized in Table III in terms of the product $H^*k_{hyd}^{1/2}$, which is the parameter typically measured in gas/liquid mass transfer experiments.

For the two related chlorinated species [$C(O)Cl_2$ and $CCl_3C(O)Cl$] a combination of studies by several groups have determined $k_{hyd} \approx 100\text{-}150 \text{ s}^{-1}$, with about a factor of two uncertainty. For $C(O)Cl_2$ the studies include aerosol chamber (65), wetted wall reactor (65), bubble column (64), and mixed solvent kinetic experiments (66). For $CF_3C(O)Cl$, bubble column (64), collected droplets (63) and mixed solvent kinetic experiments (67) have been performed. The $H^*k_{hyd}^{1/2}$ values for $C(O)Cl_2$ and $CCl_3C(O)Cl$, 0.2 and 0.9

M atm⁻¹ s⁻¹, respectively, span the range of the fluorine containing species listed in Table III.

Assuming that $k_{\text{hyd}} \approx 100 \text{ s}^{-1}$ is representative of all the halocarbonyl species, one obtains $H \approx 0.1\text{--}0.6 \text{ M atm}^{-1}$. With H and k_{hyd} values, tropospheric lifetimes for heterogeneous uptake into clouds and into the ocean can be estimated, as listed in Table III (62,68,69). The range of lifetimes reflects a conservative range of $k_{\text{hyd}} = 1\text{--}1000 \text{ s}^{-1}$. For tropospheric cloud processing, the lower limit of 5 days is indicative of atmospheric transport limitations, i.e., the time taken to transport the species into the clouds. These estimates are consistent with results of more sophisticated global assessment model calculations (68,69).

There are two conclusions to be drawn from Table III. First, and most importantly, despite the considerable uncertainty in the laboratory kinetic results, heterogeneous removal of halocarbonyl species is fast enough to have no effect on the overall halogen lifetime compared to the lifetime of the parent halocarbon. Second, tropospheric cloud rainout will predominate over deposition to the ocean. This conclusion, based on the most recent laboratory results, reverses earlier predictions of ocean dominated deposition that assumed a larger lower limit of $H > 10 \text{ M atm}^{-1}$ (62).

More precise estimates of halocarbonyl lifetimes require further study of the aqueous kinetics. While such studies would have no impact on ODP or GWP calculations (see next section), they are important for predicting rainwater concentrations and precipitation patterns of key products such as trifluoroacetic acid (68). Another example is HC(O)F; its lifetimes listed in Table III are based upon a very conservative estimate of $k_{\text{hyd}} = 0.01 \text{ s}^{-1}$ (69). Experimental studies of its aqueous kinetics are required to determine just how conservative the long (> 0.5 year) lifetime estimates are.

Ozone Depletion Potentials

In discussions of the effects of halocarbons on stratospheric ozone the concept of "ozone depletion potential" (ODP) is useful (70). Ozone depletion potential is defined as the ratio of the calculated ozone column change per mass of a given compound released to the column change for the same mass of CFC-11. ODPs for the title halocarbons have been calculated by a number of atmospheric modelling groups. Results from Fisher et al. (71) are given in Table I.

HFCs do not contain any chlorine and so have no ozone depletion potential associated with the well established chlorine based catalytic ozone destruction cycles. Speculation regarding the possible impact of HFCs on stratospheric ozone via degradation into CF₃O_x, FCO_x, and FO_x radicals, which could participate in catalytic ozone destruction cycles (49,72,73), has been shown to be unfounded (50,51,52,53,54,74,75). The ODPs of HFCs are zero.

In ODP calculations it is assumed that attack by OH radicals in the lower atmosphere removes HCFCs and that no long-lived products are formed that could transport chlorine to the stratosphere. Uncertainty regarding the potential importance of halogenated peroxy acetyl nitrates [CX₃C(O)O₂NO₂] as carriers of chlorine to the stratosphere has been resolved by a recent study by Zabel et al. (60). In the cold upper troposphere thermal decomposition of CF₂ClC(O)O₂NO₂ and CFCl₂C(O)O₂NO₂ is very slow (60). However, in the warmer lower troposphere thermal decomposition is rapid.

At 282K, [1 km altitude in U.S. Standard Atmosphere (76)] the lifetimes of $\text{CF}_2\text{ClC}(\text{O})\text{O}_2\text{NO}_2$ and $\text{CFCl}_2\text{C}(\text{O})\text{O}_2\text{NO}_2$ are 43 and 33 hrs, respectively (60). Circulation of air through the lower troposphere acts as an efficient removal mechanism of $\text{CX}_3\text{C}(\text{O})\text{O}_2\text{NO}_2$ species. There are no known HCFC oxidation products that transport significant amounts of chlorine to the stratosphere.

As seen in Table I, HCFCs are considerably less harmful towards stratospheric ozone than CFCs. However, HCFCs do transport chlorine into the stratosphere. Recognition of this fact led to the development of a schedule of production caps and application bans culminating in a complete ban on the manufacture and importation of HCFCs in the U.S. in the year 2030.

Halocarbon Global Warming Potentials

In discussions of the potential impact of HFCs and HCFCs on global warming the concept of halocarbon global warming potential is useful (77). Halocarbon global warming potential (HGWP) is defined as the ratio of the steady state calculated warming for a fixed release of gas relative to that calculated for the release of the same mass of CFC-11. HGWPs reported by Fisher et al. (77). are listed in Table I.

The HGWPs listed in Table I provide a relative ranking of the direct radiative forcing of a series of halocarbons. Indirect effects are possible if long-lived products are formed during the atmospheric degradation process. With two possible exceptions, no significant long-lived products have been reported in the gas and aqueous phase reactions involved in the atmospheric degradation of hydrohalocarbons. Both exceptions involve the potential formation of CF_3H , first, via photolysis of $\text{CF}_3\text{C}(\text{O})\text{H}$ (an oxidation product of HFC-143a) as discussed above, and second, via microbial degradation of trifluoroacetic acid (an oxidation product of HCFC-123, 124, and HFC-134a) in oxic sediments (78). As shown in Table I, CF_3H has a long atmospheric lifetime and is a potent greenhouse gas. If substantial quantities of CF_3H are released into the atmosphere during the environmental degradation of HCFC-123, 124, and HFC-134a, and 143a, the GWPs of these compounds will need to be revised upwards. Over a 500 year horizon the GWP of CF_3H is 400 times that of HCFC-123 (see Table I). Based upon current information it is not possible to quantify the potential importance of CF_3H formation via the aforementioned pathways. Further research in this area is needed.

As seen in Table I, the HGWPs scale approximately linearly with atmospheric lifetime. This is not surprising as CFCs, HFCs, and HCFCs all have similar molecular structures and chemical bonds. Hence, the strengths and positions of their infrared absorptions are similar. The impact of these species is then largely determined by the atmospheric concentration and hence the lifetime of these species.

Finally, in discussions of potential global climate change it is germane to compare the HFCs and HCFCs with the most important greenhouse gas— CO_2 . Lashof and Ahuja (79) have proposed an index of global warming potentials by which to relate the potential impact on global climate change of CFCs and their replacements to that of CO_2 . The global warming potential of CFC-11 is approximately 1300 times greater than that of CO_2 (79).

As seen from Table I, the direct global warming potentials of HFCs and HCFCs are less than that of the CFCs they will replace but substantially greater than CO_2 . For

example, the HGWP of HFC-134a is 11 times less than for CFC-12 but 350 times greater than for CO₂. To place the potential for HFCs and HCFCs to impact global climate in perspective, we need to consider their emission rates relative to CO₂. Past CFC production provides a convenient likely estimate of HFC and HCFC emissions. In 1986 global CFC production was 10⁶ tonnes (80) while the emission of CO₂ was 2 x 10¹⁰ tonnes (81). Assuming, for example, that the HGWP of HFC-134a is representative of the weighted average of HGWPs of all emitted HFCs and HCFCs, then the direct global climate forcing due to HFCs and HCFCs would be less than 4% of that due to CO₂.

Formation of Toxic/Noxious Degradation Products

The atmospheric degradation of HFCs and HCFCs gives rise to a wide variety of products (Tables II, III). The atmospheric concentration of these products will be extremely small (<< ppb). There are no known adverse environmental impacts associated with these compounds at such low concentrations. The ultimate removal mechanism for all products is incorporation into rain-sea-cloud water where hydrolysis will take place. With the possible exception of CF₃C(O)OH, the hydrolysis products are ubiquitous, naturally-occurring species that have no adverse environmental impact.

From the available toxicological data concerning CF₃C(O)OH [see discussion by Kaminsky (2)], it has been concluded that the formation of this compound from the atmospheric degradation of HFC-134a is of no concern with respect to human health (82). High concentrations of CF₃C(O)OH ($\geq 5 \times 10^{-4}$ Molar) have been reported to adversely impact wheat and tomato seedlings (83). The concentration of CF₃C(O)OH in rainwater expected from the atmospheric degradation of HFCs and HCFCs is $< 10^{-7}$ Molar (82). CF₃COOH undergoes microbial degradation in oxic and anoxic sediments (78) and will probably not accumulate in the environment.

Conclusions

A substantial body of experimental and theoretical data concerning the atmospheric degradation of HFCs and HCFCs is available. While some uncertainties exist and more research is needed, the current understanding of the atmospheric chemistry of the commercially important HFCs and HCFCs is well established. HFCs have no impact on stratospheric ozone. HCFCs have small but non-negligible ozone depletion potentials. The direct global warming potentials of HFCs and HCFCs are approximately an order of magnitude less than that of the CFCs they replace. For HCFC-123, HCFC-124, HFC-134a, and HFC-143a the possibility exists of a substantial indirect global warming potential. The yield of CF₃H from microbial degradation of CF₃COOH and photolysis of CF₃C(O)H are key uncertainties in our understanding of the global warming potentials of HFCs and HCFCs. Finally, at the concentrations expected from the atmospheric degradation of HFCs and HCFCs, none of the oxidation products are noxious or toxic.

Literature Cited

1. Molina, M.; Rowland, F. S. *Nature* **1974**, *249*, 810.
2. World Meteorological Organization Global Ozone Research and Monitoring Project, Report No. 20; Scientific Assessment of Stratospheric Ozone, Vol 1; 1989.
3. DeMore, W. B.; Sander, S. P.; Golden, D. M.; Hampson, R. F.; Kurylo, M. J.; Howard, C. J.; Ravishankara A. R.; Kolb, C. E.; Molina, M. J., Jet Propulsion Laboratory Publication 92-20, Pasadena, CA (1992).
4. Sehested, J.; Nielsen, O. J.; Wallington, T. J. *Chem. Phys. Lett.* **1993**, *213*, 457.
5. Nielsen, O. J.; Gamborg, E.; Sehested, J.; Wallington, T. J.; Hurley, M. D. *J. Phys. Chem.* **1994**, *98*, 9518.
6. Moore, S. B.; Carr, R. W., *J. Phys. Chem.* **1990**, *94*, 1393.
7. Zabel, F.; Reimer, A.; Becker, K. H.; Fink, E. H. *J. Phys. Chem.* **1989**, *93*, 5500.
8. Köppenkastrop, D.; Zabel, F. *Int. J. Chem. Kinet.* **1991**, *23*, 1.
9. Mogelberg, T. E.; Nielsen, O. J.; Sehested, J.; Wallington, T. J.; Hurley, M. D.; Schneider, W. F. *Chem. Phys. Lett.* **1994**, *225*, 375.
10. Wallington, T. J.; Hurley, M. D.; Schneider, W. F.; Sehested, J.; Nielsen, O. J. *Chem. Phys. Lett.* **1994**, *218*, 34.
11. Maricq, M. M.; Szenté, J. J.; Hurley, M. D.; Wallington, T. J. *J. Phys. Chem.* **1994**, *98*, 8962.
12. Hayman, G. D., page 65, proceedings of the STEP-HALOCSIDE/AFEAS Workshop, University College Dublin, Ireland, March 1993.
13. Hayman, G. D.; Jenkin, M. E.; Murrells, T. P.; Shalliker, S. J., page 79, proceedings of the STEP-HALOCSIDE/AFEAS Workshop, University College Dublin, Ireland, May 1991.
14. Edney, E. O.; Gay, B. W. Jr.; Driscoll, D. J. *J. Atmos. Chem.* **1991**, *12*, 105.
15. Wallington, T. J.; Hurley, M. D.; Ball, J. C.; Kaiser, E. W. *Environ. Sci. Technol.* **1992**, *26*, 1318.
16. Edney, E. O.; Driscoll, D. J. *Int. J. Chem. Kinet.* **1992**, *24*, 1067.
17. Tuazon, E. C.; Atkinson, R. *J. Atmos. Chem.* **1993**, *16*, 301.
18. Tuazon, E. C.; Atkinson, R. *J. Atmos. Chem.* **1993**, *17*, 179.
19. Sehested, J.; Ellermann, T.; Nielsen, O. J.; Wallington, T. J.; Hurley, M. D. *Int. J. Chem. Kinet.* **1993**, *25*, 701.
20. Nielsen, O. J.; Ellermann, T.; Sehested, J.; Wallington, T. J. *J. Phys. Chem.* **1992**, *96*, 10875.
21. Wallington, T. J.; Hurley, M. D.; Ball, J. C.; Ellermann, T.; Nielsen, O. J.; Sehested, J. *J. Phys. Chem.* **1994**, *98*, 5435.
22. Hayman, G. D.; Jenkin, M. E.; Murrells, T. P.; Johnson, C. E. *Atmos. Environ.* **1994**, *28*, 421.
23. Zellner, R.; Hoffmann, A.; Mörs, V.; Malms, W., page 80, proceedings of the STEP-HALOCSIDE/AFEAS Workshop, University College Dublin, Ireland, March 1993.
24. Meller, R.; Boglu, D.; Moortgat, G. K., page 130, proceedings of the STEP-HALOCSIDE/AFEAS Workshop, University College Dublin, Ireland, March 1993.

25. Nielsen, O. J.; Ellermann, T.; Bartkiewicz, E.; Wallington, T. J.; Hurley, M. D. *Chem. Phys. Lett.* **1992**, *192*, 82.
26. Carr, R. W. Jr.; Peterson, D. G.; Smith, F. K. *J. Phys. Chem.* **1986**, *90*, 607.
27. Rayez, J.-C.; Rayez, M.-T.; Halvick, P.; Duguay, B.; Lesclaux, R.; Dannenberg, J. T. *Chem. Phys.* **1987**, *116*, 203.
28. Tuazon, E. C.; Atkinson, R. *Environ. Sci. Technol.* **1994**, *28*, 2306.
29. Rattigan, O. V.; Rowley, D. M.; Wild, O.; Jones, R. L.; Cox, R. A. *J. Chem. Soc. Faraday Trans.* **1994**, *90*, 1819.
30. Batt, L.; Walsh, R. *Int. J. Chem. Kinet.* **1982**, *14*, 933.
31. Chen, J.; Zhu, T.; Niki, H. *J. Phys. Chem.* **1992**, *96*, 6115.
32. Bevilacqua, T. J.; Hanson, D. R.; Howard, C. J. *J. Phys. Chem.* **1993**, *97*, 3750.
33. Sehested, J.; Nielsen, O. J. *Chem. Phys. Lett.* **1993**, *206*, 369.
34. Turnipseed, A. A.; Barone, S. B.; Ravishankara, A. R. *J. Phys. Chem.* **1994**, *98*, 4594.
35. Chen, J.; Zhu, T.; Niki, H.; Mains, G. J. *Geophys. Res. Lett.* **1992**, *19*, 2215.
36. Sehested, J.; Wallington, T. J. *Environ. Sci. Technol.* **1993**, *27*, 146.
37. Saathoff, H.; Zellner, R. *Chem. Phys. Lett.* **1993**, *206*, 349.
38. Kelly, C.; Treacy, J.; Sidebottom, H. W.; Nielsen, O. J. *Chem. Phys. Lett.* **1993**, *207*, 498.
39. Barone, S. B.; Turnipseed, A. A.; Ravishankara, A. R. *J. Phys. Chem.* **1994**, *98*, 4602.
40. Bednarek, G.; Kohlman, J. P.; Saathoff, H.; Zellner, R. *Z. Phys. Chem. N. F.* in press.
41. Kelly, C.; Sidebottom, H. W.; Treacy, J.; Nielsen, O. J. *Chem. Phys. Lett.* **1994**, *218*, 29.
42. Chen, J.; Zhu, T.; Young, V.; Niki, H. *J. Phys. Chem.* **1993**, *97*, 7174.
43. Wallington, T. J.; Hurley, M. D.; Schneider, W. F.; Sehested, J.; Nielsen, O. J. *J. Phys. Chem.* **1993**, *97*, 7606.
44. Nölle, A.; Heydtmann, H.; Meller, R.; Schneider, W.; Moortgat, G. K. *Geophys. Res. Lett.* **1992**, *19*, 281.
45. Wallington, T. J.; Schneider, W. F.; Szente, J. J.; Maricq, M. M.; Sehested, J.; Nielsen, O. J. *J. Phys. Chem.* **1995**, *99*, 984.
46. Schneider, W. F.; Wallington, T. J. *J. Phys. Chem.* **1993**, *97*, 12783.
47. Schneider, W. F.; Wallington, T. J.; Minschwaner, K.; Stahlberg, E. A. *Environ. Sci. Technol.* **1995**, *29*, 247.
48. Wallington, T. J.; Schneider, W. F., *Environ. Sci. Technol.* **1994**, *28*, 1198.
49. Biggs, P.; Canosa-Mas, C. E.; Shallcross, D. E.; Wayne, R. P.; Kelly, C.; Sidebottom, H. W., page 177, proceedings of the STEP-HALOCSIDE/AFEAS Workshop, University College Dublin, Ireland, March 1993.
50. Nielsen, O. J.; Sehested, J. *Chem. Phys. Lett.* **1993**, *213*, 433.
51. Wallington, T. J.; Hurley, M. D.; Schneider, W. F. *Chem. Phys. Lett.* **1993**, *213*, 442.
52. Maricq, M. M.; Szente, J. J. *Chem. Phys. Lett.* **1993**, *213*, 449.
53. Fockenberg, C.; Saathoff, H.; Zellner, R. *Chem. Phys. Lett.* **1994**, *218*, 21.
54. Ravishankara, A. R.; Turnipseed, A. A.; Jensen, N. R.; Barone, S.; Mills, M.; Howard, C. J.; Solomon, S. *Science* **1994**, *263*, 71.

55. DeBruyn, W.; Duan, S. X.; Shi, X. Q.; Davidovits, P.; Worsnop, D. R.; Zahniser, M. S.; Kolb, C. E. *Geophys. Res. Lett.* **1992**, *19*, 1939.
56. Wallington, T. J.; Hurley, M. D. *Environ. Sci. Technol.* **1993**, *27*, 1448.
57. Scollard, D. J.; Treacy, J. J.; Sidebottom, H. W.; Balestra-Garcia, C.; Laverdet, G.; LeBras, G.; MacLeod, H.; Téton, S. *J. Phys. Chem.* **1993**, *97*, 4683.
58. Rattigan, O. V.; Wild, O.; Jones, R. L.; Cox, A. R. *J. Photochem. Photobiol. A: Chemistry* **1993**, *73*, 1.
59. Richer, H. R.; Sodeau, J. R.; Barnes, I., page 182, proceedings of the STEP-HALOCSIDE/AFEAS Workshop, University College Dublin, Ireland, March 1993.
60. Zabel, F.; Kirchner, F.; Becker, K. H. *Int. J. Chem. Kinet.* **1994**, *26*, 827.
61. Wallington, T. J.; Schested, J.; Nielsen, O. J. *Chem. Phys. Lett.* **1994**, *226*, 563.
62. Wine, P. H.; Chameides, W. L., p. 271-295, World Meteorological Organization Global Ozone Research and Monitoring Project, Report No. 20; Scientific Assessment of Stratospheric Ozone, Vol 1; 1989.
63. George, C.; Ponche, J. L.; Mirabel, P., page 196, proceedings of the STEP-HALOCSIDE/AFEAS Workshop, University College Dublin, Ireland, March 1993.
64. DeBruyn, W.; Davidovits, P.; Worsnop, D. R.; Zahniser, M. S., Kolb, C. E. *Environ. Sci. Technol.*, submitted for publication.
65. Behnke, W.; Elend, M.; Krüger, H. -U.; Zetzsch, C., page 203, proceedings of the STEP-HALOCSIDE/AFEAS Workshop, University College Dublin, Ireland, March 1993.
66. Ugi, I.; Beck, F. *Chem. Ber.* **1961**, *94*, 1839.
67. George, Ch.; Saison, J. Y.; Ponche, J. L.; Mirabel, Ph. *J. Phys. Chem.* **1994**, *98*, 10857.
68. Rodriguez, J. M.; Ko, M. K. W.; Sze, N. D.; Heisey, C. W., page 104, proceedings of the STEP-HALOCSIDE/AFEAS Workshop, University College Dublin, Ireland, March 1993.
69. Kanakidou, M.; Dentener, F. J.; Crutzen, P. J., page 113, proceedings of the STEP-HALOCSIDE/AFEAS Workshop, University College Dublin, Ireland, March 1993.
70. Wuebbles, D. J. *J. Geophys. Res.* **1983**, *88*, 1433.
71. Fisher, D. A.; Hales, C. H.; Filkin, D. L.; Ko, M. K. W.; Dak Sze, N.; Connell., P. S.; Wuebbles, D. J.; Isaksen, I. S. A.; Stordal, F. *Nature* **1990**, *344*, 508.
72. Francisco, J. S.; Goldstein, A. N.; Li, Z.; Zhao, Y.; Williams, I. H. *J. Phys. Chem.* **1990**, *94*, 4791,
73. Francisco, J. S. *J. Chem. Phys.* **1993**, *98*, 2198.
74. Wallington, T. J.; Ellermann, T.; Nielsen, O. J.; Schested, J. *J. Phys. Chem.* **1994**, *98*, 2346.
75. Schested, J.; Schested, K.; Nielsen, O. J.; Wallington, T. J. *J. Phys. Chem.* **1994**, *98*, 6731.
76. U.S. Standard Atmosphere, 1976, NOAA, NASA, USAF, Washington, D. C., 1976.
77. Fisher, D. A.; Hales, C. H.; Wang, W-C.; Ko, M. K. W.; Dak Sze, N. *Nature* **1990**, *344*, 513.

78. Visscher, P. T., C. W. Culbertson, and R. S. Oremland *Nature* **1994**, *369*, 729.
79. Lashof, D. A.; Ahuja, D. A. *Nature* **1990**, *344*, 529.
80. McFarland, M.; Kaye, J. *Photochem. Photobiol.* **1992**, *55*, 911.
81. *Trends '91: A Compendium of Data on Global Change*, Boden, T. A.; Sepanski, R. J.; Stoss, F. W., Eds.; Carbon Dioxide Information Analysis Center, Oak Ridge, TN: 1991, p 389.
82. Ball, J. C.; Wallington, T. J. *J. Air Waste Manag. Assoc.* **1993**, *43*, 1260.
83. Ingle, L. M. *Proc. West Virginia Acad. Sci.* **1968**, *40*, 1.

RECEIVED June 7, 1995

Chapter 4

The Atmospheric Chemistry of Iodine Compounds

Robert E. Huie and Barna Laszlo

Chemical Science and Technology Laboratory, Chemical Kinetics
and Thermodynamics Division, National Institute of Standards
and Technology, Gaithersburg, MD 20899-0001

The chemistry of iodine in the atmosphere is briefly discussed. Results of recent experiments involving the important iodine-containing radical IO are also reported, as is the thermochemistry of this species and some of its reactions.

The most important chemical fire extinguisher presently in use is CF_3Br . This compound is quite stable in the troposphere and diffuses into the stratosphere, where it is broken down by photolysis. The recent discovery that a chemical cycle involving bromine could be responsible for a considerable fraction of the halogen-induced ozone loss in the lower stratosphere(1-3) has resulted in an impending ban on the production of CF_3Br .(4) Bromine is important in stratospheric chemistry even though its concentration is exceeded by chlorine by more than a factor of one hundred. This is due to the greater efficiency of the bromine cycle and to coupling reactions which allow bromine to act synergistically on the chlorine cycle.

CF_3I has been identified as a possible replacement for CF_3Br .(5) Unlike CF_3Br , CF_3I can be removed in the troposphere by photolysis(6)



or reaction with OH(7)



The former process is probably the more important. The absorption cross section is similar to that of methyl iodide and, in the long wavelength region ($\lambda > 270$ nm),

This chapter not subject to U.S. copyright
Published 1995 American Chemical Society

increases with increasing temperature (Figure 1).(8) A recent study employing the temperature dependent cross section for CF_3I resulted in an overall atmospheric lifetime of 23 hours, assuming a uniform global surface release.(9)

A number of authors have discussed the possible tropospheric role of iodine containing species(10-14) and, in one very recent paper, the possibility of a stratospheric role has been raised.(9) In the troposphere, iodine atoms are typically involved in two sets of reactions which lead to no net change in atmospheric composition. Both start with the reaction of the iodine atom with ozone



Since I atoms can not abstract hydrogen from saturated organic compounds and do not add readily to unsaturated compounds, this appears to be their major tropospheric reaction.

The product IO can undergo photolysis



Following the photodissociation of IO, the resulting oxygen atoms will react with molecular oxygen to regenerate ozone and complete the null cycle



Alternatively, IO may react with NO



The resulting NO_2 is also readily photolyzed to return O atoms and thence O_3 . The relative concentrations of IO and I then depend on the concentrations of O_3 , NO, and the light flux, along with the rate constants for these reactions and the photolysis cross section for IO.

A number of non-active iodine reservoir species are formed in the troposphere. The most important are HOI, formed in the reaction

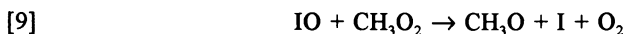


and IONO_2 , formed in the reaction



Steady-state concentrations of these species, along with the radicals I and IO, have been calculated for various NO_x concentrations.(14)

Another possibly important reaction is that of IO with alkyl peroxy radicals, particularly CH_3O_2



This reaction is similar to the reaction of ClO with CH₃O₂.(15) The importance of that reaction has been questioned, however.(16)

In the stratosphere, iodine may contribute to the destruction of ozone in a manner analogous to the much better known chlorine or bromine cycles.(17) By analogy with chlorine and bromine, the major direct effect of iodine on ozone is likely to arise from the simple cycle of reaction [3] followed by



Again by analogy with the other halogens, iodine may also interact with the water cycle by reaction [7] followed by photolysis of the product HOI

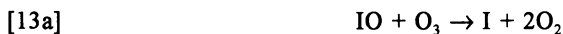


which is followed by



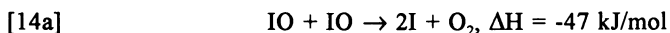
Iodine radicals also interact with the NO_x cycle by reactions [6] and [8].

In addition, IO can react with O₃

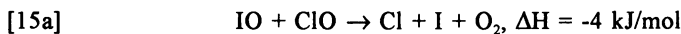


Even though the reaction is very exothermic, the rate constant for the first path is less than $1.3 \times 10^{-15} \text{ cm}^3 \text{ s}^{-1}$ at 292 K and the rate constant for the second, which is also expected to be very exothermic, is less than 2.3×10^{-16} at 323 K.(18)

IO can also undergo self-reaction(19)



or reaction with the other halogen oxide radicals ClO



or BrO

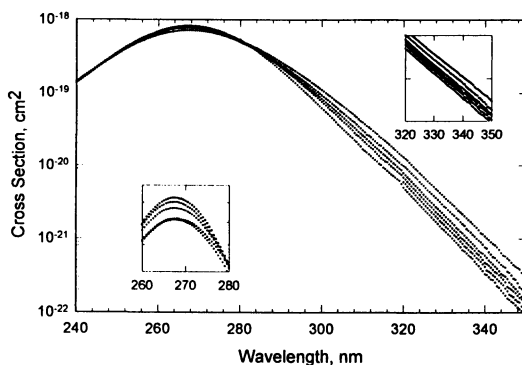


Figure 1. Absorption spectrum for CF_3I at 218, 235, 253, 273, 295, and 333 K. At the long wavelengths, the absorption cross section increases with increasing temperature.

IO SPECTRUM

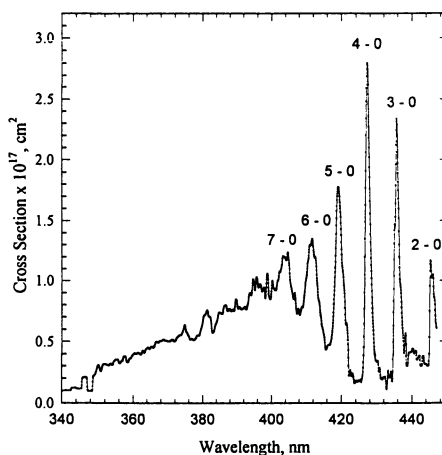
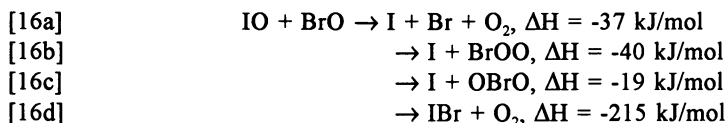


Figure 2. The absorption spectrum of the IO radical over the range 340 to 450 nm.



Of considerable importance is the observation that for all of these reactions, the reaction channel producing two halogen atoms is exothermic. (Some considerations on the thermodynamics of these species are discussed in the Appendix.) For the similar reactions of ClO with itself and with BrO, the channel leading directly to halogen atoms is endothermic. This suggests that the atom-forming branches will be of considerably greater importance in the reactions involving IO.

In order to obtain direct information on some of the reactions which may play a role in the possible effect of iodine on stratospheric ozone, we have initiated an investigation of several reactions involving iodine monoxide. In this communication, we report preliminary results of this investigation.

Experimental

The reactions were initiated by the laser-flash photolysis of N_2O at 193 nm, in the presence of 8 to 80 kPa N_2 .



The resulting oxygen atoms are allowed to react with I_2



The progress of the reaction is monitored by absorption spectrophotometry with two monochromators coupled to a transient digitizer. The details of the apparatus and the experimental procedure will be described in detail in a subsequent publication.

Results

The absorption spectrum of IO

We have measured the absorption spectrum of the IO radical from 340 to 445 nm (Figure 2). Over the spectral region 415 to 445 nm, our spectrum agrees well with previously published spectra.^(20,21) The most significant difference is that we and Stickel, *et al.* find the (2-0) peak to be significantly smaller than both (4-0) and (3-0) peaks, whereas Cox and Coker find the (2-0) peak about the same size as (3-0). We have derived absolute cross sections for IO by determining the loss of I_2 subsequent to the flash, measured simultaneously at 530 nm. The value at 427 nm, the (4-0) peak, was $2.7 \pm 0.5 \times 10^{-17} \text{ cm}^2$ (the uncertainty is twice the standard deviation from 24 experiments). This value is in good agreement with previous measurements which yielded $3.1 \times 10^{-17} \text{ cm}^2$.^(20,21,19)

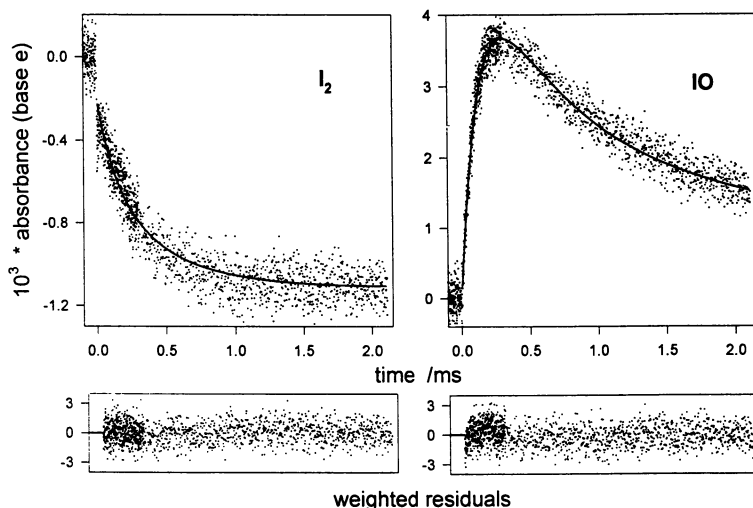


Figure 3. The loss of I_2 and the formation of IO subsequent to the flash photolysis of a mixture of 200 Pa N_2O and 80 mPa I_2 in 27 kPa N_2 . The signal is the result of an average of 2500 shots.

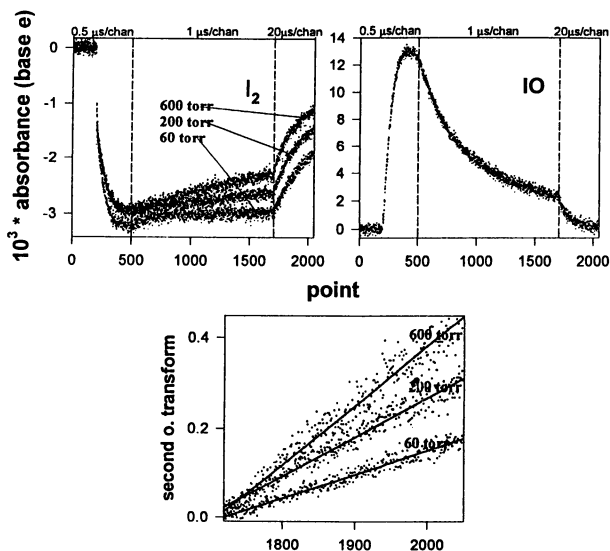


Figure 4. Temporal behavior of I_2 and of IO subsequent to the flash photolysis of a mixture of 270 Pa N_2O and 1 Pa I_2 in 8, 27, and 80 kPa N_2 . Also shown is the result of a second-order transform of the I_2 data.

In addition to the previously reported absorption of IO above 415 nm, we have identified two additional peaks at 411 and 403 nm, which we ascribe to the (6-0) and (7-0) transitions, and an underlying continuum starting around 420 nm and extending to about 350 nm. This additional absorption, weighted by the relative solar spectrum, increases the atmospheric photolysis rate by about 60%.

O + IO and O + I₂

A key reaction in the direct effect of iodine on stratospheric ozone is the reaction of O with IO, reaction 10. We have been able to obtain kinetic information on this reaction, along with the reaction of O with I₂, reaction 19, by simultaneously monitoring the formation of IO and the loss of I₂, at relatively low I₂ concentrations (Figure 3). By fitting these two curves to a model, allowing only the rate constants for O + IO and O + I₂ to vary, we obtain $k_{19} = 1.3 \times 10^{-10} \text{ cm}^3 \text{ s}^{-1}$, in excellent agreement with the previous measurement,(22) and $k_{10} = 1.2 \times 10^{-10} \text{ cm}^3 \text{ s}^{-1}$. This latter value is about four times greater than the rate constants for the comparable reactions of atomic oxygen with chlorine monoxide and with bromine monoxide.(23)

IO + IO

We have measured the rate constant for the self-reaction of the IO radical, reaction 14, by monitoring the loss of the IO absorption at 427 nm (Figure 4). Rate constants were measured over a wide range of I₂ and N₂O concentrations and over a pressure range of 8 to 80 kPa N₂. The rate constant was found to be independent of these various parameters and an average value of $8.0 \pm 1.7 \times 10^{-11} \text{ cm}^3 \text{ s}^{-1}$ was derived (the uncertainty is twice the standard deviation from 27 experiments). Although the measured rate constant for IO decay did not depend on total pressure, the extent of formation of I₂ did (Figure 4). The temporal behavior of I₂ lagged the decay of IO, indicating that the I₂ formation was not primarily from the self-reaction of IO (reaction 14c), but arose either from a secondary reaction of a product of the reaction of IO + IO, or from an enhanced rate of recombination of I atoms.

CF₃O₂ + IO

In the initial stages of this study, the reaction of O with CF₃I was used as a source of IO



A rapid loss of IO was observed, which was not purely second order, but appeared to be mixed, possibly the sum of two second-order processes. In this system, it appeared likely that in addition to the self-reaction of IO, part of the observed decay of IO was due to the reaction of IO with CF₃



O₂ was then added to suppress this reaction by the formation of CF₃O₂



Even with added oxygen, there was still an additional rapid component to the IO decay. We ascribe this to the reaction between IO and CF_3O_2



In addition, the formation of an aerosol was observed in the reaction cell with this mixture.

These observations might help explain the results of Cox and Coker(20) on the kinetics of the self-reaction of IO. In their study, CH_3I was used as an IO source, with O_2 present to remove CH_3 . They reported a very fast rate constant for reaction 14, $k = 4 \times 10^{-10} \text{ cm}^3 \text{ s}^{-1}$ and also reported the formation of an aerosol. Our results suggest that this may have been due to a rapid reaction between IO and CH_3O_2 .

Heterogeneous Chemistry

In the past few years, it has become apparent that a number of heterogeneous reactions, that is, reactions taking place on stratospheric aerosols or ice particles, are important in the effect of halogens on ozone depletion. Many of these reactions convert the halogen from an inactive to an active form. At this point, even speculation is difficult about the possible role of iodine on heterogeneous processes. It should be pointed out, however, that iodine compounds will be less volatile than the corresponding chlorine or bromine compounds, suggesting an even greater role of heterogeneous reactions. Further, the reduction potentials of iodine atoms and iodine oxides (IO, IO_2) are lower than for chlorine or bromine. Therefore electron transfer reactions leading to their regeneration might be more important. For example, the reduction potential of the I/I^- couple is 1.33 V, while for the Cl/Cl^- couple it is 2.41 V.(24) Therefore, I will be far more readily oxidized in an aerosol than Cl^- . Photolysis of iodine-containing anions in stratospheric aerosols might also play a role.

Appendix. Thermodynamics of IO and BrO.

A key piece of information in predicting the importance of possible reaction mechanisms in the interactions of IO with ClO and BrO is the heat of formation of IO. The recommended value of the heat of formation of IO is $175.1 \text{ kJ mol}^{-1}$.(25) This is based primarily on early spectroscopic measurements.(26) Other work, employing flame photometry,(27) resulted in a much lower value, $\Delta H_f = 118 \text{ kJ mol}^{-1}$. Some time ago, it was pointed out that only the lower values were compatible with the observation that the reactions of O^3P with CF_3I was very fast,(28)



This reaction has since been determined to have a rate constant of $1.1 \times 10^{-11} \text{ cm}^3 \text{ s}^{-1}$.(29) This is supported further by molecular beam observations of IO production in this reaction(30) and in reactions of alkyl iodides.(31)

Since that time, there have been additional determinations of the heat of formation of IO. Molecular beam studies of the reaction



has been used to obtain values of 222(32) and 230 kJ mol⁻¹(30) for the dissociation energy of IO, leading to $\Delta H_f = 126$ and 134 kJ mol⁻¹, respectively. Also, a potential energy surface has been constructed for IO which leads to $\Delta H_f = 106.7$ kJ mol⁻¹.(33) This latter paper also calculates $\Delta H_f = 82.3$ kJ mol⁻¹ for ClO, considerably less than the recommended value of $\Delta H_f = 102.1$ kJ mol⁻¹.

It is clear the heat of formation of IO is quite uncertain. Since the reaction of O with CF₃I is fast, the spectroscopic values are almost certainly much too high. The calculation from the potential energy surface, based on different spectroscopic measurements, are probably too low because the similar calculation for ClO appears to be too low. The most accurate results, then, are probably those from molecular beam studies. The two studies are in reasonable agreement and we have chosen to use a simple average of the two, $\Delta H_f = 130$ kJ mol⁻¹.

The recommended value of the heat of formation of BrO, 125.9 kJ mol⁻¹, also leads to a kinetic prediction which appears to be in conflict with observation. With that value, the reaction O + BrF → BrO + F is 14.6 kJ mol⁻¹ endothermic. The measured rate constant for this reaction is 1.5 × 10⁻¹³ cm³ mol⁻¹.(34) We feel that the heat of formation of this radical also should be reconsidered, but, for the present, we continue to use the recommended value.

There is also information in the literature useful in other heats of formation of species which may be of importance in some of the other reactions of interest. The free energy of formation of OBrO in the gas phase can be estimated from the value of $\Delta G_f = 144$ kJ mol⁻¹ in the aqueous phase(24) by comparison with the gas and aqueous phase values for OCIO. Taking $\Delta G_f = 120.5$ kJ mol⁻¹ for OCIO(g) and $\Delta G_f = 117.6$ kJ mol⁻¹ for OCIO(aq)(25) and assuming the same ratio applies for OBrO, we obtain $\Delta G_f = 148$ kJ mol⁻¹ for OBrO(g). Assuming the difference between ΔG° and ΔH° is the same as for OCIO (18 kJ mol⁻¹), then $\Delta H_f = 130$ kJ mol⁻¹ for OBrO.

(A similar calculation cannot be carried out for OIO. It appears to hydrate in the aqueous phase.) Also, the bond strength of BrOO has been estimated to be about 4 kJ mol⁻¹, which leads to a $\Delta H_f = 109$ kJ mol⁻¹.(35)

Acknowledgments

This work was supported in part by the United States Air Force through contract 89CS8204 and the United States Army through MIPR #M-G-164-93. Ongoing support for this laboratory is received from NASA. We thank Dr. Andrzej W. Miziolek for help and for useful discussions.

Literature Cited

- (1) Salawitch, R. J.; McElroy, M. B.; Yatteau, J. H.; Wolfsy, S. C.; Schoeberl, M. R.; Lait, L. R.; Newman, P. A.; Chan, K. R.; Lowenstein, M.; Podolske, J. R.; Strahan, S. E.; Proffitt, M. H. *Geophys. Res. Lett.* **1990**, *17*, 561.
- (2) Solomon, S. *Nature* **1990**, *347*, 347.
- (3) Brune, W. H.; Anderson, J. G.; Toohey, D. W.; Fahey, D. W.; Kawa, S. R.; Jones, R. L.; McKenna, D. S.; Poole, L. R. *Science* **1991**, *252*, 1260.
- (4) *Copenhagen amendments to the Montreal Protocol on Substances that Deplete the Ozone Layer*, 1992; Vol. 71.

- (5) Pitts, W. M.; Nyden, M. R.; Gann, R. G.; Mallard, W. G.; Tsang, W. *NIST Tech. Note 1279*, 1990.
- (6) Molina, M. J.; Tang, Y.; Scheinson, R. *Unpublished work*.
- (7) Brown, A. C.; Canosa-Mas, C. E.; Wayne, R. P. *Atmos. Environ.* **1990**, *24A*, 361.
- (8) Fahr, A.; Nayak, A. K.; Huie, R. E. *Unpublished Work*.
- (9) Solomon, S.; Burkholder, J. B.; Ravishankara, A. R.; Garcia, R. R. *J. Geophys. Res.* **1994**, *99*, 20929.
- (10) Zafiriou, O. C. *J. Geophys. Res.* **1974**, *79*, 2730-2732.
- (11) Chameides, W. L.; Davis, D. D. *J. Geophys. Res.* **1980**, *85*, 7383.
- (12) Chatfield, R. B.; Crutzen, P. J. *J. Geophys. Res.* **1990**, *95*, 22319.
- (13) Jenkin, M. E.; Cox, R. A.; Candeland, D. E. *J. Atmos. Chem.* **1985**, *2*, 359.
- (14) Barnes, I.; Bonsang, B.; Brauers, T.; Carlier, P.; Cox, R. A.; Dorn, H. P.; Jenkin, M. E.; Bras, G. L.; Platt, U., Air Pollution research Report, OCENO-NOX-CEC Project, 1991.
- (15) Simon, F. G.; Burrows, J. P.; Schneider, W.; Moortgat, G. K.; Crutzen, P. J. *J. Phys. Chem.* **1989**, *93*, 7807.
- (16) DeMore, W. B. *J. Geophys. Res.* **1991**, *96*, 4995.
- (17) Wayne, R. P. *The Chemistry of Atmospheres*; Clarendon Press: Oxford, 1991.
- (18) Buben, S. N.; Trofimova, E. M.; Spassky, A. I.; Messineva, N. A. "Study of atmospheric reactions of IO radicals. Report B. Reaction of iodine monoxide with ozone," The Institute of Energy Problems of Chemical Physics, Russian Academy of Sciences, 1994.
- (19) Sander, S. P. *J. Phys. Chem.* **1986**, *90*, 2194.
- (20) Cox, R. A.; Coker, G. B. *J. Phys. Chem.* **1983**, *87*, 4478.
- (21) Stickel, R. E.; Hynes, A. J.; Bradshaw, J. D.; Chameides, W. L.; Davis, D. D. *J. Phys. Chem.* **1988**, *92*, 1862.
- (22) Ray, G. E.; Watson, R. T. *J. Phys. Chem.* **1981**, *85*, 2955.
- (23) Ross, A. B.; Mallard, W. G.; Hellman, W. P.; Buxton, G. B.; Huie, R. E.; Neta, P. *NIST Standard Reference Database 40*, 1994.
- (24) Stanbury, D. M. *Adv. Inorg. Chem.* **1989**, *33*, 69-138.
- (25) Wagman, D. D.; Evans, W. H.; Parker, V. B.; Halow, I.; Bailey, S. M.; Schumm, R. H. *NBS Technical Note 270-3*, 1968.
- (26) Durie, R. A.; Ramsay, D. A. *Can. J. Phys.* **1958**, *36*, 35.
- (27) Phillips, L. F.; Sugden, T. M. *Trans Faraday Soc* **1961**, *57*, 914.
- (28) Herron, J. T.; Huie, R. E. *J. Phys. Chem.* **1969**, *73*, 1326.
- (29) Addison, M. C.; Donovan, R. J.; Garraway, J. *Faraday Diss Chem Soc* **1979**, 286.
- (30) Buss, R. J.; Sibener, S. J.; Lee, Y. T. *J. Phys. Chem.* **1983**, *87*, 4840.
- (31) White, R. W. P.; Smith, D. J.; Grice, R. *Chem. Phys. Lett.* **1992**, *193*, 269.
- (32) Radlein, D. S. A. G.; Whithead, J. C.; Grice, R. *Nature* **1975**, *253*, 37.
- (33) Reddy, R. R.; Rao, T. V. R.; Reddy, A. S. R. *Indian J. Pure App. Phys.* **1989**, *27*, 243.
- (34) Arutyunov, V. S.; Buben, S. N.; Chankin, A. M. *Kinet Catal* **1979**, *20*, 465.
- (35) Blake, D. A.; Browne, R. J.; Burns, G. *J. Phys. Chem.* **1970**, *53*, 3320.

RECEIVED May 11, 1995

Chapter 5

Tropospheric Degradation Products of Hydrochlorofluorocarbons and Hydrofluorocarbons

Potential Replacements for the Chlorofluorocarbons and Halons

Ernesto C. Tuazon and Roger Atkinson

Statewide Air Pollution Research Center, University of California,
Riverside, CA 92521

The products of the Cl atom-initiated photooxidations of a series of C₁-C₃ HCFCs and HFCs are summarized and discussed with respect to a generalized tropospheric reaction scheme. Direct observations of CFC₁₂CHO and CF₂ClCHO as products of CFC₁₂CH₃ (HCFC-141b) and CF₂ClCH₃ (HCFC-142b), respectively, in 100% yields are reported. The measured branching ratios of the CFC₁₂CO and CF₂ClCO radicals for decomposition versus reaction with O₂ are consistent and intermediate with those previously reported for CF₃CO and CCl₃CO.

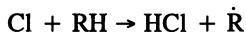
Observations of stratospheric ozone depletion at mid-latitudes as well as in the Antarctic and Arctic stratospheres during springtime (1-3) have been linked to anthropogenic emissions of Cl- and Br-containing compounds (1-3). These findings led to the 1987 Montreal protocol and its subsequent revisions at London in 1990 and Copenhagen in 1992, resulting in a phase-out of production of the Halons by January 1, 1994 and of the chlorofluorocarbons (CFCs) by January 1, 1996.

Potential hydrochlorofluorocarbon (HCFC) and hydrofluorocarbon (HFC) replacement compounds to the Halons and CFCs contain hydrogen and are designed to react with the hydroxyl (OH) radical in the troposphere (1,3,4), minimizing or avoiding the transport of chlorine and bromine to the stratosphere (1,3). These replacement compounds are largely removed by chemical reaction in the troposphere (1,3,4), and the reaction mechanisms and products formed need to be understood prior to widespread use of these compounds (4). Over the past few years we have conducted product studies of the tropospheric degradation reactions of a series of HCFCs and HFCs (5-7), and the results of these studies are described briefly here.

0097-6156/95/0611-0041\$12.00/0
© 1995 American Chemical Society

Experimental

Studies were carried out in a 5800 liter evacuable, thermostatted, Teflon-coated chamber (8) equipped with an *in situ* multiple reflection optical system interfaced to a Nicolet 7199 Fourier transform infrared (FT-IR) absorption spectrometer. Radiation of wavelength ≥ 300 nm was provided by a 24 kW xenon arc, filtered through a Pyrex pane. Because of the difficulty of maintaining high OH radical concentrations and the low rate constants for the OH radical reactions with the HCFCs and HFCs (9) reactions were initiated by reaction with Cl atoms



The initial reactant concentrations (in molecule cm^{-3} units) were typically: HCFC or HFC, $(1.2\text{-}2.5) \times 10^{14}$; Cl_2 , $(1.2\text{-}16) \times 10^{14}$; although a series of experiments to measure the formation yields of CF_2ClCHO and CFCl_2CHO from CF_2ClCH_3 (HCFC-142b) and CFCl_2CH_3 (HCFC-141b) used initial HCFC and Cl_2 concentrations of $(4.9\text{-}25.6) \times 10^{15}$ molecule cm^{-3} and 1.3×10^{14} molecule cm^{-3} , respectively (7). Most experiments were carried out at 298 ± 2 K and 740 Torr total pressure of synthetic air (80% N_2 + 20% O_2); experiments with CH_2FCF_3 (HFC-134a) were carried out over the temperature range 273-320 K and with the O_2 partial pressure and total pressure varied over the ranges 150-600 Torr and 150-740 Torr, respectively (5).

The reactants and products were monitored during the irradiations by FT-IR absorption spectroscopy, using a pathlength of 57.7 m and a full-width at half-maximum (fwhm) spectral resolution of 0.7 cm^{-1} . The identification and analysis of products were facilitated by spectral stripping, i.e., successive subtraction of absorptions using calibrated reference spectra of the known components. Calibrations with authentic samples were made by expanding measured partial pressures of the compound in calibrated 2-L and 5-L Pyrex bulbs into the reaction chamber.

The samples of HFCs and HCFCs were donated by E. I. DuPont de Nemours and Co. Inc., Allied Signal, Solvay, S. A., and Asahi Glass Co., and were generally of stated purities $\geq 99.5\%$. Samples of the highest purity available for CFCl_2CH_3 and CF_2ClCH_3 ($> 99.99\%$, Solvay S.A.) were employed. Authentic samples of CFCl_2CHO and CF_2ClCHO were prepared and purified in the authors' laboratory (7).

Results and Discussion

The series of $\text{C}_1\text{-C}_3$ HFCs and HCFCs studied, the products formed and their yields (5-7) are summarized in Table I.

The haloalkyl radical $\dot{\text{R}}$ resulting from the initial H-atom abstraction by the Cl atom (or OH radical) rapidly adds O_2 , $\dot{\text{R}} + \text{O}_2 \xrightarrow{\text{M}} \text{RO}_2$, and under the above experimental conditions where NO was absent the haloalkyl peroxy radical

Table I. Observed Products and Their Yields from the Cl Atom-Initiated Photooxidation of a Series of HFCs and HCFCs in 1 Atmosphere of Air at 298 K

HFC or HCFC		Primary Products and Yields	References
CHF ₂ Cl	(HCFC-22)	C(O)F ₂ , 100%	6
CHFC1 ₂	(HCFC-21)	C(O)FC1, 100%	6
CH ₂ FC1	(HCFC-31)	HC(O)F, 100%	6
CH ₃ F	(HFC-41)	HC(O)F, 100%	6
CH ₃ CFCl ₂	(HCFC-141b)	CFCl ₂ CHO, 100%	7
CH ₃ CF ₂ Cl	(HCFC-142b)	CF ₂ ClCHO, 100%	7
CH ₃ CHF ₂	(HFC-152a)	C(O)F ₂ , 92%; CO and CO ₂	6
CHCl ₂ CF ₃	(HCFC-123)	CF ₃ C(O)Cl, 98%	6
CHFC1CF ₃	(HCFC-124)	CF ₃ C(O)F, 100%	6
CHF ₂ CF ₃	(HFC-125)	C(O)F ₂ , ~ 100%; CF ₃ OOOCF ₃	6
CH ₂ FCF ₃	(HFC-134a)	CF ₃ C(O)F, 24%; HC(O)F, 76%; C(O)F ₂ , 8-14%; CF ₃ OOOCF ₃ and CF ₃ OOC(O)F	5 ^a
CF ₃ CF ₂ CHCl ₂	(HCFC-225ca)	CF ₃ CF ₂ C(O)Cl, 100%	7
CF ₂ C1CF ₂ CHFC1	(HCFC-225cb)	CF ₂ C1CF ₂ C(O)F, 99%; C(O)FC1, 1.0%	7

^aSome CF₃C(O)F formed by the combination reaction of CF₃CHFOO radicals; in the atmosphere the calculated yields of CF₃C(O)F and HC(O)F at 298 K and one atmosphere of air are 18% and 82%, respectively (5).

undergoes self-reaction to produce mainly the corresponding haloalkoxy radical, $2 \text{RO}_2 \rightarrow 2 \text{RO} + \text{O}_2$ (5-7). In the troposphere, the peroxy radical is expected to mainly react with NO to generate NO₂ and the alkoxy radical (4). Since the irradiations of Cl₂-HFC(or HCFC)-air mixtures were conducted in the absence of added NO_x, the formation of RONO₂, ROONO₂ and RC(O)OONO₂ class product compounds was not directly investigated in these experiments.

A generalized reaction scheme which is consistent with our product data shown in Table I, and which shows the disposition of the haloalkyl peroxy and haloalkoxy radicals under tropospheric conditions, is presented in Figure 1. The haloalkoxy radical can react via three pathways: decomposition, reaction with O₂, or Cl atom elimination. When Cl atom elimination is possible from the alkoxy

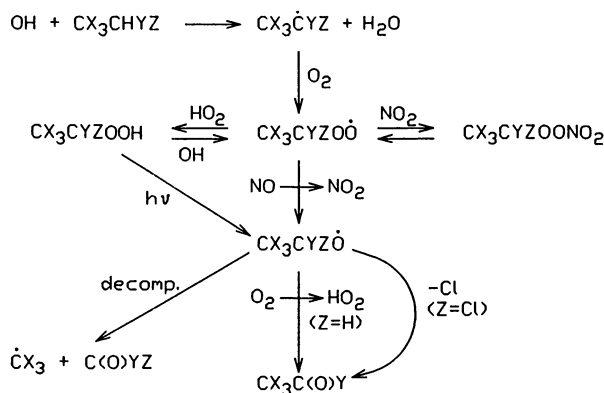


Figure 1. Generalized tropospheric reaction scheme for the HFCs and HCFCs.

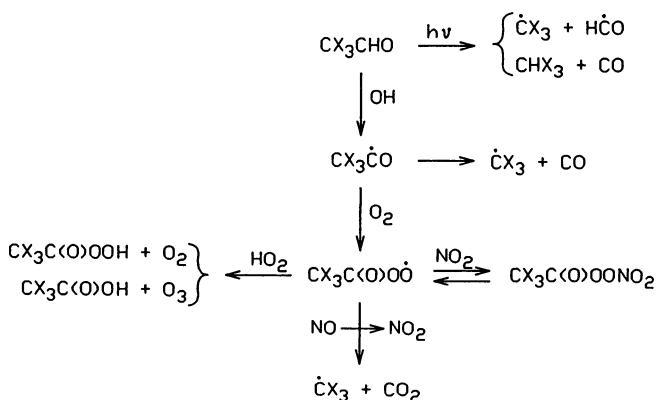


Figure 2. Generalized tropospheric reaction scheme for the haloaldehydes.

carbon, it is the dominant if not the exclusive pathway. Thus, the C₁-C₃ HCFCs listed in Table I which can form such haloalkoxy radicals lead to the formation of acid halide products in ~100% yield.

The CX₃CF₂Ö radical tends to undergo C-C bond fission as demonstrated by the case of CHCF₂CF₃ (HFC-125), which formed C(O)F₂ in ~100% yield along with further products of the ĊF₃ radical, notably the unusual trioxide CF₃OOOCF₃ under our experimental conditions. The CX₃CHYÖ radical (Y=Cl or F) undergoes both C-C bond breakage and reaction with O₂, the relative importance of which is dependent on temperature, O₂ concentration, and total pressure (and hence on altitude). This is true for the alkoxy radical CF₃CHFÖ, formed from CH₂FCF₃ (HFC-134a), with the mix of products being comprised of one- and two-carbon acyl halides and further products of the ĊF₃ radical. Our data (5) and those of Wallington *et al.* (10) and Rattigan *et al.* (11) show the CF₃C(O)F yields from HFC-134a increase with increasing altitude in the troposphere, with mainly formation of HC(O)F and products of the ĊF₃ radical at the Earth's surface and mainly formation of CF₃C(O)F at the tropopause. Further reactions of the ĊF₃ radicals in laboratory systems and in the atmosphere have been investigated (3,12,13).

Earlier experiments on the reactions of CX₃CH₂Ö radicals, such as those derived from HCFC-141b and HCFC-142b (6,14,15), could not measure the relative importance of the decomposition pathway and the reaction with O₂ which produces the haloaldehyde CX₃CHO (Figure 1). This is due to the very rapid reaction of the aldehydes with Cl atoms or OH radicals, which lead to the same carbonyl halide products as produced by the decomposition step. A determination that the haloaldehydes are formed is important with respect to the formation of peroxyacyl nitrates, which may be sufficiently stable that they could contribute to Cl transport to the stratosphere, and to the production of the C₂ acids which may be biological hazards (16). The tropospheric reaction schemes for these haloaldehydes is given in Figure 2.

Thus, photolysis experiments utilizing elevated concentrations of CFC1₂CH₃ (HCFC-141b) and CF₂C1CH₃ (HCFC-142b) in mixtures with Cl₂ in air were carried out. Product spectra from an experiment with initial concentrations of 4.9 x 10¹⁵ molecule cm⁻³ of CFC1₂CH₃ and 1.3 x 10¹⁴ molecule cm⁻³ of Cl₂ are shown in Figure 3. Intermittent irradiation was employed to provide for longer averaging times to obtain the spectra during the intervening dark periods. CFC1₂CHO was positively identified by the exact position and contour of its C=O stretch band (1782.7 cm⁻¹) as compared to the spectrum of the synthesized sample (7). The total amount of CFC1₂CH₃ reacted, which amounted to 0.8% during the total of 16-min irradiation, was determined by the sum of the observed C(O)FCl and CFC1₂CHO. With the time-concentration data obtained and the rate constant ratio k(Cl + CFC1₂CHO)/k(Cl + CFC1₂CH₃) = 2600 ± 700, derived from published rate constants (17-19), corrections for the secondary reaction of CFC1₂CHO with the Cl atom were calculated. The result was a 100% yield of CFC1₂CHO from CFC1₂CH₃ (7), indicating that at 298 K and atmospheric pressure of air the haloalkoxy radical CFC1₂CH₂Ö does not decompose but solely reacts with O₂.

A similar experiment was carried out for CF₂C1CH₃ (HCFC-142b). Figure 4 shows the spectra recorded from the photolysis of an air mixture with 2.6 x 10¹⁶

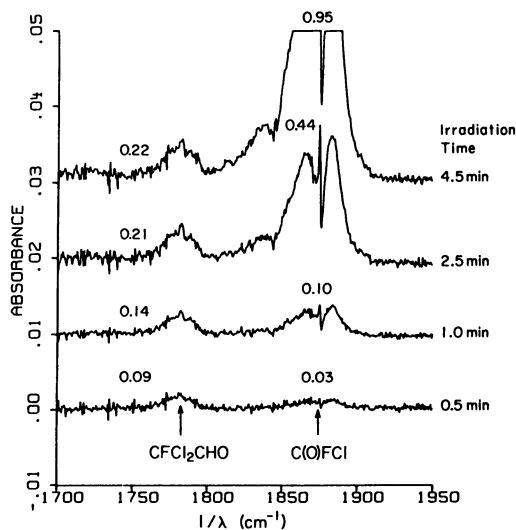


Figure 3. Product spectra from the Cl atom-initiated photooxidation of CFCl_2CH_3 . Numbers shown are concentrations in units of 10^{13} molecule cm^{-3} .

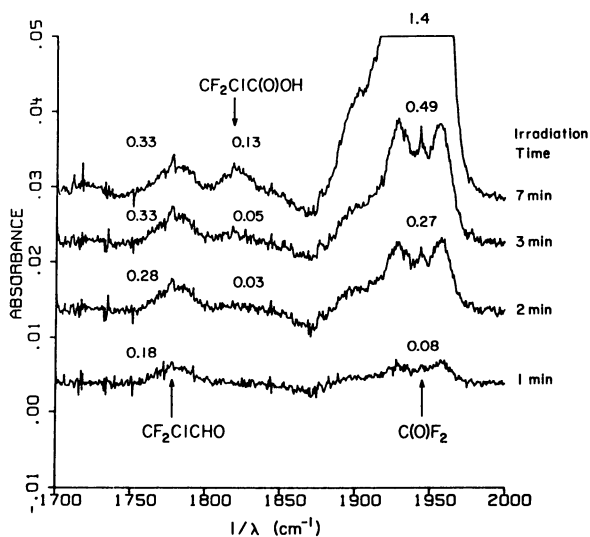
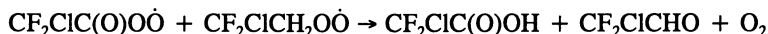


Figure 4. Product spectra from the Cl atom-initiated photooxidation of CF_2ClCH_3 . Numbers shown are concentrations in units of 10^{13} molecule cm^{-3} .

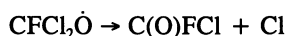
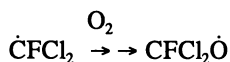
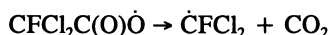
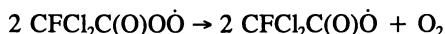
molecule cm^{-3} of CF_2ClCH_3 and 1.3×10^{14} molecule cm^{-3} of Cl_2 . The aldehyde product, CF_2ClCHO , was positively identified by the exact correspondence of its $\text{C}=\text{O}$ stretch band (1778.6 cm^{-1}) with that of the prepared sample (7). In addition to the expected formation of $\text{C}(\text{O})\text{F}_2$, $\text{CF}_2\text{ClC}(\text{O})\text{OH}$ was also observed as a product. A very small fraction of the starting compound was consumed ($\sim 0.1\%$ with 11-min total irradiation time) such that the amount of CF_2ClCH_3 reacted was calculated by the sum of the observed CF_2ClCHO , $\text{CF}_2\text{ClC}(\text{O})\text{OH}$, and $\text{C}(\text{O})\text{F}_2$ concentrations. The corrections for the secondary reactions of CF_2ClCHO with Cl which were calculated with the rate constant ratio $k(\text{Cl} + \text{CF}_2\text{ClCHO})/k(\text{Cl} + \text{CF}_2\text{ClCH}_3) = 11800 \pm 2000$, derived from literature rate constants (17-19), indicated a CF_2ClCHO yield of 167%. However, a rate constant ratio of 7400, $\sim 40\%$ lower than the above value of 11800 but within the range of errors that could occur in the measurement of rate constants for CX_3CHO (see, for example, the case of CF_3CHO ; refs. 17, 20), predicts a unit yield of CF_2ClCHO from CF_2ClCH_3 . The significant amounts of $\text{CF}_2\text{ClC}(\text{O})\text{OH}$ observed could also indicate that appreciable regeneration of the aldehyde possibly occurred via the reaction



which would then contribute to an overestimate of the correction for loss of CF_2ClCHO by reaction with the Cl atom. Overall, our experimental data strongly point to a 100% yield of CF_2ClCHO from CF_2ClCH_3 (7) and support the reaction with O_2 as the exclusive reaction channel for the $\text{CF}_2\text{ClCH}_2\dot{\text{O}}$ radical under lower troposphere conditions.

Important details of the atmospheric transformations of HCFC-141b and HCFC-142b required a study of the reactions of their respective aldehyde products CFCl_2CHO and CF_2ClCHO , specifically the disposition of the $\text{CX}_3\text{C}\dot{\text{O}}$ radicals formed from their reactions with OH radicals or Cl atoms (Figure 2). Photooxidation experiments were conducted in the 5800-L chamber at 298 K with 1 atm of air containing $(1.1\text{-}1.2) \times 10^{14}$ molecule cm^{-3} of the aldehyde and $(6.3\text{-}7.3) \times 10^{13}$ molecule cm^{-3} of Cl_2 , with spectral data being obtained after each period of short, intermittent irradiation.

As noted in Figure 2, the branching ratio of $\text{CX}_3\text{C}\dot{\text{O}}$ with respect to decomposition and reaction with O_2 can be determined by measuring the amounts of CO , CO_2 , and the $\text{C}(\text{O})\text{FCl}$ and $\text{C}(\text{O})\text{F}_2$ end products of the CX_3 radicals. In the absence of NO , the following specific reactions, illustrated for the case of CFCl_2CHO , occur:



With respect to the decomposition reaction (a) and O₂ reaction channel (b) (Figure 2), the CFCl₂C \dot{O} branching ratio was determined as 79 \pm 7% (a) and 21 \pm 5% (b), while the values for CF₂CiC \dot{O} were measured as 39 \pm 3% (a) and 61 \pm 5% (b) at 298 K and 740 Torr of air. These results are intermediate and consistent with those reported in the literature for CCl₃C \dot{O} [92% (a)] and CF₃C \dot{O} [1.3% (a)] at 298 K and 750 Torr total pressure of air (21).

Acknowledgment

The authors gratefully thank the SPA-AFEAS for financial support through Contracts CTR90-3/P90-001 and CTR91-28/P91-082 (Dr. Igor Sobolev, Project Monitor).

Literature Cited

1. *Scientific Assessment of Ozone Depletion: 1991*, World Meteorological Organization Global Ozone Research and Monitoring Project - Report No. 25, Geneva, Switzerland, 1992.
2. *Stratospheric Ozone 1993*, United Kingdom Stratospheric Ozone Review group, Department of the Environment, London, UK, November 1993.
3. *Scientific Assessment of Ozone Depletion: 1994*, World Meteorological Organization Global Ozone Research and Monitoring Project, Geneva, Switzerland, in press 1994.
4. *Scientific Assessment of Stratospheric Ozone: 1989*, World Meteorological Organization Global Ozone Research and Monitoring Project - Report No. 20, Vol. II, Appendix: AFEAS Report, Geneva, Switzerland, 1990.
5. Tuazon, E. C.; Atkinson, R. *J. Atmos. Chem.* 1992, 16, pp. 301-312.
6. Tuazon, E. C.; Atkinson, R. *J. Atmos. Chem.* 1993, 17, pp. 1799-199.
7. Tuazon, E. C.; Atkinson, R. *Environ. Sci. Technol.* 1994, in press.
8. Winer, A. M.; Graham, R. A.; Doyle, G. J.; Bekowies, P. J.; McAfee, J. M.; Pitts, J. N., Jr., In *An Evacuatable Thermostatted Environmental Chamber and Solar Simulator Facility for the Study of Atmospheric Chemistry*; Pitts, J. N., Jr. and Metcalf, R. L., Eds.; Advances in Environmental Science and Technology; John Wiley and Sons: New York, N.Y., 1980, Vol. 10; pp. 461-511.
9. Atkinson, R.; Baulch, D. L.; Cox, R. A.; Hampson, R. F., Jr.; Kerr, J. A.; Troe, J.; *J. Phys. Chem. Ref. Data* 1992, 21, pp. 1125-1568.
10. Wallington, T. J.; Hurley, M. D.; Ball, J. C.; Kaiser, E. W. *Environ. Sci. Technol.* 1992, 26, pp. 1318-1324.
11. Rattigan, O. V.; Rowley, D. M.; Wild, O.; Jones, R. L.; Cox, R. A. *J. Chem. Soc. Faraday Trans.* 1994, 90, pp. 1819-1829.
12. Sehested, J.; Wallington, T. J. *Environ. Sci. Technol.* 1993, 27, pp. 146-152.
13. STEP-HALOCSIDE/AFEAS WORKSHOP, "Kinetics and Mechanisms for the Reactions of Halogenated Organic Compounds in the Troposphere," Dublin, March 23-25, 1993, University College, Dublin, Ireland.

14. Edney, E. O.; Gay, B. W., Jr.; Driscoll, D. J. *J. Atmos. Chem.* **1991**, *12*, pp. 105-120.
15. Edney, E. O.; Driscoll, D. J. *Int. J. Chem. Kinet.* **1992**, *24*, pp. 1067-1081.
16. Ball, J. C.; Wallington, T. J. *J. Air Waste Manage. Assoc.* **1993**, *43*, pp. 1260-1262.
17. Scollard, D. J.; Treacy, J. J.; Sidebottom, H. W.; Balestra-Garcia, C.; Laverdet, G.; LeBras, G.; MacLeod, H.; Téton, S. *J. Phys. Chem.* **1993**, *97*, pp. 4683-4688.
18. Tuazon, E. C.; Atkinson, R.; Corchnoy, S. B. *Int. J. Chem. Kinet.* **1992**, *24*, pp. 639-648.
19. Wallington, T. J.; Hurley, M. D. *Chem. Phys. Lett.* **1992**, *189*, pp. 437-442.
20. Wallington, T. J.; Hurley, M. D. *Int. J. Chem. Kinet.* **1993**, *25*, pp. 819-824.
21. Barnes, I.; Becker, K. H.; Kirchner, F.; Zabel, F.; Richer, H.; Sodeau, J. In *Kinetics and Mechanisms for the Reactions of Halogenated Organic Compounds in the Troposphere*, STEP-HALOCSIDE/AFEAS Workshop, Dublin, March 23-25, 1993, pp. 52-58.

RECEIVED April 13, 1995

Chapter 6

Heterogeneous Atmospheric Chemistry of Alternative Halocarbon Oxidation Intermediates

C. E. Kolb¹, Douglas R. Worsnop¹, M. S. Zahniser¹, W. J. De Bruyn²,
Jeffrey A. Shorter², and P. Davidovits²

¹Center for Chemical and Environmental Physics,
Aerodyne Research, Inc., 45 Manning Road, Billerica, MA 01821-3976
²Department of Chemistry, Boston College, Chestnut Hill, MA 02167

Alternative halocarbons designed to substitute for chlorofluorocarbons and halons banned by the Montreal Protocol are designed to undergo oxidative degradation in the troposphere. Intermediate partially oxygenated products from currently used alternatives include carbonyl halides, haloacetyl halides and haloacetic acids. These intermediates are expected to undergo heterogeneous reactions with aqueous cloud droplets and surface waters. The chemical and physical parameters which govern the heterogeneous uptake of a range of these species by liquid water have been measured in our laboratories using droplet train/flow tube and/or bubble column techniques. The results of these experiments will be presented and compared with available results from other laboratories. Their impact on our ability to predict the atmospheric fate of halocarbon oxidation intermediates will be discussed.

Atmospheric Fate of Alternative Halocarbon Oxidation Products

Alternative halocarbons planned as substitutes for chlorofluorocarbons and halons banned by the Montreal Protocol are designed to undergo oxidative degradation in the troposphere. Intermediate partially oxygenated products from currently used or proposed alternatives include carbonyl halides, haloacetyl halides and haloacetic acids. A wide variety of atmospheric processes could participate in the removal of relatively stable degradation intermediates, including: transport to the stratosphere followed by photolysis, uptake by both tropospheric and stratospheric aerosols, uptake by cloud droplets, rainout (wet deposition), and dry deposition to vegetation, soil and dew surfaces, and to the oceans. However, recent model analyses indicate that cloud droplet and ocean uptake are the most likely removal rate determining processes. The physicochemical processes which are important in determining the rate of trace atmospheric gas uptake by liquid surfaces include gas phase diffusion, mass accommodation, solvation (Henry's law solubility), liquid phase diffusion and liquid phase reaction. The most effective removal paths and their associated physicochemical parameters are displayed in Table I. Key parameters affecting atmospheric removal rates are the mass accommodation coefficient, α , the Henry's law constant, H , and the first order hydrolysis reaction rate coefficient, k_{hyd} .

0097-6156/95/0611-0050\$12.00/0
© 1995 American Chemical Society

Table I. Atmospheric Fate Of Alternative Halocarbon Oxidation Products

Halocarbon Oxidation Produces Halocarbonyl Compounds: RX_nO (g)

$$[RX_nO = CF_2O, CCl_2O, CF_3C(O)F, CF_3C(O)Cl, CCl_3C(O)Cl]$$

Atmospheric Fate Of Halocarbonyls

$$RX_nO(g) \xrightarrow{h\nu} \text{Stratosphere} \xrightarrow{\quad} \text{Photolysis Products}$$

$$RX_nO(g) \xrightarrow[\text{Ocean}]{\text{Cloud}} RX_nO(aq) \quad \text{Accommodation by Liquid} \quad \left. \vphantom{RX_nO(g)} \right\} \alpha, H$$

$$RX_nO(aq) \xrightarrow{\quad} RX_nO(g) \quad \text{Evaporation}$$

$$RX_nO(g) \xrightarrow{\quad} RX_{n-1}O_2^- + X^- + 2H^+ \quad \text{Hydrolysis} \quad \left. \vphantom{RX_nO(g)} \right\} k_{hyd}$$

$$RX_{n-1}O_2^-(aq) \xrightarrow{\text{rain}} \text{Ocean/Land Deposition}$$

Experimental uptake data for the halocarbonyl compounds CF_2O , CCl_2O , $CF_3C(O)F$, $CF_3C(O)Cl$ and $CCl_3C(O)Cl$ will be presented and reviewed. Each of these halocarbonyl compounds is only sparingly soluble in aqueous solutions so their uptake is controlled by both their Henry's law solubility constant, H , and their hydrolysis reaction rate constant, k_{hyd} . Their uptake rate by cloud droplets or ocean surfaces is proportional to the product of these parameters, Hk_{hyd} .

The trihaloacetyl halide compounds hydrolyze to the corresponding trihaloacetic acid in aqueous environments such as cloud droplets. Since most clouds evaporate rather than precipitate, it is necessary to know the uptake coefficients for these species as well, in order to determine how soon they are likely to be reabsorbed into the aqueous phase after vaporization from a dehydrating cloud. Since these compounds are highly soluble in dilute aqueous solutions, their uptake will be controlled by their mass accommodation coefficients rather than their Henry's law constants.

Experimental Procedures

Uptake measurements in our laboratories are made either with a well documented droplet train apparatus (1), which we have used to measure uptake parameters for approximately 40 gaseous atmospheric trace species to date, or with a novel bubble column technique newly developed by our Aerodyne Research, Inc./Boston College (ARI/BC) collaboration (2). In our laboratory uptake coefficients are derived from either technique by measuring the diminution of the gas phase concentration of the trace gas species of interest as the contact time between gas a phase mixture containing that species and the liquid (aqueous) phase is varied. In both techniques the temperature and pH of the aqueous phase are varied to assess the dependence of uptake parameters on these properties. The major difference between the two techniques is the duration of the contact time between the gaseous and liquid phases. In the droplet train technique this ranges from 1 to 20 milliseconds while in the bubble column technique it typically varies from 0.1 to 1 seconds.

Both experiments measure an effective uptake coefficient, γ_{meas} , defined as :

$$\gamma_{\text{meas}} = \frac{\text{Number of molecules lost to the surface (s}^{-1}\text{)}}{\text{Number of gas - surface collisions (s}^{-1}\text{)}} \quad (1)$$

The difference in gas-liquid contact times makes allows the droplet train technique to determine γ_{meas} values in the range of 1 to 5×10^{-4} while the bubble column technique is sensitive to γ_{meas} values of order 10^{-4} to 10^{-7} . Mirabel and co-workers have recently developed a version of the droplet train method which measure the build-up of trace gases or their reaction products in the liquid phase by trapping and pooling the exposed droplets. This method extends the sensitivity of the droplet train technique to somewhat smaller values of γ_{meas} allowing them to use this method to measure uptake parameters for several of the compounds of interest to this study (3,4). Measurements of γ_{meas} as a function of contact time and other experimental parameters can be analyzed to yield a variety of fundamental physical and chemical parameters controlling uptake, including mass accommodation coefficients, Henry's law constants, reaction rate constants and liquid phase diffusion coefficients, depending on the actual parameter or parameters which control uptake for a given trace gas/liquid surface combination. This analysis process has recently been reviewed by Kolb et al. (5); this review also discusses the two experimental techniques noted above and compares their capabilities with other recently developed methods for measuring gas/aqueous surface and gas/ice kinetics. Further experimental details will not be presented here, but can be found in references 1-7.

Halocarbonyl Uptake Results

For the moderately soluble halocarbonyl compounds noted above both the droplet train and the bubble column technique directly measure the product of $Hk_{\text{hyd}}^{1/2}$ with the possibility of separately determining H from the temporal dependence of the trace gas uptake at short times. Most laboratory heterogeneous chemistry experiments are sensitive to $Hk_{\text{hyd}}^{1/2}$ not Hk_{hyd} , which is often the more atmospherically relevant parameter product (see discussion below). Some time ago we published droplet train studies of these compounds (6) showing that for the atmospherically relevant droplet pH range of 3-7 their γ_{meas} values were below 5×10^{-4} , although larger uptakes were measured for droplets with pH levels above 12. These results led us to develop the bubble column technique described in reference 2 and then to apply it to the five halocarbonyl compounds (CF_2O , CCl_2O , $\text{CF}_3\text{C(O)F}$, $\text{CF}_3\text{C(O)Cl}$ and $\text{CCl}_3\text{C(O)Cl}$) studied previously (7). Results from this study (labeled DeBruyn et al.), based on analyses of γ_{meas} , are displayed in Table II. These analyses confirmed that the time dependent uptake data are not sensitive enough to clearly determine separate values of H, so Table II contains $Hk_{\text{hyd}}^{1/2}$ values as well as an entry for H_{max} , which is the Henry's law constant needed to explain the observed uptake if the hydrolysis rate constant is zero (7). Also shown in Table II are the results, in the form of upper limits, from our previous, less sensitive droplet train uptake experiment (6).

Table II also presents results for four of the target carbonyl compounds derived from droplet train uptake experiments performed by Mirabel and coworkers (3,4) as well as other measurements of H and k_{hyd} available in the literature. Uptake parameter estimates prepared by Wine and Chameides (8) are also included. The results from Mirabel's group are derived from an analysis of droplet train uptake data that is essentially the same as that used in the Aerodyne Research, Inc./Boston College effort. Additional literature values of k_{hyd} and H for CCl_2O (which has not yet been studied by the Mirabel group) are also listed (9-12).

Table II. Solubility and Hydrolysis of Haloacetyl and Carbonyl Halides (pH 4-7)

Species/Reference	Temp. (K)	H (M/atm)	k_{Hyd} (s^{-1})	$\text{Hk}_{\text{hyd}}^{1/2}$	Hk_{hyd} ($\text{Matm}^{-1} \text{s}^{-1}$)
CF₃C(O)F					
De Bruyn et al. (7)	278	0.96 ^a	a	3.8	4.3-96
George et al.(4)	273	3.0	150	60,37	450
CF₃C(O)Cl					
De Bruyn et al. (7)	278	0.27 ^a		1.2	1.2-27
George et al.(4)	273	2.0	220	60,30	440
CCl₂O					
De Bruyn et al. (7)	278	0.15 ^a		0.66	0.68-15
	298	0.06 ^a	0.29 ^a		
Manogue/Pigford (9)	298	0.07	6 ^c	0.17	0.4
Ugi/Beck (10)	253		~100		
Behnke et al. (11)	296			0.17 ^b	3.8 ^e
Mertens et al. (12)	298		9 ^d		
	298		5.3 ^d		
CF₂O					
De Bruyn et al. (7)	278	1.0 ^a	4.3 ^a		4.7-97
George et al.(4)	273			350	
CCl₃C(O)Cl					
De Bruyn et al. (7)	278	2.0 ^a		6.9	9.1-150
George et al. (3)	274-294	2.0	500 ^f	45	1000
George et al. (3)	288		~150 ^g		
Wine/Chameides (8) (all 5 compounds)		>10	>10 ³	>0.3	>10 ⁻²
De Bruyn et al. (6) (all 5 compounds)				<50 ^f	

^aMaximum values of the parameters^bWetted wall reactor^cWater jet^dSaturated NaNO₃ aerosol^ePulse radiolysis^fDroplet train reactor^gStopped flow reactor

The uptake parameters derived from the experimental results of Mirabel and coworkers (3,4) are significantly larger than those deduced from the Aerodyne Research/ Boston College data (6,7). The degree of disagreement is illustrated in Figure 1, where actual bubble column uptake data (7) for CF₃C(O)F and CCl₃C(O)Cl are plotted along with the analytical fits to obtain $\text{Hk}_{\text{hyd}}^{1/2}$ values of 3.8 and 6.9, respectively. Also plotted are analyses of how the bubble column data would have looked if the $\text{Hk}_{\text{hyd}}^{1/2}$ values of 37 and 45 measured by Mirabel and co-workers (3,4) were correct. (Note that reference 4 also quotes an $\text{Hk}_{\text{hyd}}^{1/2}$ value of 60 obtained by an alternative analysis for CF₃C(O)F; but we have chosen to compare with the lower, more conservative value derived from separate H and k_{hyd} values quoted in the text.) However, as discussed below, both the results from the ARI/BC team and those of Mirabel and co-workers lead to the conclusion that all of the halocarbonyl compounds will be efficiently removed by and hydrolyzed in cloud droplets.

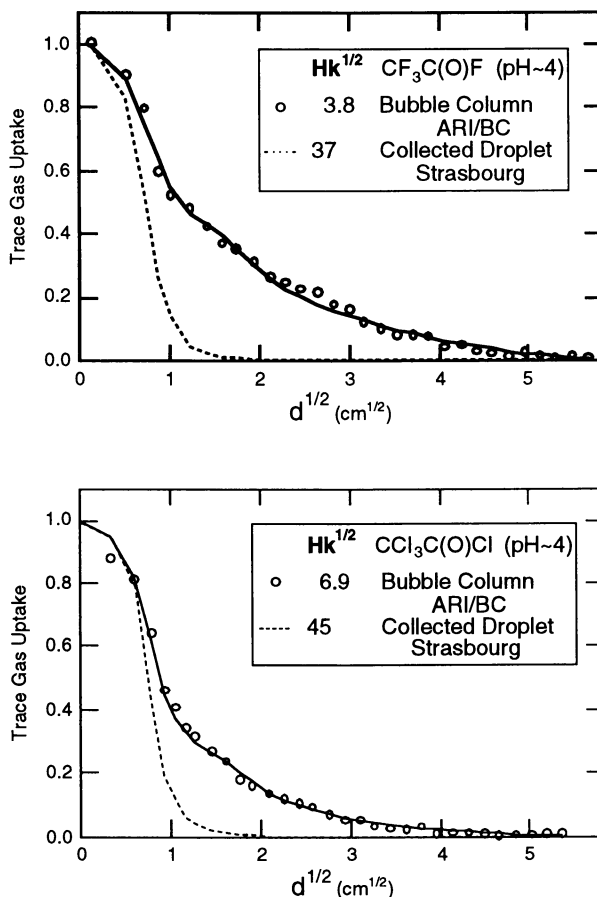


Figure 1. Comparison of ARI/BC bubble column uptake results for $\text{CF}_3\text{C}(\text{O})\text{F}$ and $\text{CCl}_3\text{C}(\text{O})\text{Cl}$ with the expected uptake if the reported $\text{Hk}_{\text{hyd}}^{1/2}$ values of Mirabel and co-workers (3,4) were correct.

Zetzsch and co-workers have performed aerosol chamber uptake experiments for CCl_2O on aqueous NaNO_3 aerosols (11). While these experiments have the advantage of directly measuring Hk_{hyd} , they suffer from some ambiguity in determining the aerosol surface area and pH. The resulting Hk_{hyd} product of $3.8 \pm 1.3 \text{ Matm}^{-1}\text{s}^{-1}$ is also shown in Table II, along with a separate measurement of $\text{Hk}_{\text{hyd}}^{1/2}$ of 0.17 from a 298 K wetted wall flow tube from the same laboratory. Finally, an older aqueous jet study by Manogue and Pigford (9) as well as a very recently published measurement of k_{hyd} using a novel pulsed radiolysis source of this reactant by Mertens et al. (12), both for CCl_2O , are included in Table II. These CCl_2O results all agree reasonably well with the ARI/BC result and disagree strongly with the very high k_{hyd} value measured by Ugi and Beck for this compound (10). This is significant because Mirabel and co-workers

use the high k_{hyd} values measured by Ugi and Beck for various halocarbonyls to lend credence to the similarly high values they obtain for $\text{H}k_{\text{hyd}}^{1/2}$ (and k_{hyd}) for CCl_2O , $\text{CF}_3\text{C}(\text{O})\text{F}$, $\text{CF}_3\text{C}(\text{O})\text{Cl}$ and $\text{CCl}_3\text{C}(\text{O})\text{Cl}$ (3,4), as well as their high k_{hyd} values obtained for $\text{CCl}_3\text{C}(\text{O})\text{Cl}$ in stopped flow bulk measurements (3). These latter stopped flow measurements, which used mixed solvents, are also suspect because they indicate a strong acid catalyzed enhancement of the $\text{CCl}_3\text{C}(\text{O})\text{Cl}$ hydrolysis rate, an effect we are unable to reproduce in our bubble column apparatus. An uptake experiment for CCl_2O by Mirabel and co-workers would be highly desirable, since it could be compared with our results as well as those of references 9-12 to determine if their adaptation of the droplet train technique has a systematic bias to high values for low uptake coefficients.

Atmospheric Fate of Halocarbonyl Oxidation Intermediates

When considering the rates of heterogeneous species removal from the atmosphere, the liquid phase diffusion time (τ_{D}) of the species into a cloud droplet has to be taken into account (5). If the species hydrolysis rate is fast compared to $1/\tau_{\text{D}}$ ($k_{\text{hyd}} \gg 1/\tau_{\text{D}}$) then the uptake rate, uptake coefficient and overall cloud processing rate are governed by the product $\text{H}k_{\text{hyd}}^{1/2}$. If $k_{\text{hyd}} \ll 1/\tau_{\text{D}}$ then tropospheric clouds can be treated as continuous 'processors' of the species. A constant fraction of the gas will be dissolved in aqueous solution in clouds, determined by H and the cloud liquid water content. The dissolved gas will be continuously hydrolyzed at a rate determined by k_{hyd} . The overall cloud processing rate will then be proportional to the product $\text{H}k_{\text{hyd}}$.

In terms of the liquid diffusion coefficient D_1 and the cloud droplet diameter d , the liquid phase diffusion time (τ_{D}) is given by:

$$\tau_{\text{D}}^{1/2} = d / 6D_1^{1/2} \quad (2)$$

For a typical cloud droplet of $\sim 10\mu\text{m}$ in diameter, $1/\tau_{\text{D}} \sim 500 \text{ s}^{-1}$. For all species under consideration $k_{\text{hyd}} < 500 \text{ s}^{-1}$ therefore tropospheric clouds act as continuous processors of the halides and the relevant uptake-determining parameter is $\text{H}k_{\text{hyd}}$.

An estimate of a global life time of the species may be calculated from the average liquid water content of the troposphere:

$$\tau_{\text{cloud}} = \frac{1}{L_c f_c RTH(k_{\text{hyd}})^{1/2}} [(k_{\text{hyd}})^{-1/2} + \tau_{\text{D}}^{1/2}] \quad (3)$$

where L_c is the average liquid water content of a cloud ($L_c \sim 0.3 \text{ g/m}^3 = 3 \times 10^{-7} \text{ cm}^3/\text{cm}^3$) and f_c is the average fraction of the global tropospheric volume containing clouds ($f_c \sim 0.15$) (17).

The overall lifetime against heterogeneous removal must also take into account uptake into the oceans, which can be described by a lifetime expression analogous to equation 3: (8)

$$\tau_{\text{ocean}} = \frac{H_A}{\text{HRT} f_E} [r_s + (D_O k_{\text{hyd}})^{-1/2}] + \tau_{\text{mix}} \quad (4)$$

where H_A is the scale height of the troposphere (8 km), f_E the fractional oceanic coverage of the earth's surface (0.7), r_s the thin film surface resistance to gas uptake on the ocean surface (170 scm^{-1}), and D_O the eddy diffusion coefficient in the ocean

surface layer ($40 \text{ cm}^2\text{s}^{-1}$). The added τ_{mix} term represents an effective mixing time within the troposphere (~ 45 days)(8). Combining equations. 3 and 4, an overall lifetime can be estimated by

$$\tau = [\tau_{\text{cloud}}^{-1} + \tau_{\text{ocean}}^{-1}]^{-1} \quad (5)$$

In Figure 2 we show plots of the tropospheric lifetime (τ) estimated from equation 5 versus k_{hyd} for the range of k_{hyd} consistent with our bubble column results (7) as well as those corresponding to the droplet train results of Mirabel and co-workers (3,4) and the work of Behnke and Zetsch (11). In calculating τ , the values of H corresponding to a given k_{hyd} were obtained from our experimental studies (7). The highlighted lines represent the range $5 < k_{\text{hyd}} < 500 \text{ s}^{-1}$, chosen to span the uncertainty in the laboratory determination of k_{hyd} . For CCl_2O , CF_3CClO , CCl_3CClO , CF_2O , and CF_3CFO , this corresponds to tropospheric lifetime ranges of approximately 5 to 50, 2 to 10, 0.2 to 2, 0.5 to 3 and 0.5 to 3 days, respectively. The results of Behnke et al. (11) with $k_{\text{hyd}} \sim 100 \text{ s}^{-1}$ yield a best estimate of $\tau \sim 12$ days for CCl_2O at 296K, in good agreement with the our results. The results of Mirabel and co-workers (3,4) for CF_2O , CCl_3 , $\text{CF}_3\text{C(O)Cl}$ and $\text{CF}_3\text{C(O)F}$ give nominal lifetimes below 0.1 days, which are much shorter than the estimates provided by our study (7).

These results can be summarized by considering the limit of slow hydrolysis ($k_{\text{hyd}} \ll 1/\tau_{\text{D}}$), in which equation 3 reduces to:

$$\tau = (\text{HRT}k_{\text{hyd}}L_c f_c)^{-1} \sim 15 (\text{H}k_{\text{hyd}})^{-1} \quad (6)$$

For the conservative estimate of $\text{H}k_{\text{hyd}} > 0.5 \text{ M atm}^{-1}\text{s}^{-1}$, this gives an upper limit to the tropospheric lifetime of the halide species of $\tau < 30$ days.

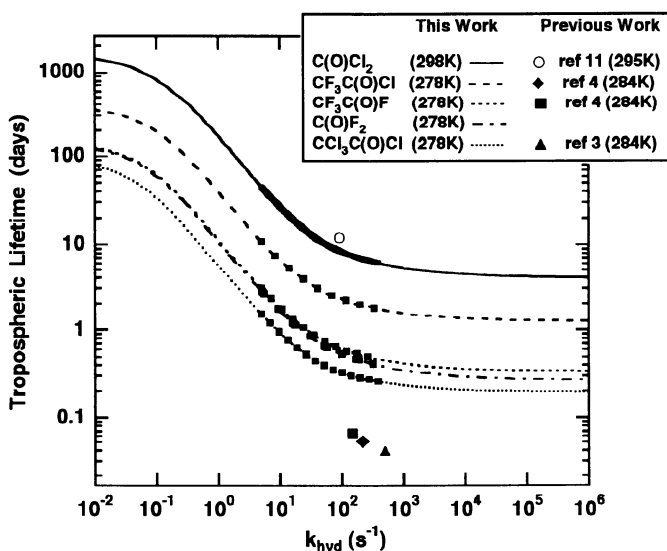


Figure 2, Tropospheric lifetimes (τ) estimated from Eq. 5 versus k_{hyd} for selected studies as summarized in Table II. The highlighted lines represent the range $5 < k_{\text{hyd}} < 500 \text{ s}^{-1}$, that was chosen to span the uncertainty in the bubble column determination of k_{hyd} in Ref. 7.

This estimate is consistent with preliminary results of global tropospheric models.¹⁸⁻²¹ Such a lifetime is in the range where modeling of global surface deposition must take into account the regional distribution of rain-out removal rates. It should be noted that equations 3 and 4 and Figure 2 are strictly applicable only for $\tau > 5$ days. At shorter lifetimes, one must take into account cloud formation probabilities. In that case, the lower limit for the atmospheric lifetime of the halogen from the alternative halocarbons would be about 10 days, limited by average tropospheric rain-out rates of the carboxylic acid or acid halide anion products.

Uptake of Haloacetic Acids

Uptake of $\text{CF}_3\text{C}(\text{O})\text{F}$ and $\text{CF}_3\text{C}(\text{O})\text{Cl}$ leads to their hydrolysis forming CF_3COOH , trifluoroacetic acid (TFA). TFA is very resistant to aqueous phase chemical degradation and will probably be re-vaporized as cloud droplets evaporate as suggested by Edney (13). In order to calculate the partitioning of TFA between the gas phase and cloud droplets the parameters governing the uptake of TFA by aqueous droplets are needed. Recently published ARI/BC droplet train uptake experiments determined the temperature dependent mass accommodation coefficients for TFA and several other haloacetic acid compounds (14). All of the measured mass accommodation coefficients for this class of compounds are large, with the value for TFA varying between 0.1 and 0.2 as the temperature ranges from ~ 290 to ~ 260 K. The Henry's law constants for TFA and the other haloacetic acids studied are sufficiently large that their uptake will be controlled by gas phase diffusion to cloud droplets given the magnitude of the measured mass accommodation coefficients. The fact that TFA (and similar haloacetic acids) will likely cycle back and forth between the gas phase and cloud droplets implies that a sufficiently fast gas phase loss process, such as reaction with OH, could become an effective destruction pathway. However, recent kinetic studies¹⁵ indicate that the reaction of OH with TFA is not rapid enough, compared with re-accommodation into cloud droplets, to destroy more than $\sim 10\%$ of atmospheric TFA. Thus, the main environmental fate of TFA will probably be wet deposition to land and ocean surfaces where it may be degraded by microbial processes.¹⁶

Summary

Measurements of uptake parameters for the halocarbonyl and haloacetic halide compounds listed in Table II confirm that their uptake rates by cloud droplets are limited by their Henry's law solubility and their aqueous phase hydrolysis rate constant, and that these parameters are sufficiently large to ensure that their tropospheric lifetimes are less than ~ 15 -30 days. Unfortunately no experimental data on the uptake parameters for other halocarbonyls, such as ClFCO or HFClO or those containing more than two carbons, are presently available, so their effective scavenging by cloud droplets, while likely, is not proven. Uptake of the haloacetic acids, including TFA, is not limited by solubility (H). Measured mass accommodation coefficients for these compounds are large, assuring their reappportioning into cloud droplets after evaporation will be limited only by gas phase transport with minor loss, at least in the case of TFA, due to gas phase reaction with OH.

Acknowledgements

We thank Dr. E.O. Edney and Prof. Peter C. Jurs for helpful discussions. Funding for this work was provided by U.S. Department of Energy Grant No. DE-FG02-91ER61208, National Science Foundation Grant No. ATM-93-10407, U.S. Environmental Protection Agency Grants No. R-815469-01-0 and CR 819733-01, the Alternate Fluorocarbon Environmental Acceptability Study, the European Chlorinated Solvent Association and the Halogenated Solvents Industry Alliance.

Literature Cited

1. Worsnop, D.R.; Zahniser, M.S.; Kolb, C.E.; Gardner, J.A.; Watson, L.R.; Van Doren, J.M.; Jayne, J.T.; Davidovits, P. *J. Phys. Chem.* **1989**, *93*, 1159-1172.
2. Shorter, J.A.; De Bruyn, W.J.; Hu, J.; Swartz, E.; Davidovits, P.; Worsnop, D.R.; Zahniser, M.S.; Kolb, C.E. *Environ. Sci. and Technol.*, in press, **1995**.
3. George, Ch.; Lagrange, J.; Lagrange, Ph.; Mirabel, Ph.; Pallares, C.; Ponche, J.L. *J. Geophys. Res.* **1995**, *99*, 1255-1262.
4. George, Ch.; Saison, J.Y.; Ponche, J.L.; Mirabel, Ph. *J. Phys. Chem.* **1994**, *98*, 10857-10862.
5. Kolb, C.E.; Worsnop, D.R.; Zahniser, M.S.; Davidovits, P.; Keyser, L.F.; Leu, M.-T.; Molina, M.J.; Hanson, D.R.; Ravishankara, A.R.; Williams, L.R.; Tolbert, M.A. In *Progress and Problems in Atmospheric Chemistry*, Barker, J.R., Ed.; Adv. Ser. Phys. Chem.; World Scientific Publ.: Singapore, 1994, in press.
6. De Bruyn, W.J.; Duan, S.X.; Shi, X.Q.; Davidovits, P.; Worsnop, D.R.; Zahniser, M.S.; Kolb, C.E. *Geophys. Res. Lett.* **1993**, *19*, 1939-1942.
7. De Bruyn, W.J.; Shorter, J.A.; Davidovits, P.; Worsnop, D.R.; Zahniser, M.S.; Kolb, C.E. *Environ. Sci. and Technol.*, in press, **1995**.
8. Wine, P.H.; Chameides, W.L. Scientific Assessment of Stratospheric Ozone: 1989, Global Research and Monitoring Project, Report No. 20, 1990, Vol. 2. 271-295.
9. Manogue, W.H.; Pigford, R.L. *A.I.Ch.E.J.* **1960**, *6*, 494-500.
10. Ugi, I.; Beck, F. *Chem. Ber.* **1961**, *94*, 1839-1850
11. Behnke, W.; Elend, M.; Krüger, H.-U.; Zetzsch, C. STEP-HALOSIDE/AFEAS Workshop Proceedings: Kinetics and Mechanisms for the Reactions of Halogenated Organic Compounds in the Troposphere, Dublin, Ireland, 1992, 203-209.
12. Mertens, R.; von Sonntag, C.; Lind, J.; Merenyi, G. *Angew. Chem. Int. Ed. Engl.* **1994**, *33*, 1259-1261.
13. Edney, E.O.; Driscoll, D.J.; Corse, E.W.; Blanchard, F.T. Proceedings of the AFEAS Workshop: Atmospheric Wet and Dry Deposition of Carbonyl and Haloacetyl Halides, Brussels, Belgium, 1992, 86-90.
14. Hu, J.H.; Shorter, J.A.; Davidovits, P.; Worsnop, D.R.; Zahniser, M.S.; Kolb, C.E. *J. Phys. Chem.* **1993**, *97*, 11037-11042.
15. Carr, S.; Treacy, J.J.; Sidebottom, H.W.; Connell, R.K.; Canosa-Mas, C.E.; Wayne, R.P.; Franklin, J. *Chem. Phys. Lett.* **1994**, *227*, 39-44.
16. Visscher, P.T.; Culbertson, C.W.; Oremland, R.S. *Nature* **1994**, *369*, 729-731.
17. Lelieveld, J.; Crutzen, P.J. *Atmos. Chem.* **1991**, *12*, 229-267.
18. Kindler, T.; Chameides, W.L.; Wine P.H.; Cunnold, D.; Alyea, F. Proceedings of the AFEAS Workshop: Atmospheric Wet and Dry Deposition of Carbonyl and Haloacetyl Halides, Brussels, Belgium, 1992, 33-43.
19. Rodriguez, J.M.; Ko, M.K.W.; N.D. Sze; Heisey, C.W. Proceedings of the AFEAS Workshop Brussels: Atmospheric Wet and Dry Deposition of Carbonyl and Haloacetyl Halides, Brussels, Belgium, 1992, 25-32.
20. Kanakidou, F.J.; Dentener, F.J.; Crutzen, P.J. Proceedings of the STEP-HALOCOSIDE/AFEAS Workshop: Kinetics and Mechanisms of the Reactions of Halogenated Organic Compounds in the Troposphere, Dublin, Ireland, 1993, 113-129.
21. Rodriguez, J.M.; Ko, M.K.W.; N.D. Sze; Heisey, C.W. Proceedings of the STEP-HALOCOSIDE/AFEAS Workshop: Kinetics and Mechanisms of the Reactions of Halogenated Organic Compounds in the Troposphere, Dublin, Ireland, 1993, 104-112.

RECEIVED June 7, 1995

Chapter 7

Evaluating the Potential Effects of Halon Replacements on the Global Environment

Donald J. Wuebbles¹, Peter S. Connell², and Kenneth O. Patten¹

¹Department of Atmospheric Sciences, University of Illinois,
105 South Gregory Avenue, Urbana, IL 61801-3070

²Global Climate Research Division, Lawrence Livermore National
Laboratory, Livermore, CA 94550

The variety of compounds being considered as replacements for halons needs to be evaluated to ensure that their use will not significantly impact the environment. This chapter examines the possibility of any concern about effects on global atmospheric ozone and climate from halons and their replacements, describes the approaches being used to evaluate these effects, and reviews existing evaluations of potential effects of these compounds on ozone and climate. These studies suggest that use of extremely long-lived gases such as perfluorocarbons and sulfur hexafluoride should be discouraged because of their potential significant effects on the radiative forcing affecting climate. Other compounds, including several HCFCs and HFCs, appear to have much less effect on ozone and climate than the compounds they would replace. Although initial studies of CF₃I indicate little concern, there remain uncertainties in its potential effects on ozone.

Under the Clean Air Act, the United States has essentially eliminated the production and import of the halons, CF₂ClBr (or H-1211), CF₃Br (H-1301), and C₂F₄Br₂ (H-2402), beginning January 1, 1994. This has been done in compliance with the international Copenhagen Agreement modification of the Montreal Protocol on Substances That Deplete the Ozone Layer (*1*). The primary environmental concern from use of halons and other bromine-containing compounds has been the potential for the bromine released from these compounds to destroy significant numbers of ozone molecules in the stratosphere. The halons being banned are part of the group of chemicals, including chlorofluorocarbons such as CFC₁₁ (CFC-11) and CF₂Cl₂ (CFC-12) and other chlorocarbons, that appear to be largely responsible for the significant decrease in stratospheric ozone observed over the last few decades (*2-4*).

In addition to the concerns about their effects on ozone, the halons and other halocarbons are also greenhouse gases, with strong absorption features in the infrared. Growing atmospheric concentrations of these gases can lead to changes in the radiative forcing on climate, and thus to potential changes in the Earth's climate (*5-7*). Although national and international policy has not yet been developed and there

0097-6156/95/0611-0059\$12.00/0
© 1995 American Chemical Society

remain significant uncertainties about the effects of human activities on climate, the concern about potential effects on climate are real and need to be considered.

A variety of industrial and government groups are currently trying to find appropriate replacements for the many important uses of halons, particularly in fire fighting applications. As part of this search, the potential effects on ozone and climate from these replacements need to be evaluated. The purpose of this chapter is to examine compounds being considered as halon replacements and the approaches being used to evaluate the potential effects of these replacements on ozone and climate.

Concentrations and Lifetimes

The tropospheric concentration of a halon or replacement compound is dependent on the rate of emission into the atmosphere and the atmospheric lifetime of the constituent. Measurements of halons H-1211 and H-1301 show that their current global mixing ratios (the ratio of its volume density or concentration to the volume density of air) are about 2.5 and 2.0 pptv (parts per trillion by volume), respectively, and are currently increasing at about 3 and 8 % per year, respectively (8, 7, 3). These rates of increase have slowed appreciably in recent years, consistent with the reduction in production and emissions of these compounds (9, 7). Despite such small concentrations, production of these compounds is being halted because of the capability of the bromine contained in these compounds to destroy ozone (see later discussion on ozone). Numerical models indicate that H-1211 and H-1301 are essentially nonreactive in the troposphere and are destroyed through photolysis in the stratosphere, resulting in atmospheric lifetimes of about 20 and 65 years, respectively (10). Because of their long atmospheric lifetimes, the destruction of these halons generally releases their bromine into the stratosphere where the bromine is most effective in affecting ozone. The long atmospheric lifetimes also imply that halons already emitted will be releasing bromine into the stratosphere for several more decades after production is stopped.

A number of compounds are being evaluated as replacements for the current uses of halons. Compounds being considered include: perfluorocarbons, such as C_2F_6 (also referred to as Fluorocarbon 116, FC-116), C_3F_8 (FC-218), C_4F_{10} (FC-31-10), and C_6F_{14} (FC-51-14); hydrofluorocarbons, such as C_3HF_7 (HFC-227ea), $C_2H_2F_4$ (HFC-134a), and CHF_3 (HFC-23); hydrochlorofluorocarbons, such as CHF_2Cl (HCFC-22), $C_2HF_3Cl_2$ (HCFC-123) and C_2HF_4Cl (HCFC-124); and several other compounds, such as CF_3I and SF_6 . A list of these compounds is given in Table I. (based on information concerning halon replacements under consideration provided by the U.S. Environmental Protection Agency). In some applications, mixtures of such compounds are being considered; only the individual compounds are examined here although the effects of a mixture can be evaluated in terms of the proper ratios of the individual effects. The atmospheric lifetime of such compounds is important to determining their potential effects on ozone and climate including calculating the indices Ozone Depletion Potentials and Global Warming Potentials.

Atmospheric Lifetime. After emission into the atmosphere, the time scale for removal of a gas, its atmospheric lifetime, is generally defined as the ratio of total atmospheric burden to integrated global loss rate. The lifetime is the time it takes for the global amount of the gas to decay to $1/e$ or 36.8% of its original concentration after initial emission into the atmosphere. The atmospheric lifetime integrates over spatial and temporal variations in the local atmospheric chemical loss frequencies for the compound. The lifetime must take into account all of the processes determining the removal of a gas from the atmosphere, including photochemical losses within the atmosphere (typically due to photodissociation or reaction with OH), heterogeneous removal processes (e.g., loss into clouds or into raindrops), and permanent removal

uptake by the land or ocean. Atmospheric lifetimes of a number of gases have been determined based on current knowledge of these loss processes; these lifetimes have recently been updated for the IPCC (7) and WMO (3) assessments.

As shown in Table I, atmospheric lifetimes of greenhouse gases of interest range from a few days (e.g., for CF_3I) to thousands of years (e.g., for SF_6 and several perfluorocarbons). In Table I, most of the values for atmospheric lifetimes are based on the recent international assessments and references therein. The lifetime for H-2402 has not been reevaluated and is based on an earlier ozone assessment (2), while lifetimes for perfluorocarbons have been evaluated by Ravishankara et al. (11). The lifetime for C_3F_8 is not available, but, using other perfluorocarbons as a guide, is likely to be on the order of 5000 years.

The atmospheric lifetimes of the perfluorocarbons and SF_6 are extremely long, implying that any emissions of these gases will remain in the atmosphere for well over a thousand years. Lifetimes of HCFCs and HFCs range from very short lifetimes for gases such as HCFC-123 that react rapidly with hydroxyl (OH) to lifetimes of comparable size to the halons. The atmospheric lifetime of CF_3I is extremely short, on the order of a few days, due to its photolysis at near-ultraviolet wavelengths (similar results found both with our model and in ref. 13).

Table I. Atmospheric lifetimes and calculated Ozone Depletion Potentials for halons and potential replacements

<i>Species</i>	<i>Chemical Formula</i>	<i>Atmospheric lifetime (years)</i>	<i>Ozone Depletion Potentials (ODPs)</i>
Halons			
H-1211	CF_2ClBr	20	5
H-1301	CF_3Br	65	13
H-2402	$\text{C}_2\text{F}_4\text{Br}_2$	22	7
HCFCs			
HCFC-22	CF_2HCl	13.3	0.05
HCFC-123	$\text{C}_2\text{F}_3\text{HCl}_2$	1.4	0.02
HCFC-124	$\text{C}_2\text{F}_4\text{HCl}$	5.9	0.03
HFCs			
HFC-23	CHF_3	250	$<4 \times 10^{-4}$
HFC-32	CH_2F_2	6.0	0
HFC-125	C_2HF_5	36	$<3 \times 10^{-5}$
HFC-134a	CH_2FCF_3	14	$<5 \times 10^{-4}$
HFC-227ea	C_3HF_7	41	0
PFCs			
FC-116	C_2F_6	10000	0
FC-218	C_3F_8	N.A.	0
FC-31-10	C_4F_{10}	>2600	0
FC-51-14	C_6F_{14}	3200	0
Other			
Sulfur hexafluoride	SF_6	3200	0
Trifluoroiodo-methane	CF_3I	<0.005	<0.008

SOURCE: Adapted from Ref. 2, 3, 7, 10

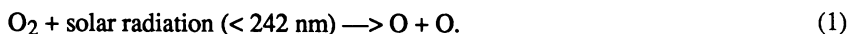
Potential Effects on Ozone

Laboratory studies, atmospheric measurements, and numerical models of the atmosphere have provided important evidence to the significant effect caused by chlorine and bromine on stratospheric ozone in the last few decades (2, 3). Understanding of the depletion of stratospheric ozone has led to the need for simple measures for comparing the impact on ozone from different compounds as a scientific guide to public policy. The Ozone Depletion Potential concept has proven to be a useful index for the effects on ozone from CFCs, halons, and their replacements.

Atmospheric Ozone. Ozone is a primary absorber of solar ultraviolet (UV) and visible radiation in the atmosphere. It is the effect of ozone in determining the amount of ultraviolet radiation reaching the Earth's surface that has largely resulted in the national and international policy actions on production of CFCs, halons and other halocarbons to protect the amount of stratospheric ozone. However, ozone is also a greenhouse gas, with a large infrared absorption band at 9.6 μm ; changes in the amount and distribution of ozone can affect the radiative forcing on climate (12).

Although ozone molecules play a vital role in the atmosphere, they are exceedingly rare, accounting for fewer than ten of every million molecules of air. Approximately 90% of the ozone in the atmosphere is contained in the stratosphere. The rest of the ozone is primarily in the global troposphere. Although ozone is a major component of photochemical smog in urban areas, this local ozone contributes very little to the global ozone budget.

Ozone is produced in the atmosphere by the rapid reaction of an oxygen atom with an oxygen molecule in the presence of any third molecule. However, the means by which the oxygen atom is primarily generated differ greatly between the troposphere and the stratosphere. In the stratosphere, the production of ozone begins with the photodissociation of an O_2 molecule, at ultraviolet wavelengths less than 242 nm,



This reaction produces two ground-state oxygen atoms that are extremely reactive and generally react with other O_2 to produce O_3 . Because O usually combines with O_2 to create O_3 , it is common practice to refer to the sum of the concentrations of O_3 and O as odd-oxygen. Ozone itself photodissociates at ultraviolet wavelengths to produce O plus O_2 , but because the O will generally react to reform O_3 , this mechanism produces no net change in the amount of odd-oxygen.

The primary destruction of odd-oxygen in the stratosphere comes from catalytic mechanisms involving various free radical species. Nitrogen oxides, chlorine oxides, hydrogen oxides, and bromine oxides participate in catalytic reactions that destroy odd-oxygen. For example, oxides of chlorine act in a catalytic way to convert O_3 and O into O_2 :



with the net effect,



Catalytic cycles involving bromine, nitrogen and hydrogen occur in a similar manner. This catalytic cycle and other catalytic cycles involving chlorine and bromine are

thought to be largely responsible for the observed decrease in stratospheric ozone over the last few decades.

Ozone in the stratosphere is therefore constantly being produced and is constantly being destroyed. As a result, the concentration of ozone results from the balance between photochemical production and catalytic destruction. The total amount of ozone will remain fairly constant as long as the destruction rate and the transport of ozone out of the stratosphere remain unchanged. This is akin to the balance maintained in a bathtub; as long as the water pouring in is balanced by the amount flowing out the drain, the water level in the bathtub will remain unchanged. However, if the strength of the ozone destruction rate changes or, in the case of our analogy, the size of the drain changes, then the amount of ozone in the stratosphere will also change. The actual distribution of ozone within the stratosphere also results from the relative strengths of winds and other processes influencing the transport of ozone and other constituents.

In addition to any trends related to human activities, the concentration of ozone in the stratosphere also varies from year to year, reflecting small shifts in the balance between ozone production and destruction. Changes in the amount of ozone can also occur naturally due to volcanic eruptions and due to changes in solar intensity (such as those occurring over the 11-year sunspot cycle).

Ozone Destruction Effectiveness. The chlorine and bromine catalytic mechanisms are particularly efficient at destroying ozone. The chlorine and bromine catalytic cycles can occur thousands of times before the catalyst is converted to a less reactive form such as HCl or HBr. Because of this cycling, relatively small concentrations of reactive chlorine or bromine can have a significant impact on the amount and distribution of ozone in the stratosphere. In the lower stratosphere, atmospheric and laboratory measurements indicate that heterogeneous chemistry on particles is leading to enhanced effects on ozone from chlorine and bromine. This heterogeneous chemistry helps convert less reactive species to the reactive forms of bromine and chlorine that can react catalytically.

Bromine is much more effective at destroying ozone in the lower stratosphere than is chlorine. Figure 1 shows the effectiveness of bromine and iodine in destroying ozone at midlatitudes relative to chlorine, and is based on calculations from the zonally averaged chemical-radiative-transport model of the global atmosphere developed at Lawrence Livermore National Laboratory. Current chemistry in the model is based on recommendations of the NASA Panel for Data Evaluation (19) with the addition of iodine chemistry based on Atkinson et al. (20) and photolysis cross-sections for CF₃I from measurements by M. Molina (private communication). As shown in figure 1, the bromine catalytic cycles are more than a 100 times more efficient than the chlorine catalytic mechanisms at destroying ozone in the lower stratosphere, especially below 20 km. However, the emissions and corresponding amount of brominated compounds or halons in the atmosphere are much smaller than those of the chlorinated compounds. As a result, while not negligible in its effect, the impact from bromine on the current atmosphere is smaller than the effects from increasing chlorine.

CF₃I and other compounds containing iodine have recently been suggested as replacements for halons. Figure 1 shows that any iodine reaching the stratosphere is even more effective than bromine and is over a thousand times more effective than chlorine at destroying ozone in the lower stratosphere. Solomon et al. (13) calculated similar results for bromine and iodine relative to chlorine from their atmospheric model. In another study, Solomon et al. (14) have suggested that natural sources of iodine, despite very small concentrations, may have played an important role in recent lower stratospheric ozone depletion through extremely fast reactions with bromine and chlorine.

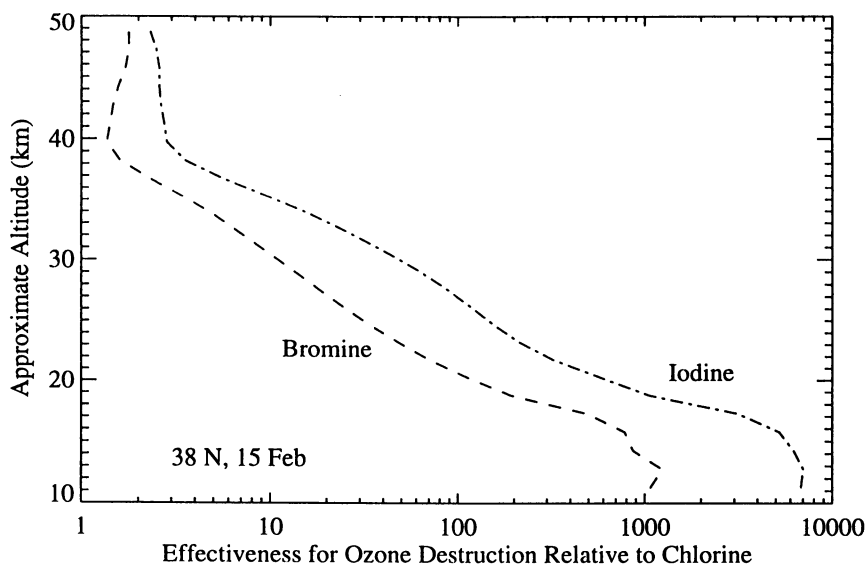


Figure 1. Calculated effectiveness of bromine and iodine to destroy stratospheric ozone at midlatitudes relative to chlorine. Based on LLNL zonally-averaged chemical-radiative-transport model; similar results also found by Solomon et al. (13).

Other suggested replacements are primarily composed of carbon, fluorine, and hydrogen. For the amounts of anticipated production and emissions, none of these compounds are likely to significantly affect ozone. It has been suggested that CF_3 radicals produced by dissociation of some of these compounds, such as from the dissociation of HFC-134a, could affect ozone; however, recent studies indicate that these radicals are unlikely to have any significant effects on ozone (3).

Ozone Depletion Potentials. The concept of Ozone Depletion Potentials (ODPs) provides a relative cumulative measure of the expected effects on ozone from the emissions of a gas (15, 2,3) relative to one of the gases of most concern to ozone change, namely CFC-11. This concept is an integral part of national and international policy considerations to protect ozone, including the Montreal Protocol and its Amendments (1) and the U.S. Clean Air Act. ODPs provide an important means for analyzing the potential for a new chemical to affect ozone relative to CFCs, halons or other replacement compounds being considered.

The Ozone Depletion Potential (ODP) of a gas is defined as the change in total ozone per unit mass emission of the gas relative to the change in total ozone per unit mass emission of CFC-11. Time-dependent ODPs can also be defined and provide information on the shorter time scale effects of a compound on ozone. However, the steady-state values have been primarily preferred and used in regulatory considerations. ODPs are currently being determined by two different means: by calculations with two-dimensional models of the global atmosphere (2, 3) and by the semi-empirical approach developed by Solomon et al (16). The two approaches give similar results.

By definition, the ODP for CFC-11 is 1.0, and the calculated ODPs for other CFCs being banned are all greater than 0.4. The Clean Air Act currently calls for policy actions on compounds whose ODPs are equal to or greater than 0.2. Table I presents steady-state Ozone Depletion Potentials for the halons and possible replacement compounds. The ODPs for halons are all extremely large, much greater than 1.0, reflecting the reactivity of bromine with ozone.

ODPs for all of the hydrofluorocarbons (HFCs), perfluorocarbons (PFCs), and sulfur hexafluoride are all near zero due to the low reactivity of the products of their dissociation with ozone. The HCFCs do contain chlorine and can affect ozone. However, the ODPs for the HCFCs being considered as halon replacements in Table I are all small, with values of 0.02 to 0.05. The effects on ozone from an unit emission of one of these HCFCs would cause less than one hundredth of the effect on ozone than the halon they would replace. The short lifetimes of these HCFCs (and their lack of bromine) results in the reduced effect on ozone.

Although iodine is extremely reactive with ozone, the ODP for surface emissions of CF_3I is less than 0.01. Because of its reactivity in the troposphere, very little iodine would be expected to reach the stratosphere from surface emissions of CF_3I . However, this value is subject to significant uncertainty in the understanding of iodine chemistry (e.g., lack of data on such reactions as IO with O_3 , ClO, or BrO) and the physical processes (e.g., the effects from convective processes in transporting iodine to the upper troposphere) affecting the iodine distribution in the troposphere and stratosphere.

Time-dependent ODPs are also useful to examine because of the insight they provide to short-term effects after emission on stratospheric ozone (while steady-state ODPs indicate integrated effects over longer time scales. As discussed in the recent international assessments (2, 3), the ODPs at short-time scales of a few years are much larger for the HCFCs than they are at steady-state. The short atmospheric lifetimes of these compounds implies that they also release chlorine in the lower stratosphere more quickly than CFC-11, and can result in a more immediate (but small) effect on ozone as compared to CFC-11. However, the time-dependent ODPs for these HCFCs are still much smaller than the halons they would replace.

Potential Effects on Climate

Much of the concern about effects of human activities on climate has centered around carbon dioxide (CO₂) because of its importance as a greenhouse gas and also because of the rapid rate at which its atmospheric concentration has been increasing. However, other greenhouse gases are contributing about half of the overall increase in the radiative forcing effect on climate (5). Because of their small concentrations, halons are currently only a minor contributor to this change in radiative forcing. It is important, however, to consider the possible role of any replacements for halons to affect future climate.

Numerical models of the climate system suggest that surface temperatures could increase by as much as 3 degrees K (best estimated range of 2 to 5 degrees K) over the next century (5, 6) due to projected changes in the concentrations of greenhouse gases. Analyses of possible future changes in climate are largely dependent on complex three-dimensional numerical models of the global climate system (atmosphere, oceans and land surface) that attempt to represent the many processes controlling climate. These models are computationally expensive and, given current computer capabilities, are severely limited in the number of calculations that can be and have been examined. The complexity of these models prohibit their extensive use in policy related analyses of greenhouse gases and their effects on climate. However, calculations made with climate models have shown, at least for well-mixed greenhouse gases, that there is approximately a linear relationship between the global-mean radiative forcing at the tropopause and the resulting change in global mean surface temperature (7). As a result, radiative forcing has become a basis for examining the potential ability of a greenhouse gas to affect climate.

Several different indices have been used as measures of the strength of the radiative forcing from different greenhouse gases. The indexing approach for greenhouse gases that has gained the widest acceptance is the Global Warming Potential concept originally developed for the IPCC (5-7).

Radiative Forcing. The radiative forcing of the surface-troposphere system (due, for example, to a change in greenhouse gas concentration) is defined (5-7) as the change in net irradiance (in Wm⁻²) at the tropopause after allowing for stratospheric temperatures to readjust to stratospheric equilibrium. The tropopause is chosen because it is considered in a global and annual mean sense that the surface and troposphere are closely coupled.

A key factor affecting radiative forcing for a gas is the location of the wavelengths for its absorption of infrared radiation. The spectral region from about 8 to 12 μm is referred to as the "window" region because of the relative transparency of the atmosphere to radiation over these wavelengths. Most of the non-CO₂ greenhouse gases with the potential to affect climate, including halons and most of their replacements, all have strong absorption bands in the atmospheric window region. Relatively small changes in the concentrations of these gases can produce a significant increase in radiative forcing.

As the concentration of a greenhouse gas becomes high, it can absorb most of the radiation in its energy bands; once any of its absorption wavelengths become saturated, it is unable to absorb more energy at that specific wavelength, and further increase in its concentration has a diminishing effect on climate. This is called the band saturation effect. For example, the radiative forcing from further increases in carbon dioxide concentrations in the current atmosphere will increase as the natural logarithm of its concentration because of this effect. Also, at the wavelengths where water vapor and carbon dioxide strongly absorb IR radiation, the greenhouse effect of other gases will be minimal. On the other hand, absorption by other gases at wavelengths that are not saturated, such as the halons or other halocarbons, varies linearly with concentration. Another important consideration in radiative absorption is

the band overlap effect. If a gas absorbs at wavelengths that are also absorbed by other gases, then the effect on radiative forcing of increasing its concentration can be diminished.

In addition to the direct forcing effect from emission of a gas into the atmosphere, the net radiative forcing can also be modified through indirect effects relating to chemical interactions on other radiatively important constituents. For example, emissions of halons result in stratospheric bromine that can destroy stratospheric ozone, which is also a greenhouse gas (Lacis et al., 1990). Such indirect effects need to be considered when evaluating potential climate effects.

Relative Radiative Forcing per Molecule or Mass. This measure compares the radiative forcing on a molecule-per-molecule basis or kilogram-per-kilogram basis of the different greenhouse gases. It is generally given relative to CO₂ or CFC-11. A radiative transfer model of the atmosphere is used to determine the radiative forcing for small perturbations of these gases relative to present-day conditions. Small perturbations are used in the calculations in order to prevent the marked nonlinear absorption of carbon dioxide, methane, and nitrous oxide from affecting the radiative forcing for these gases. Table II shows radiative forcing on a per molecule basis relative to CFC-11 for the list of halons and possible replacements.

Table II. Radiative forcing due to relevant halons and potential substitutes per unit mass and per molecule increase in atmospheric concentration relative to CFC1₃ (CFC-11). The absolute radiative forcing due to CFC-11 is 0.22 Wm⁻² per ppbv increase (5). The radiative forcing for CFC-11 is 3,970 greater than CO₂ per unit mass and 12,400 greater than CO₂ per unit molecule increase (5-7)

<i>Species</i>	<i>Chemical Formula</i>	<i>ΔF per unit mass relative to CFC-11</i>	<i>ΔF per unit molecule relative to CFC-11</i>
Halons			
H-1301	CF ₃ Br	1.19	1.29
HCFCs			
HCFC-22	CF ₂ HCl	1.37	0.86
HCFC-123	C ₂ F ₃ HC1 ₂	0.72	0.80
HCFC-124	C ₂ F ₄ HCl	0.88	0.87
HFCs			
HFC-23	CHF ₃	1.59	0.81
HFC-32	CH ₂ F ₂	1.06	0.40
HFC-125	C ₂ HF ₅	1.03	0.90
HFC-134a	CH ₂ FCF ₃	1.04	0.77
HFC-227ea	C ₃ HF ₇	0.95	1.17
FCs			
FC-116	C ₂ F ₆	1.36	1.37
FC-218	C ₃ F ₈	0.77	1.05
FC-51-14	C ₆ F ₁₄	0.75	1.84
Other			
Sulfur hexafluoride	SF ₆	2.75	2.92
Trifluoroiodo-methane	CF ₃ I	1.20	1.71

SOURCE: Adapted from Ref. 5-7

The radiative forcing of the halons and listed replacements in Table II are all within a factor of four of each other and are roughly the same order of magnitude as the radiative forcing for CFC-11. On the other hand, the radiative forcing for CFC-11 is 3,970 times greater than CO₂ on a per unit mass basis and is 12,400 times greater than CO₂ on a per molecule basis. These results suggest that all of the replacement compounds could be important greenhouse gases if their atmospheric concentrations became large enough.

Global Warming Potentials. The concept of Global Warming Potentials (GWPs) has been developed, akin to the ODP concept, as a means to provide a simple representation of the relative effects on climate resulting from a unit mass emission of a greenhouse gas (5-7). Global Warming Potentials are expressed as the time-integrated radiative forcing from the instantaneous release of a kg (i.e., a small mass emission) of a trace gas expressed relative to that of a kg of the reference gas, CO₂ (5-7):

$$\text{GWP}(x) = \frac{\int_0^n F([x(t)]) dt}{\int_0^n F([\text{CO}_2(t)]) dt} \quad (5)$$

where n is the time horizon over which the calculation is considered; $F([x(t)])$ is the radiative forcing in response to the changing concentration of species x after the pulse emission at time $t=0$; $[x(t)]$ is the time-decaying concentration of that gas; and the corresponding quantities for the reference gas are in the denominator. The radiative forcing responses are derived from radiative transfer models. The trace gas concentrations, $[x(t)]$ remaining after time t are based upon the atmospheric lifetimes of the gas in question. The reference gas has been taken generally to be CO₂, since this allows a comparison of the radiative forcing role of the emission of the gas in question to that of the dominant greenhouse gas that is emitted as a result of human activities.

The best choice of integration time horizon in evaluating GWPs has been the subject of much discussion and controversy (5-7). Unlike ODPs, the complexities of treating CO₂ and the carbon cycle prevent integration of GWPs to steady-state. There is, however, no given value of integration time for determining GWPs that is ideal over the range of uses of this concept. GWPs are generally calculated over three time horizons, for 20, 100, and 500 years. It is believed that these three time horizons provide a practical range for policy applications (6-7). GWPs determined for the longer integration period provide a measure of the cumulative chronic effects on climate, while the integration over the shorter period is representative of near term effects. GWPs evaluated over the 100-year period appear generally to provide a balanced representation of the various time scales for climatic response. The best choice of time horizon will depend on the specific analysis being considered. One needs to balance the effects of near term responses in comparing greenhouse gases with consideration of the long term persistence of any environmental effects from long-lived gases.

Direct and indirect GWPs have recently been reevaluated for the new international climate and ozone assessments (3, 7). In prior assessments (5, 6), the decay response curve for CO₂ used in evaluation of the GWPs was based on results from an "unbalanced" carbon cycle model that did not correctly calculate the current CO₂ concentration based on a realistic emission history. The new assessments base the CO₂ response curve on results from more sophisticated carbon cycle models with improved treatments of ocean and biospheric effects that are "balanced", giving a consistent determination of past and present concentrations of CO₂.

GWPs are quite sensitive to the assumed background concentration for CO₂ (18). The constant concentration background assumed in prior GWPs, and also used in the evaluation to be presented in Table III, is clearly unrealistic. This assumption implies that the emission occurs into a system in equilibrium, whereas, the carbon cycle system is currently far from equilibrium and CO₂ concentrations are likely to increase into the foreseeable future. However, the choice of which future scenario to assume is also uncertain. In the 1994 IPCC assessment, the definition for the background atmosphere is chosen to provide consistency with evaluations in earlier assessments; at the same time, as will be presented below, information is provided that allow determination of GWPs for several other assumptions of future CO₂ background concentrations.

Table III. Direct Global Warming Potentials (7)

<i>Species</i>	<i>Chemical Formula</i>	<i>Atmos. Lifetime (years)</i>	<i>Global Warming Potential (Time Horizon)</i>		
			<i>20 years</i>	<i>100 years</i>	<i>500 years</i>
CO ₂	CO ₂	*	1	1	1
Halons					
H-1301	CF ₃ Br	65	6200	5600	2200
HCFCs					
HCFC-22	CF ₂ HCl	13.3	4300	1700	520
HCFC-123	C ₂ F ₃ HCl ₂	1.4	300	93	29
HCFC-124	C ₂ F ₄ HCl	5.9	1500	480	140
HFCs					
HFC-23	CHF ₃	250	9200	12100	9900
HFC-32	CH ₂ F ₂	6	1800	580	180
HFC-125	C ₂ HF ₅	36	4800	3200	1100
HFC-134a	CH ₂ FCF ₃	14	3300	1300	420
HFC-227ea	C ₃ HF ₇	41	4500	3300	1100
PFCs					
FC-116	C ₂ F ₆	10000	8200	12500	19100
FC-51-14	C ₆ F ₁₄	3200	4500	6800	9900
Other					
Sulfur hexafluoride	SF ₆	3200	16500	24900	36500
Trifluoriodo-methane	CF ₃ I	<0.005	<5	<<1	<<<1

* Decay of CO₂ is a complex function of carbon cycle (5-7)

SOURCE: Adapted after Ref. 7

Direct GWPs. Table III presents a summary of the results for GWPs for halons and their replacements included in the new assessments (3, 7). Because their radiative forcing is of similar magnitude, the replacements with the longer atmospheric lifetimes have the largest Global Warming Potentials. In fact, the GWPs for many of the replacements are as large or larger than the GWPs for halon 1301 (other halons have not been evaluated), particularly for the shorter 20 year integration time. The shorter lived compounds, such as HCFC-123, HCFC-124, and HFC-32 have appreciably smaller GWPs, particularly at the 100 year and 500 year integration periods. The GWPs for CF_3I are extremely small (< 5 even for the short integration time) due to its few day atmospheric lifetime.

The GWPs for the perfluorocarbons and for SF_6 are all much larger than any of the values for CFCs or halons. The very long atmospheric lifetimes of these gases lead to extremely large GWPs. These large GWPs imply potentially large effects on climate over long timescales with the actual effect on climatic radiative forcing dependent on the magnitude of emissions into the atmosphere.

Indirect GWPs. Possible effects on ozone from emissions of halons or their replacements also need to be considered. Daniel et al. (17; also see ref. 3) have estimated the indirect GWPs for effects on ozone from a variety of halocarbons, including CFCs, halons, and HCFCs in an attempt to clarify the relative radiative roles of different classes of ozone-depleting compounds. Decreased ozone from CFCs and halons should primarily decrease the radiative forcing on climate. They find that the net GWPs of halocarbons depend strongly upon the effectiveness of each compound for ozone destruction. Halons are likely to have negative net GWPs while those of CFCs are likely to be positive over both 20- and 100- year time horizons (3). These analyses, however, are still subject to remaining uncertainties about the cause of ozone decreases in the ozone in the lower stratosphere, just above the tropopause.

Conclusions

The concepts of Ozone Depletion Potentials and Global Warming Potentials provide important guides to the potential effectiveness of halon replacements to destroy stratospheric ozone and to affect radiative forcing on climate. Unless the amounts of replacements produced and emitted into the atmosphere are appreciably larger than the compounds they replace, the compounds being considered as halon replacements are not expected to have any appreciable effect on stratospheric ozone.

However, the perfluorocarbons and SF_6 have extremely long atmospheric lifetimes (> 1000 years) and their large Global Warming Potentials suggest that emissions of these compounds could lead to significant concerns about radiative forcing on climate. Even individually small production (and emission) amounts of these compounds commit humanity to additional forcing on climate for thousands of years. The sum of several small sources of these compounds could produce a significant climatic forcing concern.

Acknowledgments

Work at Lawrence Livermore National Laboratory was performed under the auspices of the U.S. Department of Energy under contract No. W-7405-Eng-48. This work was supported by the National Institute for Standards and Technology and by the National Aeronautics and Space Administration, Atmospheric Chemistry Modeling and Analysis Program.

References

1. United Nations Environment Programme, *Report of the Fourth Meeting of the Parties to the Montreal Protocol on Substances that Deplete the Ozone Layer*, Copenhagen, November 23-25, 1992, Nairobi, 1992.
2. World Meteorological Organization *Scientific Assessment of Ozone Depletion, 1991*; World Meteorological Organization Global Ozone Research and Monitoring Project—Report, No. 25, Geneva, 1991.
3. World Meteorological Organization *Scientific Assessment of Ozone Depletion, 1994*; World Meteorological Organization Global Ozone Research and Monitoring Project—Report, in press, Geneva, 1994.
4. Reinsel, G. C., Tiao, G. C., Wuebbles, D. J., Kerr, J. B., Miller, A. J., Nagatani, R. M., Bishop, L., Yang, L. H. *J. Geophys. Res.* **1994**, *99*, 5449-5464.
5. Intergovernmental Panel on Climate Change (IPCC) *Climate Change, The IPCC Scientific Assessment*; Houghton, J. T., Jenkins, G. J., Ephraums, J. J., Eds.; Cambridge University Press, Cambridge, Great Britain, 1990.
6. Intergovernmental Panel on Climate Change (IPCC) *Climate Change 1992, The Supplementary Report to the IPCC Scientific Assessment*; Houghton, J. T., Callander, B. A., Varney, S. K., Eds.; Cambridge University Press, Cambridge, Great Britain, 1990.
7. Intergovernmental Panel on Climate Change (IPCC) *Radiative Forcing of Climate Change*; Cambridge University Press, Cambridge, Great Britain, 1994.
8. Butler, J. H., Elkins, J. W., Hall, B. D., Cummings, S. O., Montzka, S. A. *J. Geophys. Res.* **1992**, *359*, 403-405.
9. McCulloch, A. *Atmos. Environ.* **1992**, *26A*, 1325-1329.
10. Kaye, J., Penkett, S., *Report on Concentrations, Lifetimes and Trends of CFCs, Halons, and Related Species*, NASA reference publication 1339, Washington D. C., 1994.
11. Ravishankara, A. R., Solomon, S., Turnipseed, A. A., Warren, R. F. *Science* **1993**, *259*, 194-199.
12. Lacis, A. A., Wuebbles, D. J., Logan, J. A. *J. Geophys. Res.* **1990**, *95*, 9971-9981.
13. Solomon, S., Burkholder, J. B., Ravishankara, A. R., Garcia, R. R. *J. Geophys. Res.* **1994**, *99*, 20929-20935.
14. Solomon, S., Garcia, R. R., Ravishankara, A. R. *J. Geophys. Res.* **1994**, *99*, 20491-20499.
15. Wuebbles, D. J. *J. Geophys. Res.* **1983**, *88*, 1433-1443.
16. Solomon, S., Mills, M. J., Heidt, L. E., Tuck, A. F. *J. Geophys. Res.* **1992**, *97*, 825-842.
17. Daniel, J. S., Solomon, S., and Albritton, D. L. *J. Geophys. Res.* **1994**, *99*, in press.
18. Wuebbles, D. J., Jain, A. K., Patten, K. O., Grant, K. E. *Climatic Change 1994*, in press.
19. Demore, W. B., Sander, S. P., Golden, D. M., Hampson, R. F., Kurylo, M. J., Howard, C. J., Ravishankara, A. R., Kolb, C. E., and Molina, M. J. *Chemical Kinetics and Photochemical Data for Use in Stratospheric Modeling, Evaluation Number 10*, Jet Propulsion Laboratory, Pasadena, CA, 1992.
20. Atkinson, R., Baulch, D. L., Cox, R. A., Hampson, R. F., Kerr, J. A., and Troe, J. *J. Phys. Chem. Ref. Data* **1992**, *21*, 1125-1568.

RECEIVED July 13, 1995

Chapter 8

Halon Replacement in Aircraft and Industrial Applications

G. C. Harrison¹

Walter Kidde Aerospace, 4200 Airport Drive, Northwest,
Wilson, NC 27896-9643

The status of Halon substitutes for use in military aircraft, commercial aircraft and industrial fire extinguishing and explosion suppression applications is assessed. Both technical and regulatory influences are part of the discussion. In general, the results of this first round of Halon replacement testing shows that the search for a "drop-in" substitute has been disappointing. There are, however, alternate technologies available for use in most applications. The search will go on.

Aircraft Applications

Aircraft are inherently a high fire and explosion risk due to the large quantity of flammable fuel and other combustible fluids that are normally on-board. With the use of halon agents, principally halon 1301, and careful study of fire occurrences, the hazards have been controlled. Today's operational record shows that the fire risk is low (*1*). Giving up these remarkable agents threatens to cancel all this progress and return us to a high risk fire and explosion hazard environment. Applications readily separate into two categories, military and civilian aircraft, mainly because of the differing missions. Military aircraft must be concerned with survivability in combat situations which include fires and explosions caused by various ballistic and high energy rounds. Civilian aircraft, on the other hand, focus attention on in-flight interior cabin fires and fires resulting from impact post-crash situations. Fire extinguishing systems are used in aircraft for:

- Engine nacelles -- military and civilian
- APU (auxiliary power unit) -- military and civilian
- Fuel tank inertion -- military
- Dry bay explosion suppression --military
- Lavatory waste bins -- civilian
- Cargo compartments -- primarily civilian
- Portables, hand held -- primarily civilian

¹Current address: 903 Oak Forest Drive, Wilson, NC 27896

Engine Nacelle and APU Applications. These applications have similar fire threats and are common to both military and civilian aircraft. Fires are generally due to ignition of hydrocarbon fluids leaking from fuel or hydraulic lines. The fires are in the form of pressure sprays or puddles from accumulations in the bottom of the nacelle. Oxygen to support the combustion is available from a continuous flow of cooling air through the nacelle or APU chamber. The amount of air flow varies with the aircraft speed and altitude. The fire extinguishing system for both of these applications is similar in design. It consists of detectors to sense the presence of fire, bottles holding the extinguishing agent, a distribution system of pipes to get the agent to the fire location and a bottle opening device remotely operated. Our interest is in the bottles and the piping system since they are the parts which contain and direct the agent to the fire. Their design has been dictated by the physical properties of the agent, the dissemination rate specified by the fire suppression engineer and the minimum weight and volume restrictions set by the aircraft designer. These containers or bottles are ordinarily made of steel or stainless steel although recently titanium has been used successfully. The bottles range in volume from 40 cubic inches to 2500 cubic inches. Loading pressures vary from 360 PSIG to 825 PSIG at 70 °F. The normal pressure in Engine/APU bottles is 600 PSIG at 70 °F. Each container is designed to meet the specific requirements for a specific aircraft application. Halon 1301 is the agent most used, but there are still a few applications which use Halon 1011, Halon 1202 and even Halon 1211. The containers must meet the regulations and the corresponding fill specifications of the U.S. Department of Transportation for bottles containing pressurized liquids and gases. For Engine/APU bottles, the nominal fill density is 50 pounds per cubic foot. Nitrogen gas is added to the Halon as a superpressurizing agent to speed the discharge of the bottle contents to the fire. The distribution system is made of tubing. The size and length are determined by the bottle location with reference to the fire threat area, the volume of the fire threat space, the rate of ventilation of that space and the concentration of the agent needed for fire suppression. Lines in the fire zone are made of corrosion resistant steel. Other lines may be of aluminum alloy or corrosion resistant steel. Lines between the bottle and the discharge outlet should be as short as possible with a minimum number of fittings and turns. The preferred line length is less than 10 feet. However, in very large aircraft like the C-5, some lines are 46 feet long. The purpose of these concerns is to minimize the time to discharge the agent to the fire site. The design test for bottle discharge is listed in MIL-C-22284. It says that the charged container will be discharged through 10 feet of stainless steel tubing terminating in a tee having a total outlet area of 120 percent of the line area. Ninety percent of the contents of the container must be discharged in not more than 0.8 second. Tubing sizes are designated for containers according to their volume, the larger the bottle volume, the larger the tubing diameter. Additional design data for aircraft fire extinguishing systems is in MIL-E-22285. This document specifies the minimum quantity of Halon 1301 to be discharged into each engine. It requires that the extinguishing system be capable of producing an agent concentration of at least 6 percent by volume in

all parts of the affected zone for a minimum of 0.5 second at normal aircraft cruising condition. Another source of information is the "Design Manual on Aircraft Fire Protection for Reciprocating and Turbine Engine Installations", prepared by the Aerospace Industries Association. This manual is old but gives an historical perspective and is a generalized reference on fire prevention and suppression. Of particular interest is the discussion on fire extinguishing agents from carbon dioxide to Halon 1301, which was described at that time as limited in availability and expensive. This is useful as we are now considering a Halon 1301 replacement.

Status of Halon Replacements. In August 1990, NIST Technical Note 1279, "Construction of an Exploratory List of Chemicals to Initiate the Search for Halon Alternatives", was published by the National Institute of Standards and Technology. It contained a list of 103 chemicals which were considered candidates for replacing halons or testing the principles of fire suppression. By October 1992, a major testing program was initiated at the Wright-Patterson Air Force Base. Using pooled resources of the U.S. Air Force, Army, Navy and the Federal Aviation Administration, a comprehensive 17 month study began at NIST to select the best candidates for the full-scale fire suppression test program at Wright-Patterson Air Force Base. Based upon test data from federal laboratories, universities, private laboratories and system manufacturers; a list of 12 gaseous agents and sodium bicarbonate powder was selected for the NIST study. At its October 6-7, 1993 meeting, a selection of the following chemicals for full-scale testing at the Wright-Patterson facility was made by a Technology Transition Team which included representatives from all interested parties. According to the test plan, three candidate replacements were selected for each of two generic fire zones, engine nacelles/APU's and dry bays. The engine nacelle choices were HFC-125(C₂HF₅), HFC-227(C₃HF₇) and CF₄ (Halon 13001). The next meeting of the Technology Transition Team is scheduled for the end of October 1994. The task will be to select one of these three agents as the replacement for the final phase of testing in the Wright-Patterson program. There is already a consensus of opinion that none of these materials is really a satisfactory replacement for Halon 1301. The NIST organization is preparing a proposal for the Department of Defense to carry out a "Next Generation Fire Suppression Technology" research plan to find Halon alternatives. This will be an 8 to 10 year program. A second "Advanced Agent Working Group" is being organized by the Center for Global Environmental Technologies of the New Mexico Engineering Research Institute, University of New Mexico. This will also be a long term program. There is a real need for new and creative thinking about fire technology.

Dry Bay Explosion Suppression. Dry bays are void spaces near flammable fluids in aircraft. They may occur in the leading or trailing edge of wings and in the fuselage. These spaces frequently contain bleed-air, hydraulic, fuel or coolant lines; electrical and other cables; and various kinds of containers such as avionics equipment. Military aircraft are especially vulnerable to fire and explosion as

a result of threats from high velocity exploding warhead fragments, armor-piercing incendiary projectiles and high explosive incendiary projectiles. The protection of aircraft dry bays is one of the most critical applications of Halon 1301 and is key to survivability in combat situations. Since the impact flash from these projectiles and fragments occurs rapidly, lasting from 1 to 3 milliseconds, the extinguishing or suppression system must be able to react quickly. The conditions encountered in dry bay fire and explosion suppression are highly variable and make protection especially difficult. The dry bay is often located close to fuel tanks. Normal ventilation by design is from 2 to 40 air changes per minute, but damage by projectiles may cause a rapid increase from external air exchange or rupture of the bleed air duct. Internal structures, called clutter, create areas of low velocity or stagnant air; act as flame stabilizers and obstruct dispersion of the extinguishing agent. The fuel may be hydraulic fluid, lubricating oil, engine fuel, or a mixture. It may flow by a continuous stream, spray, or mist under high or low pressure. It may be a pool or puddle in the bottom of the bay. The agent must be effective under all of these conditions.

Many agents and dispersion techniques have been considered for use in dry bays (2-4). Among the agents tested were water, water based salt solutions, ethylene glycol water solutions, dry powders and halons. Thin dry powder packs constructed as sandwich panels were tested. They are a passive system and depend upon the ballistic impact to release and distribute the dry fire extinguishant powder. A second passive system consists of foam materials installed in dry bays and gaps that need protection. These passive techniques tend to be excessively heavy. In addition, maintenance and repair of components housed in the dry bays will be obstructed by the foam. Most active systems are the conventional pressurized container with the stored agent. A special device of this kind is a hollow thin walled stainless steel tube containing the agent, combined with a parallel linear shaped charge for agent discharge. It may be used with halons, water or dry powder. Known as an LFE (Linear Fire Extinguisher), the tube is super-pressurized with nitrogen or carbon dioxide. A separate optical detector signals the detonator initiation. Halon 1301 has been the principal agent for these applications. In the last few years, pyrotechnic devices which generate primarily nitrogen or carbon dioxide gas appear to be promising in this application. The future trend is toward a hybrid system which may generate both an inert gas and a chemically active fire suppression agent. In the writer's opinion, these devices achieve success because one uses many small units individually distributed in the space instead of a single large one with a pipe distribution system. At the same time that the Technology Transition Team selected the replacements for engine nacelles, they selected a set of agents to be candidates for dry bay extinguishment. These agents are FC-218(C₃F₈, HFC-125(C₂HF₅)) and CF₃I. HFC-227(C₃HF₇) was made an alternate.

Fuel Tank Inertion. Fuel tank inertion, like dry bay suppression, is a military need but is more susceptible to explosion. The ullage of the fuel tank, which is the vapor space above the fuel, is a contained space by design and responds more readily to explosion suppression techniques. For example, early British

explosion suppression research showed that pentane, a highly flammable gas was an effective agent. The pentane made the ullage vapor mixture over-rich and stopped the incipient explosion. Open cell polyamide foam was very successful as a fire and explosion suppressant in fuel tanks. Unfortunately, the added aircraft weight and loss of useable fuel capacity is unacceptable for many applications. A Halon 1301 system is in use which permits the pilot to flood the fuel tank ullage with inerting agent immediately before entering combat. Because the tank is vented, this inertion is only temporary.

Lavatory Waste Bins. Federal Aviation Regulation DOT 14CFR 121.308(b) requires that no person may operate a passenger carrying transport category airplane unless each lavatory in the airplane is equipped with a built-in fire extinguisher for each disposal receptacle for towels, paper or waste located within the lavatory. The fire extinguisher must be designed to discharge automatically into each disposal receptacle upon occurrence of a fire in the receptacle. Each receptacle used for the disposal of flammable waste material must be fully enclosed, constructed of at least fire resistant materials and must contain fires likely to occur in it under normal use. The ability of the receptacle to contain those fires under all probable conditions of wear, misalignment and ventilation expected in service must be demonstrated by test. Currently, all aircraft lavatory disposal receptacle fire extinguishers use Halon 1301. At the recent meeting of the FAA International Halon Replacement Working Group held in Seattle, Washington on July 26-27, 1994; a test method and apparatus were proposed for the evaluation and certification of lavatory disposal receptacle fire extinguishers. At the same time, it was shown that HFC-227ea (C_3HF_7) could be used successfully as a direct drop-in replacement for Halon 1301 in the present automatic fire extinguishers also known as "potty bottles". Once FAA certification is achieved, this could be the first application to replace Halon 1301.

Cargo Compartment. In order to evaluate the fire threat in cargo compartments, it is first necessary to understand the varying nature of these storage areas. Cargo compartments are classified into five groups, A through E. Class A compartments are small storage compartments used by air crew for personal gear. They are accessible in-flight and any fires can be controlled or extinguished with hand-held portable fire extinguishers. Class B "combi" compartments are in aircraft configured to carry both passengers and cargo. The cargo compartment is accessible in-flight. Fire protection in these compartments consists of smoke detectors and hand-held portable fire extinguishers. Some Boeing 747 aircraft with compartments as large as 17,000 cubic feet are in this category. Improvement in the fire protection for class B "combi" aircraft is probably desirable since smoke can cause a quick loss of visibility making fire fighting with portable units difficult in these large compartments. Class C compartments are located below the deck of the passenger area and vary in size from 735 to 17,000 cubic feet. This class uses a complete fire protection system.

Class D cargo compartments are also located below the deck of the passenger space. They are limited to a maximum size of 1000 cubic feet. Even though the compartment is not accessible in-flight, it has no fire extinguishing system. Instead, it relies upon a relatively air tight compartment fire resistant structure and oxygen starvation to control a fire. Class E compartments are on freight-only aircraft. They have no fire extinguishing systems, depending upon cabin depressurization to lower the oxygen concentration so that combustion is not supported. With the exception of portable units containing principally Halon 1211, cargo compartment fire extinguishing systems have used Halon 1301. The system is made up of one or more detectors, the pressurized containers mentioned above and a tube distribution arrangement. The structure and materials of construction must meet stringent flame and insulation test requirements. The Class C cargo compartment must have a liner separate from the aircraft structure. The ceiling and sidewall liner panels are tested to resist flame penetration for at least 5 minutes after application of a 1700 °F flame source. The peak temperature 4 inches above the upper surface of the horizontal test sample must not exceed 400 °F. All other materials of construction must be self extinguishing when tested vertically. Relatively large Halon 1301 containers are needed for cargo compartment applications. Some bottles are as large as 2500 cubic inches. More than one bottle may be required. The intent is to suppress flaming combustion with an initial burst of agent and then, maintain a concentration of at least 3 % by volume of Halon 1301 to inhibit flames for times as long as 180 to 210 minutes. Cargo compartments have a continuous ventilation rate due to leakage around door seals that is about one volume change per hour. Thus, it is also necessary to have a continuous flow of agent into the compartment to maintain flame inhibition. Present fire suppression options include one of the previously mentioned Halon 1301 substitutes, water sprays, inert gas from the heavy OBIGGS system (a nitrogen generating Onboard Inert Gas Generator System using membranes to separate oxygen from the air), carbon dioxide, suspended aerosols (solid particulate) and solid propellant generated gases.

Hand Held Portables. Hand fire extinguisher requirements for use in aircraft are described in the Federal Aviation Administration Advisory Circular number 20-42C dated March 7, 1984 which is still current. Referenced in this advisory are the Federal Aviation Regulations (FAR), which relate to the use of Hand Fire Extinguishers on aircraft. Provision must be made to extinguish Class A, B and C type fires as defined by the National Fire Protection Association (NFPA). Current practice is to carry at least one water portable and two Halon 1211 portable extinguishers on board commercial aircraft. For occupied spaces on small aircraft where allowable limits of Halon concentrations will be approached, Halon 1301 is the halogenated agent of choice because Halon 1301 is less toxic than Halon 1211. The location, size, type and number of extinguishers carried is carefully regulated. Frequently, an airline will choose to carry more than the minimum requirement. The Halon replacement for hand held extinguishers on aircraft must be equal to or better than the corresponding Halon extinguisher in terms of performance. Most of the cabin fires occur in the kitchen area and are

readily extinguished by the standard Halon 1211 bottle. The major concerns are seat fires that might be caused by flammable fuel in the hands of a terrorist, and the more difficult to extinguish hidden in-flight fires. A prime example of the hidden fire is that in the "cheek space" which is located below the deck of the passenger compartment and runs fore and aft along each side of the aircraft. Trash collects over time in this in-accessible area and, when ignited, may only be attacked through a narrow grillwork from above. Since one has difficulty locating the exact spot of the fire, a Halon 1211 streaming agent extinguisher is the unit of choice. For occupied spaces on aircraft, a Halon 1211 extinguisher should have a minimum capacity of 2.5 pounds (1.2 kilograms). These extinguishers must have a minimum Underwriters Laboratories rating of 5B:C, not less than 8 seconds effective discharge time, spray at least a 10-foot (3 meter) range and may be equipped with a discharge hose. For accessible cargo compartments of combination passenger/ cargo aircraft and full cargo aircraft, the Halon 1211 portable extinguishers should be at least 13 pounds (5.9 kilograms) capacity and have a minimum 2A, 40B:C rating. Specific regulations apply to the concentration of agent permitted in a compartment depending upon ventilation and occupancy. For example, in a passenger occupied compartment without ventilation or possible egress, the maximum allowable concentration of Halon 1211 is 2% by volume at 120°F. For Halon 1301, it is 5% by volume. This is a principal concern when considering the current list of potential Halon replacements. When a compartment is occupied and there is no opportunity for exiting, the maximum allowable concentration for any agent is its NOAEL (no observed adverse effect level). In a review of the EPA SNAP List, it is clear that only HFC-227ea (FM-200) has an extinguishing concentration lower than its NOAEL. FC 3-1-10 is a perfluorocarbon material with satisfactory qualities, but it has such a high GWP (global warming potential) that it is useable only when no other agent is possible. Some HCFC blends have been approved as Halon 1211 substitutes in streaming applications provided the space is "well ventilated". In the writers opinion the passenger compartment may not qualify always as a "well ventilated" space since there can be situations in an aircraft fire when the ventilation system may need to be shut down, at least temporarily.

Industrial Applications

Industrial fire protection can be divided into three kinds of general applications; fire extinguishing, explosion suppression and inertion. While these types of application are similar to those already discussed under Aircraft Applications, industrial use is not encumbered with minimum size and minimum weight restrictions. In addition, provision can usually be made for people to evacuate the fire zone. This makes possible many more alternatives. Indeed, before the discovery and development of the present halogenated agents, especially Halon 1301 and Halon 1211, fire protection was accomplished with water, water/foam, carbon dioxide and dry powder chemicals. From the 1950's until today, the Halons grew rapidly to become the agents of first choice because they extinguished fire rapidly with minimum collateral damage or cleanup after use.

Selection of a Halon replacement for industrial applications is complicated by a serious consideration of:

1. What is the type of fire threat?
2. Is the space occupied or unoccupied normally?
3. If occupied, how fast is egress?
4. How well is the space ventilated, if at all?
5. Is the fire protection portable or a fixed system?
6. How toxic are the candidate agents?
7. What is the relation of NOAEL and LOAEL to the design concentration for extinguishing?
8. What is the agent availability and price?
9. Is there a risk of future phaseout (high GWP, HCFC, or cancellation of production)?

With answers to these questions, consult the "FINAL EPA SNAP RULE" (published on March 18, 1994) and any quarterly update published thereafter. These documents list the agents which are acceptable for total flooding and streaming use along with any special restrictions. Keep in mind that agent choices are still evolving. Presidential Action number 40 has placed an increased environmental regulation concern on global warming gases expressed by the global warming potential number (GWP) assigned to each candidate agent. Some of the most promising candidates, the perfluorocarbons, were placed on severe use restriction because of their high GWP number. Active environmentalist pressure exists, especially in Europe, to phase out the production and use of HCFC's much faster than the present schedule. Each industrial application should be individually evaluated and addressed by a qualified fire protection engineer.

Total Flooding Agents. An acceptable choice for replacing Halon 1301 may be to return to older and previously used technology. Fixed extinguishing systems using carbon dioxide, water sprinklers, dry chemicals, water spray and foam solutions are regulated by OSHA with respect to safe use and pre-discharge alarms to permit satisfactory egress from occupied spaces. The NFPA provides industrial standards for such systems. New gaseous agents which are proposed as potential substitutes for Halon 1301 are listed in Table I with some of the properties that affect their selection process for applications. In addition to the agents in Table I, some alternative fire extinguishing products are being suggested. They include blends which are mixtures of the HCFC's, blends of inert gases, water mist systems, several kinds of powdered aerosols and solid propellant inert gas generators. Since these evaluations are in a continuous mode, the reader is referred to the Stratospheric Protection Division of the U.S. Environmental Protection Agency for the latest information concerning approvals and use restrictions. Reports are published quarterly in the Federal Register.

Table I. Halon 1301 Substitute Agent Choices

<i>Agent</i>	<i>ODP/GWP</i>	<i>LOAEL</i>	<i>NOAEL</i>	<i>Design Concentration</i>	<i>Remarks</i>
HFC-23	0/9000	50	30	16	high GWP
HFC-227ea	0/2050	10.5	9	7	acceptable/ occupied
HFC-125	0/3400	10	7.5	10.9	acceptable/ unoccupied
HFC-134a	0/1200	8	4	12	acceptable/ unoccupied
FC-218	0/6100	>30	30	8.8	evaluation pending
FC-3-1-10	0/5500	>40	40	6.6	high GWP
H-13001	0.01/<1	0.4	0.2	5	evaluation pending
HCFC-22	0.0.5/1600	5	2.5	13.9	phase-out 2010
HCFC-124	0.022/440	2.5	1.0	8.4	phase-out 2015
HBFC-22B1	0.74/----	1.0	0.5	5.3	phase-out 1996

At the present time, fire protection systems and portable units are commercially available which use carbon dioxide, dry chemical powders, HFC-227ea (FM-200), blends of HCFCs or a blend of inert gases (Inergen).

Streaming Agents. Streaming agents are commonly used in portable and the larger wheeled units to dump agent on a fire from a discrete distance. They may also be used mounted in large fire vehicles or as fixed systems. These agents have higher boiling points than the corresponding flooding agents so that there is more liquid in the discharge stream resulting in a much longer distance of throw. The streaming agents commonly used are water, water with foam, dry chemicals and Halon 1211. Finding a replacement for Halon 1211 is a present challenge. As with total flooding agents, replacement streaming agents must be approved for use by the EPA. These approvals are announced in quarterly updates of the SNAP Rule. The latest summary of potential Halon 1211 replacement candidates is in Table II.

Table II. Halon 1211 Substitute Agent Choices

<i>Agent</i>	<i>ODP/GWP</i>	<i>LOAEL</i>	<i>NOAEL</i>	<i>Design Concentration</i>	<i>Remarks</i>
HCFC-124	0.02/440	2.5	1	8.4	Phase-out 2015
HCFC blend C	0.02/1200	2	1	8	phase-out 2015
HCFC blend D	0.02/90	2	1	9	phase-out 2015
Gelled Halocarbon/Dry Chemical Slurries----varied mixes					
HFC-227ea	0/2050	10.5	9	7	approval pending

The first four agents in Table II have been listed as acceptable replacements for Halon 1211. HFC-227ea is listed as pending complete SNAP submission and personal monitoring data required. It is already known to be the least toxic of any of the agents in the list and has been approved as acceptable for total flooding use in occupied spaces. It should be an acceptable agent for streaming use. No HCFCs or blends of HCFCs are permitted for residential use.

Explosion Suppression and Inertion. The term "explosion" is used here in its broad sense which includes deflagration, the flame propagation through a flammable mixture containing gas, vapor and/or aerosol particles. Inertion is the prevention of ignition in the same flammable mixtures. Halon 1301 has been the agent of choice in these applications, but other agents have been used including water, Halon 1011, Halon 1211, Halon 2402, sodium bicarbonate powder and monoammonium phosphate powder. Deflagration suppression and inertion applications require the use of highly engineered systems. Those interested in more detail should read articles written by J.A. Senecal (5). Extinguishers are positioned as close as possible to likely ignition sites. The extinguishers are designed to have a high rate of discharge. A larger quantity of agent is used. All these design features are needed to overwhelm the rapidly developing deflagration or to provide sufficient agent to prevent ignition. The required agent concentration differs according to the fuel characteristics as is shown in Table III.

Table III. A Comparison of Extinguishing and Inerting Concentrations for Halon 1301

<i>Fuel</i>	<i>Extinguishing Concentration (vol%)</i>	<i>Inerting Concentration (vol%)</i>
Methane	5.0	7.7
Propane	5.2	6.7
n-Heptane	5.0	6.9

From the work of Moore et al(6), there is data to compare the inertion concentrations of several potential Halon replacements with Halon 1301 under specific conditions in a large vessel. In NFPA 12a, the recommendation is made to use 110% of the inertion concentration as the design concentration. The cardiac sensitization NOAEL and LOAEL data are included in the comparison with the inertion data in Table IV.

Table IV. Toxicity and Inertion Concentrations

<i>Agent</i>	<i>NOAEL</i>	<i>LOAEL</i>	<i>Inertion Concentration (volume%)</i>	<i>Design Concentration (volume%)</i>
Halon 1301	7.5	10	7	7.7
HFC-227ea	9	10.5	11.5	12.7
HFC-23	30	50	20.5	22.6
FC-3-1-10	40	>40	11	12.1

Because the design inertion concentration of HFC-227ea exceeds its LOAEL concentration, this compound is not a good candidate for use in occupied spaces unless the space is small enough for immediate evacuation. Its physical and thermodynamic properties are such that it might fit into present hardware with minimal changes. FC 3-1-10 is sufficiently non-toxic at concentrations greater than its design requirement to be useful as an agent in these applications. However, its GWP is so high that restrictions under the SNAP Rule make it an unlikely candidate for use. HFC-23 is also safe at concentrations higher than its design requirement. Due to its high vapor pressure, HFC-23 must be used in high strength equipment much like that required for carbon dioxide. That means a re-design of current high rate discharge equipment. Senecal(5) has also cautioned that rapid discharge of HFC-23 in high concentrations will create a potentially severe low temperature condition and a frost-bite hazard. HFC-23 has a very high GWP which puts its use in jeopardy. Since its atmospheric lifetime is only about 280 years compared to 5500 years for FC 3-1-10, the EPA is allowing its use wherever applicable given the current technical or market conditions. Clearly there is a need for a better agent for these applications. The loss of Halon 1301 and Halon 1211 as fire extinguishing agents has generated active research and development in fire technology. It is expected to bring us new and improved fire protection over the next ten years.

Literature Cited.

1. Botteri, B.P. AGARD Lecture Series No.123, 1982.
2. Wordehoff, J. AGARD Conference Proceedings No.467, Onboard Fire- and Explosion Suppression for Fighter Aircraft, 1989.
3. Wyeth, H.W.G. AGARD Lecture Series No.123, Fuel System Protection Methods, 1982.
4. Weinberg, P. AGARD Conference Proceedings No.467, US Navy Aircraft Fire Protection Technology, 1989.
5. Senecal, J.A. The International CFC and Halon Alternatives Conference 1993, pp 767-772.
6. Moore, T.A.; Dierdorff, D.; Skaggs, S.R. Large-Scale Inertion Evaluation of NFPA 2001 Agents, NMERI, The University of New Mexico, Albuquerque, NM, 1993.

RECEIVED July 25, 1995

Chapter 9

Halogenated Fire Suppression Agents

Mark L. Robin

Fluorine Chemicals Department, Great Lakes Chemical Corporation,
1801 Highway 52 Northwest, West Lafayette, IN 47906

This paper summarizes recent efforts by the industrial, academic and governmental sectors in the search for suitable replacements for Halons 1301 and 1211. The current status of potential replacement agents with regard to their fire suppression effectiveness, large scale testing, and regulatory agency approvals is detailed.

This paper reviews recent efforts in the development of replacements for the widely employed fire suppression agents Halon 1301 and Halon 1211. During the past 30 years, the use of these highly efficient, clean, nontoxic fire suppression agents has prevented the loss of human life, and these agents currently protect billions of dollars worth of equipment worldwide. However, because of their recent implication in the destruction of stratospheric ozone, the production and use of these life-saving agents is being severely restricted. As a result, intensive research efforts have been undertaken in the industrial, academic, and governmental sectors with the goal of developing replacements for these agents. This paper reviews these efforts in the area of halon replacements, covering the period from the late 1980s to the present. Several earlier reviews discussing the use of halogenated species as fire suppressants have been published, and the interested reader is directed to these past reviews (1-6).

Historic

Halogenated compounds have been employed as fire suppression agents since the early 1900s when hand-held extinguishers containing carbon tetrachloride were introduced (6). In the late 1920s methyl bromide was found to be more effective than carbon tetrachloride, and was widely employed as a fire suppressant agent by the British in the late 1930s in aircraft protection, and by the German military during World War II for aircraft and marine applications. Suppression systems employing bromochloromethane were also developed in the late 1930s, and were employed by the German Luftwaffe. Bromochloromethane was evaluated in the United States during the late 1930s to the late 1940s and was eventually employed by the US Air Force (7).

0097-6156/95/0611-0085\$12.00/0
© 1995 American Chemical Society

Although extremely effective as fire suppression agents, the relatively high toxicities of methyl bromide and bromochloromethane prompted the US Army to initiate a research program to develop an extinguishing agent which retained the high effectiveness of these agents but was less toxic. Army sponsored research at Purdue University evaluated over 60 candidate agents, most of which were halogenated hydrocarbons, for both fire suppression effectiveness and toxicity (8). As a result of these studies, four agents were selected for further evaluation: bromotrifluoromethane (Halon 1301), bromochlorodifluoromethane (Halon 1211), dibromodifluoromethane (Halon 1202), and 1,2-dibromotetrafluoroethane (Halon 2402). These further evaluations ultimately led to the widespread use of Halon 1301 in total flood and small portable applications, and the use of Halon 1211 in streaming applications.

Halons 1301 and 1211 are characterized by high fire suppression efficiency, low toxicity, low residue formation following extinguishment, low electrical conductivity, and long-term storage stability. Because the agents produce no corrosive or abrasive residues upon extinguishment, they are employed to protect areas such as libraries and museums, where the use of water or solid extinguishing agents could cause secondary damage equal to or exceeding that caused by direct fire damage. Because they are nonconducting they can be used to protect electrical and electronic equipment, and because of their low toxicity they may be employed in areas where egress of personnel may be undesirable or impossible.

Because of their unique combination of properties, the halons have served as near ideal fire suppression agents during the past 30 years. However, due to their implication in the destruction of stratospheric ozone, the Montreal Protocol of 1987 identified Halon 1301 and Halon 1211 as two of a number of halogenated agents requiring limitations of use and production, and an amendment to the original Protocol resulted in the halting of production of Halons 1301 and 1211 on January 1, 1994 (9).

Halon Replacements

The ideal halon replacement, in addition to possessing the desirable characteristics of the halons, is required to have a much lessened environmental impact with regard to its potential for ozone depletion, and also with regard to its potential for contributing to global warming. Hence, one possible set of requirements for the ideal halon replacement is as follows:

1. Highly efficient fire suppression
2. Nontoxic
3. Clean (no residue)
4. Nonconducting
5. Storage stable
6. Zero ozone depletion potential (ODP)
7. Zero global warming potential (GWP)
8. Manufacturable at reasonable cost

To date no replacement agent, halogenated or otherwise, has been found which satisfies all of the above requirements, although replacements have been found that match many of the above criteria. The various agents investigated as possible halon

replacements are discussed below, where they are divided into the chemical class of compound examined. Preliminary testing of the fire suppression characteristics of a potential candidate is typically performed employing the laboratory-scale cup burner apparatus, with n-heptane as the fuel. The cup burner apparatus has been described in detail by Hirst and Booth (10), and more recently by Sato, et. al. (11).

Bromine-Based Halon Replacements

Hydrobromofluorocarbons (HBFCs). Perhaps the first compounds considered by researchers for the replacement of the halons were the hydrobromofluorocarbons (HBFCs). The bromine atom is known to provide high fire suppression characteristics, and the fluorine atom is known to impart stability and volatility. The introduction of hydrogen into the molecular structure provides a means for tropospheric destruction of the molecule via abstraction of the hydrogen atom by tropospheric hydroxyl radicals. Destruction of the HBFC molecule in the troposphere would prevent the bromine atom from reaching the stratosphere, where it could participate in the destruction of ozone. Table I shows the properties of those HBFCs receiving attention in the scientific community. Laboratory and large scale testing of the leading candidates in this class, CHBrF_2 (12-15) and CF_3CHBrF (16) demonstrated that these agents could indeed provide fire suppression capabilities essentially equal to that of the halons.

Table I. Hydrobromofluorocarbons

<i>Formula</i>	<i>MW</i>	<i>bp (°C)</i>	<i>Ext. Conc.^a % v/v</i>	<i>ODP</i>	<i>LC₅₀ % v/v</i>
CH_2FBr_2	191.84	65 ^b	1.8 ^b	<0.2 ^b	-
CHBrF_2	130.92	-15.5 ^c	3.9 ^c	0.74 ^d	10.8(4 h) ^c
$\text{CF}_3\text{CH}_2\text{Br}$	162.94	26 ^e	3.5 ^f	-	11.7(10 m) ^g
CF_3CHBr_2	241.83	73 ^b	1.9 ^b	<0.1 ^b	1.2(30m) ^h
CF_3CHBrF	180.94	8.6 ^e	3.6 ⁱ	0.3-0.4 ⁱ	-
$\text{BrCF}_2\text{CHF}_2$	180.94	10.8 ^e	3.2 ^j	-	18.7(30 m) ^h

^aCup burner extinguishing concentration, n-heptane fuel.

^bReference 17.

^cReference 18.

^dReference 19.

^eReference 20.

^fReference 21.

^gReference 22.

^hReference 23.

ⁱReference 24.

^jReference 25.

The introduction of a hydrogen atom into the molecular structure, while providing the desired reduction in ODP, results in an increase in the toxicity of the species compared

to the totally halogenated molecule (cf. Halon 1301, 4 hour $LC_{50} = 80\%$, versus $CHBrF_2$, 4 hour $LC_{50} = 10.8\%$). Complete tropospheric destruction of HBFCs would prevent the molecule from reaching the stratosphere and participating in the depletion of ozone; however, atmospheric models predict that small amounts of HBFCs would survive transport into the stratosphere, so that while not as ozone unfriendly as molecules lacking a hydrogen atom, the HBFCs are characterized by a nonzero ODP.

Prior to legislation prohibiting the production and use of such low ODP compounds, a low, nonzero ODP was thought to be acceptable, and as a result the development of HBFCs was undertaken by several institutions. However, the classification of HBFCs as Class I substances by the US EPA, with production banned by January 1, 1996, has essentially eliminated the HBFCs from consideration as halon replacements.

Brominated Olefins. Based upon the well known rapid attack of hydroxyl radicals on double bonds, brominated olefins were proposed as possible replacements for the halons (17). Rapid reaction with hydroxyl radicals leads to shortened atmospheric lifetimes and hence a decreased ODP. Because of the difficulty in synthesizing members of this class of compounds, very few brominated olefins have been examined for flame suppression, as evidenced in Table II. Suspected high toxicities, difficult preparation and subsequent high cost of manufacture, and the nonzero ODP of these agents have essentially eliminated these agents from consideration, and no commercial interest in their use as fire suppression agents appears to exist at the present time.

Table II. Bromo-olefins^a

<i>Formula</i>	<i>MW</i>	<i>bp (°C)</i>	<i>Ext. Conc.^b</i> <i>% v/v</i>
$CH_2=CHCF_2Br$	156.96	42	-
$BrCH=CHCF_3$	174.95	40	-
$CH_2=CHCF_2CF_2Br$	206.96	55	3.5
$CH_2=CBrCF_2Br$	235.85	100	-
$CH_2=CHCFClCF_2Br$	223.42	99	4.5
$BrCH=CBrCF_3$	253.84	96	-
$CH_2=CBrCF_3$	174.95	-	8.5 ^c
$CF_2=CHCF_2Br$	192.94	35	-

^a Reference 17.

^b n-heptane.

^c Reference 26.

Nonvolatile Precursors to Fire Extinguishing Agents. In a further attempt to provide efficient suppression via inclusion of bromine in the agent, while maintaining a minimal ODP, nonvolatile bromine-containing species have been proposed which upon exposure to the flame front thermally decompose to release efficient suppression species such as HBr or the HBFCs. Table III lists several of the nonvolatile precursors

considered, along with extinguishing values from the Tyndall Air Force Base cup burner (27).

Difficult syntheses and the subsequent high cost of manufacture, and the suspected high toxicity of these agents have essentially eliminated these agents from consideration, and no commercial interest in their use as fire suppression agents appears to exist at the present time.

Table III. Nonvolatile Precursors to Fire Extinguishing Agents

<i>Formula</i>	<i>MW</i>	<i>bp (°C)</i>	<i>Ext. Conc., TAFB burner, % v/v</i>
CF ₂ BrCl	165.36	-4	1.4
BrCF ₂ CO ₂ C ₂ H ₅	202.98	170	2.2
CFBr ₂ CO ₂ C ₂ H ₅	263.89	190	1.0
BrCH ₂ CH ₂ CHBrCH ₃	215.92	175	7.9

Source: Adapted from Reference 27.

Chlorine-Based Halon Replacements

Recognizing the lessened threat to stratospheric ozone from the chlorine atom compared to the bromine atom, and realizing that impending legislation would likely lead to a banning of HBFCs, researchers turned to the investigation of the fire suppression properties of hydrochlorofluorocarbons (HCFCs), many of which were undergoing development as replacements for chlorofluorocarbons in refrigeration or foam blowing applications. HCFCs investigated as halon replacements are listed in Table IV. HCFC Blend A (trade name NAF S-III) is a blend of CF₂HCl, CF₃CHCl₂, CF₃CH₂Cl and isopropenyl-1-methylcyclohexene (weight ratio 82:4.75:9.5:3.75).

Table IV. Hydrochlorofluorocarbons

<i>Formula</i>	<i>MW</i>	<i>bp (°C)^b</i>	<i>Ext. Conc.^a</i>			
			<i>% v/v</i>	<i>ODP^d</i>	<i>NOAEL^d</i>	<i>LOAEL^d</i>
CHClF ₂	86.47	-40.7	11.6 ^d	0.05	2.5	5.0
CF ₃ CHCl ₂	152.93	28.7	6.3 ^e	0.02	1.0	2.0
CF ₃ CH ₂ Cl	136.47	-12	7.0 ^d	0.022	1.0	2.5
HCF ₂ CF ₂ Cl	136.47	-10.2	7.2 ^g	-	-	-
HCFC Blend A	92.90	-38.3 ^c	11.6 ^f	-	10	10

^an-heptane.

^bReference 20.

^cReference 28.

^dReference 19.

^eReference 29.

^fReference 30.

^gReference 31.

Except for HCFC-123 (CF₃CHCl₂), the acute inhalation toxicity of the HCFCs is relatively low (high LC₅₀), and the primary toxicological concern when employing these agents in fire suppression applications is cardiac sensitization, typically expressed as the No Observable Adverse Effect Level (NOAEL) and the Lowest Observable Adverse Effect Level (LOAEL). The National Fire Protection Association (NFPA) under NFPA Standard 2001 forbids the use of fire suppression agents in total flooding applications in normally occupied areas at concentrations exceeding the NOAEL (28). As a result, HCFC-22 (CF₂HCl), HCFC-124 (CF₃CHClF) and HCFC-123 (CF₃CHCl₂) are deemed unsuitable for use as total flooding agents in occupied areas under the criteria of NFPA 2001.

HCFC-123 has been extensively investigated as a replacement for Halon 1211 in streaming applications (32-34). Under the provisions of the Clean Air Act, HCFC-22 is scheduled for production phaseout by the year 2020, and all other HCFCs are currently scheduled for phase out by the year 2030. Hence the HCFCs can be regarded as transitional agents only.

Iodine-Based Halon Replacements

Several researchers have examined the fire suppression effectiveness of the iodofluorocarbons (35-37). Recent studies (38,39) have demonstrated that while iodine atoms readily attack ozone, the photolytic instability of the C-I bond in CF₃I results in only a small portion of the CF₃I released at ground level surviving to reach the stratosphere. As a result, CF₃I is characterized by a small, but nonzero ODP. The decreased stability of the iodofluorocarbons compared to bromine or chlorine containing fluorocarbons is reflected in their increased toxicities, as evidenced by the LC₅₀ values in Table V.

Table V. Iodofluorocarbons

Formula	MW	bp (°C) ^b	Ext. Conc. ^a			LC ₅₀
			% v/v	NOAEL	LOAEL	% v/v
CF ₃ I	195.9	-22.5 ^c	3.0	0.2 ^d	0.4 ^d	27.4(15 m) ^d
CF ₃ CF ₂ I	245.9	12	2.1	0.02 ^e	0.05 ^e	7.5(1 h) ^f
CHF ₂ I	177.9	22	-	-	-	-
(CF ₃) ₂ CFI	295.9	40	3.2	-	-	0.09(1 h) ^f
n-C ₃ F ₇ I	295.9	41	3.0	-	-	3.3(2 h) ^e
CH ₂ FI	159.9	52	-	-	-	-
n-C ₄ F ₉ I	345.9	67	-	-	-	>0.5(1 h) ^f
n-C ₆ F ₁₃ I	445.9	117	2.5	-	-	>1.35(1 h) ^f

^an-heptane; from reference 17.

^bReference 17.

^cReference 20.

^dReference 40.

^eReference 41.

^fReference 42.

While the iodofluorocarbons are extremely efficient fire suppression agents, their inherent instability, as evidenced by their relatively high inhalation toxicity, presents serious problems. One of the less toxic iodofluorocarbons on the basis of its LC₅₀, CF₃I has been shown to be an extremely potent cardiotoxicant, resulting in death to test animals at concentrations as low as 0.4 % v/v. As a result, its use in occupied areas is unlikely to be permitted. Reported storage stability problems, as well as suspected high manufacturing costs present a significant hurdle to its use in unoccupied areas, although CF₃I is currently being investigated by the National Institute of Standards and Technology (NIST) in engine nacelle and dry bay applications.

Zero ODP Halon Replacements

As the regulatory noose tightened with passing time, it became apparent that a viable halogenated fire suppression agent would be required to have a zero ODP, and hence could not contain chlorine or bromine. Hence the development of perfluorocarbon (PFC) and hydrofluorocarbon (HFC) fire suppression agents.

Research carried out at the National Institute of Standards and Technology (NIST) provides an example of this progression. In 1990, researchers at NIST identified approximately 100 gases and/or liquids thought to affect flame suppression capability (43), and also described a set of screening procedures for evaluation of potential candidates (44). This exploratory list included saturated and unsaturated halocarbons, halogenated hydrocarbons containing single and double bonded oxygen, sulfur halides, phosphorous compounds, silicon compounds, germanium compounds, metallic compounds and inert gases. Examination of these chemicals provided a basis for the search for alternatives to the current commercial halons. Further studies by NIST researchers ultimately identified thirteen core chemicals deemed suitable for investigation for the protection of engine nacelle and dry bays (21): sodium bicarbonate and twelve halogenated compounds, consisting of four PFCs, five HFCs, two HCFCs and a binary HFC blend. Following further evaluation, NIST is currently recommending three compounds for these specific aircraft applications (45): one PFC and two HFCs (CF₃CF₂CF₃, CF₃CF₂H, and CF₃CHF₂CF₃).

Perfluorocarbons. The properties of perfluorocarbons currently being evaluated as fire suppression agents are shown in Table VI. From a toxicological standpoint the PFCs are attractive, as they are generally physiologically inert, as evidenced by their low inhalation toxicity and low potential for cardiac sensitization. However, the high stability of the PFCs also leads to their being characterized by very long atmospheric lifetimes; unlike the HCFCs or HFCs, the PFCs contain no hydrogen and hence are not decomposed in the troposphere. As a result of their long atmospheric lifetimes, the global warming potential of these agents is high.

Hydrofluorocarbons. Hydrofluorocarbons evaluated as halon replacements are shown in Table VII. The introduction of hydrogen into the molecular structure significantly reduces the atmospheric lifetime, and increases the potential for cardiac sensitization compared to the fully fluorinated (PFC) analog. HFC-125 and HFC-134a, with design concentrations (cup burner plus 20%) exceeding their NOAEL

values, are not approved under NFPA 2001 for use as total flood agents in occupied areas.

Table VI. Perfluorocarbons

<i>Formula</i>	<i>MW</i>	<i>bp (°C)^a</i>	<i>Ext. Conc.^b</i>	<i>Atmospheric</i>	<i>100 Year</i>
			<i>% v/v</i>	<i>Lifetime, years^c</i>	<i>HGWP</i>
C ₂ F ₆	138.02	-78.2	8.1	>10,000	-
n-C ₃ F ₈	188.03	-36.7	6.3	-	-
n-C ₄ F ₁₀	238.04	-2.2	5.3	2600 ^d	5500 ^e
n-C ₅ F ₁₂	288.03	29.2	-	4100	-
n-C ₆ F ₁₄	338.07	58	4.4 ^e	3100	5200 ^e

^aReference 20.

^bn-heptane, Reference 21.

^cReference 46.

^dLower limit; Reference 46.

^eReference 19.

Table VII. Hydrofluorocarbons

<i>Formula</i>	<i>MW</i>	<i>bp (°C)</i>	<i>Ext. Conc.^a</i>			<i>LC₅₀ (4h)</i>
			<i>% v/v</i>	<i>NOAEL^b</i>	<i>LOAEL^b</i>	<i>% v/v</i>
CHF ₃	70.01	-82.2	12.0	30	50	66
CF ₃ CH ₂ F	102.03	-26.5	10.5	4.0	8.0	50
CF ₃ CF ₂ H	120.02	-48.5	9.4	7.5	10.0	70
CF ₃ CH ₂ CF ₃	152.04	-0.7 ^c	6.5 ^d	-	-	-
CF ₃ CHFCF ₃	170.09	-16.4	5.8	9.0	>10.5	80

^an-heptane, Reference 19.

^bReference 19.

^cReference 47.

^dReference 21.

Intermediate and Large Scale Testing

Following initial laboratory-scale screening, typically via the cup burner technique, promising candidates are naturally subjected to intermediate and full scale fire suppression testing. Extensive full scale testing of both streaming and total flooding agents has been undertaken.

Streaming Agents. A major effort under the United States Air Force Halon Alternatives Program was the development of Halon 1211 replacements. Following laboratory-scale investigations of fire suppression by the cup burner and the Laboratory-Scale Discharge Extinguishment (LSDE) apparatus (33), field testing of candidates on JP-4 pool fires up to 150 sq. ft was performed under the sponsorship of the United States Air Force. These early investigations, including the examination of

HCFC-123 (CF_3CHCl_2) and several HCFC-123 based blends, indicated that HCFC-123 could meet the needs of the USAF, but concerns over its toxicity led to further investigations involving the C_4 through C_6 PFCs (34). These field scale tests in turn demonstrated that only $n\text{-C}_5\text{F}_{12}$ and $n\text{-C}_6\text{F}_{14}$ had sufficient volatility to be employed as streaming agents, with the best performance observed with the $n\text{-C}_6\text{F}_{14}$ compound. Despite further field testing of both CF_3CHCl_2 and $n\text{-C}_6\text{F}_{14}$, Air Force groups meeting at Tyndall AFB in April of 1994 were forced to conclude that no near-term candidate was completely acceptable, and that the Air Force would retain Halon 1211 until a suitable replacement became available (48). To date a suitable replacement has not been identified.

Total Flooding Agents. Following the selection of possible candidates based upon laboratory suppression studies, candidates remaining attractive were naturally the subject of intermediate and full scale fire suppression tests. Promising candidates have also been examined in greater detail with regard to their physical, toxicological and environmental properties.

The majority of intermediate and large-scale fire suppression testing has been reported for Class B fire suppression employing the hydrofluorocarbon agents CHF_3 , $n\text{-C}_4\text{F}_{10}$ and $\text{CF}_3\text{CHF}_2\text{CF}_3$. Large-scale fire suppression testing of $\text{CF}_3\text{CHF}_2\text{CF}_3$ was reported by Robin in 1991 (15), and intermediate scale testing of $n\text{-C}_4\text{F}_{10}$ and $\text{CF}_3\text{CHF}_2\text{CF}_3$ was reported by Ferreira, et. al., in 1992 (49). These initial studies, performed by the agent manufacturers, were followed by intermediate and large scale testing by DiNunno, et. al. (50), of CHF_3 , $\text{CF}_3\text{CF}_2\text{H}$, $\text{CF}_3\text{CHF}_2\text{CF}_3$, $n\text{-C}_3\text{F}_8$, and $n\text{-C}_4\text{F}_{10}$, and intermediate scale testing of CHF_3 , $\text{CF}_3\text{CF}_2\text{H}$ and $n\text{-C}_4\text{F}_{10}$ by Sheinson, et. al., of the Naval Research Laboratories (51). Moore, et al. (30), have also reported intermediate scale testing of CHF_3 , $n\text{-C}_4\text{F}_{10}$, $\text{CF}_3\text{CHF}_2\text{CF}_3$, and HCFC Blend A. Employing standard fire growth rates and the results of their intermediate scale testing, DiNunno, et. al., have developed scaling factors for HF production as a function of fire size and have employed these to predict expected HF concentrations for slow, medium and fast fire growth rates (52). Rapid detection and discharge were concluded to result in decreased production of HF.

Full scale testing of CHF_3 , $n\text{-C}_4\text{F}_{10}$, $\text{CF}_3\text{CHF}_2\text{CF}_3$, and the HCFC Blend A were carried out by Coast Guard personnel in 1994, and full scale testing of CHF_3 , $n\text{-C}_4\text{F}_{10}$ and $\text{CF}_3\text{CHF}_2\text{CF}_3$ on the Navy's full scale fire research ship, the ex-USS Shadwell, were completed in late 1994.

A general observation from these intermediate and large scale tests is the increased production of the decomposition product HF from the HFCs and PFCs compared to Halon 1301. In general, for a given fire scenario, HF levels produced upon extinguishment by the HFCs and PFCs are approximately 5-10 times those formed upon extinguishment by Halon 1301. It is important to keep in mind, however, that many of these tests involve extremely large fires under very specialized conditions such that extinguishment by Halon 1301 itself can lead to the production of HF in amounts approaching ten thousand parts per million. For some of these fires it is questionable whether these high HF levels have any significance when consideration is given to the enormous output of heat and combustion products associated with these large fires and the damage to equipment and personnel these factors alone could cause. The generation of HF from the HFCs and PFCs can be limited by employing a more

rapid discharge, and this forms the basis for the National Fire Protection Association requirement under NFPA 2001 that such agents be discharged in less than 10 seconds. More rapid detection and system actuation can also minimize HF generation.

NIST has carried out extensive testing of C_2F_6 , $n-C_3F_8$, $n-C_4F_{10}$, cyclo- C_4F_8 , CF_3CF_2H , CF_3CH_2F , CF_3CHF_2 , $CF_3CH_2CF_3$, $CHClF_2$, CF_3CHClF and a CH_2F_2/CF_3CF_2H blend, including fire suppression, agent discharge, and compatibility studies as part of its program to develop agents for engine nacelle and dry bay applications (21). NIST is currently recommending $n-C_3F_8$, CF_3CF_2H and CF_3CHF_2 for full scale testing by the US Air Force in dry bay and engine nacelle applications.

Fire suppression testing of CF_3CHF_2 on typical electronic data processing (EDP) facility fires (wire bundles, magnetic tapes, PC boards) has demonstrated that minimal HF (< 50 ppm) is produced upon extinguishment of these Class A fires (53). As the tests were conducted under worst case conditions of zero air movement and hence long detection times, real world fire scenarios are expected to produce even less HF. This is in agreement with the conclusion of Skaggs and Moore (40) that for typical computer rooms and offices HF concentrations from suppression with the HFCs and PFCs at their design concentrations of cup burner plus 20% will be comparable to that observed with Halon 1301.

Regulatory and Approval Agency Status

In order to obtain widespread acceptance, a halon replacement must obtain the necessary governmental and fire protection industry approvals. In the United States, governmental approval of halon replacements is granted under the US EPA SNAP program. The National Fire Protection Association (NFPA), through its NFPA 2001 Standard on Clean Agent Fire Extinguishing Systems, establishes the minimum requirements for total flooding clean fire extinguishing systems. In addition, many end users require that fire suppression systems employing halon replacements be listed or approved by independent testing agencies, for example Underwriters Laboratories or Factory Mutual. The current status of the halogenated fire suppression agents with respect to regulatory and listings/approvals agencies is discussed below.

US EPA SNAP Program (19).

Streaming Agents. Halogenated fire suppression agents currently approved for use as streaming agents under the US EPA Significant New Alternatives Policy (SNAP) are shown in Table VIII. Under the current SNAP program, HCFCs cannot be employed in residential extinguishers, but are allowed in commercial, watercraft and aircraft use in portables. Under SNAP, PFCs are acceptable for nonresidential use only when other alternatives are not technically feasible. Phase out of $CHBrF_2$ is scheduled for January 1, 1996, and the HCFCs are currently scheduled for phase out in 2030. Approval of HFC-227ea in streaming applications is currently pending.

Flooding Agents. Halogenated fire suppression agents currently approved for use as total flooding agents under the US EPA SNAP program are shown in Table IX. Phase out of $CHBrF_2$ is scheduled for January 1, 1996, and the HCFCs are currently

scheduled for phase out in 2030. Although all the agents listed in Table IX are acceptable under SNAP as total flood agents in unoccupied areas, under the criteria of NFPA 2001 only CHF₃, CF₃CHF₂CF₃, HCFC Blend A and n-C₄F₁₀ are acceptable for use as total flood agents in normally occupied areas.

Table VIII. Streaming Agents Acceptable Under SNAP

<i>Agent</i>	<i>Formula</i>	<i>Trade Name</i>	<i>SNAP Acceptability</i>
HBFC-22B1	CHBrF ₂	Great Lakes "FM-100"	acceptable
HCFC-123	CF ₃ CHCl ₂	DuPont "FE-232"	acceptable
HCFC-124	CF ₃ CHClF	DuPont "FE-241"	acceptable
HCFC Blend B	a	American Pacific "Halotron I"	acceptable
HCFC Blend C	b	NAFG ^c "NAF P-III"	acceptable
HCFC Blend D	d	NAFG ^c "Blitz"	acceptable
FC-5-1-14	n-C ₆ F ₁₄	3M Co. "CEA 614"	acceptable ^e

^aPrimarily HCFC-123.

^bHCFC-123, HCFC-124, HFC-134a, and proprietary additive.

^cNorth American Fire Guardian.

^dHCFC-123 plus proprietary additive.

^ePFCs acceptable only when other alternatives are not technically feasible.

Table IX. Total Flooding Agents Acceptable Under SNAP

<i>Agent</i>	<i>Formula</i>	<i>Trade Name</i>	<i>SNAP Acceptability</i>
HBFC-22B1	CHBrF ₂	Great Lakes "FM-100"	acceptable ^a
HCFC-124	CF ₃ CHClF	DuPont "FE-241"	acceptable ^a
HCFC Blend A	b	NAFG ^c "NAF S-III"	acceptable
HFC-23	CHF ₃	DuPont "FE-13"	acceptable
HFC-125	CF ₃ CHF ₂	DuPont "FE-25"	acceptable ^a
FC-3-1-10	n-C ₄ F ₁₀	3M Co. "CEA 410"	acceptable ^d
HFC-227ea	CF ₃ CHF ₂ CF ₃	Great Lakes "FM-200"	acceptable

^aCannot be employed as total flood agent in occupied areas under NFPA 2001.

^bHCFC-123, HCFC-124, HFC-134a, and additive.

^cNorth American Fire Guardian.

^dPFCs acceptable only when other alternatives are not technically feasible.

NFPA 2001 (28). NFPA 2001 Standard on Clean Agent Fire Extinguishing Systems contains minimum requirements for total flooding clean fire extinguishing systems. Halogenated agents addressed in the standard are CHBrF₂, CHF₃, CF₃CHClF, CF₃CF₂H, HCFC Blend A, CF₃CHF₂CF₃ and n-C₄F₁₀. NFPA 2001 requires that for use as a total flooding agent in a normally occupied areas, the design concentration cannot exceed the NOAEL of the agent. Hence, the only halogenated agents approved for use in total flood systems for normally occupied areas under NFPA 2001 are CHF₃, CF₃CHF₂CF₃, n-C₄F₁₀ and HCFC Blend A.

Underwriters Laboratories/Factory Mutual. Currently UL International listings and Factory Mutual approvals have been granted for only two halogenated fire suppression agents, CF_3CHF_2 and $\text{n-C}_4\text{F}_{10}$. These listings and approvals follow the completion of stringent testing of fire suppression, system operation and materials compatibility, conducted under the direction of Underwriters Laboratories and Factory Mutual.

The Future

Based upon a consideration of current and anticipated future legislation, it is generally accepted that viable long term replacements for Halon 1301 and Halon 1211 will be required to have a zero ODP. Choices of halogenated hydrocarbons are thus narrowed to the classes of PFCs and HFCs. As happened in the case of the ozone depletion issue, concern over global warming issues will likely increase with the passage of time, and may ultimately narrow the choice even further, leaving only the HFCs as acceptable halogenated fire suppression agents. Indications of this trend are already apparent from an examination of the US EPA SNAP policy, which currently allows the use of PFCs only when other alternatives are not technically feasible.

Literature Cited

1. *Halogenated Fire Suppressants*, Gann, R. G., Ed.; ACS Symposium Series 16; American Chemical Society: Washington, DC, 1975.
2. McHale, E. T. *Fire Res. Abstracts and Reviews* **1969**, *11*, 90.
3. Ford, C. L. In *Halogenated Fire Suppressants*; Gann, R. G., Ed.; ACS Symposium Series 16; American Chemical Society: Washington, 1975; pp 1-63.
4. Engibous, D. L.; Torkelson, T. R. "A Study of Vaporizable Extinguishants"; WADC Technical Report 59-463, 1960.
5. Musik, J. K.; Williams, F. W. "The Use of Halons as Fire Suppressants-A Literature Survey"; Naval Research Laboratory, 10/5/77.
6. Wharry, D.; Hirst, R. *Fire Technology: Chemistry and Combustion*, Inst. Fire Engineers: Leicester, England, 1974.
7. Strasiak, R. "The Development History of Bromochloromethane"; WADC Technical Report 53-279, 1954.
8. "Final Report on Fire Extinguishing Agents for the Period September 1, 1947 to June 30, 1950"; Purdue Research Foundation, Contract W-44-099-eng-507.
9. Harrington, J. L. *NFPA Journal* **1993**, *March/April*, 38.
10. Hirst, R.; Booth, K. *Fire Technology* **1977**, *13*, 296.
11. Saso, Y.; Sato, Y.; Iwata, Y. *Ibid.* **1993**, *29*, 22.
12. Robin, M. L. "FM-100: An Efficient Halon Alternative For Use in Portable and Total Flooding Extinguishing Systems," Presented at the 10th Winter Fluorine Conference, ACS Fluorine Division, St. Petersburg Beach, FL, February 1991.
13. Robin, M. L. "Halon Alternatives: Laboratory Evaluation by the Cup Burner Method," Presented at the 200th National ACS Meeting, Washington, DC, August 1990.
14. Robin, M. L. "Evaluation of Halon Alternatives," *Proceedings of the 1991 Halon Alternatives Technical Working Conference*, Albuquerque, NM, April 30-May 1, 1991.

15. Robin, M. L. "Large Scale Testing of Halon Alternatives," *Proceedings of the 1991 International CFC & Halon Alternatives Conference*, Baltimore, MD, Dec. 3-5, 1991.
16. Jones, P.; Winterton, N. "Clean Agent Fire Extinguishants: Further Study of Breakdown Products," *Proceedings of the 1991 International CFC & Halon Alternatives Conference*, Baltimore, MD, December 3-5, 1991.
17. Nimitz, J. S.; Skaggs, S.; Tapscott, R. E. "Next-Generation High-Efficiency Halon Alternatives," *Proceedings of the 1991 International Conference on CFC and Halon Alternatives*, Baltimore, MD, December 3-5, 1991.
18. Robin, M. L. "Halon Alternatives: Recent Technical Progress," *Proceedings of the 1992 Halon Alternatives Technical Working Conference*, Albuquerque, NM, May 12-14, 1992.
19. *Federal Register*, Vol. 59, No. 53, Friday, March 18, 1994.
20. Smart, B. E.; Fernandez, R. E. "Fluorinated Aliphatic Compounds," In *Kirk-Othmer Encyclopedia of Chemical Technology*, 4th edition, Vol. 11, John Wiley, New York, 1994.
21. Grosshandler, W. L.; Gann, R. G.; Pitts, W. M. "Evaluation of Alternative In-flight Fire Suppressants for Full-Scale Testing in Simulated Aircraft Engine Nacelles and Dry Bays," *NIST Special Publication 861*, April 1994.
22. Robbins, B. H. *J. Pharm. Exp. Ther.* **1946**, 86, 197.
23. Davies, R. H.; Bagnall, R. D.; Bell, W.; Jones, W. G. M. *Int. J. Quantum Biology Symp.* **1976**, 3, 171.
24. Tapscott, R. E. "Replacement Agents - An Historical Overview," *Proceedings of the 1992 Halon Alternatives Technical Working Conference*, Albuquerque, NM, May 12-14, 1992.
25. Robin, M. L.; Iikubo, Y. U.S. Patent 5,080,177, 1992.
26. Skaggs, S.; Heinonen, E.; Tapscott, R. E.; Smith, E. D. "Research and Development for Total Flood Halon 1301 Replacements for Oil and Gas Production Facilities at the Alaskan North Slope," *Proceedings of the 1991 International Conference on CFC and Halon Alternatives*, Baltimore, MD, December 3-5, 1991.
27. Bannister, W. W.; Jahngen, E. G.; Kibert, C.; Nelson, D.; Mitchell, B.; Dierdorf, D. "Recent Advances in Development of Non-Volatile Precursors (NVPS) to Alternate Halon Fire Extinguishing Agents with Reduced Global Environmental Impacts," *Proceedings of the 1993 Halon Alternatives Technical Working Conference*, Albuquerque, NM, May 11-13, 1993.
28. NFPA 2001 Standard on Clean Agent Fire Extinguishing Systems, NFPA, 1994.
29. Skaggs, S.; Tapscott, R. E.; Moore, T. A. "Technical Assessment for the SNAP Program," *Proceedings of the 1992 Halon Alternatives Technical Working Conference*, Albuquerque, NM, May 12-14, 1992.
30. Moore, T. A.; Dierdorf, D.; Skaggs, S. "Intermediate Scale (645 ft³) Fire Suppression Evaluation of NFPA 2001 Agents," *Proceedings of the 1993 Halon Alternatives Technical Working Conference*, Albuquerque, NM, May 11-13, 1993.
31. Robin, M. L.; Iikubo, Y. U.S. Patent 5,137,095, 1992.
32. Brashear, W. T.; Vinegar, A. "Metabolism and Pharmacokinetics of Halon 1211 and its Potential Replacements HCFC-123 and Perfluorohexane," *Proceedings of the 1992 Halon Alternatives Technical Working Conference*, Albuquerque, NM, May 12-14, 1992.
33. Tapscott, R. E.; Floden, J. "Progress Toward Halon 1211 Alternatives," Presented at Halon and Environment '90, 2nd Conference on the Fire Protecting Halons and the Environment, Geneva, Switzerland, October 1-3, 1990.

34. Floden, J.; Tapscott, R. E. "Evaluation of Selected Perfluorocarbons as Streaming Agents," *Proceedings of the 1991 International Conference on CFC and Halon Alternatives*, Baltimore, MD, December 3-5, 1991.
35. Kibert, C. J. "Fluoroiodocarbons as Halon 1211/1301 Replacements- An Overview," *Proceedings of the 1994 Halon Options Technical Working Conference*, Albuquerque, NM, May 3-5, 1994.
36. McIlloy, A. "Ignition Suppression by CF₃Br and CF₃I of H₂/O₂/Ar- Mixtures: Detailed Studies of Time and Space Resolved Radical Profiles," *Proceedings of the 1994 Halon Options Technical Working Conference*, Albuquerque, NM, May 3-5, 1994.
37. Nimitz, J. "Trifluoromethyl Iodide and Its Blends as High-Performance, Environmentally Sound Halon 1301 Replacements," *Proceedings of the 1994 Halon Options Technical Working Conference*, Albuquerque, NM, May 3-5, 1994.
38. Solomon, S.; Ravishankara, A. R.; Garcia, R. R. *J. Geophys. Res.* **1994**, *99*, 20491.
39. Solomon, S.; Ravishankara, A. R.; Garcia, R. R. *J. Geophys. Res.* **1994**, *99*, 20929.
40. Skaggs, S.; Moore, T. A. "Toxicological Properties of Halon Replacements," Presented at the 208th ACS National Meeting, Washington, DC, August 21, 1994.
41. Skaggs, S.; Dierdorf, D.; Tapscott, R. E. "Update on Iodides as Fire Extinguishing Agents," *Proceedings of the 1993 International CFC & Halon Alternatives Conference*, Washington, DC, Oct. 20-22, 1993.
42. Ulm, K. *Spec. Chem.* **1988**, *8*, 418.
43. Pitts, W. M., et al., "Construction of an Exploratory List of Chemicals to Initiate the Search for Halon Alternatives," *NIST Technical Note 1279*, 1990.
44. Gann, R. G., et al., "Preliminary Screening Procedures and Criteria for Replacements for Halons 1211 and 130 1," *NIST Technical Note 1278*, 1990.
45. *Chemical and Engineering News*, September 19, 1994, p. 31.
46. Ravishankara, A. R.; Solomon, S.; Turnipseed, A.; Warren, R. *Science* **1993**, *259*, 194.
47. Henne, A. L.; Waalkes, T. P. *J. Am. Chem. Soc.* **1946**, *68*, 496.
48. Skaggs, S.; Dierdorf, D.; Moore, T. A. "Advanced Streaming, Agent Program," *Proceedings of the 1994 Halon Options Technical Working Conference*, Albuquerque, NM, May 3-5, 1994.
49. Ferreira, M.; Pignato, J.; Pike, M. "An Update on Thermal Decomposition Product Results Utilizing PFC-410, " Presented at the International CFC and Halon Alternatives Conference, Washington, DC , 1992.
50. DiNunno, P.; Forssell, E.; Peatross, M.; Maynard, M. "Evaluation of Alternative Agents for Halon 1301 in Total Flooding Fire Suppression Systems," *Proceedings of the 1993 Halon Alternatives Technical Working Conference*, Albuquerque, NM, May 11-14, 1993.
51. Sheinson, R. S. "Halon 1301 Replacement Total Flooding Fire Testing: Intermediate Scale," *Proceedings of the 1994 Halon Options Technical Working Conference*, Albuquerque, NM, May 3-5, 1994.
52. Hanauskas, C.; Forssell, E.; DiNunno, P. "Hazard Assessment of Thermal Decomposition Products of Halon Alternatives," *Proceedings of the 1993 Halon Alternatives Technical Working Conference*, Albuquerque, NM, May 11 14, 1993.
53. "Hazard Assessment of Thermal Decomposition Products of FM-200™ in Electronics and Data Processing Facilities," Hughes Associates, Inc., 1/16/95.

RECEIVED June 12, 1995

Chapter 10

Toxicological Properties of Halon Substitutes

Stephanie R. Skaggs¹, Ted A. Moore, and Robert E. Tapscott

Center for Global Environmental Technologies, New Mexico Engineering Research Institute, University of New Mexico, Albuquerque, NM 87131

Halon fire extinguishing agents are used throughout the world to protect valuable electronics, oil and gas production operations, military systems, as well as a number of other critical facilities. Unfortunately, halons deplete stratospheric ozone, causing destruction at 3 to 16 times the rate of CFC-11 (a common refrigerant). As a consequence, the production of halons was prohibited on December 31, 1993 by an international treaty, the Montreal Protocol. This ban on halon production resulted in a search for replacement chemicals for firefighting and explosion protection applications. Replacements must satisfy the following three criteria in order to be successful candidates: effectiveness, cleanliness, and environmental acceptability (low ozone depletion and global warming potentials). It is also necessary that a replacement agent be as non-toxic as possible relative to possible exposures and generate minimal toxic and corrosive decomposition products during the suppression event. Herein, the toxicological aspects of halon replacements are discussed. The specific toxic endpoints of concern for halocarbon candidates, as well as the kinds of toxicity testing required for halon replacements, will be addressed. The paper will also provide a summary of the toxicological properties for the most promising near term halon replacements. Associated decomposition product formation will be briefly discussed.

Toxicity Considerations

Considerations of the short- and long-term health hazards of exposure are of key importance when deciding which compounds hold potential for use in explosion and fire protection. Human and animal research indicates several principal adverse health effects caused by halocarbons. They can stimulate or suppress the central nervous system (CNS) to produce symptoms ranging from lethargy and unconsciousness to convulsions and tremors (*1*). Halocarbons can cause cardiac arrhythmias and can

¹Current address: HTL/KIN-TECH Division, Pacific Scientific, 3916 Juan Tabo, Northeast, Albuquerque, NM 87111

sensitize the heart to epinephrine (adrenaline) (2). Inhalation of halocarbons can produce bronchioconstriction, reduce pulmonary compliance, depress respiratory volume, reduce mean arterial blood pressure, and produce tachycardia (rapid heartbeat) (3). These agents can cause organ damage by degradation products of metabolism (4). Halocarbons can cause reproductive and developmental abnormalities such as infertility, fewer uterine implants, and teratogenic anomalies (5). They can also produce cancerous or mutagenic effects (6). CNS effects, cardiac sensitization, and pulmonary disorders appear to be reversible upon termination of exposure to these chemicals. Organ toxicity, reproductive effects, cancer and mutagenicity, on the other hand, are latent effects, and sequelae (delayed effects) are usual.

The immediate effects of halocarbon exposure on the nervous system, cardiovascular system, and respiratory system appear to be caused by the compound itself. However, it is thought that the latent effects that take place in specific organs, such as the liver, kidneys, and reproductive organs, are possibly caused by the degradative products formed when the halocarbons enter into metabolic processes. Both the immediate effects and the latent damage must be considered when evaluating potential candidates for firefighting.

Regulatory Considerations

Title VI of the 1990 Clean Air Act Amendments implements the restrictions imposed by the Montreal Protocol for the United States. Title VI, Section 612 requires that the US Environmental Protection Agency (EPA) enact regulations making it unlawful to replace any CFC or halon with any replacement that "may present adverse effects to human health or the environment, where the Administrator has identified an alternative to such replacement that — (a) reduces the overall risk to human health and the environment; and (b) is currently or potentially available." Section 612 requires the EPA to publish lists of both prohibited and acceptable substitutes. Risk assessments are performed under the Significant New Alternatives Policy (SNAP) program to determine the acceptability of substitutes. This indicates that toxicological considerations are a major concern when developing halon replacement agents.

Cardiac sensitization occurs at a lower concentration than the concentrations necessary to elicit toxic responses such as anesthesia or lethality. Therefore, regulatory and standard setting authorities have used cardiac sensitization thresholds as the criteria for determining acceptability for use in areas where human occupancy may occur. In addition, the phenomenon of cardiac sensitization is particularly important in firefighting because under the stress of the fire event, higher levels of epinephrine are secreted by the body which increases the possibility of sensitization.

Toxicity Tests

Toxicity testing is the most time-consuming and expensive effort in the early development of a halon replacement. Estimates indicate that the cost range for the battery of toxicity tests required to satisfy regulatory and liability issues is \$2-5 million per chemical (7). A number of toxicity tests have been suggested for halon replacement agents to facilitate a risk assessment decision. Below is the list of minimum likely toxicity tests required by the US EPA for fire extinguishing agents under the SNAP program: (8)

- Range finder of acute toxicity (such as a limit test or LC₅₀ test)
- Cardiac sensitization test
- Developmental toxicity test
- 4- or 13-week subchronic test
- Genetic toxicity screening test (such as the Ames test)
- Degradation byproduct test (not combustion toxicology)

Most of the tests listed above determine the toxicity due to short exposures. However, other longer exposure tests would likely be required to satisfy occupational concerns imposed during manufacture of the chemical and maintenance and service of the extinguisher systems.

In determining the acceptability of a replacement for a particular application, a risk assessment is performed where the toxic concentrations of the chemical are compared to the likely exposure concentrations for specific scenarios of use. For applications where human exposure is possible, a replacement agent should not be toxic at exposure concentrations. Therefore, another "test" that might be required, as determined on a case-by-case basis, is one to determine the exposure concentration during the specific use of the replacement agent.

Acute Toxicity Testing. Acute toxicity tests are usually concerned with the lethality manifested due to exposure within a relatively short time interval, usually on the order of minutes to days. Acute toxicity is often the result of a single exposure. Other manifestations besides lethality can include indications of anesthesia and eye or skin irritation. Sometimes pathological or histological examinations are performed on the test species to give indications of cause of death and tissues affected by the test chemical.

Cardiac Sensitization Testing. Cardiac sensitization potential is usually tested in dogs outfitted with electrocardiographic (ECG) measurement devices (9). The dogs are trained to accept venipuncture, ECG monitoring, and a mask over their snouts for chemical exposure. The usual test sequence, and the protocol recommended by the SNAP program, involves administering epinephrine to animals to determine the individual dog's response to pharmacological doses of the drug, then exposing them to the test chemical by inhalation, and finally administering a second dose of

epinephrine ("challenge dose") while the test chemical is being inhaled. Adverse effects are monitored on the ECG tracings. Adverse effects are considered as the appearance of 5 or more multifocal ectopic ventricular beats, fibrillation, or death. A standardized protocol is not universally accepted so variations on this method may be used, thus making comparison of studies difficult.

The lowest observed adverse effect level (LOAEL) is the lowest concentration at which an adverse toxicological effect is observed. The no observed adverse effect level (NOAEL) is the highest concentration at which no adverse toxicological effects have been observed. Since heart arrhythmia is the first acute adverse physiological effect observed after exposure to most halocarbons, cardiac sensitization has been chosen as the adverse effect on which NOAEL and LOAEL values are based for halogenated halon replacements.

Despite the acceptance of cardiotoxic threshold values in making regulatory decisions and settings standards, the NOAEL and LOAEL values determined in dogs are considered conservative for humans even in high-stress situations (10). The conservative nature of these values is contributed to several factors: (a) no certainty exists that dogs are a good model for humans for cardiac sensitization, (b) very high doses of epinephrine are used in the test method (epinephrine doses in the test animals are 10 times higher than the highest levels secreted in humans), (c) some dogs, and presumably some humans, are more susceptible to sensitization than others, and (d) two to four times more chemical is required to cause cardiac sensitization in the absence of exogenous epinephrine, even in artificially created situations of stress or fright in animals. Nevertheless, regulatory and standard-setting authorities are using results of cardiac sensitization tests to determine the acceptability of halon replacements for use in normally occupied total flood applications. If the cardiac sensitization value (LOAEL for US EPA or NOAEL for NFPA) is below the fire suppression or inertion design concentration, then the candidate is not acceptable for use in normally occupied total flood applications.

Development Toxicity Testing. During the developmental toxicity test, pregnant animals (usually rats or rabbits) are subjected to the chemical in order to determine what effect the chemical has upon the developing fetus. Dams are exposed during the period of fetal organogenesis, and litters are evaluated for a number of endpoints, including number of viable offspring, types and incidence of skeletal and visceral malformations or variations, and body weight (11). Maternal toxicity endpoints, such as organ weights and clinical histopathology, are also assessed.

Subchronic Toxicity Testing. Subchronic tests measure toxicity caused by repeated dosing over an extended time, but not such a long time period that it constitutes a significant portion of the expected lifespan of the test species. These tests provide information on essentially all types of chronic toxicity. Subchronic tests are frequently used to determine the No Observed Effect Level (NOEL), a value that is used in risk assessment calculations for occupational exposure. Although the 90-day

(13-week) subchronic toxicity test is not specific for carcinogenicity or mutagenicity endpoints, it is a definitive study that may give indications of the carcinogenic potential of highly potent mutagens and carcinogens.

Genetic Toxicity Testing. Chemical carcinogenesis is usually the result of long-term exposure to a chemical that may occur generally during industrial processing and handling. To determine the potential carcinogenicity of an agent, genotoxicity (mutagenicity) screening tests are often performed. Positive mutagenicity results alert toxicologists to the possibility of carcinogenesis and indicate the need for subchronic exposure testing to develop industrial exposure standards. Examples of genotoxicity tests are the Ames test in bacteria, mouse lymphoma test, mouse micronucleus test, unscheduled DNA synthesis test in mammalian liver cells, sex-linked recessive mutation test in fruit flies, and sister chromatid exchange test in Chinese hamster ovary cells.

Commercial Replacements for Total Flooding and Streaming

A number of halon replacement candidates have been announced by industry for commercialization. In most cases, the toxicity testing is being completed by support from the manufacturers. These manufacturers not only must determine the toxicity of the chemicals to gain regulatory approval but also to satisfy product liability. As a result, the manufacturers often support additional toxicity testing in order to address this concern. Tables I and II present summaries of the toxicological information on commercially available Halon 1301 and 1211 replacements, respectively. Developmental and subchronic results have not been determined for many of the agents yet. Table I provides manufacturer recommended design concentrations to allow comparisons with cardiac sensitization NOAEL and LOAEL values. Those agents with cardiac sensitization values above the design concentrations are suitable for use in occupied areas.

Because design concentrations are not typically thought of for streaming agents, exposure of personnel is difficult to determine and highly scenario-dependent. The EPA uses models and air monitoring data to determine if exposure levels will exceed the cardiac sensitization LOAEL during discharge of portable extinguishers. During breathing zone personnel monitoring studies of halon replacement agents, firefighters were exposed to less than 0.1% agent concentration in simulated aircraft hangar exposures during discharge of 20- or 150-LB fire extinguishers in T-dock aircraft hangers (12) and in open pit, outdoor fire scenarios fought with 20- or 150-LB fire extinguishers (13). Another study showed firefighter breathing zone concentrations less than 0.1% in real fire, simulated flightline scenarios with 150-LB extinguishers using either Halon 1211, HCFC-123, or FC-5-1-14 (14). Accordingly, in outdoor and T-hangar streaming scenarios similar to those indicated above, it is anticipated that firefighter exposure would not exceed concentrations greater than 0.1%. For streaming agents, this type of exposure information is compared to the cardiac sensitization values to determine the suitability of use in areas where human exposure might occur.

Table I. Toxicological Summary of Halon 1301 Replacements

Candidate Agent ^a	Acute Toxicity (LC ₅₀ ^b or ALC ^c), vol %	Cardiac Sensitization, vol %		Developmental Toxicity, NOAEL, ^d vol %	Subchronic Toxicity (13-wk), NOAEL, ^d vol %	Recommended Design Conc., vol %	
		N ^d	L ^e			CB ^f	IC ^g
Halon 1301 ^h	>80 ^c	5	7.5	4.95	<2.3 ⁱ	5	7.7
HBFC-22B1	10.8 ^b	0.3	1.0	N/A ^j	N/A	4.9	N/A
HFC-23	66.3 ^c	30	>50	N/A	1	16.0	22.2
HFC-125	>80 ^c	7.5	10	5	5	10.9	16.2
HFC-227ea	80 ^b	9.0	10.5	>10.5	>10.5	7.0	12.7
HFC-236fa	>13.5 ^c	10	15	N/A	N/A	6.4	N/A
HCFC-124	36 ^b	1.0	2.5	5	10.0	8.5	13.9
HCFC Blend A	64 (est)	10.0	>10	N/A	N/A	8.6	N/A
HCFC-123	3.5 ^b	1.0	2.0	0.5	N/A		--
HCFC-22	22 ^b	2.5	5.0	0.1	N/A		--
HCFC-124	36 ^b	1.0	2.5	N/A	1.5		--
FC-218	>80 ^c	30	40	N/A	>11.3 ^k	8.8	12.3
FC-3-1-10	>80 ^c	40	>40	N/A	N/A	6.0	11.8
CF ₃ I	27.4 ^l	0.2	0.4	N/A	N/A	3.6	7.2

^aAs Listed in NFPA 2001 or the US EPA SNAP List.

^bLC₅₀ = Lethal Concentration that kills 50% of rat population with a 4-hr. exposure.

^cALC = Approximate Lethal Concentration.

^dNOAEL = No Observed Adverse Effect Level.

^eLOAEL = Lowest Observed Adverse Effect Level.

^fCB = NMERI 5/8-scale cup burner using *n*-heptane with 20% safety factor or manufacturers recommended design concentration.

^gIC = Inertion concentration for propane with 10% safety factor above laboratory sphere apparatus or large-scale inertion chamber (safety factor recommended in NFPA-2001) From Reference 20.

^hHalon 1301 provided as reference.

ⁱ18-wk exposure.

^jN/A = Not Available.

^k24 hr/day for 10 days.

^lLC₅₀ 15-minute exposure.

Decomposition Product Toxicity

The toxicity of the neat agent is not the only toxicological aspect that must be considered; decomposition product generation must also be investigated. The principal toxic species produced in carbon-based fuel fires is carbon monoxide (CO) or carbon dioxide (CO₂) (15). The yield of each is strongly dependent on the burning conditions and the availability of air. Levels typically range from tens to several hundreds of ppm.

Table II. Toxicological Summary of Halon 1211 Replacements

Candidate Agent ^f	Acute Toxicity (LC ₅₀ ^b or ALC ^c), vol %	Cardiac Sensitization, vol %		Developmental Toxicity, NOAEL ^d vol %	Subchronic Toxicity (13-wk), NOAEL ^d vol %
		N ^g	L ^e		
		Halon 1211 ^f	3.2-13 ^b		
HBFC-22B1	10.8 ^b	0.3	1.0	N/A	N/A
HCFC-123	3.2 ^b	1.0	2.0	1.0	<0.5
HCFC-124	36 ^b	1.0	2.5	5	10
HCFC Blend B	N/A	N/A	N/A	N/A	N/A
HCFC-123	3.2 ^b	1.0	2.0	1.0	<0.5
HCFC Blend C	N/A	N/A	N/A	N/A	N/A
HCFC-123	3.2 ^b	1.0	2.0	1.0	<0.5
HCFC-124	36 ^b	1.0	2.5	5	10
HFC-134a	>50 ^b	4.0	8.0	4	5
HFC-227ea	80 ^b	9.0	10.5	>10.5	>10.5
FC-5-1-14	>80 ^c	40	>40	N/A	30.5 ⁱ
CF ₃ I	27.4 ^j	0.2	0.4	N/A	N/A

^aAs Listed in US EPA SNAP List.

^bLC₅₀ = Lethal Concentration that kills 50% of rat population with a 4-hr. exposure.

^cALC = Approximate Lethal Concentration.

^dNOAEL = No Observed Adverse Effect Level.

^eLOAEL = Lowest Observed Adverse Effect Level.

^fHalon 1211 provided as reference.

^gN/A = Not Available.

^h3-wk exposure.

ⁱ30-day exposure.

^jLC₅₀ 15-minute exposure.

Other toxic products may also be present depending upon the material(s) being combusted. Wood and paper fires typically produce CO and CO₂, as do hydrocarbon fuel fires. Plastics from circuit boards, cables, and fabrics, however, tend to generate other toxic products, such as hydrochloric acid (HCl) and hydrogen cyanide (HCN), in addition to CO and CO₂ (15).

Although the fire itself is hazardous and produces toxic products, adding halocarbon fire extinguishing agent increases the amount and types of combustion products. The resulting species generated are characterized as a decomposition products and can be acutely toxic. In addition to increased CO and CO₂, acid gases, such as hydrogen fluoride (HF), hydrogen bromide (HBr), and hydrogen chloride (HCl), as well as carbonyl fluoride (COF₂) are formed. Chemical intermediaries (e.g., perfluoropropene from HFC-227ea) have also been identified (16). The

concentration of toxic products generated by the current halon replacements, except CF_3I , exceeds levels generated by the existing halons by 5 to 10 times (16, 17, 18). Decomposition product amounts for CF_3I are essentially similar to Halon 1301 (Moore, T. A., personal communication, 1994) and will not be discussed further. Concentrations of decomposition products for other replacement agents have been measured at 10 to 1000 times those limits set by the Occupational Safety and Health Administration (OSHA) and other safety and health organizations (see Table III). In order to minimize the decomposition product formation, end use (application specific) analysis is critical for agent selection and in determining the proper design concentration.

Total Flood Agents. Table III compares typical measured decomposition product levels for total flood agents at two typical concentrations. As shown, at the National Fire Protection Association (NFPA 2001) recommended design concentration for total flood agents in fixed facilities (cup burner extinguishment concentration plus 20%), extremely high concentrations of decomposition products are formed. Increasing the concentration of extinguishant used to suppress the fire lowers the decomposition product concentrations, in some cases by a factor of 10, but concentrations are still above dangerous levels. Consequently, care must be taken to choose a high enough design concentration for halon replacements that minimizes the formation of toxic decomposition products. Test data and analysis indicate that for large hydrocarbon fuel fires, such as those found in large machinery spaces, the design concentration must be at least 40% above laboratory extinguishing concentrations (cup burner value, *n*-heptane) to minimize HF and COF_2 concentrations (16, 17, 18).

However, for typical computer rooms and office spaces where combustibles are not liquid hydrocarbons, analysis by DiNenno et al., using fire growth models and test data, indicates that HF and COF_2 concentrations will be comparable to Halon 1301 with design concentrations at 20% above cup burner (DiNenno, P., personal communication, 1993). These concentrations are predicted to be under OSHA limits. Agent manufacturers' test data appear to substantiate DiNenno's analysis (Register, W. D., conference presentation, 1994). It can be concluded that decomposition product concentrations are a function of agent type, fire type, fire size, and extinguishment time, and they can be minimized by proper agent design concentration determined through a correct assessment of all risks.

COF_2 has been measured at concentrations exceeding OSHA limits. Prior to recent studies using in situ methods, it was thought that the lifetime of COF_2 , generated during the extinguishment process, was sufficiently short, on the order of minutes, to preclude its consideration as a potential hazardous decomposition product. However, with the present halon replacements at design concentrations less than 140% of the cup burner value, COF_2 has been found to exceed OSHA limits and linger for over 30 minutes (16, 18). It should be noted that COF_2 has not been measured in significant amounts in any Halon 1301 baseline tests or with replacements agents where design concentrations exceeded 140% of the cup burner value.

Table III. Toxicological Summary of the Decomposition Products Generated During the Suppression of Fires With Halon 1301 and the Halon Replacements

Typical Chemical Species Resulting from Suppression with Halocarbons	OSHA	ALC	Dangerous Conc., ^c ppm	Measured Conc., ^d ppm		Measured Conc., ^d ppm	
	STEL, ^a ppm	15 min., ^b ppm		Halon 1301		Current Halon Replacements except CF ₃ I	
				At CB ^e Plus 20%	70% ^f	At CB ^e Plus 20%	40%
CO	200	N/A ^b	N/A	10	1	1000	100
HBr	N/A	4750	N/A	N/A	N/A	** ⁱ	**
HCl ^g	N/A	N/A	N/A	N/A	N/A	8000	100
HF	N/A	2500	50-250	1000	100	5000	500
COF ₂	5	1500	N/A	2	0	20	1
COCl ₂ ^g	N/A	100-150	N/A	**	**	N/A	N/A

^aOccupational Safety and Health Administration (OSHA) Short Term Exposure Limit (STEL) (15-min time weighted average).

^bApproximate Lethal Concentration for a 15-min exposure.

^cFrom Reference 5.

^dData extrapolated from Reference 18 for small to medium (0.6 to 2.5 ft²/1000 ft³) *n*-heptane fires, values tend to vary by ±10%.

^eCB = NMERI 5/8-scale cup burner w/*n*-heptane.

^fTypical existing design concentration for Halon 1301 is 5% (70% above the cup burner value for *n*-heptane).

^gPresent with chlorine containing replacements (e.g., HCFC-Blend A).

^hN/A = Not available.

ⁱ** = Not applicable for the agent considered.

Streaming Agents. Different considerations are required when evaluating the risk associated with the decomposition products from streaming agents. Typically, streaming agents are used locally to extinguish a fire. Discharging a portable extinguisher may result in a plume that may envelop unprotected personnel, especially if the fire is indoors and personnel have no easy exit available. Wind direction and obstruction that may affect plume dispersion must be considered in agent selection. An Air Force evaluation of selected near term streaming agent replacements indicates that the decomposition products are formed at concentrations 2 to 4 times higher than Halon 1211 (19). Concentrations ranged from 40 to 120 ppm for HF and 30 to 95 ppm for COF₂ when HCFC-123 and FC-5-1-14 were applied to a 150-ft² pool fire using a 150-LB Amerex flightline extinguisher.

Conclusions

The halon replacement candidates currently being considered have been tested under a number of different toxicological protocols. For the Halon 1301 replacements,

cardiac sensitization is used to evaluate whether the chemical can be applied in occupied areas where human contact is possible. Cardiotoxicity is the toxic effect that occurs at the lowest concentration compared to other toxic endpoints. The cardiac sensitization threshold is compared to the fire extinguishing design concentration and only those chemicals with threshold levels above the design concentration can be used in normally occupied areas. Consequently, HFC-23 (FE-13), HFC-227ea (FM-200), FC-218, FC-3-1-10 (CEA-410), and HCFC Blend A (NAF-SIII) are suitable for fire suppression use in occupied areas. All agents are acceptable from a toxicity basis for use in unoccupied applications.

For Halon 1211 replacements, toxic endpoints are compared to realistic exposure concentrations based on personnel monitoring levels rather than design concentrations. The levels at which humans would likely be exposed under proper use of streaming agents in scenarios that have been measured are much lower than the toxic levels (again, cardiac sensitization threshold). The streaming replacements suitable for outdoor and large aircraft hangar applications are HCFC-123 (FE-232), HCFC Blend B (Halotron I), HCFC Blend C (NAF-PIII), HCFC-Blend D (NAF BLITZ), FC-5-1-14 (CEA-614), HFC-227ea (FM-200), HFC-124 (FE-241), and CF₃I. Exposure concentrations for other scenarios must be determined to assess the suitability of these streaming agent replacements for those applications.

In addition to the neat agent toxicity, toxic and corrosive species produced during the suppression event must be considered, remembering that the fire itself is hazardous. Decomposition product formation has been shown to depend on type of fuel, fire size, system discharge time, extinguishment time, and type of agent used. Most of the current halon replacements, except CF₃I, generate 5 to 10 times greater concentrations of CO, HF, and COF₂ than Halons 1211 and 1301. In total flood applications, the toxic species can be minimized by using at least a 40% safety factor with the current halon replacements, remembering that with Halon 1301, a 70% safety factor has typically been common practice. Whether the increased amounts of these decomposition products will cause realistic problems is still under investigation. End use (application specific) assessment of all exposures and associated risks are critical for agent selection and in determining the proper design concentration.

Literature Cited

1. Clark, D. G., and Reinhardt, C. F. *The Toxicology of the Halogenated Fire Extinguishing Agents*, General Chemicals Group, Runcorn, England, n.d.
2. Aviado, D. M., and Drimal, J. *J Clin Pharmacol*, **1975**, *15*, pp. 116-128.
3. Aviado, D. M., and Micozzi, M. S. In *Patty's Industrial Hygiene and Toxicology*; Clayton, G. D., and Clayton, F. E., Ed., 3rd Edition Revised, Toxicology; John Wiley & Sons, Inc.: New York, NY, 1981, Vol IIB, pp. 3071-3115.
4. Schieble, T. M., Coasta, A. K., Heffel, D. F., and Trudell, J. R. *Anesth.* **1988**, *68*, pp. 485-494.
5. Sax, N., and Lewis, R. J., Sr., *Dangerous Properties of Industrial Materials*, 7th ed., Van Nostrand Reinhold: New York, NY, 1989, Volume III.
6. Fishbein, L. *Mut. Res.* **1976**, *32*, pp. 267-308.

7. Daly, J. J., Jr., *The Properties and Toxicology of Alternatives to CFCs*, Du Pont Chemical Company: Wilmington, DE, 1989.
8. Rubenstein, R. *Proceedings of the Halon Alternatives Technical Working conference 1992*; New Mexico Engineering Research Institute: Albuquerque, NM, 1992; pp. 70.
9. Reinhardt, C. F., Azar, A., Maxfield, M. E., Smith, P. E., and Mullin, L. S. *Arch. Env. Health* 1971, 22, pp. 265-279.
10. US Environmental Protection Agency, SNAP Technical Background Document: Risk Screen on the Use of Substitutes for Class I Ozone-depleting Substances, Fire Suppression and Explosion Protection (Halon Substitutes), US Environmental Protection Agency, Office of Air and Radiation, Stratospheric Protection Division: Washington, DC, 1994.
11. Beck, B. D., Rudel, R., and Calabrese, E. J. In *Principles and Methods of Toxicology*; Hayes, A. W., Ed.; Third Edition; Raven Press: New York, New York, 1994.
12. Meridian Research, Inc., *Assessment of Fire Fighter Exposure to HCFC-123 during Fire Extinguisher Use in Aircraft Hangars*, Submitted to American Pacific Corporation, March 1993.
13. Meridian Research, Inc., *Assessment of Fire Fighter Exposure to HCFC-123 during Extinguishant Efficiency Tests Conducted at the United States Naval Air Station in Beaufort, South Carolina*, U. S. Environmental Protection Agency, Global Change Division, Office of Air and Radiation, EPA Contract 68-D900068, Work Assignment 4-44, and American Pacific Corporation, March 1993.
14. Midwest Research Institute *Assessment of Occupational Hazards of Firefighter Training*, AL/OEMI, Armstrong Laboratory: Brooks AFB, TX, February 1993.
15. Hartzell, G. E. *Advances in Combustion Toxicology*, Technomic Publishing Co.: Lancaster, PA, 1989, Vol. 1, pp. 1-8.
16. Dierdorf, D. A., Moore, T. A., and Skaggs, S. R. *Proceedings of the Halon Alternatives Technical Working Conference 1993*, New Mexico Engineering Research Institute: Albuquerque, NM, 1993; pp. 635-644.
17. Sheinson, R. E., Eaton, H. G., Black, B., Brown, R., Burchell, H., Maranghides, A., Clark, M., Salmon, G., and Smith, W. *Proceedings of the Halon Options Technical Working Conference 1994*, New Mexico Engineering Research Institute: Albuquerque, NM, pp. 379-390.
18. Moore, T. A., Dierdorf, D. A., and Skaggs, S. R. *Proceedings of the Halon Alternatives Technical Working Conference 1993*, New Mexico Engineering Research Institute: Albuquerque, NM, 1993; pp. 115-128.
19. Floden, J. R., Scheil, G., and Klamm, S. *Proceedings of the Halon Alternatives Technical Working Conference 1993*, New Mexico Engineering Research Institute: Albuquerque, NM, 1993; pp. 645-658.
20. Heinonen, E. W. and Skaggs, S. R. *Proceedings of the Halon Alternatives Technical Working Conference 1992*, New Mexico Engineering Research Institute: Albuquerque, NM, 1992; pp. 213-223.

RECEIVED June 7, 1995

Chapter 11

Field-Scale Inertion Testing of Halon Replacements

Ted A. Moore, Stephanie R. Skaggs¹, and Robert E. Tapscott

Center for Global Environmental Technologies, New Mexico Engineering Research Institute, University of New Mexico, Albuquerque, NM 87131

The information presented describes the testing and evaluation effort undertaken by the Center for Global Environmental Technologies (CGET) to compare the most promising near-term Halon 1301 replacements for occupied areas as explosion prevention (inertion) agents. The principal application of concern was protecting the Alaskan North Slope oil and gas production facilities. The candidates were selected based on the decision by the National Fire Protection Association (NFPA) Technical Committee on Alternative Protection Options to Halons (NFPA Standard 2001) that only agents with cardiac sensitization threshold levels above the design concentration are suitable for use as total-flood agents in normally occupied areas (1). An additional criterion was that the agents have a zero ozone-depletion potential (ODP). The only commercialized candidates that met these criteria were HFC-23 (FE-13), HFC-227ea (FM-200), and FC-3-1-10 (CEA-410).

Several organizations have evaluated the inertion ability of the above listed halon replacements at laboratory scale (1, 2, 3). The laboratory apparatus consists of a small sphere in which the agent and gaseous fuel are introduced, mixed, and ignition of the mixture is attempted. Inertion is defined when there is less than a 1 lb/in² pressure increase within the apparatus.

The field-scale inertion testing of the Halon 1301 replacements entailed assessing their ability to inert explosive hydrocarbon fuel (propane and methane) atmospheres. The objective was to verify the laboratory data at larger scale.

Test Methodology

Field-scale inertion test facilities, equipment, and techniques were established. The experimental procedures developed were unique to these experiments as no other large-scale inertion work has been cited in the literature. These experiments were designed to validate the laboratory-scale inertion results of the selected chemicals, leading to a relative ranking and determination of inertion performance. Sufficient testing was performed to allow characterization of the test apparatus using propane as the fuel. Limited methane inertion tests were also performed. Fourier Transform Infrared (FTIR) Spectroscopy was used to measure agent and gaseous fuel concentrations.

Test Apparatus. The test apparatus consisted of a large oval-shaped steel chamber, data acquisition/control system, agent delivery system, fuel delivery and ignition system, and agent filling station (Figures 1 and 2). The field-scale inertion chamber (FSIC) volume was 795 ft³ (22.5 m³). The nominal internal dimensions were 18 ft x 7 ft-8 in in diameter. The

¹Current address: HTL/KIN-TECH Division, Pacific Scientific, 3916 Juan Tabo, Northeast, Albuquerque, NM 87111

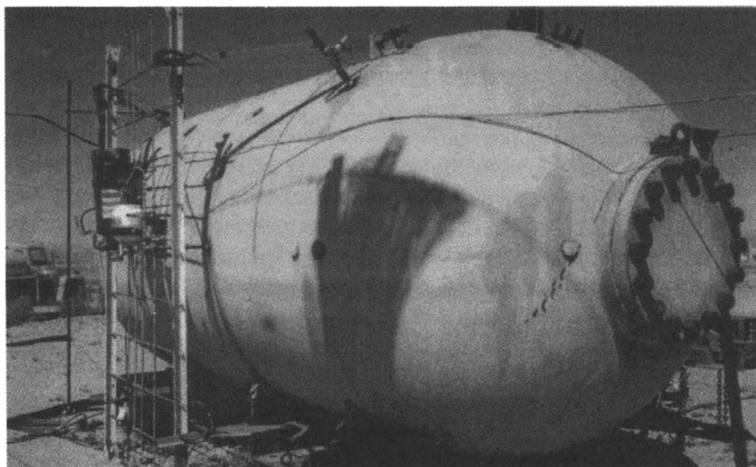


Figure 1. Photograph of the NMERI Field-Scale Inertion Chamber (FSIC).

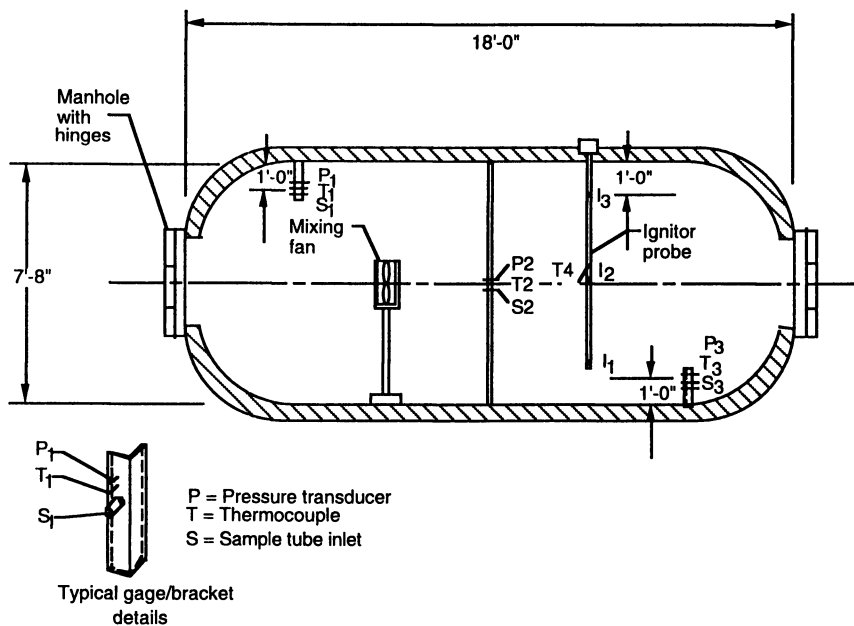


Figure 2. Interior of the NMERI Field-Scale Inertion Chamber (FSIC).

FSIC was constructed of 3-in thick steel and designed for 2000 lb/in² internal working pressure. Penetrations provided inlets for the fuel and agent, pressure transducers, thermocouples, and sampling probes. The FSIC was equipped with a mixing fan, three pressure transducers, and four thermocouples located as shown in Figure 2. Three electric matches (Imperial Chemicals, Inc. (ICI) Aerospace Model M-100, 130 J estimated effective energy for each match) were affixed to an ignitor tree. Data acquisition and equipment control were accomplished with a National Instruments Lab Windows® software-based 486 33-MHz personal computer (PC) data acquisition and control system (DA/CS). There were eight sensor input and eight output control circuits. Test data were displayed in real time for quick viewing and interpretation of results.

Sampling System. Agent and gaseous fuel concentrations were measured inside the FSIC during each test. The sampling system consisted of a Perkin-Elmer System 2000 FTIR Spectrometer, 486 33-MHz PC, Monel® and Teflon® sample tubing, a 10-cm quartz gas cell, KBr windows, a sample pump, flow meters, stainless steel solenoid valves, and miscellaneous wiring. Agent and fuel concentrations were determined to the nearest 0.2 percent by volume.

Test Conduct. The testing was conducted in three steps: (1) calibration and technique optimization, (2) baseline testing, and (3) agent evaluation. Initially, a calibration test series was performed to optimize test techniques and validate the sampling/analysis system. When it was determined that the test technique was reproducible and the analysis results matched predicted results, experiments were run to develop Halon 1301 baseline data for comparison. Testing of the NFPA 2001 candidates then began.

Test Procedures. The following general test procedures were developed: (1) Test information was recorded. (2) The agent and fuel were loaded into their respective discharge cylinders. The agent was pressurized with nitrogen to 300±5 psi. Due to the very high vapor pressure of HFC-23, no nitrogen was used with this agent. (3) The electric match ignitor tree was installed. (4) The control system was activated and a background scan of the chamber interior atmosphere was performed with the FTIR. (5) The test sequence was initiated as follows: (i) The fan was turned on and the FTIR sampling sequence was started; (ii) at 5 sec the agent was discharged; (iii) at 15 sec the fuel (propane) was discharged; however, for the methane tests, the gas was discharged directly into the FSIC to the desired concentration as measured by the FTIR; (iv) fuel and agent discharge normally were complete at 160 sec; and (v) mixing continued until 230 sec, (the FTIR data indicated that complete mixing was accomplished within 160 sec); (vi) the ignitors were initiated at 242 sec, 282 sec, and 318 sec, lower (I1), middle (I2), and top (I3), respectively; (vii) sampling with the FTIR continued until 600 sec; and (viii) the test was terminated. In the final procedures (6), the FSIC was prepared for the next test event, and the test sequence was repeated.

Concentration Calculations. The agent concentration was calculated using the FSIC temperature and information presented in NFPA 2001 (1). Figure 3 shows the agent concentration as a function of the amount discharged into the FSIC (795 ft³). The inertion concentrations are also indicated for the laboratory and field results. The agent and decomposition product concentrations were also measured in "real time" with the FTIR spectrometer. In general, the test series started with the agent concentration at 20% above the laboratory sphere flammability peak concentration for propane; the agent concentration was decreased until it was apparent that inertion was unsuccessful (e.g., an increase in temperature and pressure within the FSIC was observed). All tests were run at an approximate stoichiometric fuel concentration.

Test Results

Baseline Testing. Four baseline tests were run with Halon 1301 and propane. One baseline test was run with methane. The results are tabulated in Table I and the propane results are shown in Figures 4 and 5. The latter also shows the peak chamber overpressure as the agent concentration was increased for a stoichiometric fuel mixture in the laboratory sphere apparatus. During the Halon 1301 baseline testing, the peak chamber pressure was either greater than 200 lb/in² or zero. No tests causing an intermediate pressure rise inside the FSIC were conducted using Halon 1301. At 5.5 and 6.0 volume percent Halon 1301 temperatures greater than 1000 °C and pressures greater than 200 lb/in² were observed. The pressure gage failure point was 200 lb/in². At 6.6 volume percent Halon 1301 complete inertion was observed. The FSIC inertion value for propane is between 6.2 and 6.5 volume percent for Halon 1301. The laboratory inertion concentration at stoichiometric fuel concentration (IC_{St}) is 4.3 volume percent (Figure 4).

An interesting observation can be made about the results shown in Figure 4. During the Halon 1301 tests, the explosive fuel-air-agent mixture was either inerted or it was not. No intermediate concentration provided a partially inerted atmosphere. The pressure versus agent concentration is defined as a step function.

Figure 5 shows the laboratory flammability curve (diagram) for propane and Halon 1301. The field-scale inertion test results, the stoichiometric fuel-to-air ratio line, and the inertion concentration at the stoichiometric fuel ratio (IC_{St} value) (4.3 volume percent) have been added to the diagram.

The laboratory peak flammability value (IC_{fl}) for Halon 1301 of 6.2 volume percent compares well with the FSIC inertion value of 6.2 to 6.5 volume percent and indicates that full laboratory flammability curves must be developed to determine the appropriate inertion design concentration for realistic large-scale applications.

The Halon 1301 IC_{fl} for methane is 4.9 volume percent (3). During this test series one methane test was performed at 6.6 volume percent Halon 1301. The 6.6 volume percent Halon 1301 concentration inerted the stoichiometric methane atmosphere (Table I). The 6.6 volume percent value is equal to the IC_{fl} value plus 20%.

The NFPA 12A recommended design concentration for inertion of propane atmospheres with Halon 1301 is 6.7 volume percent, while for methane 7.7 volume percent is recommended (4). The North Slope typically uses a nominal design concentration of 7.7 volume percent. During the course of this research effort, the question was asked as to whether the 7.7 volume percent design concentration could be lowered, thus reducing the halon quantities required for protecting existing North Slope facilities. This would lead to a net reduction in the North Slope Halon 1301 requirement. Based upon the data and the discussion presented in Reference 3 (e.g., uncertainties due to ignition energy), it was recommended that the present 7.7 percent design requirement (1.18 safety factor --- 7.7 divided by 6.5) not be lowered.

Agent Evaluation. A minimum of three tests were run per candidate agent using propane as the fuel. One test per agent, at the laboratory IC_{St} plus 20%, was performed using methane. All the agents inerted the methane atmosphere. In all cases, the agent concentration to inert methane was less than the FSIC inertion value and the IC_{fl} for propane. Propane and methane test results for all the tested compounds are shown in Table I.

Figure 6 compares the IC_{St} and FSIC test data for HFC-227ea, while Figure 7 shows the laboratory flammability curve and FSIC test data for HFC-227ea. The agent FSIC inertion value for propane (11.5 volume percent) compares well with the laboratory IC_{fl} value (11.7 volume percent). The HFC-227ea IC_{St} value for methane is 8.1 volume percent. The tested FSIC methane inertion value was 9.7 volume percent (IC_{St} plus 20%). This concentration inerted the stoichiometric methane atmosphere (Table I).

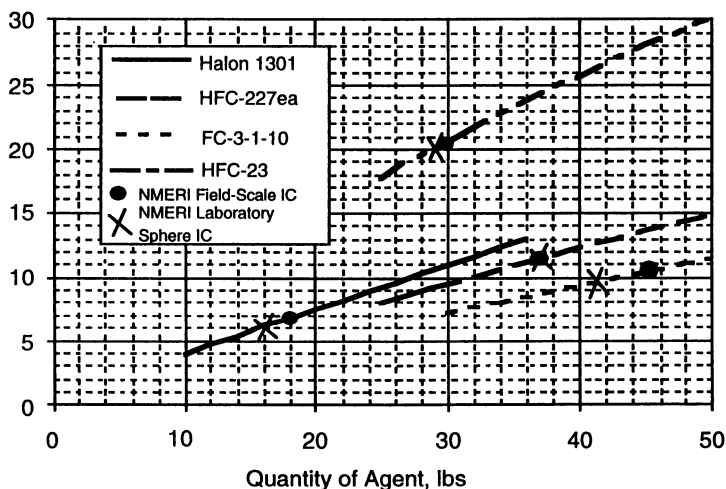


Figure 3. Agent concentration versus weight for the NMERI FSIC at 91 °F.

Table I. Field-Scale Inertion Test Results Summary

Initial Chamber Temp °F	Agent			Fuel			Peak Pressure, lb/in ²
	Agent	Amount, lbs	Conc., Vol. %	Fuel	Amount, lbs	Conc., Vol. %	
88.3	H-1301	17.7	6.6	Methane	---a	9.5	0
86.0	H-1301	13.1	5.0	Propane	3.8	4.0	>200
92.5	H-1301	15.8	6.0	Propane	3.9	4.0	>200
89.6	H-1301	17.5	6.6	Propane	3.7	4.0	0
73.9	FC-3-1-10	45	10.0	Methane	---a	9.5	0
75.2	FC-3-1-10	45	10.1	Propane	4.3	4.5	3.5
91.4	FC-3-1-10	46.6	10.7	Propane	4.3	4.1	0
77.0	FC-3-1-10	48	10.7	Propane	4.2	4.0	0
88.2	HFC-227ea	31.2	9.7	Methane	---a	9.5	0
100.4	HFC-227ea	27.2	8.8	Propane	4	4.0	40.6
91.4	HFC-227ea	31.5	9.9	Propane	4	4.0	3
95	HFC-227ea	33.3	10.5	Propane	3.8	4.0	0
91.4	HFC-227ea	34	10.6	Propane	3.7	3.9	3.4
93.2	HFC-227ea	36.1	11.2	Propane	4.1	4.0	1
91.4	HFC-227ea	40.1	12.2	Propane	4.2	4.0	0
96.4	HFC-23	24	17.3	Methane	---a	9.5	0
71.6	HFC-23	29.5	19.7	Propane	2.9	4.3	40
69.8	HFC-23	31.6	20.8	Propane	2.9	4.2	0
80.6	HFC-23	32.6	21.6	Propane	3.4	4.1	0
85.5	HFC-23	33	22.0	Propane	2.6	3.3	0

^aFuel was loaded to the desired concentration while monitoring with the FTIR.

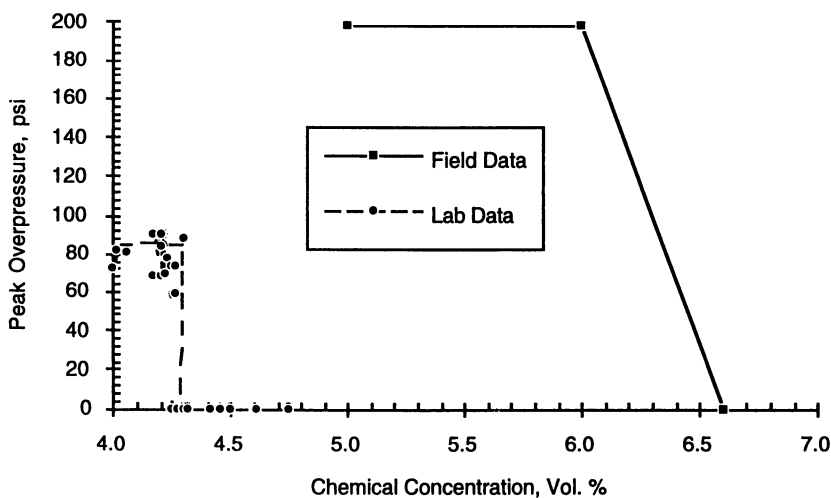


Figure 4. Peak overpressure versus Halon 1301 concentration at stoichiometric propane fuel-to-air ratio.

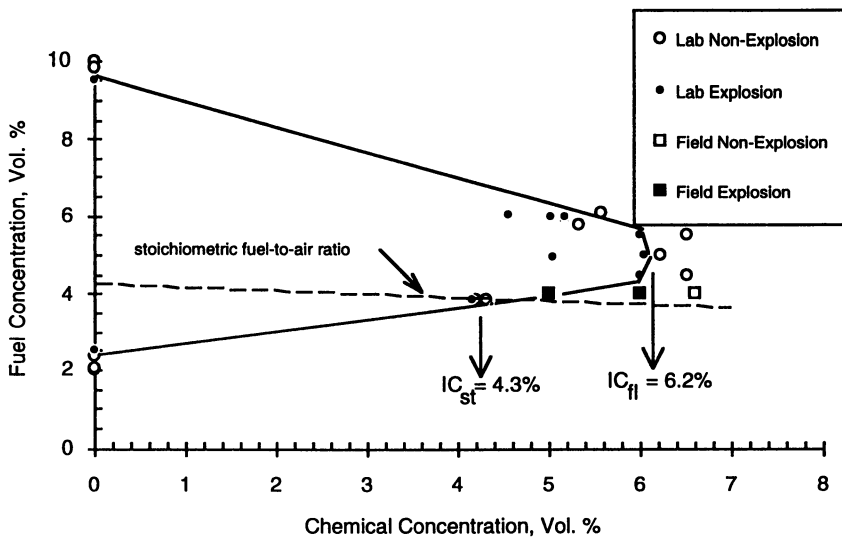


Figure 5. Laboratory flammability curve for Halon 1301 and propane with FSIC results superimposed.

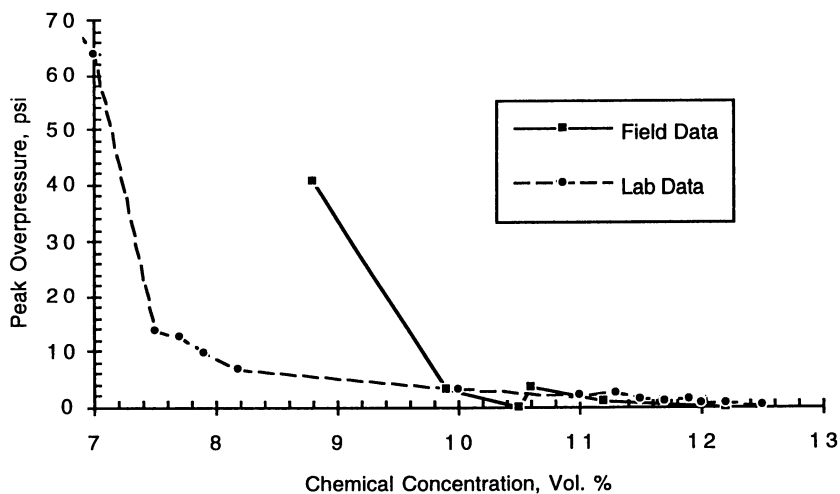


Figure 6. Peak overpressure versus HFC-227ea concentration at stoichiometric propane fuel to-air ratio.

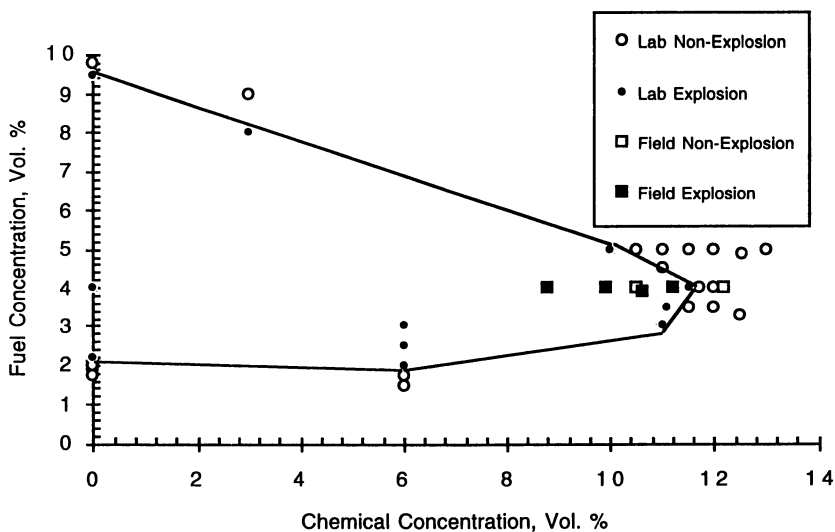


Figure 7. Laboratory flammability curve for HFC-227ea and propane with results superimposed.

The laboratory and field test data for FC-3-1-10 are compared in Figures 8 and 9. FC-3-1-10 shows the largest discrepancy between the laboratory and the field values, 9.9 volume percent (IC_{fl}) versus 10.6 volume percent (FSIC propane inertion value). The FC-3-1-10 IC_{St} value for methane is 7.8 volume percent. The tested FSIC methane inertion value was 10.0 volume percent (IC_{St} plus 28%). This concentration inerted the stoichiometric methane atmosphere (Table I).

Figures 10 and 11 present the laboratory and field test data for HFC-23. The laboratory and the field inertion concentration values compare well, 20.2 volume percent (IC_{fl}) versus 20.5 volume percent (FSIC propane inertion value), respectively. The HFC-23 IC_{St} value for methane is 14.0 volume percent. The tested FSIC methane inertion value was 17.3 volume percent (IC_{St} plus 24%). The value of 17.3 volume percent inerted the stoichiometric methane atmosphere (Table I).

Discussion

The goal of the FSIC Test Series was to compare laboratory and large-scale (field) inertion concentrations for the selected halon replacements. This goal was accomplished. There appears to be little difference between the laboratory IC_{fl} value and the field-scale inertion value, except for FC-3-1-10. Accordingly, the laboratory sphere flammability curve peak (IC_{fl}) provides a reasonable approximation of the agent concentration required to inert large volumes (spaces).

Figure 12 indicates that the laboratory and field-scale flammability diagrams may not be comparable, because explosions (flammable conditions) were encountered for Halon 1301, FC-3-1-10, and HFC-23 outside the laboratory flammability curve explosive region. That field-scale inertion was accomplished within 10% of the laboratory IC_{fl} for propane indicates that a 10% safety factor above the laboratory IC_{fl} should be adequate for inerting gaseous atmospheres in realistic large-scale applications. Table II summarizes the inertion effectiveness test results for the tested candidates.

Table II. Comparison of Test Results for The Evaluated Agents ^a

Agent	IC_{fl} , Vol. %	Propane Inertion Concentration, Vol. %		Effectiveness Relative to Halon 1301 ^b	
		FSIC Value, Vol. %	Recommended Minimum Design Conc., Vol. % ^c	Weight	Volume
Halon 1301	6.2	6.2 - 6.5	6.7 ^d	1.0	1.0
HFC-227ea	11.7	11.5	12.9 ^e	2.4	2.6
HFC-23	20.2	20.5	22.2	1.9	4.3
FC-3-1-10	9.9	10.6	10.9	2.7	2.6

^aBased upon the field-scale inertion results presented herein.

^bBased upon recommended minimum design concentration as set by NFPA Standards 12A and 2001.

^c IC_{fl} plus 10% safety factor, as recommended in NFPA 12A and 2001.

^dValue recommended in NFPA 12A, this equates to a 8% safety factor above the laboratory IC_{fl} value.

^eThe propane and methane inertion concentrations for HFC-227ea exceed the cardiac sensitization threshold levels, indicating the agent is not acceptable to protect occupied spaces as a propane and methane inerting agent.

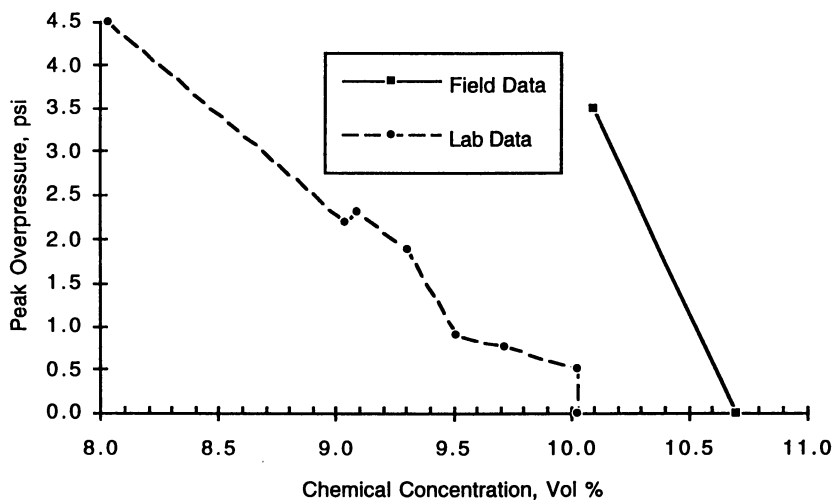


Figure 8. Peak overpressure versus FC-3-1-10 concentration at stoichiometric propane fuel-to-air ratio.

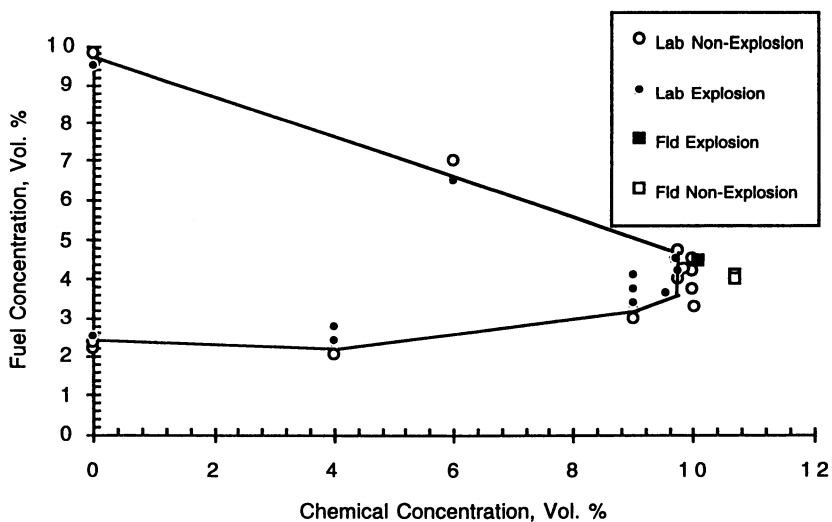


Figure 9. Laboratory flammability curve for FC-3-1-10 and propane with FSIC results superimposed.

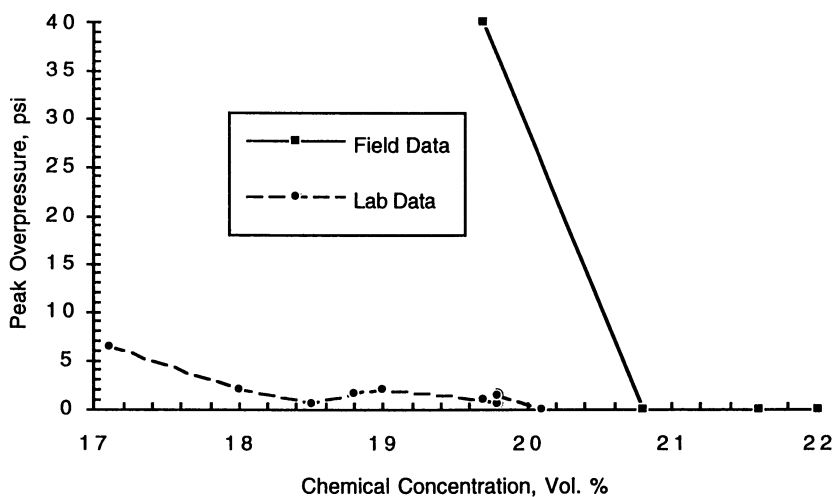


Figure 10. Peak overpressure versus HFC-23 concentration at stoichiometric propane fuel-to-air ratio.

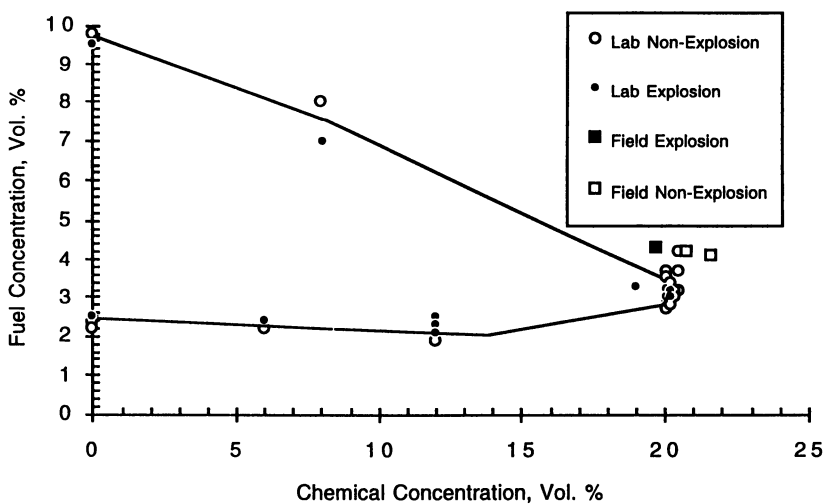


Figure 11. Laboratory flammability curve for HFC-23 and propane with FSIC results superimposed.

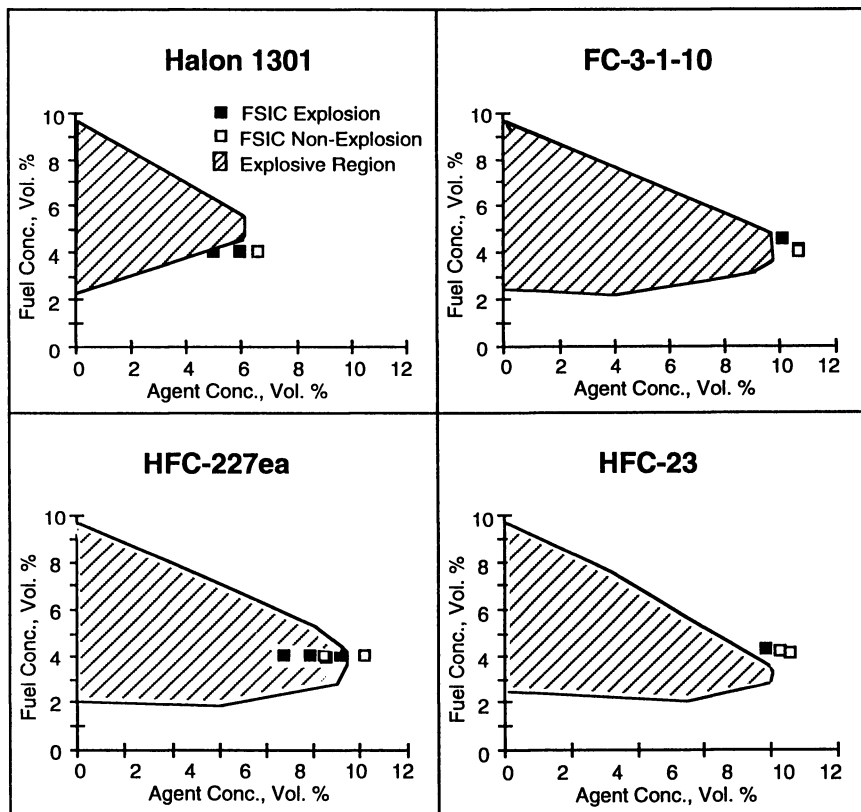


Figure 12. NMERI Laboratory Sphere flammability curves showing FSIC results.

Conclusions

A large-scale apparatus and test procedures were developed to assess the explosive inertion ability of Halon 1301 replacements. Zero-ODP NFPA 2001 agents acceptable for use in normally occupied spaces were tested. A summary of the test results for propane and methane have been presented. The FTIR sampling and analysis system proved to be very effective in identifying and quantifying agent and fuel concentrations.

The propane test results indicate that the FSIC inertion values (large-scale) for Halon 1301, HFC-23, and HFC-227ea were approximately equivalent to the laboratory flammability curve peak (IC_{fl}) values (minimum inertion concentration at the flammability peak) obtained using the NMERI Laboratory Sphere. However, the FSIC inertion value for FC-3-1-10 was found to be 10% higher than the laboratory value. No explanation for the differing results was determined. The propane inertion concentration for these agents also inerted stoichiometric methane atmospheres. These candidate agents required between 2 and 3 times more agent to achieve the same performance as Halon 1301 (Table II).

Recommendations

The following recommendations are made as a result of the field-scale tests:

- The laboratory flammability curve peak (IC_{fl}) value is representative of the inertion concentration measured at large-scale and can be used to establish design concentrations provided a minimum 10% design safety factor is applied.
- The laboratory inertion concentration at stoichiometric (IC_{st}) is not recommended for setting design concentrations.
- Additional testing of FC-3-1-10 should be performed at laboratory and large-scale to verify the propane inertion value.
- The only commercially available agents suitable for providing explosion (inertion) protection for gaseous fuel atmospheres in normally occupied spaces are HFC-23 (FE-23) and FC-3-1-10 (CEA-410).
- Additional large-scale testing should be performed to develop large-scale flammability curves and investigate ignition energy effects to fully validate the previous recommendations.

Acknowledgments

This work was supported by the Alaskan North Slope oil and gas producers and by the Air and Energy Engineering Research Laboratory of the United States Environmental Protection Agency (EPA). Technician support provided by Jesse Parra, Robert Pierson, and Hank Tsinnie is gratefully acknowledged.

Literature Cited

1. NFPA 2001, *Standard on Clean Agent Fire Extinguishing Systems, 1994 Edition*, National Fire Protection Association, Quincy, MA, 1994.
2. Skaggs, S. R., Heinonen, E. W., Moore, T. A., and Kirst, J. A., *Low Ozone-Depleting Halocarbons as Total Flood Agents; Volume 2: Laboratory-Scale Fire Suppression and Explosion Prevention Testing*, NMERI OC 92/26, September 1993. (Draft)
3. Heinonen, E. W., *The Effect of Ignition Source and Strength on Sphere Inertion Results, Proceedings of the Halon Alternatives Technical Working Conference 1993*, Albuquerque, NM, May 11-13, 1993, pp. 563-576.
4. NFPA 12A, *Standard on Halon 1301 Fire Extinguishing Systems, 1987 Edition*, National Fire Protection Association, Quincy, MA, 1987.

RECEIVED June 7, 1995

Chapter 12

Compatibility of Halon Alternatives During Storage

**Richard G. Gann¹, Carlos R. Beauchamp², Thomas G. Cleary¹,
James L. Fink², Richard H. Harris, Jr.¹, Ferenc Horkay²,
Gregory B. McKenna², Thomas P. Moffat², Marc R. Nyden¹,
Richard D. Peacock¹, Richard E. Ricker², Mark R. Stoudt²,
and William K. Waldron, Jr.²**

**¹Building and Fire Research Laboratory, Fire Science Division and
²Materials Science and Engineering Laboratory, National Institute
of Standards and Technology, Gaithersburg, MD 20899-0001**

A key facet of the evaluation of new fire suppressants is their behavior under pressure and at elevated temperature in a metal storage container with an elastomer seal. In this study, 13 candidate chemicals have been examined: C₂F₆, C₃F₈, C₄F₁₀, cyclo-C₄F₈, CH₂F₂, C₂HF₅, CH₂F₂ (60%)/C₂HF₅ (40%), C₂H₂F₄, C₃HF₇, C₃H₂F₆, CHF₂Cl, C₂HF₄Cl, and NaHCO₃. This paper presents the results of testing for thermal stability in the presence of various metals, corrosion of those metals, and effects on selected elastomers and lubricants.

Under the Montreal Protocol of 1987 and its subsequent amendments, production of new halon 1301 (CF₃Br) has been curtailed and now halted. However, the need for fire suppressants still exists for in-flight fires aboard aircraft. There, halon 1301 is now stored for up to 5 years in a metal container which is sealed with a lubricated elastomer. For high temperature applications, a metal gasket is used. The storage pressures are typically 2-4 MPa, and the temperature of the container (or bottle) during flight can range from -70 °C to +150 °C. Deleterious interaction between the chemical and the materials in the storage container could lead to leakage of the suppressant and/or failure of the container. Interaction between the chemical or its combustion by-products could also lead to weakening of downstream parts of the aircraft following a fire. Discussions with military and civilian maintenance personnel indicate that there has been no significant leakage of halon 1301 from its storage system, nor has there been evidence of significant agent deterioration during long-term storage. To avoid costly design errors, it is important that a replacement chemical be similarly stable and that the system remain intact.

Most of the chemicals under consideration (Table 1) are aliphatic halocarbons of low or zero ozone depletion potential that are being manufactured for other applications. Most were recommended by Zallen [1], considering past investigations

This chapter not subject to U.S. copyright
Published 1995 American Chemical Society

[2],[3],[4],[5]. His list was modified by the sponsors, the results of early testing, and a solicitation of additional chemicals.

Table 1. Core chemicals examined

Chemical Formula	Designation	IUPAC Name
C ₂ F ₆	FC-116	hexafluoroethane
C ₃ F ₈	FC-218	octafluoropropane
C ₄ F ₁₀	FC-31-10	decafluorobutane
cyclo-C ₄ F ₈	FC-318	octafluorocyclobutane
CH ₂ F ₂	HFC-32	difluoromethane
C ₂ HF ₅	HFC-125	pentafluoroethane
CH ₂ F ₂ (60%)/C ₂ HF ₅ (40%)	HFC-32/125	-
C ₂ H ₂ F ₄	HFC-134a	1,1,1,2-tetrafluoroethane
C ₃ HF ₇	HFC-227ea	1,1,1,2,3,3,3-heptafluoropropane
C ₃ H ₂ F ₆	HFC-236fa	1,1,1,3,3,3-hexafluoropropane
CHF ₂ Cl	HCFC-22	chlorodifluoromethane
C ₂ HF ₄ Cl	HCFC-124	2-chloro-1,1,1,2-tetrafluoroethane
NaHCO ₃ /SiO ₂ (1%)	-	sodium bicarbonate/silicon dioxide

This paper describes procedures developed for obtaining agent stability and materials compatibility data under conditions well-related to those during use [6]. It was determined that the agent storage would be initially at 25 °C and 4.1 MPa. In flight, these could rise to 150 °C and 5.8 MPa. The experimental approaches followed from an earlier study [7]. The facilities developed and knowledge gained go well beyond the specific applications to aircraft, and advance the fire suppression technology in general.

Corrosion of Metals

There are 6 forms of potential concern for the storage, distribution, and post-deployment corrosivity of fire suppressant agents on aircraft: **general corrosion**, the result of reactions over the entire exposed surface, resulting in metal thinning, reduced mechanical strength, and an altered surface appearance; **pitting corrosion**, which results in an accelerated corrosion rate in a small spot on the surface of a material; **crevice corrosion**, which occurs where the local environment does not freely mix with the bulk environment and could result in failure of joints; **intergranular corrosion**, rapid deterioration between the microcrystals formed during melt solidification of the metal, resulting in reduced mechanical strength; **environmentally-induced fracture**, crack formation at levels well below those due to mechanical stress, leading to catastrophic fracture; and **dealloying**, selective leaching of an alloying element, resulting in serious loss of mechanical strength.

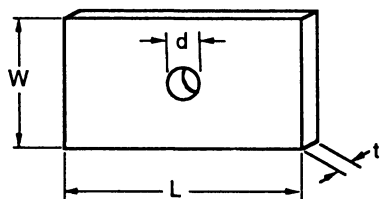
Table 2. Composition of the alloys in weight percent

Element	Nit 40	Al 6061	In 625	304 SS	CDA 172	13-8 Steel	AM 355	AISI 4130
Ni	7.1	--	61.39	8.26	0.06	8.4	4.23	0.08
Cr	19.75	0.04	21.71	18.11	0.01	12.65	15.28	0.98
Mn	9.4	0.15	0.08	1.41	--	0.02	0.8	0.51
Mg	--	1	--	--	--	--	--	--
Si	0.5	0.4	0.09	0.49	0.08	0.04	0.16	0.23
Mo	--	--	8.82	0.17	--	2.18	2.6	0.16
Nb	--	--	3.41	--	--	--	--	--
N	0.29	--	--	0.03	--	0	0.12	--
C	0.02	--	0.02	0.06	--	0.03	0.12	0.32
Be	--	--	--	--	1.9	--	--	--
Co	--	--	--	0.11	0.2	--	--	--
Zn	--	0.25	--	--	--	--	--	--
Cu	--	0.15	--	--	97.9	--	--	--
Fe	bal	0.7	3.97	bal	0.06	bal	bal	bal
Al	--	bal	0.23	--	0.04	1.11	--	0.04
g/cm ^{3a}	7.83	2.70	8.44	7.94	8.23	7.76	7.91	7.85
kg/m ³	7,830	2,700	8,440	7,940	8,230	7,760	7,910	7,850

*Nominal Density

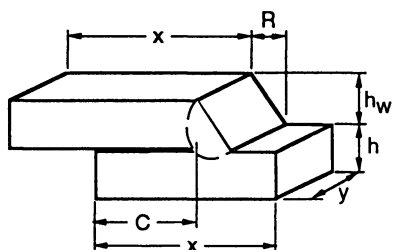
Very little is known about corrosion under elevated pressures and temperatures, the corrosivity of most of these agents to the metals used for aircraft storage containers, or the potential for significant corrosion damage to aircraft structural components by residual suppressant or by suppressant combustion products (*e.g.*, HF, NaOH). Therefore, the effects of the agents on 8 metals most typically used in suppressant storage vessels and fittings were examined. Their compositions are given in Table 2. Several different types of experiments were performed to evaluate the various forms of corrosion.

Exposure Tests. 25-day exposure tests were conducted to determine the change in mass and, in turn, to assess the rate of formation of corrosion scales or the rate of removal of metallic species by corrosion. Visual and optical microscopic examination of these samples before and after exposure allowed for the evaluation of the occurrence of pitting, intergranular corrosion and dealloying. The samples were flat, smooth, and clean surface coupons as shown in Figure 1(a) [8].



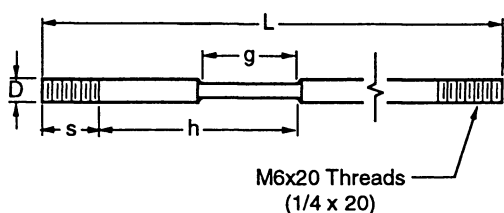
$W = 25.4 \text{ mm (1.0 in)}$
 $L = 50.8 \text{ mm (2.0 in)}$
 $t = 1.6 \text{ mm (0.0625 in)}$
 $d = 6.7 \text{ mm (0.265 in)}$

(a) General corrosion coupon design (ASTM G-01).



$x = 50.8 \text{ mm (2.0 in)}$
 $y = 50.8 \text{ mm (2.0 in)}$
 $R = 4.75 \text{ mm (0.1875 in)}$
 $C = 31.75 \text{ mm (1.25 in)}$
 $h = 3.2 \text{ mm (0.125 in)}$
 $h_w = 3.2 \text{ mm (0.125 in)}$

(b) Weld/crevice corrosion coupon design.



$D = 19 \text{ mm (0.75 in)}$
 $L = 178 \text{ mm (7 in)}$
 $g = 25.4 \text{ mm (1 in)}$
 $h = 57 \text{ mm (2.25 in)}$
 $s = 19 \text{ mm (0.75 in)}$

(c) Slow strain rate tensile sample design (ASTM E-8, G-49).

Figure 1. Design of samples used in immersion and slow strain rate tensile tests.

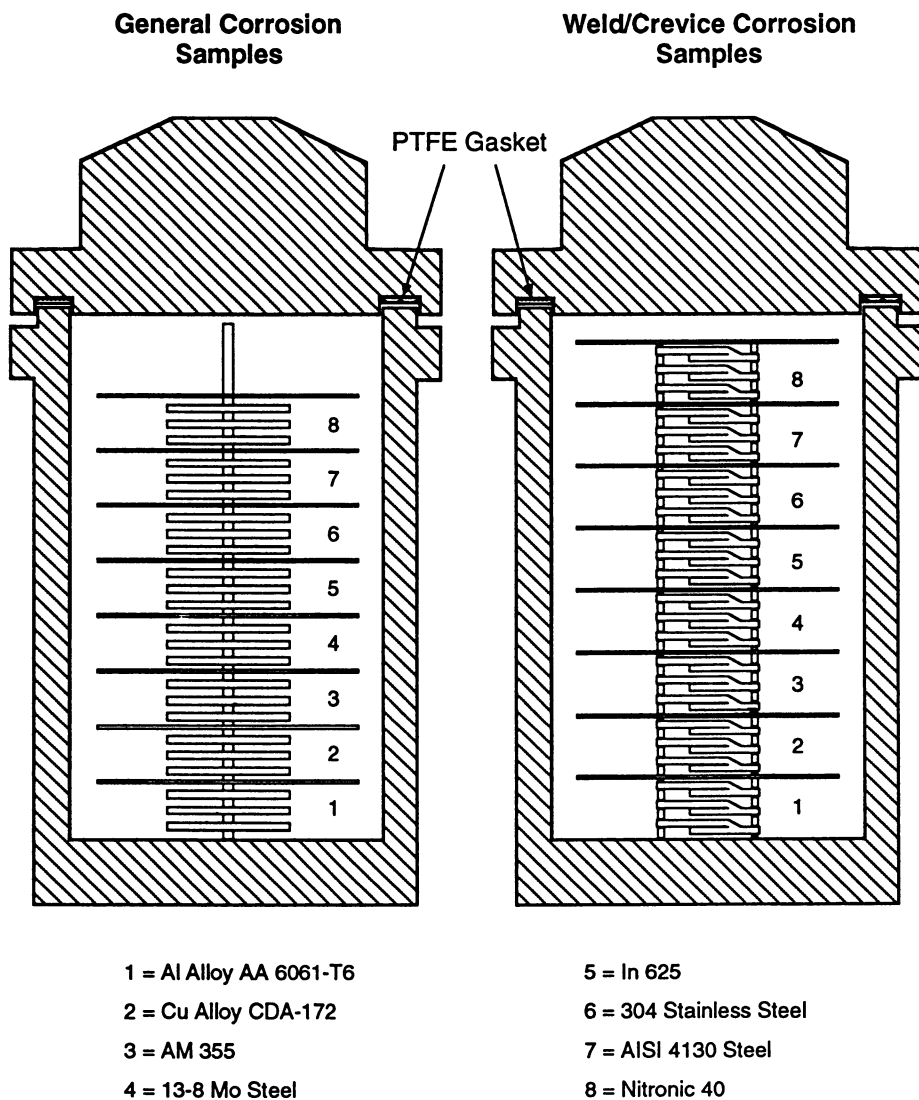


Figure 2. Immersion testing chamber used for general corrosion coupon tests and weld/crevice corrosion coupon tests.

In each exposure test, 3 pre-weighed coupons of each of the 8 alloys were mounted on a polytetrafluoroethylene (PTFE) rod with PTFE spacers between the triplicate samples as shown in Figure 2. This both separated the samples and eliminated galvanic coupling effects. The samples were placed in a PTFE liner and charged into a 2000 ml stainless steel pressure vessel. Each vessel was charged with enough neat agent to achieve a final pressure of ≈ 5.86 MPa at 150 °C. At the conclusion of the testing period, the coupons were extracted from the cooled vessels and re-weighed.

All of the mass changes were found to be relatively small and most were mass increases. Visual examination confirmed the presence of very thin surface films on many of the samples as noted by a color change.

Similar experiments were conducted to evaluate crevice corrosion, weld zone attack, and intergranular attack in the heat-affected zone. The geometry of these samples is shown in Figure 1(b) and the test chamber is shown in Figure 2.

At the end of the 25-day test period, the samples were removed from the test chambers and split along the fusion boundary. The corrosion damage within the crevice region of the 3 samples for each agent/alloy combination was then evaluated visually and statistically [9]. Seven of the agents had an alloy that showed no visible evidence of attack and all of the agents had at least three alloys with only light discoloration of the surface. Thus, the crevice/weld immersion experiments show that while there is a clear difference in the corrosivity of the agents, one can find container alloys for each of the candidates. The agents were then ranked based on the appearance of the corrosion damage in the crevice region for each alloy. The results showed the same general trend as the first analysis. Sodium bicarbonate received distinctly poor ratings here. Third, the alloys were graded based on their performance in all agents. Again, the results were consistent.

Tensile Testing. The stress corrosion cracking susceptibilities of the 8 alloys in the replacement candidates were evaluated using the slow strain rate (SSR) tensile test technique. A test involves slowly increasing the strain on the sample until failure occurs. The result for each agent is then compared to that strain required to cause failure in an inert environment.

The samples used for these experiments were machined with the tensile axis parallel to the rolling direction of the plate stock (Figure 1(c)). The vessels were 250 ml volume autoclaves similar to those used for the exposure testing, except that for these vessels, a load could be applied to the tensile specimen *in situ* under constant environmental conditions (5.86 MPa at 150 °C). The number of moles of agent was held constant for all tests.

After failure, the fracture surfaces were cut from the broken SSR samples for analysis. Scanning electron microscopy was used to evaluate the mechanism of crack propagation based on the fracture morphology. The test results were analyzed using the maximum load observed during the tensile test, the total strain to cause failure, and the reduction in area of the fracture surface. Each of these three parameters were considered relative to the value from an inert environment.

From the SSR data, every agent had at least one alloy demonstrating good performance and all but two agents had more than one. However, no alloy was unaffected by all of the agents and no agent left all the alloys unaffected. Since the alloys have different chemical compositions, surface films and corrosion susceptibilities, this is not surprising, but it indicates the importance of conducting experiments of this type.

Finally, the data from all of the tests were combined into a single matrix, which appears as Table 3. It is clear from these compiled results that there are metals that are compatible with each of the agents under consideration. Some of the metals, especially the aluminum and copper-beryllium alloys and the 355 and 4130 steels, appear riskier to use than the others. The range of choice is more limited for sodium bicarbonate than for the other agents.

Post-Deployment Corrosion. An additional set of experiments appraised the effects of deposits of a suppressant and its byproducts on potential aircraft metals. The samples were the same as in Figure 1(a) without the hole in the center.

These agents can be classified into two categories: those that will produce halogen acids (of which HF is usually the worst) and those that contain sodium bicarbonate. Sodium bicarbonate will decompose on heating to form sodium carbonate (Na_2CO_3), and on combustion to form sodium hydroxide (NaOH).

To produce a surface film rich in fluoride ions, the surfaces of the samples were first sprayed with ASTM artificial seawater (a worst-case wet environment) then sprinkled with sodium fluoride (NaF) powder while the surface was still wet. A second surface film was simulated by spraying with the ASTM seawater and sprinkling with a 50/50 mixture of sodium bicarbonate/sodium carbonate. A third set of samples was sprayed with the ASTM seawater and then sprayed with a 0.1 M solution of NaOH. Samples of alloys with the 3 treatments were then stored for 30 days at 3 different fixed relative humidities (RH): 20%, 52%, and 93%.

The samples were weighed between the cleaning and the surface pre-treatment steps, after the application of the ASTM artificial seawater, and after application of the corrosive salt(s). Following the exposure, the coupons were weighed, then rinsed in double distilled water, dried and reweighed. Finally, they were weighed again after chemical removal of the corrosion product films.

For most of the alloys the mass changes were quite small, no particular surface pretreatment was consistently worse than the others, and there was no clear trend in the magnitude of the mass change with relative humidity. For three alloys (aluminum 6061-T6, AISI 4130 steel, and Cu-Be CDA-172), the mass changes were somewhat larger. Of particular importance is the large effect of $\text{NaHCO}_3/\text{Na}_2\text{CO}_3$ on the aluminum alloy, which comprises most of the aircraft surface. Cleaning these surfaces soon after discharge of the NaHCO_3 fire suppressant would be a very beneficial practice [10],[11],[12],[13].

Table 3. Interactions of Metals During Storage. Worse of Slow Strain Rate and Weight Loss tests

NAME	NITRONIC 40	AL ALLOY 6061-T6	INCONEL 625	304 STAINLESS	CU-BE CDA 172	13-8 STEEL	AM 355 STAINLESS	AISI 4130 STEEL
HFC-236fa	GOOD	FAIR	GOOD	GOOD	FAIR	GOOD	GOOD	GOOD
HFC-32/125	GOOD	FAIR	GOOD	GOOD	FAIR	FAIR	FAIR	FAIR
HFC-227ea	GOOD	FAIR	GOOD	GOOD	FAIR	GOOD	GOOD	GOOD
HCFC-22	FAIR	FAIR	FAIR	GOOD	FAIR	GOOD	GOOD	FAIR
HFC-134a	GOOD	FAIR	GOOD	GOOD	FAIR	GOOD	FAIR	GOOD
FC-116	GOOD	FAIR	GOOD	GOOD	FAIR	GOOD	FAIR	FAIR
HCFC-124	FAIR	FAIR	GOOD	GOOD	FAIR	GOOD	FAIR	GOOD
HFC-125	GOOD	FAIR	GOOD	GOOD	FAIR	GOOD	FAIR	FAIR
FC-218	GOOD	FAIR	GOOD	GOOD	FAIR	GOOD	FAIR	FAIR
FC-31-10	GOOD	FAIR	FAIR	FAIR	FAIR	FAIR	FAIR	FAIR
FC-318	GOOD	FAIR	GOOD	GOOD	FAIR	FAIR	GOOD	GOOD
NaHCO ₃	FAIR	FAIR	GOOD	GOOD	FAIR	BAD	GOOD	FAIR

GOOD: NO SIGNIFICANT INTERACTION FAIR: MAY BE AN INTERACTION BAD: POSSIBLE PROBLEM

Storage Stability

Storing chemicals under high temperature and pressure accelerates both homogeneous reactions and heterogeneous interactions with the metal storage cylinders. These can promote the evolution of undesirable products and a concomitant loss of fire suppression effectiveness.

The most reliable way to assess storage stability of a chemical is by monitoring its degradation in the actual storage environment. Cylinders made of some of the metals were unavailable or extremely costly. Accordingly, in this project samples of each of the candidate agents were evaluated in pressurized, PTFE-lined, 1000 ml carbon steel cylinders. To simulate the interactions with actual storage bottle materials, each test cylinder contained 30 pieces (10.2 cm x 0.8 cm x 0.2 cm) of one of the 8 metals. The combined surface area of the pieces was comparable to the inside of a 1000 ml bottle. New metal pieces were used for each test. Blanks with no metal added were also run. While the 12 fluids in Table 1 and halon 1301 were studied, NaHCO_3 was not tested because it is stable under these storage temperatures and pressures. CF_3I was added to the test list.

Each vessel was filled to the saturation vapor pressure of a liquid agent at 22 °C and then pressurized with nitrogen to an initial pressure of 4.13 MPa (600 psi). FC-116 was available as a high pressure gas, and two other agents (HFC-125 and the azeotrope of HFC-32 and HFC-125) had saturation vapor pressures somewhat higher than the other agents. Therefore, these three were filled to a pressure approximating the mass filled for most of the other agents. All vessels were then stored in an oven for 28 days at 149 °C (300 °F). These tests simulate degradation that might be expected over a far longer storage time under typical use.

After cooling to ambient conditions, an infrared (IR) spectrum of the aged sample was compared to a spectrum of the original sample [14]. Degradation of the sample would be indicated by a systematic decrease in the absorbance of peaks attributable to the agent and/or the appearance of new peaks in the IR spectrum of the aged agent. The absolute signals varied between the two analyses due to sensitivity to the alignment of the Fourier transform infrared (FTIR) spectrometer. Thus, the key indicator of degradation was the formation of new compounds evidenced in the spectra.

For both the initial and final analyses before and after the exposure, a cooled cylinder was connected to the inlet of the gas cell on the FTIR system. The agent/ N_2 mixture was introduced into the gas cell to an absolute pressure of 1330 ± 10 Pa ($9.95 \pm .05$ torr). Three spectra were taken for each sample.

For all 13 agents examined, no new peaks were observed in any of the spectra. To determine whether the peaks of new compounds were being masked by the peaks from the original compound, we examined the peak heights and areas of selected peaks in the spectra before and after the 28 day storage. Again, no new compounds were identified in any of the spectra for any of the agents.

For CF_3I , an initial spectrum and two later (8-day and 28-day) spectra were available. The peak areas systematically decreased over the four-week exposure, but the changes were likely within the experimental measurement error. Since no new compounds were observed in the CF_3I spectra, the possible degradation of CF_3I deserves further examination.

The metal coupons were removed from the cylinders and examined. Changes in their appearance are given in Table 4. When the metals from the CF₃I cylinders were removed, a dark solid was apparent on the coupons, and then disappeared within seconds, perhaps solid I₂ which then sublimed. For the other metals, visual changes may be due to the prolonged heating of the metal or to interaction with the agent. For the former, effects would be observed for all of the agents (for example, the Cu/Be C82500 coupons). Interaction with the agents is far more common, with some metals affected by only a few agents and others effected by nearly all of the agents. HCFC-22 and CF₃I affected most of the metals, while for others, only the Cu/Be C82500 coupons were affected.

Table 4. Visible Changes in Metals After 28-Day Exposures at 149°C (300°F)

Agent	304 stainless steel	Nitronic-40 (21-6-9)	Inconel 625	6061-T6 aluminum	4130 alloy steel	AM 350 stainless	Cu/Be C82500	13-8 Mo stainless
HCFC-22	✓ ^a	✓	✓	✓	✓		✓	✓
HCFC-124							✓	
HFC-125							✓	
HFC-32/HFC-125							✓	
HFC-134a					✓		✓	
FC-218		✓		✓	✓		✓	
HFC-227ea					✓		✓	
FC-31-10		✓		✓	✓		✓	✓
FC-116					✓		✓	
FC-318	✓				✓		✓	
HFC-236fa							✓	
halon 1301							✓	
CF ₃ I	✓	✓	-- ^b	✓	✓	✓	--	✓

a - ✓ indicates visible change in metal appearance after exposure

b - data not available

These results indicate that for these chemicals, stability in long-term storage should not be a major deciding factor in selection of agents for further study. However, pending further study, CF₃I could be an exception.

Elastomer Seal Compatibility

Excessive swelling or deterioration of the elastomer seal (o-ring) and its lubricant in the fire suppressant storage container could lead to leakage of the agent, leaving the system unready to respond in case of fire. The elastomers and lubricants examined in this study (Tables 5 and 6) reflect the types likely to be considered for storage bottle use. Both crosslinked and uncrosslinked elastomers were studied.

Table 5. Elastomers used in swelling experiments

Elastomer	Vendor	Designation
Silicone	Colonial Rubber	Si
55% Butadiene-45% Acrylonitrile	Goodyear	N206
Fluorosilicone	Colonial Rubber	FSi
Viton E-60 Fluorocarbon	Du Pont	FKM
Neoprene	Colonial Rubber	CR
85% Butadiene-15% Acrylonitrile	Goodyear	N926

Table 6. Lubricants used in swelling experiments

Lubricant	Vendor	Designation
Krytox 240AC Fluorinated Grease	Du Pont	240AC
Braycote 600 Perfluoropolyether Grease, Low Volatility	Castrol	600
Braycote 807 Aircraft Grease MIL-G-27617, Type IV	Castrol	807

Two types of measurements were conducted to determine the proclivity of candidate agents to alter the properties of various elastomers and greases and thus assist in the identification of appropriate seals for suppressant storage containers.

Swelling. The degrees of swelling of the greases and elastomers were each determined by measuring the displacement of a quartz spring using a cathetometer as in the

experimental arrangement illustrated in Figure 3. The 2.25 l pressure vessel had two 10.2 cm diameter glass view ports 180° apart for viewing and backlighting purposes. Inside was a stainless steel spring stand with 16 fused quartz spring and pan assemblies. Temperatures were maintained by immersing each vessel in a thermostatically-heated borosilicate jar filled with silicone oil.

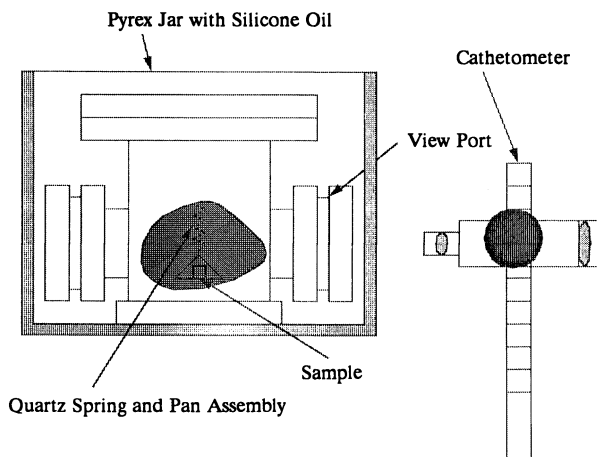


Figure 3. Schematic of the experimental apparatus for isopiestic swelling measurements

Swelling measurements were taken at four vapor pressures at 35, 70, 105, and 150 °C. FC-116 was also tested at 5 °C ($p^{\circ}=2.133$ MPa) because this fluid has a low critical temperature ($T_c = 19.7$ °C) and little swelling was observed at temperatures above T_c . The maximum pressure considered was 5.86 MPa. Saturation pressures for each temperature were determined using thermodynamic properties software [15],[16] or vendor-supplied data [17],[18],[19],[20].

The elastomer's or grease's mass uptake of the agent (solvent) was calculated from the relative displacement of the springs. Values of χ [21] for the various polymer/agent mixtures were then calculated from:

$$\ln(p/p^{\circ}) = \ln(1 - w_2) + w_2 + \chi_0 w_2^2 + \chi_1 w_2^3, \quad (1)$$

where p° is the saturation pressure of the solvent, and w_2 is the polymer weight fraction [22].

The χ ($= \chi_0 + \chi_1$) values were used to characterize the compatibility of the solvents (agents) with the polymers (elastomers and greases). The maximum swelling occurred for exposures at 35 °C, and thus these data were used in the analysis. Small χ values correspond to good solubility or, for present purposes, bad compatibility.

Table 7. Compatibility of lubricants and crosslinked elastomers based on swelling measurements in various fluorocarbon agents at 35 °C

Agent	240AC	600	807	Si	N206	Fsi	FKM	CR	N926
HFC-236fa	good ^a	good	good	fair ^b	fair	bad ^c	bad	bad	bad
HFC-32/125	good ^f	good	good ^f	fair	good ^f	good	good	good	good ^f
HFC-227ea	fair ^f	fair	fair ^f	fair ^c	good ^f	fair ^c	fair ^f	good ^c	bad
HCFC-22	fair	good	fair	fair	bad	fair	fair	good	bad
HFC-134a	good	fair	good	fair	good	fair	good	good ^f	good
FC-116 ^d	fair	fair	fair	good ^f	good ^f	good	good	good ^f	good ^f
HCFC-124	good ^f	good ^f	good	bad ^f	fair ^f	fair ^f	fair ^f	fair ^f	fair ^f
HFC-125	fair	good	good	good	good	good	fair	good	good
FC-218	good ^f	good	good	good	good	good	good	good	good
FC-31-10	fair	bad	bad	fair	fair	good	fair	good	fair
FC-318	fair	fair	fair	good	good	good ^c	good	good	fair

^a $\chi > 1.2$

^b $0.9 \leq \chi \leq 1.2$

^c $\chi < 0.9$

^dmeasured at 5 °C

^e $12.5 < CV < 20\%$ and $0.64 < \chi < 1.5$

^f $CV > 20\%$

Ratings (Table 7) were defined based on the values of χ parameters obtained from swelling measurements at 35 °C, where the swelling was the largest. Good compatibility ($\chi > 1.2$, $w_1 < 0.22$) implies that an elastomer or lubricant is acceptable for use in the fire suppressant system. Bad compatibility ($\chi < 0.9$, $w_1 > 0.38$) corresponds to excessive swelling. For values of $0.9 < \chi < 1.2$, the agent was considered to have fair compatibility with the elastomer or grease and represents a marginally acceptable system.

Durability. These measurements produced data on residual mechanical (rheological) properties of the elastomers and greases, determining their ability to maintain their elasticity. Ratings were based on the results of compression set and tensile test measurements of the elastomers and viscosity measurements of the greases. These tests provide direct information on the physical and chemical damage to the samples at extreme conditions. It is important to note that the long term exposure response of these materials cannot be extracted from the tests as performed.

The mechanical property measurements of the elastomers and greases were obtained after 1-, 2-, 4- and 6-week exposures to the agents at the extreme conditions of 150 °C and 5.86 MPa. The two pressure vessels were similar to those used for the swelling measurements, but without view ports. Inside each vessel was a compression set fixture with samples of the 6 elastomers, and a 2 ml vial for each of the three greases. The vessel was heated using a forced air oven. The o-rings used in this study were Parker size no. 2-214 and are listed in Table 8.

Table 8. Elastomers used in durability experiments

Elastomer	Vendor	Designation
Silicone	Parker	S604-70 ^a
Nitrile (standard industrial)	Parker	N674-70
Fluorosilicone	Parker	L1120-70
Fluorocarbon	Parker	V1164-75
Neoprene	Parker	C1185-70
Nitrile (low temperature industrial)	Parker	N103-70

^aThe number following the dash in the designation (compound number) represents the Shore hardness of the elastomer.

The compression set tests were conducted per standard test methods [23],[24]. The compression set C_b was calculated using the average thickness readings before and after the exposure and was expressed as a percentage of the original deflection. Bad compatibility was defined as a condition when the compression set exceeded 90% after a 2 week exposure. Elastomers have good compatibility if the compression set was less than 90% after 4 weeks. Fair compatibility (marginally acceptable) meant that the compression set was less than 90% after 2 weeks but exceeded 90% after a 4-week

exposure. If a specimen was split or broken, the agent was considered to have bad compatibility with the elastomer.

Tensile tests were conducted per standard test methods [25]. For each agent, ultimate elongation, tensile stress, and modulus measurements were taken after 1-, 2-, 4-, and 6-week exposure times at 150 °C and 5.86 MPa. A type TT-B Instron tensile testing instrument was used for this purpose. The force F was recorded at rupture and at an elongation of 100% (if the ultimate elongation exceeded 100%). If the o-ring could not be installed without breaking the specimen because of embrittlement due to the high temperature exposure, the specimen was considered to have a 100% decrease in ultimate elongation.

The elastomers were then rated as follows. Bad compatibility was defined as

Table 9. Compatibility of elastomers and lubricants based on durability ratings (G = good, F = fair, B = bad)

Agent	240AC	600	807	S604-70	N674-70 (N206)	L1120-70	V1164-75	C1185-70	N103-70 (N926)
HFC-236fa	G ^a	G	G	G (F) ^b	B (F)	G (B)	B	B	B
HFC-32/125	G	G	G	G (F)	B (G)	B (G)	B (G)	F (G)	B (G)
HFC-227ea	B (F)	G (F)	G (F)	G (F)	B (G)	G (F)	B (F)	F (G)	B
HCFC-22	B (F)	B (G)	F	B (F)	B	G (F)	B (F)	B (G)	F (B)
HFC-134a	B (G)	B (F)	B (G)	G (F)	B (G)	G (F)	B (G)	F (G)	B (G)
FC-116	F	G (F)	G (F)	G	F (G)	G	B (G)	G	B (G)
HCFC-124	G	G	G	B	B (F)	G (F)	B (F)	B (F)	B (F)
HFC-125	G (F)	G	G	G	B (G)	B (G)	B (F)	G	B (G)
FC-218	B (G)	B (G)	B (G)	G	F (G)	G	B (G)	G	B (G)
FC-31-10	B (F)	B	B	G (F)	B (F)	F (G)	B (F)	F (G)	B (F)
FC-318	B (F)	B (F)	B (F)	G	F (G)	G	G	G	F

^aIf the ratings for compression set and tensile testing were different, the worse compatibility is listed

^bIf different, the rating for swelling compatibility (Table 7) is listed in parentheses

the decrease in ultimate elongation exceeding 65% after a 2 week exposure. Good compatibility meant the decrease was less than 65% after 4 weeks. If the decrease in ultimate elongation was less than 65% after 2 weeks but exceeded 65% after a 4-week exposure, the agent was considered to have fair compatibility with the elastomer and represents a marginally acceptable system.

The rheological properties of each grease were characterized using a Rheometrics Mechanical Spectrometer Model 800. The viscosity of the greases, when measurable, did not show systematic variation with exposure time, indicating that no significant chemical degradation occurred. However, mobile substances or fractions were extracted by some of the candidate fire suppressant fluids, resulting in the

greases becoming powder-like, *i.e.*, their viscosities were not measurable. Therefore, the ratings for the lubricant compatibility were based on the following criteria. Good compatibility meant the grease did not become powder-like after a 6 week exposure. Bad compatibility meant the grease became powder-like after a 4 week exposure. Fair compatibility meant the grease's viscosity was measurable after 4 weeks, but became powder-like after 6 weeks.

Table 9 shows the compiled compatibility of the elastomers and lubricants. It is clear from the results of the durability testing that the 150 °C condition is too severe, *i.e.*, property changes for the most part were extreme. Further testing at lower temperatures will be required to provide better estimates of elastomer and lubricant durabilities. However, the data show that there are elastomer materials and lubricants that are suitable for use with each tested suppressant.

Conclusion

Procedures have been developed for appraising the mutual stability of fire suppressant chemicals and the materials of their storage containers. These methods are capable of differentiating among chemicals, elastomers and greases, and metals on the basis of their performance in close simulations of actual storage. In general, there are storage materials available for any of the 13 tested candidate suppressants, although the choices are more restrictive for some of the chemicals.

Acknowledgments

This work was sponsored as part of the Department of Defense Technology Strategy for Alternatives to Ozone-Depleting Substances by the U.S. Air Force, Navy, Army, and Federal Aviation Administration. The program was directed by Michael J. Bennett of the Wright Laboratory, U.S. Air Force.

Literature Cited

1. Zallen, D.M., Halon Replacement Study, SBIR Report No. ZIA-92-001 to Aeronautical Systems Division, Wright-Patterson AFB, Zallen International Associates, Albuquerque, February 28, 1992.
2. Purdue Research Foundation and Department of Chemistry, Final Report on Fire Extinguishing Agents, AD 654322, Purdue University, West Lafayette, IN, July 1950.
3. Pitts, W.M., Nyden, M.R., Gann, R.G., Mallard, W.G., and Tsang, W., "Construction of an Exploratory List of Chemicals to Initiate the Search for Halon Alternatives," NIST Technical Note 1279, National Institute of Standards and Technology, Gaithersburg, MD, August 1990.
4. Sheinson, R.S., Penner-Hahn, J.E., and Indritz, D., "The Physical and Chemical Action of Fire Suppressants," *Fire Safety Journal* **15**, 437-450 (1989).
5. Tapscott, R.E., Moore, J.P., Lee, M.E., Watson, J.D., and Morehouse, E.T., Next Generation Fire Extinguishing Agent Phase III, ESL-TR-87-03, Air Force Engineering and Services Center, Tyndall AFB, FL, April 1990.
6. Grosshandler, W.L., Gann, R.G., and Pitts, W.M., eds., *Evaluation of Alternative In-Flight Fire Suppressants for Full-Scale Testing in Simulated Aircraft Engine Nacelles and Dry Bays*, NIST Special Publication 861, National Institute of Standards and Technology, Gaithersburg, MD, 1994.
7. Gann, R.G., Barnes, J.D., Davis, S., Harris, J.S., Harris, Jr., R.H., Herron, J.T., Levin, B.C., Mopsik, F.I., Notarianni, K.A., Nyden, M.R., Paabo, M., and

- Ricker, R.E., "Preliminary Screening Procedures and Criteria for Replacements for Halon 1211 and 1301," NIST Technical Note 1278, August 1990.
8. ASTM, Standard Practice for Laboratory Immersion Corrosion Testing of Metals, *Annual Book of ASTM Standards Section 3, Metals Test Methods and Analytical Procedures*, Phil., PA, 1993.
 9. ASTM, Standard Guide for Applying Statistics to Analysis of Corrosion Data, *Annual Book of ASTM Standards Section 3, Metals Test Methods and Analytical Procedures*, Phil., PA, ASTM, 1993.
 10. Romans, H. B., and H. L. C., Jr., "Atmospheric Stress Corrosion Testing of Aluminum Alloys," *Metal Corrosion in the Atmosphere*, Boston, MA, ASTM, 1967.
 11. Scully, J. R., Frankenthal, R. P., Hanson, K. J., Siconolfi, D. J., and Sinclair, J. D., "Localized Corrosion of Sputtered Aluminum and Al-0.5% Cu Alloy Thin Films in Aqueous HF Solution: II. Inhibition by CO₂," *J. Electrochem. Soc.*, 137, 1373-1377, 1990.
 12. Scully, J. R., Peebles, A. D., Romig, A. D., Frear, D. R., and Hills, C. R., "Metallurgical Factors Influencing the Corrosion of Aluminum, Al-Cu, and Al-Si Alloy Thin Films in Dilute Hydrofluoric Solution," *Metallurgical Transactions A* 23A, 2641-2655, September 1992.
 13. Stoudt, M. R., Vasudévan, A. K., and Ricker, R. E., "Examination of the Influence of Lithium on the Repassivation Rate of Aluminum Alloys," *Corrosion Testing of Aluminum Alloys*, San Francisco, CA, ASTM, Phila., PA., 1990.
 14. Willis, H.A., Van der Maas, J.H., and Miller, R.G.J. (eds.), *Laboratory Methods in Vibrational Spectroscopy*, John Wiley & Sons, New York, 1987.
 15. Gallagher J., McLinden, M., Huber, M., and Ely, J., *NIST Standard Reference Database 23: Thermodynamic Properties of Refrigerants and Refrigerant Mixtures Database (REFPROP), Version 3.0*, U.S. Department of Commerce, Washington, DC (1991).
 16. Allied Signal, Inc., *Thermodynamic Properties of Refrigerants (Genie)*, SML Services, Inc. (1989).
 17. E.I. du Pont de Nemours and Co., Inc., *Thermodynamic Properties of "Freon" 116 Refrigerant*, (1968).
 18. E.I. du Pont de Nemours and Co., Inc., *Thermodynamic Properties of HFC-236fa Refrigerant*, (1993).
 19. Robin, M.L., *Thermodynamic and Transport Properties of FM-200*, Great Lakes Corporation (1992)
 20. Wilson, L.C., Wilding, W.V., and Wilson, G.M., *Thermo-Physical Properties of Perfluorobutane*, Wiltech Research Company (1992).
 21. Flory, P.J., *Principles of Polymer Chemistry*, Cornell University Press, Ithaca, New York (1953).
 22. McKenna, G.B. and Crissmann, J.M., "Thermodynamics of Crosslinked Polymer Networks: The Anomalous Peak in Swelling Activity Measurements," *Macromolecules* 1992, ed by J. Kahovec, VSP, Utrecht, The Netherlands, pp. 67-81 (1993).
 23. ASTM, Designation D 395-89, "Standard Test Methods for Rubber Property - Compression Set," *Annual Book of ASTM Standards*, 09.01, 24 (1989).
 24. ASTM, Designation D 1414-90, "Standard Test Methods for Rubber O-Rings," *Annual Book of ASTM Standards*, 09.02, 181 (1990).
 25. ASTM, Designation D 412-87, "Standard Test Methods for Rubber Properties in Tensions," *Annual Book of ASTM Standards*, 09.02, 100 (1990a).

RECEIVED July 20, 1995

Chapter 13

New Halon Replacements Based on Perfluoroalkylamines

An Approach from the Other Side of Fluorine Chemistry

K. Takahashi¹, T. Inomata¹, H. Fukaya², and T. Abe²

¹Department of Chemistry, Faculty of Science and Technology, Sophia University, 7-1 Kioi-cho, Chiyoda-ku, Tokyo 102, Japan

²Chemistry Department, National Industrial Research Institute of Nagoya, 1-1 Hirate-cho, Kita-ku, Nagoya 462, Japan

Several perfluoroalkylamines and their derivatives which include perfluoro(*N,N*-dimethylethylamine), perfluoro(*N,N*-dimethylvinylamine), perfluorotriethylamine, and *N,N*-bis(trifluoromethyl)-1,1,2,2-tetrafluoroethylamine were synthesized. They were evaluated as new Halon replacements in terms of the fire extinguishing ability by the box method and by measurements of laminar burning velocities. The inhibition mechanism of perfluoroalkylamines was suggested by a model calculation.

The destruction of ozone layer has become the most urgent global environmental problem should be resolved by international cooperation(1). The phase-out of CFCs and Halons by the end of 1999 has been decided at the international meeting(London,1990). However, the fact that the ozone layer is being destroyed far faster than scientists expected has called for the development of their alternatives as well as an acceleration of the phase-out time of CFCs by 1995 and Halons by 1993, respectively(Copenhagen).

From the view point of synthetic fluorine chemistry, perfluoroalkylamines are useful compounds having versatile utility that primarily depends on the length of the carbon chain. For example, Halon 1301 is used as the reagent for the preparation of CF₃-containing compounds(2). Its, higher homologues, perfluorooctylbromide is also useful for X-ray shielding agent for human body that have two functions of an imaging and oxygen transporting media(3). In connection with the study on the synthesis of bromine-containing perfluoroalkylamines for the development of new X-ray shielding agents, we have identified perfluoro-alkylamines and their derivatives as prospective candidates for the new Halon replacements. Because they have some degradability at the C-F bond to the nitrogen(4) and they are very low

0097-6156/95/0611-0139\$12.00/0
© 1995 American Chemical Society

toxicity in the case of perfluoroalkylamines due to their use as an artificial blood substitutes(5).

However, during this work, regulations on the use of chlorine and/or bromine-containing volatile compounds(carbontetrachloride, 1,1,1-trichloroethane, and methylbromide) were strengthened, which was led to the ban on their use from 1994 under Montreal Protocol. So, bromine-containing perfluoroalkylamines should be removed from the list of virtual candidates. However, perfluoroalkylamines, of which ODP is zero due to the absence of bromine in the molecules, are most promising, having excellent fire extinguishing ability.

This article describes the data of the synthesis of several perfluoroalkylamines and their derivatives. Fire extinguishing ability for these compounds were evaluated by a box method and by the measurement of laminar burning velocities for the development of new Halon replacements.

Preparation of Perfluoroalkylamines and Their Derivatives

Perfluoroalkylamines and their derivatives used in this experiments were all made and purified by distillation before use. The physical properties of these compounds are shown in Table I .

Preparation of Perfluoro(N,N-dimethylethylamine) and Perfluorotriethylamine.

These tertiary perfluoro alkylamines were prepared by the electrochemical fluorination of corresponding alkylamines in yield of 20-40%(6). For example, perfluoro(N,N-dimethylethylamine) was obtained from the fluorination of N,N-dimethylethylamine in 20% yield(7). Work-up of the purification for perfluoro(N,N-dimethylethylamine) was conducted in a following manner. Before the purification by a fractional distillation, the crude products(about 140 g) were treated to remove traces of compounds having -NF group and hydrogen-containing compounds by heating with a mixture composed of acetone(50 ml), water(50 ml), and NaI(2 g) at 323 K in a 500 ml Hoke cylinder, and then by heating with a mixture of an aqueous KOH solution(7 M, 40 ml) and diisobutylamine(10 ml) at 373 K for 3 hours in a Hoke cylinder, respectively. After washing with distilled water several times, the fraction(92.5 g) having a boiling point of 293-295 K was collected by distillation. The purity of perfluoro(N,N-dimethylethylamine) and of perfluorotriethylamine was 93% and 98.2% by GC analysis, respectively. Impurities were found to be perfluoroamines and polyfluoroamines, which were identified by GC-MS Spectroscopy. The latter compounds survived through the chemical treatment with strong base.

Preparation of Perfluoro(N,N-dimethylvinylamine). Perfluoro(N,N-dimethylvinylamine) was prepared by the method reported in ref.8. Pyrolysis of a dry mixture of potassium fluoride and potassium perfluoro(3-dimethyl-aminopropionate) (245 g) at 523-543 K afforded crude perfluoro(N,N-dimethylvinylamine(100 g) in 73% yield.

After washing by passing into consecutive gas washing bottles that contain diluted aqueous solution of sodiumhydrogencarbonate and water, respectively, perfluoro-(N,N-dimethylvinylamine) was purified by a low temperature distillation. The purity 98.4% by GC analysis.

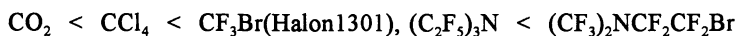
Preparation of N,N-bis(trifluoromethyl-1,1,2,2-tetra-fluoroethylamine). Pyrolysis of a dry mixture of potassium fluoride and potassium perfluoro(3-dimethylamino-propionate)(41 g) in the presence of ethyleneglycol (19.4g) in a 300ml Hoke cylinder at 443 K for 4.5 hrs afforded crude N,N-bis(trifluoromethyl)-1,1,2,2-tetrafluoroethylamine(19.4g) in 71% yield(9). The work-up was similar to that in previous section Its purity was 97.5% by GC analysis.

Evaluation of the Fire Extinguishing Ability by the Box Method

Evaluation of the fire extinguishing ability of perfluorotriethylamine, $(C_2F_5)_3N$, was tested by the box method(10). Perfluoro(N,N-dimethyl-2-bromoethylamine), Halon 1301, CO_2 , and CCl_4 were also investigated to compare with the amine.

Experimental. The test enclosure was similar to that reported in the literature(10). It was made of methacrylate resin(20x20x20 cm), which consisted of the container and the top lid. A hole(5 cm dia) was provided at the center of the lid for the introduction of agents. At one of the side wall of the container, a hole(5 cm dia) for air inlet was provided during preburn 5 cm below the center. After the preburn, this side hole was closed with a plug. It takes about 19-20 s to smother the flame if the side hole is closed after 7 s preburn and with no agent addition. The calculated amount of agent was charged in the steel cylinder(900 ml) using vacuum line, and pressurised with air to 1.5 atm by a compressor. In the center of the test enclosure, was placed a 50x5 mm metal dish that contained fuel(n-hexane). The fuel was ignited and allowed a 7 seconds preburn before the introduction of the agents. During the preburn, air was admitted into the enclosure through the side hole. After 7 seconds, the air hole was closed and the predetermined amount of the agent was introduced(Fig.1). The extinguishing time was measured between admitting the agent and extinguishment of the flame.

Results. The following order of the fire extinguishing ability(reverse order of the time) was observed for the compounds as shown in Fig.2.



Among agent tested, perfluoro(N,N-dimethyl-2-bromoethylamine) shows better fire extinguishing ability than Halon1301 and perfluorotriethylamine has comparable ability to that of Halon1301 as the fire extinguisher. So, the perfluorotriethylamine that does not have a bromine atom in the molecule was found to be a highly effective fire extinguisher. Its good fire extinguishing ability is considered to be based on the physical suppression mechanism including the third body radical

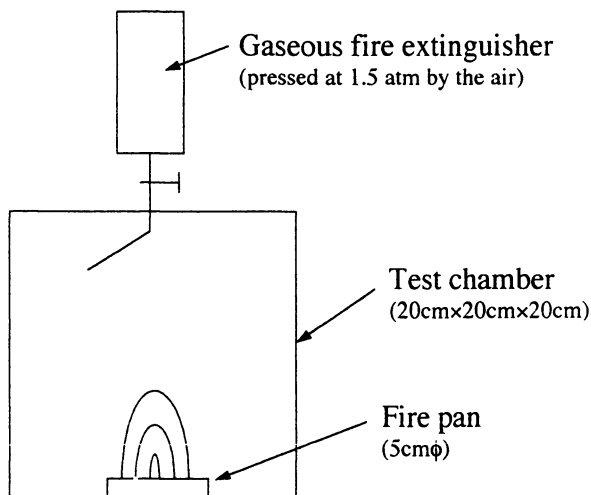


Fig.1 Schematic diagram of experimental apparatus for fire extinguishment.

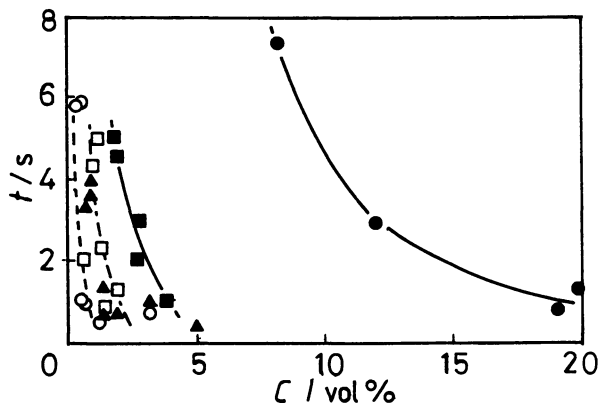


Fig.2 Evaluation of fire extinguishing ability. t is extinguishment time and C is composition of additives. ■ : CCl_4 , ● : CO_2 , ▲ : CF_3Br , ○ : $(\text{CF}_3)_2\text{NCF}_2\text{CF}_2\text{Br}$, □ : $(\text{C}_2\text{F}_5)_3\text{N}$.

one(11). The contribution of pentafluoroethyl radical that is formed because of the bond cleavage of perfluoroamine on contact with the flame zone is also expected.

Inhibition Effect of Perfluoroalkylamines on n-Heptane Flames

In order to estimate the physical and chemical effects, laminar burning velocities were measured and model calculations were performed in n-heptane flame.

Experimental. Laminar burning velocities were measured using the density ratio method. The cylindrical combustion chamber used was previously described in detail (Takahashi, K. et al. *Combust. Sci. Tech.* in press.). A mixture of n-heptane, air, and inhibitor were introduced into the chamber and ignited at the center by an electrical spark whose energy is 200-400 mJ. The velocity of propagating flame (S_s) was measured by two ion probes that were set at 1.5 cm and 3.0 cm from the center of the chamber.

As the flame propagates at constant pressure in the early stage, the laminar burning velocity (S_u) can be calculated by the expression:

$$S_u = S_s(M_b T_u / M_u T_b)$$

where M and T mean molecular weight and temperature, respectively. Subscript u and b refer to the unburned and the burned states. To estimate T_b and M_b , the adiabatic flame temperature was calculated. All measurements were carried out with an initial temperature of 298 ± 2 K and a pressure of 1 atm, using 1.87% n-heptane, 97.63% air, and 0.50% inhibitor. Perfluoroalkylamines used in this study were $(CF_3)NCF_2CF_3$, $(CF_3)_2NCF_2CHF_2$, and $(CF_3)_2NCF_2CF_2$. FM200, CH_3Br , CF_3Br , CF_4 , and CO_2 were also examined as fire-extinguishers to compare with the perfluoroalkylamines.

Model Calculation of Laminar Burning Velocity. To analyze the inhibition effect on flame propagation, a computer simulation was made using the PREMIX(12) and CHEMKIN-II(13) codes, running NEC ACOS-930 computer system. The thermochemical data, namely, heats of formation and the temperature dependencies of specific heat and entropy, were found from CHEMKIN data base(14), JANAF tables(15), NBS tables(16), and NASA compilations(17) when they were available. Those data for species that have not been published were established using theoretical methods described by Benson(18). The transport data are essentially the same as those recommended by Kee et al.(19) or were estimated using theoretical methods discussed by Svehla(20).

The present reaction scheme for hydrocarbon oxidation was constructed as suggested by Warnatz(21). R92 and R94-R97 (Table II) for C_3H_4 were added to the mechanism R1-R91 and R93(21) for H_2 , CO, and C_1 - C_3 species, because the fuel rich condition is predicted in the mixture containing inhibitor. It is well known that

Table I. Properties of polyfluoroalkylamines

Sample	b.p.(°C)	n_D^{20}	d_D^{20}
$(CF_3)_2NC_2F_5$	20~22		
$(C_2F_5)_3N$	70.3	1.262	1.736
$(CF_3)_2NCF=CF_2$	13.7(extraporated)		
$(CF_3)_2NCF_2CF_2H$	32.0(extraporated)		

Table II. Reaction Mechanism for n-Heptane Oxidation. Rate Coefficients in the form $k=AT^n \exp(-E/RT)$ in $cm^3\text{-mol-s-kJ-K}$ units.

Reaction	log A	n	E
R 92 $C_3H_6 + H \rightarrow C_3H_5 + H_2$	5.011E+12	0.00	6279.0
R 93 $C_3H_6 + O \rightarrow C_2H_5 + HCO$	3.548E+12	0.00	0.0
R 94 $C_3H_5 + O_2 \rightarrow C_3H_4 + HO_2$	6.025E+11	0.0	41800.0
R 95 $C_3H_4 + OH \rightarrow HCO + C_2H_4$	1.000E+12	0.0	0.0
R 96 $C_3H_4 + O \rightarrow HCO + C_2H_3$	1.000E+12	0.0	0.0
R 97 $C_3H_6 + OH \rightarrow CH_3HCO + CH_3$	1.000E+13	0.00	0.0
R 98 $C_7H_{16} + H \rightarrow C_7H_{15} + H_2$	4.500E+06	2.00	20900.0
R 99 $C_7H_{16} + O \rightarrow C_7H_{15} + OH$	1.400E+13	0.00	21700.0
R100 $C_7H_{16} + OH \rightarrow C_7H_{15} + H_2O$	6.500E+08	0.12	2940.0
R101 $C_7H_{15} \rightarrow CH_3 + C_3H_6 + C_3H_6$	1.600E+13	0.00	142000.0
R102 $C_7H_{15} \rightarrow C_2H_5 + C_2H_4 + C_3H_6$	1.600E+13	0.00	138000.0

Table III. Observed and Calculated Burning Velocities for n-Heptane and Methane Flames

Inhibitors	$S_W/cm \cdot s^{-1}$			
	n-heptane		methane	
	obs.	calcd.	obs.	calcd.
None	44	45	39	39
$(CF_3)_2NC_2F_5$	33	38	28	34
$(C_2F_5)_3N$	—	—	28	32
$(CF_3)_2NCF=CF_2$	34	39	29	34
$(CF_3)_2NCF_2CF_2H$	33	38	29	34
CF_3CFHCF_3 (FM200)	38	—	34	—
CF_4	39	41	37	37
CF_3Br	32	34	23	26
CH_3Br	34	35	30	31
CO_2	41	42	38	—

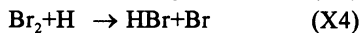
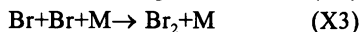
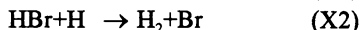
an alkyl radical formed in the initial step decomposes to smaller alkyl radicals and alkenes(22,23). However detailed a decomposition mechanism for n-heptane may be very complicated, because of the variety of the isomers. Warnatz indicated that the only realistic possibility is to find "representative reactions" and "representative species" to describe these complex processes(21). Four kinds of isomers as initial alkyl radicals are formed by elimination of H atom from n-heptane. These radicals successively decompose to smaller alkenes and alkyl radicals and finally produce CH_3 , C_2H_3 , C_2H_5 , C_3H_7 , C_2H_4 , and C_3H_6 . As the reactions including CH_3 and C_2H_5 have marked sensitivity for the burning velocity, they were chosen as "representative radicals". Rate coefficients for the reactions of H, OH, and O with n-heptane were derived from Ref.24. Since the rate coefficients for decomposition reaction of C_7H_{15} are not known, the coefficients for n- C_4H_9 were modified in the acceptable limit to fit calculated burning velocity with measured one in n-heptane-air mixture.

The reaction mechanism including bromic and fluoric species and those kinetic data were suggested by Westbrook(25) and were already listed(Takahashi,K. et al. *Combust. Sci. Tech.*, in press).

Results. The inhibition mechanism of fluorinated C_1 compounds gives us valuable information to understand that higher perfluorocarbons. So we first discuss the addition effect of C_1 compounds of which the inhibition mechanism have been well understand.

Inhibition Effect on Burning Velocities by C_1 Compounds. Table III shows the laminar burning velocities of n-heptane flames with those of methane flames containing additives. The measured burning velocity in n-heptane-air mixture agrees with previous one, 42 cm s^{-1} (26). CH_3Br and CF_3Br reduce S_u by 23% and 27 % in n-heptane flames, respectively. On the other hand, reducing ratio for CO_2 and CF_4 are less than 10%. Although CF_3Br has considerably stronger effect in methane flames than in n-heptane flames, the whole tendencies are the same in both flames.

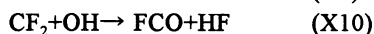
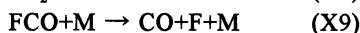
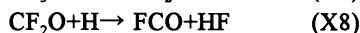
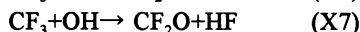
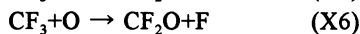
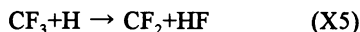
The role of bromine in bromic inhibitor has been clarified(25,27-30) as follows. $\text{RBr}(\text{CH}_3\text{Br}, \text{CF}_3\text{Br})$ is decomposed in pre-flame region by H atom that diffuses from downstream of flame(X1). HBr then acts by catalyzing the recombination of H atoms into H_2 molecules through reactions (X2)-(X4). The action decreases the rate of chainbranching reaction, $\text{H} + \text{O}_2 \rightarrow \text{OH} + \text{H}$, leading flame inhibition.



If the inhibition effect of CF_3Br is caused by this chain cycle only, the difference between CH_3Br and CF_3Br cannot be interpreted. CF_3 radical seems to contribute to high inhibition efficiency of CF_3Br .

To make clear the role of CF_3 radicals in n-heptane flame, a computer simulation was carried out for mixtures containing CH_3Br , CF_3Br , and CF_4 . Table III also shows the calculated burning velocities. For all inhibited flames, the calculated burning velocities are larger than the observed ones. However, the calculation qualitatively expresses the experimental feature in which CF_3Br has the highest inhibition efficiency and CF_4 has the lowest one in the three inhibitors.

The simulation indicates that CF_3 radicals mainly react with H, O, and OH to become F or HF that furthermore CF_2O and CF_2 finally form F or HF. F atoms are consumed right away by alkyl radicals or by fuels to produce HF. Masri also suggested that CF_3 reacts quickly to HF and CF_2O (30).



Since H, O, and OH are important chain carriers for combustion reactions, the removal of them leads to the higher inhibition efficiency of CF_3Br than that of CH_3Br . However, HF is very stable and the calculation shows the reaction (X11) proceeds to the reverse direction in whole region of flame, so that the chain cycle like as (X2)-(X4) does not form, resulting less effect of F atom in contrast with Br atom.



CF_4 can hardly affect the burning velocity. This is also true for CO_2 which has only a dilution effect under these experimental conditions. The initial step for decomposition of CF_4 is also the F atom abstraction by H atom. However, the rate of (X12) is very slow due to the small rate coefficient and CF_4 does not decompose until the post-flame region (Takahashi, K. et al. Combust. Sci. Tech. in press). Consequently, CF_4 has no chemical inhibition effect in spite of having F atoms. An inhibitor containing F atoms must easily generate C_nF_m radicals in order to have chemical inhibition effects.



Inhibition Effect of Perfluoroalkylamines. Perfluoroalkylamines reduced the laminar burning velocities of n-heptane by 23-27%, slightly less than CF_3Br but more than $\text{CF}_3\text{CHFCF}_3$ (FM200) as shown in Table III. This results indicate the possibility that the perfluoroalkylamines can replace Halons, although the effect on the burning velocity does not always reflect fire fighting ability.

Generally inhibition of flame propagation by additives takes place in both physical and chemical effects. The physical effect means dilution and the changes of transport and thermodynamic properties. The chemical one, of course, is removal of carriers for chain branching. To estimate the degree of physical effects, a calculation was carried out under assumption that the perfluoroalkylamines were chemically inert (Table III).

Since the perfluoroalkylamines are big and complicated molecules, they have high specific heats. Therefore, if the same mole fraction of additive were added to a flame, the amines can cause stronger physical effect than relatively small molecules. Calculated burning velocity in mixture containing each perfluoroalkylamine is faster than observed one but slower than both measured and calculated burning velocity in *n*-heptane. This facts mean that the perfluoroamines have not only a physical effect, but also a chemical effect.

Unfortunately, we cannot directly clarify the chemical effect due to lack of a detailed reaction mechanism including the perfluoroalkylamines and its kinetic data. However, the discussions for CF_3 in the preceding section suggest the chemical inhibition results from removal of H, O, and OH radicals by fluoric species.

Figure 3 shows the reduction in burning velocities per fluorine atom, $-S_u/N_F$, against the number of fluorine atoms, N_F , in perfluoroalkylamines and FM200. If an inhibition efficiency depends only on N_F , the plot for FM200 should be on the line extrapolating the points of perfluoroalkylamines. This tendency did not appear in the experiments. The thermal stabilities of perfluoroalkylamines and FM200 seem to lead their different inhibition efficiencies. The perfluoroalkylamines decompose through the carbon-nitrogen bond cleavage, while FM200 does through carbon-carbon bond cleavage. As the dissociation energy of C-N bond is lower than the C-C bond, perfluoroalkylamines can decompose more easily. CF_3 radicals capture the chain carriers in the flame, leading high chemical inhibition efficiencies of perfluoroalkylamines, because they produce perfluoroalkyl radicals in lower temperature region of flame.

Discussion

It is generally thought that Halons function is chemically as well as physically in fire suppression. High effectiveness in fire suppression by Halons is based on the chemical suppression mechanism due to the presence of bromine atom. In fact, the bromine-containing compounds have excellent ability for fire suppression. However, the perfluoroalkylamines tested in this experiments have comparable ability with Halon1301 and the inhibition effects cannot be explained by physical effect alone. We already discussed the role of CF_3 radical on the burning velocities in the previous sections. However, another mechanism may be possible. To explain the behavior of CF_3 radical, theoretical treatment by Gaussian 92 program using 6-31G(d) basis set was performed. It is clarified that CF_3 radical is very apt to combine with both H and OH, which behaves catalytically as a radical scavenger

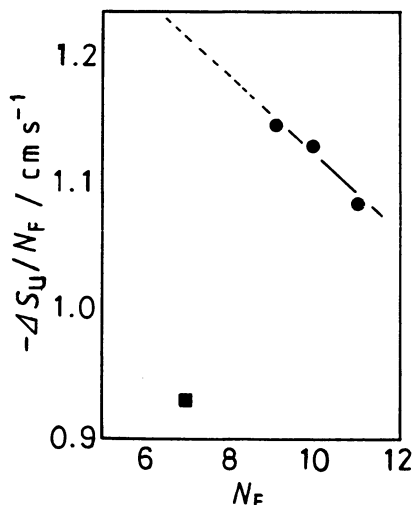
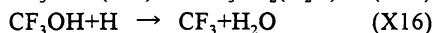
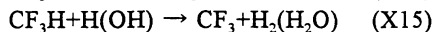


Fig.3 Reduction in burning velocity per fluorine atom($-\Delta S_u/N_F$) against the number of fluorine atom(N_F). ● : polyfluoroalkylamines, ■ : FM200.

just like the Br(Fukaya,H. and Abe,T., unpublished data). The important points are that the stabilization of the active species by the recombination reaction between CF_3 and $\text{H}(\text{OH})$ and that reproduce of CF_3 from CF_3H or CF_3OH .



This cycle resemble the fire suppression by bromine atom. A further study needs to make clear which is dominant for fire suppression by CF_3 , (X5)-(X7) or (X13)-(X16).

Although perfluorotriethylamine has almost the same efficiency as CF_3Br in the box method, perfluoroalkylamines show lower efficiency than that of CF_3Br in the measurement of burning velocity. Br atom most strongly contributes to the chemical effect and perfluoroalkylamine containing Br atom shows the best fire extinguishing ability as shown in Fig.2 and Table III. The physical effect depends on size of molecule. These facts indicate that the chemical effect intensely reveals than the physical effect for the burning velocity against for the box method.

There are some problems with perfluoroalkylamines use as a fire extinguisher. Firstly, toxicity tests are needed. Our working group has already shown that the $(\text{CF}_3)_2\text{NCF}_2\text{CF}_3$ is harmless, but the others have not been tested. Second, the influence on the environment has to be estimated. Since the chain length of the FOx cycle to ozone decomposition is much shorter than those of the ClOx and BrOx

cycles, the ODPs of the perfluoroalkylamines are nearly zero. Nevertheless the problem of global warming is left. The perfluoroalkylamines have weak C-N bonds so that they seem to give lower global warming potentials than the polyfluorocarbons, but we must quantitatively evaluate the potentials.

The boiling points of these perfluoroalkylamines are above 253 K. Therefore, the use of perfluoroalkylamines alone as a fire-extinguisher are restricted to streaming, but blending with propellants including compounds which have lower boiling points will make total flood use possible.

Literature Cited

1. Molina, M.J.; Rowland, F.S. *Nature*, **1974**, 249, pp.810.
2. Trodeux, M.; Francese, C.; Wakselman, C. *J.Chem.Soc. Perkin Trans.1.* **1990**, pp.1951.
3. Long, D.M.; Higgins, C.B.; Mattrey, R.F.; Mitten, R.M.; Multer, F.K. In *Preparation, Properties, and Industrial Application of Organofluorine Compounds*; Banks, R.E. Ed.; Ellis Horwood: London, 1982. pp139-156.
4. Hayashi, E.; Abe, T.; Nagase, S. *J.Fluorine Chem.* **1988**, 41, pp.213.
5. Blanc, M.Le.; Riess, J.G. In *Preparation, Properties, and Industrial Application of Organofluorine Compounds*; Banks, R.E. Ed; Ellis Horwood: London, 1982; pp83-138 and Blood Substitute; Loe, K.C. Ed; Ellis Horwood: Chichester, England, 1982.
6. Weinberg, N.L.; Electroorganic Chemistry; Weinberg, N.L. Ed.; In *Technique of Chemistry Volume V*; John Wiley & Sons: 1975; Part II, pp1-82.
7. Abe, T.; Hayashi, E.; Baba, H.; Nagase, S. *Nippon Kagaku Kaishi (J.Chem.Soc.Jpn)*. **1985**, pp.1980.
8. Abe, T.; Hayashi, E.; Shimizu, T. *Chem. Letters.* **1989**, pp.909.
9. Japan Kokai Tokkyo Koho 05-132451[93,132451].
10. Fukaya, H.; Hayashi, E.; Hayakawa, Y.; Baba, H.; Abe, T.; Taoda, H.; Osaki, T. *J. Environmental Chem.* **1993**, 3, pp.271.
11. Clay, J.T.; Walters, E.A.; Willcox, M.V.; Arneberug, D.L.; Nimits, J.S. *Proc. Halon alternatives technical working conference at Albuquerque*, NM, 1991, pp.79.
12. Kee, R.J.; Grear, J.F.; Smooke, M.D.; Miller, J.A. *A Fortran Program for Modeling Steady laminar One-Dimensional premixed Flames*; SAND85-8240; Sandia National Laboratories; Albuquerque, NM, 1992.
13. Kee, R.J.; Rupley, F.M.; Miller, J.A. *Chemkin-II*; SAND89-8009B; Sandia National Laboratories; Albuquerque, NM, 1989.
14. Kee, R.J.; Rupley, F.M.; Miller, J.A. *The Chemkin Thermodynamic Data base*; SAND87-8215B; Sandia National Laboratories; Albuquerque, NM, 1991.
15. Stull, D.R.; Prophet, H. *JANAF thermochemical tables*, 2nd ed.; NSRDS-NBS37; NBS, Washington D.C., 1971.
16. Wagman, D.D.; Evans, W.H.; Parker, V.B.; Schumm, R.H.; Halow, I.; Bailey, M.; Churney, K.L.; Nuttall, R.L. *The NBS tables of chemical thermodynamic properties*; NBS, Washington D.C., 1982.

17. Bahn, G.S. *Approximate thermochemical tables for some C-H and C-H-O species*; NASA CR-2178; NASA, 1973.
18. Benson, S.W. *Thermochemical Kinetics, 2nd ed.*; John Wiley, New York, NY, 1976.
19. Kee, R.J.; Dixon-Lewis, G.; Warnatz, J.; Coltrin, M.E.; Miller, J.A. *A Fortran Computer Code Package for the Evaluation of Gas-Phase Multicomponent Transport Properties*; SAND86-8246; Sandia National Laboratories, Albuquerque, NM, 1991.
20. Svehla, R.A. *Estimate viscosities and thermal conductivities of gases at high temperature*; R-132, NASA, 1962.
21. Warnatz, J. *Twentieth Symposium (International) on Combustion*; The Combustion Institute, Pittsburgh, PA, 1984, pp845-856.
22. Warnatz, J. *Combust. Sci. Tech.* **1983**, 34, pp.177.
23. Westbrook, C.K.; Pitz, W.J.; Thornton, M.M.; Malte, P.C. *Combust. Flame.* **1988**, 72, pp.45.
24. Axelsson, E.I.; Brezinsky, K.; Dryer, F.L.; Pitz, W.J.; Westbrook, C.K. *Twentyfirst Symposium (International) on Combustion*; The Combustion Institute, Pittsburgh, PA, 1986, pp783-793.
25. Westbrook, C.K. *Nineteenth Symposium (International) on Combustion*; The Combustion Institute, Pittsburgh, PA, 1982, pp127-141.
26. Gibbs, G.J.; Calcote, H.F. *J. Chem. Eng. Data.* **1959**, 4, pp.226.
27. Rosser, W.A.; Wise, H.; Miller, J. *Seventh Symposium (International) on Combustion*; The Combustion Institute, Pittsburgh, PA, 1959, pp.175-182.
28. Takahashi, K.; Inomata, T.; Moriwaki, T.; Okazaki, S. *Bull. Chem. Soc. Jpn.* **1989**, 62, pp.2138.
29. Takahashi, K.; Inomata, T.; Jinno, H. *Bull. Chem. Soc. Jpn.* **1993**, 66, pp.3503.
30. Masri, A.R. *Combust. Sci. Tech.* **1994**, 96, pp.189.

RECEIVED July 20, 1995

Chapter 14

Perfluoroalkyl Iodides and Other New-Generation Halon Replacements

Robert E. Tapscott¹, Stephanie R. Skaggs^{1,3}, and Douglas Dierdorf²

¹Center for Global Environmental Technologies, New Mexico Engineering Research Institute, University of New Mexico, Albuquerque, NM 87131

²HTL/KIN-TECH Division, Pacific Scientific, 3916 Juan Tabo, Northeast, Albuquerque, NM 87111

New-generation halon substitute candidates can be divided into two groups: tropodegradable replacements, highly efficient halocarbons with short atmospheric lifetimes, and advanced agents, non-halocarbons. At present, the most promising tropodegradable replacements are the iodides, which exhibit fire extinguishment capabilities similar to the halons. Among the advanced agents, the phosphonitriles have been shown to be superior to halons in laboratory-scale extinguishment tests.

To date, across a broad range of applications, no Halon 1301 substitute has been proven to provide total-flood protection against fires and explosions in normally occupied areas without major changes in system hardware. Moreover, few halon substitutes have been found that are as effective as Halon 1211 for streaming (e.g., portables). Much of the work to date has focused on first-generation halon replacements (1). For the most part, first-generation agents are the three families of halocarbons — hydrochlorofluorocarbons (HCFCs), hydrofluorocarbons (HFCs), and perfluorocarbons (PFCs or FCs). No chemicals within these families have an effectiveness equal to that of Halon 1301 or Halon 1211, except for very specialized scenarios. Moreover, many, if not all of these materials have some environmental drawbacks. HCFCs cause some ozone depletion, and PFCs (and to a lesser extent, HFCs) cause global warming (Table I). The HCFCs and PFCs are already facing some regulatory actions due to their perceived environmental impact.

It is extremely unlikely that any environmentally acceptable first-generation agent with an effectiveness equal to that of the existing halons will be found. There is, therefore, an increasing interest in materials other than the first-generation materials as halon substitutes. These now comprise two major areas: the tropodegradable halocarbons (2) and advanced agents (3).

³Current address: HTL/KIN-TECH Division, Pacific Scientific, 3916 Juan Tabo, Northeast, Albuquerque, NM 87111

0097-6156/95/0611-0151\$12.00/0
© 1995 American Chemical Society

Table I. Relative Properties of Halocarbon Families^a

<i>Halocarbon Family</i>	<i>Fire Exting. Ability</i>	<i>Ozone Depletion</i>	<i>Global Warming</i>	<i>Toxicity</i>
perfluorocarbons PFCs (FCs)	moderate	nil	very high, atmospheric lifetimes around 3000 years	very low
hydrofluorocarbons HFCs	moderate	nil ^b	high, lifetimes tens to hundreds of years	low to moderate, some cardiac sensitization
chlorofluorocarbons CFCs	moderate	Class I ODSs	high	low to moderate, some cardiac sensitization
hydrochlorofluorocarbons HCFCs	moderate	Class II ODSs	low to moderate, short atmospheric lifetimes	low to moderate, some cardiac sensitization
bromofluorocarbons BFCs	excellent	Class I ODSs, production ban	moderate to high	low to high, some cardiac sensitization
hydrobromofluorocarbons HBFCs	excellent	Class II ODSs	low to moderate, short atmospheric lifetimes	moderate to high
fluoroiodocarbons FICs	excellent	low, near zero	very low, atmospheric lifetimes of days	moderate to high, significant cardiac sensitization

^aFire extinguishment abilities are a summarization of data from a variety of sources, in particular from Reference 4, which contains cup burner data for 53 compounds. Sources for assessment of relative ozone depletion, global warming, and toxicity include the U.S. EPA Significant New Alternatives Program (SNAP) assessment (5) and reports of the Intergovernmental Panel on Climate Change (IPCC).

^bReference 6.

A target specification for an ideal halon replacement can be refined to that summarized in Table II.

Table II. Idealized Specification For Halon Replacements^a

<i>Property</i>	<i>Target</i>
Ozone Depletion Potential	$< 1.0 \times 10^{-3}$
Atmospheric Lifetime	< 1 year
Extinguishing Efficiency	\geq Halon (application dependent)
Toxicity	Acute endpoints (lethality, cardiac, etc.) \gg exposure concentration
Vapor Pressure (Total Flood)	$>$ Extinguishing partial pressure
Vapor Pressure (Streaming)	Sufficient for evaporation
Stability	Low decomposition under storage conditions
Materials Compatibility	Non-corrosive under conditions of use

^aThese requirements reflect the authors' opinions (7).

Tropodegradable Replacements

Tropodegradable replacements are highly effective halocarbons that have low atmospheric lifetimes, leading to near-zero global warming and ozone depletion. Examples of such materials are iodides, bromoalkenes, polar-substituted bromocarbons (e.g., aldehydes, ketones, alcohols, esters, ethers), and, possibly, aromatic bromides. Work in this area has shown that many of these compounds are, indeed, highly effective and do have negligible global environmental impacts.

Iodides. Of all of the tropodegradable replacements, iodides have been the most thoroughly investigated (8, 9). Studies have been conducted by both the Air Force and the Navy; however, relatively few reports have been released. Recent research has shown that perfluoroalkyl iodides meet many of the targets shown in Table II. In particular, some, if not all, iodocarbons have very low atmospheric lifetimes leading to low ozone depletion potentials (10) and are extremely effective fire extinguishing agents.

Toxicity Testing. Toxicity testing of CF_3I has shown a 15-minute LC_{50} of 27.4% (11) and cardiac sensitization values of 0.2% for the No Observed Adverse Effect Level (NOAEL) and 0.4% for the Lowest Observed Adverse Effect Level (LOAEL)(12). The Ames mutigenicity test is positive for 4 out of 5 strains and the mouse micronucleus test is also positive (13). On the other hand, the mouse lymphoma test was negative.

The cardiac sensitization levels of CF_3I are low, but not unprecedented (Halon 1211, CFC-11, and HCFC-123 exhibit similar values). Nonetheless, these values

preclude the use of CF_3I in total flooding of normally occupied areas. Genotoxicity results indicate that subchronic testing may be necessary to establish suitable industrial hygiene practices for manufacturing, bottle filling, and maintenance facilities.

Initial "range finder" or limit tests using rats have shown the Approximate Lethal Concentration (ALC) for $\text{C}_3\text{F}_7\text{I}$ is somewhere in the range of 3 to 5%. The 15-minute LC_{50} is 4.9 to 6.2% (14), and the 2-hour mouse LC_{50} is 3.3% (15). The cardiac sensitization values are less than 0.1% for the NOAEL and 0.1% for the LOAEL (12).

Materials Compatibility and Stability. A six month series of materials compatibility and stability test has recently been completed for CF_3I . The materials compatibility tests have been conducted in accordance with ASTM standard practices and procedures and the detailed results are reported elsewhere (9). In brief, these tests showed corrosion rates of less than 0.04 mm/yr. for the range of metals tested at temperatures of approximately 75°C, with or without the presence of water.

Fire Testing. Testing by the U.S. Navy comparing CF_3I shows shorter extinguishment times than Halon 1301 in total-flood applications (although, this could be due to differences in agent distribution) and breakdown product emission levels similar to those found for Halon 1301 and significantly lower than those found for HFC and PFC agents (16). Testing by the U.S. Air Force at Tyndall Air Force Base has shown that CF_3I is qualitatively equivalent to Halon 1211 when applied to heptane pool fires from portable extinguishers. Based on cup burner values and limited large-scale testing, a design concentration of 5.0% has been set for existing total flooding equipment (9) and 3.6% has been recommended for new equipment (1). The new-equipment design concentration is considerably lower than that of Halon 1301. The design concentration of Halon 1301, however, has historically been set higher than 120% of the cup burner value, which is used for most Halon 1301 replacements (17). It should be noted that the cup burner has been widely accepted for use in predicting design concentrations for total-flood applications; however, the utility for prediction of effectiveness of streaming agents is considerably less certain (1). The inertion concentration of CF_3I at the flammability peak for propane is 6.5%, a value essentially the same as Halon 1301 at 6.2% (9).

Other Tropodegradable Candidates. In addition to the iodides, a number of other halocarbons believed to have decreased atmospheric lifetimes due to enhancement of photolysis, reaction with tropospheric OH free radicals, and/or rainout are being studied. In the following overview, nonspecific statements on toxicity are based on general chemical knowledge and on toxicity characteristics of related chemicals (15).

Carbonyl Compounds. Carbonyl compounds include ketones, aldehydes, esters, and carboxylic acids. The presence of a polar carbonyl group greatly increases the potential for rainout from the atmosphere and promotes photolysis. Although carboxylic acids would provide the needed low atmospheric lifetime, they are corrosive and have a higher toxicity. For this reason, they have been avoided.

Compounds with halogen atoms near the carbonyl group must be avoided; α and (probably) β carbonyl compounds tend to be lachrymators and to have a high toxicity.

Alcohols. Like the carbonyl group, the presence of a hydroxyl group enhances the potential for rainout. Thus, the highly polar alcohols are expected to have a low atmospheric lifetime. Compounds with the halogen atoms near the hydroxyl group should be avoided to decrease the potential for toxicity. A typical compound is $\text{HOCH}_2\text{CF}_2\text{Br}$.

Alkenes. A relatively large amount of research has been performed on bromoalkenes as potential halon replacements (see, e.g., Table III). These materials have very short atmospheric lifetimes (due to reaction with tropospheric hydroxyl), but tend to be toxic. Halogen atoms, particularly bromine, should probably be kept away from the double bond; however, this needs further investigation. Example compounds are $\text{CH}_2=\text{CH}_2\text{-R}$ or $\text{CF}_2=\text{CF}_2\text{R}$ where "R" is CF_2Br or $\text{CF}_2\text{CF}_2\text{Br}$.

Ethers. Of all of the bromine-containing polar compounds, ethers are likely to have the lowest toxicity. Unfortunately, they also have the lowest polarity. Thus, they may not have sufficiently short atmospheric lifetimes to make them truly viable halon replacement candidates. Example compounds include $\text{F}_3\text{C-O-R}$ where "R" represents $-\text{CF}_2\text{Br}$ or $-\text{CF}_2\text{CF}_2\text{Br}$.

Aromatics. Like the alkenes, aromatics are unsaturated and react with atmospheric hydroxyl free radicals. They are, however, less reactive and whether they have acceptable atmospheric lifetimes is uncertain. It is known that chloropentafluorobenzene has a very low toxicity (18), and the same may be true for the bromo or iodo derivatives. Bromopentafluorobenzene is not readily metabolized.

Amines. Some work has been done on syntheses and fire extinguishment capabilities of tris(trifluoromethyl)amine, $\text{N}(\text{CF}_3)_3$ and related compounds (19). Most amines are pyramidal with a lone pair of electrons, making them very polar. On the other hand, tris(trifluoromethyl)amine is trigonal planar; the lone pair of electrons has no steric presence. This compound appears to have a very low toxicity, but it is also less polar than most amines, decreasing rainout potential. Fire extinguishment studies have been performed with this compound; however, the results were no better than those obtained with other first-generation agents that operate primarily by heat absorption. The addition of CF_2Br in place of one or more of the CF_3 groups would, however, give an excellent fire suppression capability. Additional work is needed on bromine-substituted perfluoroamines and related nitrogen-containing perfluoro compounds.

Cup Burner Results. Some of the compounds listed above have been recently tested. The results are reported in Table III.

Table III. Cup Burner Results for Selected Tropodegradable Agents^a

<i>Compound</i>	<i>Extinguishing Concentration, vol. % in air</i>
bromotrifluoromethane (Halon 1301)	2.9
bromochlorodifluoromethane (Halon 1211)	3.2
Iodides	
trifluoroiodomethane	3.0
pentafluoroiodoethane	2.1
heptafluoro-1-iodopropane	3.0
heptafluoro-2-iodopropane	3.2
nonafluoro-1-iodobutane	2.8
octafluoro-1,4-diiodobutane	3.0
tridecafluoro-1-iodohexane	2.5
heptadecafluoro-1-iodooctane	1.9
Bromoalkenes	
2-bromo 3,3,3 trifluoropropene	2.55
3-bromo 3,3-difluoropropene	4.5
4-bromo-3-chloro-3,4,4-trifluoro-1-butene	4.5
4-Bromo-3,3,4,4-tetrafluoro-1-butene	3.5
Aromatics	
chloropentafluorobenzene	5.1
1,3-dichlorotetrafluorobenzene	6

^aUnpublished results using the NMERI 5/8-scale cup burner with *n*-heptane fuel. Results for Halon 1301 and Halon 1211 given for reference.

Advanced Agents

With the recent investigation of the fluoroiodocarbons, the range of saturated halocarbons has been reasonably well explored for fire extinguishing ability, global environmental concerns, and toxicity. Thus, except for various mixed-halogen halocarbons such as hydrochlorofluoroiodocarbons (HCFICs), the list of potential saturated halocarbons is essentially complete with no obvious candidates remaining.

It is known that bromine, iodine, phosphorus and, at least some, transition metal organometallics can provide excellent extinguishing ability (20). Of these chemical families, all but bromine compounds, will almost certainly have low atmospheric lifetimes. Two large groups of compounds are now undergoing study:

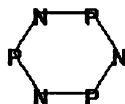
compounds containing flame inhibiting substituents that naturally lead to low atmospheric lifetimes (e.g., transition metal and phosphorus compounds) and nonhalocarbon bromides with decreased atmospheric lifetimes.

Transition Metal Compounds. It is well known that certain metal compounds are very effective in extinguishing flames (21). For example, iron pentacarbonyl ($\text{Fe}(\text{CO})_5$) may very well be one of the most effective extinguishing agents ever found (22). Moreover, chromyl chloride (CrO_2Cl_2) appears to be as much as two orders of magnitude more effective than the halons in inhibiting hydrocarbon flames (20).

Transition metals, are elements that contain incomplete d-block electronic shells in one or more of their compounds and include such elements as iron, chromium, manganese, etc. It may be that these incomplete shells aid in extinguishment by providing new catalytic pathways for oxidation/reduction that eliminate precursors for normal combustion pathways. On the other hand, it may be that particulates are generated within a fire providing heterogeneous pathways for free-radical recombination. Whatever the mechanism is, transition metal compounds appear to be highly effective.

Unfortunately, many transition metal compounds are either highly toxic (e.g., iron pentacarbonyl and chromyl chloride) or are solids, with no effective method for delivery and three-dimensional dispersion. One large group of transition metal compounds may, however, have the properties needed for effective use as fire extinguishants and, at the same time, may have acceptable toxicities. By using organic ligands containing negative charges whose sum is equal to the positive charge on the central ion, neutral transition metal compounds can be prepared. Because the overall complexes are neutral, the compounds are nonionic, a property that gives two important characteristics. First, in some cases, neutral-charged complexes containing fluorinated multidentate ligands are known to have a relatively high volatility (23). This should aid in providing three-dimensional fire and explosion suppression. Second, many neutral-charged complexes are soluble in organic liquids such as hydrofluorocarbons, providing a means for dispersion.

Phosphonitriles (Class I). In the 1990 NIST review (20), the phosphorus halides were examined and discarded as too toxic and too hydrolytically unstable for application as fire extinguishing compounds. Recently, we revisited the chemical literature in search of novel classes of phosphorus chemicals. During this review, it became obvious that the phosphonitriles should be investigated. Most of these compounds are relatively high molecular weight polymers or oligomers of the general formula $(\text{PNR}_2)_n$, where n is generally a large number. However, in the cases where n is 3 or 4, a number of relatively volatile liquid compounds or mixtures have been reported. These materials exist as two groups: compounds containing a cyclic backbone (usually containing alternating phosphorus and nitrogen atoms) and linear compounds, which have a linear chain backbone (but which also may contain cyclic substituents along the chain). The latter are often polymers whose exact structures have not been fully characterized. Examples are shown below for a six-member cyclic ring and for a four-member chain. The former example, which contains three PN units, can be designated a cyclic trimer, and the latter can be designated as a linear dimer.



Cyclic



Chain

A particularly attractive subclass of these compound is the cyclic chloro or fluorophosphonitriles with the general formula $P_3N_3Cl_xF_{6-x}$ where x ranges from zero to five (24). These compounds may be readily prepared from $P_3N_3Cl_6$ using relatively mild fluorinating conditions (25). Work has now shown that some of these materials are highly effective fire extinguishing agents (26). Liquid blends of $N_3P_3F_6$, $N_3P_3F_5Cl$, $N_3P_3F_4Cl_2$, and $N_3P_3F_3Cl_3$ give cup burner extinguishment concentrations as low as 0.3 percent (compared with 3 percent for Halon 1301). Moreover, these materials show fire extinguishing capabilities qualitatively superior to Halon 1211 in laboratory-scale streaming applications. Much work remains to be done with the phosphonitriles. In particular, laboratory syntheses are now underway to prepare some of the most promising materials for evaluation.

Silicon Derivatives. It is known that many materials containing silicon-bromide and silicon-chloride bonds are highly effective fire extinguishants. Unfortunately, such compounds hydrolyze readily in moist air releasing toxic haloacids. On the other hand, bromine substitution on fluoroalkyl groups contained in silicon and siloxane compounds, is likely to provide effective extinguishment without the problem of hydrolysis. Note that the chemistry of silicon is well understood and a large number of related silicon compounds are made commercially. It is likely that silicon-containing fire extinguishants would be manufacturable at a reasonable cost.

Conclusions

With the recent investigation of the fluoroiodocarbons, the range of saturated halocarbons has been thoroughly explored as a source of halon replacements. Within the halocarbon chemical family, no compound has been found which combines halon-like firefighting effectiveness with satisfactory global environmental and toxicological properties to meet the entire range of applications. While CF_3I meets many of the established criteria for a halon replacement, its use appears limited to Halon 1211 applications and to total flooding in unoccupied areas. These results suggest that a range of tropodegradable and non-halocarbon agents must be investigated to obtain satisfactory replacements for many critical occupied space applications such as North Slope oil production facilities and military vehicle crew compartments.

This investigation will require the synthesis and testing of a variety of compounds, some of which are not known in the chemical literature. The combination of synthesis, fire and toxicity testing requirements suggests that the actual fielding of a "perfect" new-generation agent is unlikely before the end of the century.

Literature Cited

1. Brown, J. A.; Jacobson, E.; Dvorak, L. E.; Gibson, J.; Gupta, A.; Metchis, K.; Mossel, J. W.; Simpson, T.; Speitel, L. C.; Tapscott, R. E.; Tetla, R. A. *Chemical Options to Halons*, Final Report, Task Group 6, International Halon Replacement Working Group, February, 1995.
2. Tapscott, R. E. "Second-Generation Replacements for Halon" *Proceedings, First International Conference on Fire Suppression Research*, Stockholm and Borås, Sweden, 5-8 May 1992, pp. 327-335.
3. Kibert, C. J.; Tapscott, R. E. "Five Digit Halons and Other Second Generation Agents," *Proceedings, Conference, Fire Safety - Without Halon?*, Zurich, Switzerland, 7-9 September 1994, pp. 226-236.
4. Tapscott, R. E.; Nimitz, J. S.; Walters, E. A.; Arneberg, D. L. *Halocarbons as Halon Replacements: Laboratory Testing of Halon 1211 Replacements*, ESL-TR-89-38, Vol. 3 of 5, Wright Laboratories (WL/FIVCF), Tyndall Air Force Base, FL, March, 1993.
5. *Risk Screen on the Use of Substitutes for Class I Ozone-Depleting Substances: Fire Suppression and Explosion Protection (Halon Substitutes)*, SNAP Technical Background Document, U.S. Environmental Protection Agency, Office of Air and Radiation, Stratospheric Protection Division, Washington, DC, March, 1994.
6. Ravishankara, A. R.; Turnipseed, A. A.; Jensen, N. R.; Barone, S.; Mills, M.; Howard, C. J.; Solomon, S. *Science* 1994, Vol. 263, pp. 71-75.
7. Skaggs, S. R. "Second-Generation Halon Replacements," *Proceedings, Halon Alternatives Technical Working Conference*, Albuquerque, NM, pp. 239-246, 11-13 May, 1993.
8. Skaggs, S. R.; Dierdorf, D. S.; Tapscott, R. E. "Update on Iodides as Fire Extinguishing Agents," *Proceedings, 1993 International CFC and Halon Alternatives Conference*, Washington, DC, 20-22 October, 1993, pp. 800-809.
9. Moore, T. A.; Skaggs, S. R.; Corbitt, M. R.; Tapscott, R. E.; Dierdorf, D. S.; Kibert, C. J. *The Development of CF3I as a Halon Replacement*, Final Report, Wright Laboratories (WL/FIVCF), Tyndall Air Force Base, FL, December 1994.
10. Solomon, S.; Burkholder, J. B.; Ravishankara, A. R.; Garcia, R. R. "Ozone Depletion and Global Warming Potentials of CF₃I," *J. Geophys. Res.* 1994, Vol. 99, pp. 20929-20935.
11. *Acute Inhalation Toxicity Study of Iodotrifluoromethane in Rats*, Final Report, Project No. 1530-001, Study No. 2, ManTech Environmental Technology, Inc., Research Triangle Park, NC, 1994.
12. Huntingon Research Center, UK, 1994 (unpublished results).
13. Genesys, USA, 1994 (unpublished results).
14. *Acute Inhalation Toxicity Study of Iodoheptafluoropropane in Rats*, Final Report, Project No. 1530-001, Study No. 3, ManTech Environmental Technology, Inc., Research Triangle Park, NC, 1994.

15. Sweet, D. V., Ed., *Registry of Toxic Effects of Chemical Substances*, 1985-1986 Edition; U.S. Department of Health and Human Services: Washington, DC, 1987; Vol. 3.
16. Sheinson, R. S.; Black, B.; Brown, R.; Burchell, H.; Maranghides, A.; Mitchell, C.; Salmon, G.; Smith, W. D. "CF3I - Halon 1301 Total Flooding Fire Extinguishment Comparison," *Annual Conference on Fire Research*, Gaithersburg, MD, pp. 59-60, 17-20 October, 1994.
17. *NFPA 2001 Standard on Clean Agent Fire Extinguishing Systems 1994 Edition*, National Fire Protection Association, 1 Batterymarch Park, Quincy MA, 11 February 1994.
18. Kinkead, E. R.; Culpepper, B. T.; Kutzman, R. S.; Flemming, C. D.; Wall, H. G.; Hixson, C. J.; Tice, R. R. *Evaluation of the Potential of Inhaled Chloropentafluorobenzene to Induce Toxicity in F-344 Rats and B6C3F1 Mice and Sister Chromatid Exchanges and Micronuclei Formation in B6C3F1 Mice*, Interim Report for the Period June 1988 Through June 1989, Harry G. Armstrong Aerospace Medical Research Laboratory, Wright-Patterson AFB, Ohio, September, 1989.
19. Abe, T. "Study for the Development of New Halon Alternatives," *Proceedings, 1991 Halon Alternatives Technical Working Conference*, Albuquerque, NM, 30 April - 1 May, 1991, pp. 307-310.
20. Pitts, W. M.; Nyden, M. R.; Gann, R. G.; Mallard, W. G.; Tsang, W. *Construction of an Exploratory List of Chemicals to Initiate the Search for Halon Alternatives*, NIST Technical Note 1279, Air Force Engineering and Services Laboratory, Tyndall Air Force Base, Florida, National Institute of Standards and Technology, Gaithersburg, MD, August 1990.
21. Bonne, U.; Jost, W.; Wagner, H. G. "Iron Pentacarbonyl in Methane-Oxygen (or Air) Flames," *Fire Research Abstracts and Reviews*, Symposium on Fire Control Research, National Meeting of the American Chemical Society, Chicago, IL, 3-8 September 1961, pp. 6-18.
22. Jost, W.; Bonne, U.; Wagner, H. G. *Chem. Engrg. News* 1961, Vol. 39, p. 76.
23. Moshier, R. W., and Sievers, R. E. *Gas Chromatography of Metal Chelates*; First Edition Pergamon Press: New York, NY 1965.
24. Allcock, H. R. *Phosphorus-Nitrogen Compounds*; Academic Press: New York, NY, 1972.
25. Emsly, J. and Paddock, N. L. *J. Chem. Soc. A* 1968, pp. 2590-2594.
26. Skaggs, S. R.; Kaizerman, J. A.; Tapscott, R. E. "Phosphorus Nitrides as Fire Extinguishing Agents," *Proceedings, 1995 Halon Options Technical Working Conference*, Albuquerque, NM, 9-11 May, 1995.

RECEIVED June 12, 1995

Chapter 15

The U.S. Army Requirement for a Replacement for Halon 1301

Anthony E. Finnerty

U.S. Army Research Laboratory, AMSRL-WT-TB,
Aberdeen Proving Ground, MD 21005-5066

The ban on production of Halon 1301 has serious implications for the U.S. Army. Since the early 1980s, the Army has used Halon 1301 flooding systems for fire protection in both the crew and engine compartments of ground combat vehicles. The ability of Halon 1301 to quench combat-induced fires in crew compartments quickly, so that personnel do not receive burn injuries, is of prime importance. It may be difficult to meet this performance in a replacement agent. The Army is conducting research and test programs seeking to identify an acceptable replacement agent. In addition, the Army is investigating passive approaches, such as using jackets of conventional fire extinguishing agents to surround fuel cells to provide fire protection through prevention of fire rather than by extinguishing fires after initiation.

Analyses of damage sustained by aircraft and ground combat vehicles in World War II (WW II) showed that virtually all catastrophic losses were caused by or accompanied by fire. In that time period, the U.S. Army's main fire-extinguishing agent was carbon dioxide. This material was clearly not capable of controlling the gasoline and ammunition fires that were commonly experienced in combat. In fact, it may be said that the history of air and armored warfare in WW II was the history of burning aircraft and burning vehicles. The U.S. Army realized that a more effective fire-extinguishing agent was required. A program was initiated to find a better agent.

Halons were identified as potentially useful fire-extinguishing agents as a result of research sponsored by the U.S. Army at the Chemistry Department of Purdue University in the 1940s. After much developmental work, Halon 1301 was recognized worldwide as a superior vaporizing, fire-extinguishing agent. Halon 1301 has been used extensively for total flooding applications, in which the vaporized fire-extinguishing agent is distributed uniformly throughout a volume, to extinguish any fire, regardless of its location.

This chapter not subject to U.S. copyright
Published 1995 American Chemical Society

Halon 1301 has found wide acceptance in U.S. Army weapon systems. All modern U.S. Army ground combat vehicles and many helicopters employ Halon 1301 for protection against fuel and hydraulic fluid fires. Tests of automatic fire-extinguishing systems (AFES) in armored personnel carriers have shown that, even when shaped-charge jet weapons are fired directly through a fuel cell in an occupied compartment, the AFES can detect the resulting "mist-fireball explosion" and open the solenoid valves of the Halon 1301 cylinders, releasing the high-pressure agent and extinguishing all traces of fire in less than 250 ms (see Figure 1). Data indicates that if the mist fireball explosion is extinguished in this short timeframe, any personnel present in the compartment should receive no worse than a first-degree burn (mild sunburn), even on exposed skin. If the fire is not suppressed quickly, severe burns would be expected. The low toxicity of Halon 1301 has allowed its use in both occupied (crew) and unoccupied (engine, dry bay) compartments. In addition, the U.S. Army protects many facilities (such as computer complexes) with Halon 1301.

Halon 1301 has been shown to be an excellent agent for extinguishing petroleum-type fires, although ammunition fires are still an unsolved problem.

However, when it became apparent (and was subsequently given legal status by the 1987 Montreal Protocol) that Halon 1301 could damage the ozone layer in the stratosphere, the U.S. Army decided to evaluate its uses of Halon 1301. A logical part of that evaluation was to identify those uses that could be considered critical to the combat effectiveness of the U.S. Army where no other substitute or technology was currently available.

The U.S. Army's uses of Halon 1301, which were identified as meeting the criterion previously mentioned, were the fire-extinguishing systems of ground combat vehicles and helicopters. Since the M1 tank series was fielded in the early 1980s, the U.S. Army has installed AFES in the crew compartments of new ground combat vehicles, while either AFES or manually controlled Halon 1301 systems have been used in engine compartments. Some helicopters use manually operated Halon 1301 systems to combat engine fires. Recently, driven by environmental concerns, the U.S. Army has been engaged in research and development (R&D) to find a replacement agent or system for Halon 1301 in crew compartments. Testing is underway to identify an agent or system which can be used to replace Halon 1301 in engine compartments.

Crew Compartments of Ground Combat Vehicles

To be useable for fighting fuel and hydraulic fluid (Class B) fires in occupied crew compartments, an agent must have at least the following important attributes:

1. It must have a low toxicity, so as to pose no threat to crewmembers who will be exposed to the agent during the fire-extinguishing process and may have to remain under the protection of the armor after agent discharge.
2. Any byproducts of the fire-extinguishing process should not cause injuries to crewmembers or hinder their exiting the damaged vehicle.
3. It should meet the Army's temperature range requirement of -55°C to $+71^{\circ}\text{C}$.

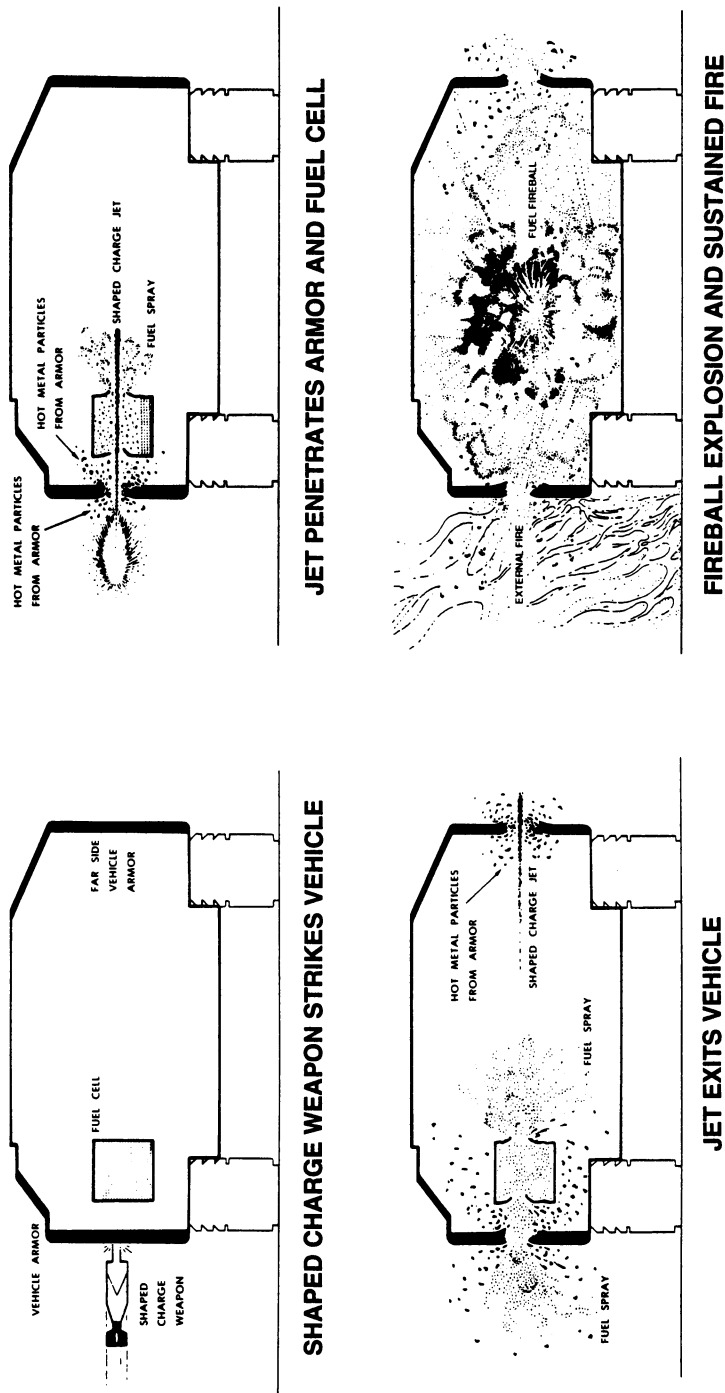


Figure 1. The mist fireball explosion.

4. It should be noncorrosive, so no damage will be done to equipment in case of an accidental discharge.

5. Any residue, after discharge, should be easily removed.

6. It must be environmentally friendly with a "zero" ozone depletion potential (ODP) and a low (acceptable) global-warming potential (GWP).

Until a suitable agent or system has been identified, the U.S. Army will use Halon 1301 from its reserves, while strong efforts will be made to minimize accidental emissions. When a suitable replacement is found, it will be installed in crew compartments, in place of Halon 1301.

Engine Compartments of Ground Combat Vehicles

The U.S. Army is confident that a replacement agent or system can be identified in the near future. Industry has shown that agents such as fluorinated alkanes, dry powders, and water mists are useful in extinguishing fuel fires. The U.S. Army Tank-Automotive and Armament Command is currently sponsoring tests conducted by the U.S. Army Combat Systems Test Activity (CSTA) at Aberdeen Proving Ground, MD, on systems currently available and under advanced development for extinguishing fuel fires in a generic engine compartment. It should be possible to provide fire protection for engine compartments equivalent to, or better than, that which Halon 1301 now provides. A replacement agent or system must be able to protect against both combat-induced fires and accidental fires due to leakage of combustible fluids. Total flood (gaseous) agents, powders, and mists are all under consideration.

It would appear that the toxicity requirements for an agent used in engine compartments could be relaxed somewhat. However, previous test experience indicates that an agent can be carried from the engine compartment into the crew compartment. Therefore, an essentially nontoxic agent is required, even for use in engine compartments. However, since the amount of agent carried into the crew compartment would not be high, irritating agents (such as powders) can be considered for use in engine compartments.

Mechanisms

In the search for halon replacements, there is a certain logic in taking the position that, as far as performance is concerned, all that is required is a knowledge of the concentration of an agent required to extinguish fire. It should then be possible to design a system to dispense an agent at the required concentration plus a safety factor. It should not be necessary to know the mechanism by which an agent extinguishes fire. A knowledge of the minimum concentration required should be sufficient. Certainly, fire safety engineers designed numerous successful fire-extinguishing systems using Halon 1301 before detailed information on mechanisms was elucidated. Typically, commercial systems were designed to dispense Halon 1301 at what is known as the cup burner concentration plus a safety factor of about 20% into an enclosure. Why should the situation be any different with halon replacement agents?

There are two main classes of mechanisms by which fire-extinguishing agents suppress fires. These are chemical mechanisms and heat-absorbing mechanisms.

Agents are said to be chemical agents if they react to remove active chemical species (free radicals) from the flame. The removal of active radicals can be on a one-to-one basis, where the chemical moiety of an agent (e.g., the fluorine atoms of C_4F_{10}) removes one active chemical species from the flame. There is the potential for the removal of ten hydrogen atoms, one for each fluorine of C_4F_{10} . But each fluorine can be responsible for the removal of only one hydrogen atom. In the case of a bromine containing agent, such as CF_3Br , the bromine atom has the ability to remove many hydrogen atoms from the flame. Therefore, the bromine moiety of CF_3Br is responsible for making Halon 1301 a catalytic chemical agent. The $CF_3\cdot$ radical of CF_3Br can also contribute to the removal of hydrogen atoms, but not in a catalytic fashion.

A heat-absorbing agent can lower the flame temperature leading to extinction of the flame. The method of heat absorption can be by heat capacity of a liquid plus heat of vaporization, plus heat capacity of the vapor, as in the case of water. A gaseous agent, such as CF_3Br does not have a high heat capacity of the vapor, yet a heat-absorption contribution to flame extinguishment is present even in the case of Halon 1301. An agent such as C_3HF_7 will have a higher heat-absorbing ability than Halon 1301 has, plus a chemical contribution, in removing free radicals from the flame. While some agents (such as water) can behave in a purely heat-absorbing way, the chemical agents (whether catalytic or not) will add heat-absorbing ability to the flame-extinguishing process. When used at a high enough concentration, a chemical agent will function in a manner similar to a heat-absorbing agent.

While many agents can function using a combination of the two main mechanisms, in many scenarios, one of the mechanisms predominates.

The Cup Burner Test

The cup burner test is carried out in an apparatus with a central tube containing a fuel such as heptane. The height of the liquid is controlled using a leveling device. Air flows through a surrounding coaxial tube. A diffusion flame is established in the apparatus. The agent to be tested is normally metered into the airflow. The amount of agent required to extinguish the flame is the cup burner extinguishing concentration for that agent. Although these apparatus are constructed in individual laboratories, there is reasonably good agreement on cup burner concentrations for various agents among different research groups.

It has been reported (Ref 1) that when Halon 1301 is used in the cup burner test, the overall fire suppression mechanism is 80% chemical and 20% heat absorption. The bromine atom of the agent is responsible for 55% of the suppression (catalytically), and the CF_3 radical is responsible for 25% of the suppression (noncatalytically). Yet these numbers on suppression can be changed by simply altering the experiments. In the cup burner experiment, the agent and air are premixed. They react with the fuel in a diffusion flame. The effectiveness of the bromine atom in removing free radicals, as shown by

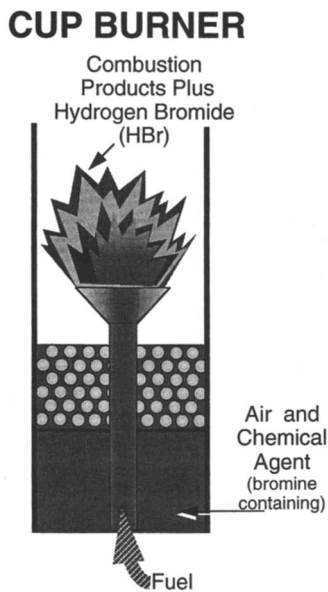


Figure 2. Cup burner test with added chemical agent.

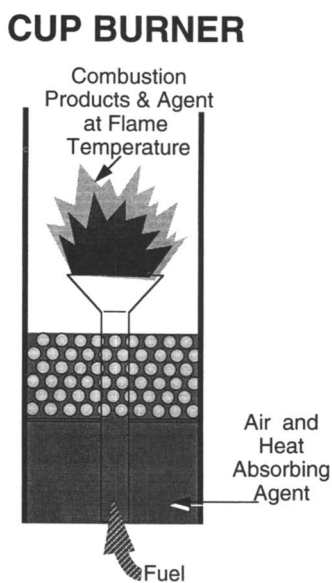
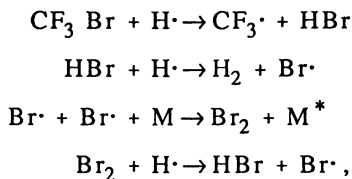


Figure 3. Cup burner test with added heat-absorbing agent.



is limited by the time the bromine is in the flame zone. The bromine can be expelled from the flame zone, due to the forced convection of the system, before it has used its full catalytic activity to remove active free radicals. Thus, HBr is a reaction product. This is shown in Figure 2. While bromine is responsible for catalytically removing free radicals from the flame, its full potential is not exploited in the diffusion flame of the cup burner apparatus. There is a chemical reserve that has not been used. This is due to the fact that the conditions of forced and natural convection do not allow sufficient residence time for the bromine to use its full power of fire suppression by the catalytic removal of fire radicals. It may be true that there is no conventional scenario in which the full power of bromine is used.

The value of the minimum concentration of Halon 1301 (or other catalytic chemical agent) required to extinguish fire, from the cup burner test, is a conservative value. The agent may be used in a real-world fire-extinguishing scenario in which it may have a long residence time. In such a scenario, the fire-suppressing ability of the bromine would be more fully exploited. In that case, a concentration of the catalytic chemical agent that is lower than the cup burner values could still extinguish the flame.

In contrast, when a heat-absorbing agent diffuses into the flame of the cup burner, the agent will come up to the flame temperature along with the other species in the flame as shown in Figure 3. Since all a heat-absorbing agent (such as water) does is experience a temperature rise (to flame temperature), the agent has done the maximum that it can do. A longer residence time in the flame would do little to increase its effectiveness. There is no reserve to exploit in a real-world fire-extinguishing scenario. It would be necessary to have conditions that would cause the entrainment of more of the agent in the flame or an unstable flame to lower the concentration requirements for a heat-absorbing agent. Such conditions would, of course, also lower the concentration requirements for a catalytic-chemical agent.

Applying a set safety factor, such as 20%, without considering the mechanisms by which a particular agent functions, can lead to a conservatively engineered system for a chemical agent and a borderline system when a heat-absorbing agent is used. The best approach is to establish agent concentrations required to extinguish fires in conditions as close to real-world conditions as possible. Designers should not rely on the cup burner concentration plus 20% rule of thumb that worked so well with Halon 1301.

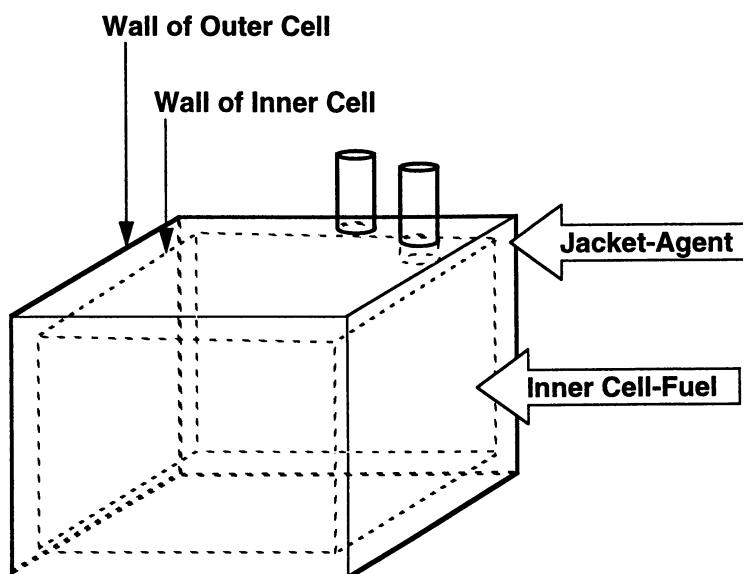


Figure 4. Jacketed fuel cell.

Jacketed Fuel Cells

Experiments have been conducted at the U.S. Army Research Laboratory (ARL) using fuel cells surrounded by jackets of fire-extinguishing agents (Ref 2). A schematic of a jacketed fuel cell is given in Figure 4. When such a cell is struck by a weapon, both fuel and agent are released simultaneously, giving a premixed fuel-air-agent mixture before ignition occurs. In firing tests of shaped charges against the jacketed fuel cells in an aluminum vehicle, strikingly different results were obtained when a heat-absorbing agent (water) was used in the jackets vs. a catalytic chemical agent (bromochloromethane [BCM]). More than twice the volume of water was required to prevent a sustained fire compared to the volume of BCM, which prevented sustained fires. When sufficient water was used, no fireball was observed and there was no evidence of high pressure inside the vehicle.

With BCM, there were large fireballs and evidence of high pressure inside the vehicle, even though there were no sustained fires. When the volume of BCM was more than doubled, there were still large fireballs and evidence of high pressure, with no sustained fires. The BCM gave surer protection from sustained fires than water gave, but the BCM could not prevent ignition and large fireballs. In contrast, when sufficient water was used, all indications are that the ignition process failed. A schematic of the situation which occurs when a heat-absorbing agent (water) is used in the jacket of the fuel cell is given in Figure 5. In contrast, Figure 6 shows the situation in which a catalytic chemical agent (BCM) is used in the jacket of the fuel cell.

When BCM was used, it did not become activated until the fireball appeared. At that point, BCM was efficient in quenching the fireball and preventing a sustained fire. For BCM to prevent the fireball, it would have to act as a heat-absorbing material. A much larger quantity of BCM would have been required than was needed to prevent sustained fire.

The designer should appreciate the differences in expected results when heat-absorbing agents vs. chemical agents are used in jackets of fuel cells, or any other situation in which the fire-extinguishing agent is premixed with fuel before ignition occurs. The heat-absorbing agent can prevent the occurrence of a fireball, but may allow the chance of a small fire which can grow into a sustained, vehicle-destroying fire. The catalytic chemical agent allows a fireball to form, but prevents sustained fires.

Figure 7 shows the contrasting situations of the ignition of a fuel-air mixture, the ignition of a fuel-air plus heat-absorbing agent mixture, and ignition of a fuel-air plus chemical agent mixture.

Powder Packs

Experiments have been performed at ARL and CSTA at Aberdeen Proving Ground (Ref. 2 and 3) using powder packs (honeycomb panels whose void volumes are filled with fire-extinguishing powder).

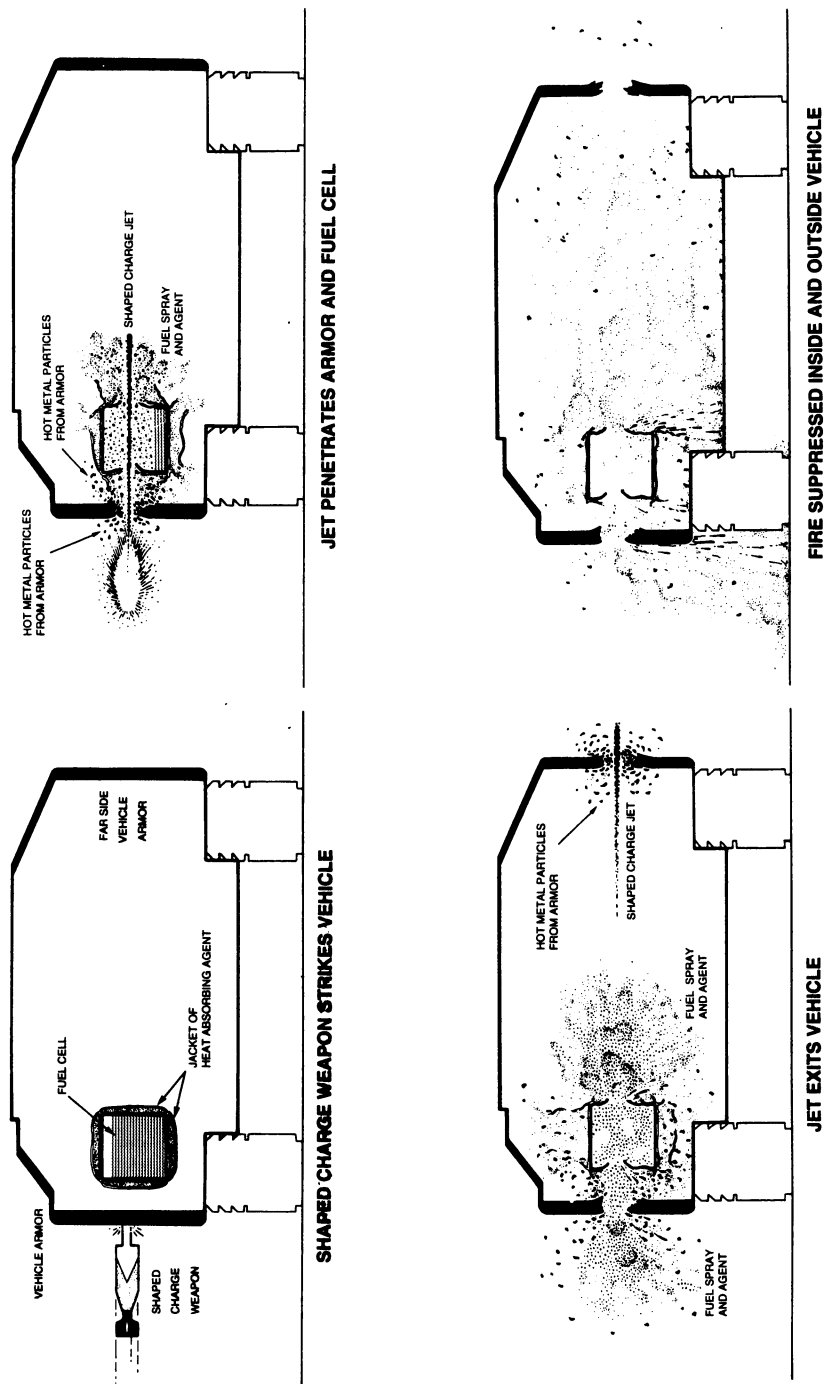


Figure 5. Heat-absorbing agent in jacket of fuel cell.

Downloaded by STANFORD UNIV GREEN LIBR on October 4, 2012 | http://pubs.acs.org
 Publication Date: May 5, 1997 | doi: 10.1021/bk-1995-0611.ch015

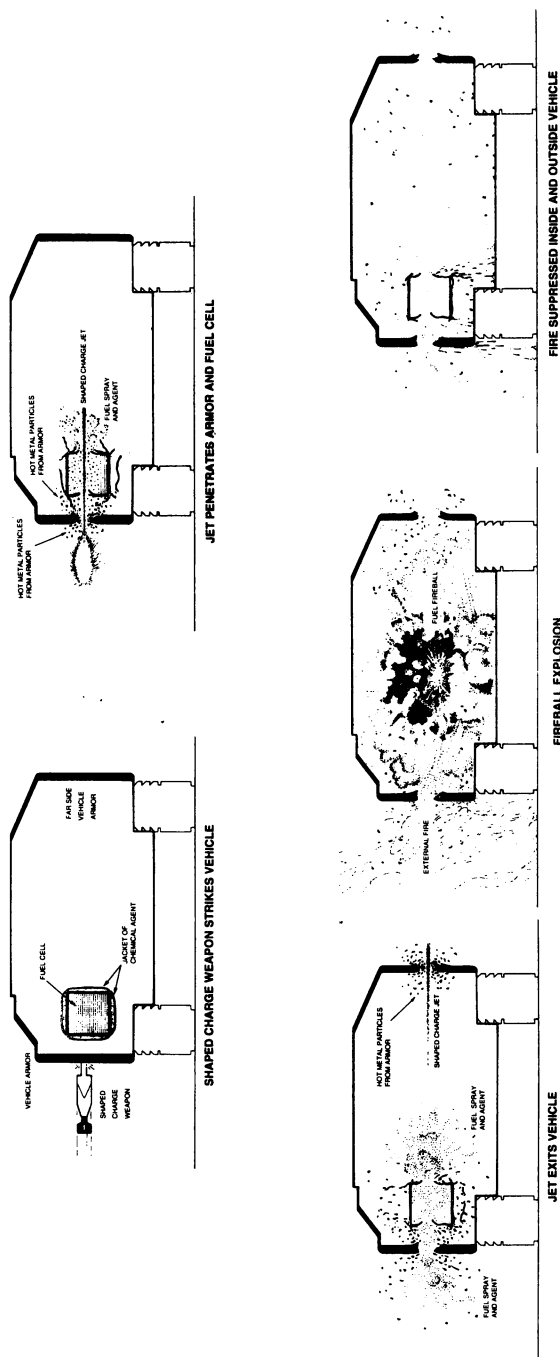


Figure 6. Chemical agent in jacket of fuel cell.

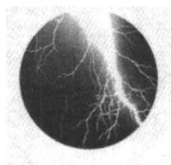
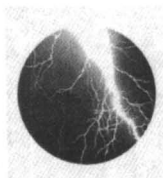
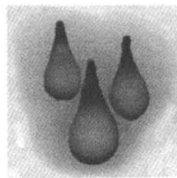
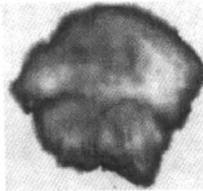
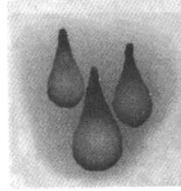
A. Fuel-Air Mixture**AIR plus FUEL****IGNITION SOURCE****FIREBALL
AND
SUSTAINED FIRE****B. Fuel-Air Mixture with Heat Absorbing Agent****AIR plus FUEL
HEAT ABSORBING
FIRE EXTINGUISHING
MATERIAL****IGNITION SOURCE****FIRE OUT****C. Fuel-Air Mixture with Chemical Agent****AIR plus FUEL
plus CHEMICAL
FIRE EXTINGUISHING
MATERIAL****IGNITION SOURCE****FIREBALL****FIRE OUT**

Figure 7. Ignition of (a) a fuel-air mixture, (b) a fuel-air mixture with heat-absorbing agent, and (c) a fuel-air mixture with chemical agent.

These panels are attached to fuel cells and hydraulic fluid reservoirs. Since the powder packs completely surround the fluid containers, an attacking weapon must break open a panel, releasing fire-extinguishing powder, in order to reach the fuel cell. Thus, fuel and fire-extinguishing powder are released at the same time. Premixing the powder with the fuel effectively suppresses the ignition process. Results indicated that panels as thin as 6 mm, filled with fire-extinguishing powder, prevented fire when cells containing hot (70° C) diesel fuel were attacked by shaped-charge devices. The large amount of powder released in the event makes powder packs suitable in unoccupied compartments only. These panels are useful only against weapon attack on fuel and hydraulic fluid containers, since the attacking weapon releases the powder. Fires are extinguished virtually instantaneously. The panels cannot extinguish fires caused by accidental leaks of combustible fluids, since there is no mechanism to release the powder.

Water Mists

The U.S. Army has started a study of water-based mists as possible halon replacement agents for engine compartments of ground combat vehicles. A prime concern is the large temperature range (-55° C to +70° C) over which the system must survive and/or function. Initially, the calcium chloride-water eutectic was chosen to give low temperature capability.

Water-based mists are attractive in that there should be little environmental concerns over their use. They should be acceptable in both normally occupied (crew) and normally unoccupied (engine) compartments. The high heat-absorbing ability of water means that mists (with small particle diameter) can be very efficient in extinguishing fires. In the engine compartments, a mist generator could be aimed at high-temperature exterior engine surfaces, thus reducing the possibility of reignitions, once an engine fire is extinguished. Additives (such as potassium iodide and potassium bromide), intended to enhance the fire-extinguishing effectiveness of the eutectic, are added and tested against hydrocarbon fires. While the results have been encouraging, much more R&D must be carried out before such a system can be installed in a combat vehicle. Water mists should be useful against both accidental and weapon-induced fires once answers have been identified concerning proper additives to prevent freezing and to increase the effectiveness of the water mist systems.

Pyrotechnic Smoke Generators

The U.S. Army is studying pyrotechnic formulations which yield fire-extinguishing smoke when the mixture burns. Devices incorporating these formulations could be strategically placed in a compartment to provide full coverage. Since it is anticipated that such devices would be small and initiated electrically, they could be put into convenient locations. The possibility of zoned coverage, by initiating only those devices in a particular area, is attractive. These devices are being considered only for nonoccupied compartments, since the fire-extinguishing smoke generated by the

devices would be quite irritating to personnel. These smoke generators should be useful against both accidental and weapon-generated fires in engine compartments and dry bays.

Problems which must be addressed include the high rate of smoke generation needed to extinguish fires quickly, while suppressing flame from the generator, to preclude being the cause of fire and/or reignitions. The buoyancy of the fire-extinguishing material, generated by an exothermic reaction, may also pose a problem. Cleanup will obviously be more difficult than when a vaporizing agent is used, although no more difficult than when powder packs are used. More research is required before pyrotechnic systems can be engineered for use in combat vehicles.

Summation

The U.S. Army is conducting research, development, and testing to identify methods of protecting against the mist-fireball explosion. Occupied space explosion protection is unique to the crew compartments of ground combat vehicles. Methods of combating engine compartment fires are also being addressed. Initiatives from industry are being studied for possible use in both crew compartments and engine compartments. The goals are to identify solutions for existing vehicles and to identify approaches which can be incorporated into the design of future vehicles. The Army must conduct proper risk analysis concerning the use of halon replacement materials/systems.

Literature Cited

1. Sheinson, R. S. "Halon Alternatives Extinguishment Pathways." Proceedings of the Halon Alternatives Technical Working Conference, Albuquerque, NM, April 30–May 1 1991, pp. 71–82.
2. Finnerty, Anthony E., and James T. Dehn. "Alternative Approaches to Fuel-Fire Protection for Combat Vehicle." ARL-TR-377, U.S. Army Research Laboratory, Aberdeen Proving Ground, MD, April 1994.
3. Finnerty, A. E., and S. Polyanski. "Using Powder Packs for Passive Fire Protection of Military Vehicles." *Journal of Fire Sciences*, May–June 1993, vol. 11, pp. 242–254.

RECEIVED August 4, 1995

Chapter 16

The U.S. Navy Halon Total Flooding Replacement Program

Laboratory Through Full-Scale

Ronald S. Sheinson

Navy Technology Center for Safety and Survivability, Naval Research Laboratory, Code 6185, 4555 Overlook Avenue, Southwest, Washington, DC 20375-5342

The Navy Technology Center for Safety & Survivability, which has evolved from the Chemistry Division, Combustion and Fuels Branch, focuses on combustion processes and fire protection issues. This chapter includes Naval Research Laboratory (NRL) efforts relevant to understanding flame suppression processes, halon replacement, fire protection and valid testing concerns. This is not a comprehensive treatment. A review of other efforts is not intended.

The NRL halon replacement effort has a long, if discontinuous, history with many participants. Halon 1301 (CF_3Br) is used in total flooding shipboard fire protection, primarily for its effectiveness in extinguishing flammable spray and cascading liquid three dimensional fires. Leaks from pressurized fuel or hydraulic lines can occur throughout propulsion engine spaces and are very difficult to combat. While Halon 1301 is very effective, as well as clean, non-conducting, and non-toxic, it does generate significant hydrogen halide acid products from fire interactions. Halon also is ineffective on smoldering combustion.

Research on finding replacements began at NRL in the 1970s, prior to stratospheric ozone environmental concerns. In 1976 NRL (*I*) estimated that Halon 1301 would be at least as potent an ozone depleter as are CFCs. The amount of halons then used was very small compared to CFCs. Dr. Homer Carhart, formerly Head of the Navy Technology Center for Safety & Survivability, felt that halon ozone depletion might become a future political issue, but was not a primary technological concern. This was prior to the realization of the magnified significance bromine containing compounds and the vast increase in halon employment. Much of the increased utilization was probably not warranted, but halon presented a clean, high-tech fire protection solution not requiring extensive analysis or planning. How much of the atmospheric bromine load is from newly released halons, especially with ongoing recent minimization efforts, remains uncertain.

This chapter not subject to U.S. copyright
Published 1995 American Chemical Society

The prime objectives for halon replacement efforts must first be on eliminating the threat of fire, limiting the damage done by a fire, and/or minimizing the deleterious effects on capabilities or functions. The next stage would be suppressing the fire by other existing means. This chapter is on replacement of the chemical CF_3Br for those cases where these basic fire protection steps were inadequate and halon-like properties really are needed. The Navy surface fleet requirement is for combating catastrophic pressurized flammable fluid fires in a manned main ship propulsion machinery space.

Early Suppression Modeling Efforts

Combustion research (2) was performed primarily via cup burner extinguishment, using CFCs, perfluorocarbons, CF_3I , model compounds, agent blends and synthetic atmospheres. All substances have a physical (heat capacity) component at a minimum by virtue of translation (kinetic) energy. If, in addition, the chemical component is very significant, the agent will typically be labeled a "chemical" agent. This research quantified physical and chemical suppression mechanisms (3). The extinction data from a series of inerts, CF_3X , SF_5X , (X is F, Cl, Br, or I) and other model compounds were used to construct an empirical linear additive model. The basis for separating out the physical and chemical components was Huggett's observation (4) that atmospheres with a heat capacity above a certain (wide) range would not allow combustion. The NRL n-heptane cup burner study allowed quantifying that "range" to a single number. If the gas mixture energy abstraction capacity, normalized per mole of oxygen, is above the energy produced from the combustion consumption of oxygen, a flame will not be able to propagate. There will not be sufficient exoergicity to achieve minimum flame propagation temperatures. Please see reference 3 and references therein for a more complete discussion.

The model allows calculation of the physical contribution from chemically acting agents. Subtraction leaves the chemical component; itself divided into radical components. There are many different specific modes of suppression simultaneously contributing to extinction. Computer calculations of premixed gas flame extinction allowed us to deconvolute heat capacity, thermal conductivity, and dilution factors. Extinction should not be attributed to oxygen starvation or heat abstraction (or chain breaking). The combined modes summed together is the relevant parameter.

The simplistic linear additive model was verified for combinations of primarily physically acting suppressants. There are deviations for mixtures with highly efficient bromine or iodine containing "chemical" suppressants. That issue has been addressed in a later model. For predominantly physically acting agents or "chemical" agents in air not combined with other agents, the linear model is a good first approximation for predicting suppression action and agent concentration requirements. Halon 1301 extinguishment of n-heptane in air was shown to be 20 % physical, and 80 % chemical, with about 25 % due to CF_3 interactions and 55 % due to Br.

It has been suggested (5) that the apparent chemical effectiveness of the halogens is due to atomic weight differences, a physical process, with correlations provided for support. However, correlation is not sufficient to prove cause. Chemical properties as well as atomic weight both change with progression down the halogen periodic chart column. Reference 5, with included symposium discussion,

presented both supporting and countering mixture examples. The NRL model, including chemistry, correctly predicts flammability for the examples. Further documentation of chemical action, suppression as a non-linear function of suppressant concentration for bromine and iodine containing molecules, is discussed in a later section.

Chemical action is clearly indicated in comparing (3) inerting and cup burner results for CF_3Br and CF_4 . Although almost identical molar volumes were required to prevent spontaneous ignition, one fifth as much CF_3Br as CF_4 was required to extinguish a cup burner flame. HF was detected from CF_3Br inhibited flames; virtually none from CF_4 inhibited flames. Spontaneous ignition inhibition depends on heat capacity - almost identical for the two compounds. Fire extinguishment adds interaction with flame chemistry. A chemical agent does not become "activated" until conditions are such that reaction or decomposition occurs.

HF production for several agents including Halon 1301 was characterized from partially suppressed cup burner fires (2), as well as for Halon 1301 total flooding extinguishment of hydrocarbon pool and spray fires in small (6) (1.8 m^3) to large (7) (625 m^3) compartments. HF concentrations from Halon 1301 extinguished small fires ranged into the hundreds of parts-per-million by volume (ppm). (All gas phase concentrations are volume/volume). The largest liquid fuel fires generated up to one half per cent HF. Comparing simultaneous *in situ* infrared HF determination with various sampling techniques highlighted (6) serious sampling / reaction difficulties. This may partially explain disparities in the literature.

Other Evaluation Efforts

Larger scale tests (up to 324 m^3) were run with inert gas (8), fine water mist (8) with and without additives, and fine dry powders. Liquid water fire extinction (9) requirements can be predicted with the linear physical model by including the latent heat of vaporization in the calculation. Performance would be optimum if vaporization occurred exclusively in the flame sheet - the goal of a properly designed water mist system. The minimum amount of water required is the same volume as liquid Halon 1301, or 2/3 the mass. However, even if that case could be reached, less than half the energy abstraction is due to vaporization. The water molecule itself has a relatively high heat capacity, based on molecular weight as it has a high number of bonds per molecular mass. Generation and transport into the flame of sufficient fluid above its gas phase equilibrium vapor pressure (i.e., in mixed gas and liquid form) is the key issue.

Powder research at NRL in the early 1980s was a breakthrough in characterizing vastly increased performance with very large increases in powder suppression efficiency with decreasing particle size. This was studied by Ewing, *et al.* (10), and Fischer, *et al.* (11), Ewing studied extinction of wood crib fires; Fischer studied methane gas burner flame extinction. Extinguishment efficiency increased tremendously for particle sizes below 20 to 30 microns, depending on the specific inorganic salt compound. Ewing, *et al.* (12,13), also observed particle size dependant efficiency factors for larger heptane pool fires (0.29 m^2 and 2.32 m^2). Very similar dependence was observed with these very different fire threats.

The effect of larger water mist particles aerodynamically entraining fine water mist particles into a fire, previously studied at NRL, was also postulated to occur with the powder extinguished heptane pool fires. Higher momentum larger particles, in the agent, drag the smaller more effective particles into the flame. Smaller particles would otherwise have to be injected with more momentum or not reach the flame sheet due to fire generated convection currents. While much understanding of combustion processes resulted, these efforts did not identify a practical halon replacement.

Extended and Non-linear Suppression Models

Renewed efforts in the late 80s included proposing CF_3H , CF_3I , and CF_2HBr as zero or low ozone depletion potential replacement candidates (14), and extended cup burner investigations. Different cup burners, protocols, or operators, will give similar, but not identical, results. Modeling involves ratios of small differences of large values. Precise, reproducible, and self-consistent data is a necessity. The NRL Cup Burner is operated in that mode, rather than as an agent screening tool.

The empirical models for calculating agent fire suppression concentration requirements were further developed (15). Changes include accounting for the combustion promoting effects of carbon, hydrogen, C-C bonds, and weighing factors for the likelihood of breaking specific atom-atom bonds. Model input consists only of compound enthalpy of heating and the numbers of each type of atom and bond. Agent requirements are typically predicted correct to better than 10 % (relative) (16).

Suppression fraction is defined as concentration of chemical used divided by the concentration required for extinguishment. A linear model postulates that the sum of all suppression fractions would be 1 at extinction. The data show a suppression fraction of $\frac{1}{2}$ for SF_6 requires addition of only $\frac{1}{3}$, not $\frac{1}{2}$, suppression fraction of CF_3Br . This non-linear factor demonstrates the very significant increase in effectiveness per molecule at lower compound concentrations. Such effects are only apparent with agent mixtures or non-air combustion systems.

Suppressant action can be divided (17) into: Physical, no chemistry; Chemical - Scavenging, reacting with a set number of flame radicals (e.g., $\text{F} + \text{H} = \text{HF}$); and Chemical - Catalytic, reacting with flame radicals via a catalytic cycle (e.g., $\text{Br} + \text{H} = \text{HBr}$, $\text{HBr} + \text{H} = \text{Br} + \text{H}_2$) and thus potentially removing a large number of species required for flame propagation. A physical mechanism produces linear, but inefficient suppression effectiveness, while catalytic reactions involving bromine and iodine containing suppressants produce high chemical effectiveness, especially at lower agent concentrations.

Weak catalytic action involving chlorine (CF_2HCl), or chemical scavenging reactions involving fluorine (CF_3H , $\text{C}_3\text{F}_7\text{H}$, C_4F_{10}), produce small or no deviations from linear behavior, respectively. Catalytically active bromine and iodine containing compounds give significant non-linear suppression efficiency plots. Br and I - hydrogen atom recombination chain lengths can be calculated (18) from the concentration dependent effectiveness data.

Free Oxygen model. This concept has been necessary for comparing large scale test results. The work of Tucker, *et al.* (19) provided the input for our "Free Oxygen"

formalism. The Free Oxygen model (20) combines the physical model with laboratory suppression data to calculate the effective (Free) oxygen concentration requiring "neutralization." It is empirical with inputs being the physical predictions and a cup burner data set for determining each agents' efficiency curve.

Model validity is shown by considering the following two mixtures (all in volume per cent): O₂ 19.7, N₂ 80.8 and O₂ 26.9, N₂ 50.8, SF₆ 21.2. Oxygen concentrations are very different. Calculated Free Oxygen values are 5.37 and 5.40 %, and Halon 1301 concentrations required for extinguishment are 2.00 and 2.03 %, respectively. Halon 1301 effectiveness is a function of Free Oxygen, increasing significantly at low values.

Extinguishment is a function of Free Oxygen, not actual oxygen, concentration. This empirical model can predict suppressant concentration requirements in agent mixtures and blends, including as a function of oxygen concentration. The additional suppressant required to protect against reflash in a post-extinguishment, carbon dioxide rich and oxygen depleted environment can also be predicted.

Air contains approximately 7 % Free Oxygen. The rest of the oxygen is "neutralized" by the need to heat the nitrogen up to a minimum flame propagation temperature. Slight decreases in oxygen, from only 21 % to 19 %, represent an approximate decrease in free oxygen from 7 % to 5 %. Knowing the oxygen (and other major component gases) concentration in a fire extinction test is crucial. The minimum agent concentration required to extinguish a fire in air can be 40 % above the agent requirement determined in 19 % oxygen. Test results can only be validly compared if under similar Free Oxygen values, or if adjustments are calculated.

Intermediate Scale Testing

Many variables specific to a particular test and suppression scenario influence fire extinguishment. Realistic fire threat scenarios need to be studied. Starting in 1991, an intermediate scale (ISC) 56 m³ compartment was instrumented for evaluation of halon-like agents (gases at ambient temperature and pressure, liquid under pressure) for flow properties, extinguishment, and acid generation. The testing was to characterize, as well as compare, replacement candidates. Wide agent concentration ranges were used to obtain failures, not just validations. Compounds tested in the 4.0x3.4x4.3 m (13x11x14 ft) compartment included Halon 1301, Halon 1211, SF₆, CF₃H (FE-13, HFC-23) and C₂F₅H (FE-25, HFC-125) from Du Pont, CF₂HBr (FM-100) and C₃F₇H (FM-200, HFC-227ea) from Great Lakes, C₄F₁₀ (CEA-410, PFC-4-10) from 3M, CF₃I, and blends.

Such large scale test facilities should undergo a scoping evaluation before designing the final experiments. There was a significant learning curve necessary to define the parameters before truly meaningful results became the norm. Rapid extinguishment of turbulent flammable liquid fires requires significantly more agent than cup burner values. There is not a well defined "success" end point as there is with the slow flow, laminar, premixed agent-air cup burner diffusion flame. Large scale tests involve higher energy release rates, self-generated convection, agent transport and mixing factors. Fire extinction times depend on agent design concentration and addition rate, and agent and oxygen local concentrations near the fire. More rapid extinguishment can minimize, but cannot eliminate, acid products.

Appropriate "success" criteria must be validated. Discharge time, nozzle type, agent distribution inhomogeneities, discharge turbulence and fire induced convection, fire type and size, and compartment boundary conditions, size and ventilation strongly influence results.

The selected size of 0.23 m² baseline n-heptane pool fire proved harder to extinguish than either smaller or larger fires. While spray fires were much easier to extinguish than pool fires, they were also easier to reignite (not as dependent on vaporization rate or igniter placement). Spray fire reignition is always attempted periodically to test for continued protection and assure against initial fire extinction by a higher agent concentration transient. Nozzle effects and inhomogeneities are pronounced (21).

Detailed results on agent discharge pipe flow characteristics (22), and agent concentrations in the compartment as a function of time and location, extinguishment and reignition data, and acid concentrations, have been collected, including during the discharge interval (21).

Intermediate scale, not-in-kind halon alternative studies are being conducted. These include characterization of water mists (23) and pyrogenic solid aerosols (24,25). While not "clean," these technologies hold promise for future maturation. Similar generation and distribution limitations apply to these pseudo-gaseous fine aerosols. Pyrogenic solid aerosols have the additional problem of buoyancy due to high temperature generation. Other generation modes are possible (25).

Intermediate Scale Results. A single test was performed (26) with CF₃I. The agent extinguished the fire more rapidly (6 seconds versus 8 seconds) than Halon 1301 at a similar concentration. This increased performance was due to agent distribution characteristics rather than improved agent effectiveness. Further evaluation was not conducted as toxicity reports ruled out usage for occupied spaces, the main shipboard need.

The agents selected for extensive intermediate scale testing were CEA-410, FE-13, and FM-200, with bench-mark tests performed with Halon 1301. A higher design concentration (calculated for agent weight, allowing for over-pressurization leakage) for similar discharge times yielded faster fire extinguishments (shorter fire out times) for all agents tested. The NRL Cup Burner (CB) values for these replacement agents and Halon 1301 are 5.2%, 12%, 6.6%, and 3.1% respectively (27). Fire out times for increasing FE-13 design concentrations with similar discharge times are listed in Table I. Higher agent design concentrations also generated lower levels of hydrogen fluoride (HF). Table II lists fire out times and maximum measured HF values for increasing FM-200 design concentrations with 5 second discharges. Acid formation was found to be very sensitive to lower agent design concentrations (CB to 1.48 x CB).

Under similar fire and discharge conditions, the replacement agents tested produced much higher acid concentrations than Halon 1301. Table III lists the fire out times and HF maximum values recorded for Halon 1301, FE-13, FM-200, and CEA-410. The total flooding tests were run with similar fire scenarios, concentrations (factor above CB), and discharge times.

Longer discharge times for similar design concentrations produced longer fire

out times due to the longer time it took the agent to reach the extinguishing concentration. This longer exposure of agent to the fire at below extinguishing concentrations caused the production of higher measured HF values.

Increasing the fire size (1.1 m² compared to 0.23 m²), for similar design concentrations and discharge times resulted in faster fire extinguishment. The lower compartment air density resulting from the higher compartment temperature, due to the larger fire, produced a higher effective agent concentration (constant agent weight). Oxygen depletion was also observed since the compartment was not adequately vented during preburn with the larger fire. The fire was ventilation controlled, facilitating its suppression (20). These two effects were responsible for the more rapid fire out times associated with the larger fires. Despite the faster fire out times, the larger heptane fire produced 3 to 5 times more HF. These higher values were due to the increased flame surface area (and increased quantity of reactive combustion species) of the larger fire. The effects of oxygen concentration and compartment temperature on agent concentration, fire out time, and HF concentration, can be seen in Table IV.

Real Scale Tests

Real scale tests (RSC), connoting similarities to actual usage significantly beyond full scale size alone, were performed aboard the Navy's fire research test ship, the *ex*-USS SHADWELL located at Little Sand Island in Mobile Bay, Alabama. These tests were designed to evaluate the feasibility of using the proposed gaseous replacement agents, aerosols, and water mist (28) systems in occupied shipboard machinery space applications. The current test compartment will serve as a test-bed for the next generation of fire suppression agents. The RSC Halon 1301 total flooding in-kind-replacement tests were conducted according to the test plan (29) to determine if the replacement agent system characteristics were satisfactory for shipboard use. These characteristics included fire suppression and reignition protection effectiveness, decomposition products formed during fire suppression, compartment agent distribution, flow/discharge characteristics, and materials compatibility.

The test compartment's enclosed volume was approximately 840 m³ (29750 ft³), 17x7-8.4x6 m (56x23-28x20 ft). Engine and intake/exhaust duct mockups were placed in the test compartment in order to simulate Navy machinery spaces. Testing consisted of compartment characterization with fires, but without agent; agent discharge without mockups or fires, agent discharge with mockups installed, and agent fire suppression discharge tests with mockups. The mockups do present very significant obstacles for proper (homogeneous) agent distribution.

The agents used were FE-13 and FM-200, with Halon 1301 bench-mark tests. Agent design concentrations, based on ISC results, varied up to 1.5 x CB. Fires' sizes ranged up to 7.5 MW. Fuel was n-heptane and/or F-76 (Navy diesel). Electrical cable and wood crib Class A fuels were also tested. The multilevel agent discharge system had 9 nozzles. The discharge system was designed using a two phase fluid flow model (22) developed from NRL agent discharge test results. For two tests, the standard (Navy) 4.1 MPa cylinder pressure (Navy halon cylinder, DOT 3AA) was increased to 8.2 MPa (with higher ullage) in order to achieve the desired shorter discharge times (6 versus 11 seconds). Flow restrictions due to the agent

**Table I. Intermediate Scale (ISC) Tests
Effect of FE-13 Design Concentration on Fire Out Time**

Design Concentration %	Discharge Time (sec)	Fire Out Time (sec)
11.5 (0.96 x CB)	7.5	40
12.7 (1.06 x CB)	8.7	30
14.4 (1.20 x CB)	5.0	13
18.2 (1.52 x CB)	5.0	6

Table II. ISC Tests: Effect of FM-200 Design Concentration on HF Production (Discharge Times: ~5 seconds)

Design Concentration (%)	Fire Out Time (sec)	HF _{max} (ppm)
8 (1.21 x CB)	10	8000
8.2 (1.24 x CB)	12	6300
8.3 (1.26 x CB)	11	5100
9.8 (1.48 x CB)	7	2500

Table III. ISC Tests: Fire Out Time and Acid Generation Comparison between Halon 1301 and FE-13, FM-200, and CEA-410

Agent	Concentration %	Discharge Time (sec)	Fire Out (sec)	HF _{max} (ppm)
CEA-410	7.6 (1.46 x CB)	5.7	6	2900
FE-13	18.2 (1.52 x CB)	5.0	6	3400
FM-200	9.8 (1.48 x CB)	5.5	7	2500
Halon 1301	4.7 (1.52 x CB)	3.1 (high ullage)	8	600

Table IV. ISC Tests: FE-13 Fire Size Effect on Fire Out and HF Production (Design Concentration: 18.2% (1.52* Cup Burner))

Fire Size (ft ²)	Discharge Time (sec)	T _{enclosure} (C) (bottom) - (top)	Agent Equil. Conc. (%)	Fire Out Time (sec)	HF _{max} (ppm)
2.5	5	30 - 50	18.4	6	3400
12	5	170 - 300	23.7	3	11000

storage cylinder bottleneck diameter (standard Navy equipment) required this approach.

RSC Results. The halon replacement agents tested proved successful in extinguishing all the fires. The observed trends from the RSC tests were similar to those from the ISC tests. A faster discharge time corresponded to shorter extinguishment times, more uniform agent concentration, and lower HF concentration. Larger fires were extinguished faster, while producing more HF. The peak HF concentration also increased with decreasing agent design concentration. Decomposition product generation was substantially higher for the replacements than for Halon 1301. Extinction times varied up to a maximum of 28 seconds for the lowest concentration FM-200 used, 8.2%. HF peaks reached 0.5% for the 1.6 MW fire, and 0.75% for the 7.5 MW fire. Please note that previous shipboard fire tests with PVC insulated cables yielded up to 5% HCl (30). Detailed results from the RSC tests can be found in reference (31-33).

The effects of compartment temperature (fire versus non-fire scenarios), discharge time, and mockups (unobstructed versus obstructed compartment) on agent concentration inhomogeneity differentials were analyzed. Both compartment temperature and mockups significantly effect agent distribution. Computer modeling is underway to simulate agent flow from nozzles and distribution in the compartment. This is needed to guide nozzle placement with respect to obstacles.

A faster discharge (6 versus 11 seconds) resulted in smaller agent concentration inhomogeneity differentials (34). The agent, however, was diluted by the additional nitrogen used for agent over-pressurization to achieve a more rapid discharge. Residual pressurant nitrogen, discharged after completion of liquid agent discharge, remained partially unmixed high in the compartment due to its lower density. Leakage in the overhead from incompletely shut ventilation ducts was also found to be significant. These factors resulted in reduced protection high in the compartment. Infrared video cameras showed that reflashes and reignitions (sustained burning) occurred in several tests, primarily in the overhead. Wood crib smoldering sometimes continued after surface burning extinguishment.

Discussion

There are very real differences between inhibited combustion, partially suppressed flames, and extinguished fires. The relative importance of the various interacting modes, chemical kinetics, energy transfer, transport, and distribution, change significantly in the transformation from laboratory reactors to full scale fires.

Chemical kinetics / hydrodynamic models of agent extinguished flames are needed. These would support and greatly extend the empirical agent requirement models previously developed. Burner experiments with various diagnostics and related computer modeling, including experiments on extinction as a function of flame stretch, are underway at NRL and a number of other locations.

An agent below the critical concentration required for extinguishment can react and/or decompose extensively. The large acid concentrations resulting from inhibited cup burner flames are not a complete measure of acid production with fire extinguishment. A very effective labile agent can extinguish the flame before

significant agent reaches the flame sheet. The quantity of reactive flame radicals present exposed to suppressant agent below its extinguishing concentration will strongly influence halide acid production.

The occupied space, zero ODP, hydrofluorocarbon and perfluorocarbon replacement candidates, CF_3H (FE-13), $\text{C}_3\text{F}_7\text{H}$ (FM-200), and C_4F_{10} (CEA-410), unlike Halon 1301, act predominantly as physical agents. NRL cup burner (n-heptane fuel) results show experimentally required extinction concentrations for these agents are 75, 85, and 90 %, respectively, of the NRL model predictions as purely physical agents. The NRL model also shows chemical effects are 75, 85, and 80 %, respectively, of the physical predictions. The total effects add to more than 100 per cent, because chemical effects include enhancement as well as suppression. In these three compounds, the competing chemical effects largely cancel out leaving residual chemical suppression of 25, 15, and 10 % of physical effectiveness, respectively.

The very large underlying chemical activity coupled with relatively inefficient extinguishment, is the reason these agents generate large quantities of HF. HF formation is part of chemical suppression as it removes a potentially active H atom, but this is a one for one scavenging reaction, not a catalytic effectiveness multiplier effect. Hydrogen fluoride concentrations are typically five to ten times greater for the zero ODP agents than for the halons. While this is a serious concern, it must be put in perspective with fire produced CO and other products. Shipboard tests involving PVC insulated cables produced higher concentration values for HCl (30) than have been observed for HF from the HFC candidate agents.

The ISC and RSC tests conducted with halon-like replacements revealed that although concentrations above cup burner can suppress flammable liquid fires, employing small safety margins ($1.2 \times \text{CB}$) can be undesirable because of longer fire suppression times and the extensive generation of decomposition products. Longer agent discharge times yield higher decomposition products as acid formation is a function of the time agent below the extinguishing concentration is exposed to the fire. Increasing fire size reduces fire out times for a ventilation controlled, high temperature environment. The already high acids associated with large flame surface areas will increase for a less oxygen limited fire.

The presence of very pronounced spatial and temporal agent and acid concentration inhomogeneities throughout the full scale test compartment confirm the need for RSC testing. The need to better quantify these inhomogeneities has led to the agent distribution modeling currently underway at NRL. These large inhomogeneities demonstrated that even a 56 m^3 (2000 ft^3) ISC compartment is not large enough to fully characterize agent distribution characteristics. Laboratory and ISC testing provide the science and engineering basis for designing, optimizing and interpreting full scale tests.

Test Results Implications

Dissemination and distribution are critical to halon replacement implementation, and real scale testing is essential in order to properly characterize agent distribution parameters. There is not a unique criteria for determining successful fire extinction for large fires, as there is with well defined laboratory cup burners. Even with cup burners, different configurations and/or operating protocols

can elicit different results; all the more so with fire (type, size, fuel), discharge, compartment, and test protocol variations in large tests.

In order to determine the desired system design concentration, the minimum acceptable agent concentration at the fire must be selected. This concentration should be based on achieving acceptable fire out times and acid generation. The system concentration is then determined by adding a factor to account for observed inhomogeneities (32) and then by adding an appropriate overall system engineering safety factor.

Remaining Issues

Does successful extinction have to occur within a certain time period? Must it be complete with no residual wisping flames? Is there a level of maximum acceptable product generation or collateral damage? Can reflashes and/or reignitions (sustained burning) be tolerated and for how long is the protection required? Is fire control or complete extinction the critical parameter? Different types of suppression agents will have different behavior with different threats. How can different agents be best compared and evaluated? All these are questions that need to be answered for each particular application before any fire suppression system selection is made. A better definition of a suppression systems' overall performance is needed in a valid selection of a retrofit or new total flooding fire (or explosion) protection system.

Conclusions

Studies continue to span and integrate areas from laboratory through full scale. This includes low pressure and atmospheric pressure counterflow burners for kinetics and extinction dynamics, generalizing the empirical models, and providing them with a more basic foundation. Detailed analysis of the real scale results is continuing, as will further intermediate and full scale evaluation under realistic conditions of new and existing approaches. Specific recommendations for shipboard usage will necessarily include consideration of the required time scale for implementation.

This chapter has presented just some of the Navy efforts on addressing its halon replacement needs. There are extensive interactions with other government agencies and commercial concerns, both within the United States and abroad. The Navy is also active (17) in Montreal Protocol efforts with members on the Halon Technical Options Committee of the United Nations Environment Program.

Independent of whether or not an application requires the use of a halon replacement or alternative system, fire protection principles should always be used first to reduce risk. Halon has become "Gucci Gas." A general solution "Son of Halon" may not exist, but the definite need for specific solutions remains. There will be different optimized solutions for different requirements. Options could, and probably will, change with future developments.

Acknowledgments

There have been many individuals and sponsors involved in these efforts. In addition to his significant contributions on large scale testing, Alexander Maranghides assisted in preparing this paper. The U.S. Naval Sea Systems Command has been the primary sponsor in recent years, including for the intermediate and real scale studies.

Literature Cited

1. Bogan, D., unpublished NRL report.
2. Sheinson, R. S., Gellene, G. I., Williams, F. W., and Hahn, J. E. "Quantification of Fire Suppressant Action on Liquid Pool Fires," Paper 18, 1978 Combustion Institute, Eastern Section Meeting, Proceedings, Miami Beach, FL, USA, November 29 - December 1, 1978.
3. Sheinson, R. S., Penner-Hahn, J. E., and Indritz, D., *Fire Safety Journal*, **1989**, *15*, pp. 437-450.
4. Huggett, C., *Combustion and Flame*, **1973**, *20*, pp. 140-142.
5. Larsen, E. R., "Halogenated Fire Extinguishants: Flame Suppression by a Physical Mechanism?", Halogenated Fire Suppressants, ACS Symposium Series; 16, Gann, R. G., Ed., American Chemical Society, Washington, DC, 1975, pp. 376-402.
6. Sheinson, R. S., and Alexander, J. I., "HF and HBr from Halon 1301 Extinguished Pan Fires," Paper 62, 1982 Combustion Institute, Eastern Section Meeting, Proceedings, Atlantic City, NJ, USA, December, 1982.
7. Sheinson, R. S., Musick, J. K., and Carhart, H. W., *Journal of Fire and Flammability*, **1981**, *12*, pp. 229-237.
8. Carhart, H. W., Sheinson, R. S., Tatem, P. A., and Lugar, J. R., "Fire Suppression Research in the U.S. Navy", Proceedings First International Conference on Fire Suppression Research, Stockholm and Boras, Sweden, May 5-8, 1992, pp. 337-357.
9. Fielding, G. H., Williams, F. W., and Carhart, H. W., "Fire Suppression - Why Not Water?," NRL Memorandum Report No. 3435, Feb., 1977.
10. Ewing, C. T., Faith, F. R., Hughes, J. T., and Carhart, H. W., *Fire Technology*, **1989**, *25*, p. 134.
11. Fischer, G., and Leonard, J. T., "The Effectiveness of Fire Extinguishing Powders Based on Small Scale Fire Suppressant Tests," Internal NRL Progress Report, 1984. Some results are reproduced in Reference 25.
12. Ewing, C. T., Faith, F. R., Romans, J. B., Hughes, J. T., and Carhart, H. W., *J. Fire Protection Engineering*, **1992**, *4*, p. 35.
13. Ewing, C. T., Faith, F. R., Romans, J. B., Siegmann, C. W., Ouellette, R. J., Hughes, J. T., and Carhart, H. W., "The Extinguishment of Class B Fires by Dry Chemicals: Scaling Studies." To be published.
14. Sheinson, R. S., and Driscoll, D. C., "Fire Suppression Mechanisms: Agent Testing by Cup Burner," Proceedings The International Conference on CFC & Halon Alternatives, Washington, DC, USA, October 10-11, 1989, Vol. II.
15. Sheinson, R. S., "Halon Alternatives Extinguishment Pathways," Proceedings Halon Alternatives Technical Conference 1991, NMERI, Albuquerque, NM, USA, April 30 - May 1, 1991, pp. 71-82.
16. Sheinson, R. S., and Baldwin, S. P., "Fire Suppression Agent Effectiveness Prediction and Implications for Fire Extinguishment Tests," 1993 Combustion Institute, Eastern Section Meeting, Proceedings, Princeton, NJ, USA, October 25-27, 1993, pp. 483-486.
17. Appendix F. Combustion and Extinguishment - An Overview of the Science. United Nations Environment Programme, Montreal Protocol 1991 Assessment, Report of the Halon Technical Options Committee, December, 1991.

18. Sheinson, R. S., Driscoll, D. C., and Baldwin, S. P., "Halogenated Fire Suppressant Action," Presented at the 203rd American Chemistry Society National Meeting, San Francisco, CA, USA, April 5-10, 1992.
19. Tucker, D. M., Drysdale, D. D., and Rasbash, D. J., *Combustion & Flame*, **1981**, *41*, p. 293.
20. Sheinson, R. S., and Driscoll, D. C., "Fire Suppressant Concentration Requirements: Agent Mixtures and Depleted/Enriched Oxygen Concentrations," 23rd International Symposium on Combustion, Abstracts Book, Orleans, France, The Combustion Institute, July 22-27, 1990, p. 204.
21. Sheinson, R. S., Eaton, H. G., Black, B., Brown, R., Burchell, H., Maranghides, A., Mitchell, C., Salmon, G., and Smith, W. D., "Halon 1301 Replacement Total Flooding Fire Testing, Intermediate Scale," Proceedings Halon Options Technical Working Conference, Albuquerque, NM, USA, May 3-5, 1994, pp. 43-53.
22. Bird, E. B., Giesecke, H. D., Hillaert, J. A., Friderichs, T. J., and Sheinson, R. S., "Development of a Computer Method to Predict the Transient Discharge Characteristics of Halon Alternatives," Proceedings Halon Options Technical Working Conference, Albuquerque, NM, USA, May 3-5, 1994, pp. 95-103.
23. Back, G. G., "An Overview of Water Mist Fire Suppression System Technology," Proceedings Halon Options Technical Working Conference, Albuquerque, NM, USA, May 3-5, 1994, pp. 327-334.
24. Sheinson, R. S., Eaton, H. G., Zalosh, R. G., Black, B. H., Brown, R., Burchell, H., Salmon, G., and Smith, W. D., "Intermediate Scale Fire Extinguishment by Pyrogenic Solid Aerosol," Proceedings Halon Options Technical Working Conference, Albuquerque, NM, USA, May 3-5, 1994, pp. 379-390.
25. Sheinson, R. S., "Fire Suppression by Fine Solid Aerosol," Proceedings The 1994 International CFC And Halon Alternatives Conference, Washington, DC, USA, October 24-26, 1994, pp. 414-421.
26. Baldwin, S. P., Brown, R., Burchell, H., Eaton, H. G., Salmon, G., St. Aubin, J., Sheinson, R. S., and Smith, W. D., "Cup Burner and Intermediate Size Fire Evaluation," Proceedings The 1992 International CFC and Halon Alternatives Conference, Washington D.C., USA, September 29 - October 1, 1992, pp. 812-815.
27. Sheinson, R. S., Black, B. H., Brown, R., Burchell, H., Maranghides, A., Mitchell, C., Salmon, G., and Smith, W. D., "CF₃I - Halon 1301 Total Flooding Fire Extinguishment Comparison," Book of Abstracts Annual Conference on Fire Research, NIST, Gaithersburg, MD, USA, October 17-20, 1994, pp. 59,60.
28. Leonard, J. T., Back, G. G., DiNenno, P. J., "Full Scale Machinery Space Water Mist Tests: Phase I - Unobstructed Space," NRL Ltr Ser 6180-0713.1, October 17, 1994.
29. Sheinson, R., Maranghides, A., and Krinsky, J., "Test Plan - Halon Replacement Agent Testing on the Ex-USS SHADWELL," NRL Ltr Ser 6180-0470.1, September 19, 1994.

30. Alexander, J. I., Bogan, D. T., Eaton, H. G., Greene, J., Paholski, J., Sheinson, R. S., Smith, W. D., Tatem, P. A., Wang, H. T., Williams, F. W., Henderson, C. M., Polito, P. L., Stone, J. P., and McLain, W. L., "Navy Electrical Cable Fire Full-Scale Fire Tests of 1985 at Mobile, Alabama," NRL Memorandum Report 6395, February 16, 1989.
31. Sheinson, R. S., Maranghides, A., Eaton, H. G., Barylski, D., Black, B. H., Brown, R., Burchell, H., Byrne, P., Friderichs, T., Mitchell, C., Peatross, M., Salmon, G., Smith, W. D., and Williams, F. W., "Total Flooding Real Scale Fire Testing with Halon 1301 Replacements," Proceedings The 1994 International CFC And Halon Alternatives Conference, Washington, DC, USA, October 24-26, 1994, pp. 324-333.
32. Maranghides, A., Sheinson, R. S., Barylski, D., Black, B. H., Friderichs, T., Peatross, M. and Smith W. D. "Total Flooding Agent Distribution Considerations," Proceedings Halon Options Technical Working Conference, Albuquerque, NM, USA, May 9-11, 1995.
33. Sheinson, R. S., Maranghides, A., Eaton, H. G., Barylski, D., Black, B. H., Brown, R., Burchell, H., Byrne, P., Friderichs, T., Mitchell, C., Peatross, M., Salmon, G., Smith, W. D. and Williams, W. F., "Large Scale (840 m³) HFC Total Flooding Fire Extinguishment Results," Proceedings Halon Options Technical Working Conference, Albuquerque, NM, USA, May 9-11, 1995.
34. Bird, E. B., Giesecke, H. D., Friderichs, T., Maranghides, A., Sheinson R. S., "Results of Benchmark Comparisons of Calculated and Measured Flow Parameters for Discharges of Halon Replacement Chemicals," Proceedings Halon Options Technical Working Conference, Albuquerque, NM, USA, May 9-11, 1995.

RECEIVED August 1, 1995

Chapter 17

Experimental Studies of Diffusion Flame Extinction with Halogenated and Inert Fire Suppressants

D. Trees¹, K. Seshadri¹, and A. Hamins²

¹Center for Energy and Combustion Research, Department of Applied Mechanics and Engineering Sciences, University of California, La Jolla, CA 92093-0411

²Building and Fire Research Laboratory, Fire Science Division, National Institute of Standards and Technology, Gaithersburg, MD 20899-0001

An experimental study was conducted to determine the effectiveness of a number of agents in extinguishing diffusion flames stabilized in the counterflowing configuration and in the coflowing configuration. These agents are considered as possible replacements for CF_3Br . Liquid fuels were burnt in the counterflowing configuration and liquid and gaseous fuels were burnt in the coflowing configuration. The oxidizer was a mixture of air and agent which was introduced into the flame at an initial temperature of 25°C or at an initial temperature of 150°C . The amount of various agents required in the oxidizing stream to extinguish the flame was measured. The relative effectiveness of these agents was evaluated in terms of their mole fraction and their mass fraction in the oxidizing stream at extinction and was compared with that of CF_3Br and N_2 . The results show that CF_3Br is the most effective agent in quenching flames followed by CF_3I among the gaseous agents tested. On a mass basis the effectiveness of all other gaseous agents tested was nearly the same as that of N_2 .

Production and use of bromotrifluoromethane (CF_3Br), a commonly used fire-suppressant has been restricted because it is known to deplete the ozone present in the stratosphere. The U.S Air Force has identified eleven gaseous agents as possible substitutes for CF_3Br , which are $\text{CF}_3\text{CH}_2\text{CF}_3$ (HFC-236fa), CHFClCF_3 (HCFC-124), CHF_2CF_3 (HFC-125), C_3HF_7 (HFC-227ea), C_3F_8 (FC-218), CHF_2Cl (HCFC-22), CH_2FCF_3 (HFC-134a), C_4F_{10} (FC-31-10), $\text{CH}_2\text{F}_2/\text{CHF}_2\text{CF}_3$ (60%/40% by volume) (HFC-32/HFC-125), cyclo- C_4F_8 (FC-318) and C_2F_6 (FC-116). An experimental study was conducted to determine the effectiveness of these agents in extinguishing diffusion flames stabilized in

0097-6156/95/0611-0190\$12.00/0
© 1995 American Chemical Society

the counterflowing configuration and in the coflowing configuration. The fuels tested were heptane and JP-8 and the oxidizer was air mixed with the agents. Experiments were also performed with CF_3Br and N_2 mixed with air. To examine the influence of the initial temperature of the oxidizing gas stream on the critical conditions of flame extinction, the experiments were performed with the oxidizing gas stream at an initial temperature of 25°C and at an initial temperature of 150°C . In the experiments performed in the coflowing configuration, in addition to heptane and JP-8, the liquid fuel JP-5, the hydraulic fluids (military specifications) 5606 and 83282, and the gaseous fuel propane were also tested. Also in the experiments performed in the coflowing configuration, the additional gaseous agents He, CO_2 , Ar, SiF_4 , CF_3H , CF_2H_2 , C_3F_8 , CF_4 , CF_2CFCl , CHCl_2F , $\text{CH}_3\text{CF}_2\text{Cl}$, CF_2CHCl , CF_2CHBr , CF_2CFBr , CH_2CHBr , and CF_3I , and the liquid agents CF_2Br_2 and CH_2BrCF_3 were tested. The jet fuels and hydraulic fluids contain many components and their composition can vary from batch to batch. The heats of combustion and the elemental composition for the fuel batch used in the experiments reported here are shown in Table I.

Table I: Fuel properties

Fuel	Heat of Combustion (MJ/kg)	Elemental Analysis		
		Mass % H	Mass % C	Mass % O
JP-5	46.3	13.3	85.4	< 0.5
JP-8	46.5	13.9	86.2	< 0.5
5606	44.0	12.6	80.5	2.03
83282	45.1	13.2	79.5	4.78
C_3H_8	50.3	18.2	81.8	0
C_7H_{16}	48.1	16.0	84.0	0

Counterflowing (1-7) and coflowing (1, 2, 7-11) configurations have been employed previously to investigate the structure and critical conditions of extinction of diffusion flames. Past experience has shown that the counterflowing configuration provides a convenient geometry for detailed, fundamental studies of the structure and mechanisms of extinction of diffusion flames (1-7). In the counterflowing configuration the reactant streams (fuel stream and the oxidizer stream) flow toward each other, and a stagnation plane is formed where the value of the normal component of the flow velocity is zero. For hydrocarbon fuels, the stoichiometry of the overall combustion process is such that the flame is stabilized on the oxidizer side of the stagnation plane. In the counterflowing configuration, the flame front (defined as the position where the temperature attains a maximum value) is approximately parallel to the stagnation plane, and the structure of the flame in the vicinity of the stagnation streamline is nearly one-dimensional. Also in the counterflowing configuration, the characteristic residence time for the reactants in the flame can be easily related to the flow velocity of the reactants. This simplifies theoretical interpretation of the experimental results. In the coflowing configuration the reactant streams flow parallel to each other and the flame is stabilized in the shear layer formed between the coflowing streams. A test burner

employing the coflowing configuration is called a "cup-burner". In the coflowing configuration the flame structure is two-dimensional and the characteristic residence time for the reactants in the flame cannot be easily related to the flow velocity of the reactants. However, the experimental data obtained by employing the cup-burner can be used to rank the relative effectiveness of various agents in quenching the flame.

Experimental Apparatus and Procedures

Counterflow Burner. Figure 1 shows schematic illustrations of the counterflow burner designed to burn liquid fuels, and the coflow cup-burner. The coun-

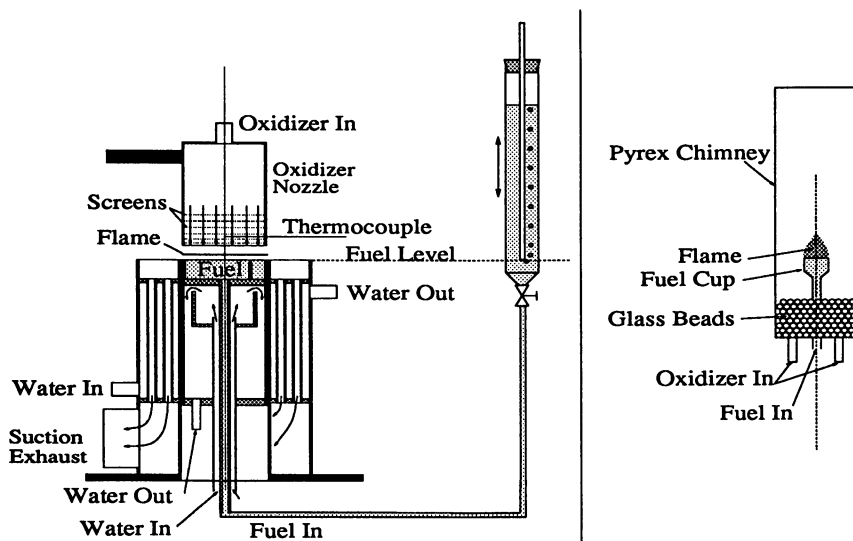


Figure 1: Schematic illustrations of the counterflow burner and the coflow cup-burner.

terflow burner consists of a fuel-cup having a diameter of 50 mm and a depth of 18mm. The fuel-cup was cooled by water to prevent boiling of the liquid fuel. The height of the liquid fuel in the cup was accurately controlled by a device similar to that designed by Bajpai (10, 11). The oxidizer duct of the counterflow burner has an inner diameter of 50.1 mm. Five layers of fine wire screens (80 mesh/cm) were placed in the oxidizer duct to reduce turbulence and to ensure a flat velocity profile at the exit of the duct. The distance between the oxidizer duct and the fuel-cup is adjustable. Experiments were performed with a separation distance of 10 mm between the surface of the liquid fuel and the exit of the oxidizer duct. Mild suction was used to pull the products of combustion from the flame into a heat exchanger surrounding the fuel-cup. Except for the fuel feeding system, the entire counterflow burner assembly was enclosed in a plexiglass box with an outlet directly connected to the exhaust to minimize exposure to the products of

combustion. A steady flame can be stabilized in this apparatus for long periods of time.

The flow rates of air and the inhibitors were measured using calibrated variable area flowmeters. Pressure gauges were placed in parallel with the flowmeters and maintained at 1.689 bar to ensure that the volumetric flow rates of the gases are not affected by the fluctuations in the output pressure from the compressed gas cylinders and by variations in stagnation pressure caused by adjusting the flow rates of the gases. The overall uncertainties in the measurements of the volumetric flow rates were estimated to be less than 5%. Experiments with preheated oxidizer streams were conducted with an electrical heater placed in the oxidizer duct to heat the gases. The temperature of the gases at the exit of the duct was measured with a thermocouple. Prior to performing the experiments, radial profiles of the temperature were measured in the heated oxidizer stream without a flame at approximately the same axial location where the flame was expected to be stabilized. These temperatures were found to vary by amounts less than 2°C in a region around the axis of symmetry whose surface area is approximately equal to that of the liquid pool.

To perform an extinction experiment, the flow rate of air was adjusted to some predetermined value and the fuel was ignited with a torch. The inhibiting agent was then added to the oxidizer stream in gradually increasing amounts until the flame extinguished abruptly. Care was taken to ensure that the system attained a steady-state after each incremental addition of the inhibitor to the oxidizer stream. The flow rates of air and the inhibitor at extinction were recorded. The tests were repeated for different flow rates of air.

The velocity of the oxidizer stream at the exit of the duct U was calculated from the ratio of the volumetric flow rate of the oxidizer to the exit area of the duct. The strain rate a is a measure of the characteristic residence time of the reactants in the flame and was calculated from the relation $a = 2U/L$ (12), where L is the separation distance between the surface of the liquid pool and the exit of the oxidizer duct. The structure of the diffusion flame depends on the value of the Damköhler number δ which is defined as the ratio of the characteristic residence time to the characteristic flow time. For small values of a the value of the characteristic residence time and the value of the Damköhler number will be large. For large values of the Damköhler number, the peak value of the flame temperature will be close to the value of the adiabatic flame temperature (13). As the value of a is increased, the value of δ and the peak value of the flame temperature will decrease. The flame will extinguish at a critical value of a at which the characteristic residence time is insufficient for chemical reactions to take place.

Coflow Burner. The coflow cup-burner shown in Figure 1 consists of a fuel-cup with an inner diameter of 28 mm, through which liquid as well as gaseous fuels were introduced. The level of the liquid fuel in the cup was controlled by a device similar to that employed in the counterflow burner. For tests with gaseous fuels, a fine wire mesh screen (40 mesh/cm) and glass beads were placed inside the fuel-cup to obtain a uniform velocity profile. The oxidizer was introduced into the burner through a Pyrex chimney, 96 mm in diameter, surrounding the fuel-

cup. The flow rates of gaseous reactants and gaseous inhibitors were measured using variable area flowmeters. To introduce liquid agents into the burner, the oxidizer line was heated to 35°C, which is above the normal boiling point of these agents. A metered nitrogen flow was used to displace the agent from a beaker placed in an ice-water bath into the heated line, where it evaporated and mixed with the oxidizing gas stream. The entire apparatus was placed in a fume hood to minimize exposure to the products of combustion.

A number of tests were performed to examine the influence of various parameters on the value of the minimum concentration of the agent required in the oxidizing stream to extinguish the flame. The parameters include the fuel-cup diameter, the volumetric flow rate and velocity of the oxidizer stream, the diameter of the chimney, and the pre-burn time of the fuel. Changes in the volumetric flow rate of the oxidizer stream and the diameter of the chimney were found to have negligible influence on the minimum concentration of the agent at extinction if the flow velocity of the oxidizer was above a certain value. Measurements were made with an oxidizer velocity of 5 cm/s. An increase in the value of the oxidizer temperature from 25°C to 35°C, which is necessary for experiments with liquid agents, had an insignificant effect on the minimum concentration of nitrogen required in the oxidizing stream to extinguish the flame. Changes in the diameter of the fuel-cup were also found to have a negligible influence on the critical conditions of extinction. The influence of preferential distillation of the multicomponent fuels tested here such as the hydraulic fuels on the critical conditions of extinction were found to be negligible for pre-burn times between 50 and 400 seconds. Therefore the experiments were carried out within this period of time.

The extinction experiments were carried out by first filling the fuel-cup with the liquid fuel. The air-flow was then turned on and the liquid fuel was ignited with a torch. The torch was immediately removed after ignition to prevent excess pre-heating of the liquid fuel. The agent was added to the oxidizing stream after 100 seconds to allow the system to attain a thermal steady-state. The inhibiting agent was then added to the oxidizer stream in gradually increasing amounts until the flame was blown away from the burner. Care was taken to ensure that the system attained a steady-state after each incremental addition of the inhibitor to the oxidizer stream. The flow rates of air and the inhibitor at extinction were recorded. The experiment was carried out several times to ensure repeatability. Considering the reproducibility of the measurements and calibrations, the uncertainty in the concentration of the agents at extinction was evaluated to be less than 10%.

Experimental Results

Counterflow Flame. Figure 2 shows the mole fraction of the agents needed to extinguish the flame as a function of the characteristic strain rate a . The fuel tested was heptane and the initial oxidizer temperature was 25°C. It was not possible to stabilize a steady flame in this apparatus for values of the strain rate below 40s^{-1} . Also it was not possible to stabilize a steady flame in this apparatus

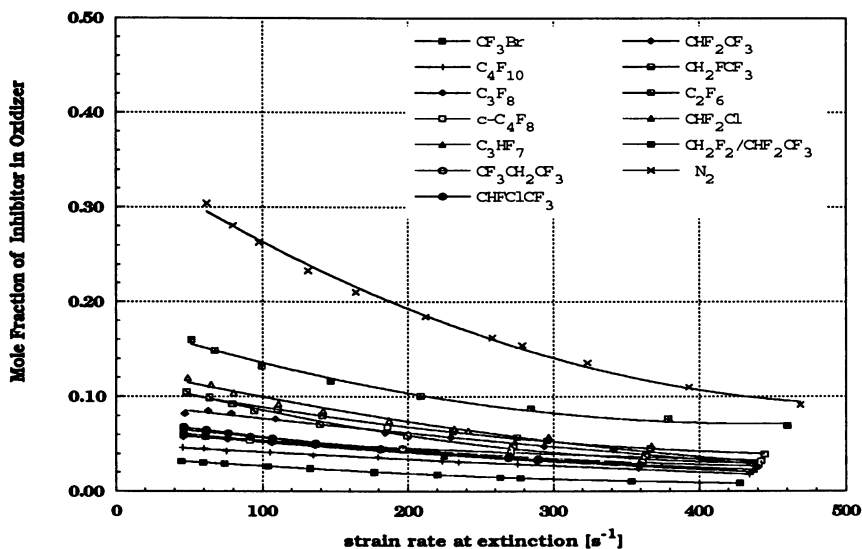


Figure 2: Mole fraction of various agents as a function of the strain rate (s^{-1}) at extinction. The fuel tested was heptane and the initial temperature of the oxidizer stream was $25^{\circ}C$.

for values of the strain rates above $550 s^{-1}$ because at these high values of a , the surface of the liquid fuel was distorted by the oxidizer gas flow, consequently the distance between fuel surface and the oxidizer duct was not uniform over the surface of the liquid pool. Therefore the measurements were made only for values of a between $40 s^{-1}$ and $550 s^{-1}$. For a given agent, the region below the curve represents conditions for which a steady flame could be stabilized in the apparatus. Figure 2 shows the concentration of the agent in the oxidizer stream at extinction to decrease with increasing values of a . Because the characteristic residence time in the flame decreases with increasing values of a , extinction can be expected to take place at lower concentrations of the agent in the oxidizer stream. For a given value of a , the mole fraction of CF_3Br required in the oxidizing stream to extinguish the flame is lower than the mole fraction of all the other agents. Therefore on a mole basis CF_3Br is considerably more effective in extinguishing the flame than all the other agents. Also on a mole basis all the agents tested here are more effective than N_2 in extinguishing the flame. Figure 2 shows that among the substitute agents tested here, C_4F_{10} which has the highest molecular weight is most effective and CH_2F_2/CHF_2CF_3 least effective in extinguishing the flame for all values of a .

For certain applications where the weight of the agent is of importance, a comparison of the mass based effectiveness of the various agents may be useful. Figure 3 replots the data shown in Figure 2 in terms of the mass fraction of the agents needed to extinguish the flame as a function a . Comparison of the data shown in Figures 2 and 3 show that the relative effectiveness of the agents

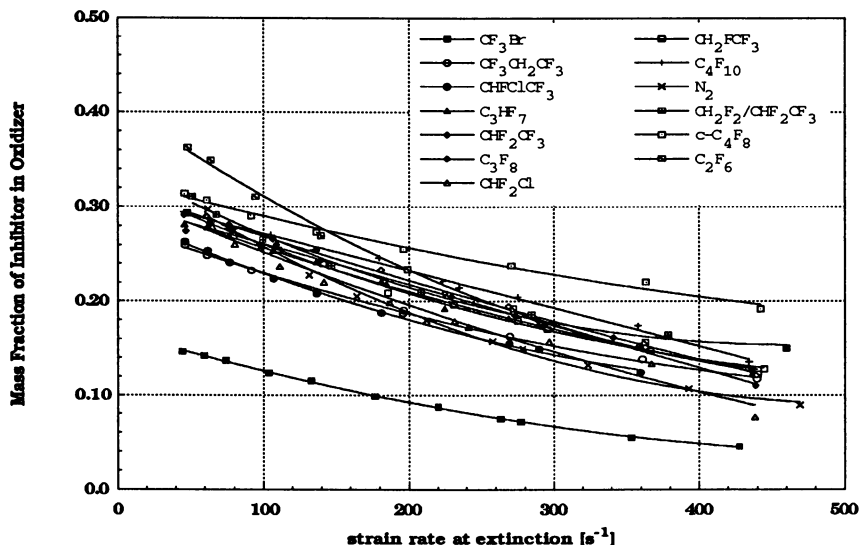


Figure 3: Mass fraction of various agents as a function of the strain rate (s^{-1}) at extinction. The fuel tested was heptane and the initial temperature of the oxidizer stream was 25°C . (Reproduced with permission from ref. 7. Copyright 1994, The Combustion Institute.)

ranked on a mole basis differ from their mass based effectiveness. On a mass basis CF_3Br is still the most effective inhibitor. Figure 3 shows that the relative effectiveness of various agents in extinguishing the flame changes for different values of a . At low strain rates $\text{CF}_3\text{CH}_2\text{CF}_3$ is most effective and C_2F_6 least effective in extinguishing the flame, whereas at high strain rates CHF_2Cl is most effective and cyclo- C_4F_8 least effective in extinguishing the flame. In fact at high strain rates only CF_3Br is more effective than N_2 in extinguishing the flame and the effectiveness of CHF_2Cl is nearly the same as that of N_2 . Figure 3 shows that, except for CF_3Br , the mass-based effectiveness of the various agents in extinguishing the flame does not differ much from that of nitrogen.

Figure 4 shows the mass fraction of the various agents required to extinguish flames burning JP-8 as a function of a . The initial oxidizer temperature was 25°C . Comparison of the data in Figure 4 with those in Figure 3 shows that JP-8 flames are easier to extinguish than heptane flames. The relative mass based effectiveness of these agents in extinguishing JP-8 flames is nearly the same as that for heptane flames. Depending on the strain rate and the agent, 65% to 93% of the amount of inhibitor required to extinguish heptane flames are needed to extinguish JP-8 flames. The differences in the amount of agent required to extinguish heptane flames and JP-8 flames are greatest at high values of a .

Figures 5 and 6 show the mass fraction of the various agents required to extinguish flames burning heptane and JP-8 respectively at an initial oxidizer temperature of 150°C . Comparisons of the data shown in Figure 5 with those in

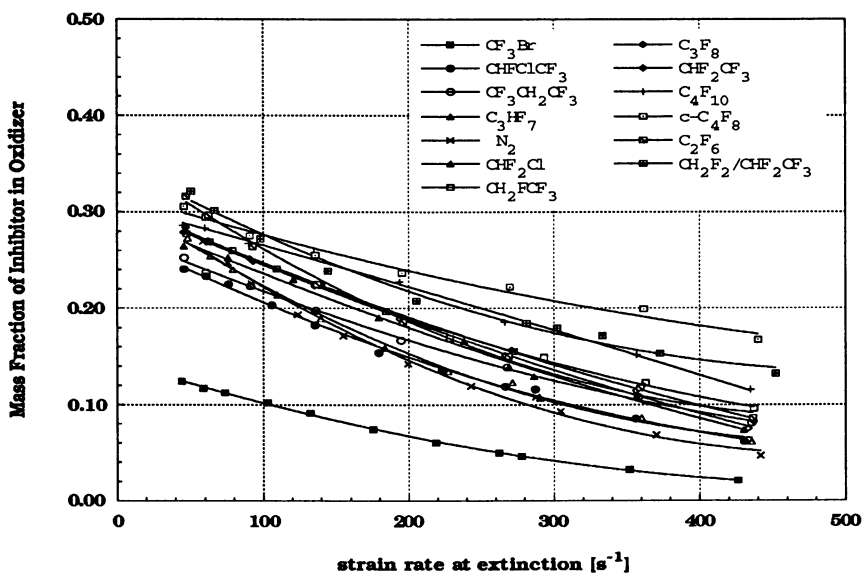


Figure 4: Mass fraction of various agents as a function of the strain rate (s^{-1}) at extinction. The fuel tested was JP-8 and the initial temperature of the oxidizer stream was 25°C.

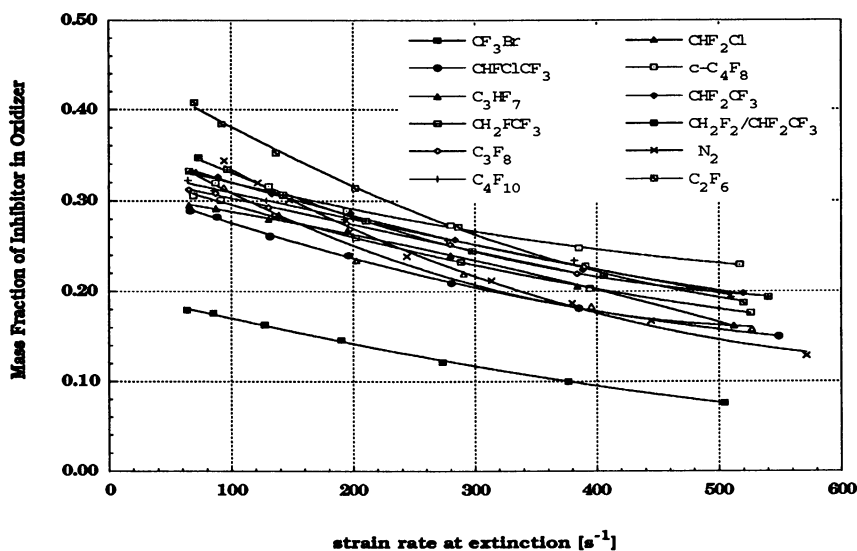


Figure 5: Mass fraction of various agents as a function of the strain rate (s^{-1}) at extinction. The fuel tested was heptane and the initial temperature of the oxidizer stream was 150°C.

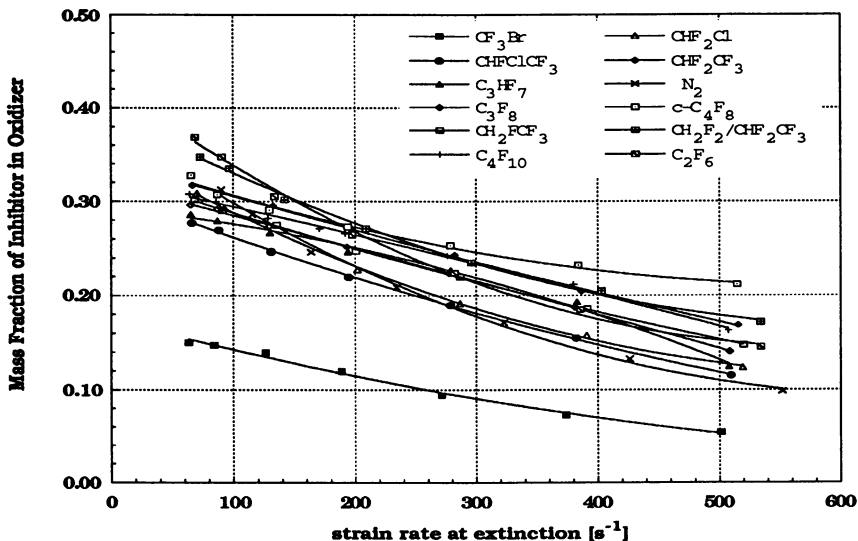


Figure 6: Mass fraction of various agents as a function of the strain rate (s^{-1}) at extinction. The fuel tested was JP-8 and the initial temperature of the oxidizer stream was 150°C .

Figure 3 and the data shown in Figure 6 with those in 4, show that the relative mass based effectiveness of the various agents is nearly the same for different initial temperatures of the oxidizer stream. The enhanced oxidizer temperature of 150°C leads to flames that require 20% to 60% more agent to extinguish them than that needed at an oxidizer temperature of 25°C . The enhanced oxidizer temperature increases the maximum flame temperature and decreases the characteristic chemical reaction time. Therefore extinction will now take place at a lower value of the flow time or at a higher value of a .

In a previous study (7) the chemical and thermal influence of the various agents on the flame was determined roughly by examining the value of the adiabatic flame temperature as a function of the strain rate at extinction. The adiabatic flame temperature was calculated from the composition of the oxidizer stream at extinction, assuming that the agent is inert (7). It was found that with the exception of CF_3Br , all the agents tested in the counterflowing configuration have a significant thermal influence on the flame (7).

Coflow Flame. Figure 7 shows the minimum mole fraction of various agents, including CF_3Br and N_2 , required to extinguish flames burning the liquid fuels heptane, JP-5, JP-8, the hydraulic fluids 5606 and 83282, and the gaseous fuel propane. The agents shown in Figure 7 were also tested in the counterflowing configuration. Propane flames are found to be most difficult to extinguish followed in most cases by heptane, the jet fuels, and the hydraulic fluids. Figure 7 shows that on a mole basis CF_3Br is most effective and N_2 least effective in extinguishing

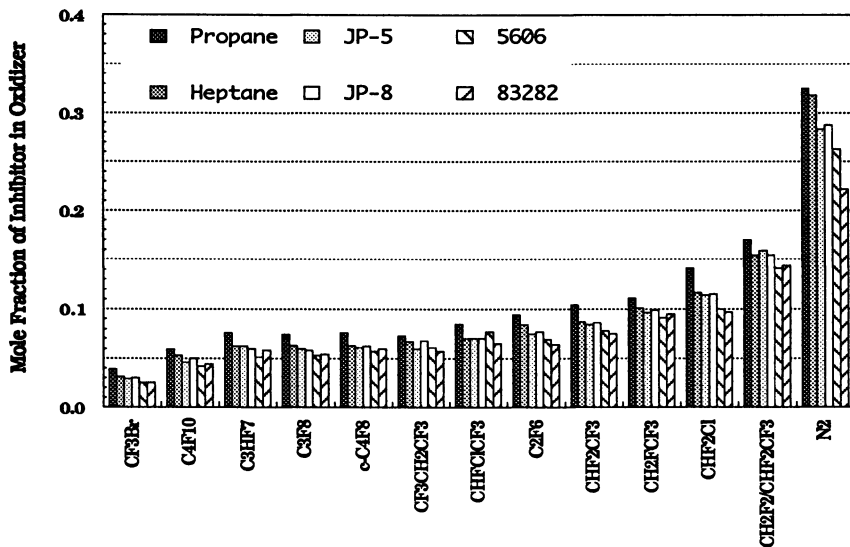


Figure 7: Minimum mole fraction of various agents required to extinguish flames burning various fuels in the coflowing configuration.

these flames. Among the substitute agents tested here on a mole basis C_4F_{10} is most effective and CH_2F_2/CHF_2CF_3 least effective in extinguishing the flames burning various fuels. Figure 8 shows the minimum mass fraction of various agents required to extinguish flames burning various fuels calculated using the data shown in Figure 7. On a mass basis CF_3Br is still the most effective inhibitor. However Figure 8 shows that the mass based effectiveness of the various substitute agents in extinguishing the flame does not differ much from that of nitrogen.

In Table II, the minimum percent mass fraction of the various agents required to extinguish flames burning heptane in the counterflowing configuration are compared with those measured in the coflowing configuration. The initial temperature of the oxidizing stream was $25^\circ C$. For the counterflow flames data measured at $a = 50 \text{ s}^{-1}$ and at $a = 360 \text{ s}^{-1}$ are shown. The values of the minimum mass fraction of the agent required in the oxidizer stream to extinguish the counterflow flames at the lower value of a agree very well with those measured in the coflowing configuration.

Table III shows the minimum mole fraction and the minimum mass fraction of a number of agents required in the oxidizer stream to extinguish coflow diffusion flames burning heptane. These agents were not tested in the counterflowing configuration. For comparison, the extinction data for CF_3Br measured in the coflowing configuration are also shown. The agents CF_2H_2 , CH_3CF_2Cl , CF_2CHCl and CH_2CHBr were found to be flammable. Therefore extinction data for these agents are not shown in Table III. From the results shown in Table III it can be observed that on a mole basis the liquid agents CF_2Br_2 and CH_2BrCF_3 are approximately as effective as CF_3Br in extinguishing flames. However, on a

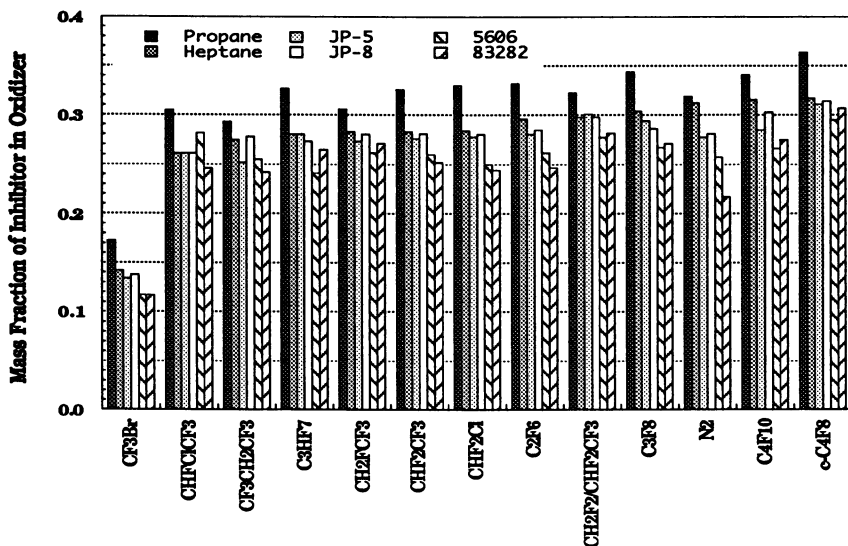


Figure 8: Minimum mass fraction of various agents required to extinguish flames burning various fuels in the coflowing configuration.

mass basis CF_3Br is still more effective than these liquid agents. In addition, if the agent dispersion is taken into consideration, the utility of agents which are liquids at room temperature is uncertain. The brominated ethenes in Table III, $\text{CF}_2=\text{CHBr}$ and $\text{CF}_2=\text{CFBr}$ are less efficient than CF_3Br on a mole basis as well as on a mass basis. On a mole basis, the iodine-containing agent CF_3I is nearly as effective as CF_3Br in extinguishing flames and more effective than all the other agents shown in Table III. Also on a mass basis CF_3I is more effective than all the substitute agents shown in Table II. Interestingly, Table III shows that on a mass basis, helium is more effective than CF_3Br in extinguishing the flame. Although helium is not particularly effective on a mole basis, it may be a practical alternative to CF_3Br in some specialized applications.

Summary and Conclusions

An experimental study was carried out to determine the effectiveness of various agents in extinguishing diffusion flames stabilized in the counterflowing configuration and in the coflowing configuration. The following remarks summarize the major conclusions of the study.

1. The relative effectiveness of various agents in extinguishing flames ranked on a mole basis differs from that ranked on a mass basis.
2. Studies performed in the counterflowing configuration show that the relative mass based effectiveness of various agents with respect to one another depends on the value of the strain rate. However, this relative mass based

Table II: Percent mass fraction of various agents at extinction.

Agent	Percent Mass Fraction at Extinction		
	counterflow		coflow
	$a = 50 \text{ s}^{-1}$	$a = 360 \text{ s}^{-1}$	
CF ₃ Br	14.5	5.4	14.2
CF ₃ CH ₂ CF ₃	25.5	13.6	27.5
CHFClCF ₃	25.9	12.5	26.1
CHF ₂ CF ₃	27.2	14.7	28.3
C ₃ HF ₇	27.9	15.4	28.0
CH ₂ FCF ₃	29.1	15.5	28.3
C ₃ F ₈	29.1	15.5	30.4
CHF ₂ Cl	29.2	12.0	28.5
C ₄ F ₁₀	29.3	16.8	31.5
N ₂	30.5	11.5	31.2
cyclo-C ₄ F ₈	30.9	21.4	31.7
CH ₂ F ₂ /CHF ₂ CF ₃	31.1	16.3	29.8
C ₂ F ₆	35.7	15.4	29.6

Table III: Mole-based and mass-based effectiveness of various agents in extinguishing heptane flames stabilized in the coflow configuration.

Type	Agent	Mass Percent	Mole Percent
inert	He	6.0	31
	CO ₂	32	23
	Ar	38	41
silicone containing	SiF ₄	36	13
HFC	CF ₃ H	25	12
	CF ₂ H ₂	^a	^a
FC	C ₃ F ₆	29	7.3
	CF ₄	37	16
HCFC	CF ₂ =CFCl	31	10
	CHCl ₂ F	32	11
	CH ₃ CF ₂ Cl	^a	^a
	CF ₂ =CHCl	^a	^a
bromine containing	CF ₃ Br	14	3.1
	CF ₂ Br ₂ (l)	16	2.6
	CH ₂ BrCF ₃ (l)	17	3.5
	CF ₂ =CHBr	24	6.0
	CF ₂ =CFBr	27	6.3
	CH ₂ =CHBr	^a	^a
iodine containing	CF ₃ I	18	3.2

^aagent observed to be flammable

effectiveness does not depend on the fuel type or the initial temperature of the oxidizer.

3. The value of the minimum concentration of the agents required in the oxidizing stream to extinguish flames depends on the fuel. Propane flames are most difficult to extinguish, followed in most cases by heptane, the jet fuels JP-8 and JP-5, and the hydraulic fluids 5606 and 83282.
4. The minimum concentration of the agents required in the oxidizing stream to extinguish flames stabilized in the counterflowing configuration at low values of the strain rate agrees well with that measured for flames stabilized in the coflowing configuration.
5. Studies performed in the counterflowing configuration as well as those performed in the coflowing configuration show that on a mass basis CF_3Br is the most effective agent in extinguishing flames. Studies performed in the coflowing configuration show that on a mass basis the effectiveness of the liquid agents CF_2Br_2 and CH_2BrCF_3 and the iodine-containing gaseous agent CF_3I in extinguishing flames is close to that of CF_3Br . The mass-based effectiveness of all other agents tested in both coflowing and counterflowing configuration is nearly the same as that of N_2 .

Acknowledgments

The research at UCSD was supported by NIST Contract # 60NANB2D1285 and by the Deutscher Akademischer Austauschdienst program HSP II. The research at NIST was supported by the U. S. Air Force, the U. S. Army, the U. S. Navy, and the FAA. We thank Professor F. A. Williams, Dr. R. Sheinson and Dr. W. Grosshandler for many useful discussions.

Literature Cited

- (1) Ford, C., in *Halogenated Fire Suppressants* (R. Gann, Ed.), Vol. 16 of ACS Symposium Series, Washington, DC, 1975, American Chemical Society, pp. 1–63.
- (2) Pitts, W., Nyden, M., Gann, R., Mallard, W., and Tsang, W., *Construction of an Exploratory List of Chemicals to Initiate the Search for Halon Substitutes*, number 1279, National Institute of Standards and Technology, U.S. Department of Commerce, 1990, pp. 14–40.
- (3) Milne, T., Green, C., and Benson, D., *Combust. and Flame* **1970**, 15, pp. 255–264.
- (4) Kent, J. H., and Williams, F. A., *Fifteenth Symposium (International) on Combustion*, The Combustion Institute, Pittsburgh, PA, 1975, pp. 315–325.
- (5) Seshadri, K., and Williams, F. A., in *Halogenated Fire Suppressants* (R. Gann, Ed.), Vol. 16 of ACS Symposium Series, Washington, DC, 1975, American Chemical Society, pp. 149–182.

- (6) Hamins, A., and Seshadri, K., *Combust. Sci. and Tech.* **1984**, 38, pp. 89–103.
- (7) Hamins, A., Trees, D., Seshadri, K., and Chelliah, H., *Combust. and Flame* **1994**, 99, pp. 221–230.
- (8) Kubin, R., Knipe, R., and Gordon, A., in *Halogenated Fire Suppressants* (R. Gann, Ed.), Vol. 16 of ACS Symposium Series, Washington, DC, **1975**, American Chemical Society, pp. 183–207.
- (9) Booth, K., Melia, B., and Hirst, R., Technical report, ICI Mond Division, Winnington Laboratory, (1973).
- (10) Bajpai, S. N., Technical report, Factory Mutual Research Corporation, Norwood, MA, (1973).
- (11) Bajpai, S. N., Technical report, Factory Mutual Research Corporation, Norwood, MA, (1974).
- (12) Seshadri, K., and Williams, F. A., *International Journal of Heat and Mass Transfer* **1978**, 21 (2), pp. 251–253.
- (13) Williams, F. A., *Combustion Theory*, Addison-Wesley, Menlo Park, CA, 2 edition, 1985.

RECEIVED July 6, 1995

Chapter 18

Effectiveness of Halon Alternatives in Suppressing Dynamic Combustion Processes

W. L. Grosshandler¹, G. Gmurczyk^{1,3}, and C. Presser²

¹Building and Fire Research Laboratory, Fire Science Division, and

²Chemical Science and Technology Laboratory, Chemical Kinetics
and Thermodynamics Division, National Institute of Standards
and Technology, Gaithersburg, MD 20899-0001

C_3F_8 is shown to require the least storage volume among twelve fluorocarbons for suppressing a quasi-detonation. CF_3I performs the best of the gaseous suppressants evaluated in a spray burner. Two experimental facilities are described as part of an effort to identify suitable replacements for CF_3Br in aircraft applications. A turbulent spray burner simulates the hazard associated with a ruptured fuel line in an engine nacelle or dry bay. A deflagration/detonation tube evaluates the ability of a gaseous agent to attenuate the pressure build-up and Mach number of a quasi-detonation.

Halon 1301 (CF_3Br) is no longer produced in the U.S., forcing the manufacturers, owners, and users of aircraft to search for an alternative fire suppressing agent (1). A research program was established at NIST to focus specifically on engine nacelle and dry bay protection. The nacelle is the portion of the airframe which surrounds the jet engine. The engine system certification process requires that enough agent be available to maintain a minimum concentration (6% by volume for halon 1301) throughout the nacelle for a 0.5 s time interval to ensure that the fire will be extinguished and not relight. Dry bays refer to normally closed spaces adjacent to flammable liquid storage areas that are vulnerable to anti-aircraft fire. The entire suppression sequence occurs in under 100 ms in the dry bay.

The experiments described here are two of dozens that were developed (2) to identify the best chemicals for subsequent full-scale aircraft fire extinguishment evaluation at Wright-Patterson Air Force Base. The discriminating factors elucidated by the test protocols were lumped into four categories: (i) agent dispersion characteristics, (ii) required storage volume, (iii) environmental factors, and (iv) operational issues. The results presented in this paper are limited to the flame suppression studies which directly impact the estimate of agent storage volume required on board the aircraft. However, the dispersion character of the different agents in cold-flow

³Current address: Science Applications Interactional Corporation, 555 Quince Orchard Road, Suite 500, Gaithersburg, MD 20878

experiments varied more extensively than the amount of the agent required for flame suppression. The agent leaves the storage vessel, pressurized with N_2 at about 4 MPa, and immediately flashes or breaks into droplets, evaporates, and mixes with ambient air. The timing of this process is critical, and can render an agent which requires less mass to extinguish a laboratory flame ineffective in suppressing an actual aircraft fire. The reader is referred to the thorough discussion by Pitts et al. (2, Section 3) for details on how the agents were screened based upon the dispersion process.

Four different flame suppression facilities were designed with the objective of examining the flame extinction properties of the agents over the whole range of conditions likely to be encountered by aircraft in flight: (i) an opposed-flow diffusion flame (OFDF) burner, (ii) a cup burner, (iii) a turbulent spray burner, and (iv) a detonation/deflagration tube. The results of the turbulent spray and deflagration/detonation suppression experiments are summarized here. The OFDF and cup burner results are discussed in a companion chapter in this Series (3). Readers should refer to the Special Publication by NIST for additional details on the suppression experiments (2, Section 4).

Fluorocarbons (FCs), hydrofluorocarbons (HFCs), hydrochlorofluorocarbons (HCFCs), and CF_3I were examined and compared to the performance of N_2 and CF_3Br . The behavior of sodium bicarbonate powder was studied in the spray burner only. All of the agents are listed with their physical properties in Table I. Air was the oxidizer, and the fuels included ethene, a jet fuel (JP-8), and a hydraulic fluid (MIL-H-83282C).

Turbulent Spray Flames

A fuel spray provides a unique opportunity for supporting a fire. Small droplets quickly evaporate and the momentum from the spray efficiently entrains the air necessary for combustion. A ruptured high pressure fuel, lubricant or hydraulic fluid line can supply a steady flow of fuel for a fire stabilized behind obstacles in the engine nacelle, or create a cloud of droplets from a punctured fuel tank adjacent to a dry bay. Extinguishment of the burning spray will occur when the critical level of agent is mixed with the air that gets entrained into the reaction zone. The process is affected by the velocity of the air flow, the rate that the agent is added to the air, the system temperature, and the agent and fuel concentrations and properties.

Experimental Facility. The spray burner facility consisted of an air delivery system, a fuel delivery system, an agent injection system, and a combustor. Figure 1 shows a cross-sectional view through the combustion zone. Air at atmospheric pressure co-flowed around the fuel tube within a 0.5 m long, 50 mm diameter stainless steel pipe. A Pyrex tube extension, 75 mm long, was used to observe the flame under confined conditions. The fuel was injected along the centerline through a pressure-jet nozzle, flush with the open end of the surrounding passage. The flame was stabilized on a 35 mm diameter steel disk attached to the nozzle body. The nominal air velocity across the burner was 33 m/s. The fuel (JP-8 or hydraulic fluid) was delivered at a rate of about 0.5 ml/s when the gauge pressure was 687 kPa.

The gaseous agents were injected impulsively into the air 0.54 m upstream of the nozzle using a computer controlled solenoid valve. Uniform dispersion across the air stream was enhanced by injecting the gas in a radial direction into a reduced diameter

Table I. Physical properties of agents evaluated (2, Section 2)

Agent		Molec. Wt., g/mole	P _v @ 25 °C, MPa	T _{bp} @ 101 kPa, °C	Sat. Liq. Density @ 25 °C, kg/m ³
Designation	Formula				
nitrogen	N ₂	28	^a	-196	^a
halon 1301	CF ₃ Br	149	1.61	-57.8	1551
halon 13001	CF ₃ I	196	0.49	-22.0	2106
FC-116	C ₂ F ₆	138	^a	-78.2	^a
FC-218	C ₃ F ₈	188	0.88	-36.8	1321
FC-31-10	C ₄ F ₁₀	238	0.27	-2.0	1497
FC-318	cyc-C ₄ F ₈	200	0.31	-7.0	1499
HFC-125	C ₂ HF ₅	120	1.38	-48.6	1190
HFC-32/125	CH ₂ F ₂ /C ₂ HF ₅	67	1.67	-52.5	1040
HFC-134a	C ₂ H ₂ F ₄	102	0.67	-26.2	1209
HFC-227ea	C ₃ HF ₇	170	0.47	-16.4	1395
HFC-236fa	C ₃ H ₂ F ₆	152	0.27	-1.5	1356
HCFC-22	CHF ₂ Cl	87	1.05	-40.9	1192
HCFC-124	C ₂ HF ₄ Cl	137	0.38	-13.2	1357
sodium bi-carbonate	NaHCO ₃	84	^b	^b	^b

^a 25 °C is above critical temperature of compound

^b solid powder, blended with silica

section of the air passage. Screens were placed downstream of the injection point to ensure complete mixing between the air and agent prior to encountering the flame zone. The amount of injected agent was controlled by varying the initial pressure and the time that the solenoid valve was open. The actual mass delivered was determined from the difference between the initial and final pressures in the storage vessel (5).

The gaseous injection system was modified to accommodate powders. The sodium bicarbonate was loaded into two nylon tees downstream of the computer-controlled solenoid valve. Straight-through ball valves isolated the powder from the burner to minimize back-flow and powder loss during loading. Compressed air stored in the agent vessel was used to propel the powder into the burner.

The independent parameters which were controlled in the spray burner facility were the air flow and temperature, the fuel flow and type, the agent composition, and the mode of injection (fixed time or fixed pressure). The particle size distribution and

the transport gas pressure were varied for the powdered NaHCO_3 . The dependent parameters in the experiments were the mass and the rate of injection required for suppression.

The protocol used to evaluate the gaseous agents incorporated a fixed injection interval of 75 ± 10 ms. The fuel spray was ignited and the air flow set to the desired level. The flame was allowed to burn for several minutes to ensure steady operation. If the air was at an elevated temperature, it was necessary to wait until the temperature at the burner stabilized. The agent storage vessel was evacuated and then flushed several times with the chemical under investigation. The pressure in the vessel was adjusted with the solenoid valve closed to a value which was expected to be insufficient to extinguish the flame. The computer control/data acquisition was initiated and the response of the flame to the injection process was observed. If the flame was not extinguished, the pressure in the agent vessel was increased and the experiment was repeated under the same operating conditions. Eventually a pressure was found which was sufficient to suppress the flame. This procedure was normally repeated four times for each agent. Additional details on the facility and its operation have been given previously (2, Section 4; 4; 5).

Experimental Results. The mass fraction of agent required to extinguish the flame, β , is defined by the average mass flow of the agent divided by the sum of the agent and air flows. The mass of agent added to the flame and the actual time interval of agent injection were determined from pressure-time traces (5).

The injection time interval had an effect on the minimum amount of nitrogen required to extinguish the flame. The closed-circles plotted in Figure 2 illustrate this effect. For these experiments, the pressure was fixed and the injection time interval was gradually increased until extinction occurred. The minimum mass of nitrogen was about 0.32 g, for a set injection period of 23 ms. Reducing the set time to 6 ms had no impact on the amount of nitrogen required to quench the flame because of the finite time response of the solenoid valve. Injection times as long as 260 ms more than tripled the amount of N_2 required. A limit was reached at long time intervals where transient mass addition was insufficient to extinguish the flame.

Nitrogen was allowed to flow continuously in one experiment, with the rate increasing until the flame was extinguished. The mass fraction of N_2 required to suppress the flame was 0.11, and is indicated by the continuous flow arrow in Figure 2. This compares to a value of 0.28 found in a cup burner (3) with the same fuel/agent combination. Less nitrogen was required for extinguishment of the spray flame because of the greater turbulence levels and reduced time available for the combustion to occur. The solid triangles also plotted in the figure are values of β that correspond to the different injection time intervals. As the time is shortened, β increases, reaching a limiting value of about 0.28. For an agent that is to be used in a transient manner, the total mass must also be considered. This is distinct from the quasi-steady state measurements taken with the cup burner apparatus, for which β is a reasonable measure of performance for a total flooding agent.

Gaseous Agent Test Series. Extinguishment experiments were first performed using halon 1301 to establish a baseline. An average over five experiments led to a CF_3Br mass of $0.44 \pm .04$ g and a β of 0.15 required for flame suppression. The

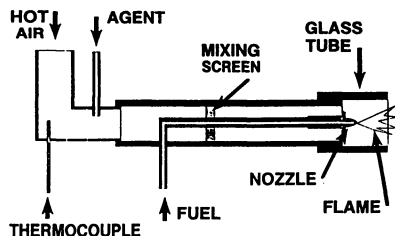


Figure 1. Cross-section of combustion zone of spray burner facility.

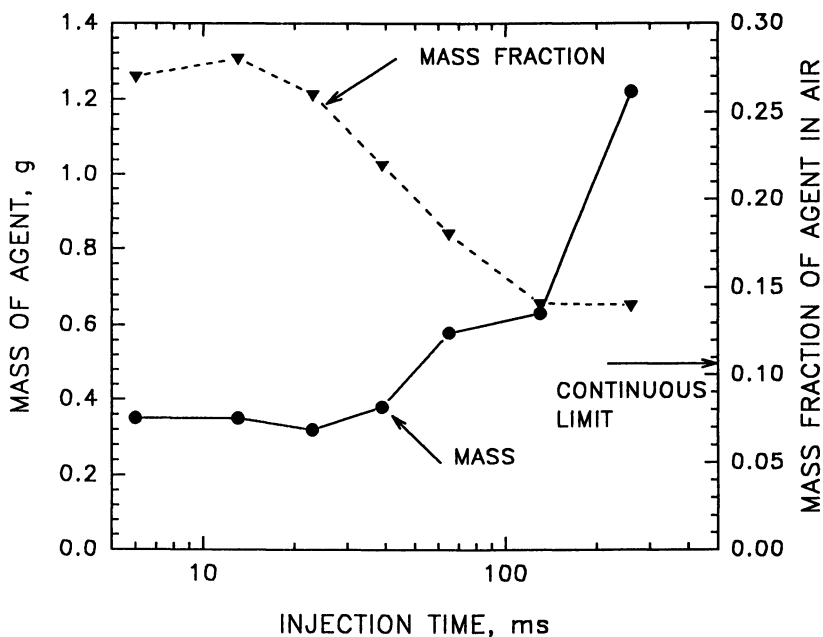


Figure 2. Effect of injection time on the total mass and mass fraction of N_2 required to extinguish JP-8 spray flame.

results of the ambient temperature air/JP-8 flame suppression experiments for all of the gaseous chemicals examined are summarized in Table II. The CF_3I required the least mass (0.54 g) and a mass fraction of 0.16, close to that of CF_3Br . Nitrogen was only slightly less effective. HCFC-22 was the next most effective, requiring 0.65 g for suppression; FC-31-10 required the most (1.00 g) material and the highest mass fraction (0.27) to extinguish the flame.

The air was preheated to 150 °C and the experiments were repeated with all of the gaseous agents except for CF_3I (4). The increase in temperature affected the flame stability in several ways. First, since the mass flow of air remained fixed, the average velocity across the air duct increased about 50% due to the drop in density. The JP-8 in the line was also warmed as it flowed through the heated air annulus. The higher temperatures and lower fuel density required the fuel pressure to be increased to deliver the same amount. However, even at a maximum fuel line pressure of 1.03 MPa-g, the mass of fuel was only 90% of the ambient temperature condition, resulting in a slightly leaner flame. The increase in air velocity and decrease in equivalence ratio somewhat destabilized the flame; but this was counteracted by the increase in enthalpy of the reactants due to the higher initial temperature.

As seen in Table II, increasing the temperature, on average, increased the amount of agent required to suppress the JP-8 spray flame by 0.04 g. The halon 1301 remained the most effective, but in relative and absolute terms, required the largest increase in mass of all the chemicals investigated. The nitrogen remained better than the other halogenated compounds, and FC-31-10 remained the least effective. It can be speculated that the relatively poorer behavior of the halon 1301 is attributable to two possible reasons: the decreased residence time of the agent in the flame, and the increased temperature near the flame front. Both physical effects could reduce the number of bromine atom/hydrogen radical interactions.

A flame could not be stabilized using MIL-H-83282C hydraulic fluid and ambient temperature air. By increasing the air temperature to 120 °C and by operating closer to stoichiometric conditions (the fuel volume flow was increased by 27% over the JP-8 flame), sufficient stability was maintained. A bluish appearance of the hydraulic fluid spray flame suggested that less soot was being formed.

There was little difference in the amount of halogenated agent necessary to suppress the hydraulic fluid spray when compared to the JP-8 flames. (See Table II, and note that neither FC-31-10 nor CF_3I were tested with the hydraulic fluid.) In particular, the amount of halon 1301 was identical to the unheated jet fuel experiments. About 10% more FC-318 was used to suppress the hydraulic fluid. By contrast, 28% less nitrogen extinguished the hydraulic fluid flame. An explanation for this unique behavior is not available.

Sodium Bicarbonate Powder Experiments. There was a definite particle size effect on the efficiency of the powder as a fire suppression agent. Table II summarizes the results. The smallest particle size powder was 2 1/2 times more effective in its fire suppression capability than the large particle size powder. There was no significant difference in performance created by changing injection pressure of the smallest particles. On the other hand, increasing the injection pressure increased the effectiveness of the large particle size by more than 20%. The enhancement in performance can be explained by the improved mixing of the powder into the flame as the injection

Table II. Amount of agent required to suppress turbulent spray flame (2, Sect. 4)

Agent	JP-8, $T_{\text{air}}=20\text{ }^{\circ}\text{C}$		JP-8, $T_{\text{air}}=150\text{ }^{\circ}\text{C}$		Hydraulic Fluid, $T_{\text{air}}=120\text{ }^{\circ}\text{C}$	
	mass, g	β	mass, g	β	mass, g	β
halon 1301	0.44	0.15	0.53	0.19	0.44	0.16
CF ₃ I	0.54	0.16	a	a	a	a
nitrogen	0.58	0.18	0.63	0.19	0.42	0.16
HCFC-22	0.65	0.20	0.70	0.23	0.70	0.24
HFC-125	0.73	0.22	0.77	0.24	0.78	0.26
HCFC-124	0.74	0.22	0.75	0.22	0.70	0.23
FC-116	0.75	0.22	0.74	0.23	0.73	0.23
HFC-134a	0.76	0.24	0.78	0.23	0.79	0.26
HFC-236fa	0.78	0.23	0.84	0.25	0.78	0.24
HFC-227ea	0.80	0.24	0.81	0.24	0.82	0.26
HFC-32/125	0.81	0.24	0.89	0.26	0.82	0.25
FC-218	0.89	0.24	0.87	0.25	0.86	0.28
FC-318	0.97	0.25	0.99	0.26	1.08	0.30
FC-31-10	1.00	0.27	1.02	0.25	a	a
NaHCO ₃ , < 10 μm	0.20	0.08	a	a	a	a
NaHCO ₃ , > 50 μm	0.52	0.18	a	a	a	a

^a not measured

pressure increases and as the particle size decreases. The β values indicate a very effective agent for small particles, and a rather average performing agent for the large particle size (2, Section 4).

High speed movies of injection of the 0-10 μm particles showed what appears to have been a uniform powder cloud passing through the burner in about 80 ms. This compared to an injection interval equal to 75 ms based upon the recorded air pressure in the storage vessel. The photographs also showed that flame extinction happened within the first 50 ms from the time the powder reached the flame. This time was independent of injection pressure, and was close to the 40 ms estimated from high speed photographs of HCFC-22 suppressing a similar flame.

Discussion of Spray Flame Experiments. If the agents are ranked according to the mass required to inhibit the flame, the order does not change by more than plus or minus one position for the three series of experiments. The exception is HFC-125, which drops two positions in both of the high temperature tests. Expressing the results in terms of the flame suppression number (FSN) is a convenient way to compare the performance of the different agents in the three series of experiments. The FSN is defined as the mass fraction of agent relative to the mass fraction of halon 1301 used to suppress the equivalent flame. For the ambient temperature JP-8 flame, the FSN ranges from about 1.4 to 2.1 for the various agents, which is about 25% less than the FSNs measured in the cup burner (3).

Minimizing the storage volume on board the aircraft is as critical as minimizing the mass of agent. The density of the saturated liquid agent at ambient temperature provides a logical conversion from the mass required to the storage volume because the saturated liquid condition at ambient temperature is close to the condition maintained when the fire extinguishing bottle is filled (assuming negligible solubility of the pressurizing gas). The volume factor, VF, is defined as the volume of the agent in the cylinder required for flame suppression normalized by the equivalent volume of halon 1301. Figure 3 compares the performance of the different agents in this fashion, using (i) ambient temperature air and JP-8 (open bars), (ii) 150 °C air and JP-8 (cross-hatch bars), and (iii) 120 °C air and hydraulic fluid (solid bars). Nitrogen requires a storage volume 36 times that of halon 1301, and is off the scale in Figure 3 because it does not liquify under typical bottle conditions. The FC-116 also rates poorly on a volume basis because its critical temperature is less than the ambient. In the figure, the density of FC-116 was calculated at 25 °C and 4.1 MPa, a typical bottle pressure. The remainder of the agents have storage volume factors between 1.5 and 2.5, depending on the agent, fuel and temperature. Of these, the HFC-32/125 mixture has the highest volume factor, and HCFC-124, HFC-227ea and HCFC-22 have the lowest. The powdered agent was not compared on a volume basis since the volume of the system depends upon the pressurizing method as much as on the volume of the powder. The superior performance of the NaHCO₃ powder is evident, however, from the value of its FSN, which is less than 0.9 (2).

Conclusions from Turbulent Spray Burner Study. The turbulent spray burner has been found to be suitable for comparing the performance of gaseous and fine powder extinguishing agents in transient operation. The facility is not overly sensitive to the air or fuel flows, and the agent delivery system is able to control accurately the injection period between 20 and 910 ms.

The following conclusions are made regarding the ability of different agents to extinguish the spray flame:

- No statistically significant difference in agent performance was found between the room temperature JP-8 and hydraulic fluid flame testing, indicating little fuel effect.
- The majority of the agents require slightly more mass to extinguish the higher temperature JP-8 flame, indicating a small temperature effect. This trend is not completely unexpected since a higher temperature leads to more rapid fuel evaporation and greater flame stability. However, the temperature effect does not alter the ranking on agent performance, with the exception of HFC-125.

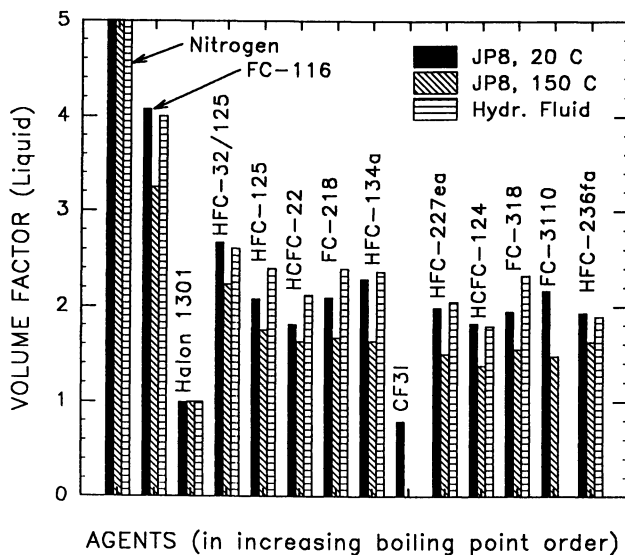
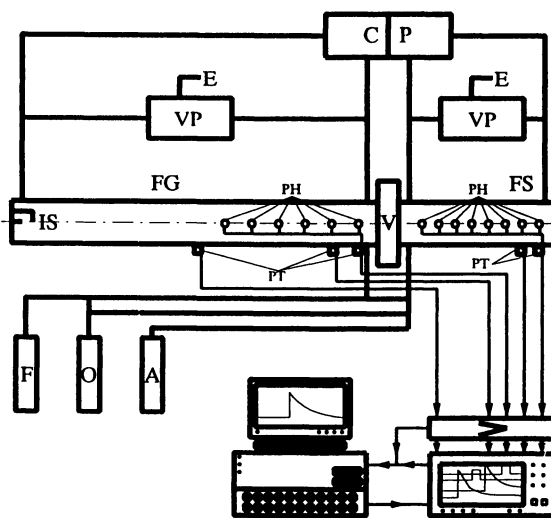


Figure 3. Volume factor (VF) based upon liquid volume of agent relative to liquid volume of CF_3Br required to extinguish turbulent spray flame.



FG - FLAME GENERATION, FS - FLAME SUPPRESSION, IG - IGNITION,
V - GATE VALVE, CP - CIRCULATION PUMP, VP - VACUUM PUMP,
PH - PHOTODIODE, PT - PRESSURE TRANSDUCER, F - FUEL,
O - OXIDIZER, A - AGENT

Figure 4. Schematic diagram showing major components of the deflagration/detonation tube facility.

- The FCs, HFCs and HCFCs all perform better in a turbulent spray burner relative to halon 1301 than is predicted from cup burner measurements. Generally speaking, almost twice as much mass and volume are needed to suppress the spray flame using the alternative agents when compared to halon.
- The amount of agent required for flame suppression decreases with increasing rate of agent injection.

Quasi-detonations

An anti-aircraft projectile entering a dry bay could lead to a situation in which a vaporizing fuel spray produces a combustible mixture which is then ignited by a glowing fragment. If the space were confined, the pressure would increase behind the reaction front, accelerating the flame. A transition to turbulence would likely occur as the flame encounters clutter in the dry bay. If the ventilation is insufficient to relieve the pressure build up, the possibility of a supersonic detonation would exist, leading to destructive over-pressures in the dry bay.

Supersonic combustion is distinct from the flames simulated in a spray burner. As a result, the effectiveness of an agent in preventing a detonation depends upon different chemical and physical mechanisms. A shock wave precedes the supersonic reaction zone. Obstructions in the flow promote intense mixing of the fresh reactants with the combustion products and cause the pressure waves to interact with the mixing region. Given enough distance, the flame can accelerate dramatically, increasing the temperature of the reaction zone behind the shock and further adding to the heat release rate. Depending upon the geometric details, the detonation wave can approach its theoretical Chapman-Jouguet velocity and accompanying high pressure ratio.

Deflagration/detonation Tube Experimental Facility. The effectiveness of a fire fighting agent in suppressing high speed, premixed combustion or a quasi-detonation can be rated by the extent to which it decelerates the propagating wave and simultaneously attenuates the hazardous shock which always precedes the combustion process. The traditional experiment in which the flame inhibitor is premixed with the fuel and air prior to ignition does not replicate the chemistry critical to the actual situation since in a dry bay the suppressing compound is injected after the combustion process has been initiated.

The two-section, deflagration/detonation tube shown in Figure 4 was designed to produce the desired environment for both the flame initiation and flame suppression regimes. The complexities and biases associated with the fluid dynamics of agent release were avoided by premixing the agent with the fuel and air in a portion of the tube distinct from where the flame is initiated. A repeatable, uninhibited turbulent flame was fully established in the driver section, the design of which was based directly upon the work of Peraldi et al., (6). In this study it was found that a 50 mm inner diameter tube with a blockage ratio of 0.43 could be used to create repeatable, high-speed flames and quasi-detonations within the first several meters of an 18 m tube. By varying the equivalence ratio of ethene/air mixtures from 0.5 to 2.1, they were able to produce flame velocities between about 600 and 1300 m/s.

The driver section used in the current project (labeled "FG" in Figure 4) was 5 m long and was equipped at the closed end with a spark plug ("IS"). This section was

filled with the combustible mixture of ethene and air. The gas handling system consisted of a vacuum pumping network ("VP" in figure); pressurized gas cylinders for the fuel ("F"), oxidizer ("O") and agent ("A"); and a dual circulating pump ("CP"). The ignition energy was delivered in a microexplosion of a tin droplet that short-circuited the tips of nichrome electrodes connected to an 80 V power supply. Spiral-shaped obstructions made of 6.4 mm stainless steel rods with a pitch equal to the inner diameter of the tube were inserted to produce an area blockage ratio of 44%. This ratio is similar to the value shown by Lee et al. (7) to promote a quasi-detonation in their facility.

The second section of the deflagration/detonation tube ("FS" in Figure 4) contained the gaseous agent along with the same fuel/air mixture used in the driver section. The diameter was the same and its length was 2.5 m. An identical spiral insert was used to maintain a high level of mixing. The two sections were separated from each other by a 50 mm inner diameter, stainless steel, high vacuum gate valve ("V"), which remained closed until just before ignition. Pressure transducers ("PT") and photodiodes ("PH") were located along the test section to monitor the strength and speed of the combustion wave. Their output was recorded on a multi-channel, digital storage oscilloscope.

Operating Procedure and Characterization. The deflagration/detonation tube was evacuated to 0.1 Pa before filling the driver and test sections separately with the desired mixtures. The fuel/air ratio and total pressure were held constant across the gate valve. The initial temperature was the ambient value. The oxidizer used in all experiments was breathing grade air. Ethene (99.5% volume purity) was chosen as the fuel because it had been demonstrated (7) that subsonic flames, quasi-detonations, and full detonations all could be obtained in a tube of this geometry simply by varying the stoichiometry.

About ten seconds prior to ignition, the gate valve was opened manually. After ignition, the flame propagated into the driver section and accelerated quickly. The flame/shock system, shown schematically in Figure 5, encountered the same combustible mixture plus agent as it passed through the gate valve and into the test section. Depending on the concentration of the agent, the flame was or was not extinguished and the pressure wave attenuated.

Mach number and pressure ratio were the two dependent parameters which were measured as a means to characterize the extent of flame suppression. The Mach number was based upon the time it took for the pressure wave to travel the distance between the two pressure transducers, normalized by the sonic velocity of the reactant gases in the test section. The pressure ratio was determined from the average amplitude of the first pressure pulse to be recorded by each transducer, normalized by the initial pressure. Consecutive pressure jumps occurred, indicating that localized explosions were present in the mixing region between the spirals. Individual runs were concluded before the shock wave reflected from the end plate and arrived back at the pressure transducers. The distance between the leading shock wave and the flame front was measured in some of the experiments from the time lag between the photodiode and pressure transducer response at the same location. The primary independent variables were agent type and concentration.

Characterization experiments were conducted with 100% nitrogen in the test

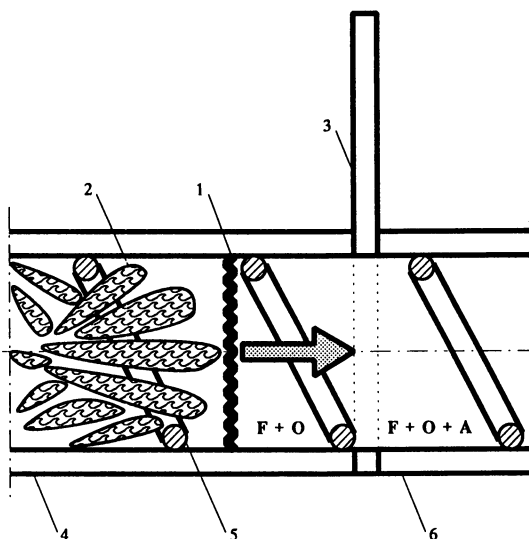
section, a 5% ethene-in-air mixture in the driver section (fuel/air equivalence ratio equal to 0.75), and the total pressure equal to 100 kPa. The incident shock wave velocity measured 2.2 m beyond the gate valve and 0.3 m from the end of the tube was 420 ± 8 m/s. The pressure ratio based upon the initial pressure rise was 2.5 ± 0.5 , and about 3.0 ± 1.0 based upon the peak increase. No significant changes in shock speed occurred for a partial pressure fraction (which is approximately equal to the mole fraction) of nitrogen in air greater than 40%. When no suppressing nitrogen was added to the test section the shock velocity attained a value of 1170 m/s. The pressure ratio based upon the initial rise, P_1/P_0 , increased dramatically at the same point as the velocity when the partial pressure of nitrogen was decreased, reaching a maximum of 18 when no nitrogen was added to the ethene/air mixture. The peak pressure ratio, which normally did not correspond to the initial pressure pulse, was around 30:1. The shock velocities and pressure ratios are presented in Figures 6 and 7 as a function of the partial pressure fraction of added N_2 in the test section for 100 kPa and two lower initial pressure conditions.

Stoichiometric and rich (equivalence ratio equal to 1.25) mixtures were ignited to determine the combustion wave parameters with no nitrogen added to the test section. The shock Mach number increased to 4.1 for stoichiometric and 4.5 for rich mixtures, and the corresponding pressure ratios were 26:1 and 35:1. With 100% N_2 in the test section the Mach number dropped to 1.3 and the pressure ratio to 3.5 when the mixture was stoichiometric.

The results of the preliminary parameter assessment led to an experimental protocol with wave speeds that were reproducible from run-to-run (to within about $\pm 2\%$). Pressures downstream of the shock wave had a higher variability ($\pm 20\%$) because of the complex shock structures created by interactions with the spiral rod inserts. More details can be found in (2, Section 4) and in the paper by Gmurczyk et al. (8).

Results and Analysis. Experiments using halon 1301 were studied and compared to an inerting agent like N_2 . Halon 1301 suppressed the flame at a partial pressure fraction of 10% to the same extent as if the test section had been completely filled with nitrogen. An unusual behavior occurred in the 100 kPa experiments when the concentration was between 2% and 3%. Both the Mach number and pressure ratio increased with the amount of CF_3Br , followed by the expected decrease for large concentrations. This reversal, while small, was greater than the uncertainty in the data.

Lean Mixtures. Attenuation of the shock speed and pressure increase by the agents was measured with the ethene/air equivalence ratio fixed at 0.75 (5.0% by volume C_2H_4), an initial absolute pressure of 100 kPa, and an initial temperature of 22 °C. It was found that the amplitude and speed of the pressure wave, and the speed of the trailing flame, were all strongly dependent on the agent type and concentration. The flame always followed the shock wave in such a way that both speeds were equal. However, when the amount of the agent in the mixture was increased, the distance between the shock and flame increased as well, up to around 100 mm as full suppression was approached. At the extinguishing concentration the radiation disappeared, which indicated the absence of the flame. In that situation the pressure wave amplitude was attenuated by a factor of eight and the wave speed by a factor of three, similar to the results for nitrogen.



1 - SHOCK WAVE, 2 - TURBULENT FLAME, 3 - GATE VALVE,
4 - DRIVER SECTION, 5 - SPIRAL INSERT, 6 - TEST SECTION,
F - FUEL, O - OXIDIZER, A - AGENT

Figure 5. Rendering of high speed turbulent flame entering test section.

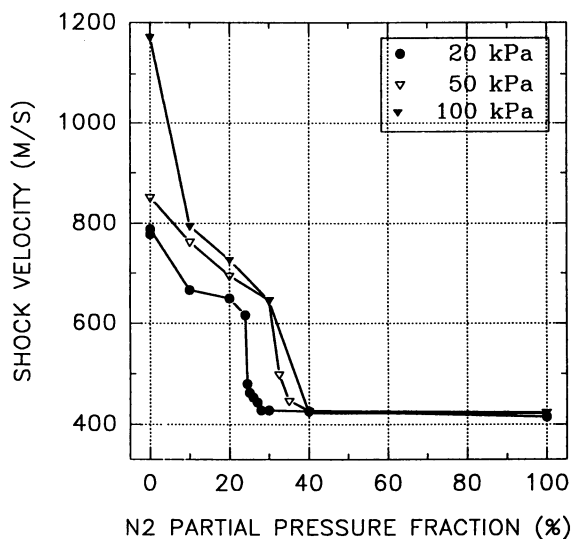


Figure 6. Effect of added nitrogen partial pressure and initial total pressure on the shock velocity in the deflagration/detonation tube.

The results for the FCs, HFCs and the HCFCs are compared in Figures 8 through 10. The pressure ratios at zero mass fraction represent the pure combustible mixture with no flame suppressing agent present. One can see that the agent mass fractions necessary for total extinguishment range from around 30% for the FCs to almost 50% for CHF_2Cl . At low concentrations the pressure ratios are higher for some agents than even the value for the pure combustible mixture. The FCs, as a class, were generally the best performers on both a partial pressure and mass fraction basis. In fact, FC-116 was superior to CF_3Br , and FC-318 was about equivalent. FC-218 and FC-31-10 slightly enhanced the pressure ratio in low concentration. This can be seen in Figure 8. FC-218 reduced the pressure ratio to less than 5:1 at a mass fraction of 0.29, which was better than with CF_3Br .

Adding hydrogen to the molecule had a significant effect on the performance of the HFCs, shown in Figure 9. The $\text{CH}_2\text{F}_2/\text{C}_2\text{HF}_5$ mixture produced peak pressures more than double the value for no suppressant. The Mach number was increased to its highest value of 4.1 when the mass fraction was 11%. It was not until the mass fraction exceeded 38% that the HFC-32/125 mixture became as effective as nitrogen in reducing the speed and pressure build-up of the shock wave. The two fluoropropanes, HFC-227ea and HFC-236fa produced the lowest pressure build-up of the HFCs and effectively reduced the shock speed.

The chlorine atom in the two HCFCs created an additional complexity because chlorine is a strong oxidizer. From Figure 10, one can see that HCFC-22 was the least effective on a mass basis of all of the agents in fully suppressing the combustion wave pressure ratio, requiring a mass fraction of over 50% in the test section. The maximum pressure ratio for HCFC-124 was 32:1 at a 23% mass fraction, which was exceeded only by HFC-125 and the HFC-32/125 mixture.

The one iodofluorocarbon tested was CF_3I . The Mach number and pressure build-up, shown in Figure 11, were reduced by about one half with partial pressure fractions in the test section of only 15 to 20%. None of the other chemicals, including CF_3Br , was able to accomplish this. Unfortunately, when the mass fraction was increased to 30%, the Mach number shot back up and the pressure ratio attained a value of 21:1, which was greater than when no CF_3I was present. This reversal, which was slight in the bromine-containing halon 1301, changed what at first appeared to be the most effective suppressing agent into one of the least effective agents. It is known that iodine atoms can cause a catalytic effect in some reactions by lowering the overall activation energy. At intermediate concentrations the possibility also exists that the iodine (and bromine) recombine, reducing their impact on the combustion process.

Stoichiometric Mixtures. To see if the relative performance of the agents was dependent upon the fuel/air ratio, a number of experiments were carried out under stoichiometric conditions. The equivalence ratio was based upon the amount of ethene in the mixture and was not adjusted to account for the contribution of the agent to the fuel or oxidizer pool. The initial pressure and temperature remained the same for the stoichiometric experiments: 100 kPa and 22 °C.

The Mach number and pressure ratio increased as the fuel/air mixture was changed from lean to stoichiometric. However, the relative behavior was not significantly altered for the FCs nor the CF_3I . That is, the pressure ratio vs. mass fraction curves were shifted upward about uniformly.

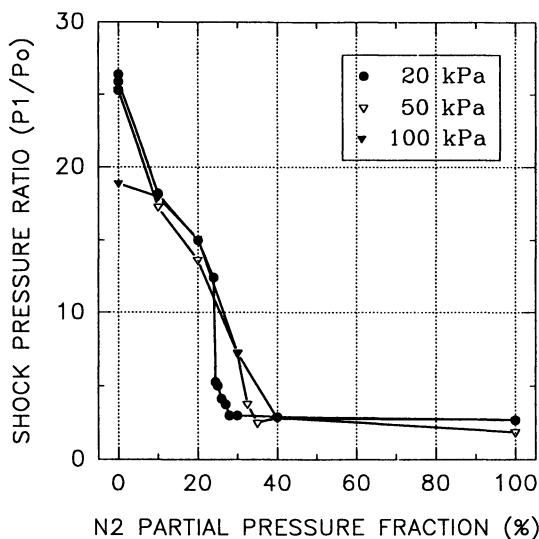


Figure 7. Effect of added nitrogen partial pressure and initial total pressure on the initial shock pressure ratio in the deflagration/detonation tube.

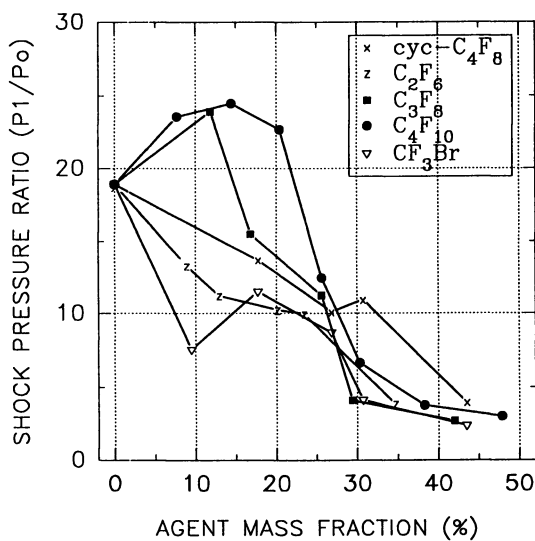


Figure 8. Reduction in pressure ratio as a function of FC mass fraction, compared to CF₃Br.

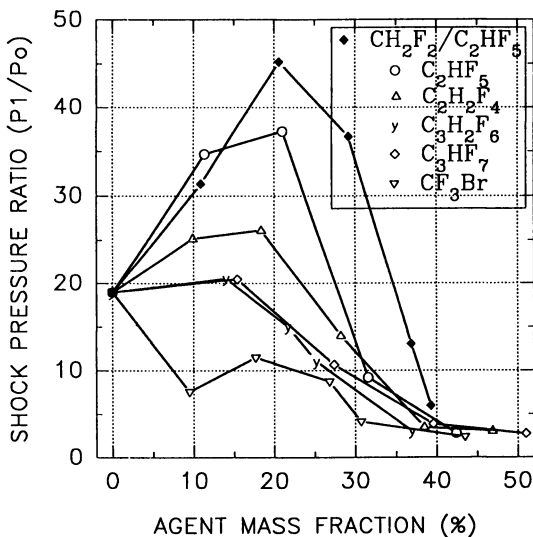


Figure 9. Reduction in pressure ratio as a function of HFC mass fraction, compared to CF_3Br .

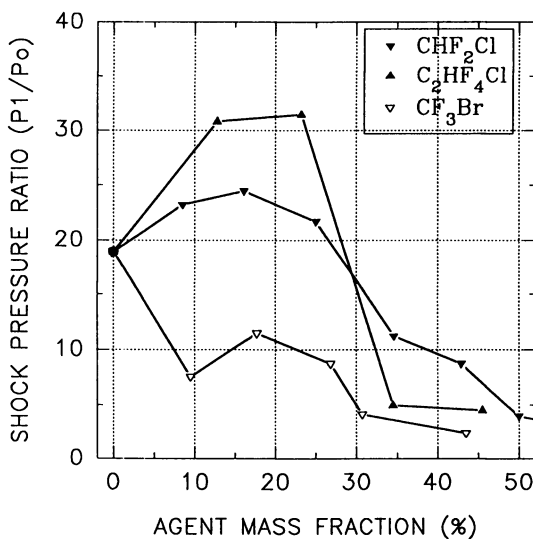


Figure 10. Reduction in pressure ratio as a function of HCFC mass fraction, compared to CF_3Br .

Downloaded by STANFORD UNIV GREEN LIBR on October 6, 2012 | http://pubs.acs.org
 Publication Date: May 5, 1997 | doi: 10.1021/bk-1995-0611.ch018

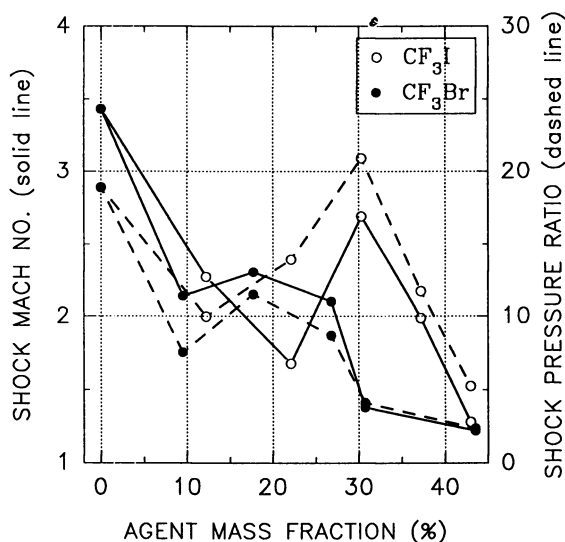


Figure 11. Reduction in shock wave Mach number and pressure ratio as a function of CF_3I mass fraction, compared to CF_3Br .

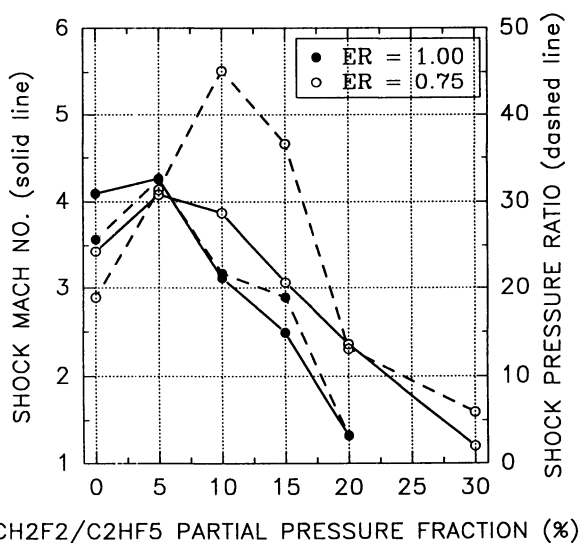


Figure 12. Effect of equivalence ratio on the reduction in shock Mach number and pressure ratio for HFC-32/125 mixture.

A distinctly different behavior occurred with the HFC-32/125 mixture, shown in Figure 12. The hydrogen atoms attached to the agent molecules had less of an enhancing effect under stoichiometric conditions ($ER = 1.0$). The over-pressure was greatly reduced when the equivalence ratio was increased, leading to a cross-over condition where both the Mach number and pressure ratio were reduced for the stoichiometric condition.

Ranking the Agents. The results that were gathered indicated the complexity of the suppression process in the deflagration/detonation tube. Because one does not know *a priori* the conditions in an actual dry bay fire zone, and because different initial conditions (i.e., pressure, temperature and fuel/air ratio) affect the amount of agent required for suppression to varying degrees, the following specific set of initial conditions was chosen at which all the agents were compared: 100 kPa, 22 °C, and 0.75 ethene/air equivalence ratio. The reduction in pressure ratio rather than the Mach number was chosen as the measure of suppression because of the direct impact of pressure on the structural integrity of the dry bay. The amount of halon 1301 required to reduce the pressure (i) to 10% and (ii) to one-half the maximum increase were used to normalize the results.

Figure 13 displays three different performance parameters calculated under these conditions: the volume factor (VF), the flame suppression number (FSN-mass) based upon the mass fraction, and the flame suppression number based upon the relative partial pressures (FSN-pp). While there were some reversals depending upon the basis of evaluation (i.e., 90% reduction FSN, 50% reduction FSN, or VF), Figure 13 (based upon 50% reduction) is representative of the relative behavior. FC-218 was clearly the best performer under the conditions tested, and the HFC-32/125 mixture and HCFC-22 were the worst. The FSN of FC-116 based upon a 50% reduction in pressure build-up was the lowest of all agents, even performing better than halon 1301. However, because hexafluoroethane does not condense at room temperature, its density is low, leading to a volume factor which is less desirable. On a mass basis nitrogen (not shown in figure) performed almost as well as halon 1301. It is also a gas at room temperature, though, and had a huge VF of 32. The CF_3I performed relatively well on a volume basis because of its high liquid density, but less well based upon the mass required.

Conclusions from the Deflagration/Detonation Study. It is necessary to emphasize that the experimental conditions in the deflagration/detonation tube differed significantly from those used in the turbulent spray flame burner. The main qualitative difference was the occurrence of a strong shock wave ahead of the flame. That wave influenced the gas dynamic, thermodynamic and chemical state of the pure combustible mixture in the driver section and the mixture containing an agent in the test section. Another feature was a high level of turbulence within the flame due to its high speed and the interactions with the spiral obstruction. The quantitative difference was a supersonic regime (relative to the undisturbed mixture) of flame/shock propagation and strong pressure changes (due to confinement and shock) during the process. Thus, the oxidizer, fuel and agent molecules were preconditioned prior to entering the flame zone.

It is concluded that suppression of highly dynamic flames can be effectively

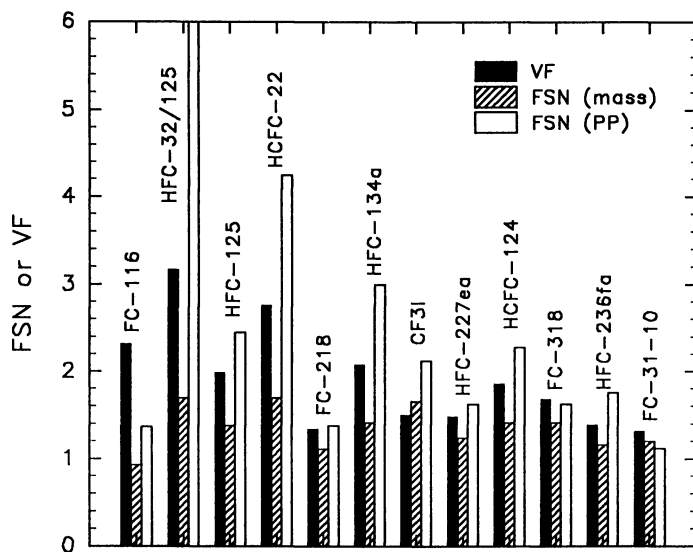


Figure 13. Flame suppression numbers and volume factors of agents examined in deflagration/detonation tube.

studied in the two-sectional tube, permitting clear discrimination of performance among various alternative extinguishing agents. The high-speed turbulent flame and the combustion zone in the quasi-detonation wave travel at the same speed as the preceding shock wave. The distance between the flame and the shock increases with the amount of an extinguishing agent. At extinguishment the flame disappears while a residual shock remains. The suppression process of the lean ethene/air mixture is pressure dependent both for chemically inert nitrogen and chemically active halon 1301. This may be related to the fact that the oxidation mechanism of ethene is known to be pressure dependent, as well.

The analysis of the suppression data for the lean ethene/air mixture leads to the division of the alternative compounds into four general categories: perfluorocarbons, hydrofluorocarbons, hydrochlorofluorocarbons, and CF_3I . The extinguishing concentrations of the more effective agents (the FCs) are around 10% by volume and 40% by weight, while less effective ones are around 20% by volume and close to 50% by weight. The least effective agent is the HFC-32/125 mixture, giving unusually high pressure ratios. HCFC-22 requires the highest extinguishing concentration of all the alternatives. The presence of a hydrogen-containing suppressant in the combustible mixture results in a significant increase in pressure ratio relative to that of the pure combustible mixture. The phenomenon occurs also for the compounds not containing hydrogen atoms at relatively lower concentrations, but the impact is not as dramatic and is generally weaker for stoichiometric relative to lean mixtures. The agent can act as an extra fuel, shifting the mixture to richer conditions.

The behavior of CF_3I is different from the other agents. At lower concentrations (10-20% by mass) the performance is the best of all the alternatives. However, at intermediate concentrations (20-30% by mass) the performance is diminished significantly. The phenomenon is independent of the equivalence ratio of the combustible mixture. The behavior at the intermediate concentrations may be attributed to a catalytic effect caused by the iodine atoms.

Summary Conclusions on Flame Suppression Effectiveness

The following observations summarize the results of the flame suppression study:

- The relative ranking of the agents depends upon whether one uses a mass basis or a volume basis.
- The relative ranking of the agents varies only slightly between the turbulent spray burner and cup burner studies done by Trees et al. (3), but a substantially different ranking results from the deflagration/detonation apparatus.
- The relative ranking of the agents is not affected much by the fuel type or air temperature.
- The quantity of agent required to suppress a flame increases with the type of burner generally in the following order:
deflagration tube < spray burner < cup burner.
- The quantity of agent required to suppress the turbulent spray flame increases with decreasing rate of agent injection.
- The quantity of agent required to attenuate the shock wave speed and pressure ratio in the deflagration/detonation tube varies with equivalence ratio, sometimes increasing as one goes from lean to stoichiometric and sometimes decreasing.

- Sodium bicarbonate was the most effective suppressant of the turbulent spray flame, requiring less mass than halon 1301. The smaller size particles were more effective.
- Iodotrifluoromethane was more effective than halon 1301 in suppressing the spray burner flame, and was less effective in attenuating the shock speed and pressure in the deflagration/detonation apparatus.
- The gaseous agents required between 1 1/2 and 4 times the storage volume of halon 1301 to suppress the different flames.
- HCFC-124 was the best performer of the gaseous agents (other than CF₃I) in suppressing the turbulent spray flame, and FC-218 was judged the best for attenuating the shock speed and pressure in the deflagration/detonation tube.
- FC-116 was the poorest performer (on a liquid storage volume basis) of the agents evaluated in the spray flame suppression tests; the HFC-32/125 mixture was the second poorest performer in the spray flame, and led to the highest over-pressures in the lean deflagration/detonation tube study.

Acknowledgments

The authors wish to acknowledge the U.S. Air Force, Navy, Army and Federal Aviation Administration for funding the Agent Screening for Halon 1301 Aviation Replacement project. The program was directed by Michael Bennett at the Wright Patterson AFB, Flight Dynamics Laboratory, Vehicle Subsystems Division, Survivability Enhancement Branch. The contributions of Isaura Vázquez, Darren Lowe and William Rinkinen to the spray burner experiments are also gratefully acknowledged.

Literature Cited

1. Harrington, J.L. *NFPA J.* March/April 1993, pp 38-42.
2. *Evaluation of Alternative In-flight Fire Suppressants for Full-scale Testing in Simulated Aircraft Engine Nacelles and Dry Bays*; Grosshandler, W.L.; Gann, R.G.; Pitts, W.M., Eds.; NIST SP 861; National Institute of Standards and Technology: Gaithersburg, MD, April 1994.
3. Trees, D.; Seshadri, K.; Hamins, A. In *Halon Replacements: Technology and Science*; Miziolek, A.W.; Tsang, W., Eds.; ACS Symposium Series; American Chemical Society: Washington, DC, 1995.
4. Vázquez, I.; Grosshandler, W.; Rinkinen, W.; Glover, M.; Presser, C. In *Fourth Inter. Symp. on Fire Safety Science*; Kashiwagi, T., Ed.; IAFSS, USA, 1994.
5. Grosshandler, W.L.; Presser, C.; Lowe, D.; Rinkinen, W., "Assessing Halon Alternatives for Aircraft Engine Nacelle Fire Suppression," *J. Heat Transfer*, in press, 1995.
6. Peraldi, O.; Knystautas, R.; Lee, J.H. In *Twenty-first Symposium (International) on Combustion*; The Combustion Institute: Pittsburgh, PA, 1986; pp 1629-1637.
7. Lee, J.H.; Knystautas, R.; Chan, C.K. In *Twentieth Symposium (International) on Combustion*; The Combustion Institute: Pittsburgh, PA, 1984; pp 1663-1672.
8. Gmurczyk, G.; Grosshandler, W.; Peltz, M.; Lowe, D. In *Chemical and Physical Processes in Combustion*; Eastern States Section of The Combustion Institute: Princeton, NJ, 1993; pp 487-490.

RECEIVED July 20, 1995

Chapter 19

Acid Gas Production in Inhibited Propane–Air Diffusion Flames

G. T. Linteris

Building and Fire Research Laboratory, Fire Science Division, National Institute of Standards and Technology, Gaithersburg, MD 20899–0001

The proposed replacements to halon 1301, mainly fluorinated and chlorinated hydrocarbons, are expected to be required in significantly higher concentrations than CF_3Br to extinguish fires. At these higher concentrations the by-products of the inhibited flames may include correspondingly higher portions of corrosive gases, including HF and HCl. To examine the chemical and transport-related mechanisms important in producing these acid gases, a series of inhibited flame tests are performed with several types of laboratory-scale burners, varying agent type and concentration. A wet-chemistry analysis of the final products of the flames using ion-selective electrodes for F⁻ and Cl⁻ provides an experimental basis for quantitative understanding of the HF and HCl production. Production rates are measured for co-flow laminar and jet diffusion flames. Systematic selection of the agent concentrations, burner type, and air flow rates allows an assessment of the relative importance of agent transport and chemical kinetics on the acid gas production rates. These experimental results are then compared to a model which estimates the maximum HF and HCl production rates based on stoichiometric reaction to the most stable products. The results demonstrate the relative significance of F, Cl, and H in the inhibitor and fuel, as well as the effect of different burner configurations.

Although the corrosiveness and toxicity of candidate fire suppressants have always been recognized as important, it has also been observed that since the most effective flame suppressants are not chemically inert the properties of their decomposition by-products are also important. Halogenated hydrocarbons are widely used and effective flame suppressants; however, the production of the most effective of these (for example halon 1301 CF_3Br and 1211 CF_2ClBr) has been discontinued. The proposed alternatives to these halons, primarily fluorinated and chlorinated hydrocarbons, are required in much higher concentrations. Consequently, they have the potential to have

This chapter not subject to U.S. copyright
Published 1995 American Chemical Society

correspondingly higher amounts of decomposition by-products. Since most hydrocarbon-based compounds at flame temperatures typically undergo both thermal decomposition and decomposition by radical attack, the formation of products other than the inhibitor itself is highly probable. The acid gases hydrofluoric (HF) and hydrochloric acid (HCl) are believed to be the most corrosive products. The objective of this research is to obtain an understanding of the chemical and physical processes of acid gas formation in inhibited flames.

Background

The halogen acid or hydrogen halide HX (where X represents the halogen) is a thermodynamically stable product in mixtures containing hydrogen and halogen atoms. Formation of acid gases in inhibited hydrocarbon flames has been studied for many years. The research can be categorized as either global measurements of HF produced in suppressed fires, or detailed flame structure measurements. Burdon *et al.* [1] ignited mixtures of fuel, air, and CH_3Br in flasks, analyzed the products and found copious amounts of HBr. Numerous premixed low pressure flame studies [2-5] used mass spectroscopy to measure the profiles of hydrogen halides and other products in hydrogen, carbon monoxide, and hydrocarbon flames inhibited by CH_3Br , CF_3Br , and CF_3H . These studies indicated conversion efficiencies of the halogens in the inhibitor into halogen acids on the order of unity. Acid gas formation in hydrocarbon-air pool fires suppressed by CF_3Br has been studied by Sheinson *et al.* [6-7]. These studies, in test volumes of 1.7 and 650 m^3 , stressed the difficulties in probe sampling for acid gases. The latter study described an in situ IR absorption method for measuring HBr and HF. To overcome these limitations and also provide time-resolved acid gas concentration data, Smith *et al.* [8] developed a new HX sampling technique and obtained HX and inhibitor concentrations as functions of time for discharge of CF_3Br into a 56 m^3 space. In a series of experiments with a variety of fuels and halogenated inhibitors, Yamashika [9] showed that the extinction time for a compartment fire sprayed with inhibitor is dependent upon the discharge rate and room volume. He then showed [10] that the amounts of hydrogen halides and carbonyl halides are also dependent upon the discharge rate. Using a simple model of acid gas formation based on the steady-state rates, he developed a model of transient acid gas formation to explain his results.

In more recent studies [11,12], CF_3Br , C_3HF_7 , and C_4F_{10} were injected into an enclosure fire and measured the HF produced using ion-selective electrodes. Di Nenno *et al.* [13] introduced halon alternatives into compartment fires and measured the HF, HCl, and COF_2 produced using Fourier transform infrared spectroscopy. These studies again confirmed the importance of injection rate and fuel consumption rate on the amount of acid gas produced. Filipczak [14] introduced CF_2ClBr and CF_3Br into a methane flame and measured the O_2 , CO_2 , H_2O , HF, HCl, HBr, and unreacted inhibitor using a mass spectrometer. Hoke and Herud [15] are currently developing a fast-response ion-selective electrode for measuring HF and HCl produced in extinguished fires in crew compartments of combat vehicles.

Previous research related to understanding acid gas formation in inhibited flames can be seen to include both detailed flame structure measurements and global measurements of HF produced in suppressed fires. The former provide the basis for obtaining a good understanding of the underlying chemical kinetics of the formation of acid gases. The global measurements provide important information on the magnitude of the acid gases produced and allow a comparison of the relative amount of acid gases formed by new halon alternatives. There remains a need to develop a fundamental basis for interpreting the data on acid gas formation in fires suppressed by halon alternatives and to understand the chemical kinetic rates of acid gas formation in diffusion flames inhibited by these alternative agents. In particular, there exists a need to understand the relationship between fuel and inhibitor type, flame characteristics, agent transport rates, and the concentrations of by-products formed.

Experimental Approach

The formation of toxic and corrosive by-products in flames suppressed by halogenated hydrocarbons may be determined by transport rates of the inhibitor into the flame, chemical kinetic rates, and equilibrium thermodynamics. These phenomena in turn will be affected by the fuel type, local stoichiometry, inhibitor type and concentration, and the characteristics of the flow field (mixing rates, strain, and stabilization mechanisms). The approach in this research is to study the influence of key parameters (inhibitor type and concentration and flame type) through systematic experiments on laboratory-scale flames. Inhibitor is added at steady-state to the fuel or air stream of co-flow diffusion flames. The diffusion flames are operated under both laminar and near-turbulent conditions to vary the mixing rates. The apparatus used to obtain these data, the results, and their interpretation are presented below.

The experiments are performed with a propane-air co-flow diffusion flame. Two burner types are used. The first is modelled after the cup burner described by Booth [16] and Bajpai [17]. The experimental arrangement is shown in Figure 1. The burner consists of a 28 mm diameter pyrex cup positioned concentrically in a 120 mm diameter 450 mm tall chimney 150 mm from the base. In these experiments with propane, the cup burner was modified for use with a gaseous fuel (liquid fuels will be tested in future experiments). The cup is filled with 1 mm diameter glass beads and covered with a stainless steel screen. The second burner consists of a 25 cm long pyrex tube with a 0.50 mm diameter opening positioned concentrically and at the same height as the cup burner, with the same chimney. The cold flow Reynolds number based on the exit velocity of the propane in the tube is 1050. This second burner, referred to here as the jet burner, is designed to provide better mixing of the inhibitor in the air stream with the fuel. Although a higher jet Reynolds number would have been desirable to achieve turbulent mixing, the flame is very close to blow-off at flows with a Reynolds number of 2000, and very little inhibitor can be added before blow-off occurs. Consequently, at these flows, it is difficult to study the effects of air stream inhibitor concentration on HF formation.

The air used is shop compressed air (filtered and dried) which is additionally passed through an 0.01 μm filter to remove aerosols and particulates, a carbon filter to remove organic vapors, and a desiccant bed to remove water vapor. The fuel gas

is propane (Matheson¹, CP) at flow rate of 0.114 l/min at 21 °C. Gas flows are measured with rotameters (Matheson 1050 series) which are calibrated with bubble and dry (American Meter Co. DTM-200A, DTM-325) flow meters. Inhibitor gases are of different purities from various suppliers. The twelve agents tested are CHClF_2 , CF_3Br , C_2HF_5 , C_2F_6 , $\text{C}_2\text{H}_2\text{F}_4$, C_2HClF_4 , C_3F_8 , C_3HF_7 , $\text{C}_3\text{H}_2\text{F}_6$, C_4F_{10} , and $\text{CH}_2\text{F}_2/\text{C}_2\text{H}_2\text{F}_4$.

Before measuring HF in the product gases, the concentration of inhibitor in the air stream necessary to extinguish the flame is determined. The inhibitor is then added to the co-flowing air stream at a concentration of either 50 or 90% of the extinguishing concentration, and the product gases are sampled for acid gas. In one series of experiments with the cup burner, the inhibitor is added to the gaseous propane stream at 70% of the concentration which would extinguish the flame.

A wet chemistry technique is used to measure the HF and HCl concentrations in the exhaust gases from the co-flow diffusion flames. A glass funnel is placed over the chimney and the exhaust gases pass through the 4.0 cm diameter neck. A quartz probe, centered in the neck, extracts a measured fraction of the product gases (approximately 0.5%), and directs the gases through polyethylene sample lines to polyethylene impingers filled with water which trap the acid gases. The sample flow is continued for a total collection time of sixty seconds. The quartz probe and sample lines are washed with water which is returned to the impinger. The sample is tested for F^- and Cl^- using ion-selective electrodes (Orion models 96-09 and 96-17B). To reduce the effects of sampling losses as have been reported by other investigators, a quartz probe and polyethylene sample lines are used, the distance from the chimney top to the bubbler is kept small (~ 10 cm) and the sample lines are washed with the bubbler fluid immediately after the sample is collected. It should be noted that since COF_2 is known to hydrolyze rapidly in the presence of water, this technique for acid gas measurement includes F from both HF and COF_2 . When HF formation is described in this paper, it actually refers to an equivalent amount of fluoride ion collected in the bubbler.

Model for Acid Gas Formation

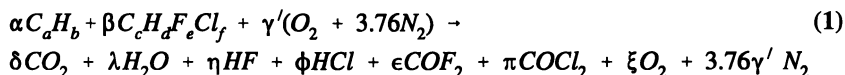
A model for the amount of acid gas formed in an inhibited diffusion flame can be developed in a manner analogous to the determination of the local equivalence ratio and structure for diffusion flames. In the classic Burke-Schumann analysis [18], the chemical reaction is assumed to occur at a sheet. This location serves as a sink for the fuel and oxidizer which are assumed to diffuse there in stoichiometric proportions based on complete reaction to the most stable products (i.e., HF formation is assumed to be controlled by equilibrium thermodynamics rather than chemical kinetics). This model will be referred to as the stoichiometric model.

¹ Certain commercial equipment, instruments, or materials are identified in this paper in order to adequately specify the experimental procedure. Such identification does not imply recommendation or endorsement by the National Institute of Standards and Technology, nor does it imply that the materials or equipment are necessarily the best available for the intended use.

In the case of a flame inhibited by halogenated hydrocarbons, a thermodynamic analysis shows that in equilibrium, the inhibitor breaks down to CO_2 , HX , and H_2O ($X = \text{halogen}$). Consequently, the inhibitor is assumed to be consumed like a fuel and form the most stable products. The assumptions used in the stoichiometric model are:

1. there is complete reaction of the inhibitor molecule with fuel and air to form the most stable products;
2. the inhibitor in the air stream which by-passes the flame sheet does not decompose through interaction with the post-combustion product gases;
3. there is no loss of acid gases to the chimney walls; and
4. the product gases are perfectly mixed.

An equation for the reaction of an arbitrary hydrocarbon with air and arbitrary halogenated hydrocarbon inhibitor is:



In this equation α is specified as is β when inhibitor is present only in the fuel stream. For inhibitor present in the air stream, β is determined by the concentration of inhibitor in the air stream and the ratio of the diffusion rates for oxygen and inhibitor.

$$\beta = \frac{\alpha(a+b/4)}{1/(\rho r) - [c + 1/4(d-e-f)]} \quad (2)$$

Where ρ is the ratio of the binary diffusion coefficient of the inhibitor in nitrogen to that of oxygen with nitrogen and r is the ratio of the concentration of inhibitor to oxygen in the air stream. An atom balance for all species provides all of the unknown coefficients, and an estimate of amount of acid gas formed per mole of fuel, $(\eta + \phi)/\alpha$, is then readily found.

The assumption that the ratio of the diffusion rates for oxygen and inhibitor controls the amount of HF that forms basically implies that the characteristic flame height over which oxygen and inhibitor react is the same (as related to assumption 2 above).

Results and Discussion

The acid gases produced are measured at inhibitor concentrations of 50 and 90% of the concentration of inhibitor found to extinguish the flame when the inhibitor is added to the co-flowing air stream in the cup burner and jet burner, and at 70% of the extinction concentration for inhibitor added to the propane fuel stream for the cup burner. Table I lists the extinction concentrations for each agent for inhibitor added

Table I. Extinction conditions for halon alternatives added to the air or fuel of co-flow propane-air cup burner and jet burner flames, and HF produced and H/X ratio with agent addition to the fuel stream.

Inhibitor	Agent Addition to Air		Agent Addition to Fuel		
	Extinction Concentration in Air (mole percent)		Inhibitor/Fuel ratio in Fuel Stream at Ext.	H/X Ratio in Flame (70% Ext.)	Fluorine Mole Fraction Collected
	jet	cup	cup	cup	cup
C_2F_6	3.8	9.4	2.5	0.76	0.43
C_3F_8	3.8	7.5	2.0	0.70	0.55
C_4F_{10}	3.2	5.0	1.6	0.70	0.38
C_4F_8	5.1	7.6	2.2	0.65	0.38
C_2HF_5	6.2	10.2	3.1	0.94	0.30
C_3HF_7	4.2	7.6	2.2	0.87	0.45
$C_2H_2F_4$	9.5	11.1	5.6	1.01	0.44
C_2HClF_4	4.2	8.6	2.6	1.33	0.42
$C_3H_2F_6$	4.0	7.2	3.5	0.88	0.30
CH_2F_2/C_2HF_5	15.5	15.2	11.8	1.03	0.37
CF_3Br	0.8	4.3	0.88	4.4	0.35
$CHClF_2$	6.7	13.8	4.3	1.82	0.55

to the air stream of both burners, and for inhibitor added to the fuel stream of the cup burner. As the table indicates, the jet burner flame typically requires about 50% less inhibitor in the air stream to extinguish the flame than the cup burner, even for identical fuel and air flows, although there are notable exceptions: CF_3Br , which requires about one fifth as much inhibitor in the jet burner than in the cup burner, and $C_2H_2F_4$ and the $CH_2F_2/C_2H_2F_4$ mixture which had nearly the same extinction concentrations. In addition to providing the necessary extinction conditions for specification of inhibitor flows at 50 and 90% of extinction, these results also demonstrate the sensitivity of the extinction conditions to the burner geometry.

The measured HF for these diffusion flames is shown in Figures 2 and 3. These figures present the HF produced (moles/min) for each inhibitor for the five burner/inhibitor combinations. The total flow is about 1 mole/min. For each inhibitor, the measured HF is plotted for the cup burner and for the turbulent jet burner with inhibitor present in the air stream at 50 and 90% the extinction value, and for inhibitor added to the fuel stream in the cup burner at 70% of the value necessary to cause extinction. The figure indicates that the amount of HF varies, for a given agent, by

a factor of about five for these two flames. For a given flame and fraction of extinction concentration of agent, the amount of HF formed varies by about ten for these twelve agents. Note that the fuel and air flow rates are held constant in these data. Chloride ion is also measured in these experiments and the results are qualitatively the same as for fluoride. For clarity of presentation, however, only the HF results are presented.

The results of the agent addition to the fuel stream are also presented in Table I. The halogen to hydrogen ratio of the inlet reactants in the fuel stream at the agent loading of the tests (70% of extinction) is listed, as is the fraction of the fluorine converted by the flame to a species which hydrolyses in the bubbler. While conversion is only 30 to 55%, there is no clear dependence on halogen to hydrogen ratio in either the parent inhibitor molecule or the reactant stream.

In order to provide insight into the controlling parameters in inhibited diffusion flames, the data of Figures 2 and 3 are presented in an alternative form in Figures 4 to 15. In these figures, the amount of HF produced is plotted as a function of the inhibitor concentration in air. The symbols represent the experimental data, while the lines marked F and H represent estimates of the fluxes of fluorine and hydrogen into the reaction zone based on the stoichiometric model described above.

Figure 4 shows the measured and estimated HF production rates in a propane-air diffusion flame for C_2F_6 in the cup and jet burners. The curve labeled F in Figure 4 is the maximum fluoride atom molar flux into the reaction sheet of the diffusion flame calculated using the stoichiometric model described above. The curve labeled F' in Figure 4 is the fluoride molar flux when the diffusion rate of the inhibitor relative to oxygen is modified to account for preferential diffusion of oxygen relative to the inhibitor using the molecular weight correction factor

$$\sqrt{W_i + W_{N_2} / W_{N_2} W_i} / \sqrt{W_{O_2} + W_{N_2} / W_{O_2} W_{N_2}} .$$

In this equation, W_{N_2} , W_{O_2} , and W_i are the molecular weights of nitrogen, oxygen, and inhibitor. The predicted fluorine and hydrogen fluxes are based on actual experimental flows which vary slightly from run to run. The slight variations in flows cause the slight discontinuities in the F and H curves as in Figure 5.

Qualitatively, the curves F and F' are seen to increase with increasing inhibitor concentration in air, and the molar flux of inhibitor into the reaction zone is lower when a lower rate of diffusion is used for the inhibitor. The curves labeled H and H' (coincident for C_2F_6) show the estimated hydrogen atom flux into the reaction zone as a function of inhibitor concentration in the air stream. Since this inhibitor does not contain hydrogen, all of the hydrogen is from the propane, and increasing inhibitor in the air stream does not increase the hydrogen flux into the flame. One would expect that the HF production rate would not be greater than the estimated flux of F or H into the reaction zone. For this inhibitor, the flame appears to be hydrogen limited above about 5% C_2F_6 in the air stream; however, when there is not enough hydrogen, the most stable product is COF_2 , which is known to rapidly hydrolyze in the presence of water, and would also appear as F' in the bubbler. Consequently, the hydrogen limit may or may not exist (depending upon whether the kinetics are fast enough to form COF_2 in the hydrogen-limited case).

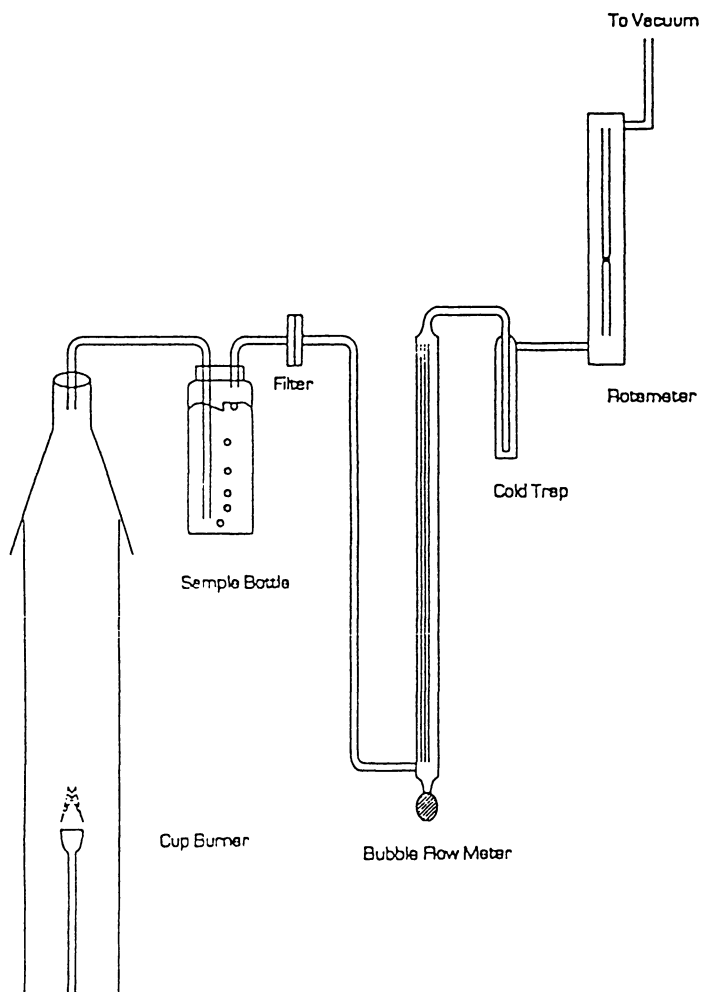


Figure 1 - Experimental apparatus for co-flow diffusion flame studies of acid gas formation in inhibited propane-air flames.

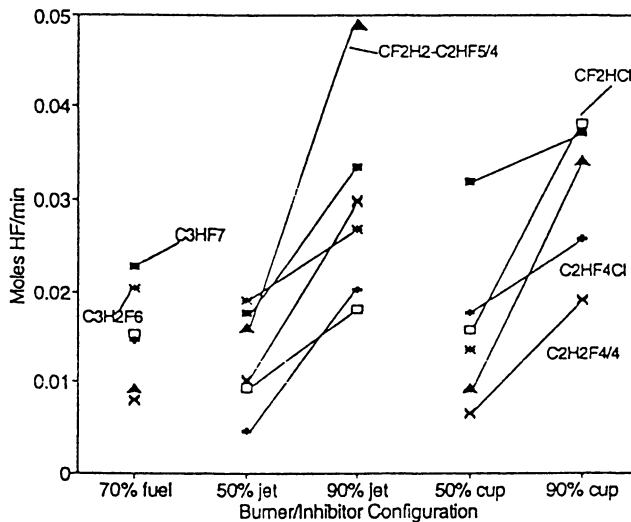


Figure 2 - Measured HF production rates in co-flow propane-air diffusion flames. Data are shown for cup and jet burners at 50 and 90% of the extinction concentration for agent added to the air stream, and at 70% in the fuel stream in the cup burner.

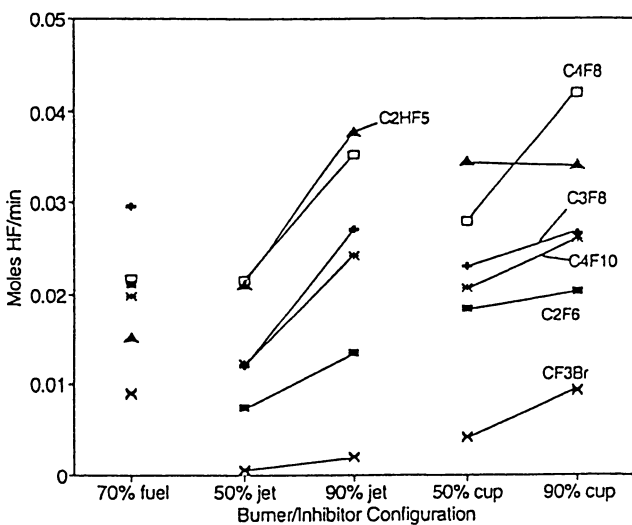


Figure 3 - Measured HF production rates as in Figure 2. Note that the curves for CF_2H_2 - C_2HF_5 and $\text{C}_2\text{H}_2\text{F}_4$ are reduced by a factor of 4.

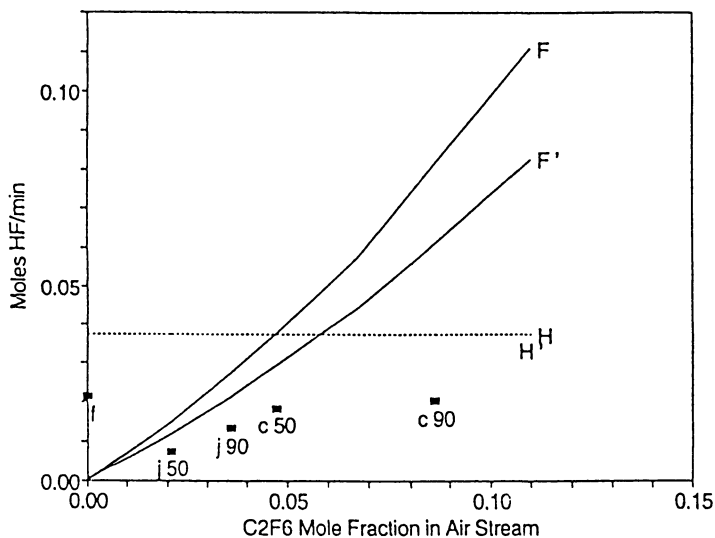


Figure 4 - Moles of HF produced as a function of the C_2F_6 concentration in the air stream for the cup (c) and jet (j) burners at 50 and 90% of extinction, and with inhibitor addition to the fuel stream (f) of the cup burner at 70% of extinction. The squares are the experimental data. The lines show the estimated fluorine (F) and hydrogen (H) flux into the reaction zone using the stoichiometric model, based on equal rates of diffusion for O_2 and inhibitor (un-primed) and with binary diffusion coefficients corrected for molecular weight variations (primed). The estimated error bars on the HF measurements are $\pm 10\%$.

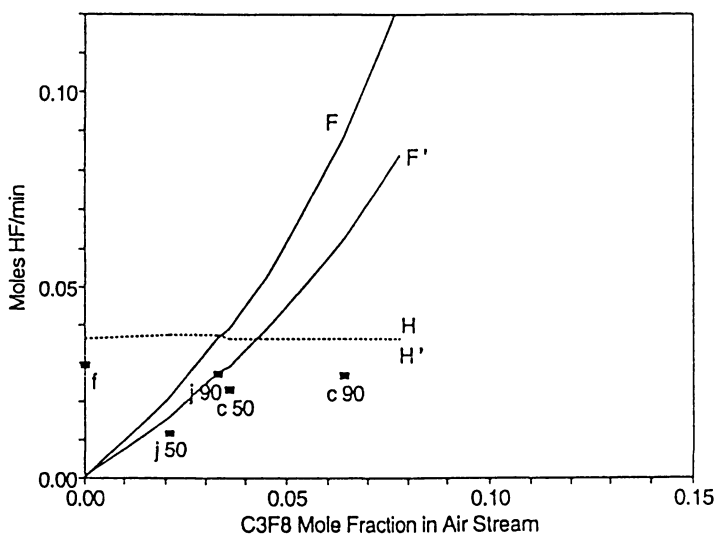


Figure 5 - Moles of HF produced as a function of C_3F_8 concentration as in Figure 4.

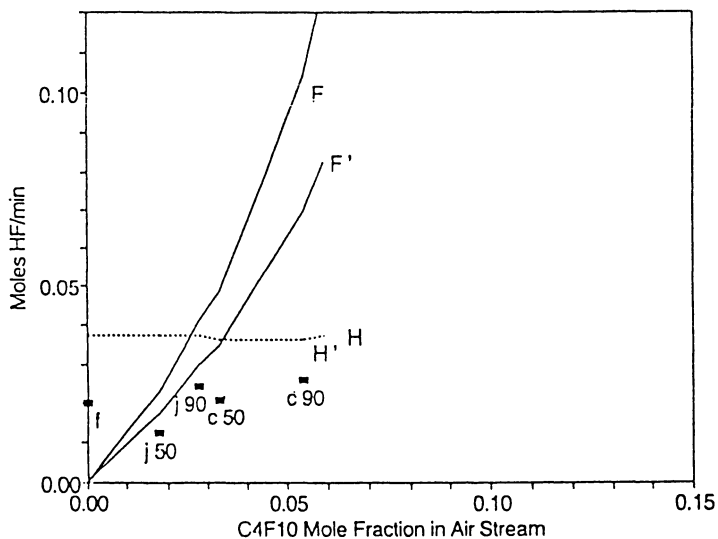


Figure 6 - Moles of HF produced as a function of C_4F_{10} concentration as in Figure 4.

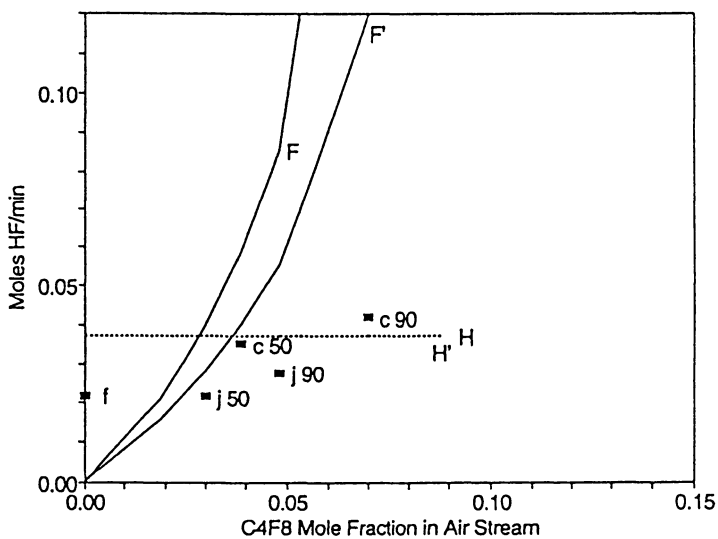


Figure 7 - Moles of HF produced as a function of C_4F_8 concentration as in Figure 4.

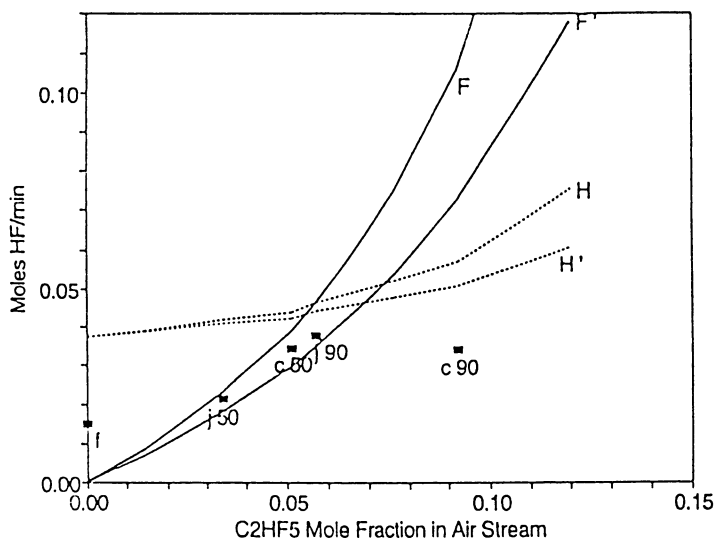


Figure 8 - Moles of HF produced as a function of C_2HF_5 concentration as in Figure 4.

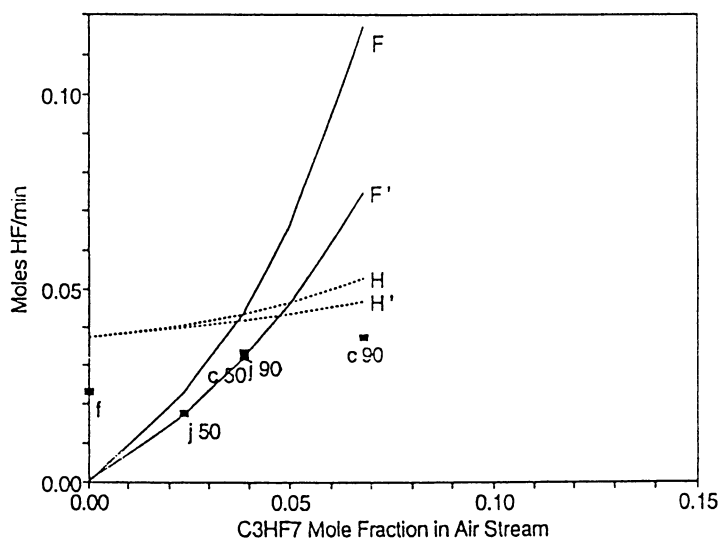


Figure 9 - Moles of HF produced as a function of C_3HF_7 concentration as in Figure 4.

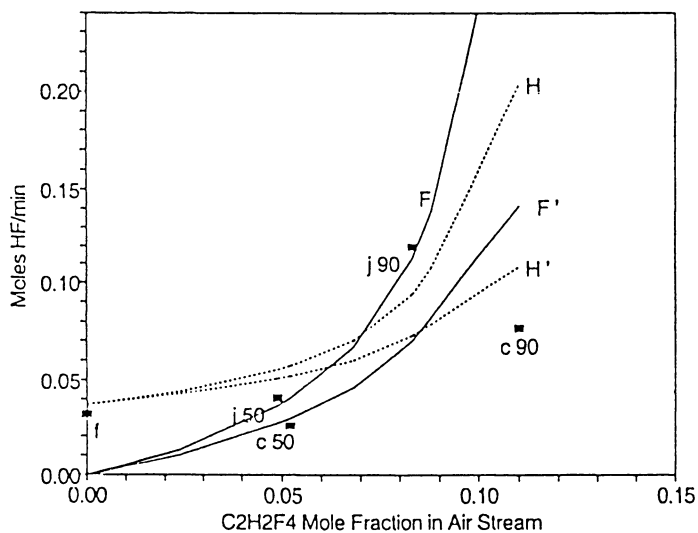


Figure 10 - Moles of HF produced as a function of $C_2H_2F_4$ concentration as in Figure 4.

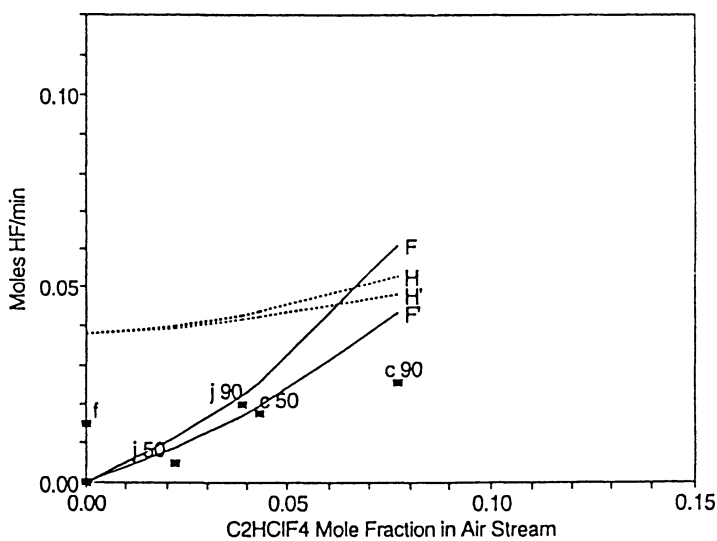


Figure 11 - Moles of HF produced as a function of C_2HClF_4 concentration as in Figure 4.

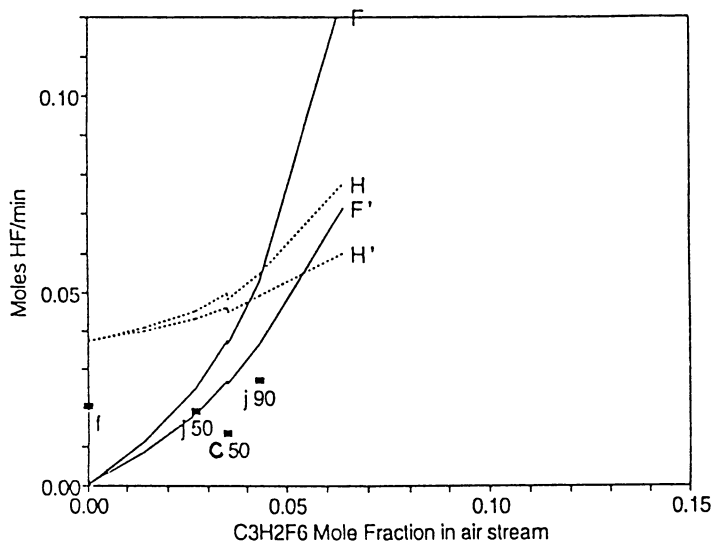


Figure 12 - Moles of HF produced as a function of $C_3H_2F_6$ concentration as in Figure 4.

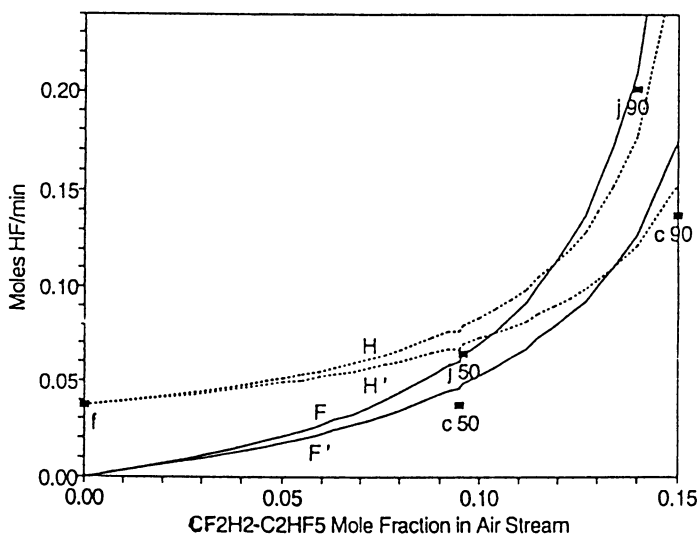


Figure 13 - Moles of HF produced as a function of CF_2H_2/C_2HF_5 concentration as in Figure 4.

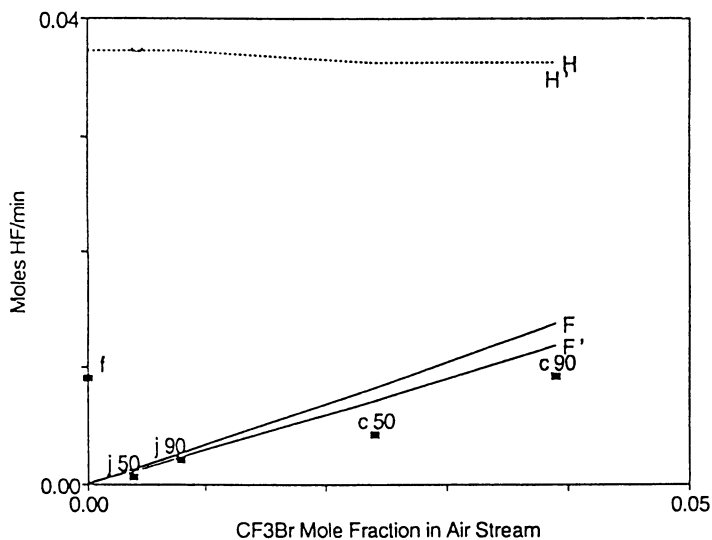


Figure 14 - Moles of HF produced as a function of CHF₂Cl concentration as in Figure 4.

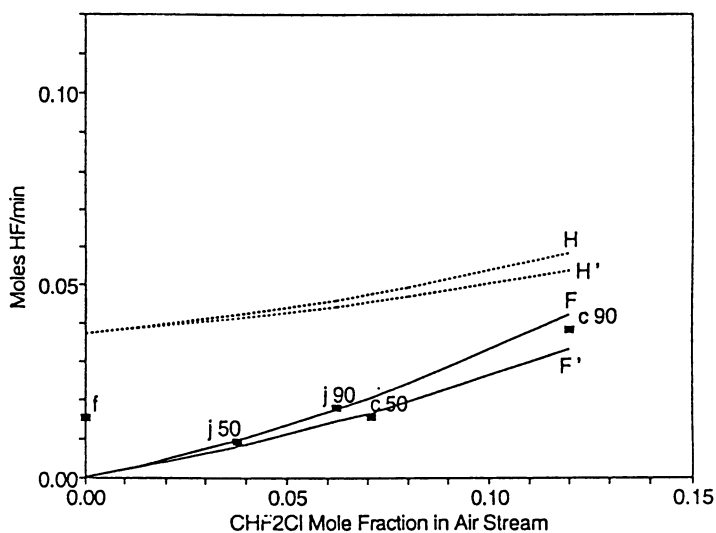


Figure 15 - Moles of HF produced as a function of CF₃Br concentration as in Figure 4.

Also shown in the figure are the experimentally measured HF production rates for the jet and cup burners (labeled c and j respectively) at 50 and 90% of the extinction concentration of C_2F_6 . As indicated, the measured quantities of HF are lower than both the fluorine and hydrogen limits, and the measured values are closer to the estimated limits when the effects of preferential diffusion (H' and F') are included as described above. The results for the inhibitor addition to the fuel stream in the cup burner (labeled f) are plotted at an inhibitor concentration of zero so that they can be included in the figure.

Although the cup and jet burner results are plotted together, the phenomenological behavior of jet burner is distinctly different from that of the cup burner. Because the flame of the jet burner first stabilizes as a co-flow diffusion flame anchored at the outlet of the jet, the heated gases have a much lower Reynolds number, keeping the flow laminar. As inhibitor is added to the air stream, the flame grows in length (as it would in increasing the fuel flow rate). Eventually, the flame lifts off the burner surface by about 5 cm to form a lifted jet diffusion flame. With further inhibitor addition, the flame eventually blows off. These blow-off concentrations are referred to as the extinction concentrations (see Table I) and are found to be much lower (about half) of the values determined for the cup burner. In the tests at 50% extinction, the flow is laminar, whereas at 90% of extinction, the flow is nearly turbulent and the flame is lifted. Transport of the agent into the flame is estimated in the stoichiometric model assuming molecular diffusion. The goal of these experiments is to compare the model's prediction of HF formation for a diffusion flame where more vigorous mixing occurs, and identify if the enhanced mixing increases the HF production. Figures 4 to 15 show that HF production in the turbulent burner at 90% of extinction is higher relative to the model prediction than the cup burner results at 90% (except for C_2F_6 and C_4F_8), but that the jet burner HF production rates are still not above the estimate of the fluorine flux based on equal transport for O_2 and the inhibitor (the curve labeled F).

When viewed as in Figures 4-15, the behavior of the alternative inhibitors falls into three categories. In the first category are the inhibitors C_2F_6 , C_3F_8 , C_4F_{10} , C_3F_8 , C_2HF_5 , and C_3HF_7 (Figures 4 to 9). For these inhibitors, at the highest inhibitor concentration tested (cup burner at 90% of extinction) the estimated hydrogen flux into the reaction zone is lower than the fluorine flux. The ratio of hydrogen to total halogen flux ranges from 0.31 to 0.68, and the H flux is not a strong function of the inhibitor concentration. For these inhibitors, the HF produced does not increase significantly when the inhibitor concentration in the air stream increases above that necessary for a hydrogen/fluorine ratio in the reaction zone of about unity (the region of where the lines marked F and H or F' and H' cross in Figures 4 to 15). A second category includes those inhibitors ($C_2H_2F_4$, C_2HClF_4 , $C_3H_2F_6$, and $CH_2F_2/C_2H_2F_4$; Figures 10 to 13) for which the estimated H and X fluxes are closer, with H/X ratios of 0.68 to 0.85. For these inhibitors, the amount of HF produced increases with increasing inhibitor concentration in the air, but the highest concentration tested corresponds F/H ratio of about unity in the reaction zone. The last category consists of CF_3Br and $CHClF_2$ (Figures 14 and 15) for which the estimated hydrogen flux is much higher than halogen flux (in a ratio of 2.3 and 1.1, respectively), and there is

estimated always to be more hydrogen than halogen in the reaction zone. For these agents, the HF produced is always increasing with higher agent concentration in the air stream.

Although the stoichiometric model is very simple and is only expected to provide an upper limit on the amount of HF formed, it is instructive to investigate the possible reasons that the measured HF production rates might be lower than the estimates. Lower HF may be measured in the experiments due to experimental difficulties, for example: loss of HF to the chimney walls, loss in the sampling system, HF undetected by the ion-selective electrodes, or imperfect mixing in the product gases. Based on exploratory parametric tests, these loss mechanisms are considered to be of secondary importance. The predicted values of the HF production do not include chemical kinetic limitations and the estimates of transport rates into the reaction zone are only approximate. Additional experiments will be performed to allow examination of these important parameters.

Conclusions

The formation rate of HF in diffusion flames is strongly influenced by the mass flux of inhibitor into the flame sheet. For diffusion flames with the inhibitor added to the air stream, there appear to be kinetic limitations to the rate of HF formation for most but not all of the agents tested which increase as the inhibitor concentration in the air stream increases. Many of the agents (for example $C_2H_2F_4$, C_2HClF_4 , $C_3H_2F_6$, CH_2F_2/C_2HF_5 , CF_3Br and $CHClF_2$) produced HF at rates within about 25% of that given by equilibrium thermodynamics in the diffusion flames tested. Most of the perfluorinated agents tested (C_2F_6 , C_3F_8 , and C_4F_{10}) and the agents C_4F_8 , C_2HF_5 and C_3HF_7 produced 0 to 35% less than the equilibrium values except when the estimated fluorine to hydrogen flux into the flame goes above unity when they show no further increase with increasing inhibitor concentration in the air stream.

Co-flow diffusion flames with inhibitor added to the fuel stream show HF production rates 30 to 55% of the values given by equilibrium thermodynamics, clearly implying kinetic limitations. Further research is needed to understand these kinetic limitations, as well as kinetic limitations present at high fluorine loading when the agent is added to the air stream.

Acknowledgments

This research was supported by the US Naval Air Systems Command; US Army Aviation and Troop Command; Federal Aviation Administration Technical Center; and the US Air Force, under the direction of Mr. J. Michael Bennett at the Wright Patterson AFB Flight Dynamics Laboratory, Survivability Enhancement Branch. The author is grateful to Y.E. Hsin and A. Liu for careful performance of the experiments.

Literature Cited

1. Burdon, M.C.; Burgoyne, J.A.; Weinberg, F.J. *Vth Symposium (Int'l) on Combustion*, Reinhold Publishing Corp., New York, NY, 1955, 647-651.

2. Wilson, W.E., Jr. *Xth Symposium (International) on Combustion*, The Combustion Institute, Pittsburgh, PA, 1965, 47-54.
3. Biordi, J.C.; Lazzara, C.P.; Papp, J.F. *XIVth Symposium (Int'l) on Combustion*, The Combustion Institute, Pittsburgh, PA, 1973, 367-381.
4. Safieh, H.Y.; Vandooren, J.; Van Tiggelen, P.J. *XIXth Symposium (International) on Combustion*, The Combustion Institute, 1982, Pittsburgh PA, 117-127.
5. Vandooren, J. F.; da Cruz, N.; P. Van Tiggelen *XXIInd Symposium (International) on Combustion*, The Combustion Institute, Pittsburgh, PA, 1988, 1587-1595.
6. Sheinson, R.S.; Musick, J.K.; Carhart, H.W. **1981**, *Journal of Fire and Flammability*, 12, 229.
7. Sheinson, R.S.; Alexander, J.I. *Fall Meeting, Eastern States Section Meeting/The Combustion Institute*, 1982, Pittsburgh, PA, Paper 62.
8. Smith, W.D.; Sheinson, R.S.; Eaton, H.G.; Brown, R.; Salmon, G.; Burchell, H.; St. Aubin, H.J. *Sixth International Fire Conference, Interflam '93*, Interscience Communications Limited, 1993, 757-764.
9. Yamashika, S. **1973**, *Report of Fire Research Institute of Japan*, 36, 7.
10. Yamashika, S.; Hosokai, R.; Morikawa, T. **1974**, *Report of Fire Research Inst. of Japan*, 38, 1.
11. Ferreira, M.J.; Hanauska, C.P.; Pike, M.T. *Halon Alternatives Technical Working Conference*, New Mexico Engineering Research Institute, Albuquerque NM, May 11-13, 1992.
12. Ferreira, M.J.; Hanauska, C.P.; Pike, M.T. *Halon Alternatives Technical Working Conference*, New Mexico Engineering Research Institute, Albuquerque NM, May 11-13, 1992.
13. Di Nenno, P.J.; Forssell, E.W.; Peatross, M.J.; Wong, J.T.; Maynard, M. *Halon Alternatives Technical Working Conference*, New Mexico Engineering Research Institute, Albuquerque, NM., May 11-13, 1992.
14. Filipczak, R.A. *Halon Alternatives Technical Working Conference*, New Mexico Engineering Research Institute, Albuquerque, NM, May 11-13, 1993, 149-159.
15. Hoke, S.H.; Herud, C. *Halon Alternatives Technical Working Conference*, Albuquerque NM, May 11-13, 1993, 185-190.
16. Booth, K.; Melina, B.J.; Hirst, R. **1973**, Imperial Chemical Industries Limited, Mond Division, Cheshire UK, 31 August.
17. Bajpai, S.N. *J. Fire and Flammability*. **1974**, 5, 255.
18. Burke, S.P.; Schumann, T.E.W. **1928**, *Ind. Eng. Chem.* 20, 998.

RECEIVED July 11, 1995

Chapter 20

Flammability Peak Concentrations of Halon Replacements and Their Function as Fire Suppressants

Naoshi Saito¹, Yuko Saso¹, Chihong Liao¹, Yoshio Ogawa¹,
and Yasufumi Inoue²

¹Fire Research Institute, Fire Defense Agency, Ministry of Home Affairs,
Mitaka, Tokyo 181, Japan

²Koatsu Company, Ltd., Itami, Hyogo 664, Japan

To evaluate fire suppression efficiency of halon replacements, flammability limits and peak concentrations of hydrocarbon-air mixtures with the suppressants have been measured by tubular flame burner system. The system gives reproducible peak concentrations and wider flammable regions than those obtained by the explosion vessel methods. Adiabatic flame temperatures of the mixtures with the suppressants at the flammability limits have been calculated to know fire suppression mechanisms. The adiabatic flame temperatures are independent of inert gases in the case where the mixtures have the equal equivalence ratio. The fact indicates the inert gases act as physical heat sinks in the flame extinguishing process. Regarding the fire suppression efficiency of the halon replacements, the adiabatic flame temperature at the limit mixture reveals that their behavior is the same as inert gases in rich mixtures. On the other hand, they play the roles as both combustible and chemical inhibitor in lean mixtures.

Since January 1994, production of bromofluorocarbon fire extinguishing agents, halons, is stopped to prevent depletion of the stratospheric ozone layer. Several potential candidates of halon replacements have been reported as fruits of many efforts of development, but the candidates have never been superior in fire suppression efficiency to halons. For the appropriate use of halon replacements, it is desirable to evaluate the fire suppression efficiency of the agents with as good reliability as possible.

Evaluation of Fire Suppression Efficiency of Halon Replacements

Today, two types of test method are used to evaluate the fire suppression efficiency. One is inerting tests and the other is flame extinguishing tests using diffusion flames. In the inerting tests, a "peak concentration" is taken as a measure of the fire suppression efficiency. Here, the peak concentration means the minimum concentration of agent in a combustible mixture that will inhibit flame propagation for any concentration of fuel. Thus, the peak concentration is one of particular points on the flammability limit curve of a fuel-air-suppressant mixture. In the case of flame

0097-6156/95/0611-0243\$12.00/0

© 1995 American Chemical Society

extinguishing tests, the agent concentration necessary to extinguish a flame of a particular fuel is called a "flame extinguishing concentration." This flame extinguishing concentration is another measure of the fire suppression efficiency. Both the peak concentration and the flame extinguishing concentration are determined practically to prevent explosions and fires, respectively.

Measurement of Flammability Limit. The flammability limit is not only a practical property of the mixture to prevent explosions, but also an interesting subject in the fundamentals of combustion science (1). Several theoretical approaches have been proposed to explain the limit (2), and there have been many experimental devices on apparatuses to measure the reliable flammability limits at the same time (3).

There are two types of measuring method about the flammability limit. One is a traditional explosion vessel method represented by an explosion burette apparatus. However, the apparatuses of the explosion vessel method have not given always repeatable and/or reliable flammability limit or peak concentration, because the limit depends on direction of flame propagation, experimental conditions for example ignition energy, accuracy in preparing gas mixtures, and the criterion of "flammability" (3). The other is a burner method using flat-flame burner, counterflow binary flame burner, or tubular flame burner (4). The burner method has been used for experimental study on the fundamental properties of flames, so there are few reports of the flammable regions and the peak concentrations of mixtures obtained by the burner method. However, the various above mentioned difficulties on the explosion vessel method can be avoided, if the burner method is employed. For example, it is possible to make gas mixtures precisely with precision flow controllers, to avoid the influence of ignition energy, and to judge the flammability clearly by the existence of flame. Besides such merits, it can be expected that downstream heat loss behind the flame is very small in the binary flame and the tubular flame. Thus, the burner method can give the repeatable and reliable results for determining flammability limits and peak concentrations.

Flammability Limits by Tubular Flame Burner System

Ishizuka (4) measured the flammability limits of fuel-air mixtures diluted with nitrogen by a tubular flame burner system. His burners are made of porous bronze cylinder. He examined various effects of wall quenching, burner scale, burner position, and injection velocity on the flammability limit or the flammable region of mixture, and observed flame shape in detail. Then he concluded that flame behavior is affected by Lewis number of the mixture, and the burner position has little effect on the flammability limit except rich propane or lean hydrogen mixtures.

When a combustible mixture is injected inward from the surface of the cylindrical burner for the burner axis, a tubular flame with circular cross section is formed in a stretched flow field. It is a sort of stretched flame like a binary flame in a stagnation flow. Since this flame is formed in a counterflow field with axial symmetry as shown in Figure 1, heat loss in downstream of the flame seems negligible. In addition, a lateral conductive loss may be smaller than a propagating flame in an explosion burette. Consequently, the flammability limits determined by a tubular flame burner give wider flammable region and higher peak concentration than the explosion burette system.

The tubular flame burner is simple in its structure and is operated easily, so it has been employed to measure the flammability limits and the peak concentrations of the mixtures with suppressants in our study. Then, the burner has been examined if it has the potential to yield reliable results.

Apparatus and Chemicals. Figure 1 is a schematic diagram of the tubular flame burner system used in this study. The system is constituted by a tubular flame burner, mass flow controllers, a gas-mixing chamber, and a buffer tank.

The burner is made of porous bronze cylinder. The dimensions of the burner are 30 mm in inner diameter, 80 mm in length, 5 mm in thickness, and $5\ \mu\text{m}$ in porosity. When rich mixtures are investigated and the burner is set up vertically, diffusion flames appear at the outside of the burner and heat the burner body. To prevent the heating, the burner is equipped with water-cooled ends of 25 mm in length, and nitrogen injection parts of 25 mm in length at both sides as shown in Figure 1.

The fuels used in the study are methane and propane for halon replacements, and additionally ethane and butane for inert gases. Nitrogen, carbon dioxide and argon are used as inert gases. Halon 1301 (CF_3Br) and three kinds of halon replacements are used as the fire suppressants. The halon replacements are HFC-23 (CHF_3), HFC-227ea ($\text{CF}_3\text{-CHF-CF}_3$) and FC-3-1-10 (C_4F_{10}). The characteristics of the agents are shown in Table I.

An oil free air compressor with a drier supplies the air to the burner in the experiments. The fuels, the inert gases, or the agents are commercial gases and their purity is more than 99 %. The flow rate of each gas and composition of mixtures are adjusted freely by the precision-type mass flow controllers.

Table I. Agent Characteristics

	Halon 1301	HFC-23	HFC-227ea	FC-3-1-10
Molecular Formula	CF_3Br	CHF_3	$\text{CF}_3\text{CHFCF}_3$	C_4F_{10}
Molecular Weight	149	70	170	238
ODP ^a	10	0	0	0
Boiling Point (°C)	-58	-82	-16	-2
Vapor Pressure at 25 °C (bar)	16.0	45.0	4.5	3.3

^a Ozone Depletion Potential

Measuring Conditions. Since the injection velocity of the gas mixture and a set-up angle of the burner affect the results of the flammability limits, such effects are investigated to decide the measuring conditions of the experiment. Here, the injection velocity stands for mean flow velocity at porous cylinder surface of the burner calculated by dividing the mixture flow rate by the area of the surface.

Effect of Injection Velocity of Mixture. Figure 2 shows the mapping of the response of methane-air flames between the injection velocity and the flammability limits under the condition of the burner set up vertically or horizontally. When the injection velocity is larger than 4-5 cm/s, the fuel concentration at the extinction limit decreases in lean mixtures and increases in rich mixtures with decreasing the injection velocity V , and the flammable concentration region of methane becomes wider. However, when the injection velocity is less than 4-5 cm/s, the flammable region becomes narrower with decreasing V . This result is consistent with Ishizuka's data (4). The relation between injection velocity and flammability limits of propane-air and butane-air mixtures show the same tendency as the methane-air limits (4) (5).

Figure 3 shows the flammable regions of the methane-air mixture diluted with carbon dioxide for a horizontal burner position and injection velocities of 5 cm/s and

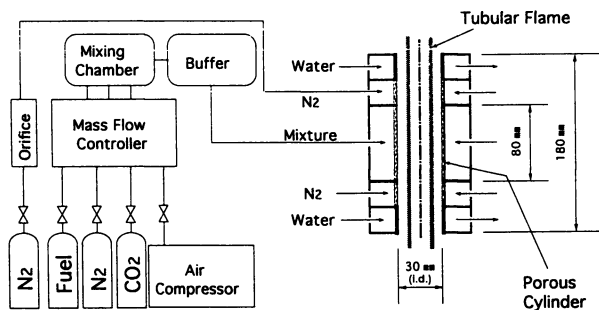


Figure 1. Tubular flame burner system

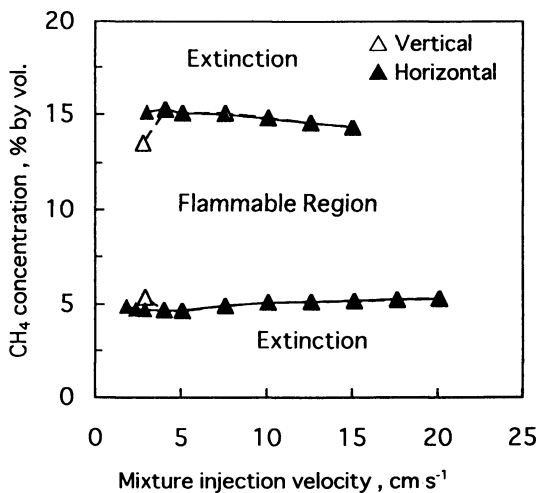


Figure 2. Stable flame regions of methane with the burner set up vertically or horizontally

10 cm/s. The flammable region clearly becomes narrow with increasing mixture injection velocity.

Figure 4 shows a dependence of the peak concentration of the methane mixture on the injection velocity. These data are obtained by both vertical and horizontal burner positions. With increasing the injection velocity, the peak concentrations almost linearly decrease for both burner positions and the differences between the peak concentrations obtained by horizontal burner and by vertical burner become small. However, the relative variations of the peak concentrations with changing the injection velocity are only -0.07 % per cm/s, thus the small variation of the injection velocity has little effect on the measurement of peak concentrations. The results show that with increasing injection velocity, the flames stabilize in the flammable region and the influence of burner position on the peak concentration decreases. It is because the effect of buoyancy on the flame becomes small relatively due to forced convection, when the injection velocity increases. In addition, heat loss to the burner also decreases. According to this consideration, large injection velocity is desirable for measuring flammability limits and peak concentrations. Increasing injection velocity, however, decreases the flammable region and peak concentration by larger flame stretch effect, then the flammability limits obtained under lower injection velocity show safer region of the mixtures on explosion.

In this study, the injection velocity of 5 cm/s is employed as a standard injection velocity condition, because not only is the flame stable enough, but also the largest and repeatable flammable region can be obtained under the injection velocity.

Effect of Set-up Angle of Burner. Figure 5 shows the flammable regions for a methane-air mixture diluted with carbon dioxide measured for both vertical and horizontal burners with an injection velocity of 5 cm/s. The flammable region obtained in the horizontal burner position is somewhat wider than that in the vertical position. At the same time, the peak concentrations measured by the horizontal burner are always larger than those by the vertical burner under the same injection velocities, as shown in Figure 4. In the case of other fuels and inert gases used here, the same results are also obtained.

In rich mixtures, diffusion flames appear at the outside of the burner outlets. If the burner is set up vertically, the diffusion flames obstruct observation of the tubular flames. On the other hand, when the burner is set up horizontally, the diffusion flames are formed above the central axis of the burner, and the diffusion flames do not hide the tubular flames in this case.

In conclusion, since the wider data on the flammability regions may be obtained and the flames are observed more easily in the horizontal burner set-up than the vertical case, the horizontal burner position is employed in the study.

Experimental Procedures. Experimental procedures are as follows. A fuel-air mixture is supplied to the burner and ignited. Then inert gas or fire suppression agent is mixed. The initial flow rate of each gas is determined so that the injection velocity at extinction will be 5 cm/s. In the case of measurement of lower flammability limits, the fuel concentration of the mixture is decreased until flame extinction occurs. For obtaining the upper flammability limit, the fuel concentration is increased until the flame disappears. The operation is repeated with increasing inert gas or fire suppressant concentration until the flame cannot exist for any fuel concentrations.

Flammable Regions of Mixtures with Inert Gas. The flammability limits and the peak concentrations of the methane and propane mixtures diluted with inert gases have been measured to confirm reproducibility of the data obtained with a tubular flame burner. Our flammable regions of the fuel-air-inert gas mixtures are displayed in Figure 6 and the measured peak concentrations of the inert gases are compared in Table II with literature data (2), (6).

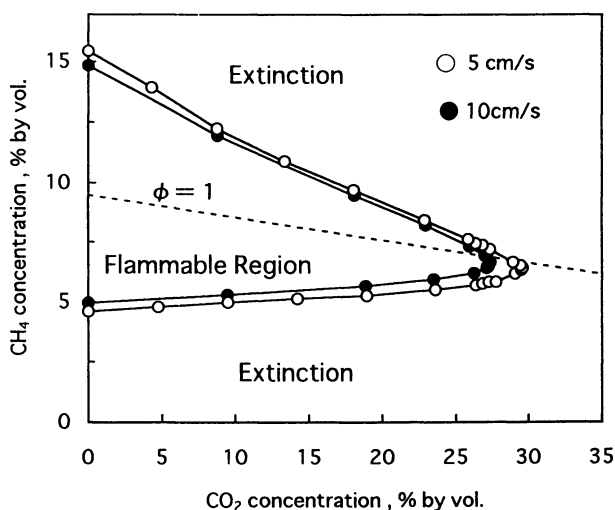


Figure 3. Extinction limits of methane flames diluted with carbon dioxide with the burner set up horizontally at the mixture injection velocity 5 cm/s and 10 cm/s

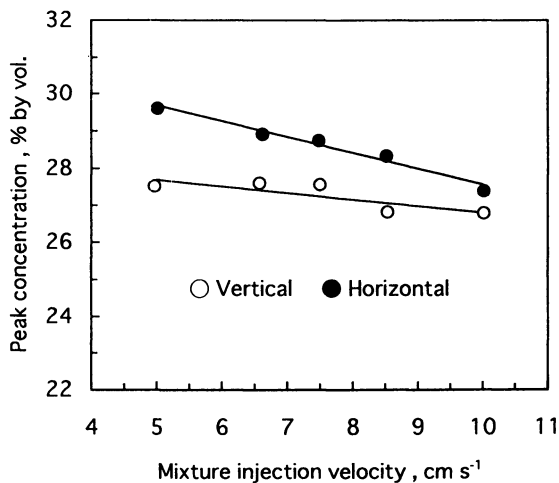


Figure 4. Peak concentration of the methane-air mixtures diluted by carbon dioxide on the mixture injection velocity with the burner set up vertically or horizontally

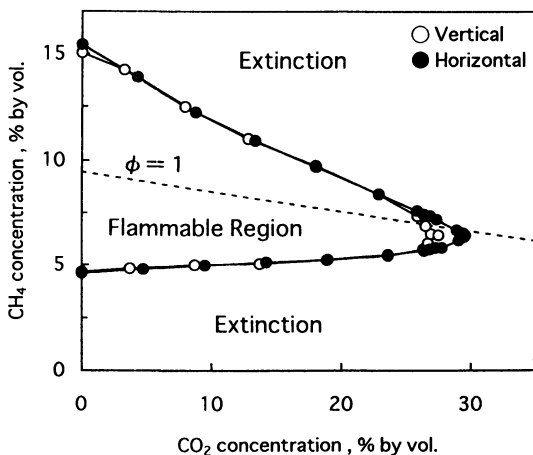


Figure 5. Extinction limits of methane flames diluted with carbon dioxide with the burner set up vertically or horizontally at the mixture injection velocity 5 cm/s

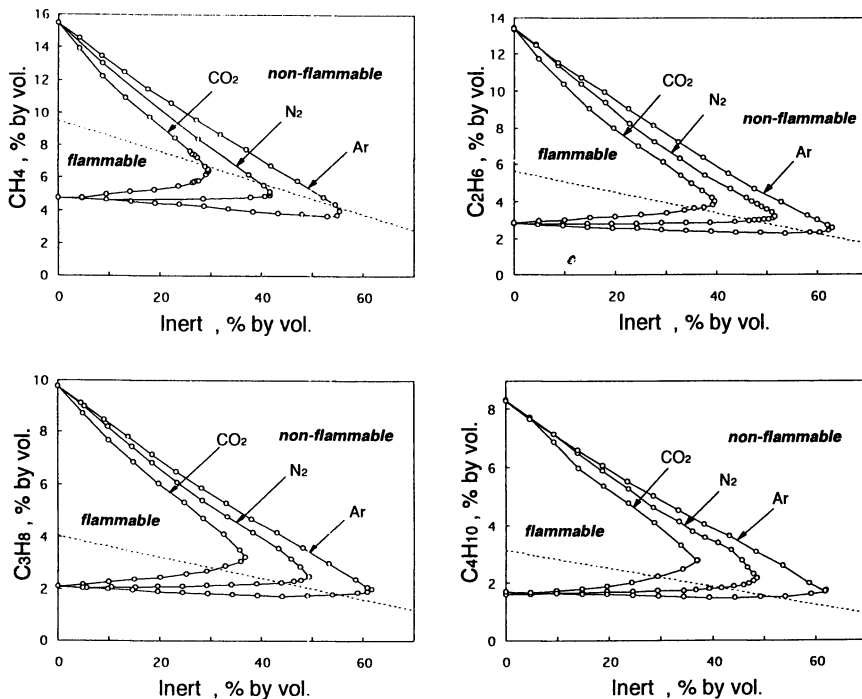


Figure 6. Flammability limits of hydrocarbon fuel-air mixtures with inert gases

In the table, the peak concentrations measured by the tubular flame burner are systematically higher than the literature data observed by the explosion burette method. The fact certifies that the tubular burner method has smaller heat loss and/or flame stretch rate than the explosion burette method as discussed in the previous section, "Flammability Limits by Tubular Flame Burner System."

Table II. Peak Concentrations of Inert Gases for Hydrocarbon Fuels

Inert gas	Peak Concentration (%)							
	Methane		Ethane		Propane		n-Butane	
	This work ^a	Ref.(2)	This work ^a	Ref.(6)	This work ^a	Ref.(6)	This work ^a	Ref.(6)
CO ₂	29.6	23	39.7	31	36.9	28	37.1	28
N ₂	41.7	37	51.6	43	49.4	42	48.6	40
Ar	55.4	44	63.1	---	61.7	---	62.0	---

^a Injection velocity : 5cm/s , Burner position : Horizontal

The results in this study have been compared and confirmed to agree well with the data reported by Ishizuka (4). These data about the lean and rich flammability limits and the peak concentrations are shown in Table III in the cases of methane and propane mixtures diluted with nitrogen. The small differences between both data seem within experimental error. This implies that repeatable and reliable flammability limits and peak concentrations can be determined by the tubular flame burner method.

Figure 7 shows comparison between the flammable regions of the methane-air-nitrogen or carbon dioxide mixtures obtained with the tubular flame burner in this study and an explosion burette. The flammable regions measured with the explosion burette are the data reported by Coward and Jones (2). The tubular flame burner method gives much wider flammable regions than the explosion burette method. This is because downstream heat loss is negligibly small compared with the explosion method. Moreover, the low strain rate condition may also contribute to the wider flammable region.

Table III. Flammability Limits and Peak Concentrations
of this work and those by Ishizuka (4)

Investigator	Burner position	CH ₄ -air-N ₂ mixtures			C ₃ H ₈ -air-N ₂ mixtures		
		Lean	Rich	Peak	Lean	Rich	Peak
This work	Vertical	4.7	15.1	41.0	2.0	9.7	47.1
	Horizontal	4.8	15.4	41.7	2.1	9.8	49.4
Ishizuka	Vertical	4.7	14.9	39.5	2.0	9.8	46.0
	Horizontal	4.7	15.1	42.4	2.0	9.5	48.8

Flammable Regions of Mixtures with Halon Replacement. The flammability limits of the methane and propane mixtures with halon 1301 or halon replacements

have been measured by the tubular flame burner made of a porous bronze cylinder. The corrosion of the burner by HF is presumed, but the corrosion does not affect the measured flammability limits at all. This fact has been confirmed by repeat measurements and verification of reproducibility of the results.

The flammable regions of the mixtures containing halon 1301 or halon replacements are shown in Fig. 8. Since all the flammable regions of the mixtures with halon replacements are wider than that of the mixtures containing halon 1301, it is obvious that the halon replacements are less effective in fire suppression than halon 1301. The flammable region of the mixtures becomes smaller and smaller with increasing the numbers of intramolecular fluorine atom of the halon replacements.

When the halon replacements are added in the combustible mixtures, the lower flammability limits shifted to the region of lower fuel concentration. For example, the flammable regions of methane-air mixtures with halon replacements are illustrated in Figure 8.

In 1993, Moore et al. (7) reported the flammable regions of propane-air mixtures with halon or halon replacements measured by the spherical vessel of NMERI, New Mexico Engineering Research Institute, of the University of New Mexico. They measured also the inerting concentrations of halon 1301 and the halon replacements for propane-air mixture by large scale test using an inerting chamber in volume of 22.5 m³. In Figure 9, the flammable regions of propane-air mixtures with halon and the halon replacements observed in this study are demonstrated with solid lines. For comparing our results with two sorts of the NMERI's data in Figure 9, the flammability limits measured by the spherical vessel are marked by dashed lines and symbols of white and black squares correspond to "non explosion" and "explosion" of the large scale inerting test results, respectively. This figure shows that the flammability limits determined by the tubular flame burner system are almost consistent with the inerting concentrations of the large scale inerting test. Thus, the tubular flame burner system gives a wider flammable region and more repeatable and reliable flammability limits than other explosion test methods.

In Table IV, the peak concentrations of halon 1301 and the halon replacements for methane or propane-air mixtures are listed and compared with the data that appear in the NFPA 2001 standard of National Fire Protection Association (8). In the table, the symbol "---" means there is no available data in the literature. There is clearly good agreement between our data and the data of the NFPA 2001 standard.

From the facts mentioned above, it can be concluded that the tubular flame burner system is an excellent apparatus to determine flammability limits because of the ease of operation and the reproducibility and reliability of the results.

Table IV. Peak Concentrations of Fire Suppressants for Hydrocarbon Fuels

Agent	Peak concentration (%)			
	Methane		Propane	
	This work ^a	Ref. (8)	This work ^a	Ref. (8)
Halon1301	6.2	---	7.6	7.7
HFC-23	20.5	20.2	20.5	20.2
HFC-227ea	11.6	---	12.1	---
FC-3-1-10	9.4	---	10.0	10.3

^aInjection velocity : 5cm/s , Burner position : Horizontal

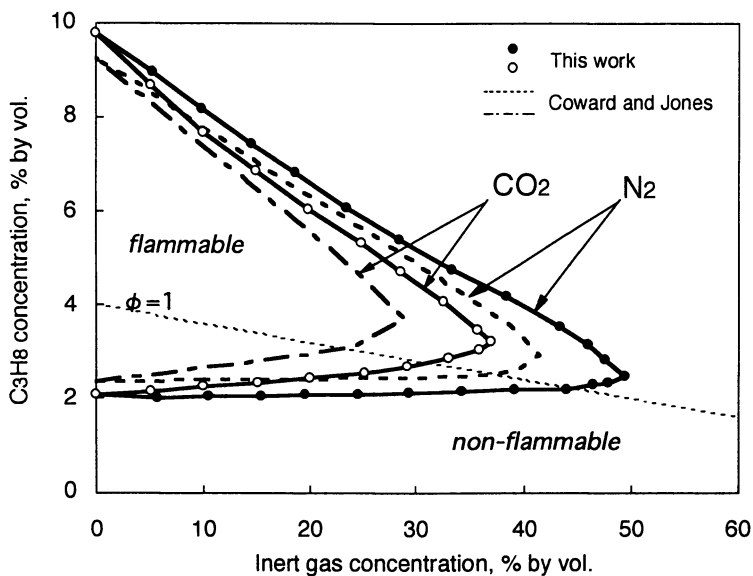


Figure 7. Flammability limits of propane-air mixtures diluted with nitrogen or carbon dioxide by this work and Coward & Jones' data (2)

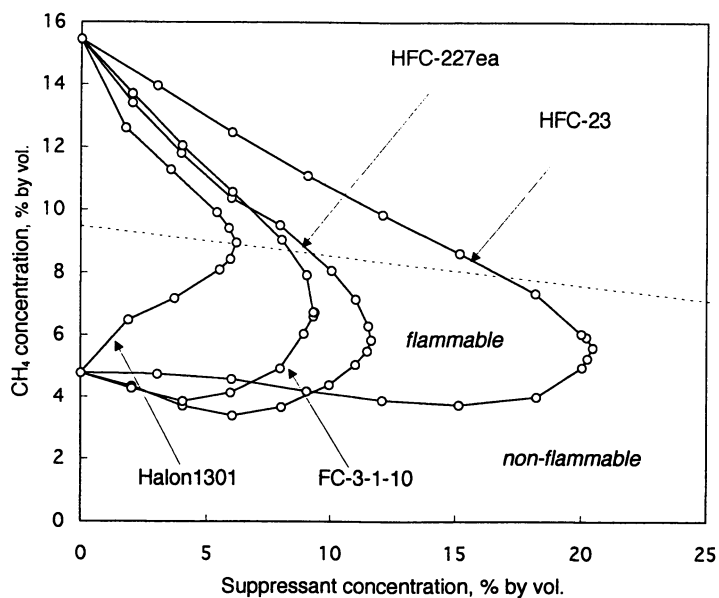


Figure 8. Flammability limits of methane-air mixtures with fire suppressants

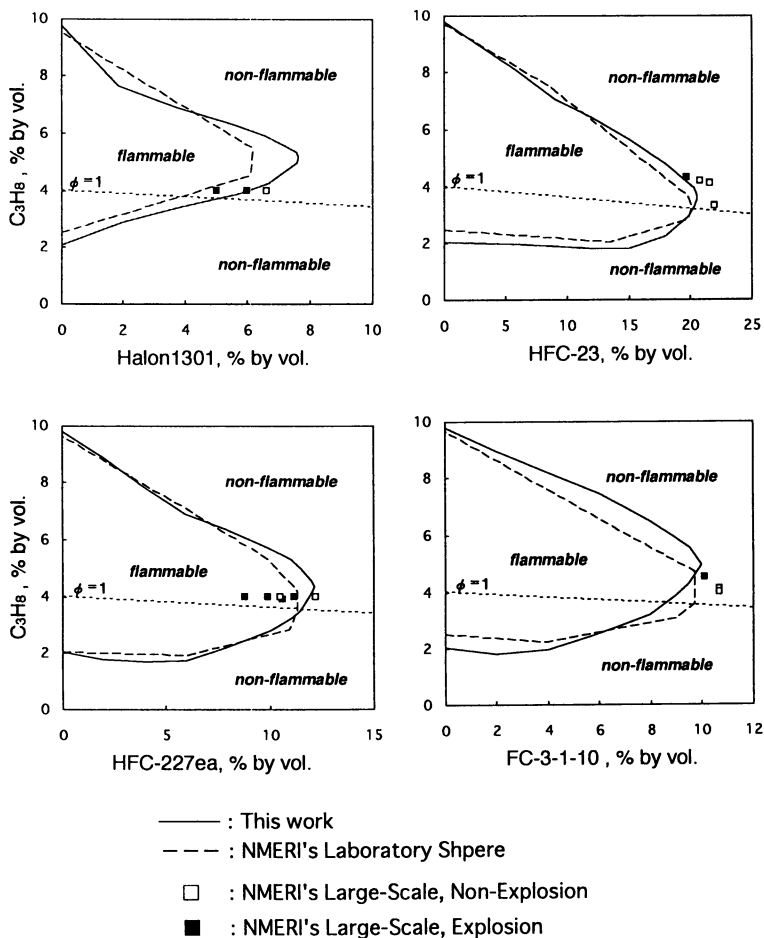


Figure 9. Comparison of flammability limits of propane-air mixtures with fire suppressants between this work and NMERI's data (9)

Downloaded by STANFORD UNIV GREEN LIBR on October 6, 2012 | http://pubs.acs.org
 Publication Date: May 5, 1997 | doi: 10.1021/bk-1995-0611.ch020

Adiabatic Flame Temperatures at the Flammability Limits

To provide a rough indication of the thermal and chemical influence of the suppressants on the flame extinction, the adiabatic flame temperatures of fuel-air-suppressant mixtures were calculated on condition that the composition of the gas mixture is on the flammability limit. The computer program for the chemical equilibrium calculations has been developed according to the method by Gordon et al. (9). In the calculations, the dissociation of the suppressant was considered and twenty kinds of equilibrium species were included as follows; H, H₂, OH, H₂O, O, O₂, N, N₂, C, CO, CO₂, Ar, F, F₂, COF₂, HF, CF₄, Br, Br₂, and HBr. The thermochemical data of JANAF have been used for the enthalpies, entropies, and specific heats of the reactants and the equilibrium species except for HFC-227ea and FC-3-1-10. For these two reactants, the thermochemical data were not available in the data of JANAF, so they have been estimated using Benson's method (10).

Additive and Adiabatic Flame Temperature of Limit Mixtures. Measurements of the flammability limits of propane-air-inert gas mixtures shown in Figure 6 were used for the calculations and the results are plotted in Figure 10. The horizontal axis represents the equivalence ratio (ϕ) of the mixture. Figure 10 shows that the calculated flame temperatures of the same equivalence ratio agree well among nitrogen, carbon dioxide and argon. This indicates that the extinction of the tubular flames of propane-air-inert gas mixtures occurs at a certain thermal condition independent of the kind of inert gas. The calculations for methane-air-inert gas mixtures also gave the same indication.

For the calculations of halon 1301 or the halon replacement-containing mixtures, measurements shown in Figure 8 and Figure 9 were used. The calculated results for methane and propane are shown in Figure 11 and Figure 12 respectively. In the calculations of the equivalence ratio, the suppressant was presumed to be inert. For comparison, both the adiabatic flame temperatures of the combustible fuel-air mixtures (shown by the dotted line) and of nitrogen-containing mixtures at the flammability limits are also shown in the Figures 11 and 12. The adiabatic flame temperatures of halon 1301-containing mixtures are much higher than those of nitrogen-containing mixtures at the same equivalence ratio. The adiabatic flame temperature by the chemical equilibrium calculation, which does not consider the reaction kinetics, becomes higher than the real flame temperature when the chemical suppression effect exists. The calculated high temperatures for halon 1301-containing mixtures indicate the large chemical suppression effect of halon 1301.

Fire Suppression Mechanisms of Halon Replacements. As shown in Figures 11 and 12, fire suppression mechanisms of the halon replacements depend on the equivalence ratio of the mixture. In the fuel rich region of $\phi > 1$, the adiabatic flame temperatures at the flammability limits of the halon replacement-containing mixtures are almost the same as those of nitrogen-containing mixtures. This indicates that the extinction of the flames of the halon replacement-containing mixtures at $\phi > 1$ occurs mainly by the thermal effect as in the case of inert gases. It is known that the considerable amount of HF is produced by decomposition of the halon replacement in the flame. Since the specific heat of HF is almost equal to that of nitrogen, the thermal suppression effect of the halon replacements can be attributed to dilution and cooling of the flame by HF. On the other hand, in the fuel lean region of $\phi < 1$, the adiabatic flame temperatures of the halon replacement-containing mixtures at the limits are remarkably higher than those of nitrogen-containing mixtures. They are rather closer to the temperatures of halon 1301-containing mixtures. It means that the halon replacements have some chemical suppression effect in addition to the thermal

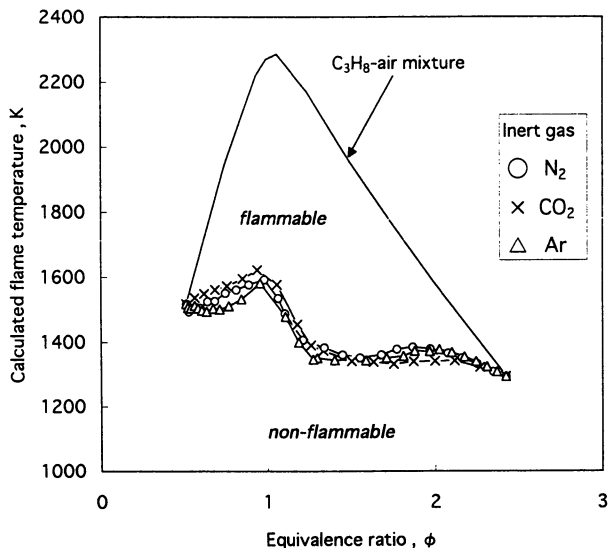


Figure 10. Calculated flame temperatures of propane-air-inert gas mixtures on flammability limits

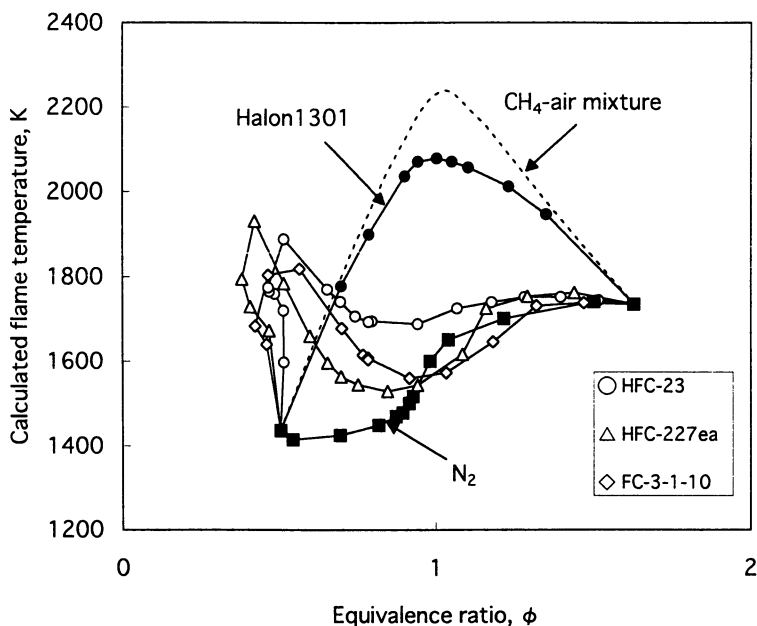


Figure 11. Calculated flame temperatures of methane-air-halon replacement mixtures on flammability limits

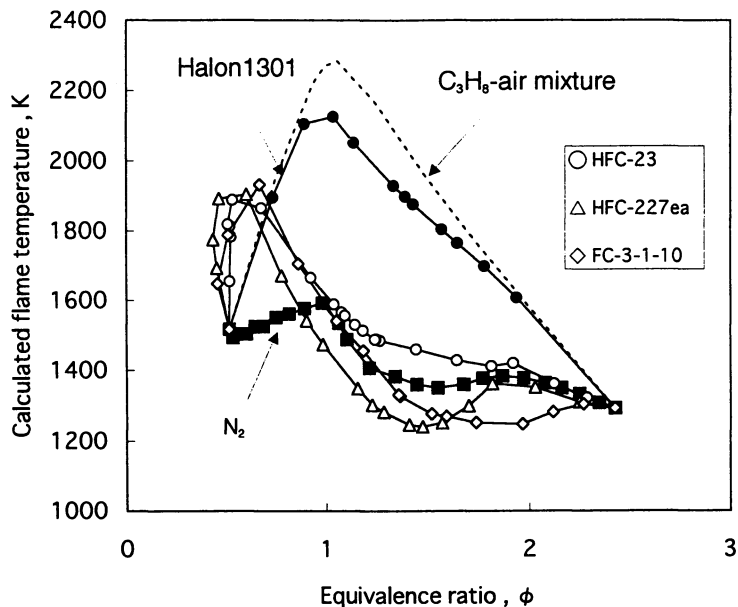


Figure 12. Calculated flame temperatures of propane-air-halon replacement mixtures on flammability limits

effect in the fuel lean region. Our results are consistent with the study by Westmoreland et al. (11), in which HFC-23 caused chemical suppression effect in methane-air flame at $\phi=0.65$. Additionally, Figures 11 and 12 show that an addition of the halon replacement extends the flammable region near the lower flammability limit to more lean direction. It means the halon replacements play a role as a combustible in the fuel lean region.

Conclusions

The tubular flame burner system can be recognized as an easily operational and reliable apparatus that is superior to the traditional explosion vessel method for measuring the reproducible flammable regions and peak concentrations of combustible mixtures.

Fire suppression efficiency of three candidates of halon replacements is determined by the tubular flame burner system. The peak concentrations of the candidates for methane and propane coincide with the corresponding data listed in the NFPA 2001 standard of National Fire Protection Association in USA. The flammable regions of propane-air mixtures with halon 1301, HFC-23, HFC-227ea, or FC-3-1-10 are larger than the data obtained by NMERI's spherical vessel, and almost agree with the inerting concentrations in 22.5 m³ NMERI large-scale inerting chamber.

Aspects of fire suppression mechanism of the new agents are investigated by calculating adiabatic flame temperatures of the mixture on the flammability limits. The compositions of mixtures along the limit curves in fuel-additive diagrams like Figure 6 are chosen for the calculation. The calculated flame temperatures of the mixtures with same equivalence ratio agree well with each other. The fact means that the flame extinction of mixtures by the inert gas occurs at a thermal condition independent of the kind of inert gas. The fire suppression mechanism of halon replacements depends on the equivalence ratio of the mixture. In rich mixtures, they act like thermal diluents and inert gases. However, in lean mixtures, they show a property like a combustible and, at the same time, it is suggested that they suppress the flames by chemical effect.

References

1. Dixon-Lewis, G. *Proc. 25th Symp.(International) on Comb.*; The Combustion Institute: Irvine, CA, 1994; (In press)
2. Lewis, B.; von Elbe, G. *Combustion, Flames and Explosions of Gases, 2nd Ed.*; Academic Press, Inc.: Oriando, Florida, 1987; pp 323, pp 709
3. Notarianni, K. A. *Preliminary Screening Procedures and Criteria for Replacements for Halons 1211 and 1201*; NIST Technical Note 1278; NIST: Gaithersburg, MD, 1990; pp 41-73
4. Ishizuka, T. *J. Loss Prev. Process Ind.* **1991**, *4*, pp 185
5. Liao, C.; Saito, N.; Saso, Y.; Ogawa, Y. *Proc. of 31th Japanese Symp. on Comb.*, The Combustion Institute Japanese Section: Tokyo, Japan, 1993; pp 183-185
6. Zabetakis, M. G. *Flammability Characteristics of Combustible Gases and Vapors*; Bureau of Mines Bulletin No. 627; Bureau of Mines, US, 1965
7. Moore, T. A.; Dierdorf, D. S.; Skaggs, S. R. *Proc. 1993 CFC & Halon Alternatives Conference*; Washington, DC, 1993
8. NFPA 2001 *Standard on Clean Agent Fire Extinguishing Systems, 1994 Edition*; Quincy, MA, 1994
9. Gordon, S.; McBride, B. J. *Computer program for Calculation of Complex Chemical Equilibrium Compositions, Rocket Performance, Incident and Reflected Shocks, and Chapman-Jouget Detonations*; NASA SP-273, Washington, DC, 1971
10. Benson, S. W. *Thermochemical Kinetics; Methods for the Estimation of Thermochemical Data and Rate Parameters, 2nd Ed.*; John Wiley and Sons: New York, 1972
11. Westmoreland, P. R.; Burgess, D. R. F. Jr.; Tang, W.; Zachariah, M. R. *Proc. 25th Symp. (international) on Comb.*, The Combustion Institute: Irvine, CA, 1994; (In press)

RECEIVED June 12, 1995

Chapter 21

Effect of Inhibitor Concentration on the Inhibition Mechanism of Fluoromethanes in Premixed Methane–Air Flames

G. T. Linteris

**Building and Fire Research Laboratory, Fire Science Division, National
Institute of Standards and Technology, Gaithersburg, MD 20899–0001**

The mechanisms of inhibition of premixed methane-air flames in the presence of difluoromethane, trifluoromethane, and tetrafluoromethane are studied. The chemistry of these agents is expected to be similar to that of agents which may be used as replacements for CF_3Br . The burning rates of premixed methane-air flames stabilized on a Mache-Hebra nozzle burner are determined using the total area method from a schlieren image of the flame. The three inhibitors are tested over an initial mole fraction from 0 to 8% at nominal values of the fuel-air equivalence ratio, ϕ , equal to 0.9, 1.0, and 1.1. The measured burning rate reductions are compared with those predicted by numerical solution of the mass, species, and energy conservation equations employing a detailed chemical kinetic mechanism recently developed at the National Institute of Standards and Technology (NIST). Even in this first test of the kinetic mechanism on inhibited hydrocarbon flames, the numerically predicted burning rates are in excellent agreement for CH_2F_2 and CF_4 and within 35% for CF_3H . The effects of inhibitor concentration on the decomposition pathway of the inhibitors and on the H, O, and OH radical production and consumption rates are discussed. The modified decomposition pathway and the reduced radical consumption explain the diminishing effectiveness of CF_3H and CH_2F_2 at higher concentrations.

Because of its destruction of stratospheric ozone, production of the widely used and efficient [1] fire suppressant halon 1301 (CF_3Br) has been discontinued, and a number of alternate agents have been proposed [2]. Since these agents are not as effective as CF_3Br , there exists a need to understand the mechanism of inhibition and suppression of these proposed alternatives (mostly fluorinated hydrocarbons and perfluorinated alkanes) to help guide the search for more effective agents. This article describes

This chapter not subject to U.S. copyright
Published 1995 American Chemical Society

measurements and numerical calculations of the reduction in burning rate of premixed methane-air flames with the addition of three fluoromethanes (CF_4 , CF_3H , and CH_2F_2) which demonstrate some of the characteristics of the alternatives, while having structures simple enough so that their chemistry can be described by a recently developed kinetic mechanism.

Early studies [3-9] of the inhibitory effect of halogenated hydrocarbons on flames were conducted in premixed systems. The premixed laminar burning rate is a fundamental parameter describing the overall reaction rate, heat release, and heat and mass transport in a flame. In addition, the reduction in the premixed flame burning rate is useful for understanding the mechanism of chemical inhibition of fires since diffusion flames often have a stabilization region which is premixed, and good correlation has been found between the reduction in burning rate and the concentration of inhibitors found to extinguish diffusion flames [10]. Premixed flame burners have flow fields which are relatively easily characterized, making interpretation of the inhibitor's effect on the overall reaction rate straightforward.

Garner *et al.* [7], Rosser *et al.* [8], and Lask and Wagner [9] measured the reduction in burning rate of various burner-stabilized hydrocarbon-air flames with addition of several halogenated methanes, halogen acids and halogen dimers. In later work, Niioka *et al.* [11] experimentally investigated the effect of CF_3Br on the extinction velocity of opposed premixed C_2H_4 flames. The inhibitory effect was found to be more effective in rich flames than in lean flames. These studies were in consensus that the magnitude of the inhibition was related to the number and type of halogen atoms present in the reactants, the concentration of the inhibitor, and the equivalence ratio ϕ ; and that the effect was generally too large to be accounted for by thermal dilution effects. This conclusion was based on supporting calculations or measurements showing that the final temperatures in the inhibited flames were not low enough to account for the burning rate reductions observed.

There have been numerous experimental studies examining the flame structure of premixed systems using mass spectrometry [12-17], and many analytical studies discussing the mechanism of inhibition of halogenated species [18-22]. In these studies the inhibition is dominated by the chlorinated and brominated species. Most of the proposed replacements for CF_3Br , however, contain only carbon, hydrogen, and fluorine. Recently, studies have examined premixed systems containing only fluorinated inhibitors. Vandooren *et al.* [23] performed molecular-beam mass spectrometer measurements in a low-pressure premixed flame of CO , H_2 , O_2 , and Ar inhibited by CF_3H , determined the destruction route for CF_3H , and obtained rate expressions for key inhibition reactions. da Cruz *et al.* [24] measured the burning rate of moist CO flames inhibited by CF_3Br , CFCl_3 , CF_2Cl_2 , CF_3Cl , CF_3H , and CF_4 , and found that the effectiveness depended most strongly on the number of Br and Cl atoms, and that the inhibitor effectiveness correlated with the rate of reaction of the inhibitor with H -atom. Using molecular beam mass spectrometer measurements in a low-pressure H_2 - O_2 flame, Richter *et al.* [25] determined the destruction pathway for CF_3H and found the reaction paths important for CO , CO_2 and CF_2O formation and CO destruction. These studies indicated that CF_3H reduces radical concentrations in the flames and inferred the important inhibition reactions to be $\text{CF}_3\text{H} + \text{H} = \text{CF}_3 + \text{H}_2$ and $\text{CF}_3 + \text{OH} = \text{CF}_2\text{O} + \text{HF}$.

None of these studies examined fluorinated inhibition in hydrocarbon flames. The present research extends the investigations of burning rate reduction to fluorinated inhibitors in hydrocarbon flames and applies a newly-developed kinetic mechanism to model the experiments. The burning rate measurements are examined as a first step in the validation of the mechanism, and the numerical results are used to study the mode of inhibition of the fluorinated agents. Emphasis is placed, in this paper, on the changes in the inhibition mechanism as the inhibitor mole fraction increases above the low values (1 to 3%) typical of previous inhibited flame burning rate measurements, to 8%, where the mechanism of inhibitor consumption is modified. A suppressed fire experiences inhibitor mole fractions in the air stream from zero to a value well above the extinction concentration of the last-surviving flamelet. Consequently, an understanding of the inhibitor consumption over a range of concentrations is of practical interest.

Methane, although its oxidation pathway is somewhat different from that of larger alkanes, was selected for study because its simple structure is amenable to modeling. As the model is further developed and tested, experiments and calculations will be performed for larger fuels and agents. Trifluoromethane CF_3H was selected because it is the smallest molecule which is representative of the fluorinated alkanes and provides the simplest species with which to understand the chemistry which is believed to proceed through the CF_3 radical. In addition, it is being considered as an agent suitable for total flooding applications because of its low toxicity. Difluoromethane CH_2F_2 is also relatively simple to model and shows the effect of higher hydrogen to fluorine ratio in the fuel and the decomposition pathway which proceeds through the species CHF and CHF_2 . Tetrafluoromethane is an example of a perfluorinated agent. These compounds have been argued to be inert (due to the absence of the hydrogen atom which is more easily abstracted than a fluorine). The fluoromethane CH_3F was not considered in the present study because it has not been suggested as a possible fire suppressant. The present research provides burning rate data useful for a first examination of the performance of the NIST fluorinated-species kinetic mechanism in hydrocarbon flames, and examines the mechanisms of inhibition implied by this mechanism as a function of initial inhibitor mole fraction for these three fluoromethanes.

Experiment

Numerous techniques exist for measuring burning rates of flames, and there are good reviews in the literature [26,27]. All of the flame and burner geometries employed, however, cause deviations from the desired one-dimensional, planar, adiabatic flame. In the present research, a premixed conical Bunsen-type nozzle burner is used. The low rate of heat loss to the burner, strain rate, and curvature facilitate comparisons of the experimental burning rate with the predictions of a one-dimensional numerical calculation of the flame structure. The burning rate in Bunsen-type flames is known to vary at the tip and base of the flame and is influenced by curvature and stretch (as compared to the planar burning rate); however, these effects are most important over small regions of the flame. Although measurement of a true one-dimensional, planar, adiabatic burning rate is difficult, the relative change in the burning rate can be

measured with more confidence. Consequently, the burning rate reduction in the present work is normalized by the uninhibited burning rate. For comparison with the results of other researchers, the absolute burning rates of the uninhibited flames are also presented.

The flame speed measurements are performed using a Mache-Hebra nozzle burner [28], consisting of a quartz tube 27 cm long with an area contraction ratio of 4.7 and a final nozzle diameter of 1.02 ± 0.005 cm. The nozzle contour is designed to produce straight-sided schlieren and visible images which are very closely parallel. The burner is placed in a square acrylic chimney 10 cm wide and 86 cm tall with provision for co-flowing air or nitrogen gas (for the present data, the co-flow velocity is zero). Gas flows are measured with digitally-controlled mass flow controllers (Sierra Model 860**) with a claimed repeatability of 0.2 % and accuracy of 1 %, which have been calibrated with bubble and dry (American Meter Co. DTM-200A) flow meters so that their accuracy is $\pm 1\%$. The fuel gas is methane (Matheson UHP) and the inhibitors are trifluoromethane (Dupont), tetrafluoromethane (PCR), and difluoromethane (Allied Signal). House compressed air (filtered and dried) is used after it has been additionally cleaned by passing it through an 0.01 micron filter, a carbon filter, and a desiccant bed to remove small aerosols, organic vapors, and water vapor. The product gas temperature of the uninhibited flames is measured with Pt/Pt 6% Rh - Pt/Pt 30% Rh thermocouples which are coated with yttrium oxide to reduce catalytic reaction on the thermocouple surface. Measurements with two bead diameters (344 and 139 μm) allow correction for radiation losses.

For the present data, the visible flame height is maintained at constant value of 1.3 cm to provide similar rates of heat loss to the burner, while the desired equivalence ratio and inhibitor concentration are preserved. An optical system provides simultaneously the visible and schlieren images of the flame. A 512 by 512 pixel CCD array captures the image which is then digitized by a frame-grabber board in an Intel 486-based computer. The flame area is determined (assuming axial symmetry) from the digitized schlieren image using image processing software. The average mass burning rate for the flame is determined using the total area method [27]. The experimental technique is similar to that used extensively by Van Wouterghem and Van Tiggelen [29]. The present burner, however, is larger, is not water-cooled, and the material (quartz) has a much lower thermal conductivity than that in ref. [29].

Model

The structure of the inhibited premixed methane-air flame was calculated using currently available techniques [30-32]. The equations of mass, species, and energy conservation were solved numerically for the initial gas compositions of the experiments. The solution assumes isobaric, adiabatic, steady, planar, one-dimensional, laminar flow and neglects radiation and the Dufour effect (concentration gradient-induced heat transfer) but includes thermal diffusion. The adopted boundary

** Certain commercial equipment, instruments, or materials are identified in this paper in order to adequately specify the experimental procedure. Such identification does not imply recommendation or endorsement by the National Institute of Standards and Technology, nor does it imply that the materials or equipment are necessarily the best available for the intended use.

conditions, corresponding to a solution for a freely-propagating flame, are a fixed inlet temperature of 298 K with specified mass flux fractions at the inlet and vanishing gradients downstream from the flame. The calculations employed a chemical kinetic mechanism recently developed at NIST [2, 33-35] for fluorine inhibition of hydrocarbon flames. Several reactions, as listed in Table 1, were modified in the present calculations to represent more recent estimations [36]. It should be noted that these rates were not modified to promote agreement with the experimental results and that these changes produce only about a one percent modification to the calculated burning rates for the present conditions. The 85-species mechanism uses a hydrocarbon sub-mechanism and adds C₁ (200 reactions) and C₂ (400 reactions) fluorochemistry. The hydrocarbon sub-mechanism has been updated, in the present work, to use GRIMECH (31 species, 177 reactions; [37]) which more closely predicts our experimental uninhibited burning rates. Although all of the reactions are not necessary to adequately describe the present flames, the comprehensive full mechanism was used for these initial calculations. Reduction of the mechanism will be performed later after more experimental validation. It should be emphasized that the mechanism adopted [33-36] for the present calculations should be considered only as a starting point. Numerous changes to both the reactions incorporated and the rates may be made once a variety of experimental and theoretical data are available for testing the mechanism.

Table 1 - Reactions changed in the present kinetic mechanism and the new parameters for the specific reaction rate constant, $k = AT^b e^{-E/RT}$, where A is the pre factor (s^{-1} , etc.); T is the temperature (K); b is the temperature dependence; and E is the activation energy (J / mol / 4.18).

<u>Reaction</u>	<u>A</u>	<u>b</u>	<u>E</u>
CF ₃ + F = CF ₄	4.00 x 10 ¹³	-0.2	0
CO + F + M = CFO + M	1.03 x 10 ¹⁹	-1.40	-487
CF ₂ O + H = CFO + HF	5.50 x 10 ⁸	1.42	19064

Results

The radiation-corrected temperature of the uninhibited flames was measured at 4 mm above the flame tip to be 2054, 2075, and 2050 (+/- 70 K) for $\phi=0.95, 1.0,$ and 1.05 respectively, while the adiabatic flame temperature is calculated to be 2191, 2229, and 2234 K (note that the inhibited flame speeds themselves were measured for a slightly wider range of equivalence ratio, 0.9 to 1.1). In these experiments, the measured final temperatures at a point slightly downstream from the reaction zone are about 150 K lower than the calculated adiabatic flame temperatures. Heat losses to the burner, although important near the rim, are not expected to be large compared to the heat release integrated over the entire flame. The quartz tube of the burner was not observed to increase appreciably in temperature during the experiments. The observed heat loss may be due to non-one-dimensional effects, radiation, or chemical non-equilibrium in the post-combustion gases. Nonetheless, since the temperature

difference is not too great, it seemed most appropriate to model the flame as freely-propagating rather than burner-stabilized (where heat losses, for example in a flat flame burner, are greater).

Figure 1 presents the measured mass burning rate (expressed as the equivalent flame velocity for flame propagation into reactants at 298 K) as a function of equivalence ratio for the uninhibited methane-air flame. For values of ϕ from 0.8 to 1.2 the data are within 5% of the results of Law [38] and of the numerical calculations.

The agreement between the experiment and model is quite good. This is expected since GRIMECH is being developed using existing experimental methane-air burning rates and the present experimental results are close to those of other researchers.

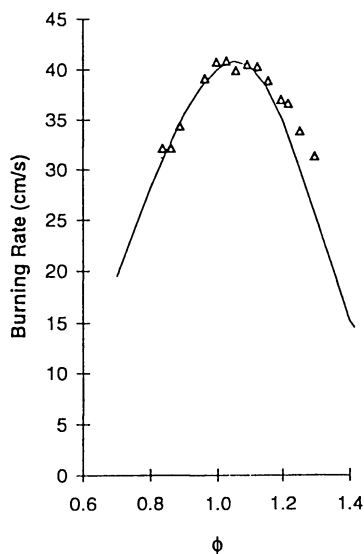
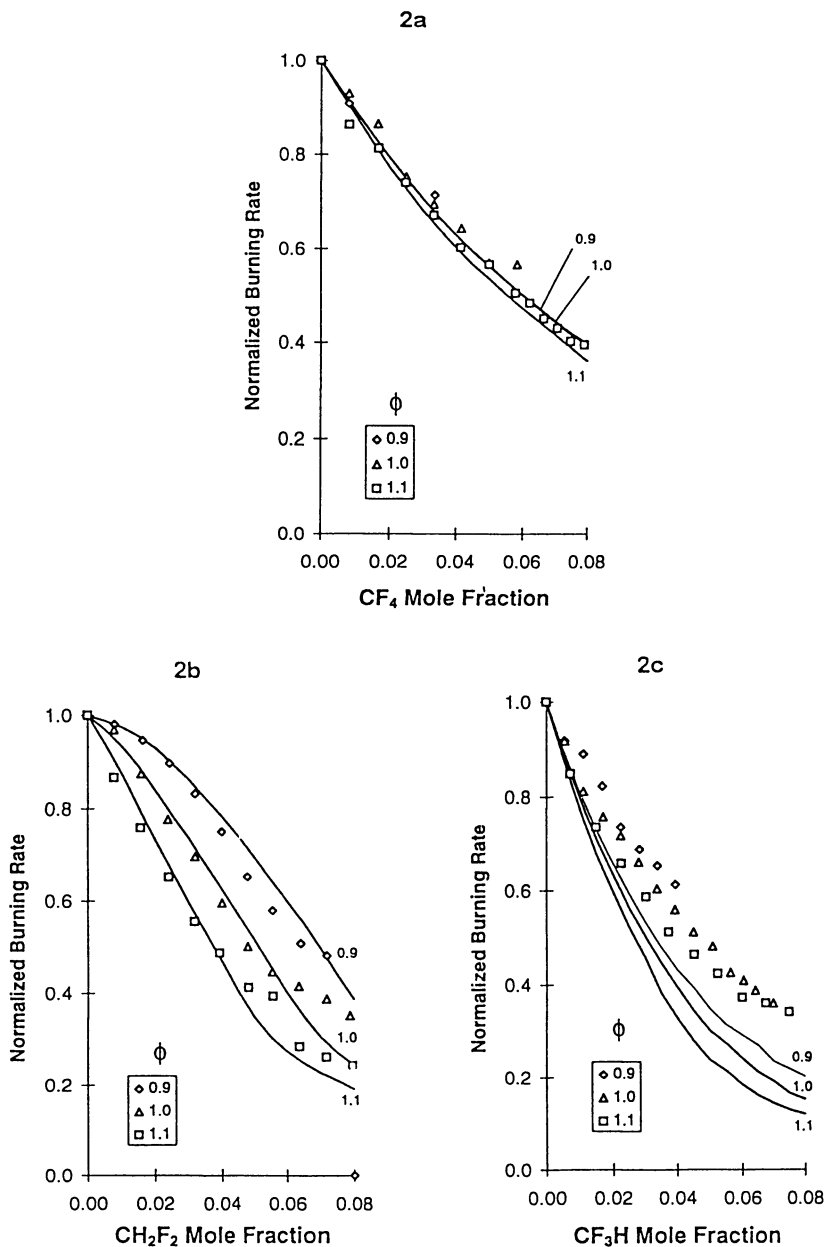


Figure 1 - Experimental burning rate (symbols) of the premixed methane-air flame in the nozzle burner as a function of fuel-air equivalence ratio, and the numerically calculated burning rate (solid line).

The results for the flames inhibited by CF_4 , CH_2F_2 , and CF_3H are presented in Figures 2a-2c respectively. The figures show the burning rate of the inhibited flame (normalized by the burning rate of the uninhibited flame) for values of ϕ of 0.9, 1.0, and 1.1 (here, the equivalence ratio is calculated based on the oxygen demand of the fuel only). Experimental and numerical results are presented for inhibitor mole fractions up to 0.08 when possible; for the lean stoichiometry and the inhibitors CF_4 and CF_3H , flames could not be stabilized for inhibitor mole fractions above about 4%.



Figures 2a, 2b, and 2c - Burning rate normalized by the uninhibited burning rate at the same stoichiometry for the methane-air flame at fuel-air equivalence ratios of 0.9, 1.0, and 1.1 as a function of the inhibitor mole fraction for CF_4 , CH_2F_2 , and CF_3H . The symbols present the experimental data, the solid lines the results of the numerical calculation (note that in Figure 2a, the lines for ϕ equal to 0.9 and 1.0 overlap).

Most of the scatter in the plots of the experimental burning rate results from flame fluctuations: the camera framing rate is 30 Hz and flame area is obtained from a single image; signal averaging would reduce this scatter. Figure 2a shows the results for CF_4 . The experiments show slightly more inhibition for richer flames as does the model. The calculated burning rate is in excellent agreement with the numerical solution. Figure 2b presents the results for CH_2F_2 . Again, rich flames show more inhibition than the lean flames but the effect is large for CH_2F_2 . The fuel effect of adding CH_2F_2 to lean flames increases the adiabatic flame temperature above the uninhibited case for low CH_2F_2 mole fractions, promoting a higher burning rate. In competition with this effect is the slower kinetics caused by presence of the fluorine compounds as discussed below. Note that although the adiabatic flame temperature is higher for lean flames with up to 5% CH_2F_2 , the burning rate is still reduced relative to the uninhibited flame. The results for CF_3H are shown in Figure 2c. The mechanism is showing the proper qualitative features of the inhibition including the dependence on stoichiometry and the reduced inhibitory effect at higher inhibitor mole fractions; however, the calculation is showing up to 35% more reduction in burning rate than is observed in the experiments.

Discussion

The results for CF_4 are not discussed in detail because examination of the reaction fluxes indicates that over the primary reaction region of the flame, the fluorinated-species reactions did not significantly affect the production or consumption of H, O, or OH. Although about 10% of the CF_4 does decompose near the primary reaction zone of the flame, most of the calculated decomposition is far downstream and fluorinated-species reactions do not significantly affect the burning rate. Rather, the effect of CF_4 is mostly to lower the heat release per unit mass of the reactants and consequently reduce the burning rate.

Previous researchers have suggested [16,22,23,25] that the overall reaction rate in premixed flames is reduced with addition of fluorinated compounds through their (and their decomposition products') reaction with hydrogen atom to form less reactive radicals and HF. Figures 2b and 2c indicate a decreasing inhibition effect with initial inhibitor mole fraction in both the experiments and the calculations for stoichiometric flames. Two approaches are used to examine this phenomenon. The numerically calculated reaction fluxes of H, O, and OH are examined here to determine the effect of increasing inhibitor mole fraction on the production and consumption of these radicals by reactions involving fluorine. Also, the consumption pathways of the inhibitor and its fragments are examined to determine changes that occur at the higher inhibitor concentrations.

Figure 3a shows the fraction of the total radical production (\cdot superscript) and consumption (\cdot superscript) for H, O, and OH by reactions involving fluorine for inhibition by CH_2F_2 . The largest effect is for hydrogen atom. The H-atom consumption increases at higher CH_2F_2 concentrations, but at a decreasing rate with

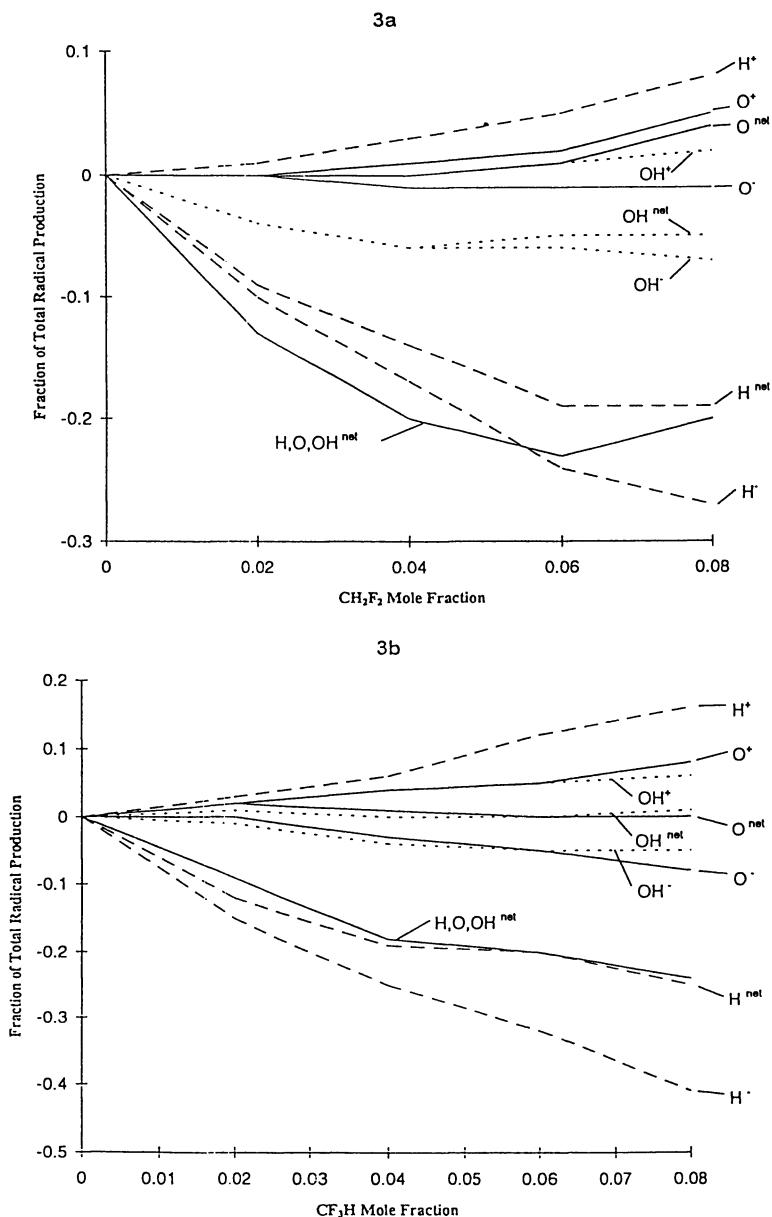


Figure 3a, b - Numerically calculated hydrogen, oxygen, and hydroxyl radical production and consumption rates from reactions involving fluorinated species as a function of initial inhibitor mole fraction for CH_2F_2 and CF_3H .

increasing inhibitor concentration. The H-atom production rate, however, increases with increasing CH_2F_2 concentration. Examination of the numerical results shows that the consumption of H-atom by the species $\text{CHF}\cdot\text{O}$, $\text{CF}\cdot\text{O}$, and CHF_2 does not increase proportionately as the CH_2F_2 concentration increases from 4 to 8%, whereas the reactions producing H-atom, $\text{H}_2 + \text{F} = \text{H} + \text{HF}$, and $\text{CF} + \text{H}_2\text{O} = \text{CHF}\cdot\text{O} + \text{H}$, increase faster than the inhibitor increase. As Figure 3a shows, the net H-atom consumption rate is approximately constant between 6 and 8% CH_2F_2 . The results for O- and OH-atom are even more pronounced: the consumption rates are approximately constant for CH_2F_2 mole fractions from 4 to 8% while the production rates of these radicals increase more rapidly over this range than they do for CH_2F_2 initial mole fractions from 0 to 4%. Between 4 and 8% CH_2F_2 , the net OH-atom consumption rate is constant, and the net O-atom production rate increases, so that there is a decrease in the sum of the H, O, and OH consumption rates from 6 to 8% CH_2F_2 . The fluorine atom concentration remains low, 2, 8, and 2 ppm at 0.5, 4.0 and 8.0% CH_2F_2 respectively. It is useful to note that the decrease in the net radical consumption does not occur until the CH_2F_2 initial mole fraction reaches just above 6%. This is also the approximate concentration at the inflection point in the burning rate for $\phi=1.0$ in Figure 2b. As discussed below, changes in the radical consumption rate for CF_3H occur at an inhibitor mole fraction of approximately 4%.

As illustrated in Figure 3b, the results for CF_3H are similar for H-atom reaction fluxes. The H-atom consumption increases at higher CF_3H concentrations, but at a slightly decreasing rate with increasing inhibitor concentration (due to the lower H-atom concentrations at higher CF_3H concentrations). In contrast, the H-atom production rates increase faster than the inhibitor initial mole fraction does (again from the reactions: $\text{H}_2 + \text{F} = \text{H} + \text{HF}$, and $\text{CF} + \text{H}_2\text{O} = \text{CHF}\cdot\text{O} + \text{H}$). The net H-atom consumption increases only slightly from 4 to 8% CF_3H . The net effect for both O and OH is small: reactions involving fluorinated species do not have a large effect on the net consumption of O and OH radicals for CF_3H concentrations up to 8%. Fluorine atom concentrations again remain low, 3, 17, and 13 ppm at 0.5, 4.0 and 8.0% CH_2F_2 respectively.

Figures 4a, b show the dominant reaction pathways for CH_2F_2 , and CF_3H for $\phi=1$ as deduced from the numerical calculations. The reaction fluxes are integrated only over the primary reaction zone of the flame (here selected to be the domain encompassing fuel and CO consumption). The arrows connect species of interest; next to the arrows are the second reacting species. The percentage of the first reactant which goes through that route is listed from top to bottom for inhibitor initial mole fractions of 2, 4, 6, and 8% respectively. From this figure we can observe the changes in the reaction pathway of the inhibitor as a function of its initial mole fraction. As shown in Figure 4a, about 82% of the initial breakdown of CH_2F_2 at low concentrations is calculated to be due to H and OH radical attack, while about 15% is due to thermal decomposition. In contrast, at 8% CH_2F_2 , reaction with H-atom is about the same, reaction with OH decreases from 50 to 22%, and thermal decomposition accounts for 44% of the CH_2F_2 destruction. The change in the consumption of $\text{CHF}\cdot\text{O}$ and $\text{CF}\cdot\text{O}$ with higher inhibitor loading is similar: the H-atom reaction is reduced moderately and destruction by thermal decomposition is two or three times higher. Formation of two-carbon fluorinated species (for clarity, not

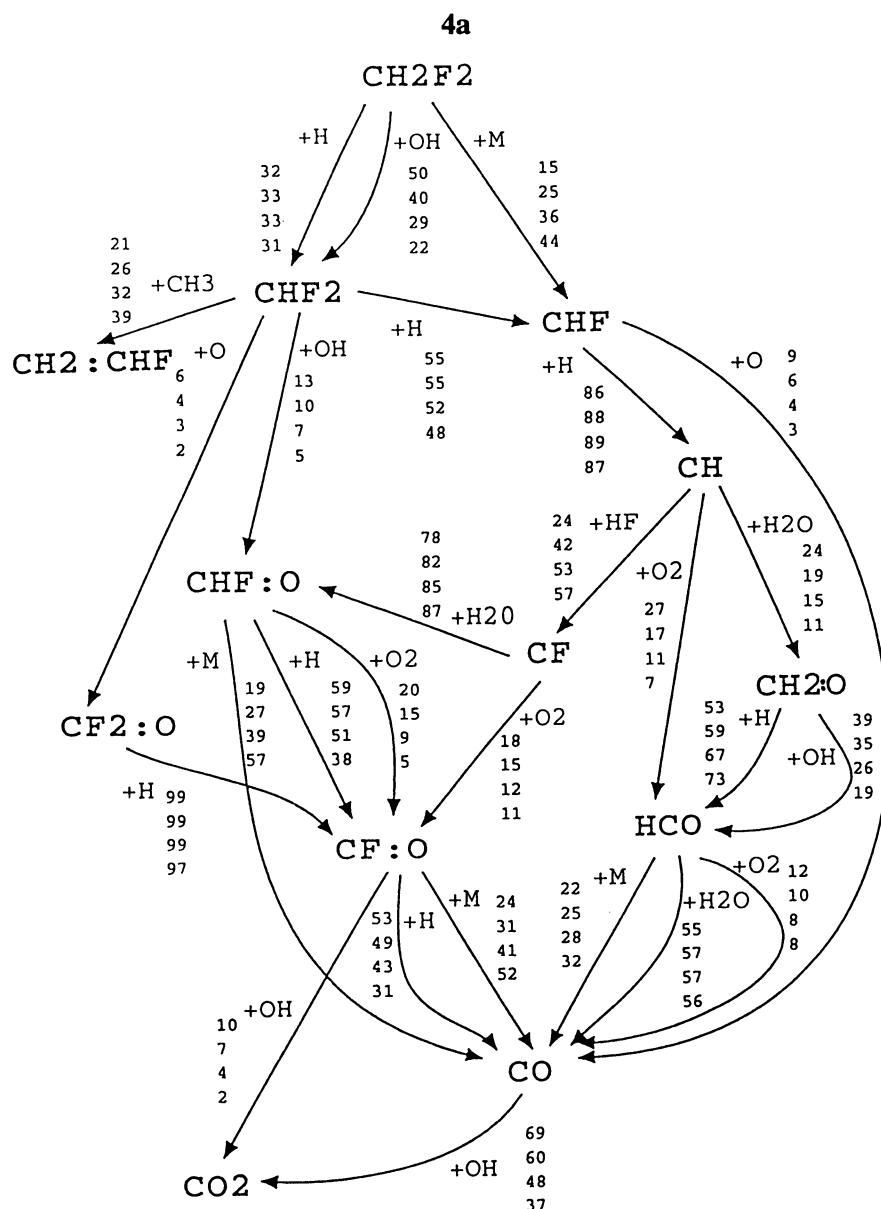
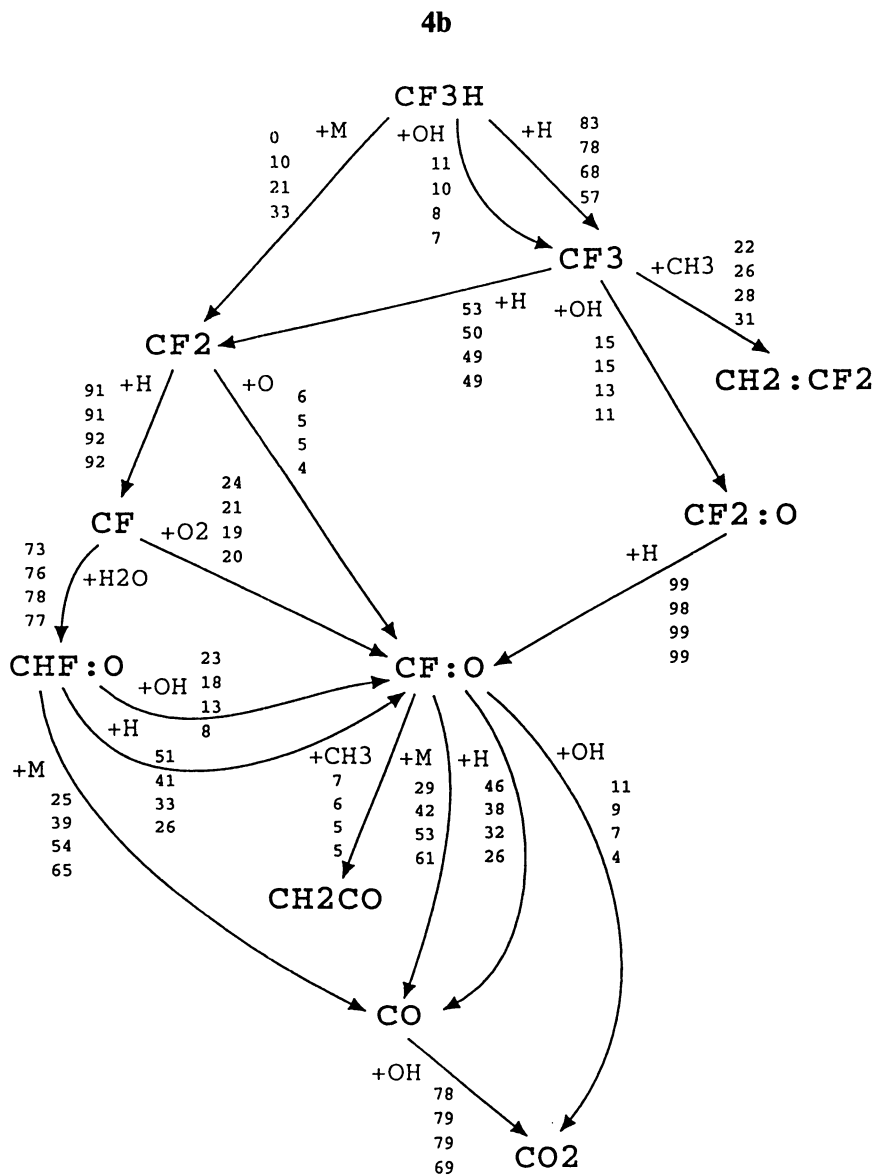


Figure 4a,b - Dominant reaction pathways for decomposition of the inhibitors CH_2F_2 and CF_3H in a stoichiometric premixed methane-air flame. The fraction of the first reactant that goes through a particular reaction path for 2, 4, 6, and 8% inhibitor is listed from top to bottom next to the arrow for the path.

Figure 4. *Continued*

shown), from CHF_2 reaction with CH_3 , is estimated to increase from 21 to 39% of the CHF_2 consumption for 2 and 8% CH_2F_2 respectively; while CHF_2 reaction with O and OH decreases by a factor of three, and reaction with H decreases only 20%. Interestingly, the consumption of CH is predicted to dramatically change. At low inhibitor loading, reaction with O_2 , H_2O and other stable species is dominant, as in uninhibited flames. At 2% CH_2F_2 , 24% of the CH is predicted to react with HF, while at 8%, this fraction is 57%.

The decomposition route calculated for CF_3H shown in Figure 4b also indicates an increasing importance for thermal decomposition reactions as the inhibitor initial mole fraction increases from 2 to 8%. Reactions of trifluoromethane with OH and H decrease by about a third, while thermal decomposition increases from 0 to 33% of its destruction. Likewise, reactions of CHF_2O and CF_2O with H- and OH-atom decrease by about a factor of two, while thermal decomposition of these species more than doubles. Reaction pathways for CF_2 , CF, and CF_3 are about the same, although reactions of CH_3 with the latter increase from 22 to 31%, so that, again, more two-carbon fluorinated species are formed at the higher inhibitor loading.

Conclusions

The reduction in burning rate has been determined experimentally and numerically for the inhibitors CF_3H , CH_2F_2 , and CF_4 in near-stoichiometric premixed methane-air flames at initial inhibitor mole fractions of 0 to 8%. Even at this early stage of development, the NIST fluorine-inhibition mechanism predicts the burning rate reduction quite well for these flames.

The numerical results have been used to examine the effects of increasing inhibitor concentration on the inhibition mechanism. A decrease in the effectiveness of the inhibitors at higher concentrations is observed for all three agents both in the experiments and in the numerical calculations. Examination of the numerical solutions indicates that for CH_2F_2 and CF_3H , consumption of the inhibitor and inhibitor fragments by radical attack is favored at low concentrations, while at inhibitor concentrations approaching 8%, thermal decomposition reactions become more important. Below about 5% inhibitor, reactions involving fluorinated species cause a net increase in the consumption rate of H, O, and OH, while above 5%, there is little additional radical consumption by these reactions. These effects are most apparent for H-atom.

Further research is necessary to test the mechanism using data from other experimental configurations. As the mechanism is further developed and refined, even closer agreement for CF_3H -inhibition of methane-air flames should be possible, and the mechanism can be extended to larger fuels and inhibitors.

Acknowledgments

This research was supported by the US Naval Air Systems Command; US Army Aviation and Troop Command; Federal Aviation Administration Technical Center; and the US Air Force. The author especially appreciates the support and technical direction of Mr. J. Michael Bennett at the Wright Patterson AFB Flight Dynamics Laboratory,

Survivability Enhancement Branch. The author is grateful to Drs. D. Burgess, W. Tsang, P. Westmoreland, and M. Zachariah for helpful conversations and for making their mechanism and publications available prior to publication; to Drs. J. Vandooren and P. Van Tiggelen for helpful suggestions concerning the experimental techniques; and to Dr. J. Hodges for help with the image processing. It is a pleasure to acknowledge the collaboration with L. Truett in making the measurements, and the assistance of Mr. Arnold Liu and Miss Cynthia Yu in writing the data acquisition and image processing software, performing the numerical calculations, and reducing the data.

Literature Cited

1. *Halogenated Fire Suppressants*; Gann, R.G., Ed.; ACS Symposium Series No. 16, The American Chemical Society, Washington, DC, 1975.
2. Nyden, M.R.; Linteris, G.T.; Burgess, D.R.F.; Jr., Westmoreland, P.R.; Tsang, W.; Zachariah, M.R. in *Evaluation of Alternative In-Flight Fire Suppressants for Full-Scale Testing in Simulated Aircraft Engine Nacelles and Dry Bays*; Grosshandler, W.L., Gann, R.G., Pitts, W.M., Eds.; *National Institute of Standards and Technology*, Gaithersburg MD, 1994; NIST SP 861, 467-641.
3. Burgoyne, J.H.; Williams-Lier, G. *Proc. of the Royal Soc.* **1948**, A193, 525.
4. Coleman, E.H. *Fuel* **1951**, 30, 114.
5. Belles, F.E.; O'Neal, C. Jr. *Sixth Symposium (Int'l) on Combustion*, The Combustion Institute, Pittsburgh, PA, 1957; 806.
6. Simmons, R.F.; Wolfhard, H.G. *Trans. Faraday Soc.* **1956**, 52, 53.
7. Garner, F.H.; Long, R.; Graham, A.J.; Badakhshan A. *Sixth Symposium (Int'l) on Combustion*, The Combustion Institute, Pittsburgh, PA, 1957; 802.
8. Rosser, W. A.; Wise, H.; Miller, J. *Seventh Symposium (Int'l) on Combustion*, Butterworths Scientific Publications, Butterworths, London, 1959; 175.
9. Lask, G.; Wagner, H.G. *Eighth Symposium (Int'l) on Combustion*, Williams and Wilkins Co., Baltimore, MD, 1962; 432.
10. Hastie, J.W. *High Temperature Vapors: Science and Technology*, Academic Press, New York, NY, 1975; 332.
11. Niioka, T.; Mitani, T.; Takahashi, M. *Combust. Flame* **1983**, 50, 89.
12. Levy, A.; Droegge, J.W.; Tighe, J.J.; Foster, J.F. *Eighth Symposium (Int'l) on Combustion*, Williams and Wilkins Co., Baltimore, MD, 1962; 524.
13. Wilson, W.E., Jr. *Tenth Symp. (Int'l) on Combustion*, The Combustion Institute, Pittsburgh, PA, 1965; 47.
14. Wilson, W.E.; O'Donovan, J.T.; Fristrom, R.M. *Twelfth Symposium (Int'l) on Combustion*, The Combustion Institute, Pittsburgh, PA, 1969; 929.
15. Biordi, J.C.; Lazzara, C.P.; and Papp, J.F. *Fourteenth Symposium (Int'l) on Combustion*, The Combustion Institute, Pittsburgh, PA, 1973; 367.
16. Biordi, J.C.; Lazzara, C.P.; Papp, J.F. *Fifteenth Symposium (Int'l) on Combustion*, The Combustion Institute, Pittsburgh, PA, 1975; 917.
17. Safieh, H.Y.; Vandooren, J.; Van Tiggelen, P.J. *Nineteenth Symposium (Int'l) on Combustion*, The Combustion Institute, Pittsburgh, PA, 1982; 117.
18. Day, M.J.; Stamp, D.V.; Thompson, K.; Dixon-Lewis, G. *Thirteenth Symposium*

- (*Int'l on Combustion*, The Combustion Institute, Pittsburgh, PA, 1971; 705.
19. Dixon-Lewis, G.; Simpson, R.J. *Sixteenth Symposium (Int'l) on Combustion*, The Combustion Institute, Pittsburgh, PA, 1977; 1111.
 20. Westbrook, C.K. *Combust. Sci. and Tech.* **1980**, 23, 191.
 21. Westbrook, C.K. *Nineteenth Symp. (Int'l) on Combustion*, The Combustion Institute, Pittsburgh, PA, 1982; 127.
 22. Westbrook, C.K. *Combust. Sci. and Tech.* **1983**, 34, 201.
 23. Vandooren, J.; da Cruz, F.N.; Van Tiggelen, P.J. *Twenty-second Symposium (Int'l) on Combustion*, 1587, The Combustion Institute, Pittsburgh, PA, 1988; 1587.
 24. da Cruz, F.N.; Vandooren, J.; Van Tiggelen, P. *Bull. Soc. Chim. Belg.* **1988**, 97:11-12, 1001.
 25. Richter, H.; Vandooren, J.; Van Tiggelen, P. *Bull. Soc. Chim. Belg.*, **1990**, 99:7, 491.
 26. Linnett, J.W. *Fourth Symposium (Int'l) on Combustion*, Williams & Wilkins, Baltimore, MD, 1953; 20.
 27. Andrews, G.E.; Bradley, D. *Combust. Flame*, **1972**, 18, 133.
 28. Mache, H.; Hebra, A. *Sitzungsber. Osterreich. Akad. Wiss., Abt.* **1941**, Ila, 150, 157.
 29. Van Wouterghem, J.; Van Tiggelen, A. *Bull. Soc. Chim. Belg.* **1954** 63, 235.
 30. Kee, R.J.; Miller, J.A.; Jefferson, T.H. *CHEMKIN: a General-Purpose, Transportable, Fortran Chemical Kinetics Code Package*, Sandia National Laboratories Report, 1980; SAND80-8003.
 31. Kee, R.J.; Warnatz, J.; Miller, J.A. *A Fortran Computer Code Package for the Evaluation of Gas-Phase Viscosities, Conductivities, and Diffusion Coefficients*, Sandia National Laboratories Report, 1983; SAND83-8209.
 32. Smooke, M.D. *J. Comp. Phys.*, **1982**, B48, 72.
 33. Burgess, D., Jr.; Tsang, W.; Westmoreland, P.R.; Zachariah, M.R. *Third Int. Conf. on Chemical Kinetics*, July 12-16, 1992, Gaithersburg, MD, 1993; 119.
 34. Westmoreland, P.R.; Burgess, D.F.R. Jr.; Tsang, W.; and Zachariah, M.R. *Twenty-fifth Symp. (Int'l) on Combustion*, The Combustion Institute, Pittsburgh, PA, 1994.
 35. Burgess, D.R.F.; Jr., Zachariah, M.R.; Tsang, W.; and Westmoreland, P.R. *Thermochemical and Chemical Kinetic Data for Fluorinated Hydrocarbons in Flames*, National Institute of Standards and Technology, Gaithersburg MD, 1994, NIST Technical Note, submitted.
 36. Burgess, D.R.F. Jr.; Tsang, W. personal communication, August, 1994.
 37. Bowman, C.T.; Frenklach, M.; Gardiner, W.; Golden, D.; Lissianski, V.; Smith, G.; Wang, H. GRIMECH, upcoming *Gas Research Institute Report*, 1995.
 38. Law, C.K. in *Reduced Kinetic Mechanisms for Application in Combustion Systems*; Peters, N.; Rogg, B., Eds.; Springer-Verlag, Berlin, 1993; 15.

RECEIVED July 1, 1995

Chapter 22

Simulation Studies on the Effects of Flame Retardants on Combustion Processes in a Plug Reactor

V. I. Babushok^{1,3}, D. R. F. Burgess, Jr.¹, Wing Tsang¹,
and Andrzej W. Miziolek²

¹Chemical Science and Technology Laboratory, Chemical Kinetics
and Thermodynamics Division, National Institute of Standards
and Technology, Gaithersburg, MD 20899-0001

²U.S. Army Research Laboratory, AMSRL-WT-PC,
Aberdeen Proving Ground, MD 21005-5066

The effect of the flame suppressants: Br₂, HBr, CH₃Br, CF₃Br, CF₃H, and C₂H₂F₄ on the ignition behavior of H₂, CH₄, CH₃OH, and C₂H₆ with air at temperatures between 900 and 2,000 K, 0.5 and 1.5 atm, equivalence ratios of 0.5 and 1.3 and additive concentrations ranging from 0 to 30% have been simulated with the Sandia Chemkin code. Dependence of ignition delay on temperature, additive concentration, pressure, and mixture composition was studied and wherever possible comparisons were made with experimental results. The decomposition of additives can promote as well as inhibit reaction. With large concentrations of additives the exothermic combustion reactions can be severely attenuated by the endothermicity of the decomposition reactions of the additive, leading in some cases to a temperature decrease. The significance of these observations in terms of mechanisms for flame inhibition is discussed.

There is much current interest in finding alternative flame retardants that do not deplete ozone. A better understanding of the chemical mechanism of suppression can serve as a guide for the selection of such compounds. At the present time, much of the knowledge on inhibition is empirical. Halogenated compounds are widely used as fire suppressants. The effect of their addition is to reduce flame speeds and narrow the limits of inflammability. On the other hand, there exists a large amount of data that indicate that many flame inhibitors may also promote the initial stages of the combustion process.

This investigation began as an attempt at developing a better understanding of the effect of inhibitors on ignition behavior through simulation studies, and indeed much of the report deals with this issue. For this purpose, we studied the influence of HBr, Br₂, CH₃Br, CF₃Br, CHF₃, and C₂H₂F₄, individually, on the ignition behavior of mixtures of methane, ethane, methanol, and hydrogen, respectively, with air at temperatures 900-2,000 K, pressures of 0.5-1.5 atm, equivalence ratios of 0.5-1.3, and additive concentrations of 0-30% by volume. Finally, we note that the simulations also yield results after the initial stages. From such results we have obtained extremely significant information bearing on the influence of larger quantities of additives on the inhibition process.

³Permanent address: Institute of Chemical Kinetics and Combustion, Novosibirsk, Russia

This chapter not subject to U.S. copyright
Published 1995 American Chemical Society

MODELING TECHNIQUES AND KINETICS DATA BASE

The main property determined from the simulation studies was the ignition delay. This is a parameter that can be and has been measured by a variety of techniques and therefore provides a good basis for comparison. In line with experimental procedures, ignition delay was characterized in terms of the following times: (a) time of achievement of maximum concentration of OH; (b) time for temperature rise of 100°K; (c) time of steep increase of temperature and changing of concentration of initial reactants; (d) time for increase in temperature for one characteristic temperature rise (RT_0^2/E), where E is the global activation energy. The uncertainty in the calculated ignition delays is between 10-30%. The limits to such studies arise at high temperatures where the reaction time is comparable to ignition delay. Calculations were carried out using the Sandia Chemkin Code SENKIN and analyzed with a National Institute of Standards and Technology (NIST) Interactive Graphics post processor. The model that is used is that of a plug reactor at constant pressure. This also corresponds to the behavior behind shock waves.

The kinetic data base contain reactions involving species with C, H, O, F, and Br atoms. The entire model includes 880 forward reactions with 98 species. The backward rates were calculated from thermodynamic equilibrium. The data base was built upon the C/H/O reaction set of Miller and Bowman(1) and Egolfopoulos et al.(2). The reactions involving C₁ and C₂ fluorinated hydrocarbons of importance in flame suppression are from the recent NIST(3) work. The set of reactions containing bromine species was based on the mechanism of Westbrook(4).

Some of the rate constants have been adjusted on the basis of the reviews of Tsang(5,6) and Baulch et al(7) and have been brought up to date using the NIST data base(8). We have added into the data base reactions involving the formation and consumption of CH₃O₂ and CH₃OOH. Adjustments of the rate constants were made in order to match existing experimental results on ignition delay times and kinetics studies on the oxidation of hydrogen, methane, formaldehyde, and methanol. Some of the important variations will be discussed in the following sections.

The reaction $\text{HO}_2 + \text{CH}_2\text{O} \Rightarrow \text{HCO} + \text{H}_2\text{O}_2$ is absent from the mechanisms of Miller and Bowman(1). Our calculations showed that this reaction is very important for reproducing ignition delays of methane at low temperatures. With large concentrations of formaldehyde, this reaction is the main source of H₂O₂ and is responsible for the propagation of the reaction chain. The rate constant that is used is based on the recommendation of Tsang et.al(5). Without this reaction, ignition delays were factors of 4 larger than that determined from the studies of Reid et al.(9) and Conti(10) et al. The reaction $\text{CH}_4 + \text{HO}_2 \Rightarrow \text{H}_2\text{O}_2 + \text{CH}_3$ influence the ignition delay of methane at low temperatures. Agreement with experimental data of Reid et al.(9) and Conti et al.(10) was achieved through use of recommendation of Baulch et al.(7).

The reactions of methyl radicals with O₂ involve three possible product channels: CH₃O+O(1), CH₂O+OH(2), and CH₃O₂(3). Most models only include the first channel. Channel 2 is used in the model of Egolfopoulos et al.(2) with a rate constant that is in fact larger than that for the first process. The introduction of this reaction decreases the ignition delay by more than a factor of 10 at 900-1000 K. The reactions $\text{CH}_3 + \text{HO}_2 \Rightarrow \text{CH}_3\text{O} + \text{OH}$ and $\text{CH}_3\text{O} + \text{O}_2 \Rightarrow \text{CH}_2\text{O} + \text{HO}_2$ lead to the same products as reaction 2, and the recommended rate constants for these reactions should be fairly accurate. The contributions from channel 2 is added to that for the other two reactions and amplifies the consequences.

A rate constant of not more than 4×10^7 cm³/(mol•s) at 900 K for channel 2 is needed to fit the data. This is a very low value in comparison with the recommendation of Baulch et al.(7) and the tabulated values in the NIST(8) compilation. For the present purposes, we use the value obtained by Ho et al. (11).

For reactions involving fluorine, an important difference from earlier recommendations is the assignment of the mechanism and rate constants for the reaction of $\text{CF}_3 + \text{O}_2$. Westbrook favors the formation of CF_2O and OF, while in the NIST work(3) and that of Vedenev et al.(12), the formation of CF_3O and O is recommended. The latter is a branching process, while the mechanism of Westbrook ultimately leads to termination. The results of Vedenev et.al. and NIST are from transition state calculations. The former leads to much larger decreases in ignition delay than would be warranted from experimental results. The NIST values, which lead to larger delays, are in better accord with experiments and are based on the most recent thermochemistry for the species in question. The basis for estimating transition state properties are probably more accurate. We have used the NIST expression $2.46 \cdot 10^{13} \exp(-23,900/RT)$ cm³/(mol•s) in our simulations.

We have updated the data base involving bromine species by adjusting the rate expressions to reflect more recent measurements. Some of these changes are as much as an order of magnitude. Westbrook's reaction set is a very abbreviated one. He assumed that because of the difference in the energy of C-H and C-Br bonds in CH_3Br molecule, the bromine atom will always be abstracted first. This leads to the omission of species such as CH_2Br , CHBr , CBr , BrO , and BrOH . We have included reactions involving CH_2Br , BrO and BrOH with rate constants similar to that for comparable Cl species. The result of these modifications was an approximate 30% change in ignition delay at low temperatures at 1% additive level and smaller effects at higher temperatures. With our more complete C/H/O/F mechanism, a much larger set of bromine reactions is warranted. However our analysis suggests that the Westbrook mechanism is fairly robust and that the important phenomena have been captured.

MODEL VALIDATION, COMPARISONS WITH EXPERIMENTAL DATA

We have calibrated our data base by comparison with the experimental results of Reid et al.(9), Conti et al.(10), Suzuki et al.(13), Hochgreb et al.(14), Skinner(15), Aronowitz et al.(16), Cathonnet et al.(17), Tsuboi et. al.(18) and Hidaka et al.(19). This includes not only ignition delay but also species concentration as a function of time. Agreement is better than a factor of 2. This is not a complete validation of all the rate constants we have used. There may be cancellation of errors. Nevertheless it is suggestive of the validity of the results derived from such calculations. The important point is that the main physical characteristics of the system are reproduced with reasonable accuracy.

RESULTS AND DISCUSSION

Temperature dependence:

Figure 1 contains results on the temperature dependence of the ignition delay for methane, methanol, ethane and hydrogen with air and 1% CF_3Br . With methane and methanol, CF_3Br always acts as a promoter. This is also the case for ethane at temperatures below 1,100K. At higher temperatures, the additive acts as an inhibitor. In the case of H_2 ,

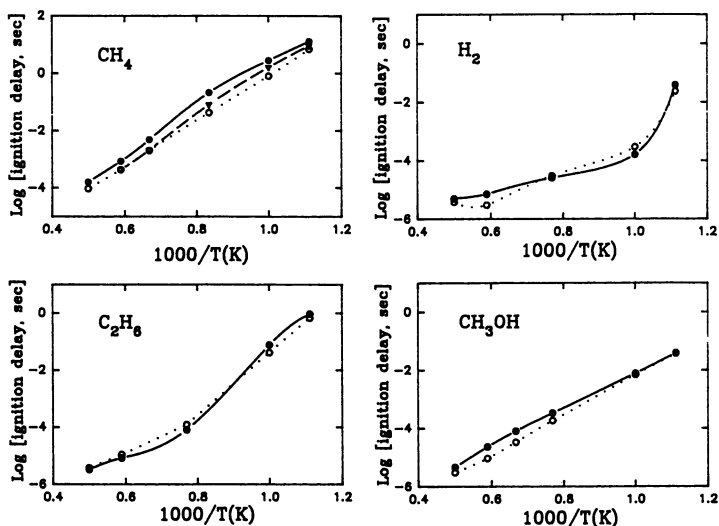


Figure 1. Temperature dependence of ignition delay in the presence of (open circle) CF₃Br and (triangle)CF₃H and absence (filled circle) of additives for stoichiometric mixtures of methane, hydrogen, ethane, and methanol at 1 atm. Additives are at 1% level. Solid lines are for pure compounds. Dotted lines are from studies with additives.

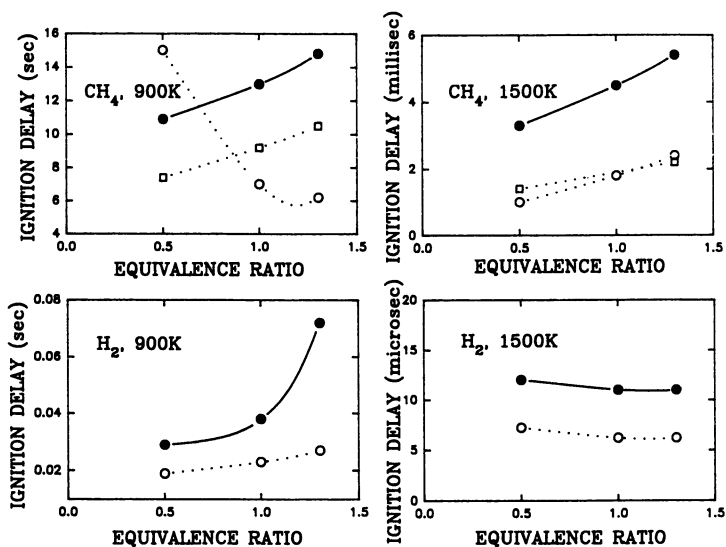


Figure 2. Dependence of ignition delay on equivalence ratio for stoichiometric methane and hydrogen with (square) CF₃H, (open circle) CF₃Br, and without (filled circle) additives at 1 atm. Additives are at 1% level. Solid lines are for pure compounds. Dotted lines are from 900 K

CF₃Br increases ignition delay only near 1,000 K. In methane, CF₃H appears to be a less effective promotor than CF₃Br. This is in agreement with the observations of Suzuki et al.(13). Significantly, for ethane they found inhibition and this was in fact reproduced and used for validating our mechanism. In general, the efficiencies become closer to each other with increasing temperature.

The results of Reid et al.(9) and Conti et al.(10) lead to ignition delay times of 10-30 secs at 900 K for stoichiometric methane mixtures at 1 atm without CF₃Br. This can be compared with the calculated results from Westbrook's model of 31 s. Our results yield a value of 13 s. Westbrook's model gives below 1,100 K with 1% CF₃Br inhibition but at higher temperatures promotion occurs. From our model promotion occurs across the whole range. Thus the present results and those of Westbrook's model span the experimental observations.

Analysis of reaction pathways and rates showed that promotion is connected with inhibitor decomposition under conditions where rates are higher than those for initiation without inhibitor. Calculations with and without initiator decomposition show that the former accelerates ignition processes and its exclusion leads to relatively weak inhibition. This is expected since inhibitor decomposition releases radicals into the system. Some characteristic results for air-methane stoichiometric mixture at 900 K, 1 atm pressure with 1% additive can be seen in Table 1.

Equivalence Ratio Dependence:

Figure 2 contains the results of simulations with variations in equivalence ratio ranging from 0.5 to 1.3 at 1 atm and temperatures 900 and 1,500 K in the presence of 1% CF₃Br for methane and hydrogen. For methane, we also include data with CF₃H as an additive. Decreases in equivalence ratio leads to decreasing ignition delay for pure mixtures. For H₂ at 1,500 K the ignition delay is weakly dependent on the equivalence ratio. In the case of H₂ at 900 K and methane at 1,500 K the general trends of increasing ignition time with equivalence ratio is similar with or without additive. The absolute magnitudes are, of course, different. It is interesting, in the latter case, the effects of CF₃H and CF₃Br are equivalent. For methane at 900 K, the effect of CF₃Br is to increase the ignition delay at low equivalence ratio. For the pure compounds and in the presence of CF₃Br our trends are in agreement with those from Westbrook's model except that our values are again somewhat lower.

Pressure Dependence:

Results of calculations for CH₄ and H₂ in stoichiometric mixtures and pressure ranges of 0.5 to 1.5 atm can be found in Figure 3. For pure methane, under all conditions the ignition delay is decreased with pressure. This follows the trend derived from Westbrook's model. However, when CF₃Br is added, as noted before, Westbrook's model leads to inhibition and we find promotion. Westbrook's model also leads to increased inhibition with pressure. In our calculations, at the highest pressures the promotion effect of the additive decreases. The general phenomena regarding pressure dependence of ignition delay is well understood in terms of the thermal nature of the ignition process and is in accord with the Semenov equation(20), $P^{nt} = A \cdot \exp(-E/RT)$, where n is the global reaction order. Stoichiometric H₂, at an initial temperature of 900 K is an exception. This is because the initial conditions of the system are near the extended second explosion limit. The effect of pressure is to pass this and go to lesser degrees of branching. Thus CF₃Br inhibits the process at lower pressures. With increasing pressure, inhibition becomes promotion.

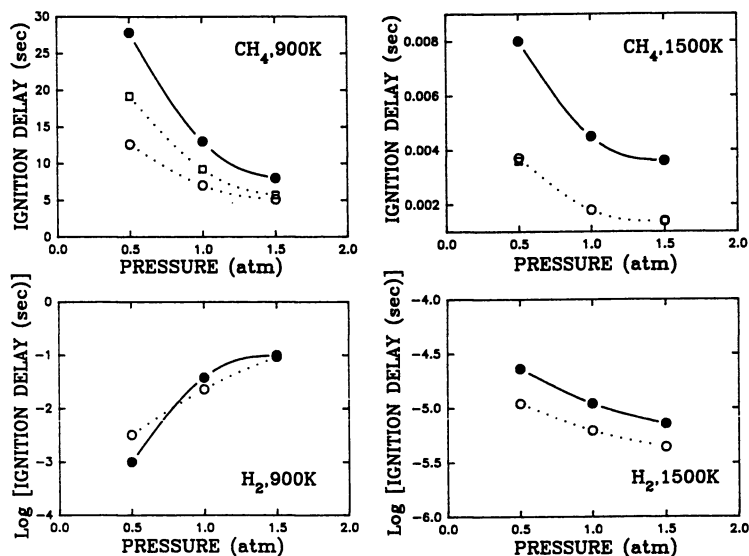


Figure 3. Dependence of ignition delay on pressure for stoichiometric methane and hydrogen mixture with (open circle) CF_3Br and (square) CF_3H and without (filled circle) additives. Additives are at 1% level. Solid lines are for pure compounds. Dotted lines are from studies with additives.

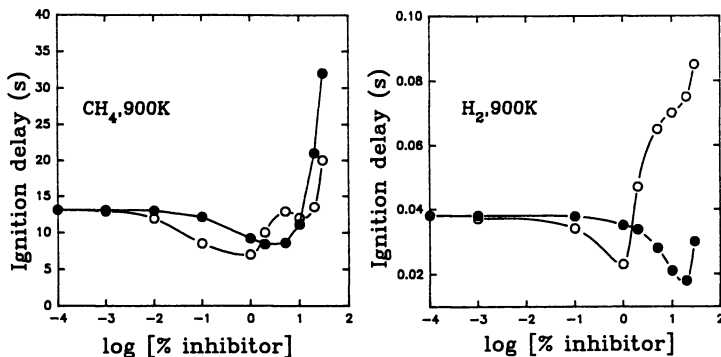


Figure 4. Dependence of ignition delay for stoichiometric methane and hydrogen mixtures at 900 K at 1 atm as a function of added inhibitors (open circle) CF_3Br and (filled circle) CF_3H .

Ignition Delay Dependence on Additive Concentration:

The results of our simulation on stoichiometric mixtures of methane and H_2 with varying quantities of CF_3Br and CF_3H can be found in Figure 4. Curves for methanol are similar to that for methane. Initially, ignition delay is decreased. A minimum or an optimum concentration for promotion is achieved at 0.5 to 2% additive concentration. Subsequently, there is a continual increase in the ignition delay. This is connected with a decrease in heat release rate and arises from the pyrolysis of the additive. In comparison, Westbrook's model for the oxidation of methane leads to inhibition at concentrations of CF_3Br as low as 0.1%. With increasing concentration, ignition delay decreases followed by increase at 5% or greater. In all cases, the increase in ignition delay is very sharp. The critical concentration is 10-30% by volume. This general phenomena has been observed by Gmurczyk et al.(21) for processes occurring in the quasi-detonation regime in ethylene/air mixtures with inhibitors such as CF_3Br and CF_3H . Lefebvre et al.(22) also needed large concentrations of inhibitors to suppress detonations.

Figure 5 contains results where HBr is used as the additive. Although the general picture is similar, with the simpler compound, it is much easier to define the important chemical processes. Attention is called to the high sensitivity of the system to very low concentrations of HBr . Our analysis of the simulation results leads to the following rationale. At low concentrations, HBr is consumed mainly via the reaction $HBr + CH_3 \Rightarrow Br + CH_4$ leading to the formation of Br atoms. Bromine atom reacts mainly with formaldehyde leading to accelerated formation of HCO through the reaction $Br + CH_2O \Rightarrow HCO + HBr$. Such a chain of reactions strongly accelerates conversion of CH_4 to HCO and then to CO . With increasing HBr concentration, the reactions $HBr + HO_2 \Rightarrow Br + H_2O_2$ and $Br + HO_2 \Rightarrow HBr + O_2$, effectively scavenge HO_2 radicals and result in decreasing rates of CH_2O and CH_3 formation. However, it is important to note that modeling with large quantities of additives may be adversely affected by failure to consider reactions involving higher molecular weight processes leading to soot formation.

Temperature behavior at high additive concentration:

The increase in ignition delay at large concentrations of inhibitors is connected with an unexpected decrease in the temperature (as large as 200 degrees) in the course of exponential temperature increase during reaction. This can be seen in Figure 6 for the reaction of 20% $CF_3H/H_2/air$ and 30% $CF_3CFH_2/CH_4/air$. This decrease in temperature leads naturally to a slower rate of reaction. After the minimum temperature, there is a slow increase until the adiabatic temperature is reached. This appears to be a general phenomena and is characterized by concentrations of additives at the 15-30% by volume level. Calculations on the basis of Westbrook's model reproduce the temperature decrease during explosion for methane and methanol oxidation with CF_3Br as the additive.

We have not noted any mention of this phenomenon in the literature. The explanation of the phenomena in terms of a two stage model of thermal explosion is however quite straightforward. One considers two processes $A \Rightarrow B + Q_1$, and $C \Rightarrow D - Q_2$, where Q_1 and Q_2 are reaction heats. The first represents the standard oxidation process (somewhat modified by the presence of the additive) and leads inevitably to an exponential increase in temperature. The second reaction, involving the decomposition of the additive, being endothermic, and with a large activation energy does not occur until a certain high

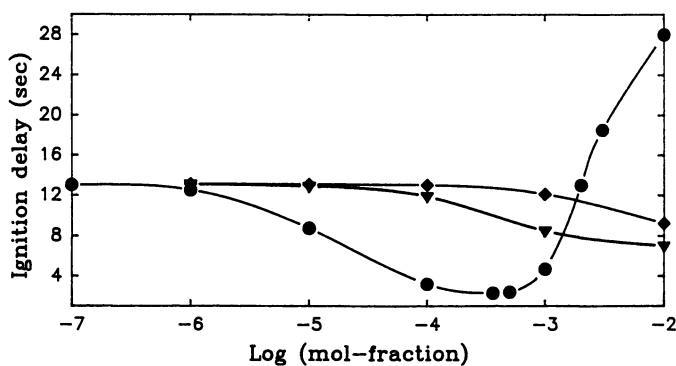


Figure 5. Dependence of ignition delay for stoichiometric methane-air mixtures at 900 K at 1 atm as a function of added inhibitors (circle)HBr, (triangle)CF₃Br, and (diamond)CF₃H.

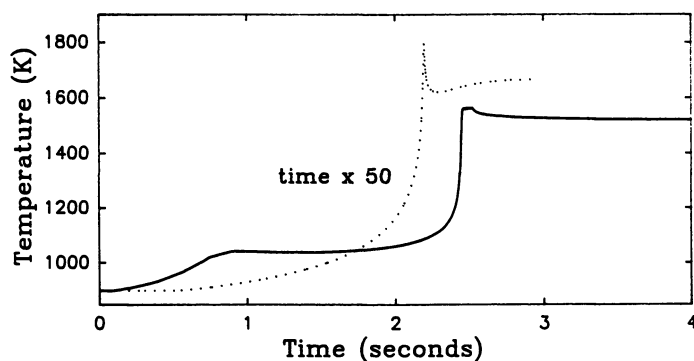


Figure 6. Dependence of mixture temperature on time for stoichiometric methane and hydrogen mixtures at 1 atm. 20% CF₃H/H₂/air, (dotted line) and 30% CF₃CFH₂/CH₄/air, (solid line)

temperature is reached. At that point, an endothermic decomposition occurs, and this absorbs much of the heat that is released. Note that the decomposition of the additive usually is connected with a large dissociation energy, hence the necessity for high temperatures. Another important property is that the decomposition products should be less reactive than the combusting mixture. In Table 2, characteristic times of unimolecular decomposition are presented for a number of inhibitors. It is seen that characteristic time of decomposition of CF_3Br of 0.1 and CF_3H of 1 ms is achieved near a temperature of 1,500 K. It has been observed that the maximum temperature may be greater or smaller than the adiabatic temperature. This is understandable in terms of different rates of heat release and the rate of reaction of the additive. Indeed, it should be emphasized that the violent changes in Figure 6 could not be possibly be simulated if only physical effects are operative. Of course the amount of additive present is very important. The consequence is however to control the magnitude of the heat of reaction. There are undoubtedly some dilution effects but the magnitude can be expected to be much smaller.

GENERAL CONSIDERATIONS

Our observations on the capabilities of flame inhibitors to decrease as well as increase induction time suggest that this is not a proper single parameter to assess the value of a compound as a fire suppressant. The former is particularly troubling since decreasing induction time is contradictory to the role of a chemical as an inhibitor. This is not surprising from a purely chemical point of view. If the stability of the inhibitor is such that appreciable quantities of reactive species are released prior to the usual conditions for the onset of combustion, then obviously there is the possibility of initiating oxidation at an earlier stage. There is indeed a large literature pertaining to the acceleratory effects arising from addition of molecules with known flame inhibiting properties to decomposing organic systems. These include slow oxidation(23-29), two-stage ignition(30), hot-wire ignition(31), exploding-wire-initiated detonation(32), ignition behind shock waves(13,33-37), and detonation (21,22,38). Presumably, there are also conditions where subsequent reactions involving radical attack on the inhibitors may prolong induction times.

Our observations of ignition delay as a function of additive concentration is of some significance. These show a shallow minimum for promotion at low concentrations followed by sharp increases in inhibitory powers as the concentration is further increased. From a chemical point of view, this must mean that there is a minimum concentration above which the chain carriers are in fact being intercepted by the inhibitor. Below this value, the process is generally that of promotion. The ultimate effect is to transform the nature of the chemistry.

The earlier work of Westbrook has identified a decrease in flame speed as a direct manifestation of inhibitory action. Although this appears to be plausible, there has not been the type of exhaustive modeling as carried out here that defines the nature of the functional relation between flame speed and additive concentrations. Obviously, decreasing the flame speed by a certain percentage does not necessarily extinguish a flame. We are currently carrying out some work to more fully explore this issue. For the present, we note that in order to fully extinguish a flame, the concentration of inhibitors must be close to that of the fuel. For example in the case of a stoichiometric mixture containing 9.5% methane, the concentration of CF_3Br necessary for extinction, from a variety of sources, ranges from 2-9%(39). In the case of propane, a 4% stoichiometric mixture requires 3-5% of CF_3Br . These observations have direct pertinence on our observations regarding the importance of

Table 1: Ignition delay for stoichiometric methane-air mixtures in the presence and absence of decomposing and non-decomposing inhibitors; 1 atm, 900K

Conditions	Ignition delay, s
CH ₄ + air	13.1
CH ₄ + air + 1%CF ₃ Br	7.0
CH ₄ + air + 1%CF ₃ Br K(CF ₃ Br=>CF ₃ +Br)=0	15.0
CH ₄ + air + 1%CF ₃ H	9.2
CH ₄ + air + 1%CF ₃ H K(CF ₃ H+M=>CF ₂ +HF+M)=0	13.8

Table 2. Characteristic time of additive decomposition at 1 atm, time in s.

T, K	1000	1500	2000
CH ₃ Br	300	2•10 ⁻³	4•10 ⁻⁶
CF ₃ Br	3	7•10 ⁻⁵	4•10 ⁻⁷
CF ₃ H	40	3•10 ⁻³	4•10 ⁻⁵
HBr	10 ⁸	80	9•10 ⁻²
Br ₂	2•10 ⁻²	2•10 ⁻⁵	6•10 ⁻⁷

endothermic decomposition reactions, setting a cap on the maximum flame temperature and even lowering it for a certain critical time period.

It should be recalled that the large-scale destruction of the inhibitor leads not only to the release of endothermicity into the reactant mixture but also the formation of new species. These may have additional inhibitory impacts. Fig. 7 illustrates the reaction pathways for CH_4 and CHF_3 conversion during the 20-30 seconds period of ignition delay starting with an initial temperature of 900 K. and at 1 atm pressure. During this time the temperature rises from 920 to 970 K. It can be seen that the CHF_3 inhibitor and its derivatives directly participate in conversion of methane and oxygen, thereby changing the reaction pathways. For example, the contribution of the reactions: $\text{CH}_3 + \text{CHF}_3 \Rightarrow \text{CF}_3 + \text{CH}_4$ and $\text{CH}_3 + \text{CF}_3 \Rightarrow \text{CH}_2\text{CF}_2 + \text{HF}$, to the overall rate of CH_3 consumption is about 50%. About 50% O_2 is consumed in the reaction $\text{CF}_2 + \text{O}_2 \Rightarrow \text{CF}_2\text{O} + \text{O}$ thus changing the oxidation of methane to that occurring in "fuel rich" conditions. CF_3 plays a very important role in converting formaldehyde to HCO and also for the decomposition of ethane via the reaction $\text{C}_2\text{H}_6 + \text{CF}_3 \Rightarrow \text{C}_2\text{H}_5 + \text{CHF}_3$. These effects arise from the fact that the additive and its decomposition fragments have reactivities that are in general not that much different from the fuel itself. Therefore it is not surprising that they should participate in the whole range of reactions that the fuel and its breakdown products can undergo. This can be readily seen from the distribution of reaction products at intermediate stages of reaction. For example at 1300 K ($T(\text{max}) = 1612$ K) we obtain the following product distribution (in percent): $\text{N}_2=46$; $\text{O}_2=6.1$; $\text{CO}_2=0.4$; $\text{CH}_4=2.2$; $\text{CHF}_3=16.9$; $\text{HF}=13.4$; $\text{CF}_2\text{O}=4.3$; $\text{H}_2\text{O}=3.5$; $\text{CO}=3.4$ (initial concentrations: $\text{CHF}_3 = 29.84$; $\text{CH}_4=6.67$; $\text{O}_2=13.3$ and $\text{N}_2=50.16$). Near the maximum temperature the analogous distribution (in percent) is: $\text{N}_2=37.7$; $\text{O}_2=0.28$; $\text{CHF}_3=2$; $\text{CO}_2=0.85$; $\text{HF}=36.6$; $\text{CF}_2\text{O}=6.1$; $\text{H}_2\text{O}=0.35$; $\text{CF}_2=1.4$; $\text{CO}=11.1$, $\text{CF}_4=1.1$. An important issue is the adequacy of the data base for the simulation systems where inhibitors are present in concentration as large as the fuel. There is need for much more work in this area.

CONCLUSIONS

We have demonstrated that flame retardants can promote as well as inhibit ignition depending on the reaction conditions. Promotion arises from the action of the decomposition products of the additives in initiating reactions and is dependent on the thermal stability of the additive and the reactivity of the decomposition product. As a result, ignition delay has a very complex dependence on concentration and reaction conditions. It is clearly unsuitable as a sole parameter for characterization of inhibitive power. Through our simulation efforts, we found that large effects appear only with large concentrations. This can lead to a stopping of rapid temperature increases during ignition and is due to the characteristic time of endothermic decomposition of the additives. The mechanism of chemical suppression of combustion at large concentrations of inhibitors appears to be due to their large heats of decomposition as well as reactions involving the interactions of the decomposition products of the inhibitor leading to the formation of less chemically active compounds. This is of course superimposed on the physical effects arising out of heat capacity and dilution effects. Finally, our simulations indicate that methane ignition is very sensitive to small changes in HBr concentration.

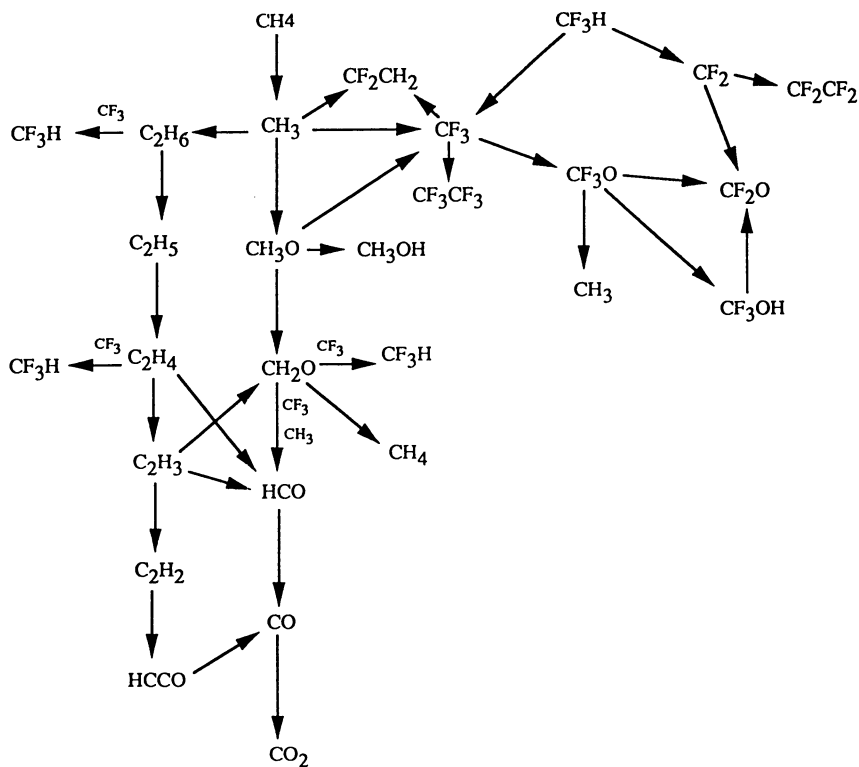


Figure 7. Reaction pathways for methane oxidation at large concentration of CF_3H additive

ACKNOWLEDGEMENTS:

This work was sponsored by the Strategic Environmental Research and Development Program (SERDP) and the Department of Defense Technology Strategy for Alternatives to Ozone-Depleting Substances by the U. S. Air Force, Navy, Army and Federal Aviation Administration.

REFERENCES

1. Miller, J. A., Bowman, C. T., *Prog. Energy and Comb.Sci.*, 15, pp.287-338, 1989
2. Egolfopoulos, F. N., Du, D. X., Law, C. K., *Combust. Sci. Technol.*, 83, pp.33-75, 1992
3. Grosshandler, W. L., Gann, R. G., Pitts, W. M. (Eds), "Evaluation of Alternative In-Flight Fire Suppressants for Full-Scale Testing in Simulated Aircraft Engine Nacelles and Dry Bays", NIST Special Publ. 861, Washington, 1994
4. Westbrook, C. K. (1983) *Combust. Sci. Technol.*, 34, pp.201-225, 1983
5. Tsang, W., Hampson, R. F., *J. Phys. Chem. Ref. Data*, 15, pp.1087-1279, 1986
6. Tsang, W., *J. Phys. Chem. Ref. Data*, 16, pp.471-508, 1987
7. Baulch, D. L., Cobos, C. J., Cox, R. A., Esser, C., Frank, P., Just, Th., Kerr, J. A., Pilling, M. J., Troe, J., Walker, R. W., Warnatz, J., *J. Phys. Chem. Ref. Data* 21, No 3., 1992
8. Mallard W. G., Westley F., Herron J. T., Hampson R. F., Frizzel D. H., NIST Chemical Kinetics Database ver. 5.0, NIST Standard Reference Database 17, Gaithersburg MD., 1993
9. Reid, I. A., Robinson, C., Smith, D. B., 20th Symp. (Int.) on Combustion, pp.1833-1843, 1984
10. Conti, R. S., Hertzberg, M., *J. Fire Sciences*, 6, pp.348-355, 1988
11. Ho, W., Yu, Q. R. Bozzelli, J. W., *Combust. Sci. Tech.* 85, pp.23-63, 1992
12. Vedeneev, V. I., Gol'denberg, M. Ya., Teitel'bom, M. A., *Kinetics and Catalysis* 28, No 5, part 2, pp.1055-1059, 1988
13. Suzuki, A., Inomata, T., Jinno, H., Moriwaki, T., *Bull. Chem. Soc. Jpn.*, 64, 3345-3354, 1991
14. Hochgreb, S., Yetter, R. A., Dryer, F. L., 23d Symp.(Int.) on Combustion, pp.171-177, 1990
15. Skinner, G. B., "Inhibition of the hydrogen-oxygen reaction by CF_3Br and CF_2BrCF_2Br ", in "Halogenated Fire Suppressants" (Gann, R. G., ed.), ACS Symp.Ser., 16, Washington, pp.295-317, 1975
16. Aronowitz, D., Santoro, R. J., Dryer, F. L., Glassman, I., 17th Symp. (Int.) on Combustion, p.633, 1979
17. Cathonnet, M., Boettner, J. C., James, H., *J. Chim. Physique*, 79, pp.475, 1982.
18. Tsuboi, T., Hashimoto, K., *Combust. Flame*, 42, pp.61-76, 1981
19. Hidaka, Y., Nakamura, T., Kawano, H., Koike, T. *Int. J. Chem. Kinet.*, 25, pp.983-993, 1993.
20. Mullins, B. P., "Spontaneous ignition of liquid fuels", Butterworths, London", 1955
21. Gmurczyk, G., Grosshandler, W., 25-th Int. Symp.on Combustion, 1994 (in press)
22. Lefebvre, M. H., Nzeyimana, E., Van Tiggelen, P. J. "Colloquium on Dynamics of Explosion and Reactive Systems", Nagoya, Japan, 1991.

23. Rust, F. F., Vaughan W. E., *Ind. Eng. Chem.*, 41, pp.2595-2616, 1949.
24. Allen, E. R., Tipper C. F. H., *Proc. Roy. Soc.(London)*, 258A, pp.251-269, 1960
25. Cullis, C. F., Fish, A., Ward, R. B., *Proc.Roy. .Soc. (London)* A276, pp.527-541, 1963
26. Kochubei, V. F., Moin, F. B., in "Inhibition of Chain Gas Reactions" (Ksandopulo, G. I., Vedennec. V. I., eds.) *Alma-Ata (in Russian)*, pp.43-49, 1971
27. Baratov, A. N., Vogman, L. P., Makeev, V. I., Poloznov, N. M., Petrova, L. D., In "Inhibition of Chain Gas Reactions" (Ksandopulo, G. I., Vedeneev, V. I.,Eds).. *Alma-Ata (in Russian)*, pp.160-172, 1971
28. Lovachev, L. A., Gontkovskaya, V. T., Ozerkovskya, N. I., *Combust. Sci. Tech.*, 17, pp.143-151., 1977
29. Parsamyan N. I., Nalbandyan A. B., in "Inhibition of Chain Gas Reactions". (Ksandopulo, G. I., Vedeneev, V. I.,eds), *Alma-Ata, in Russian*, pp.31-38, 1971
30. Moore, F., Tipper, C. F. H., *Combust. Flame* 19, pp.81-87, 1972.
31. Morrison, M. E., Scheller, K., *Combust. Flame*, 18, pp.3-12, 1972
32. Macek, A., *AIAA J.*, 1, No 8, pp.1915-1918., 1963
33. Hidaka, Y., Kawano, H., Suga, M., *Combust. Flame*, 59, pp.93-95, 1985.
34. Takahashi, K., Inomata, T., Moriwaki, T., Okazaki, S., *Bull. Chem. Soc. Japan*, 61, pp.3307-3313, 1988
35. Hidaka, Y., Suga, M., *Combust.Flame* 60, pp.233-238, 1985
36. Inomata, T., Moriwaki, T., Okazaki, S., *Combust. Flame*, 62, pp.183-191, 1985
37. Takahashi, K., Inomata, T., Moriwaki, T., Okazaki, S., *Bull. Chem. Soc. Japan*, 62, pp.636-638, 1989
38. Moen, I. O., Ward, S. A., Thibault, P. A., Lee, J. H., Knystautas, R., Dean, T., Westbrook, C. K., 20th Symp. (Int.) on Combustion, pp.1717-1725, 1984
39. Gann, R. G. (Ed.) "Halogenated Fire Suppressants" ACS Symp. Ser. 16, Washington, 1975

RECEIVED August 11, 1995

Chapter 23

The Chemical Inhibiting Effect of Some Fluorocarbons and Hydrofluorocarbons Proposed as Substitutes for Halons

F. Battin-Leclerc¹, B. Walravens¹, G. M. Côme¹, F. Baronnet¹,
O. Sanogo², J. L. Delfau², and C. Vovelle²

¹Département de Chimie-Physique des Réactions, Unité de Recherche Associée 328, Centre National de la Recherche Scientifique, INPL-ENSIC and Université de Nancy I, 1 rue Grandville, BP 451, 54001 Nancy Cedex, France

²Laboratoire de Combustion et Systèmes Réactifs, Centre National de la Recherche Scientifique and Université d'Orléans, 1C Avenue de la Recherche Scientifique, 45071 Orléans Cedex 2, France

Experimental and modelling studies of the inhibiting effects of different fluorocarbons and hydrofluorocarbons have been performed on two reaction systems:

* Oxidation of methane or ethane in isothermal reactors: contrary to CF₃Br, no effect of these fluorinated compounds on the conversion of methane was observed in a temperature range from 773 to 1573 K.

* Low pressure methane premixed flames: the efficiency of the inhibitors was quantified by measuring their effects on the flame temperature profiles and on the flame velocities. Comparisons of the flame structure between the flames with and without added inhibitor were performed for C₂F₆ and C₃F₇H.

These results were used to understand the mechanism of action of these fluorinated inhibitors and to distinguish the physical and the chemical contribution in their fire suppression effectiveness.

Due to their particularly high ozone depletion potential (O.D.P.), the production of halons, such as CF₃Br, largely used as fire-extinguishing agents, has been stopped (1-1-1994) to comply with the Copenhagen amendments of the Montreal Protocol. Previous studies (1) have indicated that viable alternative compounds to halons be found among the following types of compounds:

(a) partially chlorinated or brominated hydrocarbons such as the hydrochlorofluorocarbons (HCFCs): the addition of 11 % of CF₃CFHCl (HCFC 124) is required to extinguish an ethanol flame in a cup burner (1) and 4.1 % of CHF₂Br is required to extinguish a n-heptane flame in a cup burner (2)

(b) the perfluoroalkanes (FCs): the addition of 6.1 % of CF₃CF₂CF₃ (FC 218) is required to extinguish a n-heptane flame in a cup burner (3),

0097-6156/95/0611-0289\$12.00/0
© 1995 American Chemical Society

(c) the hydrofluoroalkanes (HFCs): the addition of 3% of CF_3H has an inhibiting effect on a $\text{H}_2\text{-O}_2$ premixed flame (4), the addition of 8.5 % of $\text{CF}_3\text{CFHCF}_3$ (HFC 227e) is required to extinguish an ethanol flame in a cup burner (1).

Compounds of type (a) will have lower ozone depletion potentials (O.D.P.) than halons since the presence of hydrogen in the molecule makes them susceptible to react with OH in the lower atmosphere (5,6). This reduces their life time in the atmosphere and a smaller fraction of the parent compound compared to the CFCs will therefore reach the stratosphere to cause ozone loss. But, nevertheless, as the presence of chlorine or bromine in the molecule does not lead to zero O.D.P., the production of these compounds are scheduled to be phased out by 2030, even sooner in the case of hydrobromofluorocarbons, to comply with the Copenhagen amendments of the Montreal Protocol.

Conversely, compounds of type (b) and (c) are considered as suitable replacements since they contain no chlorine or bromine and will therefore have no effect on ozone depletion.

Therefore, with the purpose of determining halon substitutes which have optimal properties as fire-extinguishing agents, the objectives of the present study are:

* To produce reliable experimental data concerning the ability of some representative FCs and HFCs to inhibit oxidations and flames of model hydrocarbons (mainly CH_4),

* To improve the understanding of the mechanism of the inhibition of combustions and oxidations by these FCs and HFCs and to develop correctly validated mechanistic models which permit the prediction of the inhibition induced by the addition of these halogenated compounds.

Experimental procedure

These experimental studies were performed by two complementary approaches which allowed a temperature range from 600 to 2000 K to be covered:

In this work, temperatures were regulated by P.I.D. regulators and gas flows by mass flow controllers or monitored by sonic orifices and rotameters. The halogenated compounds used in this study were provided by Elf-Atochem (France).

Inhibiting effect on oxidation reactions. The studies of the inhibiting effect of halogenated compounds on the gas-phase oxidation reactions were performed by the following methods:

* Measurement of autoignition delays of mixtures (7.8 kPa O_2 , 7.8 kPa n-pentane, 1.3 to 2.6 kPa halogenated compound) at 573 K in a batch pyrex reactor (spherical, vol: 350 cm^3) by following the temperature rise using a thermocouple located inside the vessel,

* Plotting reactant conversions versus space time for mixtures, Helium : Methane (Ethane for temperature below 900 K): Oxygen : (+ Halogenated compounds) = 1000 : 100 : 100 : (+ 2 to 8) (volumic flow), flowing through one of the two following types of isothermal flow reactors operated at atmospheric pressure:

- Jet stirred reactor (internal volume 86 cm^3) made of quartz and heated by means of electrically insulating resistors directly coiled on the vessel (7), with space times ranging from 1 to 7 seconds for temperatures from 773 to 1223 K,

- Tubular reactor (length: 52 cm, internal diameter: 0.7 or 1.5 mm) made of alumina and located in a high temperature furnace (Vecstar Furnace), with residence times in the heated area (length 15 cm) ranging from 0.5 to 50 milliseconds for temperature from 1373 to 1573 K. In these conditions, the flow was laminar and the maximum pressure drop was around 0.4 bar. The temperatures were measured using a Pt-Pt 10% Rh thermocouple located inside the tube of 1.5 mm diameter.

The analyses were performed by gas chromatography with detection by thermal conductivity (CO , CO_2 , O_2) or by flame ionisation (CH_4 , C_2H_2 , C_2H_4 , C_2H_6 , CF_3H

and CH_2CF_2). For each sample, carbon balance was checked and agreement was obtained within 5 %.

Inhibiting effect in flames. The effects of the halogenated compounds on flames were shown in the following ways:

* Measurements of the velocity in an open tubular burner (length 50 cm, i.d. 1.4 cm, these conditions ensured that a fully developed velocity profile was obtained at the burner exit) of a flame, Nitrogen : Methane: Oxygen = 122.0 : 16.3 : 32.6 (flow rate) stabilized at atmospheric pressure. The flame velocity was derived from the ratio F/A, with F: overall flow rate and A: area of the flame front measured from pictures of the flame.

* Measurements of the temperature profile on a laminar flame stabilized at a pressure of 4.2 kPa using a Pt-Pt 10% Rh thermocouple (wire diameter: 50 μm) with a refractory coating ($\text{BeO}\text{-Y}_2\text{O}_3$); the measured values were corrected by taking into account the radiative heat losses. The flames were fed by mixtures, Argon : Methane: Oxygen : (+ Halogenated compounds) = 0.681 : 0.103 : 0.216 : (until + 0.03) (mole fraction).

* Comparison of the mole fraction profiles: Two types of premixed flames have been stabilized (pressure 4.2 kPa) : Flame of type I: Argon : Methane: Oxygen = 0.49 : 0.17 : 0.34 (mole fraction), Flame of type II: Argon : Methane: Oxygen : Halogenated compounds = 0.486 : 0.168 : 0.336 : 0.01 (mole fraction). For both flames, the unburned gases velocity (at 298 K and 4.2 kPa) was equal to 53.7 cm s^{-1} . The burner could be moved vertically and the flat flame was sampled along its symmetry axis with a quartz cone (aperture diameter 0.1 mm, angle 60°). Sudden expansion across the cone orifice created a supersonic jet that preserved atoms and radicals. After selection of its central part by a skimmer and modulation by a chopper wheel, the jet entered the ionisation source of a quadrupole mass spectrometer. Care was taken to avoid fragmentation by using very low electron energies for intermediate species. Signal from the mass spectrometer had to be corrected for residual gas and isotopic contributions before conversion into mole fractions. This conversion required calibration factors obtained by direct measurements of mixtures of known composition for stable species and by calculation of ionisation cross sections for atoms and radicals. H, O and OH were calibrated by assuming partial equilibrium for some reactions of the H_2/O_2 system in the post combustion area.

The low pressure flat flame burner and molecular beam mass spectrometry (MBMS) apparatus used in this study has been described in previous publications (8,9). The burner matrix was made of a brass disc drilled with 1mm diameter holes on a 9 cm diameter circular area and cooled by water circulation.

Experimental results

Inhibiting effect on oxidation reactions

Autoignition delays in n-pentane-oxygen mixtures at 573 K. The additions of C_3F_8 (FC 218), CF_3H (HFC 23) or CF_3Br (halon 1301) as a reference, had no more effect than the additions of the same amounts of helium or nitrogen. It seemed thus that there was no inhibiting effect of halogenated compounds on the autoignition delays in n-pentane-oxygen mixtures at 573 K.

Influence on ethane oxidation between 773 and 873 K. The inhibiting influence of addition of 4 % (with respect to ethane) of CF_3Br , C_3F_8 (FC 218) and $\text{C}_3\text{F}_7\text{H}$ (HFC 227e) on the ethane oxidation has been investigated at a space time of 1.3 second, corresponding to ethane conversion from 2 to 60 %.

The addition of C_3F_8 and $\text{C}_3\text{F}_7\text{H}$ which are the most efficient non-brominated compounds during the cup burner tests (1) and that of CF_3Br has no effect both on the

conversion of the reactants (Figure 1a displays the results concerning the conversion of ethane) and on the formation of the products, C_2H_4 , CO, CO_2 and CH_4 (Figure 1b displays the results concerning CO).

Influence on methane oxidation between 973 and 1223 K. Figure 1c displays the conversion of methane without any additive, in the presence of 8% (with respect to methane) of C_2F_6 (FC 116) or C_3F_8 (FC 218) and, for comparison, with addition of 2% CF_3Br (10); Figure 1d shows the conversion of oxygen (as some HFCs led to the formation of CF_2H_2 which was not completely separated from CH_4 in the GC analyses, it was more quantitative to make this comparison on the conversion of oxygen) without any additive, in the presence of 8% CF_3H (HFC 23), C_2F_5H (HFC 125), $C_2F_4H_2$ (HFC 134a) or C_3F_7H (HFC 227e) and, to compare, with addition of 2% CF_3Br . The data in Figures 1c and 1d were obtained at a space time of 4.8 s, corresponding to methane conversion from 10 to 70 %.

These two latter figures suggest that, unlike CF_3Br , none of the FCs or HFCs studied has any inhibiting effect on the methane oxidation in this temperature range.

However, these fluorinated compounds react in the methane-oxygen system. Indeed, the analysis of CF_3H (the only reaction product which can be observed by flame ionisation detection) shows that, at 1173 K, 90% of this product is consumed. At 1173 K, the major products obtained are HF (this product has not been directly analysed but the significant erosion of the quartz end of the reactor provides an evidence of its presence), CO and CO_2 .

Influence on methane oxidation between 1373 and 1573 K. In these experimental conditions, at 1573 K, for a residence time around 1.5 ms, the methane oxidation reaches a reactant conversion higher than 90 % and leads to around 80 % CO, 10 % CO_2 and 9 % C_2H_2 .

Figure 2 displays the conversion of methane without any additive, in the presence of 8% (with respect to methane) of CF_3H (HFC 23), C_3F_7H (HFC 227e) or C_3F_8 (FC 218) and, for reference, with addition of 8% CF_3Br , at 1573 K for residence times from 0.7 to 3 ms (Figure 2a), at 1473 K for residence times from 3.5 to 12 ms (Figure 2b) and at 1373 K for residence times from 13 to 35 ms (Figure 2c).

It appears that, in this temperature range, fluorinated compounds have no effect on the methane oxidation and CF_3Br has a rather promoting effect.

It is interesting to note that at these high temperatures, the chromatographic analyses showed the complete consumption of CF_3H , but the amounts of CO and CO_2 formed are the same without and with addition of 8% (with respect to methane) fluorinated compounds and the formation of neither CF_3H nor $CF_2=CH_2$ was observed.

Inhibiting effect on flames

Study of the inhibiting efficiency. The evaluation of the efficiency of the different inhibitors studied (C_2F_6 (FC 116), C_3F_8 (FC 218), $C_2F_4H_2$ (HFC 134a), C_3F_7H (HFC 227e) and as a reference for CF_3Br) was performed by two different methods:

* Measurements of the flame maximum temperature: The maximum temperature of the flame exhibits a linear increase (inhibitors increase flame temperatures because they modify the heat transfer between the flame and the burner and because they release heat when they react as their consumption is exothermic) as a function of the inhibitor concentration (see Figure 3a in the case of C_3F_8); the slopes vary according to the inhibitor and the fresh gases velocity that is to say the initial temperature of the flame without inhibitor.

* Measurements of the flame velocity (except for C_3F_7H (HFC 227e)): An increase in the concentration of additive leads to a linear decrease in the flame velocity. The inhibitor amounts needed either to produce a temperature increase of 100 K (in a

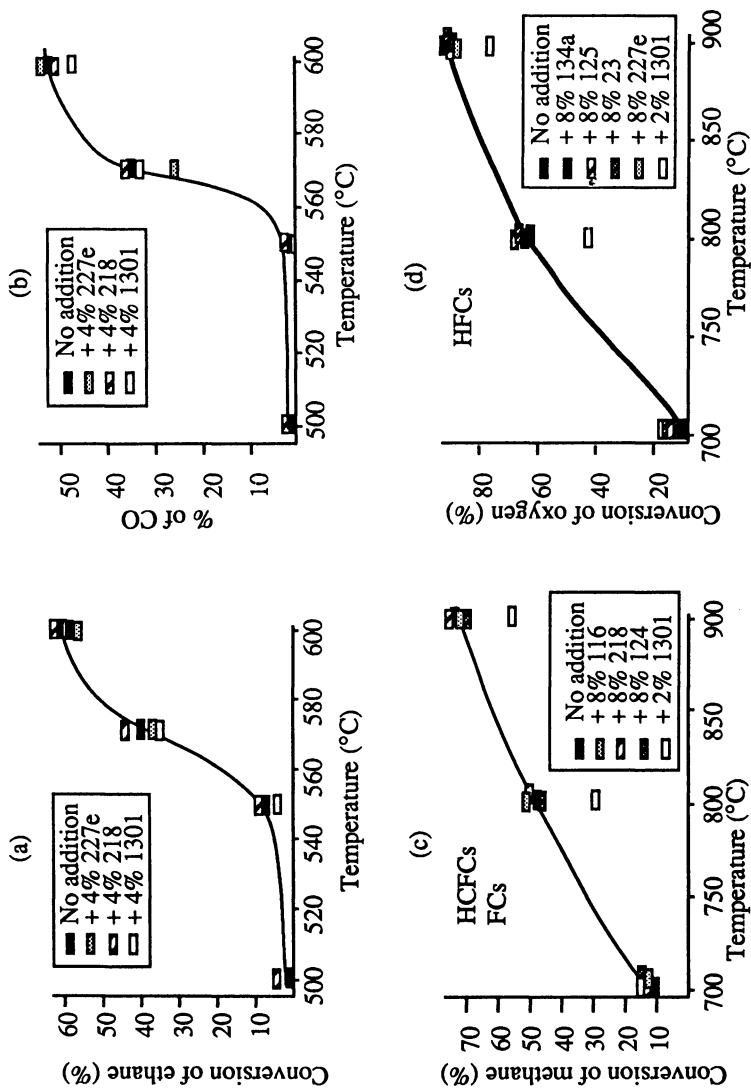


Figure 1 : Influence of the addition of halogenated compounds on the oxidation of ethane and methane between 773 and 1273K.

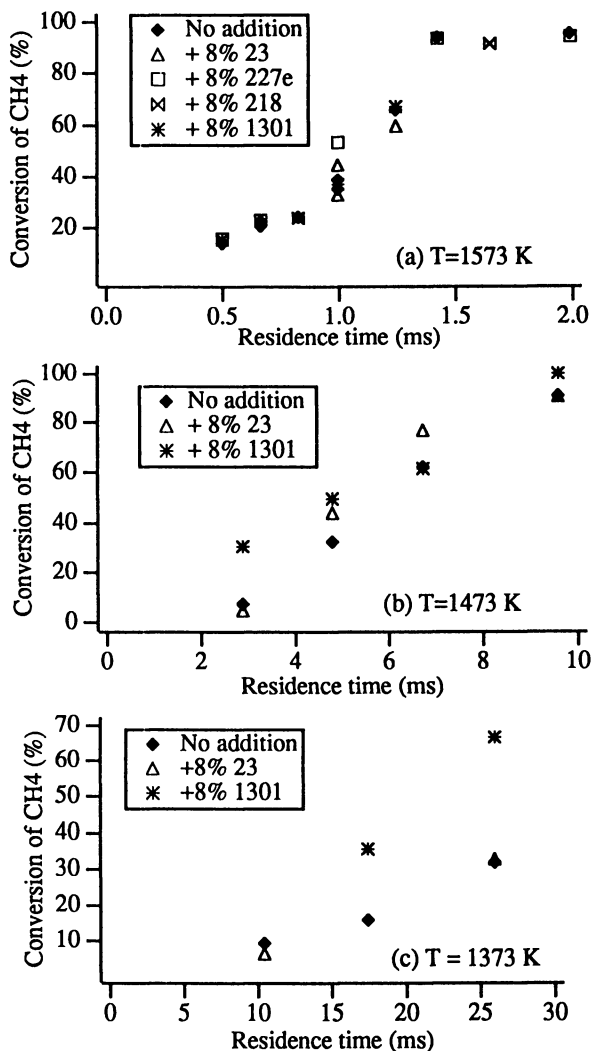


Figure 2 : Influence of the addition of halogenated compounds on the oxidation of methane between 1373 and 1573 K.

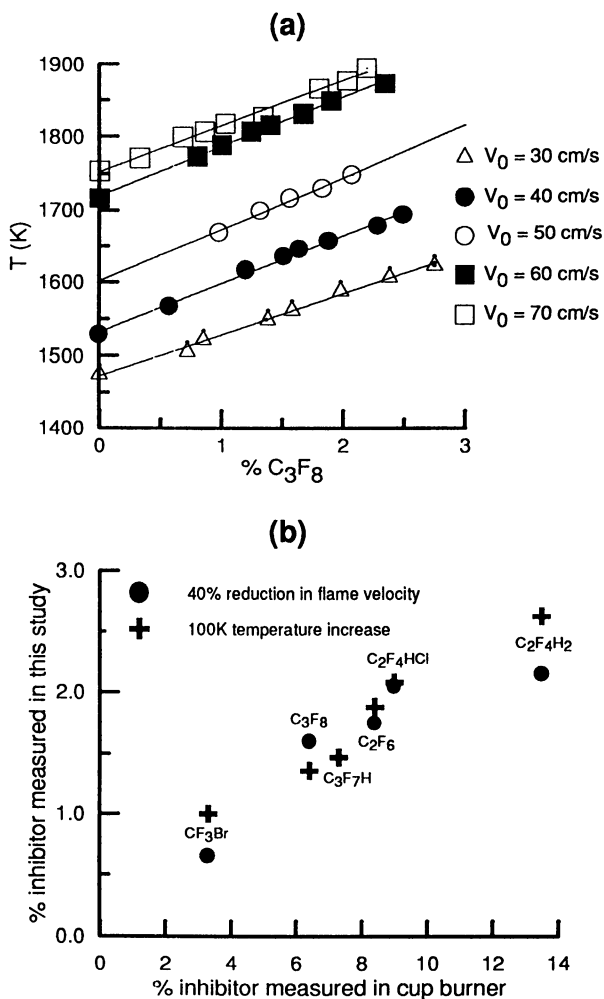


Figure 3 : a: Evolution of the maximum flame temperature versus inhibitor concentration ; b: Inhibiting efficiency deduced from the flame temperature and velocity measurements correlated with experiments performed in the cup burner.

Downloaded by NORTH CAROLINA STATE UNIV on October 1, 2012 | http://pubs.acs.org
 Publication Date: May 5, 1997 | doi: 10.1021/bk-1995-0611.ch023

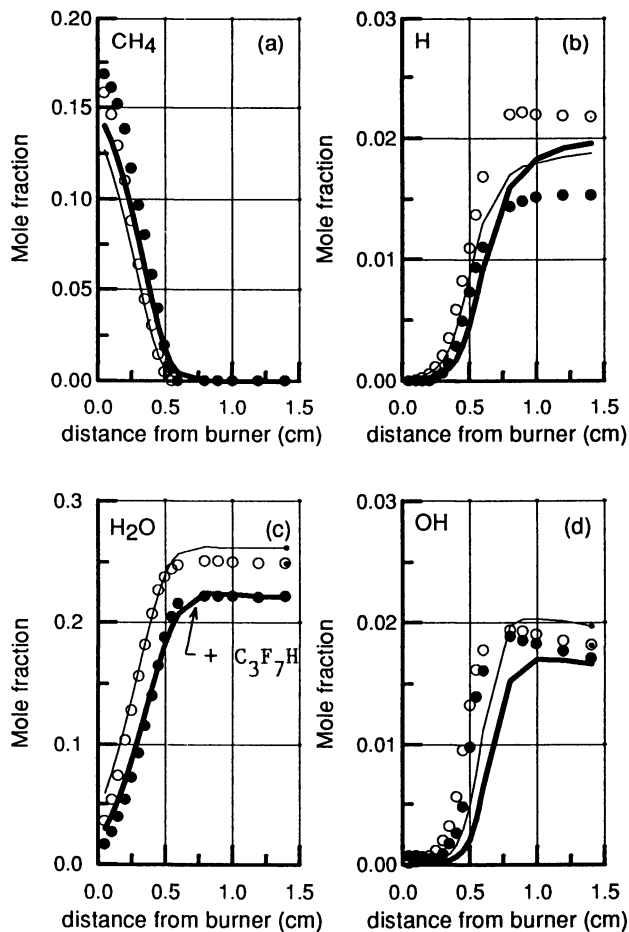


Figure 4 : Influence of C_3F_7H on species profiles in a methane flame: Comparison between model (curves) and experiments (points); the profiles with addition of C_2F_6 are to be published (28).

flame with a velocity of 50 cm s^{-1} which can be considered as close, in velocity and temperature (around 1700 K), to the diffusion flame used in the cup burner) or to give a 40 % reduction of the flame velocity, have been plotted versus the quantity of inhibitor necessary for the extinguishment of a n-heptane flame in a cup burner (11) (Figure 3b). This latter figure shows that there is a good correlation between the results of this study and those obtained in a cup burner and points out that (except for CF_3Br) the efficiency of the fluorinated compounds increases with the number of fluorine atoms in the molecule and that the presence of hydrogen does not reduce the inhibiting effect.

Flame structure determination. Comparison between the mole fraction profiles obtained in flames of type I and in flames of type II seeded respectively with $\text{C}_3\text{F}_7\text{H}$ (HFC 227e) or C_2F_6 (FC 116) showed the following effects of the additives on the species formed in methane combustion :

- * Slight delay in the consumption of methane (Figure 4a) and oxygen, and in the formation of H_2O (Figure 4c) and CO_2 ; this effect was lower in the case of C_2F_6 addition,

- * Important reduction of the formation of H_2O (Figure 4c) and augmentation of the final mole fraction of CO ,

- * Reduction of the active species concentrations, H (Figure 4b), OH (Figure 4d) and O in the burned gases.

The consumption of the fluorinated reactants (Figure 5a), (the consumption of $\text{C}_3\text{F}_7\text{H}$ was faster than that of C_2F_6) led mainly to the formation of HF (Figure 5b), CF_2O (Figure 5c) which was slowly consumed and CF_2CH_2 and CF_2 (Figure 5d) which reacted very rapidly. Minor products included CF_3 (if CF_3 was formed by cracking, it could only derive from the inhibitor and, in this case, the shape of its profile should be similar to that of the inhibitor) and CF_2H , C_2F_4 and $\text{C}_2\text{H}_3\text{F}$ in the case of $\text{C}_3\text{F}_7\text{H}$ addition. The mole fractions of CF_2CH_2 , CF_2 and CF_3 were substantially lower in the case of C_2F_6 seeded flames.

To summarize, the main results of this experimental work are:

- * No inhibiting effect of the FCs and HFCs studied on methane or ethane oxidation is observed in a temperature range from 573 to 1573 in reactors in which the physical effects had no influence,

- * An inhibiting effect of the FCs and HFCs studied, lower than that of CF_3Br , and a slight effect of these additives on the mole fraction profiles is observed in low pressure methane flames.

Modelling of the effect of C_2F_6 (FC 116) and $\text{C}_3\text{F}_7\text{H}$ (HFC 227e) in flames

With the purpose of understanding the action of fluorinated compounds, a mechanistic model of the effect of C_2F_6 and $\text{C}_3\text{F}_7\text{H}$ in flames was built and validated using the flame structure data.

Computational tools and mechanisms used. Computation of the mole fraction profiles was performed with Warnatz's code (12).

The mechanism for the methane-oxygen system was based on the mechanism proposed by Warnatz (13) for the combustion of alkanes, with minor changes aimed at updating the kinetic data for some reactions (14,15).

The mechanism of consumption of fluorinated compounds was based on a mechanism developed by Westbrook (16) to model the action of CF_3Br ; this mechanism had been previously validated against flame structure data (9). This mechanism was the first one to include the reactions induced by CF_3 and its by-products. Recent attempts of modelling using a simplified version of the mechanism written at NIST (17) were performed, but no noticeable changes were observed.

The reactions leading to CF_3 from the fluorinated reactants had to be added. In the

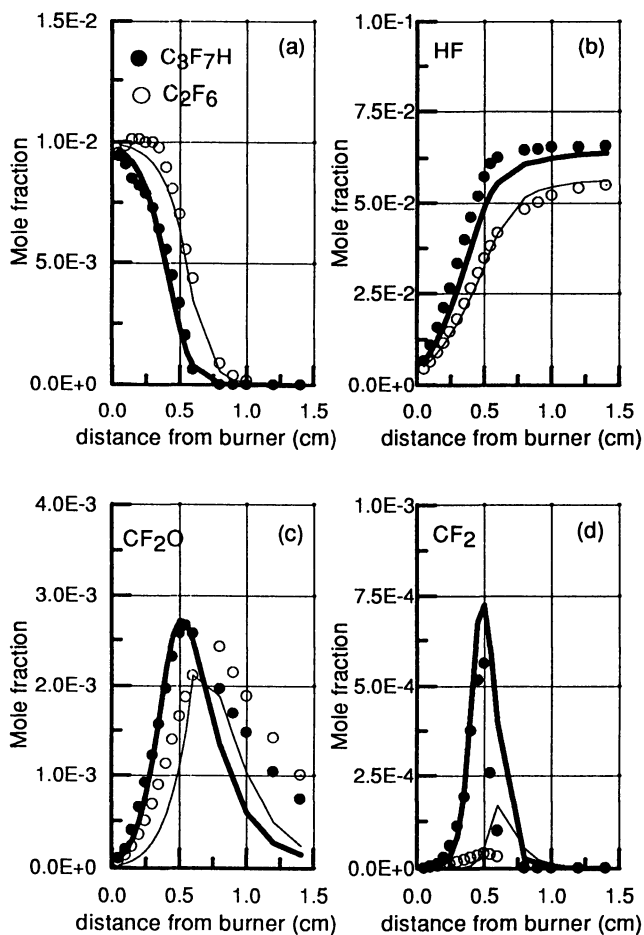
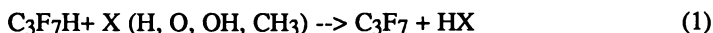


Figure 5: Halogenated species profiles in a methane flame seeded by C_3F_7H and C_2F_6 : Comparison between model (curves) and experiments (points).

case of C₃F₇H, the consumption reactions were assumed to be, by analogy with the reactions of propane :



The values of the rate constants of reactions (1) and (2) were chosen equal to those for the equivalent reactions with propane (18,19,20); the rate coefficients of reactions (3), (4) and (5) were respectively the values determined by Schug (21), by Umemoto (22) and an estimated value.

In the case of C₂F₆, the consumption reaction was:



The kinetic parameters of this reaction were calculated from the reverse reaction data using the thermochemistry.

For reactions in the fall-off pressure regime, the rate constants at 4.2 kPa were calculated using the formalism of Troe (23).

Comparisons model-experiments. Figures 4 and 5 present a comparison between the experimental and computed mole fraction profiles for flames of type I and flames of type II seeded respectively by C₃F₇H (HFC 227e) and C₂F₆ (FC 116). The agreement between the model and the experiments is globally satisfactory for almost all the species either formed in methane combustion or derived from the fluorinated reactants.

This mechanism (with recalculation of the 1 atm. rate constant for reactions in fall-off pressure regime) is used to model the effect of inhibitor addition on flame velocities and a good agreement is obtained between the measured and computed values.

This model, used to perform sensitivity analyses on flame velocities, data which were shown to be directly connected with the inhibitor efficiencies, represented then a valuable tool to understand the fire-extinguishing action of fluorinated compounds.

Discussion on the mechanism of inhibitors action

Two types of mechanism have been proposed in the literature to explain the extinguishing effect of combustion inhibitors:

- * A mechanism of physical extinguishment in which the flame would be cooled down by dilution with an inert gas,

- * A chemical action in which the inhibitor would influence the branching reactions and would prevent the flame to be self-sustained by radical multiplication.

Physical effect. A calculation of the inhibitor concentration (%) needed to extinguish a n-heptane flame in cup-burner was performed taking into account only the physical effect according to the method proposed by Sheinson (2).

Calculation method. When the heat losses decrease the flame temperature until a temperature area below 1600K (temperature below which the combustion can no more self-sustain according to Huggett (24)), the flame energy loss corresponds

mainly to the enthalpy $\Delta H'$ (normalized per oxygen mole) needed to heat the nitrogen and the inhibitor agent from 298 to 1600K which is given by equation {1}

$$\Delta H' = \Delta H'_{(\text{air})} + \left(\frac{X_A}{X_{O_2}} \right) \int_{298}^{1600} C_{PA} T dT \quad \{1\}$$

With: $\Delta H'_{(\text{air})}$: enthalpy (normalized per oxygen mole) needed to heat the nitrogen from 298 to 1600K, $\Delta H'_{(\text{air})} = 38 \text{ kcal (mol. O}_2\text{)}^{-1}$ (2),
 X_A : Mole fraction of the inhibitor agent in the gas mixture,
 X_{O_2} : Mole fraction of oxygen in the gas mixture, $X_{O_2} = 0,21 (1 - X_A)$, 0,21 being the mole fraction of oxygen in air,
 $C_{PA}^{(T)}$: Heat capacity of the inhibitor agent at temperature T.

The mole fraction of inhibitor agent is then given by equation {2}:

$$X_A = \frac{\Delta H'*(0,21) - 7,9}{\int_{298}^{1600} C_{PA}^{(T)} dT + \Delta H'*(0,21) - 7,9} \quad \{2\}$$

Comparison between experimental and calculated concentrations. As 16 % of CF_4 , compound which has only a physical effect (Sheinson had observed that addition of CF_4 in flames did not form any HF (2)), were needed to extinguish a n-heptane flame, a value of $64 \text{ kcal (mol. O}_2\text{)}^{-1}$ was deduced for $\Delta H'$; this value was used to calculate the required concentrations of the other halogenated additives.

Table I presents a comparison between the experimental and calculated concentrations of halogenated additives required to extinguish a n-heptane flame. It appears that the calculated values agree with the experimental data within about $\pm 20 \%$, except in the case of CF_3Br .

Therefore, this approach leads to think that , contrary to that of brominated compounds, the inhibiting effect of fluorinated inhibitors would be mainly due to their important heat capacity and this would explain the experimental results obtained in reactors in which the physical effects have no influence.

Table I : Experimental and Calculated Concentrations of Halogenated Additives Required to Extinguish a n-heptane Flame

A	C_{PA}					$\int_{298}^{1600} C_{PA} T dT$ (kcal/mol)	X A (calculated) (%)	X A (cup burner) (%)(1)
	300K	500K	800K	1000K	1500K			
CF_4	14,6	19,3	22,6	23,6	24,8	28,8	-	16,0
C_2F_6	25,4	33,3	38,3	39,8	41,4	47,3	10,4	8,4
C_3F_8	35,4	46,5	54,7	56,6	59,7	69,4	7,4	6,4
$\text{C}_3\text{F}_7\text{H}$	32,7	43,6	51,7	54,0	59,9	66,7	7,7	7,3
$\text{C}_2\text{F}_4\text{H}_2$	20,8	28,3	34,5	36,6	42,5	45,2	10,9	13,5
$\text{C}_2\text{F}_4\text{HCl}$	21,7	-	-	-	-	47,2 ^b	10,5	9,0
CF_3Br	16,6	-	-	-	-	32,7 ^c	14,5	3,3

^aHeat capacities ($\text{cal mol}^{-1} \text{K}^{-1}$) are estimated by using the programme THERGAS (25) based on the methods proposed by S.W. BENSON (26),

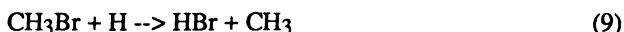
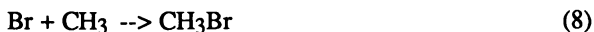
^bCalculated assuming the same temperature dependence as $\text{C}_2\text{F}_4\text{H}_2$,

^cCalculated assuming the same temperature dependence as CF_4 .

Inhibiting effect of brominated compounds. Before trying to draw a conclusion on an eventual chemical inhibiting effect of the fluorinated compounds, the mechanism of the inhibiting action of brominated compounds must be mentioned.

Previous studies in the literature (16,27) or performed in our laboratories have shown that the inhibiting effect of brominated compounds comes from the following inhibiting cycles:

* In slow oxidation systems around 1100 K (10) :



* In flames (9) :



These inhibiting cycles induced by HBr, product which is rapidly formed in the combustion of every brominated compound, bring an additional terminating channel for H atoms which directly competes with the branching step (13) and then explain the inhibiting effect of brominated compounds.



Chemical inhibiting effect of fluorinated compounds. Aiming at showing a possible chemical effect of fluorinated inhibitors in flames, simulations of flame velocities were performed by varying respectively C_{pA} and X_A (from $X_A = 1\%$), using $\text{C}_3\text{F}_7\text{H}$ as an inhibitor. The results given in Table II show that a same change in C_{pA} and X_A does not produce the same effect, the changes in X_A are more effective, which is certainly due to some influence of the chemistry in the flame.

Table II: Influence of C_{pA} and X_A on the Flame Velocity (V_f)

Parameter	$C_{pA} * 2$	$C_{pA}/2$	$X_A * 2$	$X_A/2$
$\Delta V_f/V_f$	- 0.12	+0.05	-0.37	+ 0.26

Sensitivity analyses on the flame velocities show that the main reaction channels responsible for the inhibiting effect of $\text{C}_3\text{F}_7\text{H}$ and C_2F_6 would be those involving CF_3 and CF_2 .

Indeed, the analyses of the reaction rates reveal that $\text{C}_3\text{F}_7\text{H}$ and C_2F_6 would be rapidly consumed to give CF_3 and CF_2 .

The major reaction of CF_3 would be:



and the main channels consuming CF_2 would be:



followed by the reaction of CF_2O , CF and FCO



Sensitivity analyses showed an important inhibiting effect of reaction (14), (17), (18), (20) and (21) which trap H and OH radicals to form HF. These reactions would then be responsible for a chemical inhibiting effect of fluorinated compounds taking place only in flames where the radical concentrations are very high. In these series of reactions, contrary to brominated compounds, the inhibitor would not be regenerated and therefore this chemical effect would remain relatively limited compared to the physical influence.

This modelling must be considered as a first attempt, since the mechanism proposed by C.W. Westbrook (16) would really need to be up-dated by using new kinetic data and completed by considering the new reactive species (such CF_2H ,...) which might certainly appear in reactions of hydrofluorocarbons.

Acknowledgements

Financial support from Elf-Atochem, Centre d' Application de Levallois (France) and from the European Commission, DG XII (Environment Programme) is gratefully acknowledged.

Literature Cited

1. Sallet D. (ATOCEM), European Patents n° 91404348.7, n° 91401350.3 and n° 91401349.5, 1991.
2. Sheinson R.S. and Driscoll D.C., Poster abstract, *23rd Symposium (Int.) on Combustion*, The Combustion Institute, 1990.
3. Sheinson R.S., Penner-Hahn J.E. and Indritz D., *Fire Safety J.* 1989,15, 437.
4. Richter H., Vandooren J. and Van Tiggelen P.J., *Bull. Soc. Chim. Belg.* 1990, 89 n°7, 491.
5. Gierczak T., Talukdar R., Vaghjiani G.L., Lovejoy E. R. and Ravishankara A.R., *J. Geophys. Research* 1991, 96 NO. D3, 5001.
6. Talukdar R., Mellouki A., Gierczak T., Burkholder J.B., McKeen S. and Ravishankara A.R., *Science* 1991, 252, 693.
7. Battin F., Dzierzynski M., Marquaire P.M., Côme G.M. and Baronnet F., *Bull. Soc. Chim. Belg.* 1990, 99 n°7, 473.
8. Delfau J.L., Bouhria M., Reuillon M., Sanogo O., Akrich R. and Vovelle C., *23rd Symposium (Int.) on Combustion*, The Combustion Institute, 1990, 1567.
9. Sanogo O., Thèse de l'université D'Orléans, 1993.
10. Battin-Leclerc F., Côme G.M. and Baronnet F., *Comb. Flame* 1994, 99, 11.

11. Bourgeois C., Sallet D. and Macaudière S., ELF-ATOCHEM, personal communication, 1991.
12. Warnatz J., *18th Symposium (Int.) on Combustion*, The Combustion Institute, 1981, 369.
13. Warnatz J., *20th Symposium (Int.) on Combustion*, The Combustion Institute, 1984, 845.
14. Bastin E., Delfau J.L., Reuillon M., Vovelle C. and Warnatz J., *22nd Symposium (Int.) on Combustion*, The Combustion Institute, 1988, 313.
15. Baulch D.L., Cobos C.J., Cox R.A, Esser C., Franck P., Just Th., Pilling M.J., Troe J., Walker R.W. and Warnatz J.; Evaluated Kinetic Data for Combustion Modelling, *J. Phys. Chem. Ref. Data* 1992, vol 21, n^o2 .
16. Westbrook C.K., *Combust. Sci. and Technol.* 1983, 34, 201.
17. Zachariah M.R., Westmoreland P.R., Burgess Jr. D., TsangW. and Melius C.P., National Institute of Standards and Technology, personal communication, 1994.
18. Walker R.W., *Int. J. Chem. Kin.* 1985, 17, 573.
19. Westbrook C.K., *Prog. Ener. Comb. Sci.* 1984, 10,1.
20. Hidaka Y., Oki T. and Kawano H., *Int. J. Chem. Kin.* 1989, 21 , 689.
21. Schug K.P. and Wagner H. Gg., *Ber. Buns. Phys. Chem.* 1978, 82, 719.
22. Umemoto H., Sugiyama Tsunashima S. and Sato S., *Bull. Chem. Soc. Jpn.* 1985, 58,1228.
23. Troe J., *Ber. Buns. Phys. Chem.* 1974, 78, 478.
24. Huggett C., *Comb. Flame* 1973, 20 ,140.
25. Muller C., Scacchi G. et Côme G.M. In *The role of data in scientific progress*, Glaeser P.S., Ed.; Elsevier, Amsterdam,1985.
26. Benson S.W., *Thermochemical Kinetics*, 2nd ed., John Wiley, Ed; New York 1976.
27. Biordi J.C., Lazzara C.P. and Papp J.F., *J. Phys. Chem.*1978, 82 n^o2, 125.
28. Sanogo O., Delfau J.L., Akrich R. and Vovelle C., *25th Symposium (Int.) on Combustion*, The Combustion Institute, 1994 in press.

RECEIVED June 12, 1995

Chapter 24

Flame Inhibition of Current Fire Extinguishers and of Potential Substitutes

H. Richter, P. Rocteur, J. Vandooren, and P. J. Van Tiggelen

Laboratoire de Physico-Chimie de la Combustion, Université Catholique de Louvain, Place Louis Pasteur 1, B-1348 Louvain-la-Neuve, Belgium

The replacement of the commonly used fire extinguishers CF_3Br and CF_2ClBr has prompted the search for new inhibitors that are less damaging to the ozone layer but as active to inhibit combustion. In this paper, four approaches are considered : 1) Influence of additives on the burning velocities, 2) Structures of inhibited flame , 3) Chemi-ionization in flames with inhibitors, 4) Numerical modeling of inhibited flame systems. From the data, a simplified chemical inhibition mechanism is discussed and the role of the bromine chemistry in inhibition is emphasized. All substitutes suggested so far that are harmless to the ozone layer are not efficient enough to replace halon 1301.

After the discovery of the probable contribution of chlorofluorocarbons to stratospheric ozone depletion in 1974 by Molina and Rowland [1], the scientific debate led to the regulation of most of these compounds in the Montreal Protocol [2]. Replacement of the commonly employed fire extinguishers CF_3Br and CF_2ClBr has been required also because their production was discontinued as of January 1994. The search became essential for other compounds less damaging to the ozone layer but active as flame extinguishers. To move beyond experiments which essentially check the macroscopic phenomena of fire extinction as a function of the amount of extinguisher added [3], more detailed studies have been conducted in order to reach a better understanding of the chemical and physical processes responsible for flame inhibition. Four approaches have been used:

- 1) The influence of added compounds on the burning velocities of several flammable mixtures,
- 2) The analysis of inhibited flame structures,
- 3) The chemi-ionisation in flames seeded with inhibitors,
- 4) The numerical modeling of flame systems.

0097-6156/95/0611-0304\$12.00/0
© 1995 American Chemical Society

It is worth mentioning that numerical modeling of combustion phenomena cannot be considered to be a really independent approach because it requires the knowledge of a chemical reaction mechanism with the corresponding rate coefficients of the investigated combustion system. Therefore, experiments have to be performed to check the validity of the suggested reaction mechanism, for which a large number of rate coefficients are not known to a satisfactory degree of accuracy.

1) Burning Velocities

Simmons and Wolfhard [4] as well as Garner et al. [5] were the first authors to notice the decrease of the burning velocities of ethylene/air [4] and methane/oxygen [5] flames when halogenated methane derivatives are added to the mixture of fresh gases. Rosser et al. [6] and, somewhat later, Lask and Wagner [7] reported the addition of numerous halogenated inhibitors to methane/air and n-hexane/air flames in order to measure their influence on the burning velocities. In 1963, Halpern observed that diminution of the flame propagation was proportional to the fraction of CH_3Br in the initial mixture [8], while Philips and Sudgen [9] reported the depletion of the H-atom concentrations in $\text{H}_2/\text{O}_2/\text{N}_2$ flames when amounts of Cl_2 , Br_2 , HBr or HCl were added. A first chemical inhibition model has been suggested in 1971 by Fristrom and Sawyer [10]. They considered the reactions (1) $\text{H} + \text{O}_2 \rightarrow \text{OH} + \text{O}$, (2) $\text{O} + \text{H}_2 \rightarrow \text{OH} + \text{H}$ and (3) $\text{H}_2 + \text{OH} \rightarrow \text{H}_2\text{O} + \text{H}$ as responsible for the flame propagation. An halogenated compound like CH_3X reacts by means of the reactions (4) $\text{CH}_3\text{X} + \text{H} \rightarrow \text{CH}_3 + \text{HX}$ and (5) $\text{HX} + \text{H} \rightarrow \text{H}_2 + \text{X}$. These reactions explain the decrease of the H-atom concentration in the flame front. Both processes compete efficiently with reaction (1) which is responsible for the branching process essential to explain the mechanism of flame propagation, as demonstrated by A. Van Tiggelen already in 1952 [11]. Fristrom and Sawyer also suggested an inhibition parameter Φ to quantify the flame inhibition phenomena:

$$\Phi = \frac{[\text{O}_2]}{[\text{I}]} \frac{V_0^0 - V_0^I}{V_0^0}$$

where $[\text{O}_2]$: concentration of oxygen, $[\text{I}]$: concentration of the added inhibitor, V_0^0 : burning velocity without inhibitor, V_0^I : burning velocity with inhibitor

In the 1980's, the effects of several halomethanes on the burning velocities of $\text{CO}/\text{H}_2/\text{O}_2/\text{Ar}$ mixtures were studied systematically [12, 13, 14, 15, 16]. All the cited authors were using nozzle burners at atmospheric pressure, allowing flames to be stabilized close to adiabatic conditions. Knowing the initial gas flows, they measured the flame surface by means of a schlieren technique [12] and the final flame temperatures by the sodium line-reversal method [12]. Safieh and Van Tiggelen [13] measured the influence of CF_3Br by varying the initial percentages of Ar, CF_3Br and of H_2 . They showed that the inhibition effect is related strongly to the hydrogen (H_2) content, in agreement with Fristrom and Sawyer's inhibition model. This work was

followed by an extensive comparative study [14, 15] establishing the following order of decreasing efficiency of the additive:

$\text{CF}_3\text{Br} > \text{CFCl}_3 > \text{CF}_2\text{Cl}_2 > \text{CF}_3\text{Cl} > \text{CF}_3\text{H} > \text{CF}_4$. Recently, Richter et al. [16] also checked CF_2HCl influence using the same techniques, obtaining a mean inhibition parameter lower than the one for CF_3H . Table I summarizes the mean inhibition parameters (Φ_a^m) as measured in references [13 -16].

Table I. Mean inhibition parameters (Φ_a^m) of different halogenated methanes

Inhibitor	da Cruz et al.	Safieh et al.	Richter et al.
CF_4	1.78	-	-
CF_3H	3.21	-	3.20
CF_3Cl	5.45	-	-
CF_2Cl_2	6.17	-	-
CFCl_3	7.07	-	-
CF_3Br	8.00	7.4	-
CF_2HCl	-	-	2.25

Independently, Sanogo [17] measured the influence of the addition of $\text{C}_3\text{F}_7\text{H}$ and of C_2F_6 on methane/air flames. He observed that $\text{C}_3\text{F}_7\text{H}$ and C_2F_6 are much less efficient inhibitors than CF_3Br , although $\text{C}_3\text{F}_7\text{H}$ is more active than C_2F_6 . Fristrom and Van Tiggelen [18] suggested that the overall inhibition parameter Φ of a molecule can be considered to be the sum of the contribution of the inhibition parameters Φ_i of the individual atoms or group of atoms in the inhibiting molecule. With such a method, da Cruz et al. [14, 15] have proposed the following order of inhibition efficiency:

$\Phi\text{Br} > \Phi\text{CF}_3 > \Phi\text{Cl} > \Phi\text{CF}_2 > \Phi\text{H} \approx \Phi\text{CF} > \Phi\text{F}$. However, one has to recall that the measurements of flame burning velocities represent a fairly macroscopic approach to examine and to understand inhibition phenomena. A deeper insight of the inhibition phenomena is gained from the knowledge of the individual chemical species in the flame reaction zone, and from the specific elementary reactions of the additives in the inhibited flames. For this reason, we turn now to the analysis of flame structures.

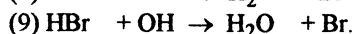
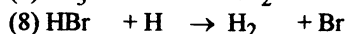
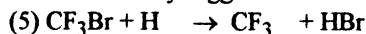
2) The analysis of detailed flame structures

The structure of a flat flame is established when the temperature profile and the concentration profiles of the individual chemical species present in the flame front are measured as functions of the distance from the burner surface. In order to enlarge the flame front, flame structures are usually measured at low pressure. The usual analytical techniques are optical and chromatographic methods as well as mass spectrometry. All studies referred to in this work are based on mass spectrometry coupled with molecular beam sampling (MBMS), a technique with the essential advantage of freezing the composition of the gaseous sample until it is analysed in the mass

spectrometer. The first microscopic studies of flame inhibition have been reported in 1965 by Wilson who added small amounts of CH_3Br , HCl , HBr and Cl_2 to low pressure methane/oxygen flames [19]. A detailed research program on chemical inhibition mechanisms was carried out between 1975 and 1978 by Biordi's group [20-28]. They studied by means of the MBMS technique the influence of the addition of 0.3 or 1.1% of CF_3Br to low pressure $\text{CH}_4/\text{O}_2/\text{Ar}$ flames. Additionally, they reported preliminary measurements about the effect of CF_2Br_2 addition [29, 30]. All data indicated a significant decrease of H - and CH_3 - radical concentrations if CF_3Br was added. Those authors noticed also the faster consumption of CF_3Br compared to the fuel CH_4 . Reaction (5) $\text{CF}_3\text{Br} + \text{H} \rightarrow \text{CF}_3 + \text{HBr}$ is responsible for CF_3Br disappearance. Biordi et al. detected also CF_2 as an intermediate species and they explained its formation by means of the reaction (6) $\text{CF}_3 + \text{H} \rightarrow \text{CF}_2 + \text{HF}$. However, the development of a detailed inhibition mechanism of CF_3Br was not possible at that time due to the following reasons:

- the combustion mechanism of the methane fuel was not yet fully established, and
- the production of species with fragments of both the fuel and the inhibitor such as CH_2CF_2 was noticed.

For these reasons Safieh et al. [31] choose to investigate a stoichiometric $\text{CO}/\text{H}_2/\text{O}_2/\text{Ar}$ flame containing 1% CF_3Br . They analysed it by means of the MBMS method and they suggested the following reactions as responsible for flame inhibition:



Reactions (5) and (8) are competing thus with the branching reaction (1). Processes (7) and (9) are consuming the chain carrier OH, essential for H_2 and CO consumption by reactions (3) $\text{H}_2 + \text{OH} \rightarrow \text{H}_2\text{O} + \text{H}$ and (10) $\text{CO} + \text{OH} \rightarrow \text{CO}_2 + \text{H}$.

In order to reach a better understanding of the inhibiting effect of the group CF_3 compared to bromine atoms, Vandooren et al. [32] analysed a CF_3H -seeded stoichiometric $\text{CO}/\text{H}_2/\text{O}_2/\text{Ar}$ flame by using the MBMS method. They showed the consumption of CF_3H by reaction (11) $\text{CF}_3\text{H} + \text{H} \rightarrow \text{CF}_3 + \text{H}_2$, as well as the slow decay of CF_2O by reaction (12) $\text{CF}_2\text{O} + \text{H} \rightarrow \text{CFO} + \text{HF}$. The relatively low inhibiting effect of CF_3H can be ascribed to the competition of reaction (11) with reaction (1) and of reaction (7) $\text{CF}_3 + \text{OH} \rightarrow \text{CF}_2\text{O} + \text{HF}$ with reaction (3) and (10). The main difference between CF_3Br and CF_3H is therefore the production of HBr in reaction (5) instead of H_2 by reaction (11): the HBr molecule acts itself as an inhibitor by reaction (8) and (9). The atomic bromine can be viewed, indeed, as an end-product.

Based upon those conclusions, Richter, Vandooren and Van Tiggelen [16, 33, 34, 35] have analysed the structures of $\text{H}_2/\text{O}_2/\text{Ar}$ flames seeded with CF_3H , CF_2HCl and CF_2Cl_2 by means of the MBMS technique. They also measured temperature profiles with a coated thermocouple using an electrical compensation for the losses by radiation. The use of the $\text{H}_2\text{-O}_2$ system as a reference flame allows examination of the process of CO and CO_2 formation from the additive molecule because the reference

system does not contain carbon. In the case of the added CF_3H , the equivalence ratio of the fresh gas mixture was varied so that the role of H, O and OH in the decay mechanism of CF_3H could be understood. Figures 1 - 6 exhibit the flame structures of a lean [16, 33, 34] and of a stoichiometric [16, 34] $\text{H}_2/\text{O}_2/\text{Ar}$ flame seeded with 3% of CF_3H . A much higher H radical concentration is noticed in the stoichiometric flame, which explains the faster CF_2O consumption by reaction

(12) $\text{CF}_2\text{O} + \text{H} \rightarrow \text{CFO} + \text{HF}$. The larger CF_2O concentration is ascribed in the lean flame to the competition between reactions (7) $\text{CF}_3 + \text{OH} \rightarrow \text{CF}_2\text{O} + \text{HF}$ and

(6) $\text{CF}_3 + \text{H} \rightarrow \text{CF}_2 + \text{HF}$. CF_2 species is consumed ultimately by processes

(13) $\text{CF}_2 + \text{OH} \rightarrow \text{CFO} + \text{H}$, (14) $\text{CFO} + \text{H} \rightarrow \text{CO} + \text{HF}$ and

(15) $\text{CFO} + \text{OH} \rightarrow \text{CO}_2 + \text{HF}$. The relative large CO concentration in the stoichiometric flame can be explained by the equilibrium (10) $\text{CO} + \text{OH} \leftrightarrow \text{CO}_2 + \text{H}$, shifted to the left as a consequence of the relatively large H concentration.

From a quantitative analysis of the flame structures, Richter et al. deduced the rate coefficients of some elementary reactions [35]. The deduction of rate coefficients [36] requires the knowledge of the individual mole fluxes and of the net reaction rates of at least one reactant or product of the investigated reaction. To compute the mole fluxes we took into account the physical processes of convection and of diffusion (thermal and molecular):

$$F_i = AN_i(v + V_i) \quad \text{eq. 1}$$

F_i : mole flux of the species i [$\text{mole cm}^{-2} \text{ s}^{-1}$]

A : expansion area ratio

N_i : concentration of the species i [mole cm^{-3}]

v : local convection velocity in [cm s^{-1}]

V_i : local diffusion velocity of the species i [cm s^{-1}]

The net reaction rate R_i of the individual species i is the gradient of the mole flux F_i :

$$R_i = \frac{1}{A} \frac{dF_i}{dz} \quad \text{eq. 2}$$

From the deduced rate coefficients for reactions (16) $\text{CF}_3\text{H} + \text{H} \rightarrow \text{Products}$ and (17) $\text{CF}_3\text{H} + \text{O} \rightarrow \text{CF}_3 + \text{OH}$ and by using an interpolated value taken from the literature for the reaction (18) $\text{CF}_3\text{H} + \text{OH} \rightarrow \text{CF}_3 + \text{H}_2\text{O}$, the relative contribution ($\%F_j$) of those individual reactions to the CF_3H consumption can be inferred by applying eq. 3 :

$$\%F_j = \frac{\int_0^{25\mu\text{m}} k_j[\text{CF}_3\text{H}][i]dz}{\sum_{j=1}^3 \int_0^{25\mu\text{m}} k_j[\text{CF}_3\text{H}][i]dz} \bullet 100 \quad \text{eq. 3}$$

The rate coefficients used are $k_{16} = 1.16 \cdot 10^{14} \exp(-8800/T) \text{ cm}^3 \text{ mole}^{-1} \text{ s}^{-1}$, $k_{17} = 1.10 \cdot 10^{12} \exp(-1600/T) \text{ cm}^3 \text{ mole}^{-1} \text{ s}^{-1}$ and $k_{18} = 2.65 \cdot 10^4 T^{2.45} \exp(-1554/T) \text{ cm}^3 \text{ mole}^{-1} \text{ s}^{-1}$, respectively. The results collected in Table II provide the importance of the different chain carriers to consume CF_3H for the lean and stoichiometric flames.

Table II. Contribution (% F_i) of H, O and OH to the CF_3H decay

flame	H	O	OH
lean	5	83	12
stoichiom.	40	42	18

Table II shows clearly how the CF_3H consumption by H is sensitive to the equivalence ratio of the feed gas mixture. Experiments with rich mixtures would confirm such a trend. Moreover, it is obvious that the contribution of O-atoms to the CF_3H initial attack cannot be neglected in a lean flame.

The structure of a stoichiometric flame containing 1% of CF_2HCl is presented in Figures 7, 8 and 9. Compared to CF_3H -seeded flames, a more rapid consumption of CF_2HCl is noticeable and CF_2O is produced also in smaller amounts than in the similar CF_3H flames. The latter observation is rationalized if the competition between reactions (19) $\text{CF}_2\text{H} + \text{O} \rightarrow \text{CF}_2\text{O} + \text{H}$ and (20) $\text{CF}_2\text{H} + \text{H} \rightarrow \text{CF}_2 + \text{H}_2$ is considered. Richter et al. [16] demonstrate also that Biordi's suggestion of the role of reaction (21) $\text{CF}_2 + \text{OH} \rightarrow \text{CF}_2\text{O} + \text{H}$ is not dominant, otherwise the difference between CF_3H and CF_2HCl additive should not be observed. Moreover, they considered the re-injection of H radicals by reaction (19) into the system as a process responsible for the smaller inhibition efficiency of CF_2HCl compared to CF_3H (see previously). A rate coefficient for reaction (22) $\text{CF}_2\text{HCl} + \text{H} \rightarrow \text{CF}_2\text{H} + \text{HCl}$ was also deduced [35]. From numerical modeling Richter et al. [37] have shown the large dependence of the initial decay of CF_2HCl on the equivalence ratio of the flame. In stoichiometric and rich mixtures, CF_2HCl is almost exclusively attacked by reaction (22) $\text{CF}_2\text{HCl} + \text{H} \rightarrow \text{CF}_2\text{H} + \text{HCl}$. On the contrary in lean flames, reaction (23) $\text{CF}_2\text{HCl} + \text{O} \rightarrow \text{CF}_2\text{Cl} + \text{OH}$ contributes for 32% and reaction (24) $\text{CF}_2\text{HCl} + \text{OH} \rightarrow \text{CF}_2\text{Cl} + \text{H}_2\text{O}$ for 25% to the initial decay of CF_2HCl .

Some mole fraction profiles measured in a stoichiometric $\text{H}_2/\text{O}_2/\text{Ar}$ flame seeded with 0.5% of CF_2Cl_2 are presented in Figure 10 [34]. A slight relative increase of the CF_2O mole fraction compared to the CF_2HCl -containing flame can be noticed. It can be explained by the exclusive formation of CF_2Cl in reaction (25) $\text{CF}_2\text{Cl}_2 + \text{H} \rightarrow \text{CF}_2\text{Cl} + \text{HCl}$ followed by the competing reactions (26) $\text{CF}_2\text{Cl} + \text{OH} \rightarrow \text{CF}_2\text{O} + \text{HCl}$ and (27) $\text{CF}_2\text{Cl} + \text{H} \rightarrow \text{CF}_2 + \text{HCl}$. Such a competition is more favourable for CF_2O formation than the competition between reactions (19) and (20) occurring in CF_2HCl -containing flames.

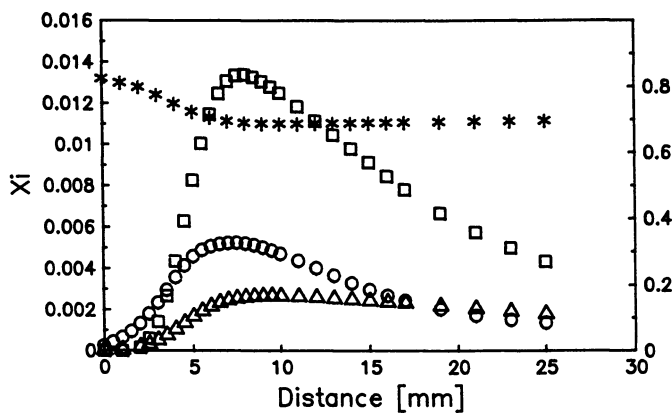


Figure 1 Mole fractions of H (O), O (\square), OH (Δ) (left scale) and O_2 (*) (right scale) in a lean flame containing 3% of CF_3H .

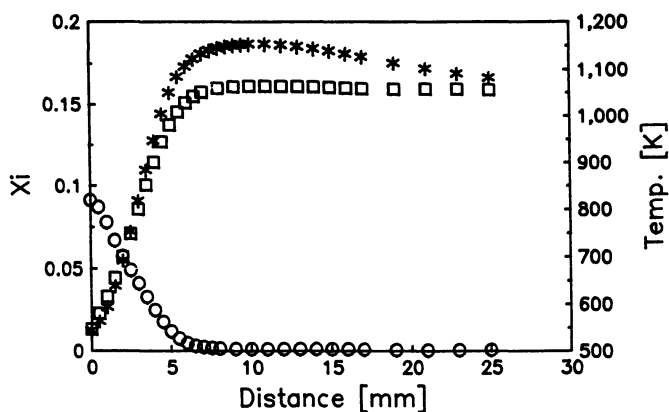


Figure 2 Mole fractions of H_2 (O), H_2O (\square) and the temperatures (*) in a lean flame containing 3% of CF_3H .

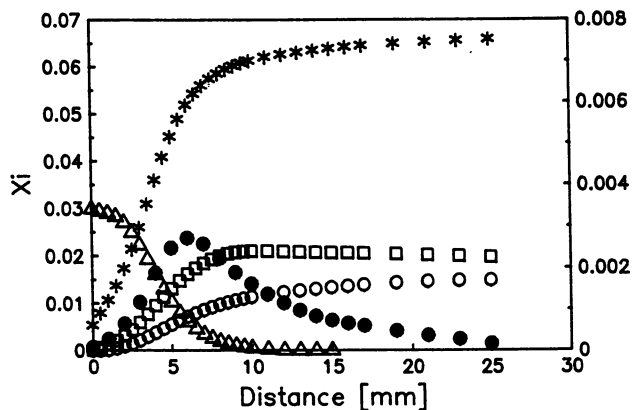


Figure 3 Mole fractions of HF (*), CO₂ (O), CF₂O (□), CF₃H (Δ) (left scale) and CO (●) (right scale) in a lean flame containing 3% of CF₃H.

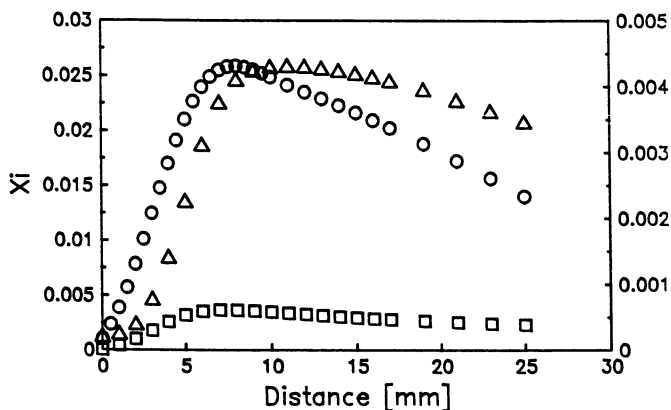


Figure 4 Mole fractions of H (O), O (□) (left scale) and OH (Δ) (right scale) in a stoichiometric flame containing 3% of CF₃H.

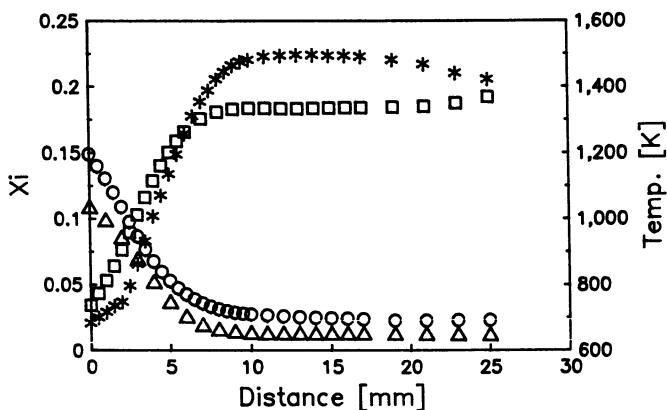


Figure 5 Mole fractions of H_2 (\circ), H_2O (\square), O_2 (Δ) and the temperatures ($*$) in a stoichiometric flame containing 3% of CF_3H .

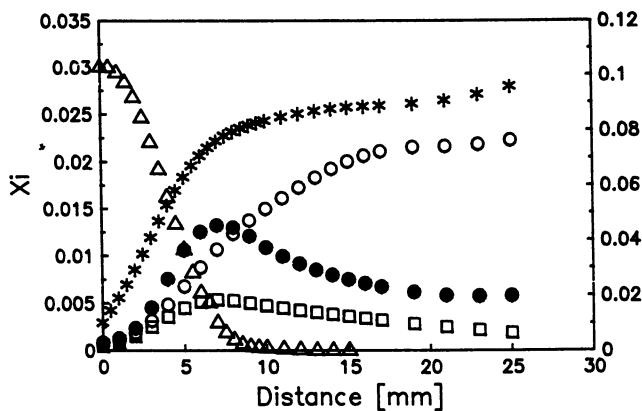


Figure 6 Mole fractions of CO (\bullet), CO_2 (\circ), CF_2O (\square), CF_3H (Δ) (left scale) and HF ($*$) (right scale) in a stoichiometric flame containing 3% of CF_3H .

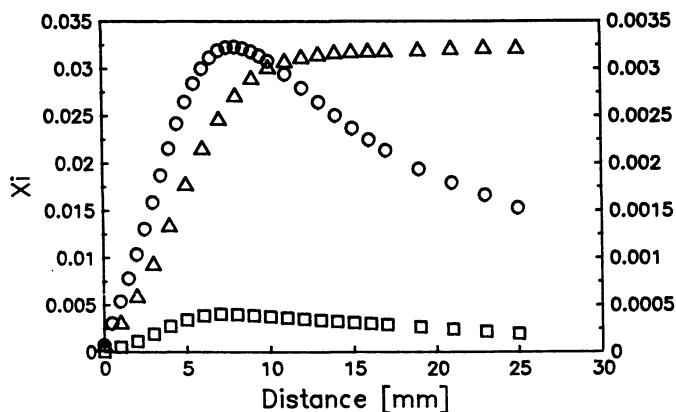


Figure 7 Mole fractions of H (O), O (□) (left scale) and OH (Δ) (right scale) in a stoichiometric flame containing 1% of CF_2HCl .

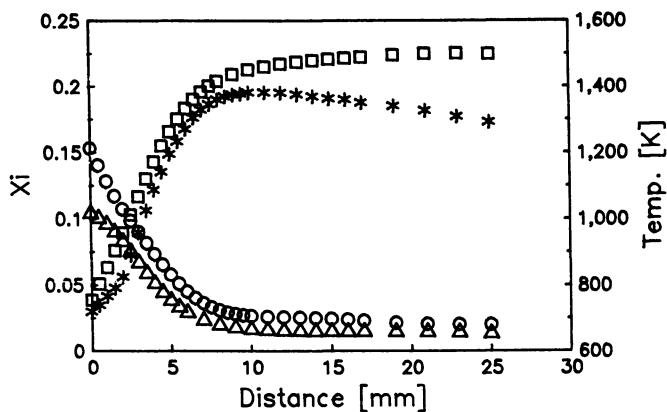


Figure 8 Mole fractions of H_2 (O), H_2O (□), O_2 (Δ) and the temperatures (*) in a stoichiometric flame containing 1% of CF_2HCl .

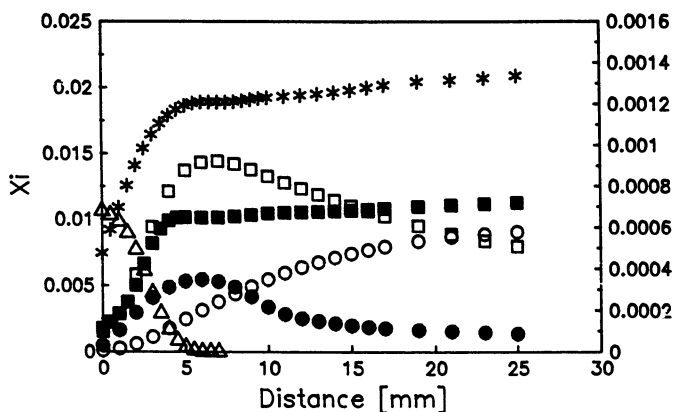


Figure 9 Mole fractions of HF (*), CO (●), HCl (■), CO₂ (O), CF₂HCl (Δ) (left scale) and CF₂O (□) (right scale) in a stoichiometric flame containing 1% of CF₂HCl.

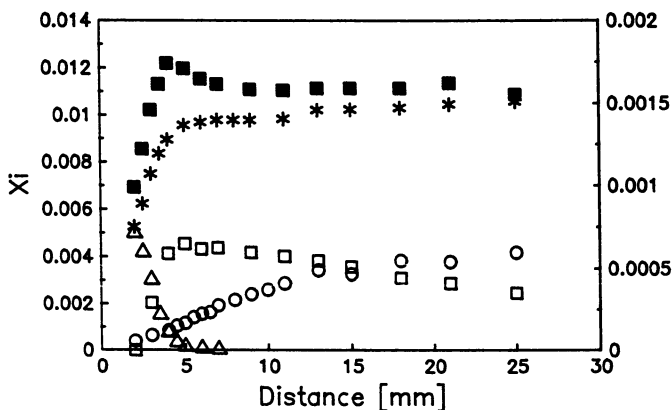


Figure 10 Mole fractions of HF (*), HCl (■), CO₂ (O), CF₂Cl₂ (Δ) (left scale) and CF₂O (□) (right scale) in a stoichiometric flame containing 0.5% CF₂Cl₂.

Finally, it should be noted that Sanogo [17] has analysed experimentally by the same MBMS technique the structures of stoichiometric methane/oxygen/argon flames seeded with CF_3Br , $\text{C}_3\text{F}_7\text{H}$ or C_2F_6 in order to understand their consumption mechanisms in hydrocarbon flames. However, it is a rather more difficult problem to solve due to the relatively complicated interaction between $\text{CH}_4\text{-O}_2$ combustion system and the additive decay chemistry.

3) Chemi-ionization in flames seeded with inhibitors

It is a well known fact that hydrocarbon-containing flames are producing ions in excess with respect to the equilibrium value [38]. It is the reaction

(28) $\text{CH} + \text{O} \rightarrow \text{CHO}^+ + \text{e}^-$ which creates the primary flame ions [39] and which is followed by ion-molecule reactions like the process

(29) $\text{CHO}^+ + \text{H}_2\text{O} \rightarrow \text{H}_3\text{O}^+ + \text{CO}$. A method to determine the overall rate of ion formation is the measurement of saturation currents [38]. In this technique a metal plate is located in front of the burner and an electrical potential is applied between the burner and the metal plate. By means of the current measurement, the quantity of charged particles produced in the flame per unit time can be determined. Rocteur and Van Tiggelen [40, 41] have applied this technique on $\text{CO}/\text{H}_2/\text{O}_2/\text{Ar}$ flames seeded with trace amounts of several halocarbons. They established the following sequence for ion formation efficiency: $\text{CF}_4 < \text{CF}_3\text{Br} < \text{CF}_3\text{Cl} < \text{CF}_3\text{H} < \text{CF}_2\text{Cl}_2 < \text{CF}_2\text{HCl} \approx \text{CH}_4$. The corresponding ionic currents I_S for flames containing 0.8% of additive are presented in Table III.

Table III. Ionic currents measured in $\text{H}_2/\text{O}_2/\text{CO}/\text{Ar}$ flames with different additives

Additive	I_S [A]
CF_4	$2 \cdot 10^{-8}$
CF_3Br	$1.2 \cdot 10^{-7}$
CF_3Cl	$2.1 \cdot 10^{-7}$
CF_3H	$2.5 \cdot 10^{-7}$
CF_2Cl_2	$3.2 \cdot 10^{-7}$
CF_2HCl	$3.5 \cdot 10^{-6}$
CH_4	$3.8 \cdot 10^{-6}$

The most surprising result is the large ionic current in flames containing CF_2HCl . Moreover, the ionic current I_S is directly proportional to the amount of additive present in the fresh gas mixture. The ionic yield (η_S) is defined by the equation

$$\eta_S = K \frac{I_S}{D_{\text{add}}} \quad \text{eq. 4}$$

with K an apparatus constant and D_{add} the volumetric flow of the additive in $\text{cm}^3 \text{ s}^{-1}$. The ionic yield (η_S) can be used to deduce an activation energy increment ΔE_+ .

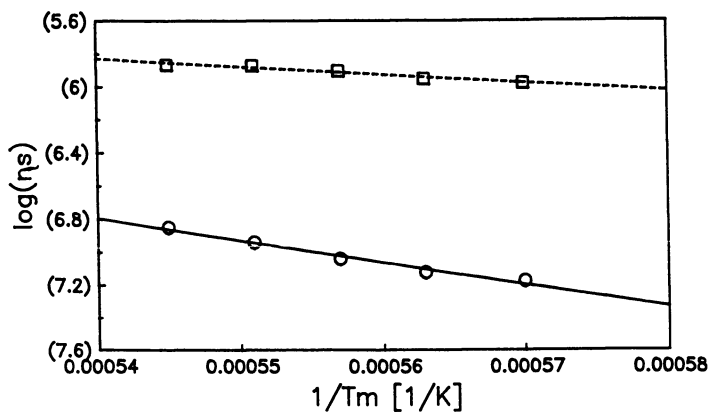


Figure 11 Determination of the global activation energy for ion production in CF_2HCl (□) and CF_2Cl_2 (○) containing flames. The parenthesis on the ordinate mean negative values of $\log(\eta_s)$.

Figure 11 exhibits the the plot of $\log(\eta_s)$ versus the reciprocal flame temperature used to determine ΔE_+ . The values for ΔE_+ are 21 kcal mol⁻¹ and 60 kcal mol⁻¹ for CF₂HCl and CF₂Cl₂, respectively. It demonstrates the role of a slow rate-determining step ((30) CF₂ + H₂ → CHF + HF) producing the CHF radical responsible for the CH formation when the compound CF_iX_i is added, as opposed to the fast radical-radical reaction (31) CF₂H + H → CHF + HF occurring when CF₂HCl is present.

4) Numerical Modeling

The mathematical description of combustion phenomena requires the use of computational codes which consider physical processes like convection, conduction and molecular diffusion as well as the detailed chemical combustion mechanism with all the pertinent rate coefficients. The pioneering application of numerical modeling to inhibition was the comparison between experimental and computed results for the structure of H₂/N₂O/N₂ flames seeded with CH₃Br or HBr by Day et al. in 1971 [42]. Those authors also checked the influence of HBr on the flame propagation velocities of H₂/O₂/N₂ flames. Westbrook [43, 44] was the first to suggest a so-called comprehensive inhibition mechanism for HCl, HBr, HI, CH₃X, C₂H₅X or C₂H₃X (with X: Cl, Br or I) as well as for CF₃Br. In the case of CF₃Br, he used principally Biordi's mechanism to compute the flame burning velocities of mixtures propagating in different fuels CH₄, C₂H₄ or CH₃OH containing inhibitors. Those computations were carried out at different pressures. Unfortunately, flame burning velocities are not very sensitive to the choice of the rate coefficients, with the exception of the branching step. Only flame structures may help to validate a complex combustion mechanism with inhibitors. The structure of a flame burning at atmospheric pressure in a stoichiometric methane/oxygen mixture containing 1% of CF₃Br was also modeled by Westbrook [43], but the lack of experimental data for flame structure at one atmosphere impeded verification of the chemical mechanism. Moreover, due to the very restricted knowledge of experimentally determined rate coefficients, Westbrook was forced to guess several rate coefficients, so that the suggested mechanism can be considered as a first attempt but not as a definite inhibition mechanism.

In order to avoid the use of a large number of evaluated rate coefficients, Richter et al. [16, 34] chose a more simple system, (i.e. H₂/O₂ mixtures), and they suggested a simple decay mechanism for CF₃H, CF₂HCl [16, 34] and CF₂Cl₂ [34] based upon experimentally validated rate constants in flames at different equivalence ratios. Their approach is detailed in [16].

A recent numerical modeling of inhibition phenomena induced by CF₃Br, C₃F₇H or C₂F₆ was undertaken by Sanogo et al. [17, 45]. They have computed flame propagation velocities for inhibited methane/air flames. The flame structures of some seeded methane/oxygen/argon flames have been calculated relying almost exclusively on the Westbrook mechanism [43, 44]. Thus, the chemical mechanism they present to explain their very impressive experimental results is only of a limited value.

Conclusions

A lot of experimental data have been gained recently to understand the macroscopic and microscopic inhibition effects of the fire extinguishers like CF_3Br and of their potential replacements like CF_3H , CF_2HCl , $\text{C}_3\text{F}_7\text{H}$ or C_2F_6 . From the state of the art, one may conclude that the most efficient flame inhibition must be attributed to the sequence of reactions (5) $\text{CF}_3\text{Br} + \text{H} \rightarrow \text{CF}_3 + \text{HBr}$, (8) $\text{HBr} + \text{H} \rightarrow \text{H}_2 + \text{Br}$, and (9) $\text{HBr} + \text{OH} \rightarrow \text{H}_2\text{O} + \text{Br}$ which is competing with the branching process (1). The inhibition effect of HBr itself has been documented in the past and acts as a catalytic cycle: reaction (8) or (9) followed by a three-body recombination step (30) $\text{H} + \text{Br} + \text{M} \rightarrow \text{M} + \text{HBr}$. Bromine is thus more efficient for inhibition because it is continuously recycled. Compounds containing only fluorine atoms such as CF_3H , $\text{C}_3\text{F}_7\text{H}$ or C_2F_6 are much less efficient inhibitors because each fluorine atom scavenges only one H atom to produce one stable molecule (HF).

Many research efforts using numerical modeling have been done also in order to suggest detailed chemical reaction mechanisms to explain the action of the investigated compounds in flames. But, due to a limited knowledge of the rate coefficients and to complexity of combustion phenomena, only mechanisms in simple burning mixtures can be considered as sufficiently validated to describe the inhibition mechanism.

It is worth to be mentioned that some studies [46, 47, 48, 49] have been performed also about the influence of halogenated methanes on detonation waves. The sequence of relative efficiency of the additives to quench or eventually to stop the detonation is similar to the one discussed above for flames.

Considering all the experimental evidence available at this stage, it is possible to conclude that no substitute compound with an inhibition efficiency similar to the one of CF_3Br (Halon 1301) can be suggested. The bromine chemistry is, indeed, essential to a chemical inhibiting action.

REFERENCES

- [1] M. J. Molina and R. Rowland, *Nature* 249, 810 (1974).
- [2] Montreal Protocol on Substances that Deplete the Ozone Layer, Final Act, UNEP (1987).
- [3] R. S. Sheinson, J. E. Penner-Hahn and D. Indritz, *Fire Safety Journal* 15, 437 (1989).
- [4] R. Simmons and H. Wolfhard, *Trans. Far. Soc.* 51, 1211 (1955).
- [5] F. H. Garner, R. Long, A. J. Graham and A. Badakhshan, 6th Symposium (International) on Combustion, p. 802, Rheinhold, New-York, 1957.
- [6] W. A. Rosser, H. Wise and J. Miller, 7th Symposium (International) on Combustion, p. 175, Butterworths, London, 1959.
- [7] G. Lask and H. Gg. Wagner, 8th Symposium (International) on Combustion, p. 432, Williams and Wilkins, Baltimore, 1962.

- [8] C. Halpern, *J. Res. Nat. Bur. Standards (U.S.)* 67A (1), 72 (1963).
- [9] L. F. Phillips and T. M. Sugden, *Can. J. Chem.* 38, 1804 (1960).
- [10] R. M. Fristrom and R. F. Sawyer, *AGARD Conf. Proceeding* 84, 12-1 (1971).
- [11] A. Van Tiggelen, *Mém. Acad. Roy. Belge (Cl. Sc.)*, XXVII (1), p. 1 (1952).
- [12] A. Van Tiggelen et al.: *Oxydations et Combustions*, Edition Technip, Paris, Vol. I (1968).
- [13] H. Y. Safieh and P. J. Van Tiggelen, *J. Chim. Phys.* 81, 461 (1984).
- [14] F. N. da Cruz, J. Vandooren and P. J. Van Tiggelen 97, 1011 (1988).
- [15] F. N. da Cruz, PhD thesis, Université Catholique de Louvain, Louvain-la-Neuve, 1988.
- [16] H. Richter, J. Vandooren and P. J. Van Tiggelen, 25th Symposium (International) on Combustion, in press, The Combustion Institute, Pittsburgh, 1994.
- [17] O. Sanogo, PhD thesis, Université d'Orléans, Orléans, 1993.
- [18] R. M. Fristrom and P. J. Van Tiggelen, 17th Symposium (International) on Combustion, p. 773, The Combustion Institute, Pittsburgh, 1979.
- [19] W. E. Wilson Jr., 10th Symposium (International) on Combustion, p. 47, The Combustion Institute, Pittsburgh, 1965.
- [20] J. C. Biordi, C. P. Lazzara and J. F. Papp, 14th Symposium (International) on Combustion, p. 367, The Combustion Institute, Pittsburgh, 1973.
- [21] J. C. Biordi, C. P. Lazzara and J. F. Papp, *Combust. and Flame* 24, 401 (1975).
- [22] J. C. Biordi, C. P. Lazzara and J. F. Papp, *J. Phys. Chem.* 80, 1042 (1976).
- [23] J. C. Biordi, C. P. Lazzara and J. F. Papp, *Combust. and Flame* 26, 57 (1976).
- [24] J. C. Biordi, C. P. Lazzara and J. F. Papp, *J. Phys. Chem.* 82, 125 (1978).
- [25] J. C. Biordi, C. P. Lazzara and J. F. Papp, *J. Phys. Chem.* 81, 1139 (1977).
- [26] J. C. Biordi, C. P. Lazzara and J. F. Papp, 15th Symposium (International) on Combustion, p. 917, The Combustion Institute, Pittsburgh, 1974.
- [27] J. C. Biordi, C. P. Lazzara and J. F. Papp, 16th Symposium (International) on Combustion, p. 1097, The Combustion Institute, Pittsburgh, 1976.
- [28] J.C. Biordi, C.P. Lazzara and J.F. Papp: *ACS Symposium Series* 16, 256 (1975).
- [29] C. P. Lazzara, J. F. Papp and J. C. Biordi, Fall Technical Meeting, The Combustion Institute, Eastern Section, 1978.
- [30] J. F. Papp, C. P. Lazzara and J. C. Biordi, Bureau of Mines RI8551, 1981.
- [31] H. Y. Safieh, J. Vandooren and P. J. Van Tiggelen, 19th Symposium (International) on Combustion, p. 117, The Combustion Institute, Pittsburgh, 1982.
- [32] J. Vandooren, F. N. da Cruz and P. J. Van Tiggelen, 22th Symposium (International) on Combustion, p. 1587, The Combustion Institute, Pittsburgh, 1988.
- [33] H. Richter, J. Vandooren and P. J. Van Tiggelen, *Bull. Soc. Chim. Belg.* 99, 491 (1990).
- [34] H. Richter, PhD thesis, Université Catholique de Louvain, Louvain-la-Neuve, 1993.
- [35] H. Richter, J. Vandooren and P. J. Van Tiggelen, *J. Chim. Phys.* 91, 1748 (1994).

- [36] J. Peeters and G. Mahnen, 14th Symposium (International) on Combustion, p. 133, The Combustion Institute, Pittsburgh, 1973.
- [37] H. Richter, J. Vandooren and P. J. Van Tiggelen, *Bull. Soc. Chim. Belg.* **103**, 355 (1994).
- [38] J. Peeters, J. F. Lambert, P. Hertoghe and A. Van Tiggelen, 13th Symposium (International) on Combustion, p 321, The Combustion Institute, Pittsburgh, 1971 and J. F. Lambert and P. J. Van Tiggelen, *Annales Soc. Sci. Bruxelles* **88** (3) p 399 (1974)
- [39] H. F. Calcote, 8th Symposium (International) on Combustion, p. 184, Williams and Wilkins, Baltimore, 1962.
- [40] Ph. Rocteur, Mémoire de licence, Université Catholique de Louvain, Louvain-la-Neuve, 1988.
- [41] Ph. Rocteur and P. J. Van Tiggelen, XIth Sym. Int. Gas Kinetics, C8, Assisi, 1990.
- [42] M. J. Day, D. V. Stamp, K. Thompson and G. Dixon-Lewis, 13th Symposium (International) on Combustion, p. 705, The Combustion Institute, Pittsburgh, 1971.
- [43] C. K. Westbrook, 19th Symposium (International) on Combustion, p. 127, The Combustion Institute, Pittsburgh, 1983.
- [44] C. K. Westbrook, *Combustion Science and Technology* **34**, 201 (1983).
- [45] O. Sanogo, J.-L. Delfau, R. Akrich and C. Vovelle, 25th Symposium (International) on Combustion, in press, The Combustion Institute, Pittsburgh, 1994.
- [46] J. C. Libouton, M. Dormal and P. J. Van Tiggelen, 15th Symposium (International) on Combustion, p. 79, The Combustion Institute, Pittsburgh, 1975.
- [47] M. Vandermeiren and P. J. Van Tiggelen, *Progress in Astronautics and Aeronautics* **114**, 186 (1988).
- [48] M. H. Lefebvre, E. Nzeyimana and P. J. Van Tiggelen, *Progress in Astronautics and Aeronautics* **153**, 144 (1992).
- [49] P. J. Van Tiggelen and L. Thill, Proceedings of Halon Alternatives Technical Working Conference, University of New Mexico, Albuquerque, May 1993, p. 48.

RECEIVED June 27, 1995

Chapter 25

Key Species and Important Reactions in Fluorinated Hydrocarbon Flame Chemistry

D. R. F. Burgess, Jr.¹, M. R. Zachariah¹, Wing Tsang¹,
and P. R. Westmoreland²

¹Chemical Sciences and Technology Laboratory, Chemical Kinetics
and Thermodynamics Division, National Institute of Standards
and Technology, Gaithersburg, MD 20899-0001

²Department of Chemical Engineering, University of Massachusetts,
Amherst, MA 01003-3110

A comprehensive chemical mechanism consisting of elementary reactions was developed to describe the destruction of fluorinated hydrocarbons and their influence on flame chemistry. This paper discusses the key species and important reactions in fluorocarbon chemistry. Emphasis is placed on identifying those species and reactions with uncertain thermochemical and rate data that impact decomposition pathways and flame chemistry. Existing fluorinated hydrocarbon thermochemical and kinetic data were utilized when available. These data were supplemented through application of empirical, QRRK/RRKM, and *ab initio* methods, since much of the data necessary to complete the reaction set does not exist or is uncertain. Plug flow simulations were used to refine the reaction set and premixed flame simulations were used to predict the effectiveness of added fluorocarbon agents on flame suppression. The mechanism briefly outlined here should be considered only a framework for future model development, rather than a finished product. Future refinements will require experimental validation by high temperature flow reactor, premixed flame, and diffusion flame measurements, as well as measurements of important, yet currently uncertain, rate constants.

The work presented here is a small part of a large effort (1) at NIST evaluating (for the United States Air Force, Navy, Army, and Federal Aviation Administration) potential fluorinated hydrocarbons and other agents as replacements for Halon 1301 (CF₃Br). Halon 1301 is very effective as a chemical extinguisher. However, it is also extremely effective for depleting stratospheric ozone. Consequently, its production and use are restricted. The major objective of this modeling work was to pro-

This chapter not subject to U.S. copyright
Published 1995 American Chemical Society

vide a chemical basis for rationalizing the relative degree of effectiveness of each candidate agent. A fundamental understanding of the chemistry of these agents in hydrocarbon flames should facilitate identification of desired characteristics of effective agents. That is, utilization of simple chemical concepts should enable screening and selection of potential agents with minimal time and human resources. In order to accomplish this goal, it was necessary to develop a chemical mechanism based on elementary reaction steps for their destruction, their participation in and influence on hydrocarbon flame chemistry, as well as for prediction of potential by-products of incomplete combustion. However, neither such a mechanism nor review of the relevant existed prior to this study. Consequently, significant effort was required in order to simply construct such a comprehensive mechanism prior to its utilization in any simulations. The focus of the mechanism development work was restricted to the chemistry involving only fluoromethanes and fluoroethanes. This includes both those candidate agents specifically being considered as replacements (i.e., CH_2F_2 , $\text{CF}_3\text{-CH}_2\text{F}$, $\text{CF}_3\text{-CHF}_2$, $\text{CF}_3\text{-CF}_3$), as well as all of the other possible fluoromethanes and fluoroethanes. Larger fluorinated hydrocarbon agents (e.g., C_3F_8) and chlorine-substituted agents (e.g., CHF_2Cl) were not specifically considered, because this would significantly increase the complexity of the chemistry.

Background. There has been a significant amount of work over many years investigating the effectiveness of halogenated fire suppressants (2-9), as well as other types of fire suppressants (10-13). We will not review this body of work, but refer the reader to these and other relevant sources. A large part of our work is based on the pioneering work in this area by Biordi and coworkers (14) and Westbrook (7). In earlier experiments on a range of candidates, CF_3Br was identified as being very effective for extinguishing flames. However, its mechanism was not understood. Biordi and coworkers measured both stable and radical species in methane flames doped with CF_3Br using a flame-sampling molecular beam mass spectrometer. Many of the relevant elementary reactions describing the decomposition of CF_3Br , its chemistry, and its influence on hydrocarbon flames were determined in this work. Westbrook developed the first comprehensive chemical mechanism to describe in detail the chemistry of CF_3Br and modeled inhibition in hydrocarbon flames. As a result of this work, it is generally agreed that flame suppression by bromine-containing compounds is a result of catalytic destruction of H atoms by Br atoms. The ability of bromine to recycle in the chemical system in the flame is directly related to the weak molecular bonds formed by bromine.

There are a variety of ways in which fire suppressants act in inhibiting hydrocarbon flames. Most of these effects are intimately related. For example, a heat loss means a temperature decrease, which causes the chemistry to slow. This results in fewer radicals being created, which decreases product formation. This means less heat generated, which results in a temperature decrease and so on. One can separate suppression effects into two general categories: physical and chemical (although there is overlap). One can define chemical effects as being directly related to the characteristics of the specific molecule (e.g., H, F, or Cl substitution), while physical effects are not. For example, heat capacity is a physical effect, since to a first approximation it is largely a function of the number of atoms in the molecule

and their connectivity, but not the identity of the molecule (*i.e.*, its composition).

There are a number of different types of chemical effects. Most of these involve different competing factors. First, all of the fluorinated hydrocarbons will eventually decompose and then burn (forming CO₂, H₂O, and HF). This liberates heat and increases flame temperatures (speeding flame chemistry). On the other hand, the agents are large molecules with many atoms. Consequently, their high heat capacities may result in a decrease in flame temperature prior to complete combustion (slowing flame chemistry). The competition between these two factors is strongly dependent upon flame conditions - the most important of which is the mechanics of mixing of the fuel and oxidizer.

Another set of competing effects involves fluorinated radicals produced by agent decomposition. These radicals are slower to burn than their pure hydrocarbon analogues, because the C-F bond is significantly stronger than the C-H bond. Consequently, reactions involving these radicals may effectively compete with analogous pure hydrocarbon chemistry by creating less "flammable" intermediates, thereby inhibiting combustion of the hydrocarbon fuel. For example, since the agents are added to the air stream, their immediate decomposition products (radicals) are formed in oxygen rich, relatively cold regions of the flame. Consequently, these radicals may be involved in termination steps, such as $\bullet\text{CF}_3 + \text{HO}_2\bullet \rightarrow \text{CHF}_3 + \text{O}_2$, slowing radical chain reactions and inhibiting the flame. These radicals also compete with hydrocarbon radicals for important H, O, and OH radicals. On the other hand, these radicals also react with stable molecules in the colder air stream (*e.g.*, O₂), generating more radicals, such as O atoms, and thereby initiating chemistry or promoting combustion of the fuel.

Mechanism Development

We constructed a large comprehensive reaction set or "mechanism" for fluorinated hydrocarbon chemistry involving C₁ and C₂ stable and radical hydrocarbon species, including partially oxidized fluorinated hydrocarbons. The mechanism should be considered only a framework for future model development, rather than a finished product. Future refinements will require experimental validation by high temperature flow reactor, premixed flame, and diffusion flame measurements, as well as measurements of important, yet currently uncertain rate constants.

Species Thermochemistry. Existing thermochemical data was compiled and evaluated. Where little or no data existed for potential species of interest (most of the radicals), we have estimated it using both empirical methods, such as group additivity (15), and also through application of *ab initio* molecular orbital calculations (16-18). For many of the radicals, we had to rely upon recent *ab initio* calculations of thermochemical data. This includes both *ab initio* calculations done as part of this project and those done previously by other workers. In all cases, significant effort was made to utilize thermochemical data for each species that was consistent with data for all other species. We have employed thermochemistry from the various evaluated sources and have cited these references below. Citations for the original sources of data can be found in the evaluated sources.

H/O/F Species. We used standard hydrogen/oxygen and hydrocarbon thermochemistry, most of which can be found in the JANAF tables (19) or in a Sandia compilation (20), as can data for F and HF. Other simple species (*e.g.*, F₂, FO•, HOF, FOF, FOO•, HOOF) were initially considered in the mechanism, but were later excluded, because they did not contribute to the overall chemistry.

Fluoromethanes and Fluoromethyl Radicals. Thermochemical data for the fluoromethanes (CH₃F, CH₂F₂, CHF₃, and CF₄) can be found in the JANAF tables (19) and have been re-examined subsequently in the Journal of Physical and Chemical Reference Data (JPCRD) (21). Recommendations for the heats of formation of the fluoromethanes have also been made by Kolesov (22). Heats of formation for CH₂F₂ and CF₄ are the best known (uncertainties of <1.5 kJ/mol) and are derived from their heats of combustion. The heat of formation of CHF₃ has a slightly higher uncertainty (4 kJ/mol) due to side reactions in its combustion. The heat of formation of CH₃F has been estimated (uncertainty of ~10 kJ/mol) employing empirical trends in heats of formation of the other fluoromethanes, since there are no experimentally-derived values (other than from appearance potentials). Although CH₃F is unlikely to be a key species in fluorinated hydrocarbon-inhibited hydrocarbon flames, as the simplest fluorinated hydrocarbon, its heat of formation is significant for benchmarking heats of formation of other fluorinated hydrocarbons. We have chosen to employ heats of formation for the fluoromethanes recommended by Kolesov with the entropy and heat capacity data found in the JPCRD review. We note that heats of formation for the fluoromethanes from our *ab initio* calculations (23) using the BAC-MP4 method (18) are within ~2 kJ/mol of the recommended values.

Thermochemical data for the perfluoromethyl radical (•CF₃) can be found in the JANAF tables (19) and have been re-examined subsequently by Rodgers (24). The heat of formation of •CF₃ has an uncertainty of ~5 kJ/mol. Experimentally derived heats of formation (from bond dissociation energies and heat of reactions) for all of the fluoromethyl radicals (•CH₂F, •CHF₂, •CF₃) can be found in evaluations by McMillen and Golden (25) and Pickard and Rodgers (26) with uncertainties of less than 10 kJ/mol. We have chosen to employ the heats of formation recommended by McMillen and Golden. For entropies at standard state and heat capacity data, we used values for •CF₃ from the JANAF tables. Since no experimentally derived entropy and heat capacity data exist (to our knowledge) for •CH₂F and •CHF₂, we used that derived from our BAC-MP4 *ab initio* calculations. We note that heats of formation for the fluoromethyl radicals from our *ab initio* calculations are within ~4 kJ/mol of the recommended experimental values.

Fluoromethylenes and Fluoromethylidyne. Thermochemical data for the closed-shell fluoromethylenes (:CHF and :CF₂) can be found in the JANAF tables (19). More recently, Rodgers (24) has recommended a value for the heat of formation of :CF₂ based largely upon kinetic data; Hsu and coworkers (27) and Pritchard and coworkers (28) have independently made a recommendation for the heat of formation of :CHF based upon heat of reaction and kinetic data; and Lias and coworkers (29) have provided values for the heat of formation of both :CHF and :CF₂ based upon appearance and ionization potentials. Unfortunately (since :CHF

and :CF_2 are important species), there are significant uncertainties in their heats of formation. The values for :CF_2 are the best (± 10 kJ/mol) and are derived from a number of different types of measurements. The uncertainty in the heat of formation for :CHF is even greater (± 30 kJ/mol) due to the lack of direct, reliable data. We used heats of formation for :CF_2 as adopted by Rodgers and for :CHF as provided by Pritchard and coworkers. For entropies at standard state and heat capacity data of both species, we used values from the JANAF tables. We note that heats of formation for both species from our BAC-MP4 *ab initio* calculations (23) are within ~ 15 kJ/mol of the recommended experimental values.

Thermochemical data for fluoromethylidyne ($\bullet\text{CF}$) can be found in the JANAF tables (19). We note that our BAC-MP4 *ab initio* heat of formation for $\bullet\text{CF}$ is within ~ 20 kJ/mol of the JANAF recommendation.

Carbonyl Fluorides and Fluoromethoxy Radicals. Thermochemical data for the carbonyl fluorides ($\text{CHF}=\text{O}$, $\text{CF}_2=\text{O}$, $\bullet\text{CF}=\text{O}$) can be found in the JANAF table. The biggest uncertainties here are for $\text{CHF}=\text{O}$ (± 20 kJ/mol) and $\bullet\text{CF}=\text{O}$ (± 10 kJ/mol), where no direct experimental data are available. Consequently, their heats of formation were calculated using average bond dissociation energies from other related compounds. We note that heats of formation for these species from our BAC-MP4 *ab initio* calculations (23) are within ~ 20 kJ/mol of the recommended experimental values, except for $\text{CF}_2=\text{O}$, where the *ab initio* value is ~ 40 kJ/mol higher. Other *ab initio* calculations (30-31) using different approaches also predict a heat of formation for $\text{CF}_2=\text{O}$ that is higher (by ~ 30 kJ/mol) than the experimental value. Because of this significant difference, both uncertainties in the experimental measurements and *ab initio* calculations warrant further examination. Given that reliable experimental data exists for the unimolecular decomposition of $\text{CHF}=\text{O}$ (32), any uncertainty in its heat of formation may be unimportant. However, under some conditions the bimolecular reaction $\bullet\text{CF}=\text{O} + \text{H}_2\text{O} \rightarrow \text{CHF}=\text{O} + \text{OH}$ (~ 80 kJ/mol endothermic) may contribute. Consequently, any uncertainty in the heat of formation of $\text{CHF}=\text{O}$ may play some role. In contrast, the heat of formation of $\bullet\text{CF}=\text{O}$ is very important, since there are no experimental data for its unimolecular decomposition (a major pathway).

We used an experimentally-derived value for the heat of formation of the perfluoromethoxy radical $\text{CF}_3\text{O}\bullet$ (33). For entropy at standard state and heat capacity data, we used that derived from our BAC-MP4 *ab initio* calculations (23). The *ab initio* heat of formation is within ~ 30 kJ/mol of the experimental value. A number of other species, such as the other fluoromethoxy radicals (*e.g.*, $\text{CH}_2\text{FO}\bullet$), fluoromethanols (*e.g.*, CF_3OH), or fluoromethylperoxy radicals (*e.g.*, $\text{CF}_3\text{OO}\bullet$), were initially considered in the mechanism (using *ab initio* thermochemical data). These species were later excluded, because they did not contribute to the overall chemistry. In many cases, these species were present in steady state concentrations and creation and destruction reactions can be combined into a single overall reaction. Although these species may be important in atmospheric chemistry, they are present in extremely low concentrations at high temperatures in hydrocarbon/air flames.

Fluoroethanes. Thermochemical data for some of the fluoroethanes can be found in the Journal of Physical and Chemical Reference Data (34) and the DIPPR compilation (35). Recommendations for the heats of formation of some of the fluoroethanes have been made by Kolesov and Papina (36) and by Pedley *et al.* (37). There are no experimentally-derived heats of formation for a number of the fluoroethanes ($\text{CH}_3\text{-CH}_2\text{F}$, $\text{CHF}_2\text{-CHF}_2$, $\text{CH}_2\text{F-CF}_3$). These have been estimated using bond or group additivity or other trends in heats of formation. However, there are significant uncertainties in these procedures, because of non-covalent or ionic contributions to these species stability due to the high electronegativity of fluorine. For example, $\text{CH}_3\text{-CF}_3$ is ~ 34 kcal/mol more stable than predicted using heats of formation of $\text{CH}_3\text{-CH}_3$ and $\text{CF}_3\text{-CF}_3$ (all three have good experimentally-derived values). The additional stabilization can be rationalized as an ionic contribution to the C-C bond strength because of large differences in net charges on the carbon atoms of the -CH_3 and -CF_3 groups due to the high electronegativity of the F atoms.

A recommendation for the heat of formation of ethyl fluoride ($\text{CH}_3\text{-CH}_2\text{F}$) has recently been made by Luo and Benson (38), based on electronegativity correlations of heats of formation of substituted alkanes, and is significantly lower (15 kJ/mol) than other values. The reasons for this significant difference warrant further examination. $\text{CH}_3\text{-CH}_2\text{F}$ is unlikely to be important as a species in the fluorocarbon-inhibited hydrocarbon flames. However, as a simple, single-substituted fluorinated hydrocarbon (like CH_3F), its heat of formation is important for benchmarking the heats of formation of other species. For example, another $\text{-CH}_2\text{F}$ substituted fluoroethane, $\text{CH}_2\text{F-CF}_3$, has no experimentally-derived heats of formation. Any uncertainties in the heats of formation and, consequently, stability of the fluoroethanes will influence product channels for fluoromethyl combinations (*e.g.*, $\bullet\text{CH}_3 + \bullet\text{CF}_3 \rightarrow \text{CH}_3\text{-CF}_3$ versus $\bullet\text{CH}_3 + \bullet\text{CF}_3 \rightarrow \text{CH}_2=\text{CF}_2 + \text{HF}$).

We used thermochemical data from the JPCRD review for the six simplest fluoroethanes ($\text{CH}_3\text{-CH}_2\text{F}$, $\text{CH}_3\text{-CHF}_2$, $\text{CH}_3\text{-CF}_3$, $\text{CH}_2\text{F-CF}_3$, $\text{CHF}_2\text{-CF}_3$, $\text{CF}_3\text{-CF}_3$). We used heats of formation for $\text{CH}_2\text{F-CH}_2\text{F}$ calculated using the C-C bond dissociation energy determined by Kerr and Timlin (39), for $\text{CH}_2\text{F-CHF}_2$ recommended by Lacher and Skinner (40), and for $\text{CHF}_2\text{-CHF}_2$ from our *ab initio* calculations. Standard state entropies and heat capacities were computed based on vibrational frequencies and moments of inertia from our *ab initio* calculations. We believe re-examination of all of the heat of formation data is warranted. For example, the heat of formation of $\text{CH}_3\text{-CF}_3$ recommended in the JPCRD review is based on old values for $\bullet\text{CH}_3$ and $\bullet\text{CF}_3$. We note that heats of formation for the fluoroethanes from our BAC-MP4 *ab initio* calculations are within $\sim 10\text{-}20$ kJ/mol of recommended values.

Fluoroethyl Radicals. There are experimentally-derived thermochemical data (24) for a few of the fluoroethyl radicals ($\text{CH}_3\text{-CF}_2\bullet$, $\text{CF}_3\text{-CH}_2\bullet$, $\text{CF}_3\text{-CF}_2\bullet$). Heats of formation for the others have been estimated using heats of formation for the fluoroethanes and C-H or C-F bond dissociation energies for $\text{CH}_3\text{-CHF}\bullet$ and $\text{CF}_3\text{-CHF}\bullet$ by Martin and Paraskevopoulos (41), for $\text{CH}_3\text{-CHF}\bullet$ by Tschuikow-Roux and Salomon (42), and for all other fluoroethyl radicals by Burgess and Zachariah (43). Thermochemistry for all fluoroethyl radicals have been calculated using *ab initio* molecular orbital theory by Tschuikow-Roux and coworkers (44-46). They

used the experimentally-derived heats of formation for the three fluoroethyl radicals recommended by Rodgers (24). For the others, they used their calculated energies in conjunction with isodesmic-homodesmic reactions (with known experimental reaction enthalpies) to provide values that approach the "true" heats of formation. We used the thermochemical data provided by Tschuikow-Roux and coworkers, because it provides a consistent set of data. However, we believe some re-examination of all of the heat of formation data (both experimental and *ab initio*) is warranted. We note that heats of formations for the fluoroethyl radicals from our BAC-MP4 *ab initio* calculations are within ~ 20 kJ/mol of the recommended values.

Fluoroethylenes and Fluorovinyl Radicals. Thermochemistry for $\text{CF}_2=\text{CF}_2$ can be found in the JANAF tables (19) and data for $\text{CH}_2=\text{CHF}$ and $\text{CH}_2=\text{CF}_2$ in the DIPPR compilation (35). Heats of formation based on ionization potentials have been determined for $\text{CHF}=\text{CHF}(E)$ and $\text{CHF}=\text{CHF}(Z)$ by Stadelman and Vogt (48). Recommendations for the heat of formation and entropy at standard state of $\text{CHF}=\text{CF}_2$ have been made by Stull *et al.* (49). We supplemented these data using the results of our BAC-MP4 *ab initio* calculations (23) to provide entropies at standard state for $\text{CHF}=\text{CHF}(E)$ and $\text{CHF}=\text{CHF}(Z)$ and heat capacity data for $\text{CH}_2=\text{CHF}$, $\text{CHF}=\text{CHF}(E)$, $\text{CHF}=\text{CHF}(Z)$, and $\text{CHF}=\text{CF}_2$.

There are no experimentally-derived thermochemical data (to our knowledge) for the fluorovinyl radicals. Consequently, we used thermochemical data from our BAC-MP4 *ab initio* calculations (23).

Other C_2 Fluorinated Hydrocarbons. The thermochemistry of the fluoroacetylenes (C_2HF , C_2F_2) can be found in the JANAF tables (19), however, with relatively large uncertainties: ± 60 kJ/mol and ± 20 kJ/mol in the heats of formation, respectively. Fluoroketenes ($\text{CHF}=\text{C}=\text{O}$ and $\text{CF}_2=\text{C}=\text{O}$) and the fluoroketyl radical ($\bullet\text{CF}=\text{C}=\text{O}$) can be formed through a number of channels (analogous to simple hydrocarbon chemistry). To assess the importance of these species and relevant reactions, we included these species in the mechanism. There are no experimentally-derived data for these species. Consequently, we used data from our BAC-MP4 *ab initio* calculations (23). A number of other partially-oxidized species, such as $\text{CH}_3\text{-CFO}$, were excluded from the mechanism based on the assumption that they would be only present in steady state concentrations at flame temperatures. For lower temperatures, this assumption should be re-examined.

Reaction Kinetics. The mechanism is too large to be described in detail here and, consequently, only a overview of important classes of reactions will be presented. Utilizing the species identified as potentially important, a grid of possible reactions was constructed. Existing chemical rate data involving these fluorinated species was then compiled and evaluated. Where rate data were available, but only over limited temperature ranges or at different pressures (for unimolecular or chemically activated steps), RRKM (50) and QRRK (51) methods were used to estimate the temperature dependencies (at 1 atmosphere) of the rates and to predict relative rates where multiple product channels were possible. Where no rate data were available for potential reactions, the rate constants were estimated by analogy to other hydrocar-

bon or substituted hydrocarbon reactions. The prefactors were adjusted for reaction path degeneracy and the activation energies were adjusted empirically based on relative heats of reaction or relative bond energies (*i.e.*, Evans-Polanyi relationships).

Initially, upper limits were used for estimated rate constants. If as a result of simulations under a variety of conditions (using different agents, flame geometries, etc.), it was observed that a specific reaction with an upper limit rate constant did not significantly contribute to the destruction or creation of any of the species in the "mechanism," then we continued to use that estimate. However, if a specific reaction contributed to the chemistry and its rate constant was an upper-limit estimate, then its value was re-examined and possibly refined. For important contributing reactions where no good analogy was available, where significant uncertainty existed in the barrier (generally reactions with tight transition states and modest-to-large barriers), or where multiple, energetically-similar product channels were possible, we calculated the geometries and energies of the transition states (23) using the BAC-MP4 *ab initio* method. RRKM methods were then applied to obtain the temperature (and pressure) dependence of the rate constant.

Hydrocarbon Chemistry. The C/H/O subset is derived from the Miller-Bowman mechanism (52) and consists of about 30 species and 140 reactions. Any other hydrocarbon mechanism could be substituted, for example the GRIMECH (53).

H/O/F Chemistry. The H/O/F subset consists of about 3 species and 8 reactions that are relatively well known. This is the chemistry of fluorine atoms with hydrogen- and oxygen-containing species, such as H₂, OH, and H₂O. There are three reactions of this type that were determined to participate in the chemistry under a variety of conditions. These reactions are the combination of H and F to form HF (and the reverse decomposition) and the hydrogen atom transfer reactions by F atoms from H₂ and H₂O.

C₁/H/O/F Chemistry. The C₁/H/O/F subset with about 150 reactions consists of chemistry of 14 species containing one carbon (and hydrogen/oxygen/fluorine) with H, O, OH, H₂O, and other flame species. It includes reactions such as unimolecular and chemically-activated decompositions of the fluoromethanes, reactions of fluoromethyls with O₂, O, and OH to form carbonyl fluorides (*e.g.*, CF₂=O) and other products, and reactions of the fluoromethylenes (*e.g.*, :CF₂) with H to form •CF and O₂, O, or OH to form carbonyl fluorides.

Fluoromethanes: Decompositions and Abstractions. Both thermally- and chemically-activated decompositions of the fluoromethanes were considered (*e.g.*, CHF₃ → :CF₂ + HF and •CHF₂ + H → :CF₂ + HF). There have been a number of measurements of the unimolecular decomposition of fluoromethanes (with HF elimination). We employed rate expressions for HF elimination from CH₃F and CHF₃ that are extended Arrhenius fits to the experimental data of Schug and Wagner (54) and Hidaka *et al.* (55), respectively. These data were obtained at different temperatures and pressures than are relevant to atmospheric flames. The experimental data were interpolated or extrapolated and fit using temperature

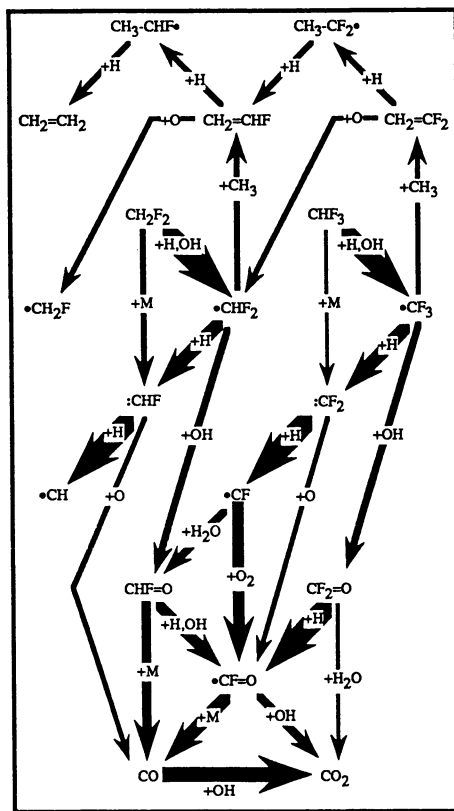


FIGURE 1. Typical Reaction Pathways for CH_2F_2 and CHF_3 Decomposition.

dependencies (T^b) that were consistent with the experimental data and our RRKM calculations. For HF elimination from CH_2F_2 , we employed a rate expression from our BAC-MP4/RRKM calculations, although there is reasonable experimental data by Politanskii and Shevchuk (56). For H_2 elimination (a minor channel) from CH_3F and CH_2F_2 , we used rate expressions from our RRKM calculations using our BAC-MP4 *ab initio* barriers (23). Fluorine atom eliminations from the fluoromethanes are negligible decomposition channels, except for CF_4 , where it is the only possible pathway. For this reaction, we used a rate expression from our RRKM calculations, based on room temperature measurements for $\text{CF}_3 + \text{F}$ by Plumb and Ryan (57).

There have been no measurements (to our knowledge) for reactions involving chemically activated or "hot" fluoromethanes other than room temperature measurements of the rate constant for $\text{CF}_3 + \text{H} \rightarrow \text{Products}$, for example Tsai and McFadden (58). We used RRKM methods with either experimental or BAC-MP4 (23) *ab initio* barriers (23) for insertion of $:\text{CHF}$ and $:\text{CF}_2$ into HF and H_2 , and the energetics of the reaction pathways to estimate values for these various reactions, as well as for the stabilized fluoromethane channels. Although there are no experimental measurements at flame temperatures for chemically-activated fluoromethane decompositions, and these are primary pathways for destruction of fluoromethyl radicals, the corresponding uncertainties in the rates are small since these combinations are barrierless.

There have been a number of measurements of H atom abstractions by H, O, and OH radicals from the fluoromethanes. For abstraction by H atoms, we fit experimental data for CH_3F (59), CH_2F_2 (60), and CHF_3 (61) using a temperature dependence ($T^{3.0}$) by analogy to methane. For abstraction by O atoms, we fit experimental data for CH_3F (62), CH_2F_2 (63), and CHF_3 (64) using a temperature dependence ($T^{1.5}$) also by analogy to methane. For abstraction by OH radicals, we used prior recommended rate expressions (65-67) that have temperature dependencies based on transition state theory. These recommendations are largely based on the experimental work of Jeong and Kaufman (68).

The fluoromethanes are primarily destroyed in hydrocarbon flames by H atom abstraction by H and OH and through unimolecular decomposition (see Figure 1). Destruction by H atom abstraction by O atoms is a minor channel. Although there is good quality experimental data, the biggest uncertainty is the unimolecular decompositions, because they are very temperature and pressure dependent. Further mechanism refinements should provide better rate expressions for these reactions.

Fluoromethyl Radical Destruction. Fluoromethyl radicals are destroyed by three general pathways whose relative contributions are sensitive to conditions: 1) they can combine with H atoms forming chemically-activated fluoromethanes that eliminate HF (creating methylene/fluoromethylenes); 2) they can react with oxygen-containing species (*i.e.*, O_2 , O, OH), resulting in the formation of fluoromethoxy radicals and carbonyl fluoride species; and 3) they can combine with methyl or fluoromethyl radicals, forming chemically-activated fluoroethanes that may be either stabilized or eliminate HF (creating ethylene/fluoroethylenes). This latter class of reactions is included with the fluoroethane (C_2) chemistry. The fluoromethyl radicals are primarily formed by H atom abstractions from the fluoromethanes. However, there are several other channels that can contribute to their formation and

are classified as C₂ chemistry. For example, CH₂=CHF + O → •CH₂F + HCO or CHF₂-CF₂• + H → •CHF₂ + •CHF₂ contribute to the formation of fluoromethyl radicals. Similarly, there are a number of other decomposition channels that can be classified as C₃ chemistry, such as •CH₂F + C₂H₄ → •CH₂-CH₂-CH₂F.

There are four potential product channels following association of fluoromethyl radicals (*e.g.*, •CHF₂) with O₂ (by analogy to hydrocarbon and chlorinated hydrocarbon chemistry). These are: 1) stabilization of the fluoromethylperoxy radicals (*e.g.*, CHF₂OO•); 2) internal abstraction of a hydrogen atom followed by O-O bond breakage (*e.g.*, CF₂=O + OH); 3) internal abstraction of a fluorine atom followed by O-O bond breakage (*e.g.*, CHF=O + OF); or 4) direct dissociation of the O-O bond (*e.g.*, CHF₂O• + O). The first channel (stabilization) should be negligible at flame temperatures, but may need to be considered at lower temperatures and for ignition delays. The second channel (H abstraction) should be a secondary pathway at flame temperatures, but clearly should be re-examined at lower temperatures. The third channel (F abstraction) can be disregarded because of the strong C-F bond (the analogous reaction is assumed to occur in chlorinated hydrocarbon chemistry). Consequently, we explicitly considered only the fourth channel (direct O-O bond dissociation). For •CF₃ + O₂ → CF₃O• + O, we estimated a rate expression from our RRKM calculations assuming no barrier in the reverse direction. For the other two fluoromethyl reactions, we assumed the fluoromethoxy radical would be present in steady state concentrations, rapidly eliminating HF, and simply used the •CF₃ rate expression after adjusting for reaction enthalpies.

For reaction of the perfluoromethyl radical (•CF₃) with O atoms (eliminating F), we used a rate constant corresponding to the room temperature value measured by McFadden and coworkers (69). For reaction of the other fluoromethyl radicals with O atoms (eliminating H), we used rate constants scaled between that for •CH₃ and •CF₃. For reaction of the fluoromethyl radicals with OH radicals, we used rate constants identical to that for •CH₃.

Fluoromethyl radicals are primarily destroyed in hydrocarbon flames through reactions with H, OH, and •CH₃ radicals (see Figure 1). Reactions with O atoms are minor channels. The biggest uncertainty here is likely to be reactions with •CH₃ radicals (HF elimination versus stabilization), which are very temperature and pressure dependent. Further refinements of this mechanism should provide better rate expressions for these reactions, benchmarking them to experimental data that exists (see brief discussion in Fluoroethane Chemistry section).

Fluoromethylene and Fluoromethylidyne Destruction. The rates of reactions for the fluoromethylenes (:CHF and :CF₂) and fluoromethylidyne (•CF) with many species are somewhat uncertain, given they are significantly slower than the analogous reactions for methylene (CH₂) and methylidyne (CH). There also appears to be conflicting experimental data on the reactivities of the fluoromethylenes and fluoromethylidyne. The fluoromethylenes can be destroyed through four pathways: 1) reaction with H atoms, where we used rate constants corresponding to the room temperature values measured by McFadden and coworkers (58,70); 2) reaction with O atoms, where we used rate constants corresponding to the room temperature values measured by McFadden and coworkers (70-71); 3) reaction with OH radicals,

where we used rate constants (for both species) corresponding to the value for $\cdot\text{CF}_2$ determined by Biordi *et al.* (72) in their flame measurements; and 4) reaction with O_2 , where we used the rate expression for $\cdot\text{CF}_2$ measured by Keating and Matula (73) and the equivalent rate expression for $\cdot\text{CHF}$ after adjusting for reaction enthalpy. The fluoromethylenes can also be destroyed via insertion into H_2O (a major flame species). We estimated barriers to reaction of 25 and 100 kJ/mol for $\cdot\text{CHF}$ and $\cdot\text{CF}_2$, respectively, from our BAC-MP4 *ab initio* calculations. The fluoromethylenes can also be destroyed via reaction with hydrocarbons (see brief discussion in Fluoroethane Chemistry section).

For reactions of $\cdot\text{CF}$ with O_2 , H, and O, we used rate expressions with reasonable prefactors and barriers that are consistent with the room temperature rate measurements of McFadden and coworkers (69,71) and Peeters *et al.* (74). We note that to date we have (mis)assigned the products of the reaction $\cdot\text{CF} + \text{H} \rightarrow \text{C} + \text{HF}$ (~ 25 kJ/mol exothermic) as $\text{CH} + \text{F}$ (~ 20 kJ/mol endothermic). This was done to eliminate C, C_2H , C_4H_2 , and other fuel rich species in order to minimize the number of species in the reaction set. If a hydrocarbon sub-mechanism is used that includes these species, the correct product channel should be used. For the reaction $\cdot\text{CF} + \text{OH} \rightarrow \text{CO} + \text{HF}$, we assumed no reaction barrier. For $\cdot\text{CF} + \text{H}_2\text{O} \rightarrow \text{Products}$, we estimated an activation energy of 70 kJ/mol by analogy to other radical+ H_2O reactions. $\cdot\text{CF}$ can also be formed via $\text{CH} + \text{HF} \rightarrow \cdot\text{CF} + \text{H}_2$ (~ 70 kJ/mol exothermic). For reaction of $\cdot\text{CF}$ with other molecules, we assumed upper limits that should be re-examined if those reactions contribute to $\cdot\text{CF}$ destruction.

The fluoromethylenes ($\cdot\text{CHF}$ and $\cdot\text{CF}_2$) are largely destroyed in hydrocarbon flames via reaction with H atoms. Reactions with O and OH radicals are minor channels. There are good quality experimental data for all of the reactions which proceed with small barriers. An open question here is the probable addition of the fluoromethylenes to ethylene. This class of reactions have been ignored in this mechanism in order to minimize the number of species in the reaction set, because these reactions would lead to the formation of C_3 fluorinated hydrocarbons. In the reaction set, fluoromethylidyne ($\cdot\text{CF}$) is largely destroyed via reaction with O_2 and H_2O . Reaction with H atoms is a minor channel. Given that there are no experimental measurements for reaction of $\cdot\text{CF}$ with H_2O , limited (and inconsistent) data for reaction with O_2 , and both of these reactions are likely to have modest barriers, these reactions provide a significant uncertainty to this reaction set. Further refinements of this mechanism should address these issues for $\cdot\text{CHF}$, $\cdot\text{CF}_2$, and $\cdot\text{CF}$.

Carbonyl Fluoride Chemistry. An important set of species to fluorocarbon species are the carbonyl fluorides ($\text{CHF}=\text{O}$, CF_2O , $\cdot\text{CF}=\text{O}$).

$\text{CHF}=\text{O}$ can be destroyed via unimolecular decomposition and H atom abstraction by H, O, and OH radicals. For the unimolecular decomposition (eliminating HF), we have fit the experimental data of Saito *et al.* (75) using an extended Arrhenius expression (using their recommended value for E_0). For the abstractions, we have substituted accepted rate expressions for the analogous $\text{CH}_2=\text{O}$ reactions. However, there is some significant uncertainty for abstraction by H atoms. The C-H bond dissociation energy in $\text{CHF}=\text{O}$ is ~ 45 -50 kJ/mol stronger than in $\text{CH}_2=\text{O}$. Consequently, as an abstraction the barrier should be somewhat

higher. On the other hand, H atom addition followed by H₂ elimination could be more facile than the pure abstraction.

CF₂=O can be destroyed via unimolecular decomposition (F atom elimination), by reactions with H atoms, through reactions with OH radicals, and potentially through reactions with H₂O. The unimolecular decomposition is likely a minor channel due to the strong C-F bond. There are a number of possible reactions with H atoms: 1) direct abstraction of a F atom abstraction; 2) addition to the oxygen followed by 1,2 elimination of HF; and 3) addition to the carbon followed by 1,1 elimination of HF. Biordi *et al.* (76) have estimated a rate constant for the net reaction of H with CF₂=O at 1800 K based on their molecular beam sampling measurements in low pressure flames. More recently, Richter *et al.* (77) has estimated a rate expression based upon measurements at several different temperatures. We have also used BAC-MP4 *ab initio* transition state calculations (23) followed by RRKM analysis to provide rate expressions for each of the possible channels. Our calculations are in excellent agreement with the experimental values and indicate the following trends: 1) the addition/1,2 elimination channel dominates (92 kJ/mol barrier); 2) the addition/1,1 elimination channel is about a factor of ten slower (101 kJ/mol barrier); and 3) the direct abstraction channel is negligible (188 kJ/mol barrier). CF₂=O may also be destroyed via addition of OH to the carbon atom followed by 1,2 elimination of HF. However, this is likely a minor channel for destruction, since from our BAC-MP4 *ab initio* transition state calculations, we estimate a barrier of ~105 kJ/mol. Because of the low reactivity of CF₂=O and the large amounts of H₂O in hydrocarbon flames, CF₂O + H₂O reactions must be considered. We have calculated rate expressions for CF₂=O + H₂O complex formation followed by HF elimination. Modeling results suggest that it is a secondary destruction pathway to the H atom addition/1,2 elimination pathway, but, nevertheless, it still needs to be considered.

The radical species •CF=O can be destroyed via unimolecular decomposition and reactions with H, O, OH, and •CH₃ radicals. Modeling results suggest that the unimolecular decomposition and the reaction with H atoms are the primary decomposition pathways (see Figure 1). For reaction with H atoms, we used a rate constant identical to that for the analogous HCO reaction. For the unimolecular decomposition, we determined a rate expression assuming a barrierless combination in the reverse direction. There is significant uncertainty in the heat of formation of •CF=O and, consequently, there is significant uncertainty in this rate. Future refinements of this mechanism should address this issue.

C₂/H/O/F Chemistry. The C₂/H/O/F subset consists of about 40 species and 400 reactions and consists of reactions analogous to those in the C₁ subset with a few exceptions (due to new types of product channels).

Fluoroethanes: Thermally and Chemically Activated Decompositions.

Both thermally- and chemically-activated decompositions of the fluoroethanes were considered, as well as stabilization of hot fluoroethanes (*e.g.*, CH₃-CF₃ → CH₂=CF₂ + HF, •CH₃ + •CF₃ → CH₂=CF₂ + HF, and •CH₃ + •CF₃ → CH₃-CF₃). There have been quite a few measurements (mainly in shock tubes) of the unimolecular decomposition of the fluoroethanes by a number of different workers (*e.g.*, 78-85).

We selected experimental values from these and other sources and used them without modification. The validity of employing these high pressure limit values should be re-examined for those fluoroethanes that have only a few fluorine substitutions, especially when using the reaction set at low pressures (and high temperatures). There have been a number of measurements for reactions of a few of the chemically-activated or "hot" fluoroethanes produced by combination of fluoromethyl radicals, for example Kim *et al.* (86). These data include (in some cases) branching ratios between product channels (*i.e.*, HF elimination versus stabilization). There are no measurements (to our knowledge) for decomposition of hot fluoroethanes following combination of fluoroethyl radicals and H atoms. We used rate expressions for all products of the hot fluoroethanes based on our RRKM calculations in order to provide a consistent set. Further refinements of this mechanism should include benchmarking the RRKM calculations to the existing experimental data.

Fluoroethanes: Fluoromethyl Disproportionation and Fluoromethylene Insertions. There has been a number of measurements of disproportionations between methyl and fluoromethyl radicals (*e.g.*, Pritchard *et al.* (87)). These studies suggest a branching ratio for disproportionation versus combination (HF elimination or stabilization) of ~10-20% at 350-500 K. We employed these data in combination with estimated barriers from our BAC-MP4 *ab initio* calculations and determined rate expressions consistent with the experimental data. The barriers to disproportionation are ~3-9 kJ/mol for reactions involving $\cdot\text{CHF}_2$ (*i.e.*, $\cdot\text{CF}_2$ product) and 14-19 kJ/mol for reactions involving $\cdot\text{CH}_2\text{F}$ (*i.e.*, $\cdot\text{CHF}$ product). The species $\cdot\text{CHF}$ and $\cdot\text{CF}_2$ may also insert into C-H bonds in methane and fluoromethanes. We used rate expressions based on estimated barriers from our BAC-MP4 *ab initio* calculations of 63 and 130 kJ/mol for insertions of $\cdot\text{CHF}$ and $\cdot\text{CF}_2$, respectively. These are rather significant when compared to $\cdot\text{CH}_3$, which inserts into C-H bonds with little barrier. Our BAC-MP4 *ab initio* calculations suggest these barriers result from ionic repulsion between the electropositive H atom on the (fluoro)methane and the highly electropositive carbon atom on the fluoromethylene. For example, the H atom on CH_4 has a Mulliken charge of +0.17 and the C atom on $\cdot\text{CF}_2$ has a Mulliken charge of +0.54. However, there is some experimental evidence to suggest that the barriers are significantly smaller (88). This apparent conflict should be addressed in future mechanism refinements.

Fluoroethanes: Abstractions. There have been a number of measurements of H atom abstractions by OH radicals from the fluoroethanes. Cohen and co-workers (65-67) have recommended rate expressions for these reactions that have temperature dependencies based on transition state theory. Their recommendations are largely based on the experimental measurements of Clyne and Holt (89) and Martin and Paraskevopoulos (41). There have been no measurements (to our knowledge) for H atom abstractions by H and O atoms from the fluoroethanes. Consequently, we utilized an empirical correlation that we determined for other H abstraction reactions. For abstraction by H atoms, we used activation energies that were a factor of 2.5 times that for the analogous abstraction by OH radicals. For abstraction by O atoms, a factor of 2.7 was employed.

The fluoroethanes are largely destroyed via unimolecular decomposition and abstraction by OH radicals. There are good quality experimental data for these reactions. Future refinements of this mechanism need only re-evaluate this work.

Fluoroethyl Radical Destruction. Fluoroethyl radicals can be destroyed via reaction with the flame species O_2 , H, O, OH, and $\bullet CH_3$. For reaction with O_2 , O, and OH, we used the accepted rate expressions for the analogous ethyl radical reactions. Reactions of fluoroethyl radicals with H atoms form hot fluoroethanes and we used rate expressions from our RRKM calculations as mentioned previously. Fluoroethyl radicals may combine with $\bullet CH_3$ to form hot fluoropropanes (which most likely will be stabilized except at the highest temperature). Fluoroethyl radicals may also disproportionate with $\bullet CH_3$ to form CH_4 and fluoroethylenes. The first channel (combination) was simply ignored in order to exclude C_3 fluorinated species from the reaction set. The rate constants for the second channel (disproportionation) was set identical to that accepted for $C_2H_5 + \bullet CH_3 \rightarrow C_2H_4 + CH_4$.

Fluoroethylene Chemistry. There are experimental measurements (90-91) for the rate of pyrolysis of two of the fluoroethylenes (eliminating HF). For the other fluoroethylenes, we used these rate expressions as benchmarks and adjusted the activation energy based on the reaction enthalpy. For pyrolysis of perfluoroethylene ($CF_2=CF_2 \rightarrow \bullet CF_2 + \bullet CF_2$), we used a rate expression from our RRKM fits to the experimental data of Schug and Wagner (92). For the other thermally and chemically activated fluoroethylene decompositions (e.g., $\bullet CHF + \bullet CHF \rightarrow CHF=CHF$ or $C_2HF + HF$), we used rate expressions from our RRKM calculations (with our estimate of the barrier to combination). Fluoroethylenes are primarily destroyed via reaction with O atoms (e.g., $CH_2=CF_2 + O \rightarrow \bullet CHF_2 + HCO$). For these reactions, we used the recommendations of Cvetanovic (93). There is some evidence to suggest (94) that the assumed methyl+formyl products (e.g., $\bullet CHF_2 + HCO$) may not be the only product channel (e.g., $CHF=CHF + O \rightarrow CHF=C=O + HF$ or $CHF=CHF + O \rightarrow CHF=O + \bullet CHF$). Future refinements should resolve this issue.

Fluoroethylenes can also be destroyed via reaction with H atoms. This includes H atom addition followed by stabilization of the fluoroethyl radical produced (e.g., $CH_2=CF_2 + H \rightarrow CH_3-CF_2\bullet$ or $CHF_2-CH_2\bullet$), as well as H atom addition followed by F atom elimination (e.g., $CH_2=CF_2 + H \rightarrow CH_2=CHF + F$). There are some experimental data for these reactions, however, there are appears to be some conflict between them. Consequently, in this mechanism, we simply employed an accepted rate expression for the H atom addition/stabilization for the analogous ethylene reaction. For the F atom eliminations, we assumed barrierless addition in the reverse direction. However, there are some significant uncertainties here. First, it is likely the barrier-to-addition will be influenced by the degree of fluorine substitution on the alpha carbon. Secondly, the efficiency of stabilization of the "hot" fluoroethyl radical will be strongly influenced by the degree of fluorine substitution. Fluoroethylenes may also be destroyed by OH addition/elimination reactions resulting in the formation of (fluoro)vinoxy radicals (e.g., $CHO-CHF\bullet$). However, in order to minimize the number of species in the reaction set, we have not consider these reactions. Future mechanism refinements should consider these.

Summary

We constructed a large comprehensive reaction set or "mechanism" for fluorinated hydrocarbon chemistry involving C₁ and C₂ stable and radical hydrocarbon species, including partially oxidized fluorinated hydrocarbons. This paper presents an overview of the thermochemical and kinetic data in the reaction set and brief documentation of the sources of the data (including estimations and calculations as part of this work). We discussed the key species and important reactions in the fluorocarbon chemistry. We attempted to identify some of those species and reactions with uncertain thermochemical and rate data that could impact the decomposition pathways and flame chemistry. The mechanism should be considered only a framework for future model development, rather than a finished product. Future refinements will require experimental validation by high temperature flow reactor, premixed flame, and diffusion flame measurements, as well as measurements of important, yet currently uncertain rate constants.

Acknowledgements

The authors wish to acknowledge support of the project "Agent Screening for Halon 1301 Aviation Replacement" by the U.S. Naval Air Systems Command, the U.S. Army Aviation and Troop Command, the Federal Aviation Administration Technical Center, and the U.S. Air Force. This program at NIST was directed by Mr. Michael Bennett of the Wright Patterson AFB Flight Dynamics Laboratory, Vehicle Subsystems Division, Survivability Enhancement Branch. The authors also wish to express their gratitude to Dr. Carl F. Melius of Sandia National Laboratories for use of the BAC (Bond Additivity Corrections) code.

Literature Cited

1. Grosshandler, W.L.; Gann, R.G.; Pitts, W.M., Eds.; "Evaluation of Alternative In-Flight Fire Suppressants for Full-Scale Testing in Simulated Aircraft Engine Nacelles and Dry Bays," *NIST Special Publication 861*, 1994.
2. Ellis, O.C.; *Nature* **1948**, *161*, 402-403.
3. Fenimore, C.P.; Jones, G.W.; *Combust. Flame* **1963**, *7*, 323-329.
4. Day, M.J.; Stamp, V.; Thompson, K.; Dixon-Lewis, G.; *Thirteenth Symposium (International) on Combustion*; The Combustion Institute: Pittsburgh, PA, 1971; 705-712.
5. Biordi, J.C.; Lazzara, C.P.; Papp, J.F.; *Fourteenth Symposium (International) on Combustion*; The Combustion Institute: Pittsburgh, PA, 1973; 367.
6. Gann, R.G.; *ACS Symp. Ser.* **1975**, *16*, 318-340.
7. Westbrook, C.K.; *Combust. Sci. Technol.* **1983**, *34*, 201.
8. Vandooren, J.F.; da Cruz, N.; Van Tiggelen, P.; *Twenty-Second Symposium (International) on Combustion*; The Combustion Institute: Pittsburgh, PA, 1988; 1587.
9. Morris, R.A.; Brown, E.R.; Viggiano, A.A.; Vandoren, J.M.; Paulson, J.F.; Motevalli, V.; *Int. J. Mass Spectrom. Ion Proc.* **1991**, *121*, 95-109.

10. Jorriksen, W.P.; Meuwissen, J.C.; *Rec. Trav. Chim.* **1924**, *38*, 589-597.
11. Fristrom, R.M.; *Fire Res. Abs. Rev.* **1967**, *9*, 125-152.
12. Creitz, E.C.; *J. Res. NBS* **1970**, *74A*, 521-530.
13. Jensen, D.E.; Jones, G.A.; *J. Chem. Soc. Faraday Trans.* **1982**, *78*, 2843.
14. Biordi, J.C.; Lazzara, C.P.; Papp, J.F.; *J. Phys. Chem.* **1978**, *82*, 125.
15. Benson, S.W.; *Thermochemical Kinetics*; Wiley: New York, NY, 1976.
16. Frisch, M.J.; Trucks, G.W.; Head-Gordon, M.; Gill, P.M.W.; Wong, M.; Foresman, J.B.; Johnson, B.G.; Schlegel, H.B.; Robb, M.A.; Repogle, E.S.; Gomperts, R.; Andres, J.L.; Raghavachari, K.; Binkley, J.S.; Gonzalez, C.; Martin, R.L.; Fox, D.J.; Defrees, D.J.; Baker, J.; Stewart, J.J.P.; Pople, J.A.; *Gaussian 92*, Gaussian, Inc.: Pittsburgh, PA, 1992.
17. Curtiss, L.A.; Raghavachari, K.; Trucks, G.W.; Pople, J.A.; *J. Chem. Phys.* **1991**, *94*, 7221.
18. Melius, C.F.; "Thermochemistry of Hydrocarbon Intermediates in Combustion: Application of the BAC-MP4 Method," in *Chemistry and Physics of Energetic Materials*; Kluwer Academic Pub.: Dordrecht, 1990.
19. Stull, D.R.; Prophet, H.; "JANAF Thermochemical Tables," *NSRDS-NBS 37*, 1971.
20. Kee, R.J.; Rupley, F.M.; Miller, J.A.; "The Chemkin Thermodynamic Data Base," *SAND87-8215B*, Sandia National Laboratories, 1987.
21. Rodgers, A.S.; Chao, J.; Wilhoit, R.C.; Zwolinski, B.J.; *J. Phys. Chem. Ref. Data* **1974**, *3*, 117.
22. Kolesov, V.P.; *Russ. Chem. Rev.* **1978**, *47*, 1145-1168.
23. Zachariah, M.R.; Westmoreland, P.R.; Burgess, D.R.F. Jr.; Tsang, W.; Melius, C.F.; *ACS Symp. Ser.* **1995**, *this volume*; and unpublished data.
24. Rodgers, A.S.; *ACS Symp. Ser.* **1978**, *66*, 296.
25. McMillen, D.F.; Golden, D.M.; *Ann. Rev. Phys. Chem.* **1982**, *33*, 493.
26. Pickard, J.M.; Rodgers, A.S.; *Int. J. Chem. Kinet.* **1983**, *15*, 569-577.
27. Hsu, D.S.Y.; Umstead, M.E.; Lin, M.C.; *ACS Symp. Ser.* **1978**, *66*, 128.
28. Pritchard, G.O.; Nilsson, W.B.; Kirtman, B.; *Int. J. Chem. Kinet.* **1984**, *16*, 1637-1643.
29. Lias, S.G.; Karpas, Z.; Liebman, J.F.; *J. Am. Chem. Soc.* **1985**, *107*, 6089.
30. Montgomery, J.A. Jr.; Michels, H.H.; Francisco, J.S.; *Chem. Phys. Lett.* **1994**, *220*, 391.
31. Schnieder, W.F.; Wallington, T.J.; *J. Phys. Chem.* **1994**, *98*, 7448.
32. Saito, K.; Kuroda, H.; Kakumoto, T.; Munechika, H.; Murakami, I.; *Chem. Phys. Lett.* **1985**, *113*, 399.
33. Batt, L.; Walsh, R.; *Int. J. Chem. Kin.* **1982**, *14*, 933-944.
34. Chen, S.S.; Rodger, A.S.; Chao, J.; Wilhoit, R.C.; Zwolinski, B.J.; *J. Phys. Chem. Ref. Data* **1975**, *4*, 441-456.
35. Daubert, T.E.; Danner, R.P.; "DIPPR Data Compilation of Pure Compound Properties," *NIST Standard Reference Database 11* **1985**.
36. Kolesov, V.P.; Papina, T.S.; *Russ. Chem. Rev.* **1983**, *52*, 425-439.
37. Pedley, J.B.; Naylor, R.D.; Kirby, S.P.; *Thermochemical Data of Organic Compounds*; Chapman and Hall: New York, NY, 1986.
38. Luo, Y.-R.; Benson, S.W.; *J. Phys. Chem.* **1988**, *92*, 5255-5257.

39. Kerr, J.A.; Timlin, D.M.; *Inter. J. Chem. Kin.* **1971**, *3*, 427-441.
40. Lacher, J.R.; Skinner, H.A.; *J. Chem. Soc. A* **1968**, *5*, 1034-1038.
41. Martin, J.-P.; Paraskevopoulos, G.; *Can. J. Chem.* **1983**, *61*, 861-865.
42. Tschuikow-Roux, E.; Salomon, D.R.; *J. Phys. Chem.* **1987**, *91*, 699-702.
43. Burgess, D.R.F., Jr.; Zachariah, M.R.; unpublished results.
44. Chen, Y.; Rauk, A.; Tschuikow-Roux, E.; *J. Chem. Phys.* **1990**, *93*, 1187.
45. Chen, Y.; Rauk, A.; Tschuikow-Roux, E.; *J. Chem. Phys.* **1990**, *93*, 6620.
46. Chen, Y.; Rauk, A.; Tschuikow-Roux, E.; *J. Chem. Phys.* **1991**, *94*, 7299.
47. Chen, Y.; Rauk, A.; Tschuikow-Roux, E.; *J. Chem. Phys.* **1991**, *95*, 2774.
48. Stadelmann, J.P.; Vogt, J.; *Int. J. Mass Spectrom. Ion Phys.* **1980**, *35*, 83.
49. Stull, D.R.; Westrum, E.F., Jr.; Sinke, G.C.; *The Chemical Thermodynamics of Organic Compounds*; John Wiley: New York, NY, 1969.
50. Robinson, P.J.; Holbrook, K.A.; *Unimolecular Reactions*; Wiley Interscience: New York, NY, 1972.
51. Dean, A.M.; Westmoreland, P.R.; *Int. J. Chem. Kin.* **1987**, *19*, 207.
52. Miller, J.A.; Bowman, C.T.; *Prog. Energy Comb. Sci.* **1989**, *15*, 287.
53. Bowman, C.T.; Frenklach, M.; Gardiner, W.; Golden, D.; Lissianski, V.; Smith, G.; Wang, H.; "GRIMECH," *Gas Research Institute Report*, 1995, in preparation.
54. Schug, K.P.; Wagner, H.G.; *Z. Phys. Chem.* **1973**, *86*, 59-66.
55. Hidaka, Y.; Nakamura, T.; Kawano, H.; *Chem. Phys. Lett.* **1991**, *187*, 40.
56. Politanskii, S.F.; Shevchuk, U.V.; *Kinet. Catal.* **1968**, *9*, 411-417.
57. Plumb, I.C.; Ryan, K.R.; *Ber. Bunsenges. Phys. Chem.* **1986**, *6*, 11.
58. Tsai, C.; McFadden, D.L.; *J. Phys. Chem.* **1989**, *93*, 2471.
59. Westenberg, A.A.; deHaas, N.; *J. Chem. Phys.* **1975**, *62*, 3321-3325.
60. Ridley, B.A.; Davenport, J.A.; Stief, L.J.; Welge, K.H.; *J. Chem. Phys.* **1972**, *57*, 520.
61. Arthur, N.L.; Bell, T.N.; *Rev. Chem. Intermed.* **1978**, *2*, 37-74.
62. Parsamyan, N.I.; Azatyan, V.V.; *Arm. Kim. Zh.* **1967**, *20*, 1.
63. Parsamyan, N.I.; Nalbanddyan, A.B.; *Arm. Kim. Zh.* **1968**, *21*, 1.
64. Jourdain, J.-L.; Le Bras, G.; Combourieu, J.; *J. Chim. Phys.* **1978**, *75*, 318.
65. Cohen, N.; Benson, S.W.; *J. Phys. Chem.* **1987**, *91*, 162-170.
66. Cohen, N.; Benson, S.W.; *J. Phys. Chem.* **1987**, *91*, 171-175.
67. Cohen, N.; Westberg, K.R.; *J. Phys. Chem. Ref. Data* **1991**, *20*, 1211-1311.
68. Jeong, K.-M.; Kaufman, F.; *J. Phys. Chem.* **1982**, *86*, 1808-1815.
69. Tsai, C.; Belanger, S.M.; Kim, J.T.; Lord, J.R.; McFadden, D.L.; *J. Phys. Chem.* **1989**, *93*, 1916.
70. Tsai, C.-P.; McFadden, D.L.; *J. Phys. Chem.* **1990**, *94*, 3298-3300.
71. Tsai, C.-P.; McFadden, D.L.; *Chem. Phys. Lett.* **1990**, *173*, 241-244.
72. Biordi, J.C.; Lazzara, C.P.; Papp, J.F.; *J. Phys. Chem.* **1978**, *82*, 125.
73. Keating, E.L.; Matula, R.A.; *J. Chem. Phys.* **1977**, *66*, 1237.
74. Peeters, J.; Van Hoeymissen, J.; Vanhaelemeersch, S.; Vermeylen, D.; *J. Phys. Chem.* **1992**, *96*, 1257-1263.
75. Saito, K.; Kuroda, H.; Kakumoto, T.; Munechika, H.; Murakami, I.; *Chem. Phys. Lett.* **1985**, *113*, 399.

76. Biordi, J.C.; Lazzara, C.P.; Papp, J.F.; *Fifteenth Symposium (International) on Combustion*; The Combustion Insititute: Pittsburgh, PA, 1974; 917-931.
77. Richter, H.; Vandooren, J.; Van Tiggelen, P.; *J. Chemie Physique*, in press.
78. Cadman, P.; Day, M.; Trotman-Dickenson, A.F.; *J. Chem. Soc. A* **1970**, 2498-2503.
79. Tschuikow-Roux, E.; Quiring, W.J.; Simmie, J.M.; *J. Phys. Chem.* **1970**, *74*, 2449-2455.
80. Tschuikow-Roux, E.; Quiring, W.J.; *J. Phys. Chem.* **1971**, *75*, 295-300.
81. Kerr, J.A.; Timlin, D.M.; *Int. J. Chem. Kin.* **1971**, *3*, 69-84.
82. Sekhar, M.V.C.; Tschuikow-Roux, E.; *J. Phys. Chem.* **1974**, *78*, 472-477.
83. Millward, G.E.; Tschuikow-Roux, E.; *J. Phys. Chem.* **1972**, *76*, 292-298.
84. Millward, G.E.; Hartig, R.; Tschuikow-Roux, E.; *J. Phys. Chem.* **1971**, *75*, 3195.
85. Tschuikow-Roux, E.; Millward, G.E.; Quiring, W.J.; *J. Phys. Chem.* **1971**, *75*, 3493-3498.
86. Kim, K.C.; Setser, D.W.; Holmes, B.E.; *J. Phys. Chem.* **1973**, *77*, 725-734.
87. Pritchard, G.O.; Follmer, D.W.; Meleason, M.A.; Shoemaker, D.D.; Perkins, J.C.; Leupp, S.L.; *Int. J. Chem. Kinet.* **1992**, *24*, 735-742.
88. DiFelice, J.J.; Ritter, E.R.; *ACS Div. Fuel Chem. Preprints* **1994**, *39*, 158.
89. Clyne, M.A.A.; Holt, P.M.; *Ber. Bunsenges. Phys. Chem.* **1979**, *75*, 582.
90. Simmie, J.M.; Tschuikow-Roux, E.; *J. Phys. Chem.* **1970**, *74*, 4075-4079.
91. Simmie, J.M.; Quiring, W.J.; Tschuikow-Roux, E.; *J. Phys. Chem.* **1970**, *74*, 992-994.
92. Schug, K.P.; Wagner, H.G.; *Ber. Bunsenges Phys. Chem.* **1978**, *82*, 719-725.
93. Cvetanovic, R.J.; *J. Phys. Chem. Ref. Data* **1987**, *16*, 261-302.
94. Gilbert, J.R.; Slagle, I.R.; Graham, R.E.; Gutman, D.; *J. Phys. Chem.* **1976**, *80*, 14-18.

RECEIVED July 27, 1995

Chapter 26

The Removal of Fluorine Atoms from Halocarbons

Jeffrey A. Manion and Wing Tsang

Chemical Sciences and Technology Laboratory, Chemical Kinetics
and Thermodynamics Division, National Institute of Standards
and Technology, Gaithersburg, MD 20899-0001

This paper is concerned with the mechanisms and rate constants for the removal of fluorine atoms from the carbon framework in halocarbons and other organics and the subsequent reactivity of the fluorine atoms at high temperature. The rationale for this interest is the decomposition of these compounds when they are used as flame suppressants and the inevitable breaking of the C-F bonds. Literature information regarding thermodynamics and kinetics related to the decomposition of halons are summarized. Some recent experiments from our laboratory using a single pulse shock tube are described. Combination with the earlier results leads to a general picture of the channels for conversion of carbon-bonded fluorine to HF as well as the factors controlling the stability of the C-F bonds in high temperature systems.

Practically all of the currently used fire suppressants and suggested short term replacements involve organic compounds with C-F bonds (1). Under use such compounds will be subject to high temperature combustion environments and some decomposition will occur. The thermodynamic endpoint for fluorinated organic compounds are mixtures of HF, H₂O and CO₂, so that at some stage C-F bonds must be broken. In this paper we wish to summarize the present state of knowledge regarding the reaction pathways for such processes and present recent experimental data from our laboratory bearing on this issue.

Such information will have implications on fire suppression chemistry. Indeed much of the additional data base required for modeling inhibited combustion systems involve reactions with fluorinated compounds and fragments. Furthermore, a number of fluorinated organic compounds have their own toxic characteristics (2) and are thus possible undesirable byproducts from combustion. Information on their rates of production in high temperature systems are therefore of considerable importance. Equally or perhaps more important in the short term, are difficulties associated with the production of toxic and corrosive HF. In any case, to properly compare the hazard

This chapter not subject to U.S. copyright
Published 1995 American Chemical Society

potential of proposed new compounds with those of the past fluorinated fire suppressants, detailed consideration of all of such factors must be made. Finally, in many combustion systems fluorinated compounds can play a very important role as a tracer or surrogate, thus serving to indicate the completeness of the combustion process. For such applications it is obviously very important to have some knowledge of reactivity of the compounds themselves, as well as the mechanisms by which they can be formed from other fluorinated compounds that may be present in the system.

The paper will begin with a summary of some basic thermodynamic information dealing with the bond energies for a number of fluorinated species (1,3-5). For bond breaking reactions in stable compounds the bond energies can be directly applied for the estimation of unimolecular rate constants. The thermodynamic feasibility of many other processes can also be deduced from such data, since reaction enthalpies are determined by the strengths of the bonds being formed and/or broken. Following the thermodynamic discussion, we next consider kinetic information dealing with the decomposition of fluorinated compounds. This will include direct measurements as well as estimates. A great deal of the quantitative information to be used here are summarized in the recent NIST report (1). By focusing on a number of key issues and molecules it is expected that the reader can obtain a better physical feeling of the pertinent phenomena, thus providing a basis for making estimates for species that have not been covered in this paper. A third section will summarize some recent measurements that we have made which impact on the issue of hydrogen atom attack on fluorinated organics. The conclusions from these data, in terms of general decomposition mechanisms, will be summarized in the final section.

Thermodynamic Background

Table I contains a summary of bond energy data dealing with a variety of fluorinated organics. The information is divided into three categories: a) stable compounds, b) unstable species, most of which are mono-radicals and c) a listing of analogous bond strengths in hydrocarbons, provided for comparison. We follow the conventional definition of the bond energy as the negative of the dissociation enthalpy. The data pertain to 298 K.

Examination of the data in Table I reveals immediately the extremely high values for the strength of the C-F bond in stable compounds. This is particularly striking when the numbers are compared with analogous C-H bonds or, for that matter, with other bonds in such compounds. Thus for closed shell molecules it will be extremely difficult to cleave a C-F bond in the unimolecular sense. In all except the simplest cases such as CF₄ there are alternative unimolecular channels that are readily available. In perfluoroethane, for example, it is obvious that the main unimolecular decomposition process will be cleavage of the C-C bond, which is 125 kJ/mol weaker than the C-F bonds. This is the same situation as with ethane, where the C-C bond is much weaker than the C-H bonds.

In fluorocarbon radicals, the bond energies of fluorines beta to the radical center are much lower than those of closed shell fluorocarbons. This difference is largely due to the formation of a pi bond concurrent with fission of the C-F bond. Thus the C-F bond in F-CF₂CF₂ is 312 kJ/mol compared with 532 kJ/mol in C₂F₆. Even in this case

Table I. Bond energies for some fluorinated organics and hydrocarbons (1,3-5)

Bond	Bond Energy (kJ/mol)	Bond	Bond Energy (kJ/mol)
F-H	568	H-H	436
F-CH ₃	464	H-CH ₂ F	437
F-CFH ₂	500	H-CHF ₂	431
F-CF ₂ H	534	H-CF ₃	444
F-CF ₃	543	H-CH ₃	439
F-CF ₂	368	H-CH ₂	439
F-CF (singlet)	517	H-CH (singlet)	391
F-C	540	H-C	340
F-CF ₂ CF ₃	532	H-CH ₂ CH ₃	420
F-C ₆ H ₅	526	H-C ₆ H ₅	466
CF ₃ -CF ₃	403	CH ₃ -CH ₃	377
CF ₂ =CF ₂	295	CH ₂ =CH ₂	667
F-CF ₂ CF ₂	312	H-CH ₂ CH ₂	152
CF ₃ -CF ₂	239	CH ₃ -CH ₂	449
F-FCO	494	H-HCO	364
F-CO	153	H-CO	71
F-CF ₂ O	110	H-CH ₂ O	94

the C-F bond is relatively strong: for example it is more than twice as strong as the analogous C-H bond in C₂H₅. Beta fission of F from fluorinated radicals, a process which would release free atomic fluorine, is thus slow in comparison with analogous reactions of hydrocarbons. As we will see, because of the high barrier to expulsion of F, alternative reaction paths will become important in many cases. Only in oxygenated radicals such as F-CO and F-CF₂O are the C-F bonds of such magnitude that ejection of F is a facile process. The above thermochemical issues have bearing on the question of how the fluorine is initially released into a reacting system. If ejected as atomic fluorine, very rapid reactions of F will ensue. In contrast, if released as HF, the exceptional strength of this bond will cause the fluorine to be effectively removed as a reactant except under extremely oxidizing conditions. In this respect fluorine differs from the other halogens, where the HX bond energies are weak enough that reactions of the type $R + HX \rightarrow RH + X$ can re-release halogen atoms into the system.

Once delivered into a mixture with hydrogen containing organics, atomic fluorine can readily abstract hydrogen to form hydrogen fluoride. On the other hand, additions of F to unsaturated organic species are also rapid and the strengths of C-F bonds are such that practically all groups can be displaced. The competition between such displacements and the abstraction of hydrogen is one of the main chemical issues in the decomposition of fluorinated flame inhibitors.

A particular and unique aspect of organic fluorine thermochemistry is the great stability of CF₂. This is readily perceived from the data on Table I where the only compounds with lower bond energies than their hydrogenated counterparts are those where bond breaking leads to the formation of CF₂. The most striking example of this is found in C₂F₄ where the strength of the carbon/carbon double bond is only 285 kJ/mol, in comparison with 667 kJ/mol in ethene. A consequence of the stability of

CF_2 is that frequently the lowest energy channel for the decomposition of highly fluorinated organic radicals involves the direct formation of CF_2 , in contrast to the situation with hydrocarbon radicals where β fissions of C-C or C-H bonds are always favored. Thus, for example, the decomposition of C_2F_5 to CF_3 and CF_2 is 80 kJ/mol less endothermic than the loss of a fluorine atom to form C_2F_4 . Similarly, Rodgers (3) has shown that in the decomposition of the $n\text{-C}_3\text{F}_7$ radical, rate constants for CF_2 and CF_3 production are not expected to be very far apart and indeed at high temperature the former channel is favored. This is quite different from decompositions of hydrocarbon radicals where formation of CH_2 is a much more endothermic and hence slower process. The general consequence of such thermochemistry is that CF_2 will be a very important species in decomposing systems where organic fluorine compounds are present.

Kinetic Data

The first section of Table II contains a summary of data on the unimolecular decomposition of a number of stable fluorinated compounds. As noted earlier, it is clear that C-F bond breaking from stable compounds cannot be an important channel for removing fluorine that is bonded on carbon. Compounds with two or more carbons can undergo carbon/carbon bond fission, which can lead to fluorine loss through subsequent reactions, but a still more likely process involves direct elimination of hydrogen fluoride through either 1,1 or 1,2 processes. Tschuikow-Roux and coworkers (6) have carried out shock tube studies on a large number of fluorinated compounds and have developed an empirical method (6) for predicting the rate expressions for HF elimination. The data show that fluoroalkanes react faster than fluoroalkenes and that the general tendency is for activation energies to increase with increasing fluorine substitution. An exception to this trend is in the case of the single carbon compounds where 1,1 elimination of HF is much faster for fluoroform (8) than for difluoromethane (11) or fluoromethane (13). Presumably this is a reflection of the great stability of CF_2 .

There are virtually no experimental data on the decomposition of fluorinated organic radicals involving the ejection of a fluorine atom. Estimates can be made on the basis of detailed balance and through the thermochemistry. As indicated earlier, in comparison to the situation for the hydrogenated analogs, β -fission of F is much more endothermic. A repercussion is that alternative decomposition channels become energetically competitive and play major roles in the chemistry. The situation for perfluoroalkyl radicals was alluded to previously. Other questions of particular interest concern the fates of fluorocarbonyl and perfluorinated methoxy radicals. These species can arise through the reactions of fluorinated methyl radicals with O_2 , OH and O. Such compounds must be important intermediates along the pathway of fluorine release into reacting systems, yet relatively slow beta-fission of F is the only likely unimolecular channel for their decomposition. In the absence of low energy unimolecular pathways, these radicals may survive long enough to react via bimolecular reactions. A possible reaction of importance is abstraction of hydrogen followed by elimination of HF. Other alternatives involve reactions with reactive radicals species.

Table II: Rate constants for some processes relevant to fluorine loss from organics

Reaction	High Pressure Rate Expression	Ref.	
Unimolecular Processes			
	(s ⁻¹)		
CF ₄ → CF ₃ + F	2×10 ¹⁷ exp(-63950/T)	Note a	
C ₂ F ₆ → 2CF ₃	1.5×10 ¹⁷ exp(-46100/T)	Note a	
CHF ₂ CHF ₂ → 2CHF ₂	4×10 ¹⁶ exp(-46000/T)	(14)	
CHF ₂ CF ₃ → CHF ₂ + CF ₃	7.9×10 ¹⁶ exp(-46450/T)	(15)	
CF ₃ H → CF ₂ + HF	1.2×10 ¹⁴ exp(-36340/T)	(8)	
CF ₂ H ₂ → CHF + HF	8.9×10 ¹² exp(-35330/T)	(11)	
CH ₃ F → Products	1×10 ¹⁴ exp(-42773/T)	(13)	
C ₂ H ₃ F → C ₂ H ₄ + HF	2.5×10 ¹³ exp(-30160/T)	(16)	
CH ₃ CHF ₂ → C ₂ H ₃ F + HF	8×10 ¹³ exp(-31170/T)	(17)	
CH ₂ FCH ₂ F → C ₂ H ₃ F + HF	2.5×10 ¹³ exp(-31300/T)	(7)	
CHF ₂ CH ₂ F → CH ₂ CF ₂ + HF	10 ¹³ exp(-32900/T)	(18)	
	→ CHFCHF (trans) + HF	1.2×10 ¹⁴ exp(-34800/T)	(18)
	→ CHFCHF (cis) + HF	3×10 ¹³ exp(-32480/T)	(18)
CH ₃ CF ₃ → CH ₂ CF ₂ + HF	2.5×10 ¹³ exp(-35800/T)	(19)	
CH ₂ FCF ₃ → CHF ₂ CF ₂ + HF	2.5×10 ¹³ exp(-35600/T)	(20)	
CHF ₂ CHF ₂ → CHF ₂ CF ₂ + HF	2×10 ¹³ exp(-34900/T)	(14)	
CHF ₂ CF ₃ → C ₂ F ₄ + HF	4×10 ¹³ exp(-36050/T)	(15)	
CH ₂ =CHF → C ₂ H ₂ + HF	1.0×10 ¹⁴ exp(-35630/T)	(21)	
CH ₂ =CF ₂ → HC≡CF + HF	2.5×10 ¹⁴ exp(-43280/T)	(22)	
Bimolecular Processes			
(including fluorination processes)			
	Rate Expression	Ref.	
	(cm ³ mol ⁻¹ s ⁻¹)		
H + CF ₄ → HF + CF ₃	1.1×10 ¹⁵ exp(-22300/T)	(9)	
H + CH ₃ F → H ₂ + CH ₂ F (Note b)	1.8×10 ¹³ exp(-4700/T)	(10)	
H + CH ₄ → H ₂ + CH ₃	5.9×10 ¹⁴ (T/298) ³ exp(-4406/T)	(12)	
CF ₂ + CF ₂ → C ₂ F ₄	8.4×10 ⁴ T ² exp(347/T)	(29)	
CF ₂ + O → Products	1.2×10 ¹³ (293 K)	(23)	
CF ₂ + H → CF + HF	2.4×10 ¹³ (298 K)	(25)	
CF ₂ + O ₂ → CF ₂ O + O	2.0×10 ¹³ exp(-13335/T)	(26)	
CF ₂ + H ₂ → Products	< 3×10 ⁵ (873 K)	(29)	
CF ₂ + CH ₄ → Products	< 2.4×10 ⁵ (873 K)	(29)	
CF ₂ + C ₂ H ₄ → Products	< 1.2×10 ⁸ (873 K)	(29)	
H + C ₆ H ₅ F → C ₆ H ₆	2×10 ¹³ exp(-5066/T)	(34)	
F + CH ₄ → CH ₃ + HF	1.8×10 ¹⁴ exp(-400/T)	(27)	
F + C ₆ H ₅ CH ₃ → C ₆ H ₅ CH ₂ + HF	8.0×10 ¹² (296 K)	(31)	
F + C ₆ H ₅ CH ₃ → C ₆ H ₅ F + CH ₃	8.0×10 ¹² (296 K)	(31)	
F + C ₆ H ₅ CH ₃ → C ₆ H ₄ FCH ₃ + H	2.0×10 ¹³ (296 K)	(31)	
F + C ₆ H ₆ → C ₆ H ₅ F + H	2.4×10 ¹³ (296 K)	(31)	

^a Calculated from the thermochemistry and rate constant for the reverse reaction (1).

^b The original authors assumed the reaction to be H + CH₃F → CH₃ + HF. We believe this to be incorrect (see text).

Data on bimolecular reactions relevant to fluorine removal are scarce. Some reactions can be ruled out on the basis of the thermochemistry. Abstraction of F by OH or O from C_2H_5F , for example, is endothermic by 213 and 219 kJ/mol respectively. On the other hand, abstraction of fluorine by H atom or methyl radical is exothermic and hence more likely. No data are available on the reaction of methyl, but in the literature there are two reports on abstraction of F by atomic hydrogen from fluorinated methanes. Kochubei and Moin (9) reported a high activation energy of 185 kJ/mol for the abstraction of F from CF_4 by atomic hydrogen, while Westenberg and de Haas (10) found a barrier of 39 kJ/mol for the $H + CH_3F$ reaction. Both studies monitored only the disappearance of starting material and the reaction mechanism was assumed to be abstraction of F. This is most disturbing in the study of Westenberg and de Haas since no attempt was made to distinguish the abstraction of fluorine from that of hydrogen. Notice, too, that on a per hydrogen basis, their reported rate constant is about equal in rate with $H + CH_4 \rightarrow H_2 + CH_3$ (12). In any case, although the C-F bonds in CF_4 are somewhat stronger than that in CH_3F , it is unlikely that the two rate expressions for fluorine abstraction are as different as the data suggest. This implies that there must be a problem with one of the studies, thus providing the rationale for the experiments that will be described subsequently. Based on our results and as indicated in Table II, we will argue that the data on CH_3F pertain to abstraction of H and not F as suggested by the original authors.

In addition to bimolecular reactions between radicals and molecules, radical-radical processes can be important in some instances. The thermal stability of methyl and fluorinated methyl radicals, for instance, means that in high temperature systems fast combination processes will represent an important removal channel. This bonding process liberates roughly 400 kJ/mol as excess internal energy. Until removed by bimolecular collisions, this energy is of course available to drive unimolecular reactions of the complex. Since the barrier to HF elimination is typically less than 290 kJ/mol, it is apparent that HF can be expelled from the recombination complex in a chemically activated process. Note that for unsubstituted hydrocarbons such four-center decomposition channels are more endothermic and therefore unimportant. In fluoroalkanes, the importance of the chemical activation channel is determined by the rate of HF elimination relative to collisional loss of the excess energy and hence will depend heavily on the temperature and pressure of the system.

RRKM calculations and estimates of weak collision effects provide a framework for estimating the required rate constants. A summary of the calculated results for the combination $CF_3 + CH_3$ are shown in Figures 1 and 2. Figure 1 shows the results at 1 atmosphere pressure as a function of temperature while Figure 2 shows the pressure dependence at 1200 K. Our calculations indicate that the excited complex $(CF_3CH_3)^*$ leads to three product channels: A: $(CF_2CH_2 + HF)$, B: the thermalized fluoroalkane (CF_3CH_3) , and C: $(CF_3CH_2 + H)$. A fourth channel, $CH_3F + CF_2$, was also considered but found to be unimportant. The two most important processes were found to be elimination of HF and thermalization of the complex. Ejection of a hydrogen atom was relatively minor under all conditions. As shown in Figure 1, at a pressure of 1 atmosphere, elimination of HF is the dominant channel at temperatures greater than 500 K. Surprisingly, at the highest temperatures the rate constant for HF production begins to drop. This reflects the fact that, for competing processes, the pre-exponential

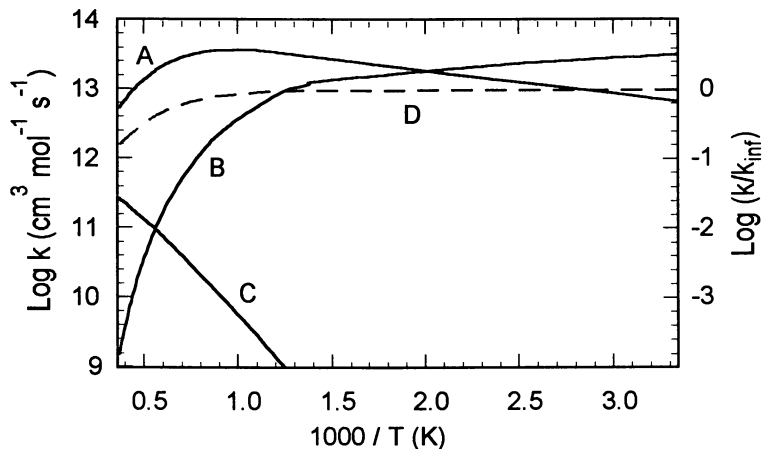


Figure 1. Rate constants as a function of temperature for recombination processes of methyl and trifluoromethyl at 1 atm pressure: A: $\text{CF}_3+\text{CH}_3 \rightarrow \text{CF}_2\text{CH}_2+\text{HF}$; B: $\text{CF}_3+\text{CH}_3 \rightarrow \text{CF}_3\text{CH}_3$; C: $\text{CF}_3+\text{CH}_3 \rightarrow \text{CF}_3\text{CH}_2+\text{H}$; D: $\log k/k_{\text{inf}}$ ($\text{CF}_3+\text{CH}_3 \rightarrow \text{Products}$), dashed line and refers to y-axis on the right.

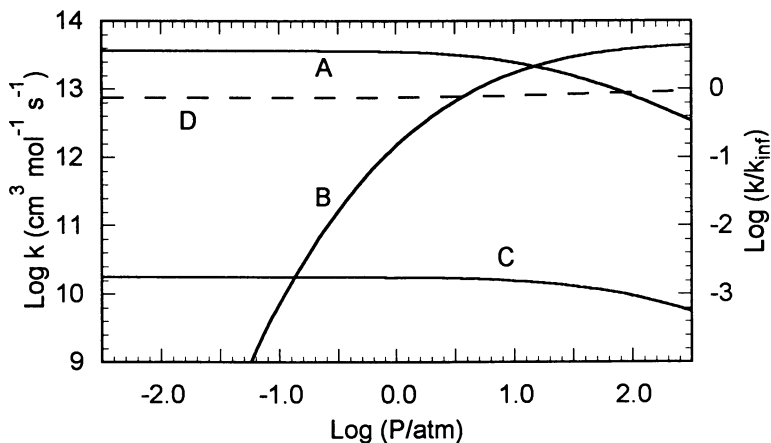


Figure 2. Rate constants as a function of pressure for recombination processes of methyl and trifluoromethyl at 1200 K: A: $\text{CF}_3+\text{CH}_3 \rightarrow \text{CF}_2\text{CH}_2+\text{HF}$; B: $\text{CF}_3+\text{CH}_3 \rightarrow \text{CF}_3\text{CH}_3$; C: $\text{CF}_3+\text{CH}_3 \rightarrow \text{CF}_3\text{CH}_2+\text{H}$; D: $\log k/k_{\text{inf}}$ ($\text{CF}_3+\text{CH}_3 \rightarrow \text{Products}$), dashed line and refers to y-axis on the right.

factors assume greater significance as the temperature increases while the importance of the activation energies is decreased. Note that the A-factor for bond breaking is much larger than that for HF elimination. Thus what is being observed at higher temperatures is the increasing importance of the C-C bond breaking reaction (reverse of the combination process) as a decomposition channel. In other words, despite the presence of an exothermic decomposition channel, fall-off phenomena become very important.

The basic results in Figure 1 are characteristic of all the various cross combination reactions of fluorinated methyl radicals with each other. Nonetheless, there are some important differences. Because the activation energy for HF elimination tends to increase with increasing fluorination, as does the heat capacity of the molecule, the importance of the stabilization channel extends to higher temperatures for such compounds. For exact rate constants it is necessary to carry out RRKM/master equation calculations using as a basis the high pressure rate expressions and an appropriate energy transfer parameter. In the present case we have used the functional form: $\langle \Delta E \rangle_{\text{down}} = 100(T/300) \text{ cm}^{-1}$, where $\langle \Delta E \rangle_{\text{down}}$ is the average energy removed per collision (the so-called step size down) and T is the temperature in Kelvin. Because $\langle \Delta E \rangle_{\text{down}}$ determines how many collisions are needed to deactivate the complex, the magnitude of this parameter is very important. Except at extremely low or high pressures, $\langle \Delta E \rangle_{\text{down}}$ is a dominant parameter controlling the calculated rates for the various processes. We have derived its magnitude and temperature dependence from correlations of unimolecular fall-off data (28). Nevertheless, it must be stressed that our values are estimates. What is really needed are accurate high temperature chemical activation measurements for the validation of procedures and input parameters. At the present time the highest temperatures at which careful chemical activation experiments have been carried out are at 400 K.

The importance of CF_2 has been mentioned earlier. The great thermodynamic stability of the singlet ground state is accompanied by chemical inertness in comparison to radicals or hydrogenated carbenes. Note that the rate constant (29) for recombination of CF_2 is relatively small. Reaction rates with closed shell species are also very small. Reaction with O_2 for instance has a reported (26) activation energy of 110 kJ/mol. The reactions of CF_2 with H_2 , CH_4 and C_2H_4 appear even less favorable with only upper rate limits having been established (29). The implication here is that unlike singlet carbenes such as CH_2 insertion rate constants must be extremely small. Indeed the upper rate limit for reaction with CH_4 at 873 K is consistent with an activation energy of greater than 140 kJ/mol. In contrast, reactions of CF_2 with radicals such as O (23), OH (24), and H (22) are fast and appear to have little or no barriers. In these later cases the presumption is that addition is the main process and is followed by the decomposition of the hot adducts.

When fluorine atoms are released into a system containing C-H bonds a very important and rapid reaction is abstraction leading to the formation of HF. This is a very exothermic process and is not likely to be reversed as is the case for other halogens. Some typical rate constants are given in Table II. Note that the limited data available indicate that, on a per-H basis, hydrogen is abstracted from methane four times as fast as from the methyl group of toluene. This is unlikely and suggests that their remain some uncertainties in the rate constants. Despite this it is clear that

abstraction of H is a fast reaction. An alternative reaction for atomic fluorine involves addition onto a site of unsaturation in any organic compound. Under combustion conditions this will lead inevitably to the ejection of the group *ipso* to the fluorine adduct. These two-step displacements lead to the production of very strongly bonded unsaturated fluorine compounds. Some data on the rate constants for fluorine addition can be found in Table II. This step is the rate determining step for the addition/ejection sequence of reactions. Obviously, knowledge of the ratio of rate constants for abstraction and displacement is very important in determining the amount of organic fluorine compounds that may be formed in an inhibited combustion system.

Ebrecht et al. (31) have determined the various channels for fluorine atom attack on toluene and benzene at room temperature. Results are summarized in Table II. It appears that displacement of the hydrogen is the predominant process at room temperature. At higher temperatures it may well be that abstraction of H will become more important. Notice that the rate constants for displacement are near gas kinetic even at room temperature, which implies that the barrier for fluorine addition must be very low, less than about 4 kJ/mol.

Data on the reaction of radicals with unsaturated fluorinated compounds are sparse. Reaction of OH with C₆F₆ has been studied by several groups, most recently by McIlroy and Tully (32), who also examined reaction with C₃F₆. The initial reaction is well established to be addition, but the fate of the adduct at higher temperatures is uncertain. Displacement of F is one possibility although the thermochemistry suggests that most additions will not lead to displacement. The experimental data (32), however, show no evidence for reversibility of the OH addition step even at 830 K, the highest temperature studied. This would seem to suggest that the adduct reacts via some pathway other than displacement of F or expulsion of OH. One possibility is that direct or indirect elimination of HF is important.

Oxygen atom is known to add to C₂F₄ with a barrier of only a few kJ/mol (33), but there are no data on the reaction at high temperatures. At low temperatures and pressures, CF₂ is a product (33), and this is a likely pathway under combustion conditions. There are no reports of the reaction of O with C₆F₆. Displacement of F by O is slightly exothermic in the case C₆H₅F, so this type of reaction could be important. However, since there are alternative reaction pathways for the adduct radical, experimental data at high temperatures are needed.

The reaction of hydrogen atom with fluorobenzene has been studied by Manion and Louw (34) who determined the rate expression for defluorination.

Kinetic Experiments

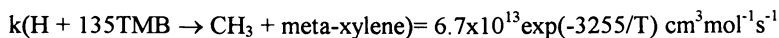
We have recently carried out some experiments with the aim of obtaining rate constants for hydrogen atom attack on fluorinated organics. As noted earlier, abstraction of fluorine from an organic by hydrogen atoms is an exothermic process. Thus it cannot be ruled out on the basis of thermodynamics. Indeed the degree of exothermicity is very similar to that for abstraction of the other halides and it is well established that such abstractions are very facile processes.

Abstraction of F is a possible mode of reaction for all fluorinated organics. In the case of a fluorine group adjacent to a site of unsaturation there is the additional

possibility that H can displace F via an addition/elimination sequence. In this case the net reaction is endothermic. This differs from analogous displacements of groups such as chlorine or methyl, since the latter two reactions are exothermic. Under the high temperature conditions of our experiments the addition of hydrogen is not reversible for the exothermic reactions. The group is always displaced and the reaction rate is determined solely by the rate of hydrogen addition to the substituted carbon. For chlorinated unsaturated compounds, measured displacement rate constants are slower than for expulsion of a methyl group (35,37). This reflects the larger barrier to hydrogen addition. For the analogous situation with fluorine, the barrier to losing hydrogen is lower than that for fluorine. This means that addition of hydrogen can be readily reversed. The rate constant for fluorine displacement will thus be smaller than for addition. The ratio of displacement/addition will depend on the thermochemistry and the relative barriers for the addition of H and F.

Issues related to the abstraction and displacement of F have recently been directly addressed through single pulse shock tube studies. Figure 3 shows a schematic of the apparatus (3a), together with the wave diagram (3b), and the graph of the heating curve at the indicated point of the shock tube (3c). On the high pressure side of the diaphragm is hydrogen which serves as the driver gas, while the low pressure side contains the reactants diluted to typically 100-10,000 ppm in argon. As indicated, rupture of the diaphragm generates a shock wave which propagates down the tube, compressing and heating the gas. The shock wave reflects off the back surface of the tube and heats the gas a second time before the wave energy is dissipated and absorbed by the dump tank. For our purposes the shock tube can be considered a pulse heater. Depending on the experimental conditions, the gas is heated to 950-1200 K for about 500 microseconds before it is cooled by re-expansion. Note that surface reactions are unimportant since the reaction time is much shorter than the time required for diffusion of species to the reactor walls. The temperature of the gas during the reaction can be determined by following the decomposition of an appropriate molecule whose rate parameters are well known. Such use of a "chemical thermometer" removes one of the major uncertainties in shock-tube experiments. Immediately following the shock, a series of valves and sample loops allow analysis of the product mixture via gas chromatography. The entire apparatus and sampling system is heated to prevent condensation of less volatile components of the samples. In our studies we vary the concentrations of the various components in order to test for interference from secondary processes. Further details of the system may be found elsewhere (30).

In the present experiments the procedure involves thermally decomposing dilute mixtures of hexamethylethane, a hydrogen atom source, in the presence of two target molecules, the fluorine compound of interest and a standard, 1,3,5-trimethylbenzene (135TMB), whose rate constants for hydrogen atom attack are well known (30):



Note that in the present case meta-xylene can only be formed from hydrogen induced displacement of methyl. Thus the ratio of meta-xylene to a unique product formed

tetrafluoroethene, respectively. These are the exclusive products from the respective intermediates since the only alternative to chlorine expulsion is loss of F, which in each case is about 155 kJ/mol more endothermic. Because the alkenes can be shown to be stable products under our conditions (35), the ratio of these two species gives the branching ratio for the overall reaction. Using the expression given above for formation of meta-xylene from 135TMB, the rate constants indicated in Figure 4 can be derived.

As shown, the dominant channel is abstraction of chlorine, for which we obtain

$$k(\text{H} + \text{DCFE} \rightarrow \text{CF}_2\text{-CF}_2\text{Cl} + \text{HCl}) = 2.1 \times 10^{14} \exp(-5839/T) \text{ cm}^3 \text{ mol}^{-1} \text{ s}^{-1}$$

Uncertainties in comparative rate studies of this type have previously been discussed in detail (18). The overall uncertainty is estimated to be about a factor of 1.4 in the rate constant, 10 kJ/mol in the activation energy, and a factor of three in the pre-exponential factor. Although relatively few data are available for comparison, the parameters for chlorine abstraction from DCFE are similar to those obtained for other chlorinated species (36,37).

Chlorotrifluoroethene, the product resulting from abstraction of F, was not detected at temperatures below 1100 K and was present only as a trace product thereafter. The observed levels were so low that we were unable to determine if its formation was due to reaction 1 or whether it resulted from secondary reactions or impurities. Hence we were only able to determine a maximum rate constant, obtaining

$$k_1(1100 \text{ K}) \leq 7 \times 10^9 \text{ cm}^3 \text{ mol}^{-1} \text{ s}^{-1}$$

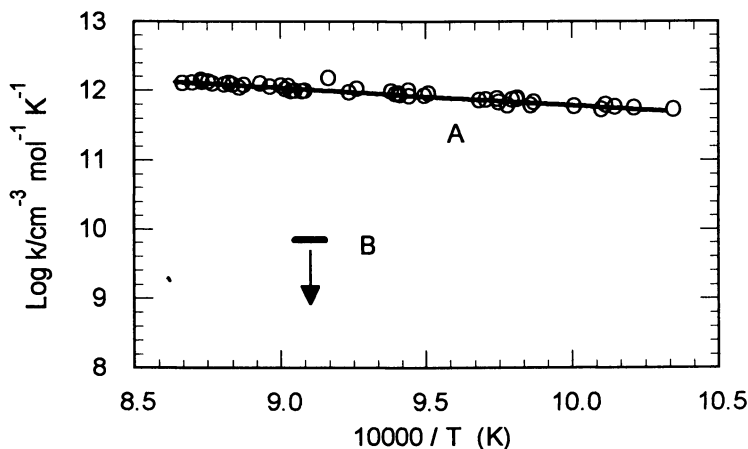


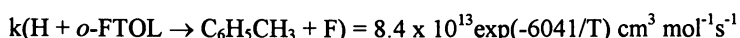
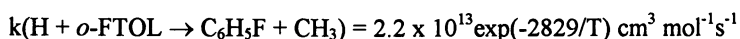
Figure 4. Rate constants for attack of H atom on dichlorotetrafluoroethane (DCFE). A: $\text{H} + \text{DCFE} \rightarrow \text{F}_2\text{C-CClF}_2 + \text{HCl}$; B: $\text{H} + \text{DCFE} \rightarrow \text{CClF-CClF}_2 + \text{HF}$; The line refers to the maximum rate constant derivable from our data.

If the pre-exponential factor is assumed to be $1 \times 10^{15} \text{ cm}^3 \text{ mol}^{-1} \text{ s}^{-1}$, we calculate $E_1 \geq 110 \text{ kJ/mol}$. On a per-F basis, our rate constant is at least 140 times slower than the measured rate for the $\text{H} + \text{CH}_3\text{F}$ reaction (Table II). Such a large difference is unreasonable if the reaction with fluoromethane were $\text{H} + \text{CH}_3\text{F} \rightarrow \text{CH}_3 + \text{HF}$ as assumed by the original (10) authors. We feel the most likely explanation is that their data are correct, but refer to the reaction $\text{H} + \text{CH}_3\text{F} \rightarrow \text{CH}_2\text{F} + \text{H}_2$. Our maximum rate constant is about 3 orders of magnitude larger than that calculated from the Arrhenius parameters of Kochubei and Moin (9) for $\text{H} + \text{CF}_4$.

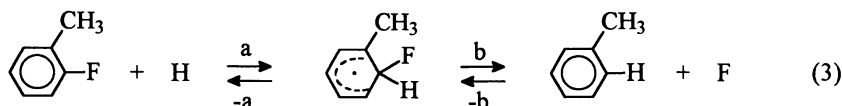
The main point is that abstraction of fluorine from DCFE by atomic hydrogen is a slow reaction despite the reaction exothermicity. Rates for other fluorinated compounds are not expected to be very different. Since the hydrogen case is the most favorable of the metathesis reactions involving abstraction of F, it is unlikely that any radical typically present in combustion systems can rapidly abstract fluorine from a closed shell species in the gas phase.

Displacement of Fluorine by Atomic Hydrogen. The above data suggest that abstraction of fluorine is unlikely, yet defluorination of fluorobenzene has been reported in the literature (34) and been suggested to occur by such a mechanism. Because the previous study involved a flow system where wall reactions could not be entirely ruled out, we have investigated the defluorination of *ortho*-fluorotoluene using the shock tube methodology. In our experiments we monitor defluorination by observing the formation of toluene. Because both displacement and abstraction of F would directly or indirectly result in toluene production, our experiment is unable to distinguish between the two mechanisms. However, as discussed below, we believe displacement is nearly the exclusive process under our conditions.

Using demethylation of 1,3,5-trimethylbenzene as our standard, we obtain the results shown in Figure 5 and listed below.



The uncertainties in our rate expressions are about 1.4 in the rate constants, 10 kJ/mol in the activation energies, and a factor of three in the pre-exponential factors. Our rate constant for defluorination of *o*-fluorotoluene is similar to that reported for fluorobenzene (34). The present data show that over our temperature range of 990-1160 K defluorination is 4-7 times slower than demethylation but still occurs with an appreciable rate. Removal of fluorine from aromatics is only a factor of 3-4 slower than dechlorination (35,37). If, on a per fluorine basis, the rate of fluorine abstraction is assumed equal to the maximum rate which we determined for DCFE, our measured defluorination rate is more than a factor of 200 larger than can be accounted for by abstraction of F. This strongly suggests that the mechanism must be displacement:



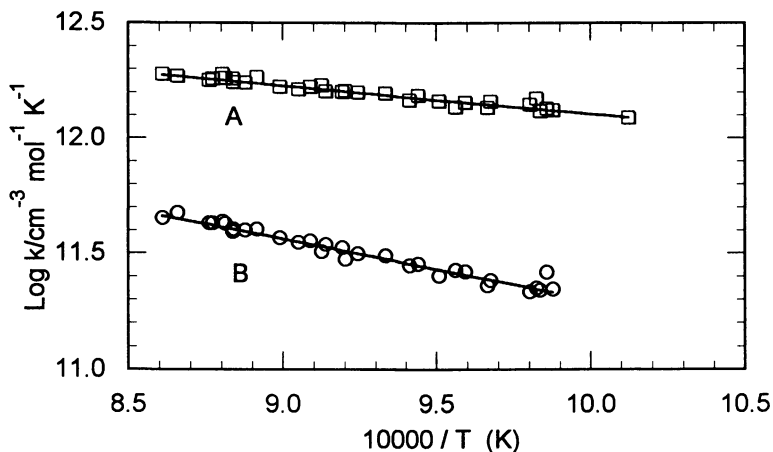


Figure 5. Rate constants for attack of atomic hydrogen on *ortho*-fluorotoluene (o-FTOL). A: $\text{H} + \text{o-FTOL} \rightarrow \text{C}_6\text{H}_5\text{F} + \text{CH}_3$; B: $\text{H} + \text{o-FTOL} \rightarrow \text{C}_6\text{H}_5\text{CH}_3 + \text{F}$.

Overall, reaction 3 is endothermic by about 54 kJ/mol at 1000 K (39). Decomposition of the cyclohexadienyl radical intermediate will therefore be a competitive process with $k_a > k_b$. What we have measured is the rate constant for the overall process, given by $k_3 = k_a k_b / (k_a + k_b)$. Our data are not very sensitive to the activation energy for hydrogen atom addition: smaller barriers lead to faster addition rate constants, but also greater reversibility. The overall rate is more sensitive to the sum of the overall reaction endothermicity and the barrier for fluorine addition, E_{3b} . Notice that our measured activation energy, 50 kJ/mol, is close to the reaction endothermicity. In the absence of further data we cannot solve explicitly for the individual rate constants, but within the uncertainties the data are consistent with the thermochemistry and a barrier of near zero for addition of F. As noted earlier the required low barrier for F addition is consistent with the large rate constant for this process near room temperature (31). The primary consequence of a mechanism involving displacement rather than abstraction is that the reaction leads to the release of atomic fluorine into the system, rather than immediately locking up the fluorine as HF.

From the thermochemistry we can calculate the rate constant for the reverse of reaction 3. We have estimated the thermodynamic properties of *o*-fluorotoluene based on the known (39) values for fluorobenzene and toluene, which at 1050 K leads to:

$$k(\text{C}_6\text{H}_5\text{CH}_3 + \text{F} \rightarrow \text{H} + \text{o-FTOL}) = 3 \times 10^{13} \exp(+400/T) \text{ cm}^3 \text{ mol}^{-1} \text{ s}^{-1}$$

The slightly negative activation energy is a consequence of the low barrier to fluorine addition and the increasing reversibility of the fluorine addition step at higher temperatures, i.e. the ratio k_{3b}/k_{3a} increases with temperature. After adjustment for statistical factors, similar parameters would be expected for the displacement of

hydrogen from other aromatic hydrocarbons. Notice that the derived rate constant has a magnitude similar to that expected for abstraction of hydrogen from saturated hydrocarbons (see Table II). With regard to fluorination of products of incomplete combustion (PICs), which are generally unsaturated species, the more pertinent but unresolved issue is the rate constant for hydrogen abstraction from sp^2 hybridized carbon. It is the relative rate of abstraction to displacement for such species that will in large part determine to what extent PICs can be fluorinated under conditions of partial combustion.

Conclusions and General Trends

The results summarized above give a general picture of how fluorine atoms are converted to HF in a combustion system. Except for the direct elimination of HF through unimolecular decomposition, fluorine is removed with much more difficulty than other halogens or hydrogen. Our experimental studies have shown that, despite the exothermicity of the reaction, abstraction of fluorine by atomic hydrogen is characterized by a very high activation energy and hence small rate constant. It thus differs from the other halides, which are readily abstractable. In aromatics, it appears that addition of hydrogen atom to a fluorine substituted site occurs with a rate that is similar to that found for other groups. The subsequent ejection of fluorine is endothermic, however, so that the addition reaction is reversible, in contrast with expulsion of other groups such as chlorine or methyl. Despite this, the rate constant for fluorine displacement is only a factor of three to four smaller than that for chlorine.

It is clear that direct radical attack on C-F bonds is not a facile channel for the removal of fluorine from the carbon framework. Indirect channels therefore become operational. For partially fluorinated molecules these may include radical attack on the more susceptible parts of the molecule. Other alternatives, and the only ones available for perfluoroalkanes, are unimolecular carbon-carbon bond fission followed by reactions of the carbon-centered radicals. It is at this stage that oxygenated fluorine containing organics appear to be formed. Some details of the subsequent reactions of such species remain unclear, but processes leading to their ultimate oxidation are generally slower than for the hydrocarbons. The broad picture outlined above contrasts greatly with that for the hydrocarbons where decomposition is frequently initiated by abstraction of hydrogen followed by the rapid decomposition of the radical, thereby releasing more radicals into the system. In the absence of such chemistry, it is not surprising that fluorinated hydrocarbon are in every way much more thermally stable than the comparable hydrocarbons. This may have an additional serious implication with regard to the formation of unwanted byproducts of incineration. In systems where fluorine is present the products of incomplete combustion are likely to initially contain fluorine and in general be more stable than those formed in hydrocarbon systems. This is reinforced by the propensity of atomic fluorine to add to unsaturated systems. Continued fluorination of these species will lead to progressively less reactive compounds. This issue is of concern since some fluorinated compounds are highly toxic. A key remaining question relates to the reactivity of atomic fluorine with unsaturated organic compounds. Specifically, it is expected that a crucial expression is the ratio for hydrogen abstraction to addition of F.

Acknowledgements

This work was sponsored by the Strategic Environmental Research and Development Program (SERDP).

References

1. Nyden, M. R., Linteris, G. T., Burgess, D. R. F., Westmoreland, P. R., Tsang, W., and Zachariah, M. R., "Flame Inhibition Chemistry and the Search for Additional Fire Fighting Chemicals" in "Evaluation of Alternative In Flight Fire Suppressants for Full-Scale Testing in Simulated Aircraft Engine Nacelles and Dry Bays" (Grosshandler, W. L., Gann, R. G. and Pitts, W. M., ed.) NIST SP 861, pp 467-621.
2. Lewis, R. J., "Sax's Dangerous Properties of Industrial Materials", 8th ed., Van Nostrand, Reinhold, New York, 1992
3. Rodgers, A. S. "Thermochemistry of Fluorocarbon Radicals" in "Fluorine-Containing Free Radicals, Kinetics and Dynamics of Reactions" (Root, J., ed.) ACS Symposium Series 66, American Chemical Society, Washington DC, 1978.
4. Stull, D. R. and Prophet, H., "JANAF Thermochemical Tables" 2nd Edition. NSRDS-NBS 37, US Government Printing Office, Washington DC, 20402, 1971.
5. Benson, S. W., "Thermochemical Kinetics", 2nd Edition, John Wiley and Sons, New York, 1976.
6. Tschuikow-Roux, E. and Maltman, K. R., *Int. J. Chem. Kin.*, **1975**, *7*, 363
7. Kerr, J. A. and Timlin D. M., *Int. J. Chem. Kin.*, **1971**, *3*, 427
8. Schug, K. P., Wagner, H. Gg., Zabel, F., *Ber. Bunsenges. Phys. Chem.*, **1979**, *83*, 167.
9. Kochubei, V. F. and Moin, F. B., *Kinet. Katal.*, **1970**, *11*, 864.
10. Westenberg, A. A. and deHaas, N., *J. Chem. Phys.*, **1975**, *62*, 332.
11. Politanskii, S. F., and Shevchuk, V. U., *Kinet. Catal., Eng. Lang. Ed.*, **1968**, *9*, 411.
12. Tsang, W., and Hampson, R. F., *J. Phys. Chem. Ref. Data*, **1986**, *15*, 1087.
13. Schug, K. P., and Wagner, H. Gg., *Z. Phys. Chem. (Neue Folge)*, **1973**, *86*, 59.
14. Millward, G.E., Hartig, R., and Tschuikow-Roux, E., *J. Phys. Chem.*, **1971**, *75*, 3195.
15. Tschuikow-Roux, E., Millward, G. E., and Quiring, W. J., *J. Phys. Chem.*, **1971**, *75*, 3493.
16. Cadman, P., Day, M. and Trotman-Dickenson, A. F., *J. Chem. Soc. A*, **1970**, 2498.
17. Tschuikow-Roux, E., Quiring, W.J., and Simmie, J. M., *J. Phys. Chem.*, **1970**, *74*, 2449.
18. Sekhar, M.V.C., and Tschuikow-Roux, E., *J. Phys. Chem.*, **1971**, *75*, 3493.
19. Tschuikow-Roux, E., and Quiring, W.J., *J. Phys. Chem.*, **1971**, *75*, 295.
20. Millward, G.E., and Tschuikow-Roux, E., *J. Phys. Chem.*, **1971**, *76*, 292.
21. Simmie, J. M., Quiring, W.J., and Tschuikow-Roux, E., *J. Phys. Chem.*, **1970**, *74*, 992.
22. Simmie, J. M., and Tschuikow-Roux, E., *J. Phys. Chem.*, **1970**, *74*, 4075.
23. Tsai, C. and McFadden, D. L.; *J. Phys. Chem.*, **1990**, *173*, 241.
24. Biordi, J. C.; Lazzara, C. P.; and Papp, J. F.; *J. Phys. Chem.*, **1978**, *82*, 125.
25. Tsai, C. and McFadden, D. L.; *J. Phys. Chem.*, **1989**, *93*, 2471.
26. Keating, E. L.; and Matula, R. A., *J. Chem. Phys.*, **1977**, *66*, 1237.
27. Atkinson, R., Baulch, D. L., Cox, R. A., Hampson Jr., R. F., Kerr, J. A., and Troe, J., *J. Phys. Chem. Ref. Data*, **1992**, *21*, 1125.

28. Tsang, W., *Combustion and Flame*, **1989**, 78, 71.
29. Murell, T. P., Battin-LeClerc, F., and Hayman, G. D., "Kinetics of the Reactions of CF₂ Radicals" in Abstracts, "13th International Symposium on Gas Kinetics" University College, Dublin, Ireland, 1994, pp 23.
30. Tsang, W. "Comparative Rate Single Pulse Shock Tube in the Thermal Stability of Polyatomic Molecules," in "*Shock Tubes in Chemistry*, A. Lifshitz ed., Marcel Dekker, 1981, pp 59.
31. Ebrecht, J., Hack, W., and Wagner, H. Gg., *Ber. Bunsenges. Phys. Chem.*, **1989**, 93, 619.
32. A. McIlroy, A. and Tully, F. P., *J. Phys. Chem.*, **1993**, 97, 610.
33. R. J. Cvetanovich, *J. Phys. Chem. Ref. Data*, 16, 261, 1987.
34. Manion, J. A. and Louw, R., *J. Phys. Chem.*, **1990**, 94, 4127.
35. Manion, J. A. and Tsang, W., to be published.
36. Cui, J.P., He, Y. Z, Tsang, W., *J. Phys. Chem.*, **1989**, 93, 724.
37. Tsang, W. and Walker, J. A., *Twenty-Third Symposium (International) on Combustion*, The Combustion Institute, Pittsburg, PA, 1991, pp 139.
38. "Selected Values of Properties of Hydrocarbons and Related Compounds", TRC Tables, Thermodynamics Research Center, Texas A&M University, College Station, TX, Data sheets 20, 90, 1010, and 3290.

RECEIVED May 11, 1995

Chapter 27

Theoretical Prediction of Thermochemical and Kinetic Properties of Fluorocarbons

M. R. Zachariah¹, P. R. Westmoreland², D. R. F. Burgess, Jr.¹,
Wing Tsang¹, and C. F. Melius³

¹Chemical Sciences and Technology Laboratory, Chemical Kinetics and Thermodynamics Division, National Institute of Standards and Technology, Gaithersburg, MD 20899-0001

²Department of Chemical Engineering, University of Massachusetts, Amherst, MA 01003-3110

³Sandia National Laboratories, P.O. Box 969, Livermore, CA 94551-0969

An ab-initio quantum chemistry procedure has been applied to the development of a database for thermochemistry and kinetics of C/H/F/O species. This information has been used to construct a chemical kinetic mechanism for the prediction of the behavior of fluorocarbons as flame suppressants. Bond-additivity corrected (BAC) Mollet-Plesset many-body perturbation theory (MP4) calculations have been performed to obtain a large body of thermochemical data on both closed-and-open shell fluorocarbon species. In addition, data on transition state structures for reactions have also been generated and rate constants based on RRKM analysis have been derived. Comparisons between theory and experiment for both thermochemistry and kinetics show excellent agreement. Calculated bond dissociation energies have been correlated to Mulliken charge distribution and have been used to understand bond energy trends in terms of electrostatic effects and molecular conformation.

CF₃Br is a highly effective agent for the suppression of flames, whose activity is generally considered to be derived by bromine atom's activity in catalytically removing H atoms. The nature of CF₃Br's (Halon 1301) environmental impact (ozone depletion potential), however, has prompted a search for alternative agents for flame suppression. The most promising replacement candidates seem to be fluorocarbons and hydrofluorocarbons, which have recently been evaluated in a critical study conducted at NIST under the auspices of the Air Force and other agencies [1]. As an aid to the testing and subsequent selection procedure, a theoretical model based on the application of detailed chemical kinetics has been developed [2-4]. Because the available thermochemical and kinetic data were not sufficient to the task, we have undertaken to calculate thermochemical data for a large set of stable and radical species along with a critical evaluation against experiment. In addition, for selected reactions deemed to be important, transition states were determined and used to calculate rate constants based on reaction rate theory (RRKM/master equation) methods.

This chapter not subject to U.S. copyright
Published 1995 American Chemical Society

Calculation Methodology

All calculations were performed using the BAC-MP4 procedure outlined by Melius [5]. This procedure involves ab initio molecular orbital calculation using the Gaussian series of programs [6], followed by application of a bond additivity correction (BAC) procedure to the ab initio calculated energy. The essence of the BAC procedure is to enable one to calculate energies at accuracies sufficient for chemical applications, without the need to resort to large basis sets or configuration interaction terms. This is a particularly important issue when the goal is the generation of a sufficiently complete data set for detailed chemical modeling.

Equilibrium geometries, vibrational frequencies and zero point energies were calculated at the HF/6-31G(d) level. Single point energies were calculated at the MP4/6-31G(d,p) level, to which the BAC procedure was applied. In the BAC method, errors in the electronic energy of a molecule are treated as bond-wise additive and depend on bonding partner and distance. The energy per bond is corrected by calibration at a given level of theory against molecules of known energy as listed in Table 1.

Melius [5] has shown that for any molecule $A_k-A_i-A_j-A_l$, the error in calculating the electronic energy can be estimated through a bond correction of the form.

$$E_{BAC}(A_i-A_j) = f_{ij} g_{kij} g_{ijl} \quad (1)$$

$$\text{where } f_{ij} = A_{ij} \exp(-\alpha_{ij} r_{ij}) \quad (2)$$

and A_{ij} and α_{ij} are calibration constants that depend on bond type and r_{ij} is the bond length at the Hartree-Fock level.

$$\text{and} \quad g_{kij} = (1 - h_{ik} h_{ij}) \quad (3)$$

is the second-nearest neighbor correction

where

$$h_{ik} = B_k \exp(-\alpha_{ik} (r_{ik} - 1.4 \text{ \AA})) \quad (4)$$

TABLE 1: Bond Additivity Correction Parameters

Bond	Calibration Species	MP4/6-31G(d,p)//HF/6-31G(d)			B_k
		A_{ij}	α_{ij}	Atom Type	
C-H	CH ₄	38.61	2.0	H	0
C-C	C ₂ H ₆ , C ₂ H ₂	1444.1	3.8	C	0.31
O-H	H ₂ O	72.45	2.0	O	0.225
C-O	CH ₃ OH, CH ₂ O	175.6	2.14	F	0.33
H-F	HF	84.21	2.0		
C-F	CF ₄	143.29	2.1		
H-H	H ₂	18.98	2.0		

For open shell molecules, an additional correction is needed due to contamination from higher spin states. This error is estimated using an approach developed by Schlegel in which the spin energy correction is obtained from [7] :

$$E_{\text{spin}} = E(\text{UMP3}) - E(\text{PUMP3}) \quad (2)$$

For closed-shell species having a UHF instability

$$E_{\text{spin}} = K S (S+1) \quad \text{where } K = 10.0 \text{ (kcal/mol)} \quad (3)$$

The transition state for a reaction was obtained in the usual way, by searching a geometry with one negative eigenvalue (saddle point on the potential energy surface), followed by steepest-descent reaction path analysis to ensure the calculated transition state corresponds to the appropriate reactants and products. BAC corrections are assigned in the same manner as with the equilibrium structures. Where needed, RRKM/master equation analysis was employed using the calculated transition state to obtain reaction rate constants.

Results

Equilibrium Thermochemistry

Heats of formation for C_1 and C_2 fluorocarbons have been calculated and, where possible, compared with available experimental data or other calculations. Table 2 summarizes the species for which calculations have been performed and their associated heats of formation. Of the over 90 species calculated to date, 44 were compared with available literature data, resulting in an average deviation of 6.5 kJ/mol (1.6 kcal/mol).

One of the key issues arising in this work turned out to be the heat of formation of carbonyl difluoride. Of the over 90 species calculated, carbonyl difluoride gave by far the largest deviation of 37.2 kJ/mol in the heat of formation at standard state. The previously accepted JANAF value is -635 kJ/mol, as compared to our calculated value of -598.2 kJ/mol.

During the course of this work, large basis sets and a limited number of G2 calculations were used to find a possible error in smaller basis sets, electron correlation or the BAC corrections. However, two independent calculations cast doubt on the validity of the accepted JANAF number. Schnieder and Wallington [8] have recently completed a study of the thermochemistry of CF_2O and related compounds using QCI-based calculations and have concluded that the discrepancies they observe can only be explained by experimental error. They recommended a value of -607.3 ± 7 kJ/mol, which is consistent with our -598.2 kJ/mol value. Montgomery et al. [9] have independently come to the same conclusion based on calculations using the CBS method and determined a value for the heat of formation at 298 K of -608.6 kJ/mol. On the basis of these independent calculations, we proceed on the assumption that while one cannot definitely conclude that the experimental number is wrong, it is unlikely that *ab-initio* calculations using different approaches that have demonstrated high accuracy for other fluorocarbons, should produce an error of the magnitude necessary for the JANAF assignment to be correct. In general, however, the agreement with experiment (where available and appropriate) was excellent.

General Chemical Features

The bond dissociation energies for C-F, C-H and C-C are shown in the figures below. In addition, we have plotted the Mulliken charge difference for comparison purposes. The Mulliken charge analysis is a procedure for assigning the relative local charge to an atom. As such, it can be used as an indicator of covalent versus ionic character.

Beginning with the fluoromethanes, the C-H and C-F bond dissociation energy (BDE) is plotted (Figure 1a,b) versus number of fluorine atoms and the absolute value of the associated difference in Mulliken charges $\Delta = |\delta_i - \delta_j|$ between the bonding atoms. For C-H BDE's, addition of the first fluorine will decrease the bond dissociation energy, but upon subsequent substitution of fluorines the BDE begins to increase again. This correlates very well with the Mulliken population analysis. In methane, carbon is an electron acceptor and is slightly ionic. Addition of one fluorine decreases ionic character and so also the BDE. Further addition of fluorine changes the character of carbon from an electron acceptor to an electron donor returning the C-H bond to a more ionic behavior and therefore a stronger bond. The C-F bond by contrast shows a monotonic increase in BDE with fluorine substitution which again correlates well with the Mulliken population analysis. In both cases, our calculations compare very favorably with experiment as shown in the figures.

Figure 2a,b shows the BDE for the C-C bond in substituted ethanes as well as the Mulliken analysis. As is clear, the C-C BDE increases upon successive addition of fluorine to the same carbon. The molecule with the highest BDE $\text{CH}_3\text{-CF}_3$, also has the largest difference in Mulliken charges between the carbons, in keeping with the increased ionic character.

One intriguing point to note is that the BDE for $\text{C}_2\text{F}_6 > \text{C}_2\text{H}_6$! One's intuition might suggest the opposite. The explanation comes from the fact that as defined, the BDE is really a measure of the relative stability between radical and parent and not the intrinsic bond strength. The explanation for the anomalous behavior between C_2F_6 , C_2H_6 and for the other symmetrically substituted fluoroethanes is that progressing from CH_3 to CF_3 , the radical goes from planar (sp^2) to pyramidal (sp^3). As such when the CF_3 radical is formed from a bond breaking event, it is already at its equilibrium conformation. By contrast, the methyl radical goes from an sp^3 when bonded in ethane to sp^2 , and must undergo a conformational rearrangement to lower energy. We have calculated the energy of these conformational relaxations to be about 80 kJ/mol in ethane (40 kJ/mol per methyl fragment). The CHF_2 and CH_2F fragments were calculated to have conformational energies of 6 and 22 kJ/mol, respectively. If one adds back this conformational energy to the BDE we can define an intrinsic bond energy which for ethane is in fact larger than the perfluoroethane, in keeping with one's expectations.

While not shown here, we have used this analysis to calculate the relative contribution of the ionic and covalent components to the C-C bond energy. By first adjusting for the conformational correction, we can obtain an absolute measure of the ionic component by subtracting the BDE energy, between the symmetrically (no ionic character) and asymmetrically substituted fluoroethanes. This difference correlates linearly with the Mulliken charge difference. This analysis indicated that indeed the intrinsic C-C bond strength in $\text{C}_2\text{H}_6 > \text{C}_2\text{F}_6$, even though the BDE shows the opposite to be true.

Table 2. BAC-MP4 Enthalpy of Formation kJ/mol

SPECIES	BAC-MP4	EXPT	REF
CH ₃ F	-233.9	-237.8	A
CH ₂ F ₂	-451.0	-452.9	A
CHF ₃	-699.6	-693.3	A
CF ₄	-934.3	-933.1	A
•CH ₂ F	- 31.4	- 32.6	B
•CHF ₂	-247.3	-247.7	B
•CF ₃	-471.5	-464.8	B
:CHF	131.7	125.5	C
:CF ₂	-203.3	-182.0	C
•CF	236.4	255.2	C
CHF=O	-395.0	-376.6	C
CF ₂ =O	-598.3	-638.9	C
•CF=O	-182.8	-171.5	C
CH ₂ FO•	-194.6		
CHF ₂ O•	-405.8		
CF ₃ O•	-628.4	-655.6	D
CH ₂ FOH(E)	-412.1		
CH ₂ FOH(Z)	-420.9		
CH ₂ FOH(G)	-430.1		
CHF ₂ OH(G)	-672.0		
CHF ₂ OH(E)	-684.5		
CF ₃ OH	-918.8		
CH ₃ OF	-91.9		
CH ₂ FOF	-260.1		
CHF ₂ OF	-520.9		
CF ₃ OF	-749.4		
•CHFOH	-239.4		
•CF ₂ OH(E)	-456.5		
•CF ₂ OH(G)	-463.2		
•CH ₂ OF	-42.3		
•CHFOF	-308.8		
CF ₃ OOH	-807.5		
CH ₂ FOO•	-172.8		
CHF ₂ OO•	-401.2		
CF ₃ OO•	-627.6		
CF(O)OH	-615.0		
CF ₂ (OH) ₂	-903.0		
CF ₂ (O)OH	-620.7		
FCO ₂	-336.5		

Table 2; continued

SPECIES	BAC-MP4	EXPT	REF
CHF=CH*(Z)	124.3		
CHF=CH*(E)	123.0		
CH ₂ =CF*	109.2		
CHF=CF*(Z)	-41.0		
CHF=CF*(E)	-42.7		
CF ₂ =CH*	-67.8		
CF ₂ =CF*	-216.3		
C ₂ HF	118.0	125.5	C
C ₂ F ₂	31.8	20.9	C
•C ₂ F	454.0		
CHF=C=O	-147.3		
CF ₂ =C=O	-290.4		
•CF=C=O(E)	69.0		
CH ₂ F-CHO(Z)	-322.6		
CH ₂ F-CHO(E)	-328.9		
CHF ₂ -CHO(E)	-525.1		
CHF ₂ -CHO(Z)	-538.9		
CF ₃ -CHO	-774.5		
CH ₂ F-CO*(Z)	-169.9		
CH ₂ F-CO*(E)	-172.8		
CHF ₂ -CO*(Z)	-377.4		
CF ₂ -CO*(Z)	-610.0		
CF ₂ -CO*(E)	-611.3		
CH ₃ -CH ₂ F	-272.4	-263.2	E
CH ₂ F-CH ₂ F	-446.9	-431.0	F
CH ₃ -CHF ₂	-505.4	-500.8	E
CH ₂ F-CHF ₂	-671.5	-643.5	G
CH ₃ -CF ₂	-755.2	-745.6	E
CHF ₂ -CHF ₂	-890.4	-860.6	H
CH ₂ F-CF ₂	-913.4	-895.8	E
CHF ₂ -CF ₂	-1124.2	-1104.6	E
CF ₂ -CF ₂	-1357.0	-1342.6	E
CH ₂ F-CH ₂ *	-56.2	-48.1	H
CH ₂ -CHF*	-75.6	-78.2	J
CH ₂ F-CHF*	-247.3	-235.6	H
CHF ₂ -CH ₂ *	-280.7	-285.8	H
CH ₃ -CF ₂ *	-300.0	-302.5	I
CH ₂ F-CF ₂ *	-460.1	-438.9	H
CHF ₂ -CHF*	-459.8	-451.4	H
CF ₂ -CH ₂ *	-527.2	-517.1	I
CHF ₂ -CF ₂ *	-673.2		
CF ₂ -CHF*	-702.8	-680.7	J
CF ₃ -CF ₂ *	-907.5	-891.2	L
CH ₃ =CHF	-139.3	-138.9	K
CHF=CHF(Z)	-301.2		
CHF=CHF(E)	-302.1		
CH ₂ =CF ₂	-340.2	-336.8	L
CHF=CF ₂	-485.8		
CF ₂ =CF ₂	-653.5	-658.6	C

NOTE: Complete Reference Information available on page 373.

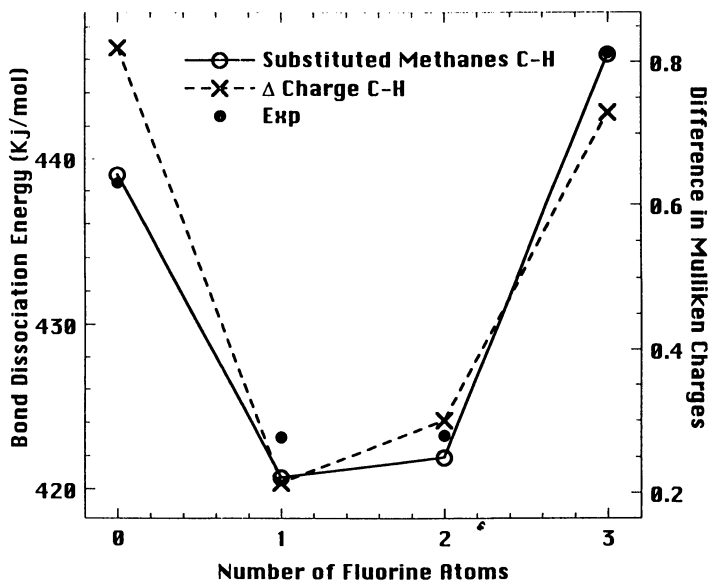


FIG. 1a. Calculated C-H BDE, experimental data and absolute value of difference of Mulliken charges between C-H as a function of fluorine substitution in fluoromethanes.

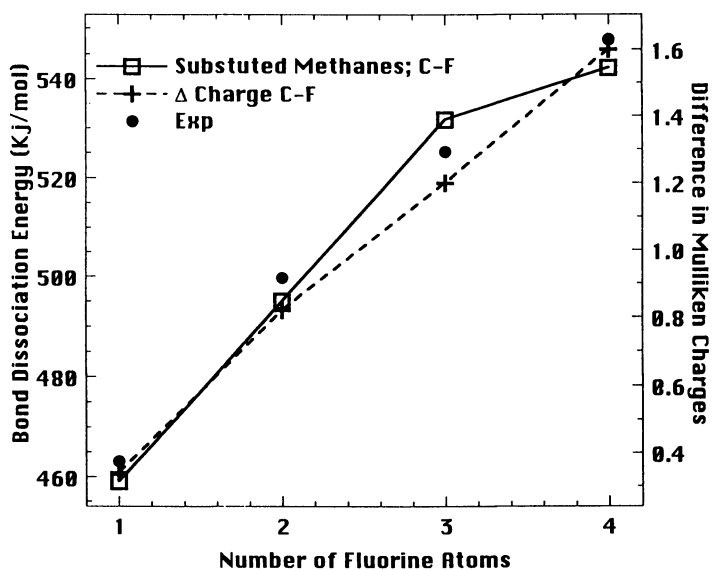


FIG. 1b. Calculated C-F BDE, experimental data and absolute value of difference of Mulliken charges between C-H as a function of fluorine substitution in fluoromethanes.

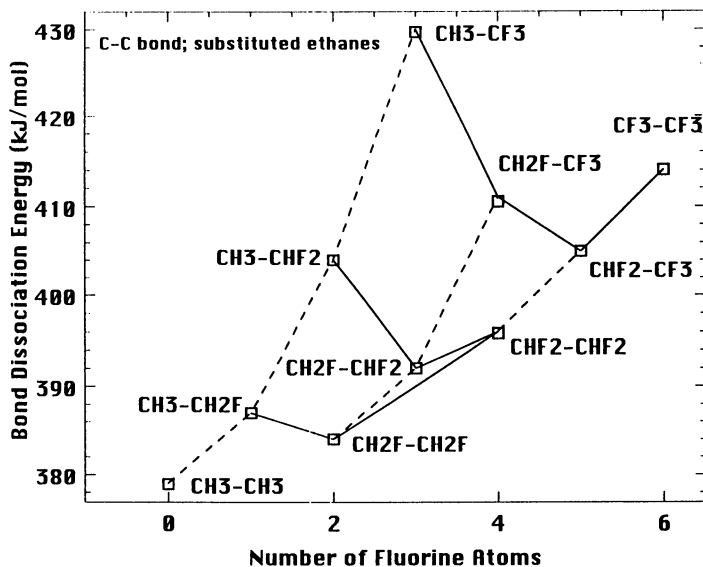


FIG 2a. C-C BDE as a function of number of fluorine atoms

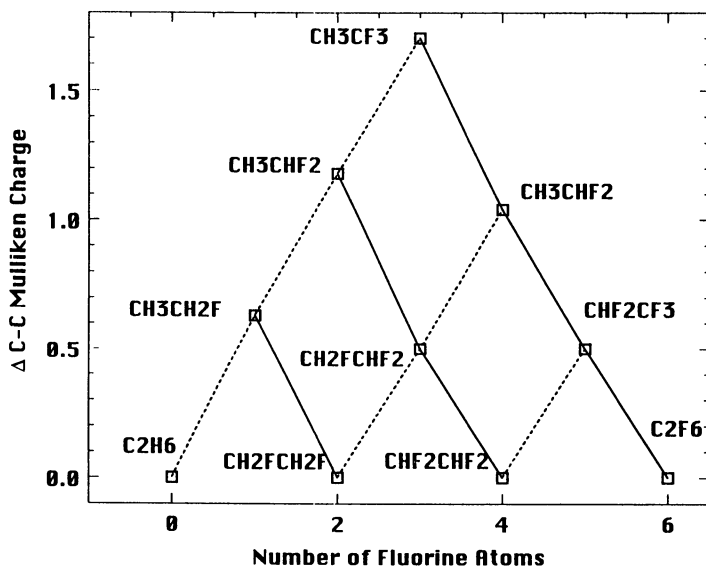


FIG 2b. Absolute value of difference in Mulliken charges between carbons in substituted ethanes.

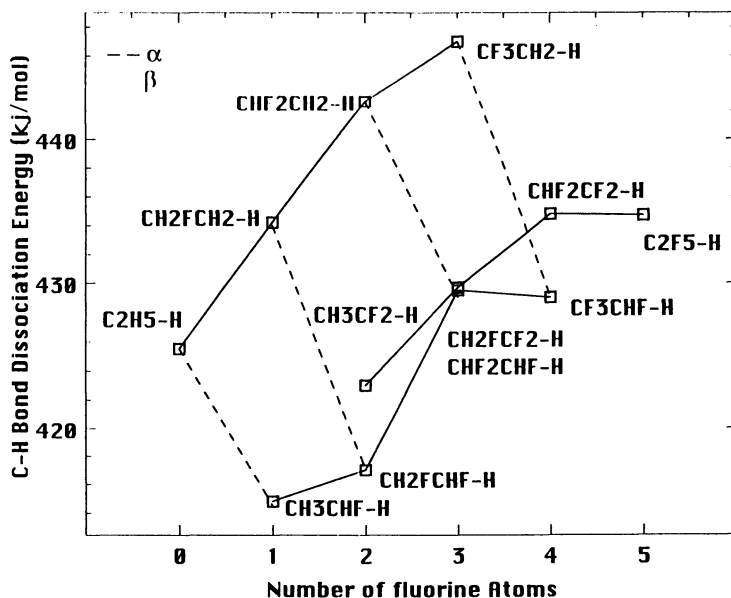


FIG 3a. C-H BDE for substitute ethanes as a function of number of fluorines

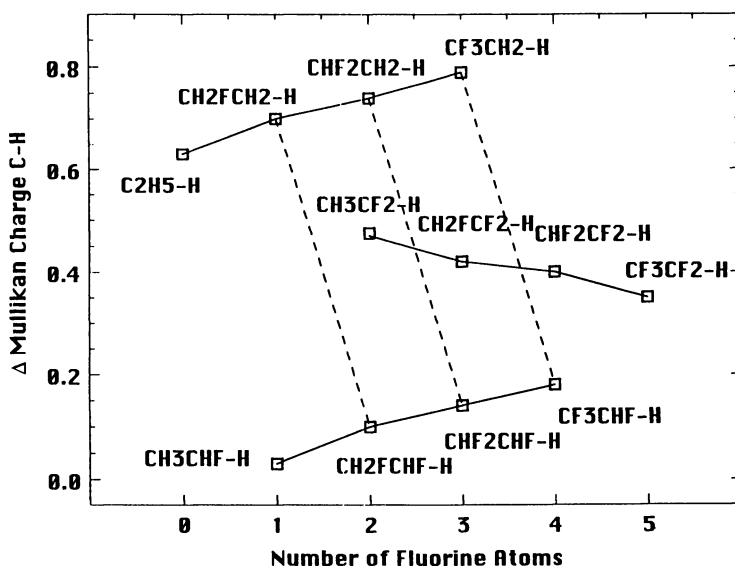
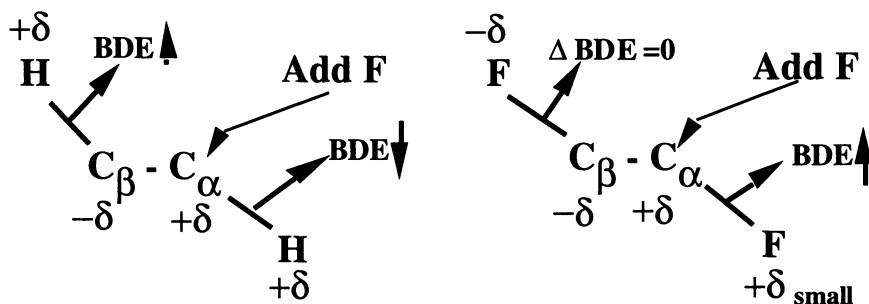


FIG 3b. Absolute value of difference in Mulliken charges between C-H in substituted ethanes.

The C-H and C-F BDE's are presented in Figures 3 and 4. As was the case for the fluoromethanes, the Mulliken charges generally correlate well with the BDE's. The basic trend observed are that fluorine substitution on the α carbon decreases the C-H BDE and increases the C-F BDE. On the other hand fluorine substitutions effect on the β carbon is to increase the C-H BDE and has virtually no effect on the C-F BDE. Substituted ethylenes showed similar trends to those discussed for the ethanes.



Transition States

The energetic properties for transition states are tabulated in Table 3. Transition state energies are presented as heats of formation in an analogous fashion to the equilibrium properties of molecules.

Reactions involving substituted methanes are summarized in Figure 5 as a function of number of fluorines. The most favored unimolecular decomposition process is HF elimination, followed by H_2 elimination, with F_2 elimination highly unlikely. In general, the more highly fluorine-substituted, the lower the activation barrier to decomposition. The effect can be quite significant, particularly for the HF elimination case where the activation barrier decreases by over 50 kJ/mol in going from CH_3F (367 kJ/mol) to CHF_3 (314 kJ/mol). Comparison with experimental data where available is quite good and follows the calculations in both qualitative trends and quantitative results.

Attack by H atoms favors abstraction of H, with activation barriers (in the 40 - 50 kJ/mole range) that are relatively insensitive to fluorine substitution. In contrast, fluorine abstraction by H requires a barrier about two and a half times as large as H abstraction and clearly indicates an increase in barrier height with increased fluorine substitution.

There are numerous studies on the thermal decomposition of CF_3H using the shock tube technique [10-14]. It is clear that even at the highest pressures the reactions are still in the pressure-dependent regime. Schug et al. [10] have carried out an extrapolation of their results to obtain the limiting high-pressure rate expression for HF elimination from CF_3H ($1.2 \times 10^{14} \exp(-36300/T) \text{ s}^{-1}$). An Arrhenius plot of the results can be found in Figure 6 along with our calculation based on transition state theory. In a

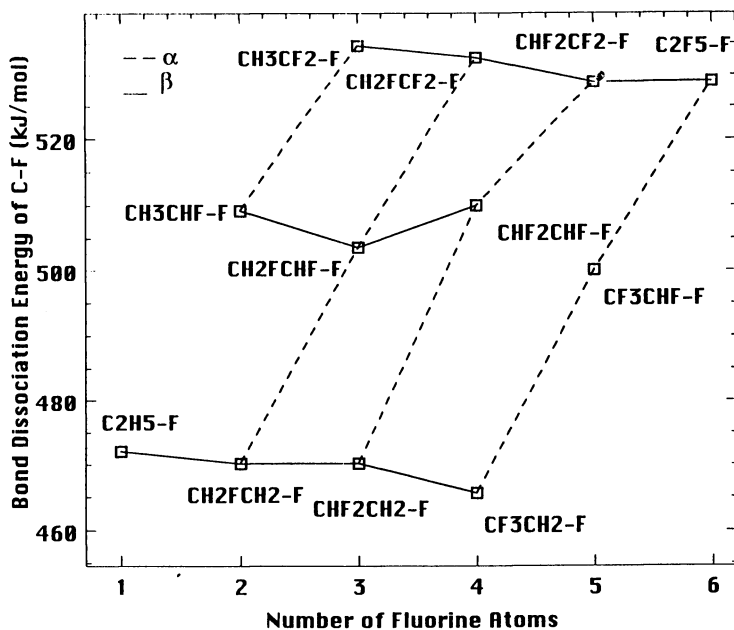


FIG 4a. C-F BDE for substituted ethanes as a function of number of fluorines

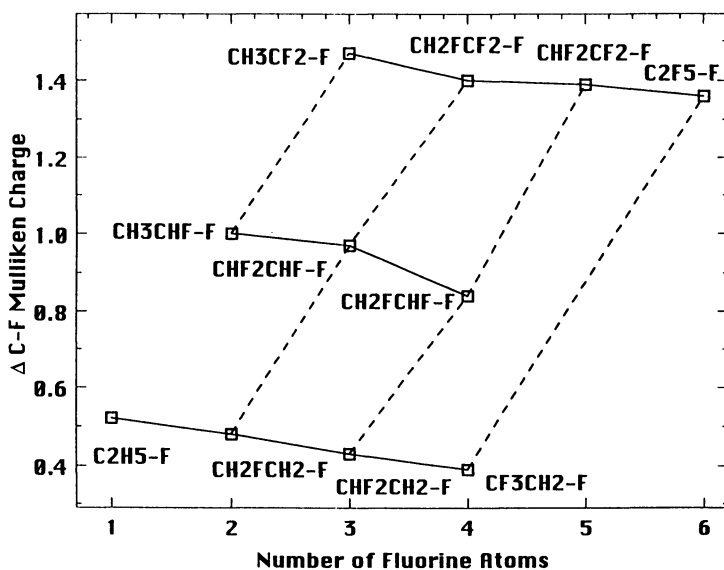
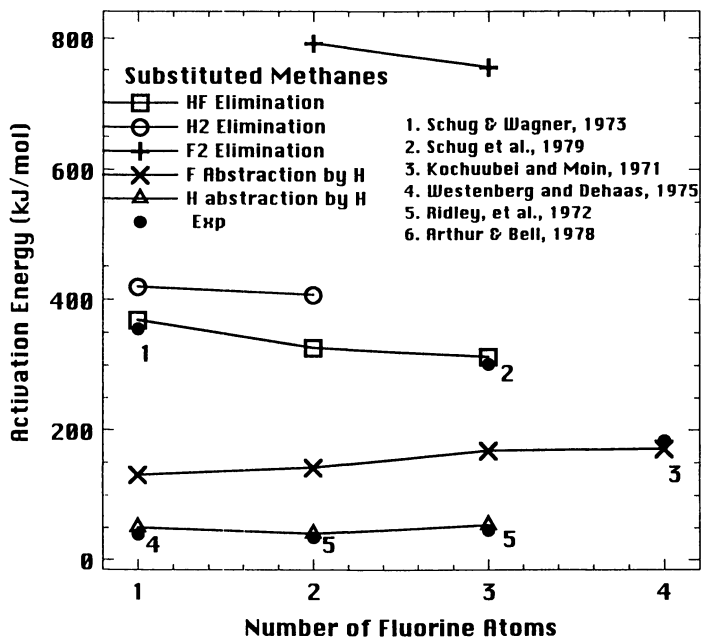


FIG 4b. Absolute value of difference in Mulliken charges between C-F in substituted ethanes.

Table 3. BAC-MP4 Transition State Calculations kJ/mol

TRANSITION STATE		ΔH_f^\ddagger	E_a
CH ₃ F	→ :CH ₂ + HF	120.8	354.5
	→ :CHF + H ₂	182.2	416.3
CH ₂ F ₂	→ :CHF + HF	-121.8	329.2
	→ :CF ₂ + H ₂	-51.9	465.8
	→ :CH ₂ + F ₂	346.0	797.3
CHF ₃	→ :CF ₂ + HF	-388.3	311.1
	→ :CHF + F ₂	52.2	751.9
CF ₄	→ CF ₂ +F ₂	-310.0	624.0
CF ₃ OH	→ CF ₂ =O + HF	-741.8	177.6
CH ₂ FO•	→ •CH=O + HF	-109.6	84.6
CH ₂ FO•	→ CF ₂ =O + F	-19.2	175.1
CHF ₂ O•	→ •CF=O + HF	-248.6	157.0
CHF ₂ O•	→ CF ₂ =O + H	-328.9	76.6
•CF ₂ OH(E)	→ •CF=O + HF	-300.0	163.0
	→ CF ₂ =O + H	-315.2	147.9
	→ CHF ₂ O•	-301.9	161.0
CH ₃ -CH ₂ F	→ CH ₂ =CH ₂ + HF	-4.6	267.7
CHF ₂ CHF ₂	→ CH ₂ F ₂ + :CF ₂	-375.5	507.8
CH ₄	+ :CF ₂ → CH ₃ -CHF ₂	-97.2	181.0
CH ₄	+ :CHF → CH ₃ -CH ₂ F	129.5	72.7
CH ₃ F	+ H → •CH ₂ F + H ₂	29.2	45.1
	→ •CH ₃ + HF	111.0	127.2
CH ₂ F ₂	+ H → •CHF ₂ + H ₂	-189.3	43.9
	→ •CH ₂ F + HF	-87.0	146.4
CHF ₃	+ H → •CF ₃ + H ₂	-431.0	50.5
	→ •CHF ₂ + HF	-317.6	164.2
CF ₄	+ H → •CF ₃ + HF	-545.2	171.2
CF ₂ =O	+ H → •CF=O + HF	-229.7	150.8
	→ •CF ₂ OH	-314.7	65.3
	→ CHF ₂ O•	-328.5	51.4
CF ₂ =O	+ H ₂ O → FC(O)OH + HF	-718.9	121.2
	→ CF ₂ (OH) ₂	-714.4	125.8
CF ₂ O	+ OH → F ₂ CO(OH)	-547.5	113.3
F ₂ CO(OH)	→ FCO ₂ + HF	-473.5	147.9
FCO(OH)	→ CO ₂ + HF	-489.0	125.8
CH ₃ -CHF•	→ CH ₂ =CH• + HF	216.7	292.2
CH ₂ F-CH ₂ •	→ CH ₂ =CHF + H	98.3	154.5



NOTE: Complete Reference Information available on page 373.

FIG 5. Activation barriers for unimolecular decomposition and H atom attack of fluoromethanes as a function of number of fluorine atoms.

similar fashion, we compare the extrapolated experimental rate constants from Schug and Wagner [14] for the thermal decomposition of CH_3F to $\text{CH}_2 + \text{HF}$ with those derived on the basis of transition state theory based on BAC-MP4 calculations. Once again there is excellent agreement in the rate constants within the error limits of the extrapolated high-pressure rate constants. From these results we conclude that for organic fluorine dehydrofluorination, BAC-MP4 calculations of the transition state leads to unimolecular rate constants that are probably within a factor of 3 of the true values.

For carbene insertions ($^1\text{CH}_2$, ^1CHF , $^1\text{CF}_2$) we use the singlet state of CH_2 for comparison because the ground state for the fluorocarbenes are singlet. The results are summarized in Figure 7. Singlet CH_2 is well known to insert into virtually any molecule. Insertion by CHF has moderate barriers of up to 45 kJ/mol, while insertion of CF_2 involves much higher activation barriers of between 85 kJ/mol for insertion into HF to 280 kJ/mol for insertion into CH_2F_2 . The implications are that highly fluorinated compounds would produce longer lived CF_2 , which, rather than insert as would be the case for methylene, would preferentially be oxidized.

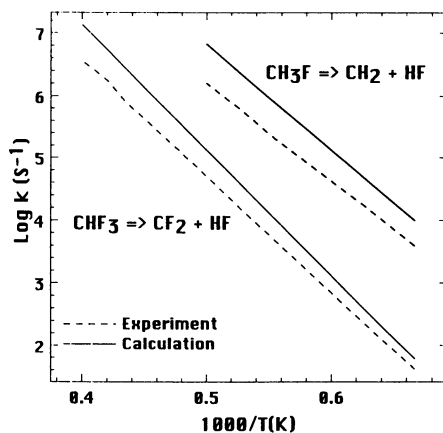


FIG 6. Comparison of experiment and theoretical calculation of limiting high pressure rate constants for HF elimination from fluoromethanes.

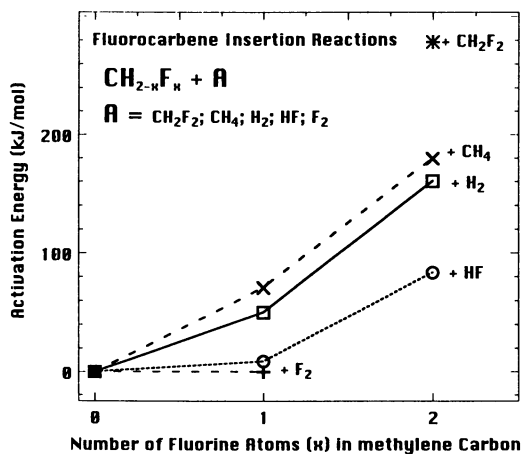


FIG 7. Activation barriers for insertions of ${}^1\text{CH}_2$, ${}^1\text{CH}_2$, and ${}^1\text{CF}_2$.

We have also undertaken an extensive study of the reactions of $\text{CF}_2\text{O} + \text{H}$ and H_2O to be published elsewhere [15], which indicated that the H atom reaction should be the most important under typical flame conditions. The analysis has led to a predictive rate constant for the H atom attack leading to $\text{CFO} + \text{HF}$, in excellent agreement with both the seminal work of Biordi [16] and more recent data obtained by Richter et al. [17].

Conclusions

A bond additivity correction procedure has been applied to a large body of ab initio molecular orbital computations on fluorocarbon molecules. Where available, the computations have been compared with literature values and show overall excellent agreement. Transition state computations have also been used to obtain barrier heights for reaction and have been subsequently used to obtain reaction rate constants from RRKM/master equation analysis. The results of the work suggest that heavy reliance on computational chemistry methods can under appropriate circumstances lead both to chemical insight and to thermochemical and kinetic data with requisite chemical accuracy, which could otherwise be unattainable by experimental methods, given time and resource constraints. The results presented here bode well for the wider use of these methodologies for a wider range of chemical systems of environmental interest.

References

1. Nyden M.D., Linteris, G.T., Burgess Jr, D., Westmoreland, P.R., Tsang, W., M.R., Zachariah, M.R., "Flame Inhibition Chemistry and the Search for Additional Fire Fighting Chemicals" in *Evaluation of Alternative In-Flight Fire Suppressants for Full-Scale Testing in Simulated Aircraft Engine Nacelles and Dry Bays*, Ed. W. Grosshandler, R. Gann, W. Pitts, Pages 467-641, Report # NIST SP 861 (1994)
2. Burgess Jr., D., Tsang, W., Zachariah, M.R., and Westmoreland, P.R., "Fluorinated Hydrocarbon Flame Suppression Chemistry" to appear in *ACS Symposium on Fuel Chemistry* (1994)
3. Westmoreland, P.R., Burgess Jr., D.R.F., Tsang, W., and Zachariah, M.R., "Kinetics of Fluoromethanes in Flames" to appear in the *25th Symposium (International) on Combustion* (1994)
4. Burgess Jr., D.R.F., Tsang, W., Zachariah, M.R., and Westmoreland, P.R., "Kinetics of Fluorine-Inhibited Hydrocarbon Flames", *Proceedings of the Halon Options Technical Working Conference*, 489-501 (1994)
5. Melius, C.F., and Binkley, J.S., *Twenty-First Symposium (International) on Combustion*, 1953 (1986)
6. M. J. Frish, M. Head-Gordon, G. W. Trucks, J. B. Foresman, H. B. Schlegel, K. Raghavachari, M. A. Robb, J. S. Binkley, C. Gonzalez, D. J. DeFrees, D. J. Fox, R. A. Whiteside, R. Seeger, C. F. Melius, J. Baker, L. R. Martin, L. R. Kahn, J. Stewart, S. Topiol, J. A. Pople, Gaussian90, Gaussian Inc., Pittsburgh, Pa (1990).
7. Schlegel, H.B., *J. Chem. Phys.* **84**, 4530 (1986)
8. Schnieder, W.F., and Wallington, T.J., *J. Phys. Chem.* **98**, 7448 (1994)
9. Montgomery Jr., J.A., Michels, H.H., and Francisco, J.S., *Chem. Phys. Lett.*, **220** 391 (1994)]

10. Schug, K.P., Wagner, H. Gg., and Zabel, F., *Ber. Bunsenges. Phys. Chem.*, **85**, 167 (1979)
11. Hidaka, Y., Nakamura, T., and Kawano, H., *Chem. Phys. Lett.*, **187**, 40 (1991)
12. Tschuikow-Roux, E., *J. Phys. Chem.*, **42**, 3639 (1965)
13. Modica, A. P., and LeGraff, J.E., *J. Chem. Phys.* **44**, 3375, (1966)
14. Schug, K.P., and Wagner, H. Gg., *Z. Phys. Chem.* **86**, 59 (1973)
15. Zachariah, M.R., Tsang, W., Westmoreland, P.R., and Burgess Jr. D.R.F., "Theoretical Prediction of the Thermochemistry and Kinetics of Reactions of CF₂O with Hydrogen atom and Water", submitted.
16. Biordi, J.C., Lazzara, C. P. and Papp, J.F., *Fifteenth Symposium (International) on Combustion* 917 (1974)
17. Richter, H., Vandooren, J., and Van Tiggelen, "Kinetics of the Consumption of CF₃H, CF₂HCL and CF₂O in H₂/O₂ Flames", *J. Chemie Physique*, in press

References for Table 2

- a. Rodgers, A.S; Chao, J.; Wilhoit, R.C.; Zwolinski, B.J.; *J. Phys. Chem. Ref. Data* **1974**, 3, 117.
- b. McMillan, D.F.; Golden, D.M.; *Ann. Rev. Phys. Chem.* **1982**, 33, 493.
- c. Stull, D.R.; Prophet, H.; *JANAF Thermochemical Tables*, **1971**, NSRDS-NBS 37.
- d. Batt, L.; Walsh, R.; *Int. J. Chem. Kin.* **1982**, 14, 933-944.
- e. Chen, S.S.; Rodger, A.S.; Chao, J.; Wilhoit, R.C.; Zwolinski, B.J.; *J. Phys. Chem. Ref. Data* **1975**, 4, 441-456.
- f. Daubert, T.E.; Danner, R.P.; "DIPPR Data Compilation of Pure Compound Properties," *NIST Standard Reference Database 11* **1985**.
- g. Pedley, J.B.; Naylor, R.D.; Kirby, S.P.; *Thermochemical Data of Organic Compounds*; Chapman and Hall: New York, NY, 1986.
- h. estimated using group additivity and/or bond dissociation energies.
- i. Rodgers, A.S.; *ACS Symp. Ser.* **1978**, 66, 296.
- j. Martin, J.P.; Paraskevopoulos, G.; *Can. J. Chem.* **1983**, 61, 861-865.
- k. Pedley, J.B.; Rylance, J.; *Sussex-N.P.L. Computer Analysed Thermochemical Data. Organic and Organometallic Compounds*; University of Sussex: Brighton, England, 1977.
- l. Stull, D.R.; Westrum, E.F., Jr.; Sinke, G.C.; *The Chemical Thermodynamics of Organic Compounds*; John Wiley: New York, NY, 1969.

References for Figure 5

- Westenberg, A.A.; deHaas, N.; *J. Chem. Phys.* **62**, 3321-3325 (1975).
 Ridley, B.A.; Davenport, J.A.; Stief, L.J.; Welge, K.H.; *J. Chem. Phys.* **57**, 520 (1972).
 Arthur, N.L.; Bell, T.N.; *Rev. Chem. Intermed.* **2**, 37-74 (1978).
 Kochubei, V.F.; Moin, F.B.; *Kinet. Catal.* **11**, 712 (1971).
 Schug, K.P.; Wagner, H.Gg.; *Z. Phys. Chem.* **86**, 59-66 (1973).
 Schug, K.P.; Wagner, H.Gg.; Zabel, F.; *Ber. Bunsenges. Phys. Chem.* **83**, 167 (1979).

RECEIVED July 20, 1995

Author Index

- Abe, T., 139
Andersen, Stephen O., 8
Atkinson, Roger, 41
Babushok, V. I., 275
Baronnet, F., 289
Battin-Leclerc, F., 289
Beauchamp, Carlos R., 122
Burgess, D. R. F., Jr., 275,322,358
Cleary, Thomas G., 122
Côme, G. M., 289
Connell, Peter S., 59
Davidovits, P., 50
De Bruyn, W. J., 16,50
Delfau, J. L., 289
Dierdorf, Douglas, 151
Fink, James L., 122
Finnerty, Anthony E., 161
Fukaya, H., 139
Gann, Richard G., 122
Gmurczyk, G., 204
Grosshandler, W. L., 204
Hamins, A., 190
Harris, Richard H., Jr., 122
Harrison, G. C., 74
Herron, John T., 1
Horkay, Ferenc, 122
Huie, Robert E., 31
Inomata, T., 139
Inoue, Yasufumi, 243
Kolb, C. E., 50
Laszlo, Barna, 31
Liao, Chihong, 243
Linteris, G. T., 225,260
Manion, Jeffrey A., 341
McKenna, Gregory B., 122
Melius, C. F., 358
Metchis, Karen L., 8
Miziolek, Andrzej W., 1,275
Moffat, Thomas P., 122
Moore, Ted A., 99,110
Nielsen, Ole J., 16
Nyden, Marc R., 122
Ogawa, Yoshio, 243
Patten, Kenneth O., 59
Peacock, Richard D., 122
Presser, C., 204
Richter, H., 304
Ricker, Richard E., 122
Robin, Mark L., 85
Rocteur, P., 304
Rubenstein, Reva, 8
Saito, Naoshi, 243
Sanogo, O., 289
Saso, Yuko, 243
Schneider, William F., 16
Sehested, Jens, 16
Seshadri, K., 190
Sheinson, Ronald S., 175
Shorter, Jeffrey A., 16,50
Skaggs, Stephanie R., 99,110,151
Stoudt, Mark R., 122
Takahashi, K., 139
Tapscott, Robert E., 99,110,151
Tiggelen, P. J. Van, 304
Trees, D., 190
Tsang, Wing, 1,275,322,341,358
Tuazon, Ernesto C., 41
Vandooren, J., 304
Vovelle, C., 289
Waldron, William K., Jr., 122
Wallington, Timothy J., 16
Walravens, B., 289
Westmoreland, P. R., 322,358
Worsnop, Douglas R., 16,50
Wuebbles, Donald J., 59
Zachariah, M. R., 322,358
Zahniser, M. S., 50

Affiliation Index

- Aerodyne Research, Inc., 16,50
 Boston College, 16,50
 Centre National de la Recherche Scientifique, 289
 Ford Research Laboratory, 16
 Great Lakes Chemical Corporation, 85
 Koatsu Company, Ltd., 243
 Lawrence Livermore National Laboratory, 59
 Ministry of Home Affairs (Japan), 243
 National Industrial Research Institute of Nagoya, 139
 National Institute of Standards and Technology, 1,31,122,190,204,225,260,275,322,341,358
 Naval Research Laboratory, 175
 Pacific Scientific, 151
 Risø National Laboratory, 16
 Sandia National Laboratories, 358
 Sophia University, 139
 U.S. Army Research Laboratory, 1,161,275
 U.S. Environmental Protection Agency, 8
 Université Catholique de Louvain, 304
 University of California—La Jolla, 190
 University of California—Riverside, 41
 University of Illinois—Urbana, 59
 University of Massachusetts, 322,358
 University of New Mexico, 99,110,151
 Walter Kidde Aerospace, 74

Subject Index

A

- Abstraction of F, atomic hydrogen, 349–353
 Acid gas production in inhibited propane–air diffusion flames
 behavior categories of inhibitors, 240–241
 effect of mixing, 238
 experimental description, 226–227,232f
 extinction concentrations for added inhibitor, 229–230
 future work, 241
 HF produced
 vs. inhibitor concentration in air, 231,234–239
 vs. inhibitor vs. burner, 230–231,233f
 model, 228–229
 previous studies, 226–227
 Acute toxicity testing, description, 101
 Additive flame temperature, limit mixtures, 254–256f
 Adiabatic flame temperatures at flammability limits
 fire suppression mechanisms of halon replacements, 254,256
 Adiabatic flame temperatures at flammability limits—*Continued*
 limit mixtures, 254–256f
 measurement procedure, 254
 Air–methane flames, inhibitor concentration effect on inhibition mechanism of fluoromethanes, 260–272
 Air–propane diffusion flames, acid gas production, 225–241
 Aircraft, halon applications, 74–80
 Alcohols, toxicity, 155
 Alkenes
 cup burner testing, 155–156
 toxicity, 155
 Alkyl peroxy radicals, reaction with iodine compounds, 32–33
 Alternative halocarbon oxidation intermediates, heterogeneous atmospheric chemistry, 50–57
 Amines, toxicity, 155
 Aqueous-phase chemistry, hydrochlorofluorocarbons and hydrofluorocarbons, 22–24

Affiliation Index

- Aerodyne Research, Inc., 16,50
 Boston College, 16,50
 Centre National de la Recherche Scientifique, 289
 Ford Research Laboratory, 16
 Great Lakes Chemical Corporation, 85
 Koatsu Company, Ltd., 243
 Lawrence Livermore National Laboratory, 59
 Ministry of Home Affairs (Japan), 243
 National Industrial Research Institute of Nagoya, 139
 National Institute of Standards and Technology, 1,31,122,190,204,225,260,275,322,341,358
 Naval Research Laboratory, 175
 Pacific Scientific, 151
 Risø National Laboratory, 16
 Sandia National Laboratories, 358
 Sophia University, 139
 U.S. Army Research Laboratory, 1,161,275
 U.S. Environmental Protection Agency, 8
 Université Catholique de Louvain, 304
 University of California—La Jolla, 190
 University of California—Riverside, 41
 University of Illinois—Urbana, 59
 University of Massachusetts, 322,358
 University of New Mexico, 99,110,151
 Walter Kidde Aerospace, 74

Subject Index

A

- Abstraction of F, atomic hydrogen, 349–353
 Acid gas production in inhibited propane–air diffusion flames
 behavior categories of inhibitors, 240–241
 effect of mixing, 238
 experimental description, 226–227,232f
 extinction concentrations for added inhibitor, 229–230
 future work, 241
 HF produced
 vs. inhibitor concentration in air, 231,234–239
 vs. inhibitor vs. burner, 230–231,233f
 model, 228–229
 previous studies, 226–227
 Acute toxicity testing, description, 101
 Additive flame temperature, limit mixtures, 254–256f
 Adiabatic flame temperatures at flammability limits
 fire suppression mechanisms of halon replacements, 254,256
 Adiabatic flame temperatures at flammability limits—*Continued*
 limit mixtures, 254–256f
 measurement procedure, 254
 Air–methane flames, inhibitor concentration effect on inhibition mechanism of fluoromethanes, 260–272
 Air–propane diffusion flames, acid gas production, 225–241
 Aircraft, halon applications, 74–80
 Alcohols, toxicity, 155
 Alkenes
 cup burner testing, 155–156
 toxicity, 155
 Alkyl peroxy radicals, reaction with iodine compounds, 32–33
 Alternative halocarbon oxidation intermediates, heterogeneous atmospheric chemistry, 50–57
 Amines, toxicity, 155
 Aqueous-phase chemistry, hydrochlorofluorocarbons and hydrofluorocarbons, 22–24

- Army's requirement for Halon 1301 replacement, *See* U.S. Army's requirement for Halon 1301 replacement
- Aromatics
cup burner testing, 155–156
toxicity, 155
- Atmospheric chemistry
alternative halocarbon oxidation intermediates, heterogeneous, *See* Heterogeneous atmospheric chemistry of alternative halocarbon oxidation intermediates
hydrochlorofluorocarbons and hydrofluorocarbons, 17–24
iodine compounds
absorption spectrum of IO, 34*f*,35,37
 $\text{CF}_3\text{O}_2 + \text{IO}$, 37–38
experimental procedure, 35
heterogeneous chemistry, 38
 $\text{IO} + \text{IO}$, 36*f*,37
 $\text{O} + \text{IO}$ and $\text{O} + \text{I}_2$, 36*f*,37
reactions in troposphere, 32–33,35
thermodynamics of IO and BrO, 38–39
- Atmospheric fate, halocarbonyl oxidation intermediates, 55–57
- Atmospheric lifetime, definition, 60
- Atmospheric ozone, potential effects of halon replacements, 62–63
- Atomic hydrogen
abstraction of F, 349–353
displacement of F, 350–351,353–355
- Autoignition delays, role of halon replacements, 291
- Auxiliary power unit, application of halons as fire-extinguishing systems, 75–76
- B**
- Banking, halon, description, 14
- N,N*-Bis(trifluoromethyl-1,1,2,2-tetrafluoroethylamine), preparation, 141
- Bond additivity corrected Mollet–Plesset many-body perturbation theory, theoretical prediction of thermochemical and kinetic properties of fluorocarbons, 358–372
- Box method, fire-extinguishing ability evaluation, 141–143
- BrO, thermodynamics, 38–39
- Brominated olefins, halon replacements, 88
- Bromine-containing compounds
environmental concerns, 59–60
role of anthropogenic emissions, 41
- Bromine-containing halon(s)
need for replacements, 2
regulatory control, 1–2
- Bromine-containing halon replacements
brominated olefins, 88
hydrobromofluorocarbons, 87–88
nonvolatile precursors, 88–89
- Bromine-containing perfluoroalkylamines, ban on use, 140
- Bromine role
chemical inhibiting action of fire extinguishers, 304–318
stratospheric chemistry, 31
- Bromotrifluoromethane
gaseous agents as possible substitutes, 190
restriction of production and use, 190
- Burning velocities, flame inhibition of fire extinguishers and potential replacements, 305–306
- C**
- $\text{C}_1\text{H/O/F}$, reaction kinetics, 329
- C_2F_6
diffusion flame extinction, 190–201
storage compatibility, 122–137
- $\text{C}_2\text{H}_2\text{F}_4$, storage compatibility, 122–137
- $\text{C}_2\text{HF}_4\text{Cl}$, storage compatibility, 122–137
- C_2HF_5 , storage compatibility, 122–137
- $\text{C}_2\text{H/O/F}$, reaction kinetics, 334
- C_3F_8
diffusion flame extinction, 190–201
storage compatibility, 122–137
- C_3HF_7
diffusion flame extinction, 190–201
storage compatibility, 122–137
- C_4F_{10}
diffusion flame extinction, 190–201
storage compatibility, 122–137

- Carbon dioxide, use as fire-extinguishing agent, 161
- Carbonyl compounds
examples, 154
toxicity, 154–155
- Carbonyl fluorides
reaction kinetics, 333
thermochemistry, 326
- Cardiac sensitization testing,
description, 101–102
- Cargo compartments, application of halons
as fire-extinguishing systems, 78–79
- C–F bonds, breakage, 341–355
- CF_2
rate constant for recombination, 348
stability, 343–344
- CF_3Br , *See* Halon 1301
- $\text{CF}_3\text{CH}_2\text{CF}_3$, diffusion flame extinction,
190–201
- CF_3I , removal in troposphere, 31–32, 34*f*
- CH_2F_2 , storage compatibility, 122–137
- $\text{CH}_2\text{F}_2/\text{CHF}_2\text{CF}_3$, diffusion flame extinction,
190–201
- CH_2FCF_3 , diffusion flame extinction,
190–201
- Chemical effects
definition, 323
types, 324
- Chemical inhibiting effect of
fluorocarbons and hydrofluorocarbons
experimental description, 290–291
inhibiting effect
flames, 292, 295–299
oxidation reactions, 291–294*f*
mechanism
calculation method, 299–300
experimental and calculated
concentrations, 300
fluorinated compounds, 301–302
physical effect, 299
- Chemical kinetics–hydrodynamic modeling,
U.S. Army's requirement for Halon 1301
replacement program, 183
- Chemical mechanisms of fire-extinguishing
agents, description, 165
- Chemiiionization, flames seeded with
inhibitors, 315–317
- CHF_2CF_3 , diffusion flame extinction,
190–201
- CHF_2Cl
diffusion flame extinction, 190–201
storage compatibility, 122–137
- CHFClCF_3 , diffusion flame extinction,
190–201
- Chlorine-containing compounds, role of
anthropogenic emissions, 41
- Chlorine-containing halon replacements,
description, 89–90
- Chlorofluorocarbons
flame inhibition, 304–318
regulation, 306
replacements, 16
role in ozone depletion, 1
search for replacements, 306
stratospheric ozone impact, 16
- Cl atom initiated photooxidations of
 C_1 – C_3 hydrochlorofluorocarbons and
hydrofluorocarbons, 41–48
- Class(es), halon replacements, 5–6
- Class II substance, definition, 12
- Clean Air Act Amendments of 1990,
function, 11
- Clean Air Act of 1977
elimination of halon production and
import, 59
role of EPA in stratospheric ozone
protection, 11
- Climate, potential effects of halon
replacements, 66–70
- Coflow burner, description, 192*f*–194
- Coflow flame, description, 198–201*t*
- Coflowing configurations, description,
191–192
- Combustion processes in plug reactor,
flame retardant effect, 275–286
- Compatibility, halon replacements during
storage, 122–137
- Consumer, halon use reduction, 10
- Corrosion, description, 123
- Counterflow burner, description, 192–193
- Counterflow flame, description, 194–198
- Counterflowing configuration,
description, 191
- Crevice corrosion, description, 123

Crew compartments of ground combat vehicles, U.S. Army's requirement for Halon 1301 replacement, 162,164

Cup burner, description, 191

Cup burner test

tropodegradable halon replacements, 155–156

U.S. Army's requirement for Halon 1301 replacement, 165–167

Cyclo-C₄F₈

diffusion flame extinction, 190–201

storage compatibility, 122–137

D

Dealloying, description, 123

Decomposition products, toxicity, 104–107

Design concentration, definition, 12

Destruction of ozone layer, resolution urgency, 139

Development toxicity testing, description, 102

Diffusion flame extinction with halogenated and inert fire suppressants

coflow burner, 192*f*–194

coflow flame, 198–201*t*

coflowing configuration, 191–192

counterflow burner, 192–193

counterflow flame, 194–198

counterflowing configuration, 191

experimental description, 190–191

fuel properties, 191

Difluoromethane, concentration effect on inhibition mechanism in premixed methane–air flames, 260–272

Direct global warming potentials, halons and replacements, 69–70

Displacement of F, atomic hydrogen, 350–351,353–355

Dry bay(s), description, 204

Dry bay explosion suppression, application of halons as fire-extinguishing systems, 76–77

Dynamic combustion process suppression agents, 205,206*t*

effectiveness, 223–224

experimental description, 204–205

Dynamic combustion process suppression—*Continued*

quasi-detonations, 212–223

turbulent spray flames, 205–213

E

Effective uptake coefficient, definition, 52

Elastomer seal compatibility, halon replacements, 132–137

Engine compartments of ground combat vehicles, U.S. Army's requirement for Halon 1301 replacement, 164

Engine nacelles, application of halons as fire-extinguishing systems, 75–76

Environment, importance of halon replacement, 2–3

Environmental impact, hydrochlorofluorocarbons and hydrofluorocarbons, 18*t*,21*t*,23–26

Environmentally induced fracture, description, 123

Equivalence ratio, role in flame-retardant effects on combustion processes in plug reactor, 278*f*,279

Ethane oxidation, role of halon replacements, 291,293*f*

Ethers, toxicity, 155

Explosion

definition, 83

suppression and inertion, 83–84

Exposure testing, storage compatibility of halon replacements, 124–127

F

FC–3–1–10, inertion testing, 117,118*f*

Field-scale inertion testing of halon replacements

agent evaluation, 113,116–119

base-line testing, 113–115*f*

comparison of laboratory vs. field-scale results, 117,120*f*

experimental description, 110

methodology

apparatus, 110–112

concentration calculations, 112,114*f*

- Field-scale inertion testing of halon replacements—*Continued*
methodology—*Continued*
procedures, 112
sampling system, 112
recommendations, 121
- Fire-extinguishing ability evaluation by box method
experimental procedure, 141,142*f*
results, 141–143
- Fire-extinguishing agents, mechanisms, 164–165
- Fire-fighting agents
need for halon replacement, 2
requirements, 2
- Fire suppression, fundamental chemistry, 5
- Fire-suppression agents, halogenated, *See* Halogenated fire-suppression agents
- Fire-suppression efficiency of halon replacements, evaluation methods, 243–244
- Fire-suppression mechanisms, halon replacements, 254,256
- First-generation halon replacements, examples, 153
- Flame(s), inhibiting efficiency of halon replacements, 292,295–299
- Flame chemistry, fluorinated hydrocarbon, *See* Fluorinated hydrocarbon flame chemistry
- Flame extinction phenomenology, halon replacements, 4
- Flame-extinguishing concentration, measurement of fire suppression efficiency, 244
- Flame front, definition, 191
- Flame inhibition of fire extinguishers and potential replacements
analysis of inhibited flame structures, 306–315
approaches, 304–305
burning velocities, 305–306
chemiionization in flames seeded with inhibitors, 315–317
numerical modeling, 317–318
- Flame maximum temperature, measurements, 292,295*f*
- Flame retardant effects on combustion processes in plug reactor
additive concentration effect on ignition delay, 280–283
effect of equivalence ratio, 278*f*,279
effect of pressure, 279–280
effect of temperature, 277–279,284*t*
effect on flame speed, 283,285
experimental description, 275
kinetics data base, 276–277
model validation, 277
modeling techniques, 275
reaction pathways, 285,286*f*
temperature behavior at high additive concentration, 281–284*t*
- Flame speed, role in flame-retardant effects on combustion processes in plug reactor, 283,285
- Flame suppression mechanism, halon replacements, 4–5
- Flame velocity, measurements, 292–297
- Flammability limit of halon replacements
adiabatic flame temperatures, 254–256
measurement methods, 244
measurement using tubular flame burner system, 244–253
- Flooding agents, SNAP approvals, 94–95
- Fluorinated hydrocarbon flame chemistry
experimental objective, 322–323
future work, 337
influencing factors, 323–324
mechanism development
reaction kinetics, 328–336
species thermochemistry, 326–328
previous studies, 323
- Fluorine atom removal from halocarbons
abstraction of F by atomic hydrogen, 348–353
addition reaction, 349
bond energies, 342–343
displacement of F by atomic hydrogen, 350–351,353–355
experimental description, 342
importance for fire suppression chemistry, 341–342

- Fluorine atom removal from halocarbons—
Continued
 kinetics
 bimolecular reactions, 346
 radical–radical processes, 346
 unimolecular decomposition, 344–345
 O addition, 349
 rate constant
 vs. pressure, 346–348
 vs. temperature, 346–348
 thermochemistry, 343–344
 toxicity, 355
- Fluoroacetylenes, thermochemistry, 328
- Fluorocarbons
 effectiveness in dynamic combustion
 process suppression, 204–223
 theoretical prediction of thermochemical and kinetic properties, 358–372
- Fluoroethanes
 abstractions, 335–336
 decomposition, 334–335
 fluoromethyl disproportionation and fluoromethylene insertion, 335
 thermochemistry, 327
- Fluoroethyl radicals
 destruction, 336
 thermochemistry, 327–328
- Fluoroethylenes
 reaction kinetics, 336
 thermochemistry, 328
- Fluoroiodocarbon, halon replacement, 152–156
- Fluoroketenes, thermochemistry, 328
- Fluoroketyl radicals, thermochemistry, 328
- Fluoromethanes
 inhibitor concentration effect on inhibition mechanism in premixed methane–air flames, 260–272
 reaction kinetics, 329–331
 thermochemistry, 325
- Fluoromethoxy radicals, thermochemistry, 326
- Fluoromethyl radicals
 destruction, 331–332
 thermochemistry, 325
- Fluoromethylenes
 destruction, 332–333
 thermochemistry, 325–326
- Fluoromethylidyne
 destruction, 332–333
 thermochemistry, 325–326
- Fluorovinyl radicals, thermochemistry, 328
- Free oxygen model, suppression, 178–179
- Fuel tank inertion, application of halons as fire-extinguishing systems, 77–78
- G
- Gas-phase chemistry of hydrofluorocarbons and hydrochlorofluorocarbons
 conversion of haloalkanes into halogenated carbonyl compounds, 17–21
 reactions of halogenated carbonyl intermediates, 20*f*–22
- Gaseous agent test series, turbulent spray flames, 207,209,210*t*
- General corrosion, description, 123
- Genetic toxicity testing, description, 103
- Global environment, halon replacement effects, 59–70
- Global lifetime of species, calculation, 55
- Global warming potentials
 concept, 68
 potential effects of halon replacements, 68–70
- Greenhouse gases, role of halons and bromine-containing compounds, 59–60
- H
- Haloacetic acids, uptake, 57
- Haloalkanes, conversion into halogenated carbonyl compounds, 17–21
- Halocarbon(s)
 fluorine atom removal, 341–353
 properties, 151,152*t*
- Halocarbon global warming potentials
 definition, 25
 hydrochlorofluorocarbons and hydrofluorocarbons, 18*t*,25–26

- Halocarbon oxidation intermediates,
heterogeneous atmospheric chemistry,
50–57
- Halocarbons, uptake, 52–55
- Halogen oxide radicals, reaction with
iodine compounds, 33
- Halogenated carbonyl compounds,
conversion of haloalkanes, 17–21
- Halogenated carbonyl intermediates,
reactions, 20f–22
- Halogenated fire suppressants, diffusion
flame extinction, 190–201
- Halogenated Fire Suppressants*,
description, 1
- Halogenated fire-suppression agents
bromine-based halon replacements, 87–89
chlorine-based halon replacements, 89–90
experimental description, 85
future, 96
halon replacements, 86–87
history, 86
intermediate and large-scale testing, 92–94
iodine-based halon replacements, 90–91
NFPA 2001 Standard on Clean Agent Fire
Extinguishing Systems approvals, 95
regulatory and approval agency status, 94
SNAP approvals
flooding agents, 94–95
steaming agents, 94,95t
- Underwriters Laboratories/Factory Mutual
approvals, 96
- zero ozone depletion potential halon
replacement, 91–92
- Halon(s)
environmental concerns, 59–60
regulation, 11–14
use as fire-extinguishing agents,
161–162
- Halon 1211 replacements, toxicological
summary, 103,105t
- Halon 1301
advantages, 162
diffusion flame extinction, 190–201
effectiveness in dynamic combustion
process suppression, 204–223
fire-suppression effectiveness, 1
flooding shipboard fire protection, 177
- Halon 1301—*Continued*
impending ban on production, 31
ozone layer damage, 162
search for replacements, 358
storage conditions, 122
U.S. Army's requirement for replacement,
162–174
- Halon 1301 replacements, toxicological
summary, 103,104t
- Halon 13001, effectiveness in dynamic
combustion process suppression,
204–223
- Halon Alternatives Consortium,
function, 10
- Halon applications
aircraft, 74–80
industry, 80–84
- Halon bank(s), establishment, 9
- Halon banking, description, 14
- Halon production, ban, 99
- Halon production phase-out
consumer use reduction, 10
future work, 11
history, 8–11
military use reduction, 10
- Halon replacements
applications, 3–4
chemical inhibiting effect, 289–302
classes, 5–6
criteria, 99
decomposition byproduct importance,
225–226
development, 13
effectiveness in dynamic combustion
process suppression, 204–224
environmental aspects, 2–3
examples, 289–290
field-scale inertion testing, 110–121
fire-suppression mechanisms,
254,256
flame extinction phenomenology, 4
flame-suppression mechanistic
studies, 4–5
flammability peak concentrations,
242–256
fundamental chemistry of fire
suppression, 5

- Halon replacements—*Continued*
- global environment
 - atmospheric lifetime, 60–61
 - effects on climate
 - global warming potentials, 68–70
 - radiative forcing, 66–67
 - relative radiative forcing per molecule or mass, 67–68
 - surface temperature, change, 66
 - effects on ozone, 62–63
 - examples, 60,61*t*
 - experimental objective, 60
 - ozone depletion potentials, 65
 - ozone destruction effectiveness, 63–65
 - tropospheric concentration, 60
 - idealized specification, 151,153
 - metal organometallics, 156–157
 - need, 2
 - nomenclature, 6
 - policy, 2
 - properties, 151,152*t*
 - regulation, 11–14
 - requirements, 2
 - storage compatibility, 122–137
 - technology required, 4
 - testing, 3–4
 - toxicological properties, 99–108
 - transition metal compounds, 157–158
 - tropodegradable replacements, 153–156
 - Halon total flooding replacement program,
 - See* U.S. Navy's halon total flooding replacement program
 - Hand-held portables, application of halons
 - as fire-extinguishing systems, 79–80
 - HCl, production by halon replacements, 225–241
 - Heat-absorbing mechanisms of fire-extinguishing agents,
 - description, 165
 - n*-Heptane, inhibition effect of perfluoroalkylamines, 143–148
 - Heterogeneous atmospheric chemistry of alternative halocarbon oxidation intermediates
 - examples, 50
 - experimental description, 51–52
 - hydrolysis, 52–53
 - Heterogeneous atmospheric chemistry of alternative halocarbon oxidation intermediates—*Continued*
 - removal processes, 50–51
 - solubility, 52–53
 - tropospheric lifetime, 55–57
 - uptake
 - haloacetic acids, 57
 - halocarbonyls, 52–55
 - Heterogeneous deposition,
 - hydrochlorofluorocarbons and hydrofluorocarbons, 22–24
 - HF, production by halon replacements, 225–241,341–355
 - HFC–23
 - acceptability as fire protection agent, 13
 - inertion testing, 117,119*f*
 - HFC–227ea, inertion testing, 113,116*f*
 - H/O/F, reaction kinetics, 329
 - H/O/F species, thermochemistry, 325
 - HOI, formation, 32
 - Hydrobromofluorocarbons, halon replacements, 87–88
 - Hydrocarbon(s), reaction kinetics, 329
 - Hydrocarbon flame chemistry, fluorinated,
 - See* Fluorinated hydrocarbon flame chemistry
 - Hydrochlorocarbons, halon replacement, 289
 - Hydrochlorofluorocarbons
 - aqueous-phase chemistry, 22–24
 - design function, 41
 - effectiveness in dynamic combustion process suppression, 204–223
 - gas-phase chemistry, 17–22
 - halocarbon global warming potentials, 18*t*,25–26
 - heterogeneous deposition, 22–24
 - OH radical attack, 16–17
 - ozone depletion potentials, 18*t*,24–25
 - replacement(s), 89–90
 - replacement for chlorofluorocarbons, 16
 - toxic/noxious degradation product formation, 21*t*,23*t*,26
 - tropospheric degradation products, 41–48
 - use for halon replacement, 2–3

- Hydrofluoroalkanes, chemical-inhibiting effect, 289–302
- Hydrofluorocarbons
- aqueous-phase chemistry, 22–24
 - design function, 41
 - effectiveness in dynamic combustion process suppression, 204–223
 - gas-phase chemistry, 17–22
 - halocarbon global warming potentials, 18*t*, 25–26
 - heterogeneous deposition, 22–24
 - OH radical attack, 16–17
 - ozone depletion potentials, 18*t*, 24–25
 - replacement for chlorofluorocarbons, 16
 - toxic/noxious degradation product formation, 21*t*, 23*t*, 26
 - tropospheric degradation products, 41–48
 - use for halon replacements, 2–3
 - zero ozone depletion potential halon replacements, 91–92
- Hydrogen halide, formation, 226
- I
- Indirect global warming potentials, halons and replacements, 69–70
 - Industry, halon applications, 80–84
 - Inert fire suppressants, diffusion flame extinction, 190–201
 - Inert gas systems, risk assessment, 13
 - Inertion, definition, 83, 110
 - Inertion testing, field scale, halon replacements, 110–121
 - Inhibited flame structures, analysis, 306–315
 - Inhibition effect of perfluoroalkylamines on *n*-heptane flames
 - burning velocity inhibition
 - C₁ compounds, 144*t*–146
 - perfluoroalkylamines, 146–148*f* - experimental procedure, 143
 - model calculation of laminar burning velocity, 143–145
- Inhibition mechanism of fluoromethanes in premixed methane–air flames, effect of inhibitor concentration, 260–272
- Inhibition parameter
- definition, 305
 - values, 305–306
- Inhibitor concentration effect on inhibition mechanism of fluoromethanes in premixed methane–air flames
- CF₄ effect, 267
 - compound selection, 262
 - decomposition reaction pathways for CH₂F₂ and CF₃H, 269–272
 - experimental burning rate vs. equivalence ratio, 264–265
 - experimental description, 260–263
 - future work, 272
 - model, 261–262
 - normalized burning rate, 265–267
 - previous studies, 261
 - radical production and consumption rates for CH₂F₂ and CF₃H, 267–269
- Intergranular corrosion, description, 123
- Intermediate-scale testing, U.S. Army's requirement for Halon 1301 replacement, 179–184
- International Cooperation, phase-out of halon production, 8–11
- IO, thermodynamics, 38–39
- Iodides
- cap burner testing, 155–156
 - fire testing, 154
 - materials compatibility and stability, 154
 - toxicity testing, 153–154
- Iodine-based halon replacements, description, 90–91
- Iodine compounds, atmospheric chemistry, 31–39
- Iodofluorocarbons, halon replacements, 90–91
- IONO₂, formation, 32
- J
- Jacketed fuel cells, U.S. Army's requirement for Halon 1301 replacement, 168–172

K

Kinetic properties of fluorocarbons, *See* Thermochemical and kinetic properties of fluorocarbons

L

Laminar burning velocity, calculation, 143–145

Lavatory waste bins, application of halons as fire-extinguishing systems, 78

Liquid-phase diffusion time, calculation, 55

Lowest observable adverse effect level, 12

M

Mass spectrometry coupled with molecular beam sampling, analysis of inhibited flame structures, 306–315

Metal corrosion, role in storage compatibility of halon replacements, 123–129

Metal organometallics, halon replacements, 156

Methane–air flames, inhibitor concentration effect on inhibition mechanism of fluoromethanes, 260–272

Methane oxidation, role of halon replacements, 291–292, 294f

Military, halon use reduction, 10

Mist fireball explosion, U.S. Army's requirement for Halon 1301 replacement, 162, 163f

Mole flux of species, calculation, 308–309

Montreal Protocol, phase-out of halon production, 8–11

N

N₂, diffusion flame extinction, 190–201

Nacelle, description, 204

NaHCO₃, storage compatibility, 122–137

Navy's halon total flooding replacement program, *See* U.S. Navy's halon total flooding replacement program

Net reaction rate, calculation, 308

NFPA 2001 Standard on Clean Agent Fire Extinguishing Systems approvals, halogenated fire suppression agents, 95

Nitrogen, effectiveness in dynamic combustion process suppression, 204–223

NO, reaction with iodine compounds, 32

Nomenclature, halon replacements, 6

Nonhalocarbon alternative agents, risk assessment, 13

Nonvolatile precursors, halon replacements, 88–89

Numerical modeling, flame systems, 317–318

O

O₃, reaction with iodine compounds, 33

Occupational Safety and Health Administration, halon regulation, 12

Organic compounds with C–F bonds, bond breakage, 341

Oxidation intermediates of halocarbons, heterogeneous atmospheric chemistry, 50–57

Ozone, *See* Stratospheric ozone

Ozone depletion, role of chlorofluorocarbons, 1

Ozone depletion potentials definition, 24, 65

hydrochlorofluorocarbons and hydrofluorocarbons, 18t, 24–25

potential effects of halon replacements, 65

role in halon regulation, 11

strategies, 11

Ozone destruction effectiveness, potential effects of halon replacements, 63–65

P

Peak concentration, measurement of fire-suppression efficiency, 243

Perfluorinated carbons, acceptability as fire protection agent, 13

Perfluoroalkanes, chemical-inhibiting effect, 289–302

- Perfluoroalkyl iodides, halon replacement, 3,152–156
- Perfluoroalkylamines
advantages as halon replacements, 139–140
applications, 139,149
CF₃ radical role in fire-suppression ability, 147–148
efficiency as fire extinguisher, 148
experimental description, 140
fire-extinguishing ability evaluation by box method, 141–143
inhibition effect on *n*-heptane flames, 143–148
physical properties, 140,144 \dagger
preparation, 140–141
toxicity, 149
- Perfluorocarbons, zero ozone depletion potential halon replacements, 91,92 \dagger
- Perfluoro[*N*-(dimethylethyl)amine], preparation, 140
- Perfluoro[*N*-(dimethylvinyl)amine], preparation, 140–141
- Perfluorotriethylamine, preparation, 140
- Phosphonitriles, halon replacements, 157–158
- Photolysis, iodine compounds, 32
- Physically acting agents/techniques, description, 5–6
- Pitting corrosion, description, 123
- Plug reactor, flame-retardant effects on combustion processes, 275–286
- Policy, halon replacements, 2
- Powder packs, U.S. Army's requirement for Halon 1301 replacement, 169,173
- Powdered aerosol systems, risk assessment, 13
- Premixed methane–air flames, inhibitor concentration effect on inhibition mechanism of fluoromethanes, 260–272
- Pressure, role in flame-retardant effects on combustion processes in plug reactor, 279–280
- Propane–air diffusion flames, acid gas production, 225–241
- Pyrotechnic smoke generators, U.S. Army's requirement for Halon 1301 replacement, 173–174
- ## Q
- Quasi-detonations
characterization procedure, 214–215,216 f ,218 f
conclusions, 221,223
deflagration/detonation tube experimental facility, 212 f –214
lean mixtures, 215,217,218–220 f
operating procedure, 214,216 f
performance of agents, 221,222 f
process, 213
stoichiometric mixtures, 217,220–221
- ## R
- Radiative forcing
definition, 66
potential effects of halon replacements, 66–67
- Reaction(s), fluorinated hydrocarbon flame chemistry, 328–336
- Reaction kinetics, fluorinated hydrocarbons, 328–336
- Real-scale testing, U.S. Navy's halon total flooding replacement program, 181–184
- Regulation, halons and halon replacements, 11–14
- Relative radiative forcing per molecule or mass, potential effects of halon replacements, 67–68
- Replacements for halon, *See* Halon replacements
- Risk balancing approach on health and safety issues, description, 11–12
- ## S
- Self-reaction, reaction with iodine compounds, 33

- SF₆, potential effects on global environment, 59–70
- Significant New Alternatives Policy (SNAP) program
- approvals, halogenated fire suppression agents, 94–95*t*
 - function, 11
 - halon banking, 14
 - halon regulation, 11–14
- Silicon derivatives, halon replacements, 156
- Sodium bicarbonate, effectiveness in dynamic combustion process
- suppression, 204–223
- Sodium bicarbonate powder experiments, turbulent spray flames, 209–210
- Species, fluorinated hydrocarbon flame chemistry, 324–328
- Steaming agents, SNAP approvals, 94,95*t*
- Storage compatibility of halon replacements
- chemical(s), 122–123
 - chemical compositions, 124
 - elastomer seal compatibility
 - durability, 135–137
 - elastomers, 132
 - lubricants, 132
 - swelling, 132–135
- experimental description, 123
- metal corrosion
- exposure testing, 124–127,
 - forms, 123
 - postdeployment corrosion, 128
 - tensile testing, 127–129*t*
- storage stability, 130–131
- Stratospheric ozone
- depletion, 8
 - potential effects of halon replacements, 62–65
 - role
 - EPA in protection, 11
 - halons and bromine-containing compounds, 59
- Stratospheric ozone depletion, role of anthropogenic emissions of Cl- and Br-containing compounds, 41
- Stratospheric ozone impact, chlorofluorocarbons, 16
- Streaming agents
- decomposition product toxicity, 107
 - halon replacement, 82–83
 - testing, 92–93
- Subchronic toxicity testing, description, 102–103
- Suppressant action, classification, 178
- Suppression fraction, definition, 178
- Suppression modeling, U.S. Army's requirement for Halon 1301 replacement program, 175–185
- Surface temperature, potential effects of halon replacements, 66
- T
- Technology, halon replacements, 4
- Temperature role
- flame-retardant effects on combustion processes in plug reactor, 277–279,284*t*
 - fluorine atom removal from halocarbons, 346–348
- Tensile testing, storage compatibility of halon replacements, 127–129*t*
- Testing, halogenated fire suppression agents, 92–94
- Tetrafluoromethane, concentration effect on inhibition mechanism in premixed methane–air flames, 260–272
- Theoretical prediction, thermochemical and kinetic properties of fluorocarbons, 358–372
- Thermochemical and kinetic properties of fluorocarbons
- calculation methodology, 359–360
 - chemical features, 361,364–368
 - equilibrium thermochemistry, 360,362–363*t*
 - experimental description, 358
 - transition states, 367,369–372
- Thermodynamics, IO and BrO, 38–39
- Title VI of U.S. Clean Air Act of 1990, function, 11
- Total flooding agents
- decomposition product toxicity, 106–107
 - halon replacement, 81–82
 - testing, 93–94

- Total flooding replacement program, *See*
U.S. Navy's halon total flooding
replacement program
- Toxic/noxious degradation product
formation, hydrochlorofluorocarbons
and hydrofluorocarbons, 21*t*,23*t*,26
- Toxicity, tropodegradable halon
replacements, 155–156
- Toxicity tests
acute toxicity testing, 101
cardiac sensitization testing, 101–102
development toxicity testing, 102
genetic toxicity testing, 103
subchronic toxicity testing, 102–103
- Toxicological properties of halon
replacements
commercial replacements for total
flooding and streaming, 103
data, 103–105*t*
decomposition product toxicity,
104–107
experimental description, 99
regulatory considerations, 100
toxicity considerations, 99–100
toxicity tests, 101–103
- Transition metal compounds, halon
replacements, 157–158
- Trifluoromethane, concentration effect on
inhibition mechanism in premixed
methane–air flames, 260–272
- Tropodegradable compounds, halon
replacements, 153–156
- Troposphere, iodine reactions, 32–33,35
- Tropospheric degradation products of
hydrochlorofluorocarbons and
hydrofluorocarbons
aldehyde regeneration, 47
experimental procedure, 42
photolysis experiments, 45–47
photooxidation experiments, 47–48
products and yields, 42–43
reaction schemes, 43–45
- Tropospheric lifetime
calculation, 56
halocarbon oxidation intermediates,
56–57
- Tubular flame burner system for
flammability limit measurement
apparatus, 244–246*f*
effect of injection velocity of mixture,
245–248*f*
effect of setup angle of burner,
248,249*f*
experimental description, 245,247
flammable regions of mixtures
with halon replacement, 250–253
with inert gas, 247–252*f*
- Turbulent spray flames
conclusions, 211,213
effect of injection time on total mass and
mass fraction of N₂, 207,208*f*
experimental facility, 205–207,208*f*
gaseous agent test series, 207,209,210*t*
process, 205
sodium bicarbonate powder requirements,
209–210
volume factor of agents, 211,212*f*
- U
- Underwriters Laboratories/Factory Mutual
approvals, halogenated fire suppression
agents, 96
- United Nations Environment Programme,
halon use concerns, 10
- U.S. Army's requirement for Halon 1301
replacement
CO₂ use, 161
crew compartments of ground combat
vehicles, 162,164
cup burner test, 165–167
engine compartments of ground combat
vehicles, 164
Halon 1301 use, 161–162
jacketed fuel cells, 168–172
mechanisms, 164–165
mist fireball explosion, 162,163*f*
powder packs, 169,173
pyrotechnic smoke generators,
173–174
water mists, 173

- U.S. Environmental Protection Agency (EPA)
environmental media criteria for halon regulation, 12–13
halon use concerns, 9–10
role in stratospheric ozone protection, 11
solicitation of guidance from organizations, 13–14
- U.S. Navy's halon total flooding replacement program
chemical effects, 183–184
chemical kinetics/hydrodynamic models, 183
determination of requirements, 185
early suppression modeling efforts, 176–177
extended suppression model, 178–179
history, 175
intermediate-scale testing procedure, 179–180
results, 180–182, 184
minimum acceptable agent concentration determination, 185
nonlinear suppression model, 178–179
- U.S. Navy's halon total flooding replacement program—*Continued*
objectives, 176
physical effect, 184
powder research, 177–178
real-scale testing, 181–185
- V
- Vienna Convention of Ozone Layer Protection, description, 9
Volume factor, definition, 211
- W
- Water mists, U.S. Army's requirement for Halon 1301 replacement, 173
- Z
- Zero ozone depletion potential halon replacements
development, 91
hydrofluorocarbons, 91–92
perfluorocarbons, 91, 92